

Actinide Separations

Publication Date: April 16, 1980 | doi: 10.1021/bk-1980-0117.fw001

Actinide Separations

James D. Navratil, EDITOR
International Atomic Energy Agency


Wallace W. Schulz, EDITOR
Rockwell Hanford Operations

Based on a symposium
sponsored by ACS Division of
Industrial and Engineering Chemistry
at the ACS/CSJ Chemical Congress
(177th ACS National Meeting),
Honolulu, Hawaii,
April 3–5, 1979.

A C S S Y M P O S I U M S E R I E S **117**

AMERICAN CHEMICAL SOCIETY
WASHINGTON, D. C. 1980



Library of Congress  Data

Actinide separations.

(ACS symposium series; 117 ISSN 0097-6156)

"Based on a symposium sponsored by ACS Division of Industrial and Engineering Chemistry at the ACS/CSJ Chemical Congress (177th ACS national meeting), Honolulu Hawaii, April 3-5, 1979."

Includes bibliographies and index.

1. Actinide elements—Congresses. 2. Separation (Technology)—Congresses.

I. Navrátil, James D., 1941— . II. Schulz, Wallace W. III. American Chemical Society. Division of Industrial and Engineering Chemistry. IV. Series: American Chemical Society. ACS Symposium series; 117.

TK9350.A3 621.48'335 79-23956
ISBN 0-8412-0527-2 ACSMC8 117 1-609 1980

Copyright © 1980

American Chemical Society

All Rights Reserved. The appearance of the code at the bottom of the first page of each article in this volume indicates the copyright owner's consent that reprographic copies of the article may be made for personal or internal use or for the personal or internal use of specific clients. This consent is given on the condition, however, that the copier pay the stated per copy fee through the Copyright Clearance Center, Inc. for copying beyond that permitted by Sections 107 or 108 of the U.S. Copyright Law. This consent does not extend to copying or transmission by any means—graphic or electronic—for any other purpose, such as for general distribution, for advertising or promotional purposes, for creating new collective works, for resale, or for information storage and retrieval systems.

The citation of trade names and/or names of manufacturers in this publication is not to be construed as an endorsement or as approval by ACS of the commercial products or services referenced herein; nor should the mere reference herein to any drawing, specification, chemical process, or other data be regarded as a license or as a conveyance of any right or permission, to the holder, reader, or any other person or corporation, to manufacture, reproduce, use, or sell any patented invention or copyrighted work that may in any way be related thereto.

PRINTED IN THE UNITED STATES OF AMERICA

**American Chemical
Society Library
1155 16th St. N. W.**

In Washington, D. C. 20036

ACS Symposium Series; American Chemical Society: Washington, DC, 1980.

ACS Symposium Series

M. Joan Comstock, *Series Editor*

Advisory Board

David L. Allara

Kenneth B. Bischoff

Donald G. Crosby

Donald D. Dollberg

Robert E. Feeney

Jack Halpern

Brian M. Harney

Robert A. Hofstader

W. Jeffrey Howe

James D. Idol, Jr.

James P. Lodge

Leon Petrakis

F. Sherwood Rowland

Alan C. Sartorelli

Raymond B. Seymour

Gunter Zweig

FOREWORD

The ACS SYMPOSIUM SERIES was founded in 1974 to provide a medium for publishing symposia quickly in book form. The format of the Series parallels that of the continuing ADVANCES IN CHEMISTRY SERIES except that in order to save time the papers are not typeset but are reproduced as they are submitted by the authors in camera-ready form. Papers are reviewed under the supervision of the Editors with the assistance of the Series Advisory Board and are selected to maintain the integrity of the symposia; however, verbatim reproductions of previously published papers are not accepted. Both reviews and reports of research are acceptable since symposia may embrace both types of presentation.

PREFACE

Actinide separation techniques and methods play a very important role in analysis and production of nuclear materials, reprocessing of nuclear fuels, nuclear waste management, and other aspects of the nuclear fuel cycle. Professionals from several disciplines—analytical chemists, chemical engineers, process chemists, etc.—make much use of this technology.

This Symposium has been organized about new concepts, new systems, and new developments in actinide separations methodology. Much of the work reported here is based on fundamental actinide chemistry developed since the Manhattan Project days. The chapters in this volume describe ion exchange, solvent extraction, precipitation, pyrochemical, photochemical, and other methods of actinide separations as well as application of these separation methods to power reactor fuel reprocessing and recovery of actinides from waste solutions.

The purpose of this Symposium has been to bring together information concerning actinide recovery, partition, and purification on an international basis from various disciplines and viewpoints. The result of this interchange, it is hoped, will be to spark ideas for improvement and development of new separation techniques and methods for all aspects of actinide technology.

Vienna, Austria

JAMES D. NAVRATIL

Richland, Washington
June 20, 1979

WALLACE W. SCHULZ

INTRODUCTION

The actinide elements consist of naturally occurring thorium, protactinium, and uranium and the synthetic transuranium elements neptunium to lawrencium, inclusive. The actinide elements neptunium to einsteinium, inclusive, are manufactured in weighable quantities by irradiation of uranium in nuclear reactors and are isolated by chemical means. The first chemical process for the isolation of neptunium and plutonium, the Bismuth Phosphate Process, was developed and put into plant-scale operation during World War II. This actinide separations process was replaced by the Redox Process, developed during and after the war. The Redox Process was in turn replaced by the Purex Process, which by now has become the classic method for recovering and purifying uranium, neptunium, and plutonium from irradiated nuclear reactor fuels. Diverse chemical separations processes, specially tailored for the purpose, are used to recover and purify transplutonium elements.

Plutonium is manufactured in megagram quantities; neptunium, americium, and curium in kilogram quantities; californium in gram amounts; berkelium in 100-milligram amounts; and einsteinium in milligram quantities. Chemical separations play a key role in the manufacture of actinide elements, as well as in their recovery, and analysis in the nuclear fuel cycle. This collection of timely and state-of-the-art topics emphasizes the continuing importance of actinide separations processes.

Berkeley, California

GLENN T. SEABORG

Neptunium (V) Anionic Exchange in Sulfate-Sulfuric Acid Solutions

J. REGO, J. GARRISON, and R. CARVER

Lawrence Livermore Laboratory, Livermore, CA 94550

The purpose of this study was to investigate the anionic exchange behavior of neptunium(V) in sulfate-sulfuric acid, because neptunium is often present as a contaminant during the separation of other actinides (1). Sulfuric acid systems are seldom utilized in industrial processes, but are often used as part of a laboratory analytical procedure. Literature on neptunium in HClO_4 , HCl , HCl-HF , and HNO_3 is quite complete, but the information on the H_2SO_4 system is sketchy at best. There is one report (2) that neptunium(V) is adsorbed strongly on Dowex 2 resin from 0.1 N to 1 N H_2SO_4 . Our measurements indicate that there is very little adsorption of Np(V) on Dowex 1 resin even at low concentrations of sulfate-sulfuric acid. We believe the differences in chemical structure of the two resins are not sufficient to explain the disparity in adsorption.

Experimental

^{237}Np traced with ^{239}Np ($t_{1/2} = 2.35$ days) was used to measure the amounts of Np adsorbed on anion exchange resin. The ^{239}Np was selected because of availability and convenience in detection. The ^{239}Np tracer was prepared by extraction from a ^{243}Am solution into thenoyltrifluoroacetone (TTA). The Np in the organic TTA was washed three times with 1 N HCl -0.4 N HI . The Np was then back-extracted into 9 N HCl .

The (V) oxidation state for all Np solutions was achieved by digesting with dilute HNO_3 before boiling to near dryness with H_2SO_4 and diluting to 0.1 N sulfuric acid (3, 6).

Five standard solutions of increasing concentrations of H_2SO_4 were prepared: 0.05, 0.1, 0.4, 0.8, and 4.2 N. From each of these solutions six aliquots were taken. To five of these aliquots a weighed and increasing amount of Na_2SO_4 was added. A measured amount of ^{237}Np traced with ^{239}Np was added to all six aliquots.

The concentrations of the sulfuric acid ranged from 0.05 N to 4.2 N. The total sulfate concentration ranged from 0.05 N to 8 N.

0-8412-0527-2/80/47-117-003\$05.00/0

© 1980 American Chemical Society

In Actinide Separations; Navratil, J., et al.;

ACS Symposium Series; American Chemical Society: Washington, DC, 1980.

The final solutions were mixed and then added to weighed amounts of anion exchange resin in a 15-ml centrifuge cone.

The resin had been prepared from commercial Dowex-1 (1 x 8), chloride form, that had been graded for particle size by selecting the fraction with a settling rate of 30-70 mm/min. The resin was first converted to the hydroxide form by washing with dilute NaOH, rinsing with water, and then converted to sulfate form by washing with dilute H₂SO₄. The resin was air-dried at room temperature before use.

Each mixture of resin and neptunium sulfate solution was mixed by mechanical shaking and was allowed to equilibrate overnight. This time interval is long, compared to the duration of an analytical procedure. The liquid was then filtered away from the resin, and the residual radioactivity of a measured aliquot of the liquid was compared to an identical solution that had not been added to any anion exchange resin. The radioactivity measurements were performed in an end-window NaI crystal counter shielded with lead. The acidity of each solution was measured by titration with a standard base.

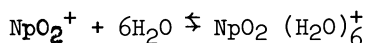
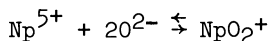
Results and Discussion

The neptunium adsorption on the resin was calculated from the measurements of ²³⁹Np not adsorbed according to the following equation:

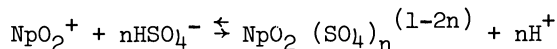
$$K_D = \frac{[\text{Total } ^{239}\text{Np} - ^{239}\text{Np}_{(\text{liquid})}]/\text{gm resin}}{^{239}\text{Np}_{(\text{liquid})}/\text{ml}}$$

Values for the calculated K_D 's are listed in Table 1. Where replicate measurements were made, the individual results are reported. A computer was used to generate a graph of the data (Fig. 1).

Neptunium(V) exists as a neptunyl ion and either hydrates or complexes (3, 4) as shown below:



If sulfate complexing occurs, the following process is predicted:



This process has been studied using spectrophotometry and oxidation potential shift, and no formation of a sulfate complex has been found (5).

TABLE I
Data for Measured and Calculated

Acid Conc.	H ₂ SO ₄ 0.05 N			H ₂ SO ₄ 0.12 N			H ₂ SO ₄ 0.41 N			H ₂ SO ₄ 0.86 N			H ₂ SO ₄ 4.2 N		
	Np Count Rate	Normality Total Sulfate	K _D	Np Count Rate	Normality Total Sulfate	K _D	Np Count Rate	Normality Total Sulfate	K _D	Np Count Rate	Normality Total Sulfate	K _D	Np Count Rate	Normality Total Sulfate	K _D
2 g	2056	4.0	0.87	2156	4.1	0.05	2256	4.4	0.18	2274	4.8	0.13	2317	8.02	0
1 g	2031	2.1	0.98	-	-	-	-	-	-	-	-	-	2404	6.06	0
1 g	1999	2.1	1.05	2046	2.1	0.9	2215	2.5	0.30	2373	2.8	0	2378	6.20	0
0.25	1974	0.58	1.22	2068	0.4	0.8	2278	0.94	0.12	2385	1.4	0	2466	4.83	0
0.25	1984	0.58	1.23	2040	0.6	0.9	2239	0.92	0.24	2401	1.4	0	2452	4.74	0
0.06	2009	0.17	1.06	2114	0.2	0.7	2341	0.5	0	2259	1.0	0.18	2470	4.45	0
0.06	2008	0.15	1.07	2058	0.2	0.8	2296	0.6	0.06	2377	1.0	0	2396	4.45	0
0.02	2061	0.09	0.84	2167	0.14	0.5	2335	0.5	0	2395	0.9	0	-	-	-
0.02	2113	0.08	0.68	2185	0.14	0.4	2259	0.5	0.18	2413	0.9	0	-	-	-
0.0	2090	0.06	0.76	2196	0.10	0.4	2298	0.4	0	2489	0.86	0	2426	4.40	0

The ²³⁹Np activity available to each sample was 2320 cts/min/ml.

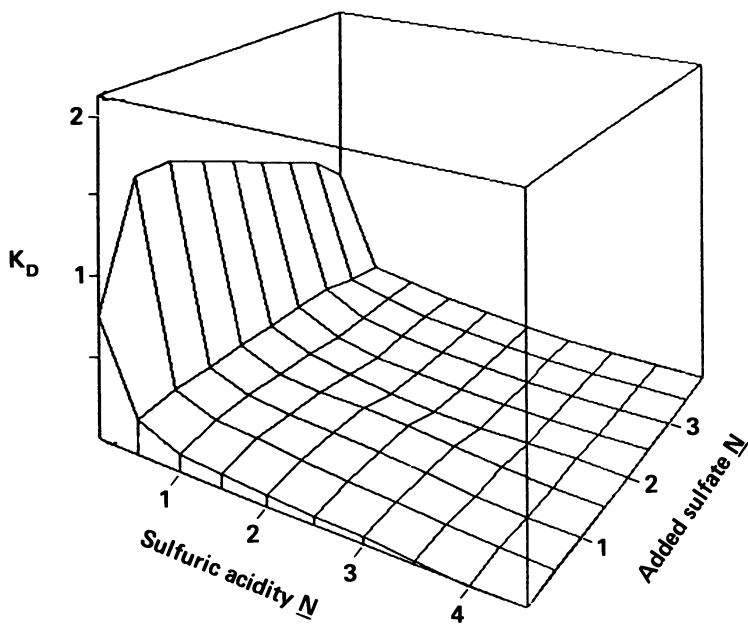


Figure 1. $Np(V)$ adsorption in total sulfate

Conclusion

The most significant difference between Dowex 1 and Dowex 2 resin is in the order of selectivity of the hydroxide ion. All other mechanical variables between the two resins, such as pore size, shrinkage, capacity and water content, are negligible differences. We conclude that these differences are insufficient to explain the disparity of adsorption of neptunium.

We have measured the adsorption of Np(V) on Dowex 1 anion exchange resin from solutions of sulfuric acid that had increasing amounts of sulfate salts added. We found that Np(V) did not adsorb significantly at any acid or sulfate concentrations. The measured K_D 's are largest at low concentrations of sulfate and sulfuric acid. The K_D 's decreased as both the sulfate or sulfuric acid concentrations increased.

Literature Cited

1. Carver, R.; Dupzyk, R., Lawrence Livermore Lab. Internal Rept. NCDTN-78-1, 1978.
2. Wish, L.; Rowall, M., U.S. Naval Radiological Defense Lab. Rept. USNRDL-TR-117, NS-081-001, 1956.
3. Burney, G.; Harbour, R., "Radiochemistry of Neptunium," U.S. AEC Technical Information Center, Oak Ridge, TN, NAS-NS-3060, 1974.
4. Mikhailov, V., "Analytical Chemistry of Neptunium," Halsted Press, NY, 1973.
5. Ai-Niaimi, N.; Wain, A.; McKay, H., J. Inorg. Nuc. Chem., 1970, 32, 2331.
6. Sjoblom, R.; Hindman, J., J. Am. Chem. Soc., 1951, 73, 1744.

RECEIVED June 27, 1979.

Work performed under the auspices of the U.S. Department of Energy by the Lawrence Livermore Laboratory under contract number W-7405-eng-48.

Recovery of Plutonium Traces from Nitric Acid-Fluorhydric Acid Solutions by Sorption onto Alumina

J. ADROALDO DE ARAÚJO and ALCÍDIO ABRÃO

Chemical Engineering Center, Energetic and Nuclear Research Center,
Cx Postal 11049, Pinheiros, S.P., Brazil

Sorption of plutonium traces onto alumina from uranyl nitrate solutions has been investigated. Several methods have been previously proposed for the recovery of plutonium traces from reprocessing solutions. Those methods include ion exchange (1,2), solvent extraction (3,4) and, extraction chromatography (5,6).

Several hydrous oxides, such as those of aluminum, silicon and, iron have been used to extract traces ions. Nevertheless, the sorption mechanism is not definitively established. Those oxides probably exhibit some ion exchange capacity among their properties and they can act as anionic or cationic exchangers and sometimes both. The separation of plutonium traces in the presence of HF by sorption onto an alumina column is based on its chemical similarities with thorium and lanthanide elements reported by Abrão (7). In this case only thorium and rare earths are sorbed onto alumina from nitric acid-fluoride solutions while uranium remains in the effluent.

The redox methods are well known for the purification and concentration of plutonium from the Purex process solutions. This paper deals with three different oxidation states of plutonium Pu(III), Pu(IV), and Pu(VI) in HNO₃-HF systems. The chromatographic column method using alumina has been applied successfully to the separation of plutonium when uranyl nitrate solution containing 0.1-0.3M HF was percolated through the column.

EXPERIMENTAL

All ²³⁹Pu solutions used during the runs were prepared from a standard solution (Amersham/Searle), of 1 uCi/ml (160 µg/ml) specific activity. The uranium solutions were obtained by dissolution of nuclear grade uranium oxides. One ml of Al₂O₃ chromatographic grade was conditioned according BROCKMANN (8) with 0.8M HNO₃ in glass columns 0.6cm in diameter and 20cm long. The experiments were followed by alpha spectrometry after the plutonium was extracted with 0.5M TTA/XYLOL. The samples for quantitative determination were prepared by electroplating according to WENZEL and HERZ (9). The alpha energy measurement was made by a

0-8412-0527-2/80/47-117-009\$05.00/0
© 1980 American Chemical Society

surface barrier detector associated with a ORTEC multichannel analyser. The plutonium oxidation states were determined by a photometric method using ARSENAZO III. The determinations were carried out with a double beam PERFIN-FLMER spectrophotometer using quartz microcells.

The first experiments were carried out to understand the performance of plutonium in an $\text{Al}_2\text{O}_3 - \text{HNO}_3$ medium. This was done by percolation of 25 ml of ^{239}Pu solution in 0.8M HNO_3 with alpha activity of 55,000 + 235 (counts/2000 sec/ml), through a glass chromatographic column (i.d. 6mm) containing 1 ml of Al_2O_3 .

All runs were made with 0.8M HNO_3 solutions with a Pu alpha activity of 10,000 + 316 (counts/2000 sec/ml) and, HF concentration ranging from 0.1 to 0.3M.

The feed solution for the Al_2O_3 column has the following composition: $1.5 \times 10^{-8}\text{M}$ ^{239}Pu ; alpha activity = 230,000 + 480 (counts/2000/sec/20ml); 0.8M HNO_3 ; 0.1 - 0.3M HF; uranyl nitrate 47.6 g U/l; 0.005M FeSO_4 and 0.04M NaNO_2 . Pu(IV) was obtained in this solution by previous reduction of total plutonium to Pu(III) with Fe(II) followed by oxidation with nitrite. No interference of uranium was observed in the process. To avoid the interference of ^{234}Th (a uranium daughter) on the measurements of plutonium, it was previously removed by percolating the solution into another alumina column before the addition of ^{239}Pu .

RESULTS AND DISCUSSION

The results (Table I) show that only 1% of the plutonium is retained by the alumina from 0.8M nitric acid and therefore plutonium must likely be complexed to be sorbed. Figure 1 shows a typical plutonium breakthrough curve from 0.8M nitric acid.

Table I. Plutonium Retention from 0.08M HNO_3 onto Al_2O_3

Exp.	^{239}Pu retained (%)
1	1.8
2	1.0
3	0.8
4	0.9
5	1.1

Table II shows that the plutonium sorption onto Al_2O_3 is around 87% and it was demonstrated that with the aid of fluoride ions the recovery of plutonium traces from waste solutions was possible.

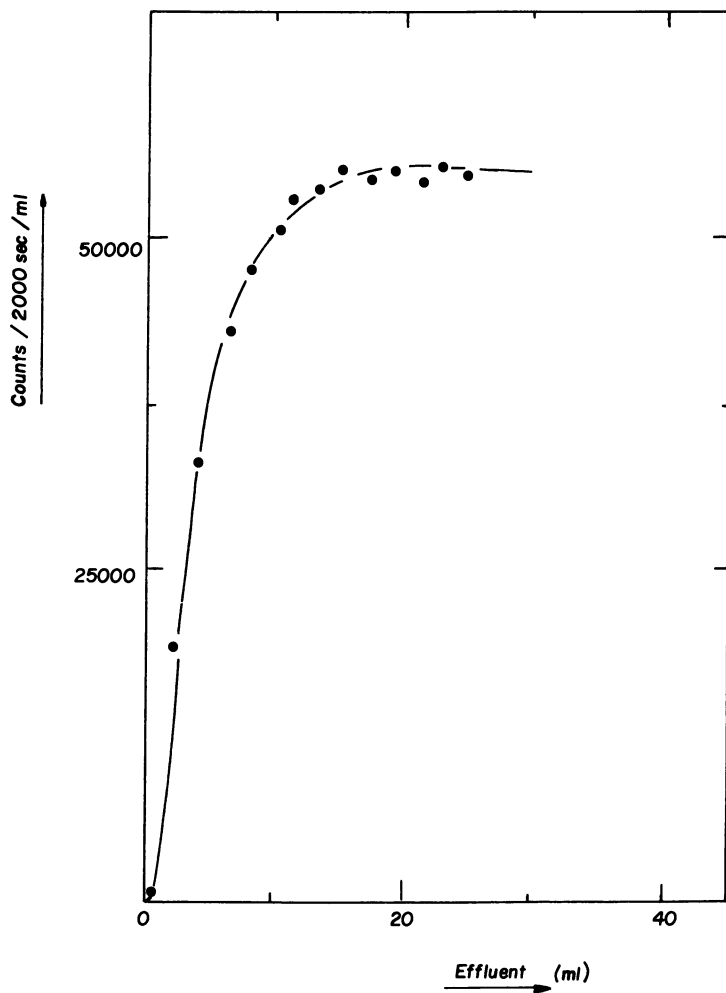


Figure 1. Breakthrough curve of Pu onto Al₂O₃ column; feed: 25 ml ²³⁹Pu-0.8M HNO₃; ²³⁹Pu activity = 55,000 ± 235 counts/2000 sec/ml; column = 1 ml Al₂O₃; flow rate = 0.8 ml/min/cm².

Table II. Effect of HF on Pu Retention on Al_2O_3

HF (M)	^{239}Pu ret. (%)	D.F. (^{239}Pu)
0.1	85.7	7.0
0.1	85.5	6.9
0.1	86.1	7.2
0.2	84.4	6.4
0.2	84.8	6.5
0.3	89.6	9.5
0.3	89.4	9.5

As was observed in the first experiments, plutonium was not completely sorbed onto alumina from 0.1 to 0.3M HF. So the next step was to examine the possibilities of adding redox agents to maintain a single oxidation state. A concentration of 0.1M HF was chosen because this is enough HF to complex all the plutonium ($Pu \sim 10^{-8}M$) in the feed solution and will not cause significant corrosion effects on the glass column. Some of the redox agents used and the average yields of plutonium recovery are given in Table III. Tetravalent plutonium is better sorbed than Pu (III) or Pu (VI). The three oxidation states of plutonium were determined spectrophotometrically by complexing Pu with ARSENAZO III (10) in nitric acid medium by adapting the method of NEMODRUCK and collaborators (11,12).

Table III. Effect of Pu oxidation states on sorption. Feed solution: $^{239}Pu \sim 100,000 + 316$ counts/2000 sec/10 ml; 0.8M $HNO_3 \sim 0.1M$ HF column: i.d. 6mm; vol. 1 ml Al_2O_3 .

Pu Valence	Redox agent in the loading solution	Pu ret. (%)	D.F. (^{239}Pu)
III	0.2M $NH_2.NH_2 - 0.2M NH_2.OH.HCl$	65.0	2.8
VI	conc. $HC10_4$	69.7	3.6
IV	0.01M $NaNO_2$	87.2	7.8
IV	0.03M $NaNO_2$	89.0	9.0
IV	0.1M $NH_2.NH_2 - 0.01M NaNO_2$	90.9	11.0
IV	0.002M $Fe(NO_3)_3 - 0.1M NH_2.OH.HCl - 0.02M NaNO_2$	92.3	13.0
IV	0.005M $FeSO_4 - 0.04M NaNO_2$	97.8	47.2

A set of laboratory experiments proved that the most effective and consistent method to elute plutonium from the alumina was by reducing plutonium to trivalent state in nitric acid. The collected data (Table IV) present good results when 3M $HNO_3 - 0.005M FeSO_4$ solution was used as elutriant. Ap-

proximately 95% of the plutonium was recovered at room temperature (25°C). To determine if the temperature could improve the plutonium desorption, the elution was done with the same elutrient at 25 and 50°C. Figure 2, shows these curves and, at 50°C, the elution presents a sharper peak while the curve at 25°C exhibits some tail.

Table IV. Plutonium elution from Al_2O_3 column at 25°C.

Elutrient	Pu eluted (%)
(M) HNO_3	
1	62.9
2	65.3
3	78.9
4	70.6
5	22.6
6	15.7
(M) HNO_3 - (M) $FeSO_4$	
1 0.005	80.8
2 0.005	81.3
3 0.005	94.7

To demonstrate the validity of this procedure for the recovery of trace amount of plutonium from dilute solutions, 30 liters of solution with a specific activity of ^{239}Pu 135 + 12 (counts/2000/sec/ml) was percolated through a small column containing 10 ml of Al_2O_3 . About 97% of plutonium were sorbed onto the alumina.

The experiments have shown that trace sorption of Pu(IV) onto Al_2O_3 is almost complete from 0.8M HNO_3 - 0.1M HF. The stabilization of Pu(IV) state was obtained by prior reduction to Pu(III) and reoxidation to Pu(IV) using Fe(II) and nitrite.

The Al_2O_3 column loaded with plutonium was satisfactorily washed with an 0.1M HNO_3 - 0.05M HF solution for the removal of the last traces of uranium and other elements not sorbed. The effluents contained less than 0.01% of plutonium. Washing the column with an 0.8M HNO_3 - 0.05M HF solution resulted in 0.1% of plutonium activity in the effluent. This indicates that the column should be washed with more dilute nitric acid. The effectiveness of elution with HNO_3 plus a reducing agent at room temperature and 50°C was confirmed in both cases. As Pu(IV) is more sorbed onto alumina than the other plutonium oxidation states, it was reduced to Pu(III) to improve the elution. On the other hand HNO_3 is the most convenient medium for further uses of plutonium, so for that reason nitric acid (1-6M) was selected as elutrient. Pure 3M HNO_3 at room temperature eluted 79% of plutonium. A 3M HNO_3 - 0.005M $FeSO_4$ solution was chosen as eluting agent and, the elution yield

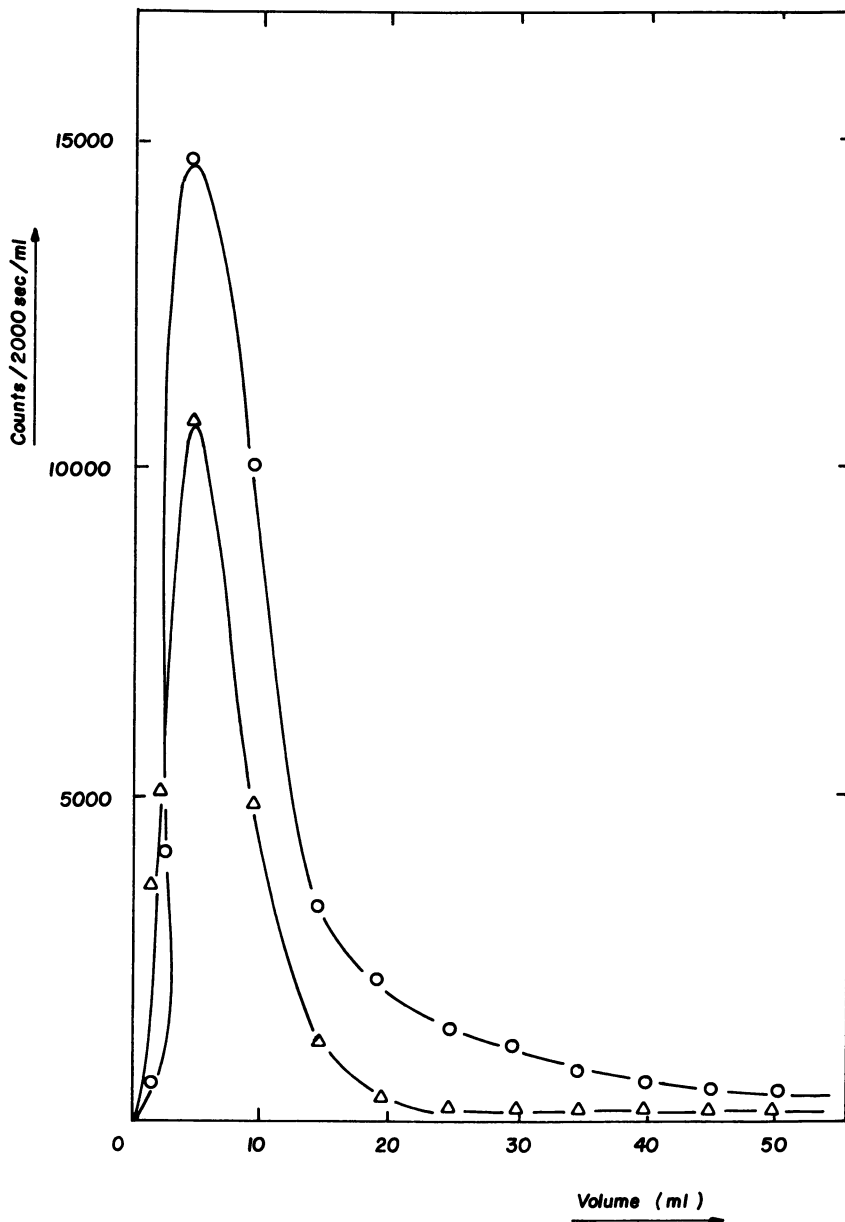


Figure 2. Elution curve of ^{239}Pu from Al_2O_3 column; $\text{Al}_2\text{O}_3 = 1$ ml; flow rate = 1.4 ml/min/cm 2 , surface barrier detector: (O) 3M HNO_3 - 0.005M Fe^{2+} , temperature $\sim 25^\circ\text{C}$; (Δ) 3M HNO_3 - 0.005M Fe^{2+} , temperature $\sim 50^\circ\text{C}$.

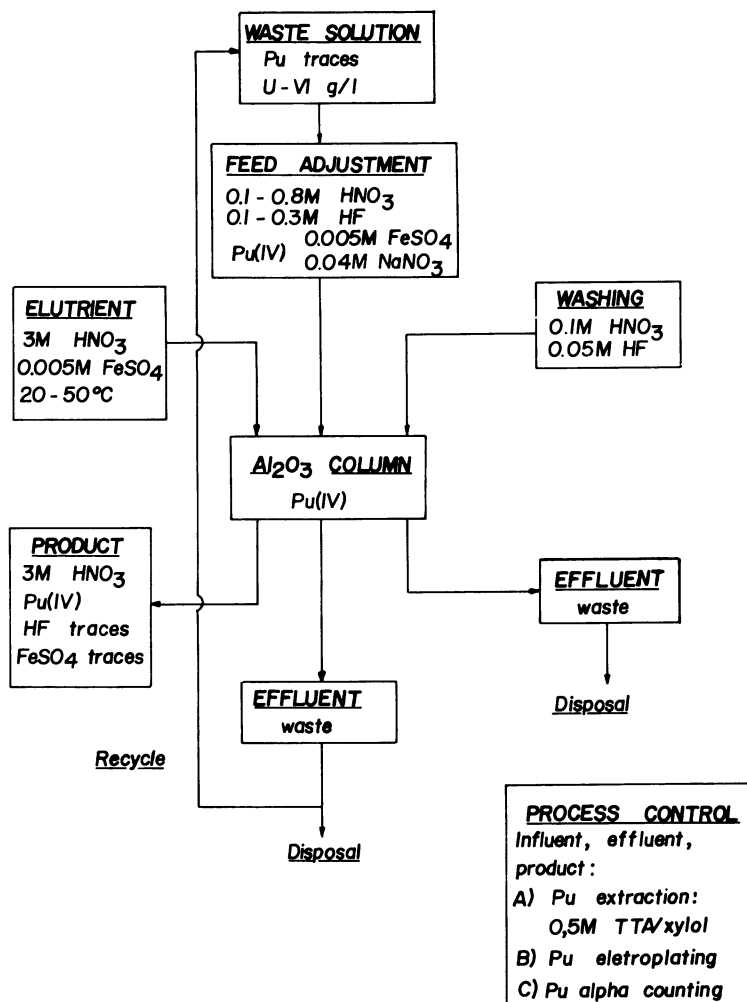


Figure 3. Proposed flowsheet for recovery of Pu traces from reprocessing solutions

being improved to about 95%. Also the temperature has some influence in the elution.

The descontamination of plutonium traces from macroquantities of uranyl nitrate by sorption of Pu(IV) onto an Al_2O_3 column was easily and successfully accomplished. Percolation of a 0.8M $UO_2(NO_3)_2$ solution, 0.8M in HNO_3 and 0.3M in HF traced with plutonium-239, the Pu was sorbed while uranium passed through the Al_2O_3 column.

CONCLUSION

The successful experiments for the retention of plutonium onto alumina from HNO_3 -HF solution gave enough confidence to recommend the proposed method to separate traces of plutonium from waste solutions in the presence of macroamounts of uranium (VI). Of course, only macroamounts of thorium, uranium (IV) and rare earths are serious interfering ions, since they precipitate with HF. The behavior expected for neptunium in the same system should be similar to plutonium, thorium and rare earths. The retention of neptunium from HNO_3 -HF solutions is in progress. The sorption yield for Pu was around 95%. The sorption mechanism is not well established. Figure 3 shows the proposed flowsheet for recovery of Pu traces from reprocessing waste solutions.

LITERATURE CITED

1. Aikin, A.M. Chem. Engng. Progr. 1957 53, 82.
2. Billiau, R., Lafontaine, I., Mostin, N., Zamorani, E. Proc. Symp. chimie des traitements des combustibles irradiés par voie aqueuse, Bruxelles, 1963.
3. Howells, G.R., Hughes, T.G., Mekey, D.R., Saddington, K. ETR report 222, March, 1968.
4. Merril, E.T., Stevenson, R.L. HW report 38684, 1955.
5. Eschrich, H. Hundere, I. ETR report 222, March, 1968.
6. Siekiersk, S., Fidelis, I. J. Chromatog. 1960, 4, 60.
7. Abrão, A. IEA report 217, June, 1970.
8. " The Merck index ", 8 ed. Rahway, N.J. Merck & Co., 1968, 46.
9. Wenzel, V., Herz, D. KFA-Jülich, ICT Jahresbericht für den Zeitraum von 1 Juli 1972 bis 30 Juni 1973, 1973, 115.
10. Milynkova, M.S., Savvin, S.B. Russ J. Anal. Chem. 1967, 22, 308
11. Nemodruk, A.A., Gluklova, L.P. Russ J. Anal. Chem. 1963, 18, 85.
12. Nemodruk, A.A., Kochetkova, N.F. Russ. J. Anal. Chem. 1962, 17, 333.

RECEIVED May 25, 1979.

Application of Inorganic Sorbents in Actinide Separations Processes

WALLACE W. SCHULZ

Rockwell Hanford Operations, Richland, WA 99352

JOHN W. KOENST

Mound Facility, Monsanto Research Corporation, Miamisburg, OH 45342

DAVID R. TALLANT

Sandia Laboratories, Albuquerque, NM 87185

Plant-scale applications of organic ion exchange resins, both anion and cation, in actinide recovery, separation, and purification processes are well established. Typical anion resin applications include tailend purification and concentration of plutonium and neptunium recovered by the Purex process and recovery and separation of ^{237}Np and ^{238}Pu from irradiated neptunium targets. (1) Cation exchange resins are used in ^{241}Am recovery and purification processes and, also, in pressurized systems, to recover and purify kilogram amounts of ^{244}Cm and ^{243}Am . (2)

For several good reasons - poor hydraulic behavior, unsatisfactory sorption kinetics, unavailability, in some cases, of commercial quantities, etc., - inorganic sorbents, in contrast to their organic counterparts, have not been used extensively in the backend of the nuclear fuel cycle. Also, such production-scale applications of inorganic exchangers as have been made have been concerned much more with sorption of particular fission products (e.g., ^{137}Cs) than with separation or purification of actinides.

This paper summarizes the present status of research which is currently underway at several U. S. Department of Energy laboratories - Rockwell Hanford Operations, Mound Facility, and Sandia Laboratories, Albuquerque - to explore the properties and characteristics of two inorganic sorbents, bone char (a form of calcium hydroxyapatite) and sodium titanate [$\text{Na}(\text{Ti}_2\text{O}_5\text{H})$], in decontaminating liquid waste streams from actinides and in separating americium and curium from lanthanides. Success in this research might lead to a potential breakthrough in plant-scale application of inorganic exchangers in actinide separation schemes.

Sorbent: Preparation-Source-Properties

Bone Char. Bone char, a form of calcium hydroxyapatite [$\text{Ca}_{10}(\text{PO}_4)_6(\text{OH})_2$], is the commercial name given a natural product

0-8412-0527-2/80/47-117-017\$05.00/0

© 1980 American Chemical Society

made from granulated cattlebone. In the United States this material is currently available in granular form from Stauffer Chemical Corporation at a cost of approximately \$1.00/kg (\$0.50/lb). The chemical composition of the commercial product along with some pertinent physical properties is listed in Table I; the Ca/P weight ratio in bone char is 2.153 compared to 2.156 in pure calcium hydroxyapatite. Additional information on some other properties of bone char is given elsewhere.(3)

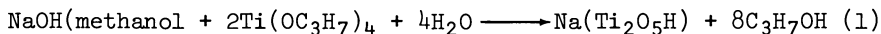
TABLE I

SELECTED PHYSICAL PROPERTIES OF
BONE CHAR AND SODIUM TITANATE

<u>Property</u>	<u>Bone Char</u> (a)	<u>Sodium Titanate</u>
Bulk density (g/cm ³)	0.641	0.35
Surface area (m ² /g)	110-120	200-400
Pore volume (cm ³ /g)	0.25-0.30	
Average particle size (mm)	1.1	0.25

(a) Composition: 7.0-8.5% C; 24.3-25.0% Ca; 0.4-0.6% Fe;
0.02-0.03% Al; 0.50-0.7% Mg; 14.8-15.2% P.

Sodium Titanate, Niobate, and Zirconate. Preparation and properties of the inorganic cation exchangers Na(Ti₂O₅H), Na(Nb₂O₆H), and Na(Zr₂O₅H) have been intensively studied by R. G. Dosch and his colleagues at Sandia Laboratories.(4,5) These ion exchange materials are synthesized via the hydrolytic reaction of NaOH and water with the metal alkoxides Ti(OC₃H₇)₄, Nb(OC₂H₅)₅, and Zr(OC₄H₉)₄ as illustrated for preparation of sodium titanate (Eqn 1).



Titanium isopropoxide and NaOH are reacted in a molar ratio of 2:1, respectively, with the titanium isopropoxide added to the NaOH-methanol solution with stirring. Subsequently, hydrolysis is done by pouring the mixture into an acetone-water mixture containing 8.5 vol% water; one liter of the acetone-water mixture is required for each mole of titanium. The hydrolyzed material is coarse and can be easily and rapidly vacuum filtered through a 50 micrometer frit. After drying at ambient temperature under vacuum, dried titanate powder is then screened with the material which passes a Number 40 U. S. Standard sieve and is retained on a Number 140 U. S. Standard sieve being the desired fraction. Some properties of sodium titanate powder are listed in Table I.

Sodium zirconate and sodium niobate exchangers have been prepared only in small laboratory-scale batches and their properties have been far less well characterized than those of

sodium titanate. Kilogram quantities of -40+140 mesh sodium titanate powder, synthesized according to Equation 1, have been prepared by Cerac, Inc., Milwaukee, Wisconsin. Also, a cooperative research program between Rockwell Hanford Operations and Sandia Laboratories is underway to develop pellet-forms of titanate with better hydraulic properties than the powder. Two such forms currently being tested are 1.6 mm diameter cylinders prepared by room temperature extrusion of water-wet powder and titanate-loaded macroreticular anion exchange resins.

Equilibration of sodium titanate, sodium niobate, and sodium zirconate with dilute HNO_3 solutions converts them to the respective hydrogen forms $\text{H}(\text{Ti}_2\text{O}_5\text{H})$, $\text{H}(\text{Nb}_2\text{O}_6\text{H})$, and $\text{H}(\text{Zr}_2\text{O}_5\text{H})$. (Vacuum dried, -40+140 mesh hydrogen form exchangers were used in some of the work reported here.) Titanate, zirconate, and niobate exchangers exhibit varying stabilities toward HNO_3 solutions. The titanate sorbent is stable in $<0.01\text{M}$ HNO_3 but dissolves, to a small extent, when contacted with 0.1M HNO_3 for a week. When contacted with 0.5M HNO_3 for two days, a few percent of the zirconate exchanger dissolves; the zirconate form appears to be completely stable in $<0.5\text{M}$ HNO_3 . Finally, niobate exchanger is indefinitely stable in 0.5M HNO_3 and dissolves only very slowly, if at all, in 2.5M HNO_3 .

Sorbent Applications: Chemistry and Processes

Bone Char Decontamination of Mound Facility Waste Streams.

Both bench and pilot plant scale studies have been performed to investigate the application and integration of bone char in schemes to remove alpha activity (^{238}Pu , ^{239}Pu , ^{233}U) from various aqueous waste streams generated at the Mound Facility. These studies have culminated in installation and successful operation of a plant-size bone char column for tertiary treatment of the Mound Facility low-risk waste stream. Highlights of the Mound experience with bone char, based on results reported in part elsewhere, (6,7,8) are briefly summarized in this paper.

Mound Facility Low-Risk Waste. Approximately 3×10^5 l of low-level waste are generated weekly at the Mound Facility. This particular waste stream is essentially local hard water which has been demineralized and then used in various chemical processes involving the radionuclides ^{238}Pu and ^{233}U . The first step in decontaminating the low-risk wastes entails addition of small amounts of calcium and iron salts followed by addition of NaOH to pH 11.5 to precipitate iron and calcium hydroxides and carbonates. The clarified effluent from the precipitation step is then passed through a 200 micrometer sand filter to yield a solution containing, typically, 0.4 d/min/ml alpha activity.

Two columns, each 0.6 m diameter and 1.4 m high (Figure 1) and each containing about 230 kg of bone char, are planned for further decontamination of the effluent from the sand filter. Figure 2 illustrates the flow diagram of the bone char tertiary

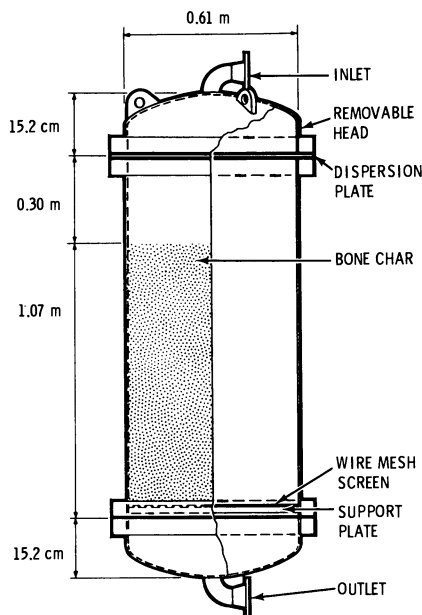


Figure 1. Bone char column used in tertiary treatment of mound facility low-risk waste

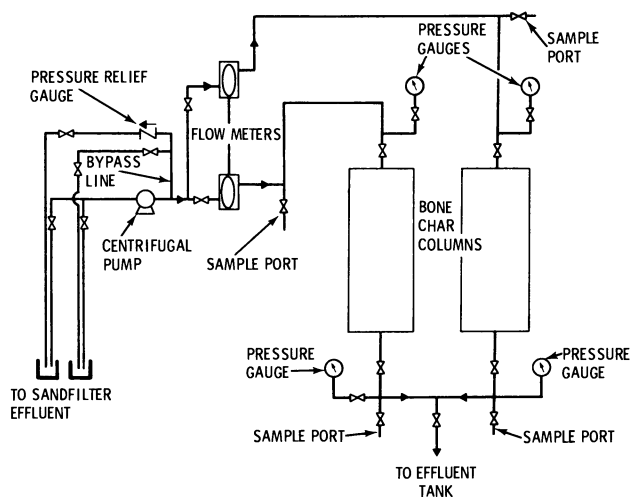


Figure 2. Flow diagram for plant-scale bone char tertiary treatment of mound facility low-risk waste

treatment system designed to operate at flows up to 190 l/min and at pressure drops as high as 345 kPa. One of the two plant-scale bone char beds was designed, installed, and put into operation in June, 1977. Its performance has been very satisfactory with column effluents routinely containing less than 0.1 d/min/ml alpha activity. It is anticipated that the bone char in this column will be changed out some time in 1979.

The criteria used in designing the full-scale treatment system were based on data obtained from a pilot-plant study using a 0.38 m dia. by 0.61 m high bed of bone char operated at a rate of about 40 l/min. Feed to the column contained an average 0.18 nCi/l alpha activity while the effluent contained about 0.09 nCi/l total alpha. This bed of bone char satisfactorily decontaminated 2.1×10^5 l of feed before saturation.

Mound Facility Caustic Waste. About 6000 l of so-called caustic waste containing 0.5 to as much as 8 mg Pu/l are generated yearly at the Mound Facility. The bulk (90 vol%) of this particular waste stream consists of a 4 wt% NaOH solution used as a scrubber in the corrosive off gas system. The remainder originates as filtrates from NH_4OH precipitation of $\text{Pu}(\text{OH})_4$ (8 vol%) and miscellaneous alkaline wastes including analytical samples and incinerator off gas scrubber solutions. The composite caustic waste has a pH in the range 8 to 13 and generally contains a moderate amount of suspended solids. Currently, for disposal purposes, 38 l of the caustic waste is sorbed on 680 kg of Fuller's earth contained in a 208 l drum.

Results of one of a series of pilot plant tests made to develop and test a sorption system for decontamination of the caustic waste are plotted in Figure 3. The pilot plant system consisted of two cartridge filters designed to retain, respectively, 100 and 1 μm diameter particles and four bone char beds each 5.08 cm diameter by 0.51 m high. A total of 367 l of actual waste adjusted to pH 8 and spiked to 8 mg/l ($\sim 3 \times 10^{11}$ d/min/ml) plutonium was flowed at a rate of 20 ml/min through the pilot plant system. The pressure drop across the cartridge filters averaged about 14 kPa for the entire run while the drop across the four bone char columns was approximately 55 kPa. After passage of 356 column volumes of feed, the effluent from the final bone char column contained 63 d/min/ml corresponding to an overall system decontamination factor (DF) of $\sim 4.8 \times 10^9$. Much of this decontamination was provided by the two cartridge filters which removed 99+% (DF = 4.3×10^4) of the alpha activity.

Results from the pilot plant studies were used to design a conceptual plant-scale system for treating the caustic waste. This conceptual design includes two cartridge filters, each 0.51 m high, containing 5 or 6 filter elements capable of retaining 100 and 1 μm diameter particles, respectively. The effluent from the cartridge filters then flows, at a rate of about 11 l/hr, through three interconnected beds of bone char, each 15.2 cm diameter by 0.71 m high and each containing about

14 kg of sorbent. The total system is designed to reduce the plutonium concentration of about 3200 μ g of feed to <100 d/min/ml before replacement of sorbents or filters. An important factor in design of the plant sorption system was that each component be sized so that it could be installed in an existing facility without major modifications and so that, when spent, it could be conveniently disposed of in 208 μ g drums in full compliance with existing regulations for transuranium wastes. As of this writing, no decision has yet been made for installation and operation of the proposed plant-scale caustic waste treatment system.

Sodium Titanate Decontamination of Hanford PRF Waste. The Hanford Plutonium Reclamation Facility (PRF) receives and stores all sorts of unirradiated plutonium metallurgical scrap (alloys, metal, and compounds) and processes the scrap to recover and purify plutonium. Equipment and operating details of the PRF have been described elsewhere. (9,10) In usual PRF operation the plutonium-bearing scrap is dissolved in a HNO_3 -HF solution. After addition of $\text{Al}(\text{NO}_3)_3$ to complex fluoride ion and to provide salting strength, plutonium is recovered by solvent extraction with a 20% TBP (tri-n-butylphosphate)- CCl_4 solvent. Subsequently, a 30% DBBP (dibutylbutyl phosphonate)- CCl_4 solvent extraction process (2) is used to recover most of the residual plutonium and 50-60% of the ^{241}Am from the aqueous raffinate from the TBP extraction scheme.

The aqueous waste from the DBBP extraction process, still containing small but significant amounts of plutonium and ^{241}Am , is diluted with a large volume of waste water from other PRF operations to produce the PRF salt waste (Table II). When evaporated to dry salts, the PRF salt waste contains, typically 1000 to 2000 nCi/g of alpha emitters.

In normal operation, the PRF generates about 120 m^3 of salt waste solution per month. Currently, this waste solution is made alkaline and routed to underground storage tanks where it mixes with other Hanford defense waste liquors. An alternative waste treatment scheme is desirable to avoid converting large volumes of non-actinide waste to retrievable actinide waste (>10 nCi alpha activity/g) and also to help make the PRF independent of future tank farm management operations.

Figure 4 illustrates in schematic form the precipitation-exchange process devised and developed for reducing the actinide concentration of the PRF salt waste, when solidified, to or below 10 nCi/g. This process involves: (a) Addition of NaOH to the slightly acid PRF salt waste to precipitate iron, calcium, and magnesium hydroxides and remove 80-90 percent of the plutonium and >99.9 percent of the ^{241}Am ; and (b) Passage of the clarified alkaline supernate liquor from the precipitation step through a bed of -40+140 mesh sodium titanate powder to reduce the concentration of both plutonium and ^{241}Am to below their Maximum Permissible Concentration (11), 0.005 and 0.004 $\mu\text{Ci}/\mu\text{g}$, respectively, in water in an uncontrolled zone. The

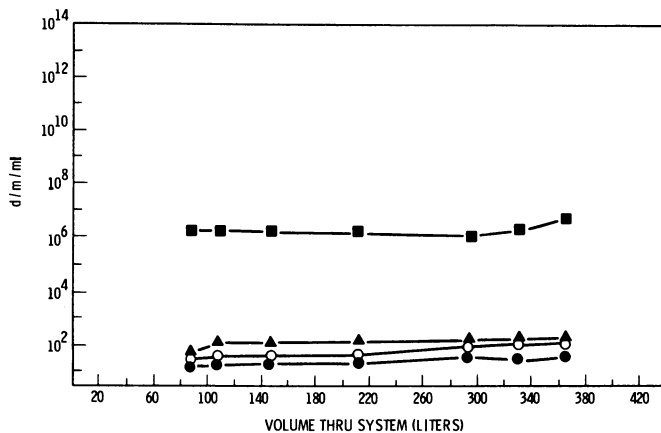


Figure 3. Pilot plant test of combined filtration-bone char decontamination of mound facility caustic waste: (■) after filters, (▲) after first bone char column, (○) after second bone char column, (●) after fourth bone char column. Conditions: pH = 8; flow = 20 ml/min; total bed height, 2.0 m of 275- μ bone char; diameter of bed, 5.1 cm; initial [Pu], 8 mg/L (3×10^{11} d/m/ml).

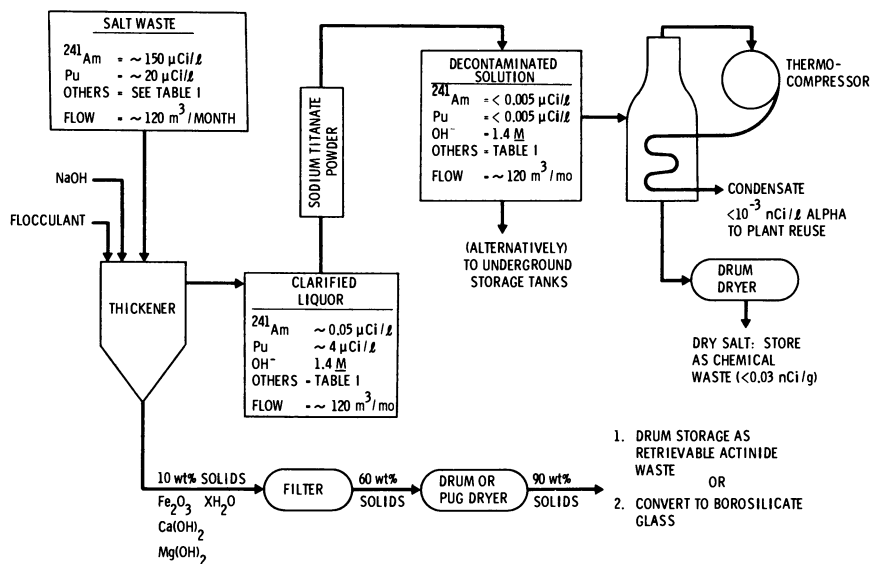


Figure 4. Precipitation-ion exchange scheme for removal of actinides from Hanford PRF salt waste

TABLE II

COMPOSITION OF ACTUAL AND SYNTHETIC ACTINIDE
PROCESS WASTE SOLUTIONS

Component	HANFORD PRF SALT WASTE		Synthetic Waste
	Batch 1	Batch 2	
NO_3^- , <u>M</u>	1.92	2.32	2.09
Na^+ , <u>M</u>	0.93	1.09	1.30
Al^{3+} , <u>M</u>	0.32	0.17	0.24
Mg^{2+} , <u>M</u>	0.0065	0.031	0.019
NO_2^- , <u>M</u>	(a)	0.028	(b)
Ca^{2+} , <u>M</u>	0.0058	0.019	0.012
Fe^{3+} , <u>M</u>	0.0053	0.0060	0.0057
Cr^{3+} , <u>M</u>	(a)	0.00028	0.0003
Ni^{2+} , <u>M</u>	(a)	0.00022	0.0002
SiO_3^{2-} , <u>M</u>	0.0031	(a)	0.0008
F^- , <u>M</u>	(a)	(a)	0.005
pH	0.88	0.40	0.84
^{241}Am , $\mu\text{Ci}/\ell$	144	262	270
Pu , $\mu\text{Ci}/\ell$	~ 16 (c)	20(c)	85(c)

(a) Not Determined
(b) Not Added
(c) As ^{239}Pu

precipitation-ion exchange decontamination process depicted in Figure 4 has been extensively and satisfactorily bench-scale tested with both actual and synthetic PRF salt waste. Highlights of these laboratory tests are discussed here; detailed results are provided in References 12 and 13.

The efficiency of freshly precipitated iron hydroxide in scavenging plutonium and other actinides from aqueous waste solutions is well known. Processes based on two or more cycles of iron hydroxide precipitation have long been used successfully at the U. S. Department of Energy Rocky Flats and Los Alamos sites to effectively decontaminate actinide-containing waste solutions generated at those sites. (14,15,16)

The PRF salt waste solutions contain, typically, 0.1 to 0.3M $\text{Al}(\text{NO}_3)_3$. To eliminate any possibility of permanently precipitating gelatinous, hard-to-separate $\text{Al}(\text{OH})_3$, it is desirable in the precipitation step to adjust the PRF salt waste

to 1-2M OH⁻. Even at these terminal hydroxide ion concentrations, which are much higher than those employed (e.g., pH 7-12) at Los Alamos and Rocky Flats in precipitation decontamination of alpha waste liquors, americium and plutonium are still effectively carried by the hydroxide precipitate. Furthermore, metal hydroxide scavenging of ²⁴¹Am from PRF salt waste is highly insensitive to changes in precipitation temperature (25 vs 60°C), agitation time (0.5 vs 4 hr), and the order of combination of waste and NaOH.

A single precipitation of iron and other metal hydroxides from PRF salt waste solution yields a stream containing, generally, <50 nCi/g but more than the desired 10 nCi/g total alpha activity. The exact chemical species of the residual concentration of ²⁴¹Am and plutonium in this alkaline (1-2M OH⁻) stream are, of course, not known. From its strong uptake by the cation exchanger sodium titanate (Table III) americium is believed to be present as a positively charged aquated or hydroxylated ion.

The results in Table III are particularly significant in that they clearly demonstrate how passage of the clarified alkaline solution from the precipitation step through a single bed of sodium titanate exchanger provides excellent further decontamination from both plutonium and americium. Limited availability of actual PRF salt waste solution for experimental work permitted passage of only about 1000 column volumes (CV) of alkaline feed through a 2.0 ml bed of titanate powder. As stated in Table III, however, almost 4000 CV of feed prepared from synthetic salt waste were passed through a 2.0 ml bed of sodium titanate. In both cases, all the decontaminated effluent contained <0.004 μCi/l ²⁴¹Am and <0.005 μCi/l plutonium. These latter values are, as noted earlier, the MPC's of ²⁴¹Am and ²³⁹Pu in water in an uncontrolled zone. Indeed, the ²⁴¹Am concentration in the bulk of the titanate-treated effluent was only about 0.1 of the MPC value.

Judging from the results presented in Table III, a single 0.04 m³ (0.15 m diameter) bed of titanate powder should adequately decontaminate all the PRF salt waste generated in a month. J. Nowak (5) at the Sandia Laboratories has successfully set up and operated, without observing excessive pressure drops, 0.1 m diameter by 1.22 m high beds of 40-140 mesh titanate powder. This experience suggests that 0.15 m diameter by 2.26 m high (0.04 m³) titanate powder beds for decontaminating alkaline PRF salt waste could also be prepared and operated satisfactorily. If not, a series of critically safe 0.15 m diameter beds of suitable height and volume could be used to provide the requisite sorption capacity.

On the basis of using only 0.04 m³ of titanate powder per month, approximately 180 kg (dry weight basis) of spent powder would be generated in one year. Titanate powder loaded with ²⁴¹Am and plutonium could be dried, drummed, and stored as a retrievable transuranium waste. Alternatively, using technology

TABLE III

SORPTION OF ACTINIDES FROM ALKALINE PRF SALT WASTE SOLUTION AND BY SODIUM TITANATE POWER

Run Conditions: Clarified supernatant liquor from liter-scale precipitation tests with either synthetic or actual PRF salt waste flowed [at 25°C and 4-5 column volumes (CV)/hr] through 2.0 ml beds (0.5-0.7 cm dia) of 40-140 mesh sodium titanate.

Actual PRF Waste (a)				Synthetic PRF Waste (b)			
241Am Sorption		Pu Sorption		241Am Sorption		Pu Sorption	
Cumulative CV	241Am $\mu\text{Ci}/\ell$	Cumulative CV	Pu(c) $\mu\text{Ci}/\ell$	Cumulative CV	241Am $\mu\text{Ci}/\ell$	Cumulative CV	Pu(c) $\mu\text{Ci}/\ell$
24	<0.0024	505	0.0040	405	<0.0002	405	<0.0010
105	0.0021	778	0.0026	739	<0.00023	739	<0.0010
223	0.0020	954	0.0040	1049	<0.00017	2832	<0.0010
261	<0.0033			1359	<0.00017	3242	<0.0010
337	<0.0033			1609	<0.00017	3562	<0.0010
462	<0.0030			1899	<0.00022		
505	<0.0038			2217	0.00037		
548	<0.0053			2522	0.00042		
681	<0.0052			2832	0.00053		
778	<0.0045			3242	0.00070		
914	<0.0057			3562	0.00082		
954	<0.0062			3892	0.00159		

(a) Feed to titanate column contained 0.039 $\mu\text{Ci}/\ell$ ^{241}Am and 3.9 $\mu\text{Ci}/\ell$ Pu

(b) Feed to titanate column contained 0.0314 $\mu\text{Ci}/\ell$ ^{241}Am and 11.1 $\mu\text{Ci}/\ell$ Pu

(c) As ^{239}Pu

developed at the Sandia Laboratories (17), the spent titanate powder could presumably be converted to an immobile monolithic form by hot pressing at $\sim 1100^{\circ}\text{C}$. Some preliminary results obtained at Sandia Laboratories and discussed later in this paper suggest it may be possible to elute actinides from loaded titanate beds with dilute HNO_3 . Such elution and regeneration, if indeed possible, would greatly reduce the amount of spent titanate exchanger to be handled.

Approximately 300 kg of dried metal hydroxide solids would be produced per month from decontamination of 120 m^3 of PRF salt waste. These solids could be drummed and stored at Hanford as a retrievable alpha waste. Techniques for incorporating the metal hydroxide solids in an immobile borosilicate glass have been developed also. (12)

The laboratory-scale studies reported here were initiated prior to the ^{241}Am -loaded cation exchange resin explosion which occurred in the PRF in 1976. Scrap reprocessing and other production operations in the PRF are currently suspended while the entire facility undergoes a comprehensive cleaning and safety review. Future plant-scale application, if any, of the precipitation-sodium titanate sorption process discussed in this paper has been deferred until cleanup operations are completed and decisions are made about the future role of the PRF facility. Finally, incorporation of a tailend sodium titanate polishing step into processing schemes presently used to clean up alpha bearing salt wastes generated at other U. S. Department of Energy sites (e.g., Rocky Flats, Los Alamos) would be an obvious extension of the technology discussed here.

Separation of Am-Cm From Lanthanides. An experimental program, directed by the Oak Ridge National Laboratory, to determine the feasibility of and to develop technology for partitioning high-level Purex process waste into actinide and fission product fractions has recently been undertaken at several U. S. Department of Energy laboratories. (18) One product, typically, from such actinide partitioning processes is an aqueous solution containing americium and curium heavily contaminated with lanthanide elements. Separation of the Am-Cm from the large mass of rare earths is necessary and desirable for future reactor burn-up of the Am and Cm. As part of the "actinide partitioning" program, limited and preliminary batch tracer distribution tests were performed at Sandia Laboratories to investigate the suitability of using the inorganic sorbents $\text{H}[\text{Ti}_2\text{O}_5\text{H}]$, $\text{H}[\text{Zr}_2\text{O}_5\text{H}]$, and $\text{H}[\text{Nb}_2\text{O}_6\text{H}]$ to effect a chromatographic separation of Am-Cm from selected rare earth ions.

A series of batch equilibrations was carried out to determine the relative affinities of selected lanthanides and actinides for niobate, zirconate, and titanate ion exchange materials as a function of pH. These affinities are expressed as distribution coefficients K_d (19), where:

$$K_d = \frac{(\text{Fraction of Tracer on Ion Exchanger})}{(\text{Fraction of Tracer in Solution})} \times \frac{(\text{ml of solution})}{(\text{g of Ion Exchanger})}$$

Adjustment of pH was accomplished by addition of dilute NaOH or HNO₃. Typically, one milliequivalent of ion exchanger (∞0.35 g niobate, ∞0.37 g zirconate, ∞0.25 g titanate) contacted about 15 ml of solution containing an appropriate radionuclide. In each case, the maximum loading was less than 1% of the ion exchanger capacity. After equilibration, the pH's of the solutions were measured. The solutions were then filtered and counted to determine the fraction of tracer remaining in solution. In those instances in which most of the radioactive tracer was removed from solution, desorption of nuclides from the ion exchange material was investigated by adding to the solids 15 ml of 0.1M HNO₃ (zirconate and titanate) or 0.5M HNO₃ (niobate), equilibrating the mixture, filtering, and counting the solution. In both sorption and desorption experiments, sorbents were contacted with test liquids for five days at 20-28°C. This equilibration time reflected personal convenience and is believed to be much longer than that required to reach equilibrium.

Figures 5-7 present results of batch sorption experiments for three actinides and four lanthanide elements. For clarity, data points for the actinide elements have been connected by solid lines. The accuracy of the K_d values is estimated to be within ±10% for 5 ml/g <K_d<10⁵ ml/g but degrades rapidly outside these limits. Two aspects of the results plotted in Figures 5-7 are particularly significant. The rapid increase in K_d and pH implies that, with the possible exception of neptunium, the radionuclides tested can be quantitatively sorbed and then eluted from these inorganic ion exchange materials by pH adjustment. This implication is supported by the desorption experiments discussed later. Second, for each exchanger across the pH range studied, americium, curium, and (at low pH) neptunium were more strongly sorbed than any of the lanthanides. Note that the ordinates in Figures 5-7 are on a logarithmic scale. In these tests distribution ratios for neptunium remained high even at low pH's whereas those for trivalent actinides and lanthanides fell off almost linearly with decreasing pH. In this latter connection it must be pointed out that the sorption behavior of neptunium in these experiments was followed by analysis for ²³⁹Np in the presence of its alpha-emitting parent ²⁴³Am. The oxidation state of the neptunium thus produced is not known.

Results of experiments conducted to investigate HNO₃ desorption of tracer amounts of selected radionuclides sorbed on the various inorganic ion exchangers are presented in Table IV. The percentages listed are the averages of two, three, or, in some cases, four desorption tests. The maximum recovery

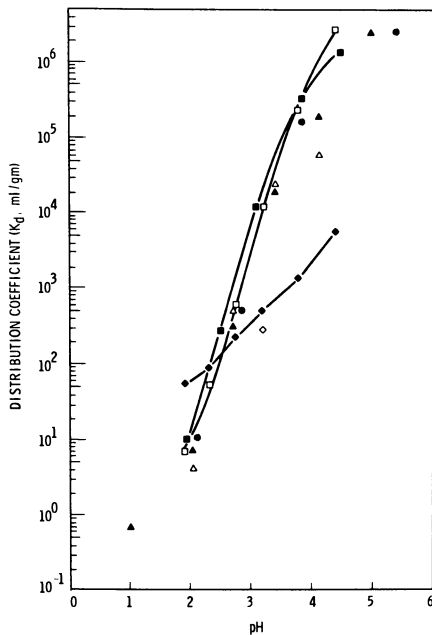


Figure 5. Affinity of $H(Ti_2O_5H)$ sorbent for selected lanthanides and actinides at various pH's: (\blacklozenge) Np, (\square) Am, (\blacksquare) Cm, (\bullet) Eu, (\blacktriangle) Gd, (\diamond) La, (\triangle) Pm.

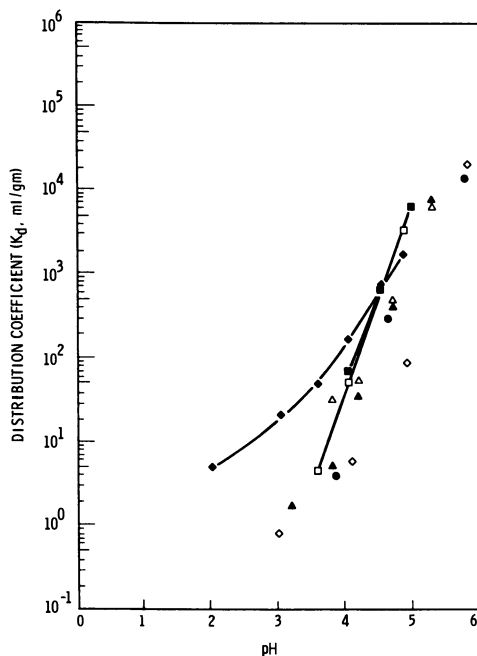


Figure 6. Affinity of $H(Zr_2O_5H)$ sorbent for selected lanthanides and actinides at various pH's: (\blacklozenge) Np, (\square) Am, (\blacksquare) Cm, (\bullet) Eu, (\blacktriangle) Gd, (\diamond) La, (\triangle) Pm.

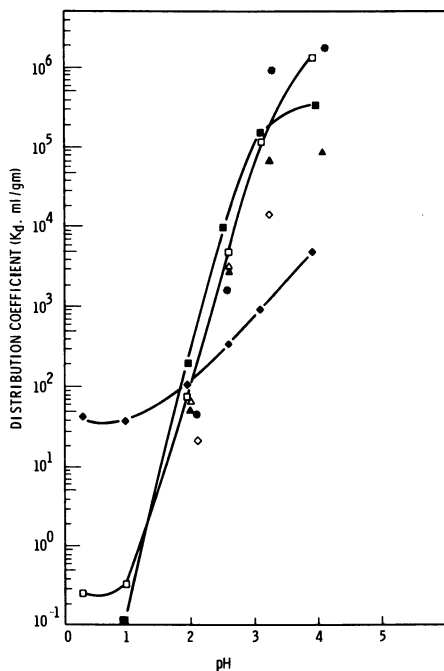


Figure 7. Affinity of $H(Nb_2O_6H)$ sorbent for selected lanthanides and actinides at various pH's: (◆) Np, (□) Am, (■) Cm, (●) Eu, (▲) Gd, (◇) La, (△) Pm.

expected in each test was about 90%. Recovery was limited by: (a) Loss of ion exchange material containing sorbed radioactivity during filtering after the load contact; (b) Dilution of the desorption solution with small volumes of the solution remaining in contact with the ion exchanger after filtering; and (c) Absorption of some radioactivity on the walls of the polyethylene vials used to contain the solid exchanger and liquid solutions. In view of these experimental limitations, the recoveries given in Table IV are believed to correspond to complete or nearly complete removal of sorbed radionuclides.

TABLE IV

BATCH HNO₃ RECOVERIES OF RADIONUCLIDES SORBED ON
INORGANIC ION EXCHANGERS

Elution conditions: 0.25 to 0.37 g of exchanger containing sorbed radionuclide contacted 5 days at 20–28°C with 15 ml of either 0.1M HNO₃ (zirconate and titanate) or 0.5M HNO₃ (niobate).

Ion Exchanger	% Recovered				
	Eu	Gd	Pm	Cm	Am
Niobate	90.6	98.4	89.8	77.1	89.7
Zirconate	91.9	93.6	86.8	80.3	89.0
Titanate	80.0	93.8	84.6	80.1	90.2

According to Nachod and Schubert (19) two sorbable species can be separated from each other by column elution chromatographic techniques provided the ratio of their K_d 's (separation coefficient) is 1.2 or greater. On this basis, from Figures 5–7 there is a pH range for each of the three exchangers - titanate, zirconate, and niobate - where partitioning of Am, Cm, and Np from lanthanide elements appears feasible. Enthusiasm for use of columns of sodium titanate, sodium zirconate, and sodium niobate for partitioning actinides from lanthanides must be tempered however by the present lack of any information about concentration effects and sorption and desorption kinetics. These and other important factors must be investigated in much more intensive studies than those conducted to date.

Acknowledgements

The important contributions of R. Zane Lawson (Sandia Laboratories); Paul Hammitt and Judy Watts (Rockwell Hanford Operations); and D. E. Blane, E. L. Murphy, and W. R. Herald (Mound Facility) to the experimental and pilot plant studies reported here are gratefully acknowledged. We, W. W. Schulz and D. R. Tallant, would also like to thank Dr. R. G. Dosch of Sandia Laboratories for kindly supplying sodium titanate, niobate, and zirconate sorbents and also for generously sharing his expert knowledge of the properties of these inorganic exchangers.

Literature Cited

- Schulz, W. W.; Benedict, G. E., "Neptunium-237 Production and Recovery," U. S. Atomic Energy Commission Technical Information Center, Oak Ridge, TN., 1972; pp 45–48.
- Schulz, W. W., "The Chemistry of Americium," Technical Information Center Energy Research and Development Administration, Oak Ridge, TN., 1976; pp 251–252.

3. Silver, G. L.; Koenst, J. W., U. S. Energy Research and Development Report MLM-2384, Mound Facility, Miamisburg, Ohio, 1977.
4. Chem. Eng. News, 1976, 54, (No. 2), 32.
5. Lynch, R. W., Ed., U. S. Energy Research and Development Report SAND-76-0105, Sandia Laboratories, Albuquerque, NM, 1976.
6. Blane, D. E.; Murphy, E. L., U. S. Energy Research and Development Administration Report MLM-2244, Mound Laboratory, Miamisburg, Ohio, 1975.
7. Blane, D. E.; Murphy, E. L., U. S. Energy Research and Development Administration Report MLM-2371, Mound Laboratory, Miamisburg, Ohio, 1976.
8. Blane, D. E.; Herald, W. R., U. S. Department of Energy Report MLM-2534, Mound Facility, Miamisburg, Ohio, 1978.
9. Bruns, L. E., Chem. Engrg. Progr. Sym. Ser., 1957, 63, 156.
10. Bruns, L. E., Plutonium-Uranium Partitioning by a Reflux Extraction Flowsheet in "Proceedings, ISEC 71," Society of Chemical Industry, London, 1971; Vol. 1, p. 186.
11. Code of Federal Regulations, Title 10, Part 20.
12. Schulz, W. W., U. S. Department of Energy Report RHO-SA-23, Rockwell Hanford Operations, Richland, Washington, 1978.
13. Schulz, W. W., Trans. Amer. Nucl. Soc., 1978, 28, 363.
14. Emelity, L. A.; Christenson, C. W.; Kline, W. H., "Operational Practices in the Treatment of Low- and Intermediate-Level Radioactive Wastes: Argonne and Los Alamos Laboratories," in "Practices in the Treatment of Low- and Intermediate-Level Radioactive Wastes," IAEA, Vienna, 1966, p. 187.
15. Christenson, C. W.; Emelity, L. A., J. Water Pollution Control Fed., 1970, 1343.
16. Ryan, E. S.; Vance, J. N.; Maas, M. E., "Aqueous Radioactive Waste Treatment Plant at Rocky Flats," in "Practices in the Treatment of Low- and Intermediate-Level Radioactive Wastes," IAEA, Vienna, 1966, p. 517.
17. Lynch, R. W.; Dosch, R. G.; Kenna, B. T.; Johnstone, J. K.; Nowak, E. J., U. S. Energy Research and Development Administration Report SAND-75-5907, Sandia Laboratories, New Mexico, 1976.
18. Croff, A. G.; Tedder, C. W.; Drago, J. P.; Blomeke, J. O.; Perona, J. J., U. S. Department of Energy Report ORNL/TM-5808, Oak Ridge National Laboratory, Oak Ridge, TN, 1977.
19. Nachod, F. E.; Shubert, J.; eds., "Ion Exchange Technology," Academic Press, New York, 1956; p. 419.

RECEIVED July 2, 1979.

Transplutonium Elements Production Program

Extraction Chromatographic Process for Plutonium Irradiated Targets

J. BOURGES, C. MADIC, and G. KOEHLI

Departement de Genie Radioactif, Service des Etudes de Procedes,
Section des Transuraniens, Centre d'Etudes Nucleaires de Fontenay-aux-Roses,
B.P. N 6-92260 Fontenay-aux-Roses, France

The French transplutonium elements production program (essentially ^{243}Am and ^{244}Cm) is based on the treatment of plutonium-aluminum alloy targets irradiated in the Celestin reactors at Marcoule. At the time of chemical treatment, these targets (which initially contained approximately 400 g of ^{239}Pu) contain 44 g of ^{242}Pu , 8.5 g of ^{243}Am , 7.5 g of ^{244}Cm , and about 340 g of fission products, including ≈ 240 g of lanthanides, chiefly the elements La, Ce and Nd (1).

The process initially developed for the chemical treatment of targets was based on liquid-liquid countercurrent extraction in nitric medium (2, 3, 4). Problems were encountered in using this process, due essentially to the formation of interface fouling and stable emulsions. Since no simple method of eliminating these stable emulsions could be found, this process was transposed to the extraction chromatography technique (which in principle, is not subjected to emulsion formation) and applied to the treatment of irradiated Pu-Al targets. Extraction chromatography has found many uses in the separative chemistry of actinides elements, dealing essentially with analytical applications (5). However, this technique has been used for the purification of ^{241}Am and ^{244}Cm on the scale of 30 g and 6 g respectively (6) using a Talspeak type process (7). In a production scheme, extraction chromatography has the drawback of being a discontinuous technique. Owing to its simplicity of implementation, this technique was nevertheless found to be competitive with liquid-liquid extraction for production of transplutonium elements on the scale of a few grams.

EXPERIMENTAL

Equipment

All the chemical treatments were carried out in hot cells equipped with remote manipulators, in view of the nuclear properties of the isotopes involved (^{243}Am , $^{242-244}\text{Cm}$, ^{252}Cf and fission products). All the experiments, including separation of americium and curium, required shielding for α , β , γ , and the neutrons from

0-8412-0527-2/80/47-117-033\$05.00/0

© 1980 American Chemical Society

In Actinide Separations; Navratil, J., et al.;

ACS Symposium Series; American Chemical Society: Washington, DC, 1980.

spontaneous fission (^{242}Cm , ^{244}Cm , ^{252}Cf) and from the action of α particles on light elements. The Petrus cell (8) protected by 80 cm thick walls of baryta concrete is ideal for these manipulations.

The chromatographic equipment includes : a) plexiglas columns packed with GAS CHROM Q or Celite 545 impregnated with extractant, b) Sonal or Prominent proportioning pumps, c) storage tanks for various solutions. The column is filled by successive additions and repeated packing of the dry stationary phase. Once the packing is completed and the top cover cemented, the column is placed in the hot cell, where it undergoes pre-equilibrium designed to produce the chemical conditions required for fixation and to expel the air. The three column models routinely used in preparative chromatography are described in Table I.

TABLE I
Characteristics of extraction chromatography columns.

Diameter (mm)	Effective height (mm)	Mass of stationary phase (g)	Interstitial volume (ml)
42	320	250	250
42	640	500	500
62	670	1100	1000

PREPARATION OF STATIONARY PHASE

Two materials marketed by Applied Science Lab. were employed, Celite 545 and GAS CHROM Q with particle size distribution from 110 to 140 μ and a specific area of about $1 \text{ m}^2 \cdot \text{g}^{-1}$. Celite 545 is made hydrophobic by treatment with dimethyldichlorosilane. Impregnation of the stationary phase materials by TBP, TOA, HDEHP, and HD(DiBM)P were carried out as follows : a mass of material is placed in contact with a solution of extractant in hexane, the solvent is then evaporated under reduced pressure by means of a Buchi Rotavapor rotary evaporator. Impregnation levels in the final mixture are respectively : TBP = 27 %, TOA = 25 %, HDEHP = 20 % and HD(DiBM)P = 30 %.

REAGENTS

The reagents HNO_3 ; $\text{Al}(\text{NO}_3)_3$, $9\text{H}_2\text{O}$ and LiNO_3 (Prolabo) are of technical grade, $\text{K}_2\text{S}_2\text{O}_8$, AgNO_3 (Prolabo), DTPA (K and K laboratories, USA), TBP (Osi), TOA (Fluka) and HDEHP (Union Carbide) are pure analytical grade. We synthesized HD(DiBM)P using the method described in (9). The aluminum nitrate solution deficient in nitrate ions. $\text{Al}(\text{NO}_3)_{3-x}(\text{OH})_x$ was prepared by destruction at 100-120°C of NO_3^- ion by formol (2 moles HCHO per NO_3^- ion to be destroyed).

IRRADIATED TARGETS

The main characteristics of irradiated targets are given in Table II.

TABLE II
Characteristics of the experimental target and industrial targets irradiated.

	Target	
	PuO ₂ /Al	Pu/Al
<u>Irradiations conditions</u>		
. mass of fertile material (g)	2.56	400
. integrated flux (n.kb ⁻¹)	30	11.28
<u>Cooling time</u>	5 years	3 years
<u>Dissolution material balance</u>		
. volume (liters)	1	88
. activity of emitters (β,γ Ci.l ⁻¹)	15	350
. emitters (g) :		
. ²⁴² Pu	0.200	44
. ²⁴³ Am	0.100	8.53
. ²⁴⁴ Cm	0.265	7.44

RESULTS AND DISCUSSION

The transplutonium elements are obtained by neutron irradiation of ²³⁹Pu or heavier isotope base targets in thermalized flux zones. Reactors safety conditions necessitate dilution of the plutonium by aluminum, both for the plutonium metal base targets and for oxide base targets. The objective of the process is the recovery of residual plutonium and the separation of transplutonium elements. After dissolution of the irradiated targets in nitric acid solution, the plutonium can be extracted easily by tertiary ammonium nitrate. We selected trioctylammonium nitrate to do this, owing to its low melting point, the distribution coefficient compatible with quantitative extraction, and the good mass capacity of inert stationary phases loaded with this extracting agent. The elution medium adopted was a sulfonitric solution : CH₂SO₄ = 0.75M, CHNO₃ = 0.2 M.

The separation of transplutonium elements from the lanthanides constitutes the delicate phase of chemical treatment, owing to their comparable affinities for the usual extractants : HDEHP, TBP and TLAHNO₃. Among all the systems described in the literature and covered by a recently published critical compilation (10), we selected those which appeared to be much suitable for adaptation to extraction chromatography : the Talspeak process (7) and the

processes developed at CEN-FAR (4). The separative performances of the three systems, based on the use of the complexant DTPA are grouped in Table III. In all cases it was observed that the separation factors $\alpha = D(\text{Ln}^{3+}) \cdot D(\text{Am}^{3+})^{-1}$ were sharply higher in the presence of DTPA. The Talspeak process achieves good lanthanide/transplutonium separation, whereas the two remaining systems only achieve good separation of trivalent actinides from light lanthanides including europium with TBP, promethium with TLAHNO₃.

TABLE III
Separation factors $\alpha = D(\text{Ln}^{3+}) \cdot D(\text{Am}^{3+})^{-1}$
for some chemical systems

element	Talspeak		TBP		TLAHNO ₃	
	α_i	$\alpha(\text{DTPA})$	α_i	$\alpha(\text{DTPA})$	α_i	$\alpha(\text{DTPA})$
La	(3.9)	380	0.80	1800	6.0	2300
Ce	5.4	140	0.86	52.0	3.5	660
Pr		(75)	1.06	12.5	2.3	73
Pm	(10)	(75)	1.1	5.8	1.2	9
Eu	48	91	1.3	2.0	0.83	1.13
Tb			1.5	1.4	0.43	0.90
Er			1.02	1.4	0.20	0.43
Tm		(8000)	0.93	1.4	0.19	0.33
Yb			0.74	1.4	0.17	

Operating conditions :

- . Talspeak organic phase : HDEHP = 0.2 M in DiPB
(7) aqueous phase : 1 M lactic acid pH = 3 (α_i),
+ DTPA ($5 \cdot 10^{-2}$ M) (α DTPA)
- . TBP organic phase : TBP (40% vol.) in dodecane
(4) aqueous phase : LiNO₃ = 4 M (α_i) + DTPA = 0.25 M
= Al³⁺ (α DTPA),
- . TLAHNO₃ organic phase : TLAHNO₃ (40% vol.) in dodecane
(50%), chlorobenzene (50%)
(4) aqueous phase : LiNO₃ = 6 M (α_i) + DTPA = 0.25 M
= Al³⁺ (α DTPA).

NOTE : The separation factors noted () were estimated from the graphs of (7).

The Talspeak process and the CEN-FAR TBP process were transposed to extraction chromatography. European researchers (6) have adapted the Talspeak process for the final purification of ²⁴¹Am and ²⁴⁴Cm at the scale of a few grams. Hence our intention is to use this experiment to treat hot targets.

The use of this process in extraction chromatography was tested on a real solution corresponding to a fraction of the

dissolution liquors of an industrial target. The preliminary operations to transplutonium/lanthanide separation are the following: a) batch extraction of ^{242}Pu by TlAHNO_3 (15 % by vol.)/dodecane, b) adjustment of the solution to $\text{Al}(\text{OH})^{2+} = 0.1 \text{ M}$, c) batch extraction of lanthanides and transplutonium elements by TBP (30 % vol.)/dodecane, d) re-extraction of trivalent elements by 2N HNO_3 or 1 M lactic acid (pH : 3), e) adjustment to 1 M lactic acid (pH : 3) in case of nitric re-extraction. Two separations were carried out involving 30 and 800 mg of ^{244}Cm . Following the fixation stage in columns packed with a mixture of HDEHP (20 % wt)/G.C.Q., the material was scrubbed by a solution with composition : 1 M lactic acid (pH = 3) ; elution was then performed by an eluent of composition: Clactic acid = 1 M, $\text{CDTPA} = 5.10^{-2} \text{ M}$, pH = 3. The ^{244}Cm elution curves are shown in figure ①, and correspond to experiments which were carried out in two days. The elution curves exhibit a considerable trail in both cases. In the first experiment (figure ①a), nitric elution of the column reveals 24 % of the initial curium present with all the lanthanides. This retention is repeated in the second experiment (figure ①b) to a greater extent : presence of two ^{244}Cm peaks with complexating elution. These occurrences can be ascribed to a slow ^{244}Cm desorption rate. In these conditions, this high ^{244}Cm retention prohibits the use of this system for the quantitative recovery of transplutonium elements. Furthermore, lactic solutions containing a large amount of curium and lanthanides deteriorate rapidly under the action of intense radiolysis : blackening of the solution and appearance of precipitates. In view of these mediocre results, the use of this system was discontinued.

CEN-FAR TBP process : a chromatographic separation process includes three successive stages for which the chemicals conditions are to be determined : fixation, scrubbing and elution.

Fixation : figure ② shows the effect of free acidity and NO_3^- ion deficiency on K_D (Cm^{3+}) for concentrated solutions containing aluminum nitrate. Extraction is carried out by TBP impregnated on G.C.Q. (1. m.mole TBP g. loaded stationary phase). K_D (Cm^{3+}) can be observed to be highly sensitive to acidity in the neutral region ; the maximum K_D (Cm^{3+}) (≈ 250) is obtained for an NO_3^- ion deficiency equal to 0.05 ± 0.05 . This result is similar to that obtained in liquid-liquid extraction.

Scrubbing can be carried out simply by using a salting out solution of $\text{LiNO}_3 = 8 \text{ M}$, which achieves the elimination of certain fission products, but especially that of aluminum, whose presence is detrimental to satisfactory elution owing to the complexation reaction : $\text{Al}^{3+} + \text{YH}_5 \rightleftharpoons \text{AlY}^{2-} + 5\text{H}^+$ (where $\text{YH}_5 = \text{DTPA}$).

Elution : The use of solution with composition $\text{CDTPA} = 0.25 \text{ M}$, $\text{CAL}^{3+} = 0.25 \text{ M}$, $\text{CLiNO}_3 = 4 \text{ M}$ (4) to carry out elution does not appear to be realistic. In actual fact, the distribution coefficient are too sensitive to a slight variation in the ratio $\text{CDTPA} . \text{CAL}^{3+}$, which is reflected by a large variation in the retention volumes of the elements to be separated. The elimination of Al from

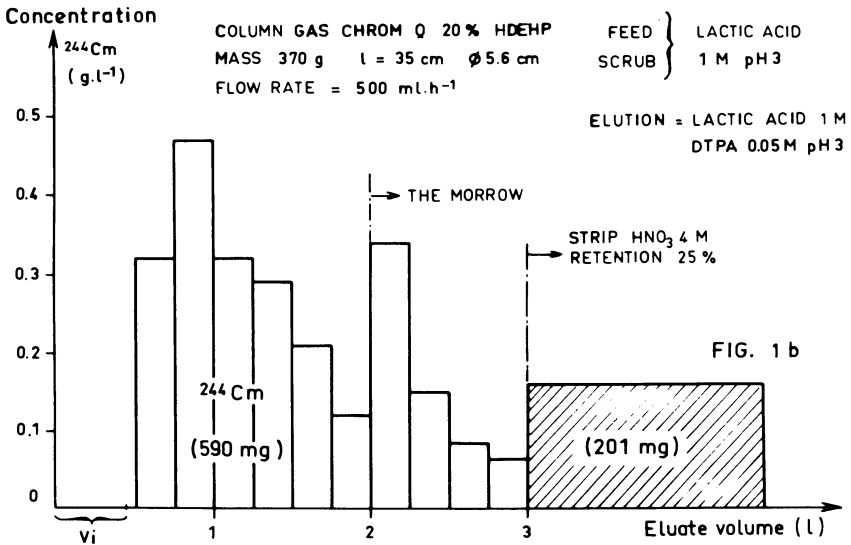
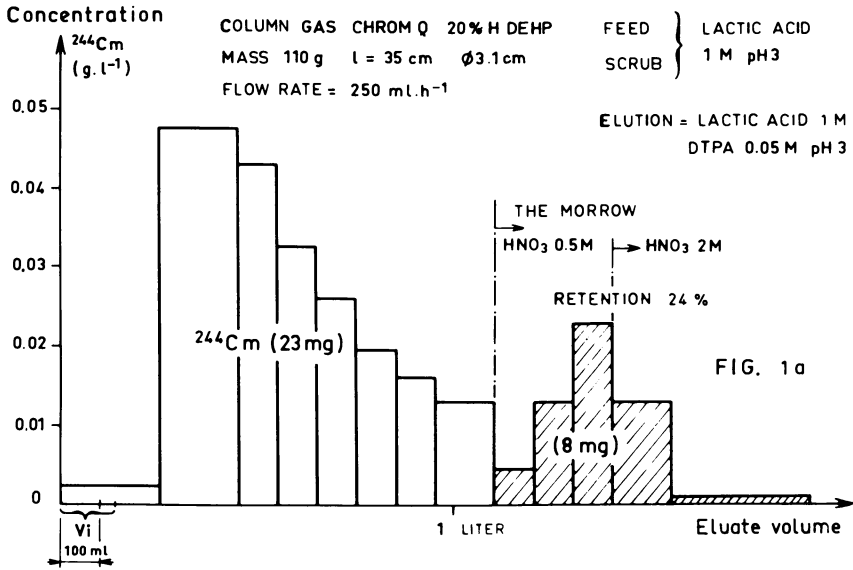


Figure 1. Elution curves for ^{244}Cm : (a) first experiment; (b) second experiment.

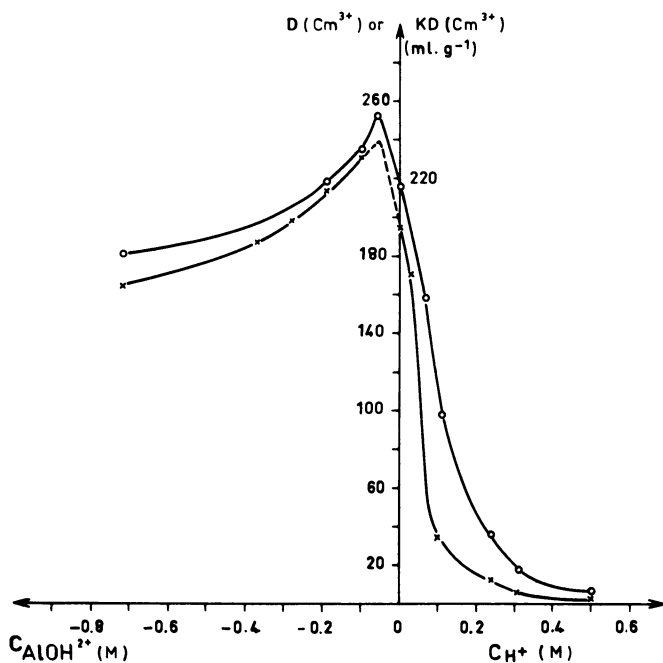


Figure 2. Effect of free acidity and NO_3 -ion deficiency on $K_D(\text{Cm}^{3+})$

the elution solution requires a higher LiNO_3 concentration and a decrease in the pH, to make it possible to obtain distribution coefficients which are compatible with good separation. Figure ③ shows the elution curve for actinide/lanthanide separation carried out in small column ($l = 5.5$ cm, $\phi = 4$ mm) using 250 mg of loaded stationary phase (TBP 27% by weight/G.C.Q.). The separation factors observed are : $\alpha_{\text{Am}}^{\text{Eu}} = 1.8$; $\alpha_{\text{Cm}}^{\text{Am}} = 2.53$, which in the case of (Am, Eu) couple is close to the value obtained by liquid-liquid extraction and given in Table III. While the separation factors obtained are encouraging, the resolution of the elution peaks are mediocre. The use of this separation system requires recycling of the median fractions. It is then possible to obtain high distribution coefficients $K_D(\text{M}^{3+})$ by adding aluminum nitrate to the eluate, thus neutralizing the complexing power of DTPA over the element to be extracted. After fixation in these new conditions, a new cycle can be carried out. To summarize, the conditions adopted to carry out transplutonium/lanthanide separation are grouped in Table IV.

TABLE IV
*Transplutonium/lanthanide separation
in column packed with a TBP 27% by wt/GCQ mixture*

stage	solution composition
fixation	
. 1st cycle	$(\text{Al}(\text{NO}_3)_3) = 1.8$ M ; $(\text{H}^+) = (0 \pm 0.05)$ M
. 2nd and following cycles	$(\text{LiNO}_3) = 7$ M ; $\text{DTPA} = 0.1$ M ; $(\text{Al}^{3+}) = 0.5$ M
scrubbing	$(\text{LiNO}_3) = 8$ M
elution	$(\text{LiNO}_3) = 7$ M ; $\text{DTPA} = 0.1$ M ; $\text{pH} = 1.2$

The possibility of applying extraction chromatography using TBP to the treatment of hot targets was attempted on the dissolution liquor of an experimental PuO_2/Al target described in Table II. After batch extraction of ^{242}Pu using a TLAHO_3 solution, the lanthanides/transplutonium elements separation is carried out among the experimental conditions defined in Table IV.

The following results are obtained : a) lanthanide and transplutonium fixation occurred in the sequence : heavy lanthanides (Eu) > transplutoniums > light lanthanides (Ce), (134 ^{137}Cs), (103 ^{106}Ru) and aluminum escape partially. b) in the scrubbing stage, a fraction of the cesium and ruthenium is eliminated with the aluminum. c) the transplutonium elements are eluted in the order : Cf, Cm, Am ; europium is eluted directly after Am. d) nitric stripping of the column contains ^{144}Ce , ruthenium and cesium. The elution curve is given in figure ④. The actinides are thus rid of most of lanthanides and other fission products in a single cycle.

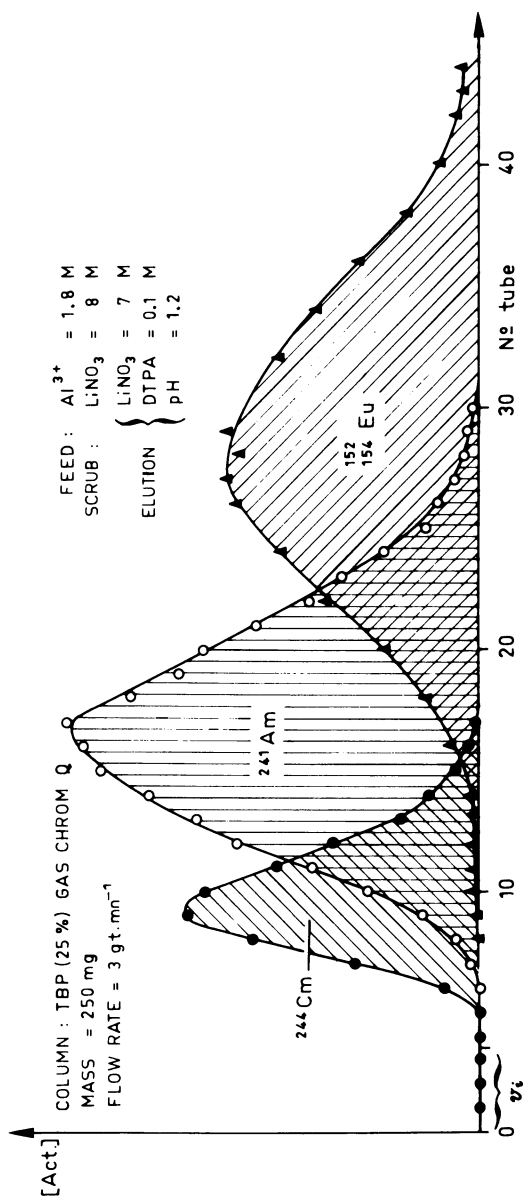


Figure 3. Elution curve for actinide-lanthanide separation

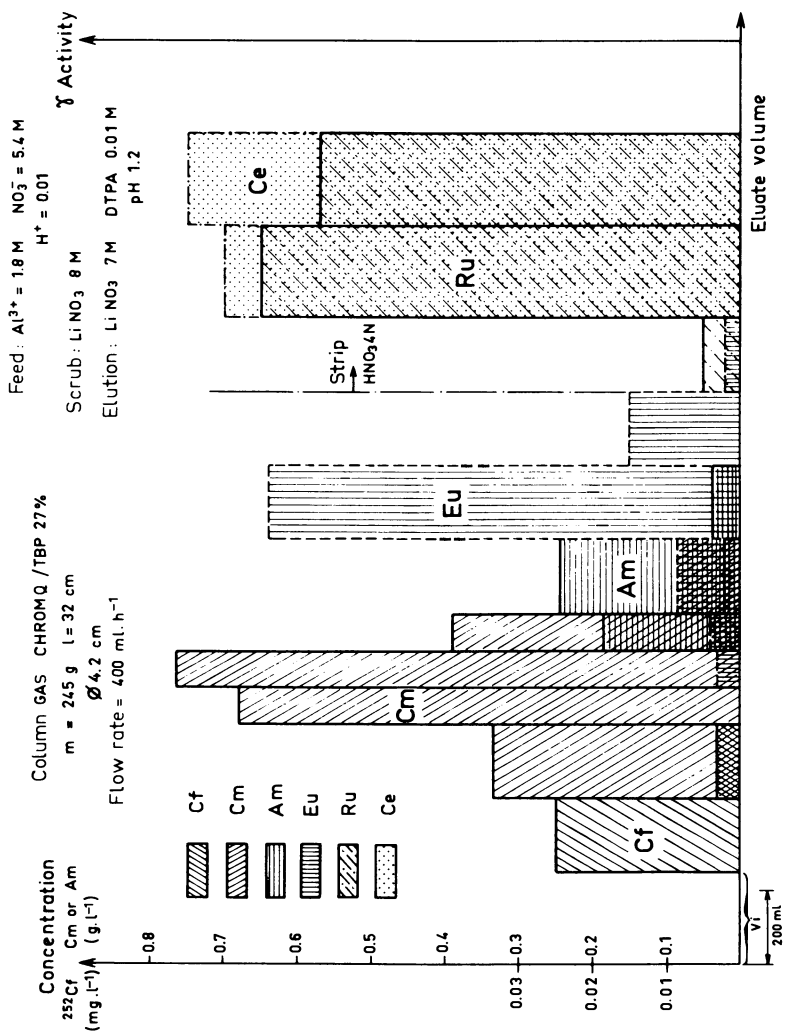


Figure 4. Elution curve for transplutonium-lanthanide separation

The fission product decontamination factors for the three transplutonium fractions collected, i.e. 5 μg of ^{252}Cf , 253 mg of ^{244}Cm , 50 mg of ^{243}Am are given in Table V.

TABLE V
*Fission product decontamination factors
of fractions ^{252}Cf , ^{244}Cm and ^{243}Am .*

	californium 252	curium 244	américium 243
DF Ce	$> 7.5 \cdot 10^4$	150	170
DF Eu	$> 5 \cdot 10^3$	280	115
DF Ru	750	12.6	50
DF Cs	$5 \cdot 10^3$	272	580

No retention of α emitters was observed during this treatment, and the separation factors of transplutonium elements in relation to europium are respectively : $\alpha_{\text{Cf}}^{\text{Eu}} = 11.2$; $\alpha_{\text{Cm}}^{\text{Eu}} = 1.83$; $\alpha_{\text{Am}}^{\text{Eu}} = 1.23$. The good performance levels obtained with this TBP process let us to select it to develop a process applicable to the treatment of industrial targets.

The dissolution of an industrial target (Pu-Al) in nitric acid gives a solution whose main characteristics are given in figure ⑤. Chemical treatment of this solution includes three successive phases : a) high activity β, γ (H.A) = separation of plutonium and separation of transplutonium elements from most of the light lanthanides (figure ⑤) ; b) medium activity β, γ (M.A) = decontamination of transplutonium elements from lanthanides and the first stages of Am/Cm separations (figure ⑥) ; c) low activity β, γ (L.A) = final Am/Cm separations and purification of ^{243}Am and ^{244}Cm produced (figure ⑦). The use of the chromatographic technique allows recovery of actinides with good yields in H.A. treatment (see Table VI).

TABLE VI
Performance of "high activity" separations

	dissolution liquors (V=88l)		final solutions (V =12l; V =20 l)		yield %	DF ^{Am, Cm} pF
	g	Ci.l ⁻¹	g	mCi.l ⁻¹		
^{242}Pu	44		39.5 (1)		90	
^{243}Am	8.55		8.25 (2)		96.5	
^{244}Cm	7.44		7.18 (2)		96.5	
^{144}Ce		23.9		2560 (2)	39	
^{125}Sb		1.66		14.8 (2)		$4.77 \cdot 10^2$
$^{103}_{106}\text{Ru}$		75.5		130 (2)		$2.5 \cdot 10^3$
$^{134}_{137}\text{Cs}$		194.7		9.4 (2)		$9 \cdot 10^4$
$^{152}_{154}\text{Eu}$		6.11		1500 (2)		17
^{60}Co		0.066		-		-

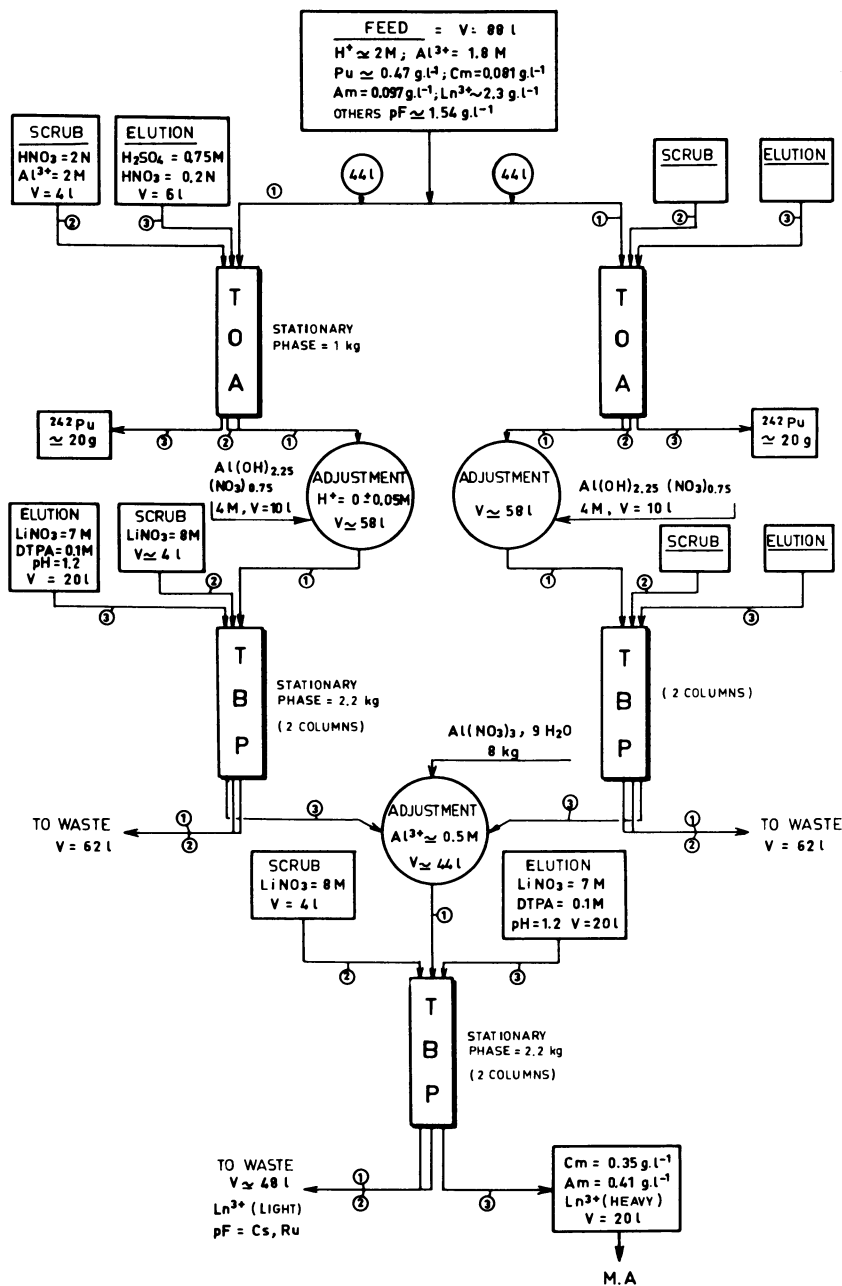


Figure 5. Dissolution of a Pu-Al target in HNO_3

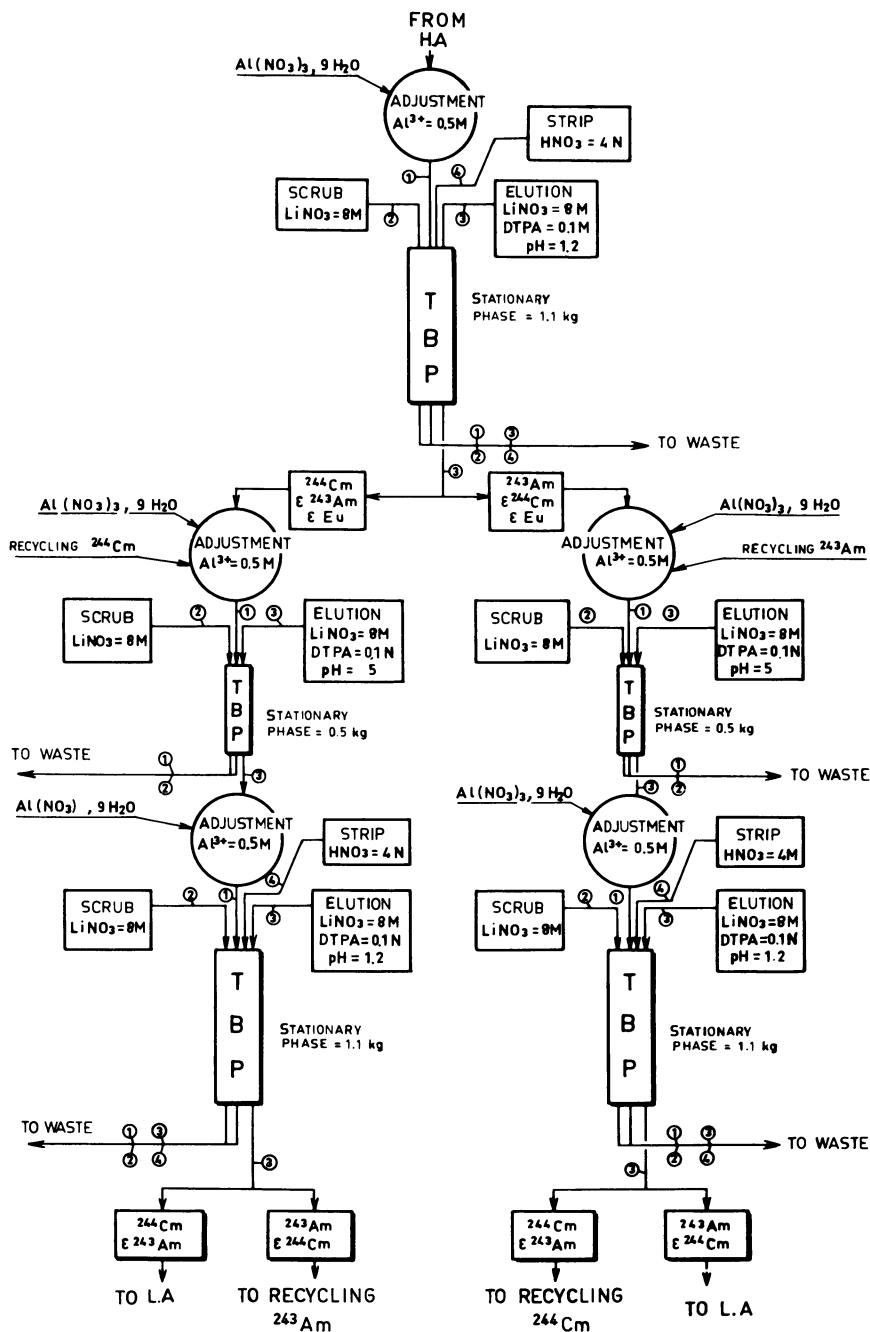


Figure 6. First stages of Am-Cm separations

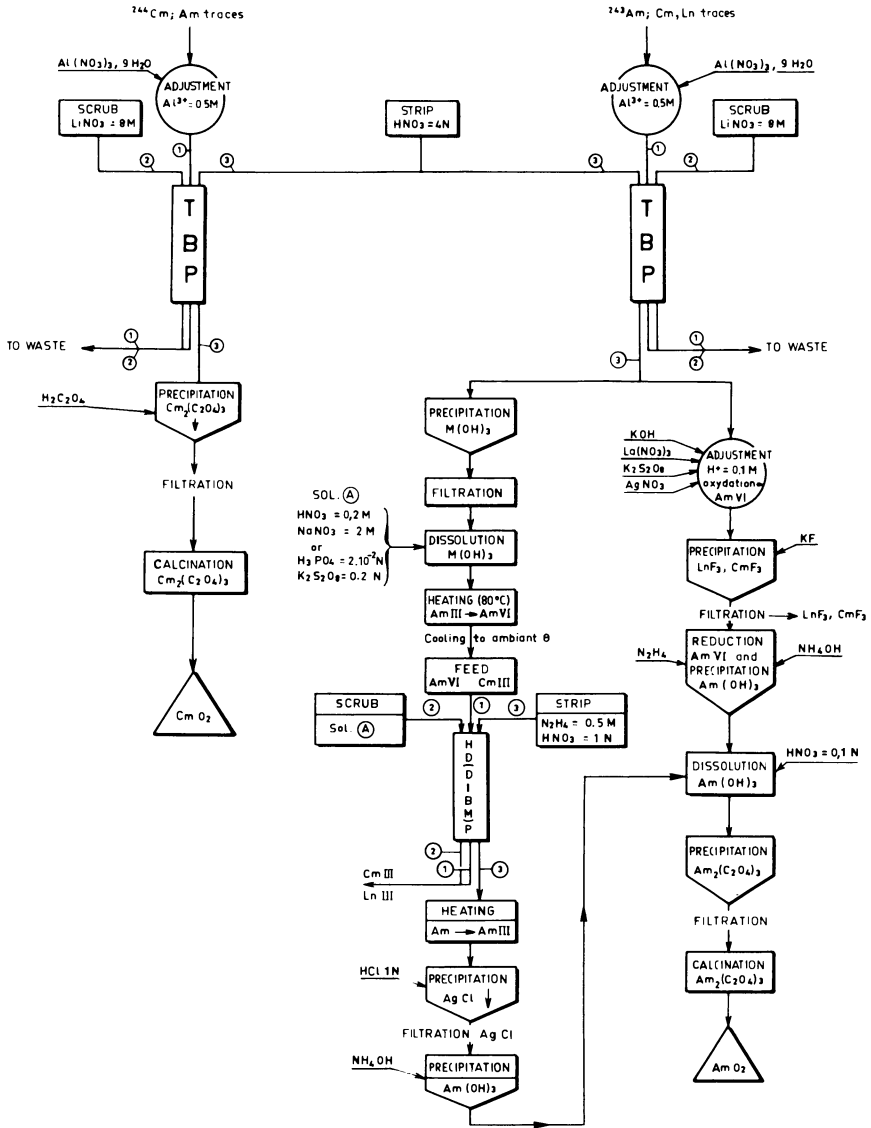


Figure 7. Final Am-Cm separations and purification of ^{243}Am and ^{244}Cm

Solution (1) :

Sulfonitric solutions of ^{242}Pu (^{242}Pu was determined by radiometry, the weights of ^{242}Pu noted above are thus approximate values).

Solution (2) :

Solution of transplutonium elements obtained at the end of high activity treatment.

At the end of this stage, the transplutonium elements are rid of most of the light lanthanides and other fission products, it may be observed that, contrary to the data in Table III, the decontamination factors of the transplutonium elements in Ce and Eu are comparable. An example of good separation of the couple Am/Cm in M.A. treatment is given in figure (8). At the end of the L.A. treatment ^{244}Cm is pure as shown in Table VII.

TABLE VII
Isotopic composition of purified curium
(3g lot)

mass number	mass fraction	
	before analytical separation	after analytical separation
242	0.0043	≈ 0.0043
243	0.006	≈ 0.0017
244	0.9565	0.9605
245	0.0133	0.0133
246	0.0218	0.0218

^{243}Am obtained from the TBP cycles contains about 20% by weight of trivalent elements, mainly Gd, Y and traces of curium. It is purified after oxidation of the americium to Am(VI), either by precipitation of fluorides MF_3 in the presence of an inactive carrier by the method recommended by S.G. Proctor (11), or by extraction chromatography on HD(DiBM)P (figure 7). Let us describe the extraction chromatographic process.

The process is based on the application of the outstanding properties of bis (2,6-dimethyl, 4-heptyl)phosphoric acid (H.D(DiBM)P investigated by G.W. Mason; A.F. Bollmeier and D.F. Peppard (9) in liquid-liquid extraction to the separation Am(VI)/Cm(III) in minute quantities. Our purpose is to adapt this process to the separation Am(VI)/Cm(III) in macro quantities by the technique of extraction chromatography. The main stages of the process are following : a) oxidation of americium : americium and curium from the TBP columns are precipitated in hydroxide form and filtered to eliminate radiolysis products. These fresh hydroxides are taken up by a solution of the following composition : $\text{CHNO}_3 = 0.2 \text{ M}$, $\text{CNaNO}_3 = 2 \text{ M}$ or $\text{CH}_3\text{PO}_4 = 2 \cdot 10^{-2} \text{ M}$ (12), $\text{CK}_2\text{S}_2\text{O}_8 = 0.2 \text{ M}$, $\text{CAgNO}_3 = 2 \cdot 10^{-2} \text{ M}$. After the americium and curium go into solution, the solution is raised and then kept at 80°C for 30 minutes. b) chromatographic separation : after cooling at ambient temperature for 10 minutes,

**American Chemical
Society Library
1155 16th St. N. W.**

In Washington, D. C. 20036

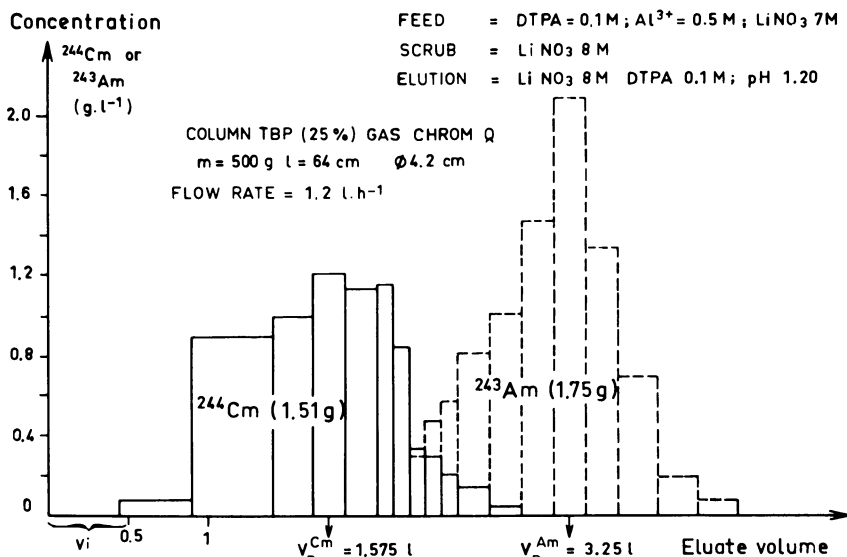


Figure 8. Separation of Am-Cm in M.A. treatment

this solution is injected into a column loaded with a mixture of HD(DiBM)P (30% wt)/G.C.Q previously treated by the oxidizing solution until maintenance of the Ag^{2+} coloration in the effluent solution. Americium in oxidation state VI is fixed, giving a ring of a greenish color. The column is then scrubbed with the oxidizing solution. The americium is eluted by a solution of composition: $\text{CN}_2\text{H}_5\text{NO}_3 = 0.5 \text{ M}$, $\text{CHNO}_3 = 1 \text{ M}$. The Am VI fixation band is discolored by reduction with the appearance of Am(III) and Am(V) in solution. The results obtained in the purification of a lot of about 3 g of ^{243}Am are presented in Table VIII, where one may note the high curium decontamination factor of the americium.

Let us now make some general comments and remarks on this process.

Column behaviour : In high activity medium the TOAHNO₃ column operates at 50% of its exchange capacity, or about 20 g of plutonium. The two TBP columns mounted in series have an exchange capacity of 110 g of lanthanides (mean atomic weight 150 g), allowing the fixation of the lanthanides present in a half target. This behaviour is certainly not obtained and it may be estimated that a large fraction of light elements escapes in the fixation stage. In actual fact, a single pair of columns is sufficient for the second purification cycle, which groups all the americium and curium present in the target. This escape of light lanthanides can be explained by the preferential fixation of the Am/Cm couple. In me-

TABLE VIII
*Am(VI)/Cm(III) separation by extraction chromatography
 on a HD(DiBM)P (30 % weight) (GAS CHROM Q column).*

Nature of solution	^{243}Am	^{244}Cm	Recovery yields %		Decontamination factors	
	mg	mg	^{243}Am	^{244}Cm	Cm(Am)	Am(Cm)
Feed	3038	284				
Loading + washing	*	296	*	104	27***	
^{243}Am stripping	2927	0.137	96.34	0.048		2.10^3

*not mesurable ***estimated from the recovery yield of Am
 column : H = 270 mm ; Φ = 34 mm
 127 g of HD(DiBM)P (30% weight)/G.C.Q.

dium activity, only 20% of the chromatography column capacities were employed. The following observations are related to the stability of the columns under irradiation : a) In H.A. β, γ (350 Ci. l^{-1}) appearance of preferential paths and degassing of solutions due to radiolysis. Destruction of stationary phase : blackening and partial collapse of the bed. Partial clogging of columns by fouling (insoluble fission products?). Drop in exchange capacity of the column associated with observations 1 and 2. All these occurrences require replacement of the columns every 3 or 4 cycles. In M.A. or L.A. β, γ (10 Ci. l^{-1} to 100 $\mu\text{Ci.}l^{-1}$) the occurrences described above also appear, but to a lesser extent. In this case it is essentially the high activities of α emitters remaining in the column which damage it and require its replacement when about 1 kg of stationary phase has fixed a cumulative activity of 820 Ci of α emitters. The phenomenon of radiolysis is very important for curium solutions with composition $\text{CLiNO}_3 = 7 \text{ M}$, $\text{CDTPA} = 0.1 \text{ M}$, $\text{C}^{244}\text{Cm} > 0.5 \text{ g.}l^{-1}$ at pH = 5. The addition of aluminum nitrate to aged curium solution causes intense liberation of gases (nitrous vapors) and considerable foam formation. These occurrences are certainly related to the formation of NO_2^- ions (stable at pH 5) under the action of radiolysis ; these ions are converted into nitrous acid, which is instable at higher acidities. The addition of nitric acid before aluminum nitrate prevents the undesirable formation of these foams.

CONCLUSIONS

The treatment of irradiated plutonium targets by extraction chromatography allowed the purification of the isotopes ^{243}Am and ^{244}Cm on the scale of few tens of grams. This process proved to be extremely simple and flexible, and yielded results which are reproducible in time. The chief advantage of the TBP process over the HDEHP process in high and medium activity conditions lies in the

rapid absorption/desorption kinetics of the elements to be purified and in the separation of americium from curium, which largely offsets its lower selectivity for lanthanide elements. It is certainly possible to improve the performance of this process by : a) optimization of the characteristics of the stationary phase, b) improvement in the filling technique and in hydraulic operation of the columns, c) on-line analysis of americium (the "key" element in actinide/lanthanide separation) in the eluate.

The application of extraction chromatography with HD(DiBM)P to the purification of ^{243}Am at the end of treatment makes the process more consistent, eliminates the delicate stages implemented in hot cell, and considerably improves final product quality.

LITERATURE CITED

1. Orth, D.A.; Mc Kibben, J.M.; Prout, W.E.; Scotten, W.C.; Proceedings of the International Solvent Extraction Conference, The Hague, Society of Chemical Industry, London 1971.
2. Berger, R.; Koehly, G.; Musikas, C.; Pottier, R.; Sontag, R.; Nucl. App. Tech. 1970, 8, 371.
3. Koehly, G.; Madic, C.; Faudot, G.; Sontag, R.; BIST, 1973, 185, 31.
4. Koehly, G.; Berger, R.; Symposium sur les éléments transuraniens, Liège, 1969, 91.
5. Braun, T.; Ghersini, G.; "Extraction chromatography", Elsevier, Amsterdam 1975.
6. Buijs, K.; Müller, W.; Reul, J.; Toussaint, J.C.; EUR 504e, 1973.
7. Weaver, B.; Kappelman, F.A.; J. Inorg. Nucl. Chem., 1968, 30, 263.
8. Sontag, R.; Koehly, G.; CEA Report R-4470, 1973.
9. Mason, G.W.; Bollmeier, A.F.; Peppard, D.F.; J. Inorg. Chem., 1970, 32, 1011.
10. Schulz, W.W.; "The chemistry of americium" TID 26971, 1976.
11. Proctor, S.G.; J. Less. Com. Metals, 1976, 44, 195.
12. Musikas, C.; Germain, M.; Bathellier, A.; This symposium 25.

RECEIVED September 24, 1979.

Plutonium Peroxide Precipitation: Review and Current Research

P. G. HAGAN and F. J. MINER

Rockwell International, Rocky Flats Plant, P.O. Box 464, Golden, CO 80401

Plutonium was first discovered by Seaborg, MacMillan, Kennedy and Wahl on December 14, 1940. In September 1942, the first pure compound of plutonium, PuO_2 , was prepared by Cunningham and Werner. Since that time plutonium has been studied extensively and its production, recovery, and purification have been well established.

A prime responsibility of the Rocky Flats Plant since it was built by the Atomic Energy Commission some 25 years ago has been the recovery and purification of plutonium. This recovery and purification has been done using an aqueous process. One of the major steps in that process is the precipitation of plutonium peroxide. This step converts the plutonium from an aqueous to a solid form for further processing and conversion to metal.

Plutonium can also be converted to a solid form by other precipitants such as oxalate or fluoride: flow sheets have, in fact, been developed for these reagents. However, peroxide was selected over other precipitants at Rocky Flats for two reasons: (1) no additional impurities are introduced by the use of H_2O_2 as the precipitant and (2) the peroxide precipitation reaction is quite specific for plutonium. Significant purification of plutonium can be realized by precipitation of plutonium peroxide. This purification is especially useful for removing americium, which is present in the process stream as a result of the beta decay of ^{241}Pu .

Plutonium peroxide was investigated by Hamaker and Koch, (1) Hopkins, (2) and Koshland, et al. (3) in the 1940's and Leary (4) in the early 1950's. This work showed that the composition of the precipitate varied and often incorporated anions from the solution from which it was precipitated. These investigations, as well as other work (5), also showed that the peroxide precipitate exists in both hexagonal and cubic crystalline forms. Although both forms are compounds of Pu(IV) , they have slightly different O^-/Pu ratios (6). The cubic form can be colloidal and therefore is less suitable for process application than the hexagonal form. The acidity of the solution has an effect on the

0-8412-0527-2/80/47-117-051\$05.00/0

© 1980 American Chemical Society

crystal structure with the cubic being favored at low acidities.

There are some data that indicate sulfate ion aids in the formation of a more easily filtered plutonium peroxide precipitate. Ganivet (7) found, for instance, that peroxide precipitated from a nitric acid medium containing sulfate had better settling characteristics than precipitates from comparable solutions to which no sulfate was added. However, sulfate in the precipitate is undesirable, because of the corrosive effects it can have on processing equipment. Mainland, et al, (8) showed that by careful control of the precipitation parameters, it was possible to effectively precipitate peroxide in the absence of sulfate.

The solubility of plutonium peroxide in nitric acid media (6,7,8,9) is a function of the acid concentration as well as the concentrations of H_2O_2 and foreign ions. Typical solubilities range from 7 to 1190 mg plutonium per liter as the acid concentration varies from 1.2 to 5.2N (7).

These investigations, as well as others over the past three decades at Rocky Flats and at other sites, indicate that there are a number of individual variables that affect the physical and chemical characteristics of plutonium peroxide. The work in this area that is available in the unclassified literature has been summarized by Cleveland (10). A review of the literature indicates a lack of any planned investigative program that encompasses all of the variables. This type of investigation is important, especially from a production process viewpoint, for it would verify the relative importance of the individual variables, as well as any significant interactions between them.

Over the years there have been a number of investigations at Rocky Flats with the goal of improving the production plutonium peroxide precipitation process. In many cases it was difficult to interpret the results since the work was conducted in process equipment, often during process runs, and control of the many process variables was difficult or impossible. Therefore, a laboratory-based experimental program was undertaken with the objective of identifying the variables that have a significant effect on the peroxide precipitation process as used at Rocky Flats, ranking these variables in order of their effect, and, from the trends observed, selecting levels for the variables to optimize the production process. The results of this investigation are summarized in this paper.

Experimental

Based on experience at Rocky Flats and information from the literature, six of the variables deemed most important in the precipitation of plutonium peroxide were selected for investigation. These six, and the ranges over which they were investigated, are identified in Table I.

It should be noted that the concentrations of HNO_3 and H_2O_2

TABLE I
 VARIABLES AND LEVELS USED IN INVESTIGATING
 THE PRECIPITATION OF PLUTONIUM PEROXIDE

Variable	Level	Statistical Designation
X_1 : HNO_3 concentration	1.8M	-1
	2.5M	0
	3.1M	+1
X_2 : H_2O_2 concentration	2.9M	-1
	3.9M	0
	4.9M	+1
X_3 : Impurities concentration	Present	-1
	Absent	+1
X_4 : Digestion time	30 min	-1
	60 min	0
	90 min	+1
X_5 : Rate of H_2O_2 addition	1.8 ml/min	-1
	1.2 ml/min	0
	0.6 ml/min	+1
X_6 : Temperature	22°C	-1
	14°C	0
	6°C	+1

given in Table I are the concentrations that exist in the final solutions. These are more meaningful values, as far as the precipitation of plutonium peroxide is concerned, than are the initial concentrations of the reagents.

The following variables were held constant throughout the experiments.

1. Plutonium concentration (in HNO_3 feed solutions): 43 g/l.
2. Total volume: 35.4 ml.
3. Pattern of H_2O_2 addition: The total amount of H_2O_2 was added at the predetermined rate, i.e., there was no change in the rate during the addition of the H_2O_2 , nor were there extended time intervals between the addition of portions of the H_2O_2 .

Filtration rate and the plutonium concentration in the filtrate were the dependent variables measured in the experiment. These were selected because they are the process variables that most directly measure the efficiency of the production precipitation process and are therefore a direct measure of operating efficiency of the process.

Reagents and Equipment. The plutonium used in the experiments was prepared by dissolving electrorefined plutonium metal in HCl, then converting to HNO_3 medium using an anion exchange resin column. The solutions were checked spectrophotometrically for the presence of Pu(VI) (11). Any Pu(VI) present was destroyed by the addition of a minimal amount of H_2O_2 . If this initial addition of H_2O_2 did not eliminate the Pu(VI), the treatment was continued until all of the Pu(VI) was converted to Pu(IV). Reagent grade HNO_3 was then added to adjust the solutions to the required plutonium and HNO_3 concentrations.

The H_2O_2 used was the same as used in the production operations. It was manufactured by Shell Chemical and contained 11.8 moles H_2O_2 per liter.

Impurities were added to the plutonium nitrate solution as a mixture. The individual metal ion impurities and their concentrations in the HNO_3 -plutonium solution were as follows: Fe, 0.31 g/l; Cr, 0.04 g/l; Ni, 0.06 g/l; Cu, 0.03 g/l; Pb, 0.02 g/l. The particular metal ions used as impurities, and their concentrations, were based on analyses of a series of production plutonium nitrate feed solutions. The impurity solution was made by dissolving either the metal (Fe), or the nitrate salts (Cr, Ni, Cu, and Pb), in 3M HNO_3 . When impurities were required in a run, 1 ml of this solution was added. When they were not, 1 ml of 3M HNO_3 was added to maintain a constant volume.

Water circulated from a constant temperature bath was used to control the temperature. The buret used in adding the H_2O_2 was jacketed so that water could be circulated through it. The beaker containing the plutonium- HNO_3 solution was placed in a small water bath cooled with coils containing water from the

constant temperature bath. An acid resistance transducer connected to a digital temperature readout meter was used to measure the temperature of this plutonium-containing solution.

A "Filterometer" was used to measure the filterability of the plutonium peroxide precipitate. This equipment, designed especially for this work, consisted of a calibrated tube (from a 100 ml buret) attached to a funnel-type support containing a wire screen. A Millipore filter (Solvinert, 1.5 μ m mean pore size) was supported by this screen. The tip of the funnel extended down into a 500 ml Erlenbeyer filter flask and a constant vacuum of 5.08 cm of Hg was applied through the side arm of the flask. The time required for a measured quantity (approximately 30 ml) of the peroxide slurry to be filtered was recorded.

A new Millipore filter was required for each experiment. In order that the filtration time be a measure of the filterability of the plutonium peroxide only, the filtration characteristics of each of the Millipore filters should be the same. However, there were large variations in flow rates of water between filters. Two steps were taken to eliminate as much of this variability as possible. First, filters were pretested. Using a vacuum of 2.54 cm of Hg, a filter had to permit the passage of 50 ml of water through the Filterometer within a time range of 28 to 37 seconds. If the filtration time exceeded 37 seconds, the filter was discarded. If the time was less than 28 seconds, it was combined with another filter and tested again. If the time for the combined filters fell within the time range, they were used. If not, they were discarded. The second step taken to eliminate variability--in this case the variability within the 28 to 37 second range--involved the use of relative rather than absolute filtration times. Relative filtration times were calculated as follows (12):

$$\frac{\text{plutonium peroxide slurry } (\sim 30 \text{ ml}) \text{ filtration time, sec}}{\text{water (40 ml) filtration time, sec}}$$

In a run, for example, in which the filtration time for water was 33 seconds and for plutonium peroxide 96 seconds, the relative filtration time is 2.91.

The volume of the plutonium peroxide slurry varied slightly depending upon the experimental conditions. This variance ranged from 29.4 to 31.6 ml with an average of 30.1 ml. (These are buret readings and they do not include the volume of the section of the Filterometer containing the filter). To correct for this variation in volume, the relative filtration time calculated above was multiplied by the factor

$$\frac{30.1 \text{ ml}}{\text{measured slurry volume, ml}}$$

This corrected relative filtration time was the time used in the

statistical evaluation of the experiments for filterability.

The concentration of plutonium in the filtrate, which is a measure of the completeness of precipitation and so the amount of plutonium recycle required, was determined coulometrically. These concentrations were used in the statistical evaluation of the experiments as a measure of the completeness of precipitation.

Experimental Design. The experimental design used in the investigation was a fractional mixed factorial for five variables at 3 levels and one variable at 2 levels. A full factorial design would have required 486 runs. This fractional factorial design required only 70 runs, three of which were duplicates used to measure the precision of the experimental methods.

Procedure. An experimental run was conducted as follows: The levels for each of the six variables were determined from a Master Run Sheet on which all 70 runs were arranged in a random sequence. For convenience, these levels were noted on a Run Sheet used to record all information about this particular run. Twenty milliliters of the HNO_3 -plutonium solution of the required HNO_3 concentration were measured by pipet and transferred to a 100 ml polyethylene beaker. A plastic beaker was used in preference to a glass one because the plutonium peroxide slurry could be transferred to the Filterometer without retention of any of the precipitate on the beaker wall. If impurities were required for the run, 1 ml of the impurity solution was added. If they were not, 1 ml of 3M HNO_3 was added. The beaker containing the HNO_3 , plutonium, and impurities was placed in a small water bath where it was cooled to the desired temperature. The beaker remained in this water bath throughout the precipitation and digestion, and the solution was stirred continuously. Hydrogen peroxide, cooled to the required temperature, was added at the predetermined rate. The measurement of digestion time began with the addition of the H_2O_2 .

Just prior to the end of the digestion time, water cooled to the required temperature was added to the slurry if necessary to bring it up to volume. This addition of water was necessary for runs using the two lower H_2O_2 concentrations - 7.7 ml of water for 2.9M H_2O_2 , and 4.3 ml for 3.9M H_2O_2 . The water compensated for the differences in the initial volumes of H_2O_2 .

At the end of the digestion time the plutonium peroxide slurry was transferred to the Filterometer. The volume of the slurry was measured to the nearest milliliter and the time required for filtration to the nearest second. The volume of the filtrate was also measured to the nearest milliliter and then diluted with an equal volume of concentrated HNO_3 . This HNO_3 dissolved any plutonium peroxide present and prevented any post precipitation. The filtrate was then analyzed coulometrically for plutonium. From the filtration time, slurry volume, and the plutonium analysis data, the relative filtration time and the

plutonium concentration in the filtrate were calculated.

Results

The data obtained from the experiments were used to develop an equation that relates either the relative filtration time or the plutonium concentration in the filtrate to the six variables selected for investigation. The equation, which is given in Table II in abbreviated form, considers the main effects of the six variables (X_1, X_2, \dots, X_6) as well as all possible first order or two-factor interactions ($X_1X_2, X_1X_3, \dots, X_5X_6$).

In the equation, Y is either the relative filtration time or the plutonium concentration in the filtrate, depending upon which experimental data are used. The X 's are statistical designations of the particular variables as given in Table I, i.e., $X_1 = \text{HNO}_3$ concentration, $X_2 = \text{H}_2\text{O}_2$ concentration, etc. The b 's are coefficients which were derived from the experimental data obtained in the work. The b values are tabulated in abbreviated form in Table II. The equation can be used to calculate either the relative filtration time or the plutonium concentrations in the filtrate at any specific value of a variable as long as that value is within the range that was used for that variable in the experiment. This calculation is made by substituting the desired value for the appropriate X in the equation. The absolute value is not substituted into the equation, but rather a number between -1 and +1 that is proportional to the spacing within the range of the variables investigated. For instance, the range of temperature investigated was 22° (-1) to 6° (+1) [see Level and Statistical Designation columns in Table I]. To obtain data for temperatures of 18° and 10° , -0.5 and +0.5 would be substituted, respectively, for X_6 .

The predicted relative filtration times and the plutonium concentrations in the filtrates were computed for a number of combinations of X 's. The series of curves that follow (Figures 1 through 12) were adapted from curves plotted by the computer and are useful in showing some of the relationships that exist. They do not by any means include all of the curves that were drawn, but rather selected ones that are useful in indicating trends.

Each of the following figures show the effect of changes in two of the variables on either the relative filtration time (Figures 1 through 6) or the plutonium concentration in the filtrate (Figures 7 through 12). One of the variables being investigated is given on the abscissa and the other in the legend for each figure. The rest of the data in the legend indicate the values used for the remaining four variables which were held constant for the calculation.

TABLE II
GENERAL EQUATION AND
VALUES OF COEFFICIENTS

$$Y = b_0 + b_1X_1 + b_2X_2 + \dots + b_6X_6 \\ b_7X_1X_2 + b_8X_1X_3 + \dots + b_{12}X_2X_3 + \\ b_{13}X_2X_4 \dots + b_{16}X_3X_4 + \dots \\ b_{19}X_4X_5 + \dots + b_{21}X_5X_6.$$

<u>Coefficient</u>	<u>Relative Filtration Time</u>	<u>Pu Concentration in Filtrate</u>
b ₀	14.04	1.263
b ₁	-15.97	1.118
b ₂	- 0.1633	-0.8838
.	.	.
b ₆	3.821	-0.1670
b ₇	3.763	-1.148
b ₈	-1.016	0.4061
.	.	.
b ₁₂	-1.801	-0.1717
b ₁₃	-1.666	-0.01744
.	.	.
b ₁₆	-0.2749	-0.2299
.	.	.
b ₁₉	-5.960	-0.06681
.	.	.
b ₂₁	-2.568	-0.2157

Figures 1–12. Effect of variables on relative filtration time, specific conditions listed below.

Figure 1. Impurities, present; digestion time, 60 min; H_2O_2 addition rate, 1.2 ml/min; temperature, 14°C; $[H_2O_2]$: (□) 2.9M, (×) 3.9M, (○) 4.9M.

Figure 2. Impurities, present; digestion time, 60 min; $[H_2O_2]$, 2.9M; temperature, 14°C; H_2O_2 addition rate: (□) 1.8 ml/min, (×) 1.2 ml/min, (○) 0.6 ml/min.

Figure 3. Impurities, present; digestion time, 60 min; H_2O_2 addition rate, 1.2 ml/min; $[H_2O_2]$, 2.9M; temperature: (□) 22°C, (×) 14°C, (○) 6°C.

Figure 4. $[H_2O_2]$, 2.9M, digestion time, 60 min; temperature, 14°C; $[HNO_3]$, 2.5M; impurities: (□) present, (○) absent.

Figure 5. Impurities, present; $[H_2O_2]$, 2.9M, temperature, 14°C; $[HNO_3]$, 2.5M; digestion time: (□) 30 min, (×) 60 min, (○) 90 min.

Figure 6. Impurities, present; digestion time, 60 min; H_2O_2 addition rate, 1.2 ml/min; $[HNO_3]$, 2.5M; $[H_2O_2]$: (□) 2.9M; (×) 3.9M, (○) 4.9M.

Figure 7. Impurities, present; $[H_2O_2]$, 2.9M; H_2O_2 addition rate, 1.2 ml/min; temperature, 14°C; digestion time: (□) 30 min, (×) 60 min, (○) 90 min.

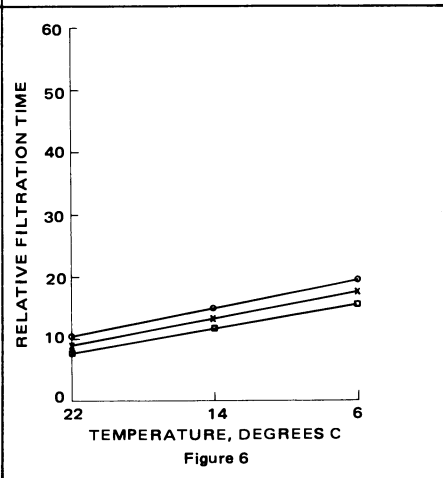
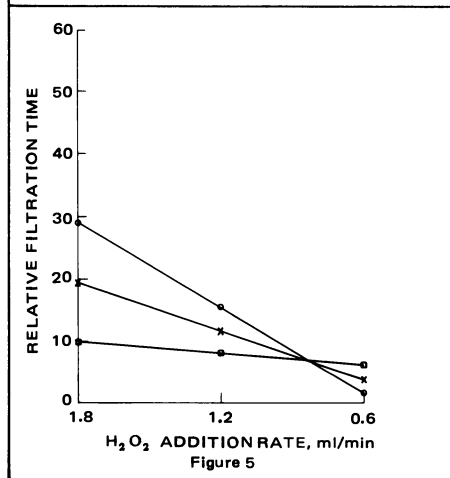
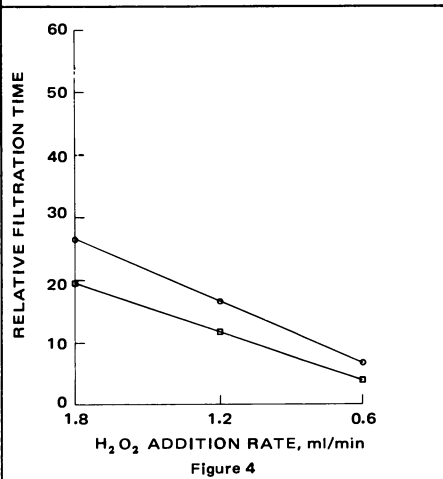
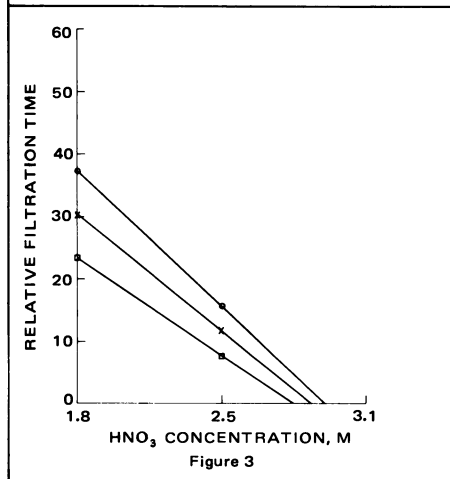
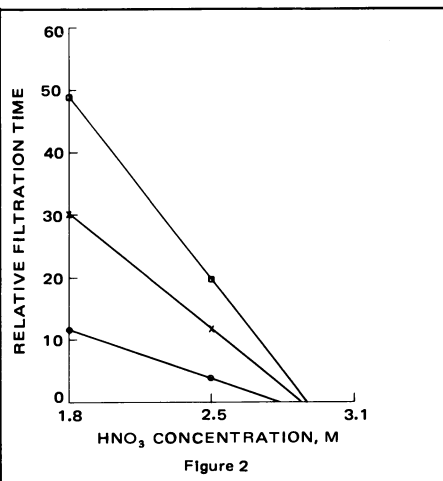
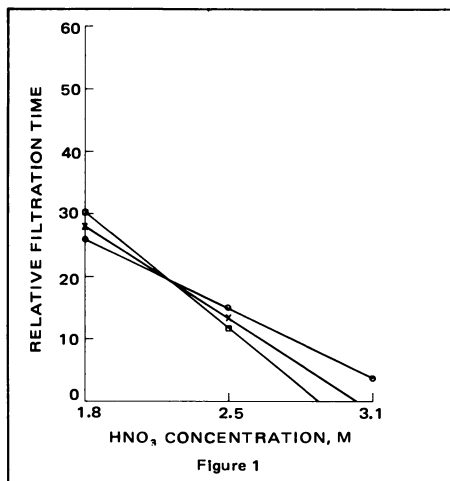
Figure 8. Impurities, present; digestion time, 60 min; H_2O_2 addition rate, 1.2 ml/min; temperature, 14°C; $[HNO_3]$: (□) 1.8M, (×) 2.5M, (○) 3.1M.

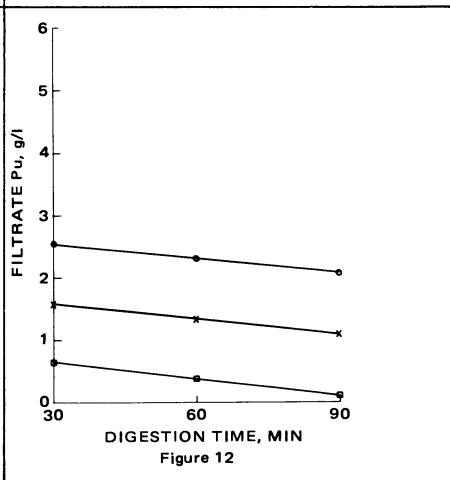
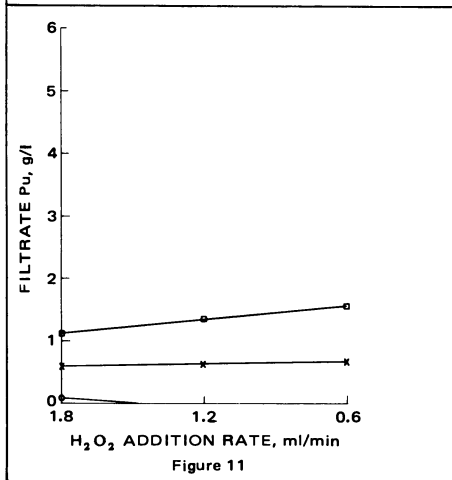
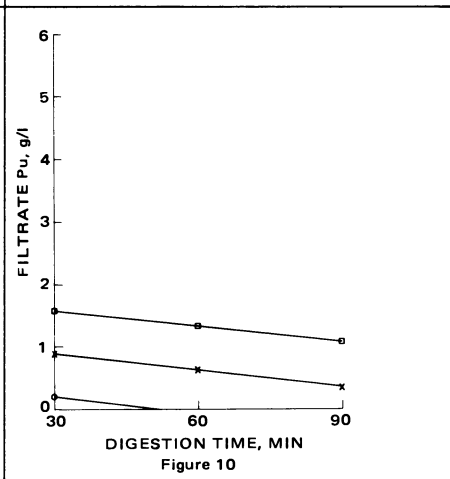
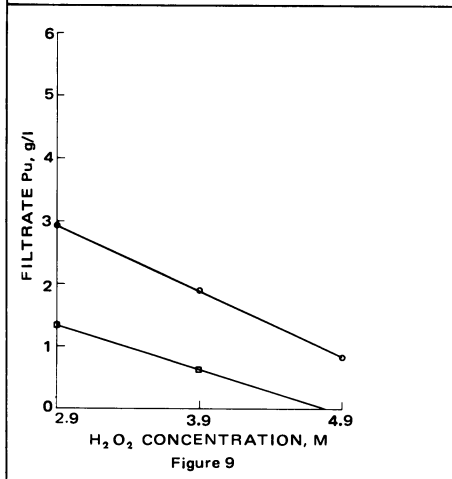
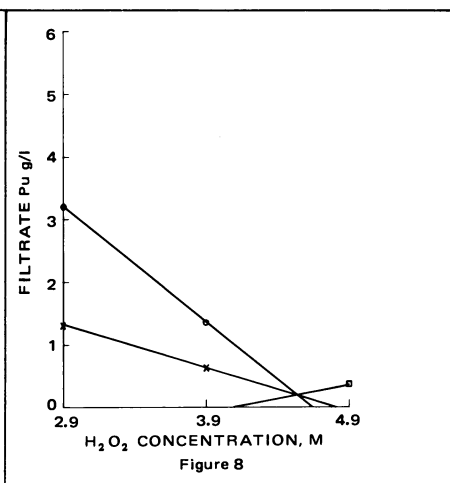
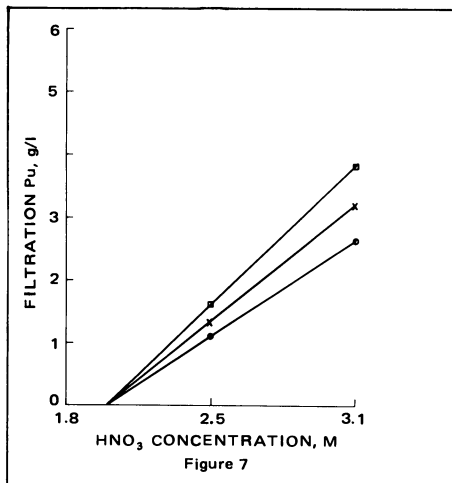
Figure 9. Digestion time 60 min; H_2O_2 addition rate, 1.2 ml/min; temperature, 14°C; $[HNO_3]$, 2.5M; impurities: (□) present, (○) absent.

Figure 10. Impurities, present; H_2O_2 addition rate, 1.2 ml/min; temperature, 14°C; $[HNO_3]$, 2.5M; $[H_2O_2]$: (□) 2.9M, (×) 3.9M, (○) 4.9M.

Figure 11. Impurities, present; digestion time, 60 min; temperature, 14°C; $[HNO_3]$, 2.5M; $[H_2O_2]$: (□) 2.9M, (×) 3.9M, (○) 4.9M.

Figure 12. Impurities, present; H_2O_2 addition rate, 1.2 ml/min; $[H_2O_2]$, 2.9M; $[HNO_3]$, 2.5M; temperature: (□) 22°C, (×) 14°C, (○) 6°C.





Effect of Variables on Relative Filtration Time

Nitric Acid Concentration. The nitric acid concentration has a major effect on the relative filtration time. This is indicated by the generally steep slopes of the plots in Figures 1, 2, and 3. Irrespective of the other variables, the relative filtration time decreases as the nitric acid concentration increases. The interaction between the nitric acid concentration and the hydrogen peroxide addition rate is notable (Figure 2). At low acid concentrations, there is a considerable difference in filtration times between the three levels of the hydrogen peroxide addition rate. But as the acid concentration increases, this difference decreases dramatically.

Hydrogen Peroxide Addition Rate. As the hydrogen peroxide addition rate decreases, the relative filtration time decreases. Again, this occurs irrespective of the other variables (Figures 4 and 5). There is the interesting interaction between the hydrogen peroxide addition rate and the nitric acid concentration as noted above. In addition, the reaction between the hydrogen peroxide addition rate and the digestion time as it effects the filtration time is somewhat out of the ordinary (Figure 5). At the shortest digestion time, the relative filtration time is essentially constant as the hydrogen peroxide addition rate decreases. But at the longest digestion time, the relative filtration time is some seven times greater at the fastest hydrogen peroxide addition rate than it is at the slowest addition rate.

Temperature. As the temperature decreases, the relative filtration time increases (Figure 6). The increase is relatively small, however.

Digestion Time. Generally, the shortest digestion time gives the shortest relative filtration time (Figure 5).

Impurity Concentration. In all cases, when metallic impurities are present the relative filtration time is shorter than when they are absent (Figure 4). The differences, however, are not great.

Hydrogen Peroxide Concentration. Generally, the lowest hydrogen peroxide concentration gives the shortest relative filtration time (Figures 1 and 6). However, the differences in relative filtration time between the various hydrogen peroxide concentration levels are very small.

Effect of Variables on the Plutonium Concentration in the Filtrate

Nitric Acid Concentration. The concentration of nitric acid

has a major influence on the plutonium concentration in the filtrate just as it has on the relative filtration time. The plutonium concentration in the filtrate generally increases with an increase in the acid concentration irrespective of the other variables (Figures 7 and 8). The only exception is at the highest hydrogen peroxide concentration where the reverse is true (Figure 8).

Hydrogen Peroxide Concentration. Generally, as the hydrogen peroxide concentration increases, the plutonium concentration in the filtrate decreases (Figures 8, 9 and 10). There is a reversal of this relationship, however, at the lowest acid concentration (Figure 8).

Impurity Concentration. The plutonium concentration in the filtrate is less when impurities are present than when they are absent (Figure 9).

Hydrogen Peroxide Addition Rate. Although the effect is small, the slower the rate of hydrogen peroxide addition, the higher the concentration of plutonium in the filtrate (Figure 11).

Digestion Time. The longer the digestion time, the lower the concentration of plutonium in the filtrate (Figures 10 and 12). The decrease in the plutonium concentration is not very great, however.

Temperature. Generally, the plutonium concentration in the filtrate increases as the temperature decreases (Figure 12).

Discussion

The objective of this investigation was to identify those variables that have an effect on the precipitation of plutonium peroxide, rank these variables in order of their effect, and then select levels for each of the variables that will give an optimum precipitation of plutonium peroxide.

The identification of those variables that have a major effect on plutonium peroxide precipitation was done in two ways. The first way used t-test values associated with each variable. The comparative magnitude of these values indicates the relative importance of the variable. The second way involved a subjective evaluation of the relative importance of each of the variables based on a visual comparison of the graphs constructed from the experimental data (Figures 1 through 12 plus a couple of dozen other comparable graphs that could not be included in this paper because of space limitations). The results of the subjective evaluation indicate that only the nitric acid concentration and the rate of hydrogen peroxide addition have a major effect on the relative filtration time. The other four variables influence the

relative filtration time, but to a lesser extent. The nitric acid, hydrogen peroxide, and impurity concentrations have the major effects on the plutonium concentration in the filtrate. The other three variables have a lesser effect.

Unfortunately, a change in one variable can have a desired effect on the relative filtration time, but an undesirable effect on the plutonium content of the filtrate. This is the situation with nitric acid. Increasing the nitric acid concentration improves the filterability of the precipitate but at the same time increases the plutonium content of the filtrate. This same type of situation exists, but to a lesser degree, for all the other variables except the digestion time and the impurity concentration.

The t-test data for both relative filtration time and plutonium concentration in the filtrate are given in Table III. The larger the value associated with a variable, the more significant is the effect of that variable. On this basis, the variables that are most important to the relative filtration time are the nitric acid concentration and the rate of hydrogen peroxide addition. The variables most important to the plutonium concentration in the filtrate are the nitric acid, hydrogen peroxide and impurity concentrations. Thus, the t-test data is in general agreement with the subjective evaluation.

The variables can be ranked in order of importance based on the relative magnitude of the t-test data given in Table III.

TABLE III
RELATIVE EFFECT OF VARIABLES
t-test Data

Variable	Value Relative Filtration Time	Value Pu Concentration in Filtrate
HNO ₃ concn.	8.021	4.896
H ₂ O ₂ concn.	0.093	4.401
Impurity concn.	0.417	3.488
Digestion time	0.764	1.860
Rate H ₂ O ₂ addition	4.242	2.318
Temperature	1.523	0.586

The variable that is most important to the relative filtration time is the nitric acid concentration. This is followed by the rate of hydrogen peroxide addition. The remaining four variables are of less importance, and, in fact, are not statistically significant. The critical t value for significance at the 95% confidence level is 2.013 and these four variables have t values lower than this.

Two variables are about equally important as far as the plutonium concentration in the filtrate is concerned. They are the nitric acid concentration and the hydrogen peroxide concentration. These are followed in order of importance by the impurity concentration and the rate of hydrogen peroxide addition. The remaining two variables are not statistically significant.

The t -test data, as well as the subjective evaluation, show that the plutonium concentration in the filtrate is more sensitive to the variables of the precipitation than is the relative filtration time.

There were no significant first or second order interactions between variables that effected either the relative filtration times or the plutonium concentrations in the filtrate.

Conclusions and Recommendations

Based on results obtained in this investigation, the levels shown in Table IV are recommended for the six major variables in the plutonium peroxide precipitation process. These levels were selected to give the best compromise between the fastest filtration time for the plutonium peroxide precipitate and the lowest concentration of plutonium in the filtrate.

The experimental work showed that increasing the HNO_3 concentration decreases the filtration time but increases the plutonium concentration in the filtrate. A compromise was therefore necessary in arriving at the values given. If a minimum plutonium concentration is required in the filtrate, the acidity could be lowered to 1.9M with an approximate doubling in the filtration time.

The H_2O_2 concentration has little effect on filtration time. However, the higher the H_2O_2 concentration, the less plutonium lost to the filtrate. Concentrations higher than the 22 moles/mole Pu recommended (at least up to 30 molar which was the highest investigated) would be beneficial if reagent costs are not excessive and production capacity exists for destroying the excess H_2O_2 in the filtrate.

Although the effect is not large, filtration time is shorter and the plutonium concentration in the filtrate is lower if metallic impurities are present. From a practical standpoint this means, simply, that some impurities can be present in the plutonium feed solution. Since different impurities can have different effects on the catalytic decomposition of H_2O_2 , the

TABLE IV
RECOMMENDED LEVELS FOR MAJOR VARIABLE
IN PLUTONIUM PEROXIDE PRECIPITATION

<u>Variable</u>	<u>Recommended Level</u>
HNO ₃ concentration	2.3 to 2.7 M ^a
H ₂ O ₂ concentration	22 moles/mole Pu
Impurities	Present
Digestion Time	30 min
H ₂ O ₂ Addition Rate	2 moles/min/mole Pu in feed
Temperature	14°C

a Concentration after H₂O₂ added to HNO₃-Pu feed solution.

impurities present in the feed solution should be known along with their concentrations.

The slowest rate of H₂O₂ addition investigated gives a plutonium peroxide precipitate with the fastest filtration time. The rate of addition has very little effect on the plutonium concentration in the filtrate.

The temperature has little effect on the filtration time. The minimum concentration of plutonium in the filtrate is obtained at 22°C. However, 14°C is recommended since decomposition of H₂O₂, which could be catalyzed by impurities present, would be slower at 14°C than at 22°C.

The effect of digestion time on both the filtration time and the plutonium content in the filtrate is minor, so the shortest digestion time investigated is recommended.

The recommended levels for each of the six variables are based on experiments in which the plutonium peroxide precipitations were made by a batch process rather than by a continuous process. However, the recommendations would be applicable, basically, to either process.

Acknowledgement

This work was performed under a contract with the U.S. Department of Energy. DE-AC04-76DP03533

Literature Cited

1. Hamaker, J. W.; Koch, C. W. in Seaborg, G. T.; Katz, J. J.; Manning, W. H., Eds., "The Transuranium Elements", NNES, IV, 14B, McGraw Hill, New York, 1949, pp. 666-681.
2. Hopkins, Jr., H. H. in Seaborg, G. T.; Katz, J. J.; Manning, W. H., Eds., "The Transuranium Elements", NNES, IV, 14B, McGraw Hill, New York, 1949, pp. 949-951.
3. Koshland, Jr., D. E.; Kroner, J. C.; Spector, L. in Seaborg, G. T.; Katz, J. J.; Manning, W. H., Eds., "The Transuranium Elements", NNES, IV, 14B, McGraw Hill, New York, 1949, pp. 731-739.
4. Leary, J. A., USAEC Report LA-1913, 1954.
5. Anonymous, Euratom Report EURAEC-790, 1963.
6. Leary, J. A.; Morgan, A. N.; Maraman, W. J., Ind. Eng. Chem., 1959, 51, 27.
7. Ganivet, M., French Report CEA-1592, 1960 (English transl., USAEC Report HW-TR-53).
8. Mainland, E. W.; Orth, D. A.; Field, E. L.; Radke, J. H., Ind. Eng. Chem., 1961, 53, 685.
9. Anonymous, Euratom Report EURAEC-705, 1963.
10. Cleveland, J. M.; "The Chemistry of Plutonium", Gordon and Breach, New York, 1970, pp. 306-310, 531-535.
11. Hagan, P. G.; Miner F. J., USAEC Report RFP-1391, 1969.
12. Burney, G. N.; Tober, F. W., Ind. Eng. Chem., Process Des. Develop., 1965, 4, 28.

RECEIVED August 9, 1979.

Work performed under U.S. Government contract number DE-AC04-76DP03533.

Actinide Extractants: Development, Comparison, and Future

R. R. SHOUN and W. J. McDOWELL

Oak Ridge National Laboratory, Oak Ridge, TN 37830

Actinide Separations Milestones

In 1805 Bucholz noted that uranyl nitrate is very soluble in diethyl ether (1), and in 1842 Peligot purified uranyl nitrate by recrystallization from ether (2). These documented instances of the dissolution of an inorganic material in an organic solvent formed the basis for a method to separate and purify large quantities of high-purity uranium and plutonium for the Manhattan Project by solvent extraction, initially using ether as an extractant. One of its first uses was to isolate element 94 (plutonium) in the Chicago Metallurgical Laboratory during the period 1942-1944. This objective was accomplished by ether extraction of uranyl nitrate, leaving the plutonium in the aqueous phase. In one instance, 300 lb of neutron-irradiated uranyl nitrate was separated batchwise by using 2- and 3-liter separatory funnels (3).

In addition to the actinide separations needs that were recognized in the 19th century and the first half of the 20th century, a multitude of other separations problems currently need to be resolved. For example, we are now faced with the problem of separating several new (man-made) actinides from the other actinides, or other groups of elements, for analytical, environmental, and nuclear waste handling purposes. These needs have added special urgency to the necessity for developing methods for separating actinides from a wide range of undesired ions. It is hoped that this review will not only serve to correlate the reference material in a useful manner, but also provide an understanding of the appropriate combination of moieties needed to make the most efficient separations agents for specific applications, and thereby contribute to the development of better extractants.

Natural successors to diethyl ether as an extractant were various ethers, polyethers, and alcohols such as dibutyl carbitol, known as "triether," dibutoxytetraethylene glycol, known as "pentaether," and ketones such as methyl isobutyl ketone, known as "MIBK" or "hexone" (4). Most applications for the ether extractants required the addition of high concentrations of

0-8412-0527-2/80/47-117-071\$05.00/0

© 1980 American Chemical Society

salting agents to the aqueous phase to effect transfer of the desired metal species into the extractant phase. This was a disadvantage both economically and in handling and disposing of the aqueous raffinate for purposes other than analytical applications.

Seeking other ether-like, aqueous-immiscible compounds with electron-donor, coordinative properties led to the recognition that tributyl phosphate (TBP) had outstanding qualities as an extractant for uranyl, thorium, and cerium(IV) nitrates from solutions containing additional nitrate ion. This represented a major milestone in the development of new reagents for solvent extraction (4,5). TBP is presently being used in an important process (Purex) for separating and purifying uranium and plutonium from spent fuels in nitric acid solution.

TBP has gained wide acceptance in separations processes for nuclear fuel reprocessing and waste handling because of its excellent extraction characteristics and ready availability; however, it has some disadvantages with respect to radiation stability and aqueous-phase solubility. At least two homologs of TBP, trihexyl phosphate (THP) and tri-(2-ethylhexyl) phosphate (TEHP), are excellent extractants, are less aqueous soluble, and do not exhibit the tendency toward third-phase formation observed when thorium is extracted by TBP (6,7). Other electron-donor alkyl phosphates with extraction properties similar to TBP, such as dibutyl phenylphosphate (DBPP) and di-*sec*-butyl phenylphosphonate (DSBPP), are both radiation-stable and show higher extraction power for uranium and plutonium. In spite of the advantages of such compounds, TBP remains largely supreme in its application because of established use and commercial availability.

The alkyl phosphoric acids were first recognized as excellent actinide extractants because dibutyl phosphoric acid existed as an impurity in TBP (8). They extract well from unsalted solutions and from systems such as sulfate in which TBP is ineffective. Organophosphorus acids are thus suitable for uranium hydrometallurgical applications where ore is leached with sulfuric acid. The Dapex process is an example in which bis(2-ethylhexyl) phosphoric acid (HDEHP) is used alone or in synergistic combination with neutral organophosphorus compounds for uranium and vanadium recovery (9,10).

The alkyl amines offer greater selectivity than organophosphorus compounds in many applications, particularly in uranium hydrometallurgy. Amine extraction is typified by the Amex process, which uses a tertiary or branched secondary amine to extract uranium from sulfate leach liquors (11). A similar process based on the use of a primary or straight-chain secondary amine (sometimes modified with an organic-soluble alcohol) has given good results in thorium recovery (12).

Amines can also be used to separate the trivalent actinides from the chemically similar trivalent lanthanides. In the Tramex process, a tertiary amine is used as the extractant from 10 to 12 M LiCl, 0.1 to 0.3 N AlCl₃, and 0.01 M HCl (13,14). The development

of the Talspeak process was an important advance in lanthanide-actinide separation. Here, the liquid cation exchanger HDEHP is used to extract the lanthanides from a solution containing carboxylic acids and other aqueous-soluble complexing agents that preferentially retain the trivalent actinides in the aqueous phase. This process, which has the advantage of being less corrosive than Tramex, has had widespread application since its development in 1964 (15,16).

Although a variety of extractants have been studied and tested for their suitability in analytical separations of actinides, perhaps the most recent milestone in the process use of actinide extractants is the application of the bidentate carbamoylmethylphosphonates (17,18,19). The pioneering work on these compounds was done 15 years ago by Siddall (20,21). Their principal advantage is their ability to extract the trivalent, tetravalent, and hexavalent actinides from considerably more concentrated nitric acid media than other extractants.

The extraction chemistry of the more important reagents will be examined, and their characteristics compared, in the following section.

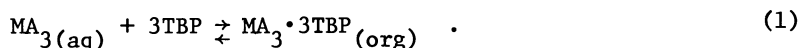
Classes of Extractants

Coordinative Extractants

All neutral, electron-donor extractant ligands, L, bind neutral metal salts, such as salts of the trivalent actinides, MA₃, by completing the coordination requirements of the metal, M, to give an adduct MA₃·nL. This is true of extractants such as ethers, the alkyl phosphate esters, the phosphine oxides, the amine salts, and all extractants that require transfer of a charge-equivalent amount of anion to the organic phase to form the extracted species.

Ethers. Although ethers hold an important historical place in actinide extraction, they are not used extensively at present. They are weak-Lewis-base coordinative extractants, whose chemistry has been adequately covered in earlier reviews (22).

Monodentate phosphate compounds. The monodentate phosphate compounds are stronger Lewis bases and have a higher coordinating ability than ethers. Their basicity is in the order: phosphate < phosphonate < phosphinate < phosphine oxide. Typical of their behavior is the extraction of actinide nitrates by TBP, which has been reported (23) as:



Extraction by any trialkyl phosphate, phosphonate, phosphinate, or phosphine oxide would be similar. In general, compounds

containing carbon-to-phosphorus bonds give higher D 's than the corresponding esters. For example, phosphine oxides, with three carbon-phosphorus bonds, give higher D 's for $\text{UO}_2(\text{NO}_3)_2$, UO_2SO_4 , UO_2Cl_2 , $\text{Th}(\text{NO}_3)_4$, and $\text{Pu}(\text{NO}_3)_4$ than does TBP, which has no carbon-phosphorus bonds (24). The order of extraction of trivalent actinides by TBP at 5 M HNO_3 is: $\text{Am} < \text{Cm} < \text{Bk} < \text{Cf} \approx \text{Es}$ (25).

A comparison of the effect of the structure of phosphate esters on uranium extraction from nitrate media shows that the esters from secondary alcohols give higher uranium distribution coefficients (D_U 's) than those from primary alcohols, phenyl esters extract uranium less strongly than alkyl esters, and benzyl esters are intermediate in extractant strength for uranium (24).

The usual effect of increasing the acid concentration is reported to be an increase in the D_M (due to increased amounts of the extractable MA_3 in the aqueous phase) followed by a decrease in the D_M (due to formation of the extractant- HNO_3 adduct), resulting in a maximum extraction at an acid concentration between 2 and 6 M . However, one study has noted an increase in americium extraction at nitric acid concentrations from 12 to 16 M . These data are not consistent with the usual view of americium distribution dependence on nitric acid and nitrate concentration, and the authors hypothesize that a TBP- HNO_3 adduct, which is a stronger extractant for americium than TBP alone, is formed above 8 M HNO_3 and an organic-phase complex of $\text{Am}(\text{NO}_3)_3 \cdot n(\text{TBP} \cdot m\text{HNO}_3)$ is formed rather than $\text{Am}(\text{NO}_3)_3 \cdot n\text{TBP}$ (26). While one may not absolutely discount this possibility, additional factors such as the extraction of $\text{HAm}(\text{NO}_3)_4$ and deviations from ideal activities in such concentrated acid solutions should definitely be considered.

The phosphine oxide most commonly used as an extractant is trioctylphosphine oxide (TOPO). The order of extraction of U(VI) from mineral acid by TOPO is: $\text{HNO}_3 > \text{HCl} > \text{HClO}_4$ (27). Extensive information on extraction with this reagent has been compiled (28).

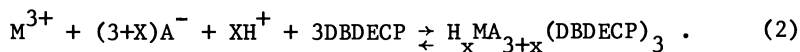
Recent papers (29) report the use of TOPO for the extraction of actinium from nitrate media. The maximum extraction coefficient from >2.0 M NaNO_3 at pH 2 with 0.05 M TOPO in cyclohexane was noted to be greater than 10^3 , and the extracted complex was reported as $\text{Ac}(\text{NO}_3)_3 \cdot 4\text{TOPO}$ (30).

The maximum actinium extraction from chloride solutions by 0.1 M TOPO--cyclohexane was found to be from 8 M LiCl at pH 2 ($D_{\text{Ac}} = >10$). The extracted compound in this system has been reported as $\text{Li}_2\text{AcCl}_5 \cdot 2\text{TOPO}$ (30). Reagent dependencies for americium extraction from slightly acidic 1 M LiCl with TOPO indicated that the extracted species is $\text{AmCl}_3 \cdot \text{TOPO}$, while $\text{AmCl}_3 \cdot 3\text{TOPO}$ is indicated when the aqueous phase is 5 M LiCl . The number of extractant molecules associated with the Am species was not constant over the LiCl concentration range 1 to 5 M , and nonintegral values of 1.2 and 2.7 were obtained at 1 M LiCl and 5 M LiCl , respectively. These results suggest a mixture of organic-phase species (31).

Bidentate phosphate compounds. The organophosphorus bidentate extractants are neutral species extractants that undergo no keto-enolization and have no exchangeable hydrogens (as is the case in extraction by the bidentate diketones). They contain either two P=O groups or one P=O and one C=O group. The carbamoylmethylphosphonates (CMPs) and carbamoylphosphonates (CPs) are examples of the latter, while the tetraalkyldiphosphonates and tetraalkyldiphosphinedioxides [or bis-(disubstituted phosphinyl)-alkanes] are examples of the former.

It has been noted (from acid and water extraction data) that the phosphoryl groups of the diphosphonates do not act independently of each other (20). Thus extraction power is not a simple function of phosphoryl group concentration. With more than one bridging methylene between phosphoryl groups, extraction is significantly poorer than expected for that phosphoryl concentration. This suggests the necessity of special steric requirements such as possibly the classical six-membered chelate ring (27,32). Nitric acid is extracted by bidentate compounds and, in most cases, competes with the metal extraction at higher acidities (>8 M). Comprehensive studies of acid extraction and its effect on metal ion extraction have been reported (21).

The extraction of Cm and Es by dibutyl(diethylcarbamoyl)-phosphonate (DBDECP), which has no bridging methylene group between the carbamoyl and phosphoryl groups, is in the order: $\text{HClO}_4 > \text{HNO}_3 > \text{HCl}$. DBDECP appears unique in that it shows third-power reagent dependence and provides a distribution coefficient which increases rapidly with acid concentration even above 8 M. This suggests either that there is no competition from acid-compound formation with the extractant or that an acido complex of the metal is extracted as in Eq. (2) (20,33):



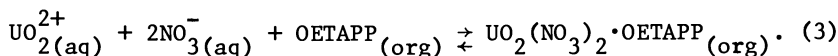
The latter possibility is supported by references, suggesting the existence of anionic trivalent actinide species at acid concentrations greater than 5 M (34).

The order of extraction of U(VI) from mineral acids by bis-(di-n-hexylphosphinyl) alkanes is: $\text{HClO}_4 > \text{HCl} > \text{HNO}_3$. The fact that this order is the reverse of the order observed for TOPO is explained by the difference in the ability of the monodentate TOPO and the bidentate compounds to saturate the uranium coordination sphere. Apparently, TOPO is unable to replace all the water in the weakly bound (but more organophilic) uranium perchlorate complex, whereas the bidentate compound has this capability (27). Numerous descriptive studies of the extraction behavior of these compounds for uranium and thorium systems can be found in the literature (27,35-39).

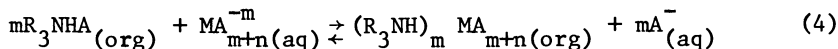
Work with the organophosphorus bidentate vinylene diphosphine, in which the phosphoryls are bridged $\text{>P(O)CH} = \text{HC(O)P<}$, illustrates the importance of steric considerations in the extraction of uranyl

nitrate. Extraction by cis and trans isomers was markedly different. Extraction by the cis-tetratoxylylvinylene diphosphine dioxide was $\sim 10^5$ greater than that shown by the trans isomer; the latter has about the same extraction power as the monoxide. In addition, the D_U shown by cis-tetraphenylvinylenediphosphine dioxide is three orders of magnitude greater than that shown by the analogous dioxide with a flexible ethylene bridge (40).

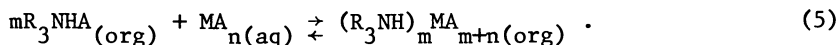
The organophosphorus bidentate octaethyltetraamidopyrophosphate (OETAPP), a compound of the type $R_2P(O)NH(O)PR_2$, is noted for the extraction of uranium from HCl as well as HNO_3 . The maximum D_U reported is about 105 from 4 to 5 M HNO_3 , or 8 M HCl. The likely equilibrium expression suggested is (41):



Alkyl ammonium compounds. High-molecular-weight amines are very useful actinide extractants in both analytical and process applications. Salts of primary, secondary, and tertiary amines, as well as quaternary ammonium bases RNH_2 , R_2NH , R_3N , and R_4N^+ , are commonly used. These compounds, which are often thought of as anion exchangers, may also be considered as neutral-species coordinators since equivalent equilibrium expressions can be written based on either mechanism. That is,



for extraction by exchange of the anion of the amine salt for a negatively charged complex of the metal MA_{m+n}^{-n} (n is the charge of the metal); or, assuming addition of the neutral alkyl ammonium salt to the neutral-metal species:



These two mechanisms cannot be distinguished by equilibrium studies, but kinetic studies (42) have shown that both can operate under appropriate conditions.

Salts of the tertiary amines have found wide application in the extraction of actinides. They are used extensively in the hydrometallurgical recovery of uranium from sulfate leach liquors of uranium ore and in the separation of uranium and thorium in sulfate systems (11,12). Plutonium(IV) is separated effectively from uranium and most other ions in a nitrate system (43). Among the transplutonium actinides, Am(III) is extracted from concentrated LiCl by tertiary amines, very slightly by secondary amines, and negligibly by primary amines (44). The trivalent transplutonium elements are almost inextractable from HNO_3 in the absence of salting-out agents, but nitrate salts often increase extraction more rapidly than the third-power dependence expected from the extraction of MA_3 . For example, the D_{Cm} increases proportionally to the seventh power of the $LiNO_3$ concentration in HNO_3 when

extracted by 0.6 M Alamine-336 [a mixture of trioctyl and tri-decyl amines (C_8-C_{10})] (12,13). The effectiveness of such salting agents appears to be inversely proportional to the ionic radius; that is, for D_{Cm} , $Li^+ > Na^+ > NH_4^+$ and $Be^{2+} > Mg^{2+} > Ca^{2+}$.

Trialkyl amines from C_8 to C_{20} have been studied for their potential suitability in the extraction of Am, Cm, and Cf from $LiNO_3$ and $NaNO_3$. With the longer-chain amines, there is a lower dependence of D_M on extractant concentration and salting-out agent concentration. This suggests that the larger, more sterically hindered extractant molecules permit a smaller number of ligands to surround the metal, thereby leaving free coordination sites in the complex filled with water. As an example of this selectivity, trioctyl amine provides a satisfactory Am-Cm separation but a poor Am-Cf separation; with longer-chain amines, the Am-Cm separation deteriorates, while the Am-Cf and Cm-Cf separations improve substantially (45). Several publications on actinides separations by tertiary amines are available studying Pu(VI) and Pu(III) extraction (46); Np(V), Np(VI); Pu(VI), U(VI) (47); and Am, Cm (48,49).

In certain applications, the quaternary ammonium salts have advantages over tertiary amines for actinide extractions. Quantitative extraction of the transplutonium elements from nitrate media by quaternary ammonium salts can be achieved with a lower aqueous-phase nitrate concentration than is required for tertiary amines; thus, aluminum nitrate may be used instead of lithium nitrate. The separation factor between Am and Cm can be as high as three in a quaternary ammonium nitrate system (50). The effect of the length of the alkyl chain on Cm, Am, Bk, Cf, and Es extraction by alkyldioctylammonium nitrates suggests that steric factors substantially influence the extraction selectivity (51). A comparison of the extraction of tetravalent and hexavalent actinides by tetraheptyl ammonium nitrate shows that tetravalent ions are more easily extracted than hexavalent ions: e.g., $Pu(IV) > Np(IV) > Th(IV) > Np(VI) > Pu(VI) > U(VI)$. Symmetrical quaternaries usually show higher extraction power than unsymmetrical ones (52). An excellent review of amine extraction may be found in (42).

Sulfoxides. Sulfoxides (R_2SO) are neutral electron-donor-type molecules similar to the phosphine oxides. A significant volume of work has shown that long-chain dialkylsulfoxides may have considerable potential utility in actinide separations. Extraction behavior from nitrate systems is similar to that of TBP for some sulfoxides; in addition, they offer the possibility of producing less troublesome degradation products than TBP. However, these compounds are not presently available in commercial quantities, and we lack the experience with them that has been amassed with TBP.

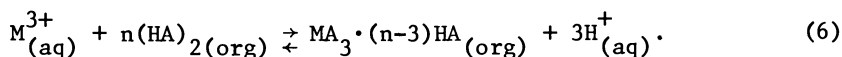
Di-n-pentyl sulfoxide (DPSO) in benzene preferentially extracts uranium over thorium from 5 M HCl containing a neutral salting-

out agent, yielding a separation factor of 3690. The extracted species for thorium is reported to be $\text{ThCl}_4 \cdot 2\text{DPSO} \cdot \text{HCl}$. Homologs dioctylsulfoxide (DOSO) and diphenyl sulfoxide ($\text{D}\phi\text{SO}$) yield complexes with the formulas $\text{ThCl}_4 \cdot 2\text{DOSO}$ and $\text{ThCl}_4 \cdot 3\text{D}\phi\text{SO}$, respectively. The extraction of a monoacidic $\text{ThCl}_4 \cdot \text{HCl}$ species by DPSO and a neutral species by DOSO is indicated (53).

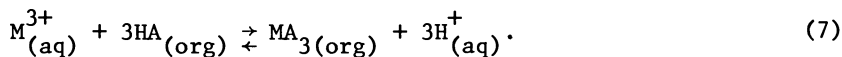
Two papers report the uranyl species extracted by DOSO to be $\text{UO}_2(\text{NO}_3)_2 \cdot 2\text{DOSO}$ (54,55). The order of strength of extraction of uranyl nitrate is: diheptyl > decyl benzyl > diphenyl: the extraction coefficient from three diluents is in the order: benzene > carbon tetrachloride > chloroform. In studies of the extraction of Pa(V) and U(VI) from HCl media by DPSO, $\text{D}\phi\text{SO}$, and DBSO, the order of extractant strength was found to be: DPSO > DBSO > $\text{D}\phi\text{SO}$. This suggests that the extracted species were $\text{PaOCl}_3 \cdot 3\text{R}_2\text{SO}$ or $\text{Pa}(\text{OH})_2\text{Cl}_3 \cdot 3\text{R}_2\text{SO}$ (56). Dipentyl sulfoxide was investigated as an extractant to separate the actinides Th(IV), U(VI), and Pa(V) from the trivalent lanthanides La, Ce, Pm, Eu, and Tb. Actinide extraction is at a maximum at 7 M HCl, and there is little or no lanthanide extraction at this acid concentration (57).

Cation Exchange Extractants

Alkyl phosphoric acids. Perhaps the largest single group of extractants for actinides are the alkylphosphoric acids of three main types: dialkylphosphoric acids, dialkylphosphonic acids, and dialkylphosphinic acids $(\text{RO})_2\text{P}(\text{O})\text{OH}$, $(\text{RO})\text{R}'\text{P}(\text{O})\text{OH}$, and $\text{R}_2\text{P}(\text{O})\text{OH}$, respectively. Monoalkyl (diacidic) representatives of each type exist, but these compounds are rarely used because of their water solubility and difficulty in stripping. Alkyl phosphoric acids usually form dimers or higher aggregates in nonpolar solvents such as benzene or n-hexane (58). The extraction of a trivalent actinide by a dialkylphosphoric acid such as HDEHP in a nonpolar diluent may be described by the reaction



In a polar solvent in which the dialkylphosphoric acid is primarily a monomer, trivalent actinide extraction has been described as (59):



The dialkylphosphoric acid most commonly used and studied for trivalent actinide extraction is probably HDEHP. Even though this compound is not as strong an extractant as some other straight-chain analogs, it offers advantages such as low aqueous-phase solubility, less tendency to third-phase formation, and ready availability.

In americium and curium extraction from chloride solutions by HDEHP in n-heptane, dependence of the extraction coefficient on hydrogen ion concentration and HDEHP concentration indicates an

extracted species stoichiometry of $\text{M}(\text{HA}_2)_2$. In benzene, the indicated species is $\text{M}(\text{HA}_2)_3$. An example of the effect of steric hindrance may be seen for the extraction of Am^{3+} and Cm^{3+} by the isomers bis-*n*-octylphosphoric acid (HDOP), bis-2-ethylhexylphosphoric acid (HDEHP), and bis-2,2-dimethylhexylphosphoric acid (HDNOP); the order of decreasing D_M for americium is HDOP > HDEHP > HDNOP (60). Diisodecylphosphoric acid (HDIDP) is reported to be a stronger extractant than HDEHP for the trivalent actinides (61).

HDEHP is also used as a tool in the study of aqueous complexation. One of the more unusual of such studies is the examination of the complex formation of nobelium with citrate, oxalate, and acetate ions and comparison with other divalent ions. Nobelium was found to resemble Ca and Sr, being slightly more like Sr (62).

Since HDEHP is both a cation exchanger and a coordinator in most extraction situations, coordinated water must be removed from the metal ion in the extraction. Because this sometimes leads to a slow reaction step, the kinetics of HDEHP extraction is important. The kinetics of the Talspeak process (14,15) has been investigated (63); the kinetics of $\text{Am}(\text{III})$ and $\text{Th}(\text{IV})$ extraction by HDEHP in an unstirred system has also been studied (64).

Dioctylphenyl phosphoric acid (HDOPP) has been found to be a more powerful extractant from mineral acids than HDEHP (65,66). The distribution coefficient of U(VI) from sulfuric acid solutions is three to five times higher with HDOPP than with HDEHP under the same conditions. Extraction of U(VI) from mineral acids by HDOPP is in the order: $\text{HClO}_4 > \text{HNO}_3 > \text{HCl} > \text{H}_2\text{SO}_4$ (67). Acidity and reagent dependencies at low reagent loadings and metal-to-reagent ratios under fully loaded conditions indicate the formation of compounds such as $\text{UO}_2\text{A}_4\text{H}_2$ and $(\text{UO}_2)_n\text{A}_{n+2}\text{H}_2$ for the two respective conditions, as has been the case for HDEHP in earlier work (68).

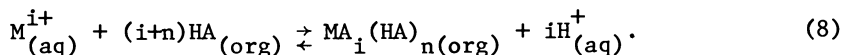
The addition of an ether linkage in the alkyl chains of dialkylphosphoric acids has been found to increase its extractive power for trivalent actinides, resulting in an extractant that is more effective from acid solutions than is HDEHP (69). Bis(hexoxyethyl)phosphoric acid (HDHöEP) is a compound of this type that has been studied extensively (70,71). The ether linkage may contribute to the coordination of the metal ion, resulting in the formation of a seven-membered ring.

In the extraction of trivalent actinides, the dialkylphosphonic acids behave in a manner similar to that observed for the dialkylphosphoric acids. However, in some systems, they offer a greater intergroup separation between lanthanides and actinides. The separation of Cf and Cm from nitric acid solutions has been studied using 2-ethylhexylphenylphosphonic acid [HEH(ΦP)] and 1-methylheptylphenylphosphonic acid [HMeH(ΦP)]. ORNL has developed a process for intergroup actinide separation, called Hepex, based on the use of HEH(ΦP) (72,73).

One study concludes that the organic-phase species resulting from $\text{Am}(\text{III})$ and $\text{Cm}(\text{III})$ extraction by HEH(ΦP) are a 3:2 mixture of $\text{MA}_3 \cdot \text{HA}$ and $\text{MA}_3 \cdot 2\text{HA}$, while Cf is extracted exclusively as $\text{MA}_3 \cdot \text{HA}$ (74).

Sulfonic acids. Sulfonic acids are very strong cation exchange extractants for a wide variety of metal ions. However, their use in process applications as liquid extractants (although extensively used as resinous cation exchangers) has been quite limited because of the difficulty of obtaining reagents that have sufficiently high organic solubility and sufficiently low distribution to the aqueous phase when in the salt (particularly the alkali salt) form. The usable compounds that are presently available are dinonyl naphthalene sulfonic acid (HDNNS) and didodecyl naphthalene sulfonic acid (HDDNS). The first of these has been used extensively in studying aqueous complexes of actinides (75,76). Stability constants for the sulfate and fluoride complexing of U(VI), Np(VI), and Pu(VI) were found to follow the order: U(VI) > Np(VI) > Pu(VI) (77).

Diketones. Beta-diketones such as acetylacetone, benzoylacetone, and isopropyltropolone are well known for their applications in analytical extraction of actinides. These compounds are weak acids due to tautomerization; thus they can act as cation exchange extractants. Trivalent actinide [M(III)] extraction by the reagent (HA) at low aqueous acid concentration where the compound behaves both as cation exchanger and coordinator probably follows the reaction



In high-acid systems where the compound can be only a neutral bidentate coordinator, the reaction would be expected to be:



Since fluorinated β -diketones are more acidic than nonfluorinated compounds, they have useful extraction coefficients from more acidic solutions (78).

The extraction of Pa(IV) by benzoylacetone (HBA) from perchloric acid and sodium perchlorate was investigated in a recent study of the equilibria in diketone extraction. The indicated reaction is reported to be the same as that given in Eq. (8), where $M^i = PaO_2^{2+}$ or $Pa(OH)_2^{2+}$ (79). Diketones have also been used in the study of aqueous complexation. Oxalate (80), sulfate, and fluoride complexing of Np(IV), Pu(IV) and Th(IV) have been studied by thenoyl trifluoroacetone (TTA) extraction. The D_M is always higher when TTA is dissolved in benzene than when it is dissolved in *n*-hexane (81), which is contrary to the usual observation of higher *D*'s in aliphatic diluents.

Synergistic mixtures. A solvent extraction system is said to be synergistic when the distribution coefficient obtained from a mixture of extractants is greater than the sum of distribution coefficients of each extractant alone. Such systems are usually

mixtures of cation exchange extractants and coordinative extractants, and the synergistic effect is thought to operate by an enhancement of the ease with which the coordination sphere of the metal can be satisfied. Two methods of accomplishing this have been proposed for trivalent actinides (78). In the first, the synergist, S, replaces coordinated water on an extracted metal complex, thus making the resulting complex more organophilic. In the second, the original extracted complex is simply coordinatively unsaturated and the synergist adds to the complex, thereby enhancing its stability.

There are a number of practical synergistic systems that make use of organophosphorus compounds. A classic example is the combination of HDEHP and TOPO. The TOPO is thought to replace water or HDEHP in the coordination sphere of the metal. Some early work in this area included a study of the extraction of uranium in such systems (82). Commercial processes now exist for the recovery of uranium from wet-process phosphoric acid utilizing synergistic systems (83,84). Descriptive studies of such systems have also been made (85,86).

Examples of TTA synergism with Aliquat 336-S chloride show a strong synergistic effect for Am, Cm, and Cf. The extracted species is represented as an organic-phase ion pair $[M(TTA)_3 \cdot Cl]^{-}A^{+}$, where A^{+} is the quaternary ammonium ion (87). For TTA-TOPO extraction of Cm, the extracted species is reported as $Cm(TTA)_2 X \cdot (TOPO)_2$, where X is NO_3^- or $HS_2O_8^{2-}$ (88). Synergism was first reported in the open literature (TTA + TBP) in 1954 (89), and the investigation of additional synergistic systems was described soon thereafter (90,82).

Synergistic systems have also been reported in which one of the adducts is in the aqueous phase. The combination of TOPO (in CCl_4) and benzoic acid (in aqueous and organic) was shown to extract uranium with a synergistic effect. The organic-phase adduct was reported to be $UO_2(ClO_4) \cdot C_6H_5COO \cdot 2TOPO$. An optimum benzoic acid/TOPO ratio exists, above which compound formation between TOPO and benzoic acid decreases the synergistic effect (91).

In recent years, the pyrazolones have been shown to be excellent extractants in synergistic combination with TBP and TOPO. The extraction of both Pu(IV) (92) and Am (93) by 1-phenyl-3-methyl-4-benzoyl-5-pyrazolone (ΦMBP) with TBP shows significant synergistic effects. Three pyrazolones in combination with TOPO and TBP are compared for the extraction of U(VI) in (94). Two pyrazolones exhibiting improved solubility characteristics, 1-phenyl-3-methyl-4-decanoyl-5-pyrazolone (ΦMDP) and 1-phenyl-3-methyl-4-tert-butylbenzoyl-5-pyrazolone ($\Phi MBBP$), have been synthesized and tested in synergistic combination with TOPO. The results show that ΦMDP is significantly more soluble in n-hexane and thus allows higher extractant concentrations to be prepared. The reagent dependence is 3.2 power to ΦMDP and 5 power for $\Phi MBBP$ with 2:1 pyrazolone:TOPO solutions in DEB for americium extraction from glycolic acid or nitric acid (95).

Future Actinide Extractants

In considering the possibilities for new and better actinide extractants, one must ask the question, "In what way is the extractant to be made better?" The answer will vary, of course, depending on the particular need or application. For example, hydrometallurgists may want a reagent that is more selective for uranium over iron in sulfate systems. Nuclear fuel reprocessing may require high radiation stability. Nuclear waste management would need a reagent which would extract actinides from highly acid nitrate systems, possibly having the ability to reject trivalent lanthanides. How are these various requirements to be met?

Selectivity appears to be best in those systems which take advantage of differences in coordinative requirements of the metal ion (e.g., in the extraction by alkylammonium salts). The coordinative neutral species extractants are the next most selective. Least selective are the cation exchange extractants; however, those that offer coordinative possibilities are more selective than those that do not. Bidentate extractants offer enhanced extraction strength because of their ability to form chelate-type rings. No class of extractants is known to have clearly superior radiation stability, although aromatic molecules are generally thought to be less susceptible to radiation damage. Reagents that are both cation exchangers and strong acids, such as the sulfonic acids, should be superior extractants from highly acid solutions. Unfortunately, no member of this sulfonic acid class that is sufficiently organophilic has been made available.

Added to the primary effect of the functional group are the effects of the size, placement, and branching of the organic portion of the molecule. Sufficient organic "weight" must be added to the functional group(s) so that the extractant molecule, and whatever salts and adducts it forms in the extraction process, are soluble in a reasonably simple high-flash-point organic diluent. Also, the reagent as well as its salts and adducts must have a very low distribution to the aqueous phases to be used. A rough approximation is that a molecular weight of about 300 is required, but the effect of a given organic loading is highly dependent on its form. Straight-chain aliphatics tend to make most compounds too insoluble in the organic phase before their distribution to the aqueous phase becomes low enough; thus aromatic, and especially branched aliphatic, radicals are much better groups to add to an extractant molecule. The addition of branched radicals, however, limits the ability of the functional group to approach the metal ion and the number of extractant molecules that can be grouped around the ion. For this reason, it is often desirable that the branching be somewhat removed from the functional group. The selectivity of extractants may be altered by the type of organic groups substituted on the functional group, with the more sterically hindered (highly branched) extractants tending to favor larger ions or ions having strong coordinative bonding.

The question then arises, "Is it possible to tailor new, more powerful, and more selective extractants for the actinide element?" The answer must certainly be yes. A wealth of information now exists as a basis for future research and development in new extraction systems, and the possibilities have hardly been touched. It does appear, however, that a more organized approach to the problem will be required than has been typical in the past. The systematic changes to be made in the structure of extractant molecules, using past experience as a basis, will require the cooperation of synthetic organic chemists and solvent extraction chemists. Such efforts should be pursued more intensively in the future.

Which functional groups appear to be most promising in the preparation of new and better extractants? Both sulfonic acids and sulfoxides offer promising, unexplored possibilities because of the very strongly acidic nature of the former and the coordinating ability of the latter. Fluorinated β -diketones appear promising as versatile chelating extractants if the aqueous solubility can be reduced to a sufficiently low volume for process applications and acid strength can be increased to the point where they are useful from acidic solutions. Synergistic combinations offer continuing fields for interesting exploration, even with available reagents. One of the more interesting possibilities may be the combination of organic-phase cation exchangers with the size-specific crown ethers to produce size-specific or selective synergistic mixtures.

Many years ago, someone in the AEC organization commented that, "Surely this solvent extraction problem has been solved by now." The possibilities of solvent extraction appear to be a very long way from exhaustion even now.

Acknowledgment

Research sponsored by the Division of Chemical Sciences, U.S. Department of Energy under contract W-7405-eng-26 with the Union Carbide Corporation.

5. Literature Cited

1. Bucholz, C. F. J. Chem. von. A. F. Gehlen 1805, 4(17), 134.
2. Peligot, E. Ann. Chim. Phys. 3rd Series 1842, 5, 5-47.
3. Seaborg, G. T. Berkeley, CA, May 1978, USERDA Report PUB-112.
4. Coleman, C. F.; Leuze, R. E. J. Tenn. Acad. Sci. 1978, 53(3), 102-107. References [1], [2], [3] contained therein.
5. Warf, J. C. J. Am. Chem. Soc. 1949, 71, 3257-3258.
6. Private communication, W. D. Arnold, Oak Ridge National Laboratory, Oak Ridge, TN, January 1979.
7. Arnold, W. D. In: Oak Ridge, TN, November 1975, USERDA Report ORNL-5111, p. 56.
8. Stewart, D. C. Livermore, CA, January 1950, Report UCRL-585.
9. Blake, C. A.; Brown, K. B.; Coleman, C. F. Oak Ridge, TN, May 1955, AEC Report ORNL-1903.

10. Blake, C. A.; Crouse, D. J.; Coleman, C. F.; Brown, K. B.; Kelmers, A. D. Oak Ridge, TN, December 1956, AEC Report ORNL-2172.
11. Brown, K. B.; Coleman, C. F.; Crouse, D. J.; Denis, J. O.; Moore, J. G. Oak Ridge, TN, May 1954, AEC Report ORNL-1734.
12. Crouse, D. J.; Brown, K. B.; Arnold, W. D. Oak Ridge, TN, December 1956, AEC Report ORNL-2173.
13. Baybarz, R. D.; Weaver, B. S.; Kinser, H. B. Nucl. Sci. Eng. 1963, 17, 457-462.
14. Leuze, R. E.; Baybarz, R. D.; Weaver, B. Nucl. Sci. Eng. 1963, 17, 252-258.
15. Weaver, B.; Kappelmann, F. A. Oak Ridge, TN, 1964, AEC Report ORNL-3559.
16. Weaver, B.; Kappelmann, F. A. J. Inorg. Nucl. Chem. 1968, 30, 263-272.
17. McIsaac, L. D.; Baker, J. D.; Tkachyk, J. W. Idaho Falls, ID, August 1975, ERDA Report ICP-1080.
18. Schulz, W. W. Hanford, WA, 1973, ERDA Report ARH-2901.
19. Schulz, W. W. Hanford, WA, 1974, ERDA Report ARH SA-203.
20. Siddall, III, T. H. J. Inorg. Nucl. Chem. 1963, 25, 883-892.
21. Siddall, III, T. H. J. Inorg. Nucl. Chem. 1964, 26, 1991-2003.
22. Sekine, T.; Hasegawa, Y. "Solvent Extraction Chemistry"; Marcel Dekker, Inc.; New York and Basel, 1977.
23. Healy, T. V.; McKay, H. A. C. Rec. Trav. Chem. des Pay-bas 1956, 75, 730-736.
24. Higgins, C. E.; Baldwin, W. H.; Ruth, J. M. Oak Ridge, TN, July 1952, AEC Report ORNL-1338.
25. Best, G. F.; Hesford, E.; McKay, H. A. C. J. Inorg. Nucl. Chem. 1959, 12, 136.
26. Zemlyanukhin, V. I.; Savoskina, G. P. Radiokhimiya 1961, 3(4), 411-416. English Translation: Sov. Radiochem. 3, 182-188.
27. Mrochek, J. R.; Banks, C. F. J. Inorg. Chem. 1965, 27, 589-601.
28. White, J. C.; Ross, W. J. Oak Ridge, TN, February 1961, NAS-NRC Report NAS-NS 3102.
29. Karlova, Z. K.; Rodionova, L. M.; Pyzhova, Z. I.; Myasoedov, B. F. Radiokhimiya 1977, 19(1), 38-41. English Translation: Sov. Radiochem. 19, 31-33.
30. Karolova, Z. K.; Rodionova, L. M.; Pyzhova, Z. I.; Myasoedov, B. F. Radiokhimiya 1977, 19(1), 42-45. English Translation: Sov. Radiochem. 19, 34-36.
31. Harmon, H. D.; Peterson, J. R.; McDowell, W. J.; Coleman, C. F. J. Inorg. Nucl. Chem. 1976, 38, 155-159.
32. Shoun, R. R.; McDowell, W. J.; Weaver, B. "Proceedings of ISEC '77," Toronto, Sept. 1977, in press.
33. Aly, H. F.; Latimer, R. M. J. Inorg. Nucl. Chem. 1970, 32, 3081-3089.
34. Horwitz, E. P.; Bloomquist, C. A. A.; Sauro, L. J.; Henderson, D. J. J. Inorg. Nucl. Chem. 1966, 28, 2131-2324.

35. Mrochek, J. E.; O'Laughlin, J. W.; Sakurai, H.; Banks, C. V. J. Inorg. Nucl. Chem. 1963, 25, 955-962.
36. Mrochek, J. E.; O'Laughlin, J. W.; Banks, C. V. J. Inorg. Nucl. Chem. 1965, 27, 603-623.
37. Mrochek, J. E.; Richard, J. J.; Banks, C. V. J. Inorg. Nucl. Chem. 1965, 27, 625-629.
38. Parker, J. R.; Banks, C. V. J. Inorg. Nucl. Chem. 1965, 27, 583-587.
39. Parker, J. R.; Banks, C. V. J. Inorg. Nucl. Chem. 1965, 27, 631-640.
40. Berkman, Z. A.; Bertina, L. E.; Kabachnik, M. I.; Kossykh, V. G.; Medved, T. Ya.; Nesterova, N. P.; Rozen, A. M.; Yudina, K. S. Radiokhimiya 1975, 17(2), 210-214. English Translation: Sov. Radiochem. 17, 213-216.
41. Jankowska, M.; Kulawik, J.; Mekulski, J. J. Radioanal. Chem. 1976, 31, 9-29.
42. Coleman, C. F. At. Energy Rev. 1964, 2(2), 3-54.
43. Wilson, A. S. Progress in Nuclear Energy Series, III, Process Chemistry 1961, 3, 211.
44. Moore, F. L. Anal. Chem. 1966, 38, 510.
45. Derevyanko, E. P.; Chudinov, E. G. Radiokhimiya 1977, 19(2), 205-214. English Translation: Sov. Radiochem. 19, 172-179.
46. Juznic, S.; Senegacnik, M. J. Radioanal. Chem. 1976, 30, 419-424.
47. Swarup, R.; Patil, S. K. J. Inorg. Nucl. Chem. 1976, 38, 1203-1206.
48. Myasoedov, B. F.; Shkimev, V. M.; Kochetkova, N. E.; Chmutova, M. K.; Spivakov, B. Ya. Radiokhimiya 1975, 17(2), 234-237. English Translation: Sov. Radiochem. 17, 237-240.
49. Nikolaev, V. M.; Lebedev, V. M.; Kovantsev, V. N. Radiokhimiya 1977, 19(5), 692-697. English Translation: Sov. Radiochem. 19, 575-580.
50. Chudinov, E. G.; Pirozkhov, S. V.; Stepanchikov, V. I. Radiokhimiya 1971, 13(2), 208-215. English Translation: Sov. Radiochem. 13, 208-214.
51. Derevyanko, E. P.; Pirozkhov, S. V.; Shudinov, E. G. Radiokhimiya 1975, 17(2), 291-296. English Translation: Sov. Radiochem. 17, 295-299.
52. Swarup, R.; Patil, S. K. Radiochem. Radioanal. Lett. 1977, 29(2), 73-82.
53. Mohanty, S. R.; Reddy, A. S. J. Inorg. Nucl. Chem. 1975, 37, 1977-1982.
54. Korpak, W. Nukleonika 1964, 9, 1.
55. Fedoezzhina, R. P.; Buchikhin, E. P.; Zarubin, A. I.; Kaneviskii, E. A. Radiokhimiya 1974, 16(5), 638-641. English Translation: Sov. Radiochem. 16, 626-629.
56. Reddy, A. S.; Ramakrishna, V. V.; Patil, S. K. Radiochem. Radioanal. Lett., 1977, 28(5-6), 445-452.
57. Reddy, A. S.; Reddy, L. K. Sep. Sci. 1977, 12(6), 641-644.
58. Peppard, D. F.; Mason, G. W.; Driscoll, W. J.; Sironen, R. J. J. Inorg. Nucl. Chem. 1958, 7, 276-285.

59. Marcus, Y.; Kertes, A. S. "Ion Exchange and Solvent Extraction of Metal Complexes"; Wiley-Interscience: London, New York, Sydney, Toronto, 1969.
60. Mason, G. W.; Metta, D. N.; Peppard, D. F. J. Inorg. Nucl. Chem. 1976, 38, 2077-2079.
61. Tachimori, S.; Sato, A.; Nakamura, H. J. Nucl. Sci. Technol. 1978, 15(6), 421-425.
62. McDowell, W. J.; Keller, O. L.; Dittner, P. E.; Tarrant, J. R.; Case, G. N. J. Inorg. Nucl. Chem. 1976, 38, 1207-1210.
63. Kasimov, F. D.; Nikolaev, V. M.; Kasimov, V. A.; Skobelev, N. G. Radiokhimiya 1977 19(4), 442-446. English Translation: Sov. Radiochem. 19, 363-366.
64. Choppin, G. R.; Nash, K. L. Rev. Chim. Miner. 1977, 14(2), 230-236.
65. Barketov, E. S.; Vorob'eva, V. V.; Zaitsev, A. A.; Petukhova, I. V.; Spiriyakov, V. I.; Filimonov, V. T. Radiokhimiya 1977, 19(4), 467-471. English Translation: Sov. Radiochem. 19, 382-385.
66. Elesin, A. A.; Karaseva, V. A.; Ivanovich, N. A.; Zaitsev, A. A. Radiokhimiya 1974, 16(6), 772-777. English Translation: Sov. Radiochem. 16, 758-761.
67. Nagle, R. A.; Murthy, T. K. S. Sep. Sci. Technol. 1978, 13(7), 597-612.
68. Baes, Jr., C. F.; Zingaro, R. A.; Coleman, C. F. J. Phys. Chem. 1958, 62, 134.
69. Horwitz, E. P. In: Oak Ridge, TN, October 1977, ERDA Report ORNL/TM-6056, Ed. Tedder, D. W.; Blomeke, J. O.
70. Peppard, D. F.; Mason, G. W.; Griffin, G. J. Inorg. Nucl. Chem. 1965, 27, 1683-1691.
71. Mason, G. W.; Bollmeier, A. F.; Peppard, D. F. J. Inorg. Nucl. Chem. 1967, 29, 1103-1112.
72. Weaver, Boyd; Shoun, R. R. J. Inorg. Nucl. Chem. 1971, 33, 1909-1917.
73. Weaver, Boyd; Shoun, R. R. Ind. Eng. Chem. Proc. Des. Dev. 1971, 10(4), 582.
74. Barketov, E. S.; Zaitsev, A. A.; Filimonov, V. T. Radiokhimiya 1975, 17(3), 338-393. English Translation: Sov. Radiochem. 17, 383-387.
75. Baisden, P. A.; Choppin, G. R.; Kinard, W. F. J. Inorg. Nucl. Chem. 1972, 34(6), 2029-2032.
76. Khopkar, P. K.; Narayankutty, P. J. Inorg. Nucl. Chem. 1968, 30, 1957-1962.
77. Patil, S. K.; Ramakrishna, V. V. J. Inorg. Nucl. Chem. 1976, 38, 1075-1078.
78. Myasoedov, B. F.; Guseva, L. I.; Lebedev, I. A.; Milyukov, M. S.; Chmutova, M. K. "Analytical Chemistry of Transplutonium Elements," John Wiley and Sons, New York and Israel Program for Scientific Translations, Jerusalem, 1974. A translation from Russian of "Analiticheskaya Khimiya Transplutoniyevykh Elementov", Izdatel'stvo "Nauka", Moskova, 1972.

79. Ludqvist, R. Acta Chem. Scand. 1975, 29(2), 231-235.
80. Bagawde, S. V.; Ramakrishna, V. V.; Patil, S. K. J. Inorg. Nucl. Chem. 1976, 38, 1669-1672.
81. Bagawde, S. V.; Ramakrishna, V. V.; Patil, S. K. J. Inorg. Nucl. Chem. 1976, 38, 2085-2089.
82. Blake, C. A.; Horner, D. E.; Schmitt, J. M. Oak Ridge, TN, February 1959, USAEC Report ORNL-2259.
83. Hurst, F. J.; Crouse, D. J.; Brown, K. B. Ind. Eng. Chem. Proc. Des. Dev. 1972, 11(1), 122.
84. Hurst, F. J.; Crouse, D. J. Ind. Eng. Chem. Proc. Des. Dev. 1974, 13(3), 286.
85. Bunus, F. T.; Talanta 1977, 24, 117-120.
86. Bunus, F. T.; Domocos, V. C.; Dumitrescu, P. J. Inorg. Nucl. Chem. 1978, 40, 117-121.
87. Khopkar, P. K.; Mathur, J. N. J. Inorg. Nucl. Chem. 1977, 39, 2063-2067.
88. Fardy, J. J.; Buchanan, J. M. J. Inorg. Nucl. Chem. 1976, 38, 149-154.
89. Cunningham, J. G.; Scargill, D.; Willis, H. H. 1950, British Report AERE, C/M215.
90. Blake, C. A.; Coleman, C. F.; Brown, K. B.; Baes, C. F.; White, J. C. Proc. 2nd U.N. Intern. Conf. Peaceful Uses At. Energy, Geneva 1959, 28, 289.
91. Konstantinova, M. Anal. Chim. Acta 1977, 90, 195-197.
92. Chmutova, M. K.; Pribylova, G. A.; Myasoedov, B. F. Radio-khimiya 1975, 17(2), 220-226. English Translation: Sov. Radiochem. 17, 224-229.
93. Chmutova, M. K.; Pribylova, G. A.; Myasoedov, B. F. Radio-khimiya 1977, 19(2), 215-221. English Translation: Sov. Radiochem. 19, 180-185.
94. Rao, G. N.; Arora, H. C. J. Inorg. Nucl. Chem. 1977, 39, 2057-2060.
95. Weaver, B.; Shoun, R. R. Oak Ridge National Laboratory unpublished data, January 1979.

RECEIVED June 20, 1979.

Research sponsored by the Division of Chemical Sciences, U.S. Department of Energy under contract W-7406-eng-26 with the Union Carbide Corporation.

Demonstration of the Potential for Designing Extractants with Preselected Extraction Properties: Possible Application to Reactor Fuel Reprocessing

G. W. MASON and H. E. GRIFFIN

Chemistry Division, Argonne National Laboratory, 9700 South Cass Avenue, Argonne, IL 60439

From the knowledge of the extractant characteristics of both neutral and mono-acidic phosphorus-based organic compounds now available, it is possible to tailor-make extractants for a specifically desired separation of two metals. The present study is concerned with neutral mono-nuclear, phosphorus-based extractants for use in affecting the mutual separation of U(VI) and Th(IV).

Liquid-liquid extraction (LLE) systems using neutral phosphorus-based organic compounds have been the subject of extensive study since Warf (1) first reported the use of tributyl phosphate, TBP, as a useful extractant for cerium(IV), uranyl and thorium nitrates. After more than twenty years, liquid-liquid extraction systems (such as the Purex and Thorex processes) employing TBP dissolved in a suitable diluent versus an aqueous HNO₃ phase remain the most widely accepted systems for reactor fuel reprocessing.

The use of extractants of the same general type as tributyl phosphate, i.e., neutral extractants containing the P=O coordinating group, but designed with specially selected extraction properties should have many advantages in the development of LLE systems which may be applicable to reactor fuel reprocessing.

The importance of the acidic and steric properties of mono-acidic phosphorus-based extractants in the extraction of metals has been well established. The work of Mason, Peppard, et al. (2, 3) has shown that combined acidic and steric effects which result from altering the structure of the acidic extractants may be varied to give a wide range of extraction constants (K_S) for specific metals. $K_S = K[H^+]^a/F^b$, where K_S is a constant characteristic of the system, K is the distribution ratio, H is the hydrogen ion concentration in the equilibrated aqueous phase, F is the concentration of extractant in the equilibrated organic phase, a and b are the respective hydrogen ion and extractant dependencies. Recent studies, to be published, involving the

0-8412-0527-2/80/47-117-089\$05.00/0

© 1980 American Chemical Society

extraction of actinides (III), (IV) and (VI) and lanthanides (III) in which the steric properties of the extractants are varied, while keeping their acidities essentially constant, show that steric hindrance within the extractant molecule is the most important property effecting separation factors of metals in different oxidation states. The possibility of predicting the basicity of the P=O of neutral phosphorus-based compounds from the pK_A values of related monoacidic acids has been demonstrated by previous studies in this laboratory (4,5,6).

The above information plus the published work of researchers such as that of Siddall, Burger and Rosen (7,8,9,10) should allow one to state with confidence that liquid-liquid extraction systems may be designed for specific process applications. By varying the type and mode of bonding (*i.e.*, COP or CP bonds) of organic groups in neutral phosphorus-based organic compounds, it is possible to exploit the changes in steric and inductive effects which result in the desired modification of extraction behavior. The purpose of this study is to demonstrate the potential for such an approach.

Experimental

The symbols used to represent the phosphorus-based organic compounds are in accordance with previous usage (11,12) in which H represents a theoretically ionizable hydrogen; T and D the prefixes tri- and di-; G a generalized organic group and P the phosphorus atom. Thus, TGP, DG[GP] and G[DGP] represent the neutral phosphate, $(GO)_3PO$, phosphonate, $(GO)_2(G)PO$, and phosphinate esters, $(GO)(G)_2PO$, respectively; HDGP, HG[GP] and H[DGP] are the corresponding monoacidic acids. The enclosure of G, organic groups, in brackets indicates that the groups are attached to the phosphorus by CP bonds in contrast to COP bonds of G groups not enclosed by brackets. G groups represented by multiple characters are enclosed in parentheses.

Individual compounds used in this study are symbolized as TBP {tributyl phosphate, $(C_4H_9O)_3PO$ }, DB[BP] {dibutyl butyl phosphonate, $(C_4H_9O)_2(C_4H_9)PO$ }, B[DBP] {butyl dibutyl phosphinate, $(C_4H_9O)(C_4H_9)_2PO$ }, DA[AP] {diamyl amyl phosphonate, $(C_5H_{11}O)_2 \cdot (C_5H_{11})PO$ }, DB[(CH)P] {dibutyl cyclohexyl phosphonate, $(C_4H_9O)_2 \cdot (C_6H_{11})PO$ }, DB[(ClM)P] {dibutyl chloromethyl phosphonate, $(C_4H_9O)_2(ClCH_2)PO$ }, T(4-MPe-2)P {tri(4-methylpentyl-2) phosphate, $[(CH_3)_2CHCH_2CH(CH_3)O]_3PO$ }, D(4-MPe-2)[BP] {di(4-methylpentyl-2) butyl phosphonate, $[(CH_3)_2CHCH_2CH(CH_3)O]_2(C_4H_9)PO$ }, D(4-MPe-2) \cdot [iBP] {di(4-methylpentyl-2) isobutyl phosphonate, $[(CH_3)_2CHCH_2CH(CH_3)O]_2[(CH_3)_2CHCH_2]PO$ }, D(4-MPe-2)[PP] {di(4-methylpentyl-2) propyl phosphonate, $[(CH_3)_2CHCH_2CH(CH_3)O]_2(C_3H_7)PO$ }, and D(EB)[(EB)P] {di(2-ethylbutyl) 2-ethylbutyl phosphonate, $[(C_2H_5)_2 \cdot CHCH_2O]_2[(C_2H_5)_2CHCH_2]PO$ }.
 The concentration unit formality, F , is defined as the number of formula weights of solute contained in 1 liter of solution.

The distribution ratio of a given nuclide is defined as the concentration of that nuclide in the organic phase divided by the concentration of nuclide in the aqueous phase of two mutually-equilibrated sensibly-immiscible liquid phases, the concentration of nuclide being on an atom basis as reflected in counting rates, alpha, beta or gamma.

The pK_A values (used in this paper) of phosphorus-based acids in 75% ethanol were determined in a comprehensive study, to be reported elsewhere, of the relationship of pK_A to structure and composition in $(X_1)(X_2)PO(OH)$ and $(X)PO(OH)_2$ compounds using a method described previously (5).

Source, Preparation and Purification of Materials. The TBP, DB[BP] and DB[(ClM)P] were obtained from Commercial Solvents Corporation and Stouffer Chemical Company, respectively. The DA[AP] and DB[(CH)P] were obtained from Hooker Chemical Corporation. The T(4-MPe-2)P, D(EB)[(EB)P], D(4-MPe-2)[BP], D(4-MPe-2)[(iB)P], D(4-MPe-2)[PP] and B[DBP] were prepared in this laboratory. The reagent grade (99% minimum purity) dodecane used as a carrier diluent was obtained from Aldrich Chemical Company.

The commercially obtained extractants were purified by a modification of a method previously described (13) for the purification of TBP. The undiluted extractant was stirred with an equal volume 6 M HCl at room temperature for 1 hour and scrubbed with two equal volume portions of water. The aqueous phases were discarded, and the organic phase was stirred for 1 hour with 1 M NaOH at room temperature. The aqueous phase was discarded, and the organic (extractant) phase was diluted to 30 percent by volume with *n*-heptane. The *n*-heptane solution was scrubbed with 6 one-half volume portions of distilled water. The water phases were discarded, and the *n*-heptane was removed from the organic phase by evaporation in an open beaker at room temperature. The purified product was freed from traces of *n*-heptane, H₂O and alcohols (formed in the purification step) by pumping for eight hours at 10⁻² mm pressure and at room temperature.

The neutral phosphonate esters, D(EB)[(EB)P], D(4-MPe-2)[BP], D(4-MPe-2)[(iB)P] and D(4-MPe-2)[PP] were prepared by the Michaelis-Arbuzov Reaction in which alkyl halides were reacted with previously prepared trialkyl phosphites. The neutral phosphate, T(4-MPe-2)P, was prepared by a conventional esterification method in which 4-methyl-2-pentanol was reacted with POCl₃ in the presence of pyridine. The temperature during the reaction was kept below 15°C to prevent disproportionation of the alkyl group. The neutral phosphinate ester, B[DBP], was prepared by esterification of dibutyl phosphorus oxychloride, (C₄H₉)₂POCl, in the presence of pyridine.

The same general method as described for the purification of the commercially obtained extractants was used to purify the neutral phosphorus-based extractants prepared in this laboratory.

Alpha-active 1.6×10^5 -yr ^{233}U ($^{238}\text{U}:^{233}\text{U}$ mass ratio less than 0.03) and alpha-active 7.8×10^4 -yr ^{230}Th ($^{232}\text{Th}:^{230}\text{Th}$ mass ratio equals 10) were obtained from Argonne National Laboratory stocks. By methods described previously, the uranium (11) and thorium (14) tracers were purified from daughter activities just prior to use.

Determination of Distribution Ratios. The distribution ratio, K , was determined radiometrically as described previously (11) with the following exceptions. The aqueous and organic phases were mixed 4 minutes in culture tubes with teflon lined screw caps using a Thermodyne vortex mixer equipped with a specially designed tube holder. The organic phases were pre-equilibrated before use by contacting each organic phase with two equal volume portions of barren aqueous phase (i.e., an aqueous phase containing all constituents except the radioactive tracer). Aliquots of the aqueous and organic phases were measured into a glass scintillation vial containing 10 ml of Beckman Ready-Solv GP scintillation cocktail and counted in a Beckman LS 100C scintillation counter. All distribution ratios were determined at $22 \pm 2^\circ\text{C}$.

Results and Conclusions

The wide range of separation factors, $K_{\text{U}}/K_{\text{Th}}$, for the extraction of U(VI) and Th(IV) from 2.00 M HNO_3 into eleven selected neutral phosphorus-based extractants shown in Table I, demonstrates the potential for designing extractant systems for specific metal separations. The separation factors range from 0.71 for B[DBP] to 162 for D(4-MPe-2)[iBP]: a $K_{\text{U}}/K_{\text{Th}}$ ratio of 228.

The data of Figure 1 show that, in the absence of steric effects, the extraction of both U(VI) and Th(IV) increases as the basicity of the coordinating P=O of the neutral extractant increases. The increase in the extraction of Th (3×10^3) which is an order of magnitude greater than the increase for U (3×10^2) leads to an inversion of their extraction for B[DBP], the most basic of the extractants studied. (From the data of previous studies (4,5), the basicity of the P=O is assumed to increase as the pK_A of the corresponding monoacidic acid increases. The corresponding monoacidic acid is a compound which contains an OH group in place of one of the ester groups. For example, HDBP is the corresponding acid for TBP.) Of the homologous series of neutral phosphate, phosphonate and phosphinate extractants, respectively, TBP, DB[BP] and B[DBP], the extractant that gives the best separation factor for U(VI) and Th(IV) is TBP. The TBP molecule also has the least basic P=O of the series. It is apparent that changing only the basicity of the extractant has little useful advantage in the separation of U(VI) and Th(IV).

The distribution ratios of the extraction of U(VI) and Th(IV) into a highly hindered phosphate extractant, T(4-MPe-2)P,

Table I. Extraction of Uranium and Thorium into Several Neutral Phosphorus-Based Organic Extractants from 2.00 M HNO_3 . Extractant Solutions are 1.00 F in Dodecane

Extractants	Distribution, K		Separation Factor, K_U/K_{Th}
	Uranium	Thorium	
TBP	17.5	1.74	10.1
T(4-MPe-2)P	3.26	0.15	21.7
DB[BP]	249	61	4.1
DA[AP]	295	70.5	4.2
DB[(CH)P]	245	23.8	10.3
DB[(ClM)P]	3.71	0.54	6.9
D(4-MPe-2)[BP]	362	3.12	116
D(4-MPe-2)[(iB)P]	56.8	0.35	162
D(EB)[(EB)P]	245	18.1	13.5
D(4-MPe-2)[PP]	374	2.89	129
B[DBP]	1175	1656	0.71

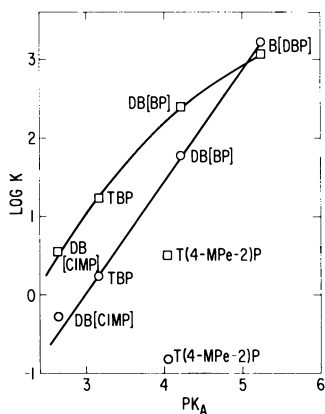


Figure 1. Distribution ratio, K, of the extraction of U (VI) (\square) and Th (IV) (\circ) from 2.00M HNO_3 into 1.00F solutions of several phosphorus-based extractants in dodecane diluent vs. the pK_A of their corresponding HDGP, HG[GP], or H[DGP] acids (Example: HDBP corresponds to TBP).

are low, 3.26 and 0.15 respectively, regardless of the relatively high basicity of the $P=O$. Therefore, the data for this extractant do not fit the curves of the plot of $\log K$ versus pK_A of Figure 1. The large effect of steric hindrance on the extraction of U(VI) and Th(IV) and on their separation factors is shown by these data and the data for the highly hindered phosphonate extractants, D(4-MPe-2)[BP], D(4-MPe-2)[PP], and D(4-MPe-2)[iBP] given in Table I.

It should be noted that the linear curve for Th(IV) compared to the markedly concave curve for U(VI) (see the plot of $\log K$ versus pK_A of Figure 1) indicate a difference in the mechanism of extraction for these two metals.

The extractant dependencies of the extraction of U(VI) and Th(IV) as shown in Figure 2 and Figure 3, are second power and third power, respectively, for DA[AP] and D(4-MPe-2)[BP] extractant phases versus low HNO_3 aqueous, *i.e.*, 0.125 M HNO_3 and 0.50 M HNO_3 for the two systems, respectively. For the non-ideal solution range at concentrations of extractant greater than 0.50 F, the curves depart from integral slopes. The dependencies depart markedly from integral slopes when 2.00 M HNO_3 is used as the aqueous phase, the departure being greatest at high extractant concentrations. Since the portion of extractant tied up by HNO_3 remains constant at a specific HNO_3 concentration, the difference in dependency for the extraction from the aqueous 2.00 M HNO_3 phase is probably due to the change in the nature of the complexing environment caused by the high HNO_3 concentration in the organic phase.

The advantage from the improved separation factors at low extractant concentrations, shown in Figures 2 and 3, is greatest in processing systems in which the extraction of high concentrations of metal is not required.

The HNO_3 dependencies of the extraction of U(VI) and Th(IV), shown in Figure 4, should be considered of operational significance only since several parameters vary simultaneously as the equilibrium aqueous HNO_3 concentration is varied. For example, NO_3^- activity and nitrate complexing of metals in the aqueous and the free extractant concentration in the organic phase may vary as the aqueous HNO_3 concentration is varied.

The difference in the HNO_3 dependency for the extraction of U(VI) and Th(IV) into D(4-MPe-2)[BP], curves A and D of Figure 4 and into DA[AP], curves B and C of Figure 4, results in a substantial difference in separation factor for these metals at low and high HNO_3 concentrations. The separation factors for their extraction range from 65 to 400 for D(4-MPe-2)[BP] and 4.5 to 32 for DA[AP]. The improvement in separation factors at low HNO_3 concentrations is a real advantage for processes in which hydrolysis of the metals at low acid concentration is not a problem.

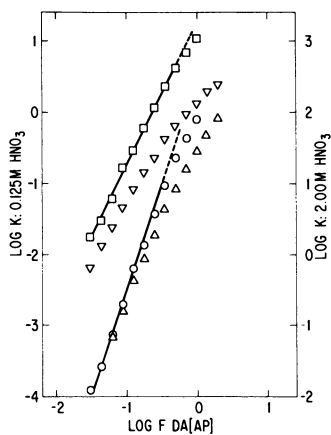


Figure 2. Extractant dependency of the extraction of U (VI) and Th (IV) into a dodecane solution of DA[AP] from: [(□) U, (△) Th] 0.125M HNO_3 ; [(▽) U, (○) Th] 2.00M HNO_3 .

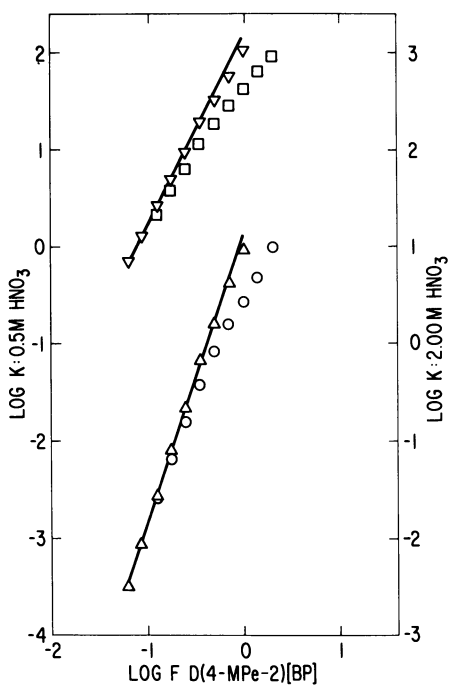


Figure 3. Extractant dependency of the extraction of U (VI) and Th (IV) into a dodecane solution of D(4-MPe-2) [BP] from: [(▽) U, (△) Th] 0.50M HNO_3 ; [(□) U, (○) Th] 2.00M HNO_3 .

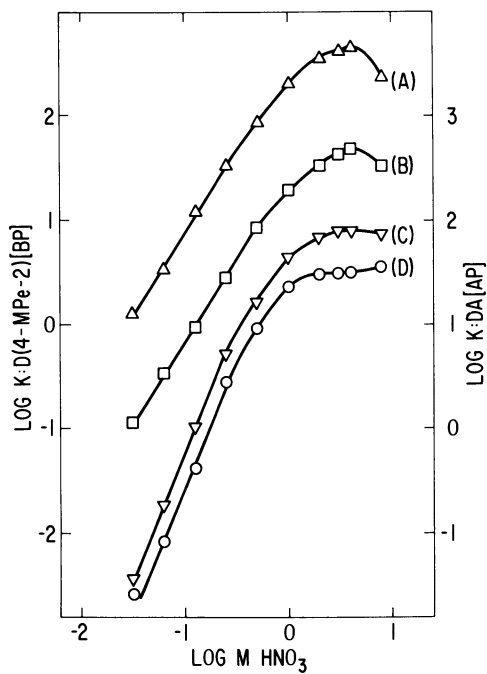


Figure 4. HNO_3 dependency of the extraction of U (VI) and Th (IV) into a dodecane solution of: [(B) U, (C) Th] 1.00F DA[AP]; [(A) U, (D) Th] 1.00F D(4-MPe-2) [BP].

Although the separation factors for the extraction of U(VI) and Th(IV) into DA[AP] and D(4-MPe-2)[BP] differ greatly (a factor of 28) due to the difference in steric properties of the extractants, the parameters of extractant dependencies, Figures 2 and 3, and HNO₃ dependencies, Figure 4, show a parallel relationship for the two extractants. The apparent independence of these parameters from the steric properties of the extractant greatly simplifies the selection of an extractant and the specific concentrations of extractant and HNO₃ required for a desired separation.

Discussion

Some of the advantages of using neutral phosphorus-based organic extractants of the same general type as tributyl phosphate, TBP, designed with specially selected extraction properties in the development of LLE systems for use in reactor fuel reprocessing are:

(1) The distribution ratios for the extraction of the elements to be recovered (uranium and thorium, for example) may be optimized such that both elements can be efficiently extracted then selectively stripped into HNO₃. Optimizing the distribution ratios eliminates the necessity of adding complexing agents to the aqueous phase for selective stripping of the metals.

(2) Since the extractants are of the same general type as TBP, systems based on their use would involve essentially the same well established technology as required for the use of TBP.

(3) The high metal to extractant ratio for these extractants allows high metal loading of the extractant phase, thus reducing the required inventory of extractant.

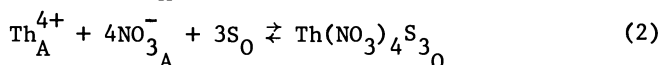
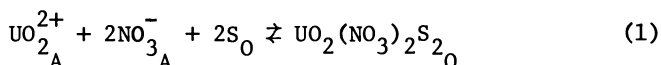
(4) The methods of production of neutral phosphorus-based compounds is well known.

The widely different extraction of U(VI) and Th(IV), actinides (III) and lanthanides (III) as a function of the acidity and steric hindrance of monoacidic phosphorus-based extractants, shown in previous studies (2,3), led to the study of the effect of varying the structure of neutral phosphorus-based compounds on their behavior as extractants. The inverse relationship in the order of substituent base-increasing power and acid-increasing power of the same substituents in phosphorus-based organic compounds, established by previous studies (4,5,6), indicate the potential for predicting the basicity of the P=O in neutral phosphorus-based compounds from existing pK_A values for corresponding monoacidic compounds. Although the availability of basicity data for neutral phosphorus-based compounds is limited, the large volume of published pK_A data for phosphorus-based organic acids should make prediction of the basicity of a large number of such compounds possible.

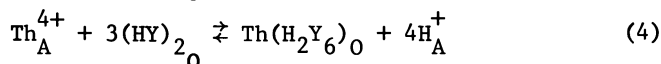
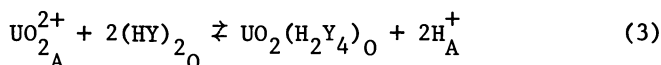
There is no apparent correlation between the extraction of U(VI) and the pK_A or steric properties of monoacidic phosphorus-based acids, but the range of its K_S values is relatively small compared to the corresponding ranges for Th(IV), actinides (III) and lanthanides (III). The range of K_S values representing both acidity and steric effect is 2.7×10^5 ($< 2 \times 10^2$ for most extractants) for the extraction of U(VI) compared to 3.3×10^{14} for Th(IV) and $> 1.7 \times 10^{10}$ for Am(III) for the extractants reported (2,3).

In the extraction studies, to be reported elsewhere, involving the use of monoacidic phosphonate extractants of the (GO)(ClCH₂)PO(OH) type (where G represents phenyl groups with various substituents) with essentially constant acidities but with varying amounts of steric hindrance within the extractant molecule, the range of K_S values was 2.6×10^7 for Th(IV) and 22 for U(VI). Thus, steric hindrance within the extractant molecule was established as a very important factor in LLE separations.

As might be expected from the relative stoichiometries involved,



compared to



(where S and HY represent one mole of neutral extractant and one monomeric unit of acidic extractant, respectively, and A and O represent the aqueous and organic phases, respectively), the effect of steric hindrance on separation factors is much larger for U(VI) and Th(IV) for acidic extractants than for neutral extractants. A logical extension of this research would be a study in which the acidity and steric effects for neutral phosphorus-based extractants are correlated with these effects for their corresponding monoacidic acids.

Literature Cited

1. Warf, James C. J. Am. Chem. Soc., 1949, 71, 3257.
2. Mason, G. W.; Lewey, S. McCarty; Gilles, D. M.; and Peppard, D. F. J. Inorg. Nucl. Chem., 1978, 40, 683.
3. Mason, G. W.; Bilogram, I.; and Peppard, D. F. J. Inorg. Nucl. Chem., 1978, 40, 1807.

4. Cook, A. Gilbert and Mason, G. W. J. Inorg. Nucl. Chem., 1973, 35, 2093.
5. Peppard, D. F.; Mason, G. W.; and Andrejadish, C. M.; J. Inorg. Nucl. Chem., 1965, 27, 697.
6. Cook, A. Gilbert and Mason, G. W. J. Org. Chem., 1972, 37, 3342.
7. Siddall III, T. H. Ind. Eng. Chem., 1959, 51, 41.
8. Burger, L. L. J. Phys. Chem., 1958, 62, 590.
9. Siddall III, T. H. J. Am. Chem. Soc., 1959, 81, 4176.
10. Rosen, A. M.; Nikolotova, Z. I.; and Kartasheva, N. A. Proceedings International Solvent Extraction Conference (September, 1977).
11. Peppard, D. F.; Mason, G. W.; and Lewey, S. J. Inorg. Nucl. Chem., 1965, 27, 2065.
12. Peppard, D. F.; Mason, G. W.; Bollmeier, A. F.; and Lewey, S. J. Inorg. Nucl. Chem., 1971, 33, 845.
13. Peppard, D. F.; Mason, G. W.; and Maier, J. L. J. Inorg. Nucl. Chem., 1956, 3, 215.
14. Peppard, D. F.; Mason, G. W.; and McCarty, S. J. Inorg. Nucl. Chem., 1959, 13, 138.

RECEIVED June 29, 1979.

Work performed under the auspices of the Office of Basic Energy Sciences of the Department of Energy under contract number W-31-109-eng-38.

Solvent Extraction of Transplutonium Elements from Acid Solutions by Polydentate Neutral Organophosphorus Compounds and from Alkaline Solutions by Quarternary Ammonium Bases and by Alkylpyrocatechols

B. F. MYASOEDOV, M. K. CHMUTOVA, and Z. K. KARALOVA

V. I. Vernadsky Institute of Geochemistry and Analytical Chemistry,
USSR Academy of Sciences, Moscow, USSR

Various classes of reagents for quantitative extraction of TPE are widely used. However, these extractants either extract TPE only from weakly acid media (chelate-forming reagents, amines, organophosphoric acids), or require a great amount of salting out agents (neutral monofunctional organophosphorus compounds).

The purpose of the present work consists in the investigation of polydentate neutral organophosphorus compounds as extractants for isolation and concentration of TPE from acid solutions and quaternary ammonium bases and alkylpyrocatechols for isolation and separation of TPE and rare earth elements from alkaline solutions.

Extraction of transplutonium elements from acid solution

It is well-known that certain bidentate neutral organophosphorus compounds are far better extractants than their monodentate analogues (1,2).

Bidentate organophosphorus compounds have recently attracted still more interest as it was found that some of them can be used for removing long-lived TPE from waste nuclear fuel element solutions in order to eliminate the potential danger brought about by TPE accumulation (3). The methods developed have shown that these reagents are fairly promising. It has been still necessary, however, to search for reagents with even higher extraction capacity and low solubility in water whose production and refinement would be as simple as possible.

We have studied a number of neutral bi-, tri- and tetradentate organophosphorus compounds as ex-

0-8412-0527-2/80/47-117-101\$05.00/0

© 1980 American Chemical Society

tractants of TPE, Eu and U, in two aspects: (i) the dependence of extraction capacity and (ii) the dependence of selectivity on the reagent structure.

Bidentate neutral organophosphorus compounds were synthesized in the laboratory of organophosphorus compounds, USSR Academy of Sciences as described in (4-11), the tri- and tetradentate compounds as described in (11). The reagents were dissolved in chloroform or dichloroethane.

The reagents used for the extraction from 1-15 M HNO_3 may be divided into two groups: (1) Bidentate reagents with a linear bridge between the functional P=O groups (12,13) and the reagents in which the methylene group hydrogen is substituted for some other atom or group. (2) Bi-, tri- and tetradentate reagents in which the residues of *o*-, *m*- and *p*-xylene, mesitylene and durrole (11) serve as bridges connecting the P=O functional groups.

As an example, let us take the simplest dioxide of the first group, i.e. tetraphenylmethylenediphosphine dioxide $(\text{Ph})_2\text{P}(\text{O})\text{CH}_2\text{P}(\text{O})(\text{Ph})_2$ (I) and trace the effect of modifications in its structure on the extracting capacity with respect to TPE and Eu.

As the bridge elongates to two methylene units $(\text{Ph})_2\text{P}(\text{O})(\text{CH}_2)_2\text{P}(\text{O})(\text{Ph})_2$ (II), the distribution coefficients decrease by approximately a factor of 10^3 (Figure 1).

Substitution of the ethylene bridge by vinylene bridge arrests the P=O group in *cis*-position and brings about a thousandfold increase in the distribution coefficients, $(\text{Ph})_2\text{P}(\text{O})\text{CH}=\text{CHP}(\text{O})(\text{Ph})_2$ (III) (figure 2).

As it has been shown for uranium(VI) (14), if the P=O groups are bound together by a vinylene bridge arresting them in *trans*-position (IV) or by an acetylene bridge $(\text{Ph})_2\text{P}(\text{O})\text{C}\equiv\text{CP}(\text{O})(\text{Ph})_2$ (V) (Figure 2), the reagents stop behaving as bidentates and the distribution coefficients sharply decrease.

CH_3 -groups introduced into *p*-positions of benzene rings attached to the phosphorus atoms in (III) make the reagents more basic and more nucleophilic; $(\text{ToI})_2\text{P}(\text{O})\text{CH}=\text{CHP}(\text{O})(\text{ToI})_2$ (VI) is a somewhat better extractant of TPE and Eu in comparison with reagent (III).

We should note that these facts refer primarily to extraction from solutions where the HNO_3 concentration is less than 5M. For instance, the distribution coefficients of all the elements (D_{TPE}) by

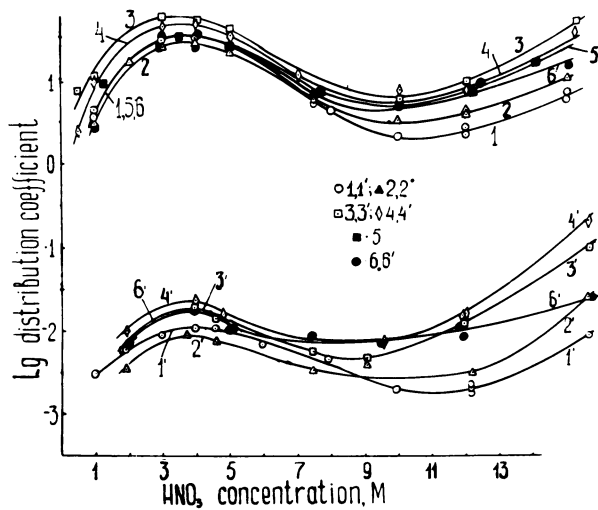


Figure 1. Extraction of trivalent Am (1,1'), Cm (2,2'), Bk (3,3'), Cf (4,4'), Es (5), and Eu (6,6') by 0.025M chloroform solutions of reagents I (1-6) and II (1'-6') as a function of HNO_3 concentration.

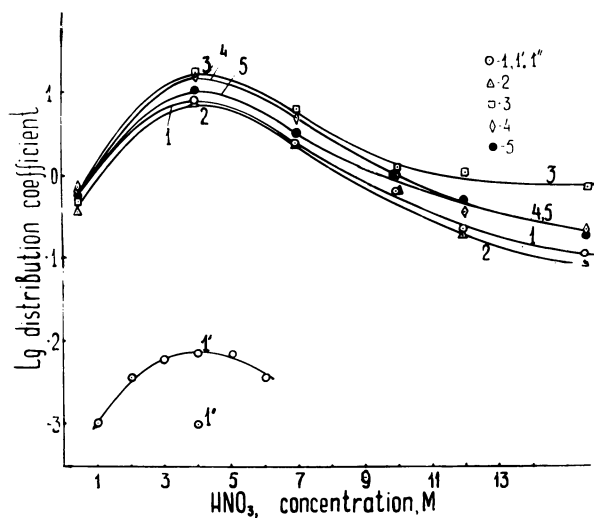
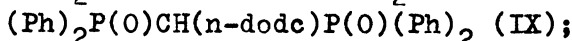
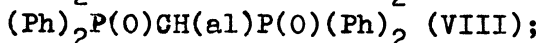
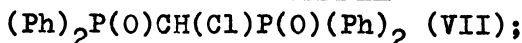


Figure 2. Extraction of trivalent Am (1,1', 1''), Cm (2), Bk (3), Cf (4), and Eu (5) by 0.025M chloroform solutions of reagents III (1-5), IV (1'), and V (1'') as a function of HNO_3 concentration.

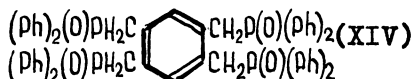
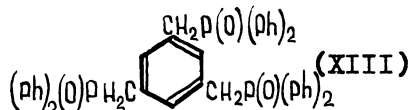
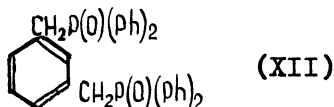
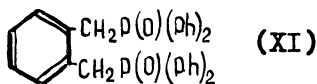
extraction from 14-15 M HNO_3 with the help of reagent (II) do not differ as greatly from those observed with the reagents (III) and (VI) as in moderately acidic media.

Substitution of hydrogen in the dioxide (I) methylene bridge for other atoms or groups Cl, allyl (al), n-dodecyl (n-dodc) and vinylidene:



$(\text{Ph})_2\text{P}(\text{O})\text{C}(\text{=CH}_2)\text{P}(\text{O})(\text{Ph})_2$ (X) has been found to decrease the extraction capacity in all the instances. Substituents of the methylene bridge hydrogen take no part in formation of compounds being extracted but, according to the induction properties, affect their stability.

Also studied was the extraction capacity of another group of reagents (11), i.e.



The dioxide containing a p-xylene fragment as a bridge proved insoluble in chloroform and dichloroethane.

The extraction capacity in this group was primarily dependent on relative positions of functional groups in the bridge. For instance, the dioxide (XI) ability to extract Am(III) proved about 3×10^3 times weaker than that of dioxide XII. The presence of three P=O groups, even if their mutual arrangement is favourable, like in (XIII) where they occupy metapositions with respect to each other, or of four groups (two couples in meta-position, reagent XIV) does not lead to any substantial increase in distribution coefficients of TPE and Eu, (Figure 3). This is probably due to sterical factors, changing basicity of the functional groups, etc.

It is easy to see that the best extractant of TPE is tetraphenylmethylenephosphine dioxide (I). Dioxide I appears to have extraction ability superior to that of all the currently known bidentate neutral

organophosphorus compounds. Hence we have investigated it in more detail (15).

Experiments on TPE extraction by dioxide from nitric acid solutions containing nitrates have shown that this reagent can be used for quantitative group extraction and concentrating of TPE from solutions containing 1-15 M HNO₃ and arbitrary amounts of Li, Al, Na or NH₄ nitrates. Table 1 gives some examples of Am concentrating up to the hundredfold.

Table 1

Americium extraction from nitric acid solutions by 0.1 M chloroform solution of reagent I

org.	Extraction, %			
aq.	1M HNO ₃	3M HNO ₃	1M HNO ₃ - 1M Al(NO ₃) ₃	1M HNO ₃ - 1.8M Al(NO ₃) ₃
1:10	-	-	-	99.9
1:20	94.9	-	98.6	93.0
1:50	92.0	98.5	97.0	-
1:100	-	98.0	93.0	89.0

The reagent is poorly soluble in nitric acid solutions; it is resistant to the acid and radiolysis. The reagent solutions in chloroform retain their high ability of TPE extraction from 1-15 M HNO₃ after receiving a portion of γ -radiation as high as 75 Wt/h per 25 ml. The reagent solutions may be repeatedly used for quantitative TPE extraction. The back-extraction of TPE is performed by an ammonium carbonate solution or by water after the organic phase has been just once washed by an Al(NO₃)₂OH solution.

Another problem we were interested in was the selectivity of the reagents studied.

It is known that the reagent selectivity is significantly influenced by fragments preventing individual groups from free rotation and more or less arresting functional groups positions and therefore

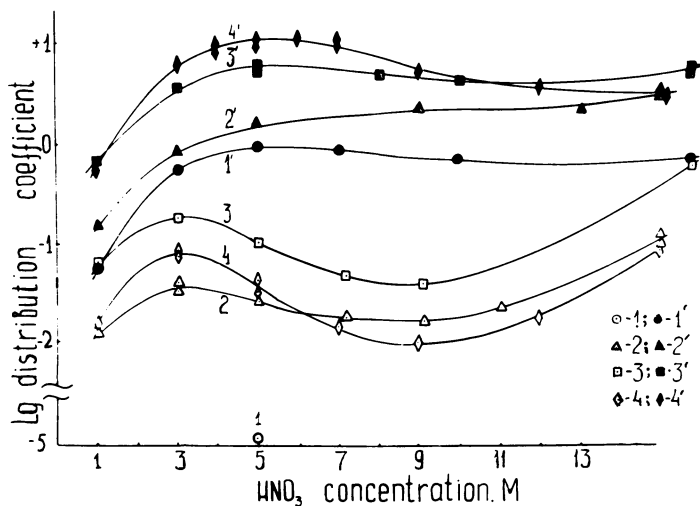


Figure 3. Extraction of trivalent Am (1-4) and hexavalent U (2'-4') by 0.025M chloroform solutions of reagents XI (1,1'), XII (2,2'), XIII (3,3'), and XIV (4,4') as a function of concentration.

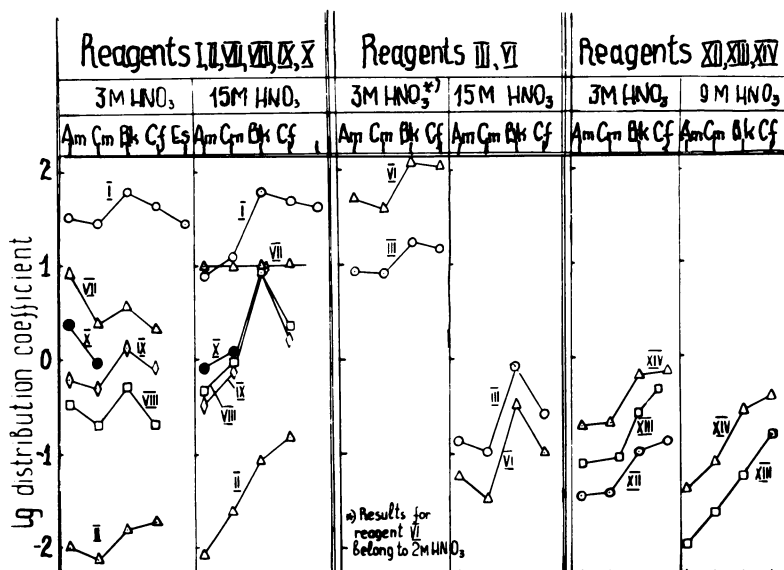


Figure 4. Distribution coefficients of trivalent TPE in the neutral organophosphorus compound-chloroform-nitric acid systems. The Roman numerals correspond to numbers of reagents in the text.

controlling the size of the chelate rings (11, 12, 13).

Here are some results on reagents containing rigid bridge fragments. In a series of compounds with the same functional groups and the same substituents to the phosphorus atoms the selectivity of dioxides containing flexible saturated bridges (reagents I and II) differed from that of dioxides with non-saturated (vinylene) bridges, which restrict the freedom of P=O groups mutual orientation (reagents III and IV). The latter reagents are relatively more selective with respect to berkelium; in the extraction from concentrated HNO₃ the factor of Bk/Cm separation reaches 10 (Figure 4).

A similar effect can be provided by introducing substituents into the methylene bridge of dioxide I; thus in all the cases the factors of TPE separation both from each other and from Eu are growing in diluted (3M) as well as in concentrated HNO₃. The only exclusion is extraction by chloro-derivative VII from 15 M HNO₃ when the distribution coefficients of all the TPE are the same. Incidentally, this reagent displays appreciable selectivity with respect to Am extraction from 1-5 M HNO₃; the factor of Cm/Am separation is about 5 and that of Am/Eu separation is about 7.5. The selectivity of reagents containing *o*- and *m*-xylene, durrole and mesithylene bridges was found to depend only on mutual arrangement of P=O groups in the bridge regardless of their number (11). Figure 3 illustrates that dioxide XI, in which the functional groups are in *o*-positions with respect to each other is highly selective to U(VI), the U/Am separation factor reaching about 8×10^4 .

The polydentate reagents XII, XIII and XIV provide relatively high Am/Eu and practically the same separation factors (about 12 for all the three reagents, Figure 4). It appears that TPE and Eu complex formation with these compounds occurs essentially on account of P=O groups in mutual *m*-positions which is evidently responsible for the high factors of TPE separation from each other and of Eu separation from Am.

Uranium extraction by dioxide XI is very selective; the extraction by tetraoxide XIV is more selective than that by reagents XII and XIII. This can be explained in terms of complex formation involving not only the P=O groups of substituents in *m*-positions but also the groups of substituents in mutual *o*-positions.

Extraction of transplutonium elements from alkaline solutions

Extraction from basic media being complicated by formation of low soluble precipitates. On the other hand, many elements can exist in alkaline solutions in the form of stable soluble complexes, which under appropriate conditions may be transferred into the organic phase. As we have shown (16, 17, 18, 19) it is possible to extract actinides and lanthanides from very alkaline media by using aliquat 336 and 4(α , α -dioctylethyl)pyrocatechol (DOP). α -Oxycarbonic acids and some of aminopolycarboxylic acids were employed to keep the ions of hydrolyzing elements in alkaline solutions. It was found that the mechanism of extraction strongly depends on the nature of the extractant. Aliquat transfers ions into the organic phase in the form of an ionic associate consisting of the metal compound with the complex-forming agent as the anion, and the extractant as the cation. DOP extracts actinides and lanthanides from the alkaline solutions in the form of chelates, the same as in case of rare elements (20).

Extraction by aliquat 336. We have found (16, 17) that aliquat 336 can extract actinides and lanthanides from very alkaline media as complexes with α -oxycarbonic acids and with aminopolycarboxylic acids.

The extent of extraction depends on the alkali concentration and on concentration of the complex-forming ligand. Figure 5 shows results on Am and Eu extraction in the presence of dioxydiaminebutanetetraacetic acid (DOBTA) and tartaric acid vs. alkali concentration. The extraction is the most complete at $C_{\text{NaOH}} \leq 1 \text{ M}$ from the DOBTA solution and at $C_{\text{NaOH}} \leq 0.5 \text{ M}$ from the tartaric acid solution.

In the latter case the decrease in extraction with increasing alkali concentration is more pronounced. It appears that complexes with aminopolycarboxylic acids are more stable than those with α -oxycarbonic acids probably on account of greater mobility of oxy-group hydrogen of complex-forming ligand. Eu seems to form more hydrolyzable complexes than Am, since the latter displays higher distribution coefficients.

Studies on the degree of complex-forming agents concentration on the extent of europium microamount extraction have shown that the extraction occurs even from very diluted solutions of complex-forming

agents, and is almost insensitive to variations of DOBTA concentration in the region from 10^{-5} to 10^{-2} M, and to those of tartaric acid in the range from 10^{-2} to $\approx 5 \times 10^{-2}$ M.

Extraction of elements from alkaline solutions is significantly affected by the nature of the complex-forming agent, by the number and mutual arrangement of hydroxylic groups in its structure. Above 0.3 M alkali concentration europium is better extracted with monocarbonic acids than with dicarbonic ones. Dicarbonic oxyacids promote extraction the better the more OH^- groups they contain. For instance, distribution coefficients of europium in the 0.5 M NaOH-trioxyglutaric acid are twice as high as in the 0.5 M NaOH-tartaric acid system. The results indicate that aromatic aminopolycarboxylic acids provide for europium extraction over a wider range of the alkali concentrations than the aliphatic ones.

In alkaline solutions trivalent actinides and lanthanides form rather stable complexes with tartaric acid and DOBTA. The complexes undergo no appreciable decay during long keeping of the solutions; for instance, Eu and Am complexes with DOBTA in 0.5-1 M NaOH are stable for more than a month.

The degree of the metal extractions depends on its concentration. For example, with increasing europium concentration the distribution coefficients in the alkali-DOBTA system decrease, while in the alkali-tartaric acid system a maximum at 7×10^{-4} M Eu concentration is observed. As we suggested the enhancement in the metal distribution coefficient is evidently due to the metal polymerization in the organic phase, and the decrease is caused by polymerization in the aqueous phase, which eventually results in low extractable polymer form. The latter assumption is supported by the fact that as the alkali concentration increases the maximum on extraction curves undergoes a shift towards lower concentration of the metal.

The preliminary data on the composition of the compounds being extracted are given. Experiments on ion transfer have shown that the metal being extracted is a part of the anionic complex fragment. As suggested by the logarithmic dependence of distribution coefficients on the extractant concentration, at high alkali concentration the metal/extractant ratio in the compound being extracted is 1:1. The compound being transferred into the or-

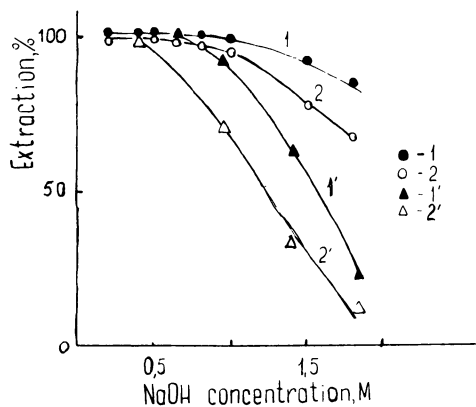


Figure 5. Extraction of Am(III) (1,1') and Eu(III) (2,2') in the presence of 2×10^{-3} M DOBTA (1,2) and 2.5×10^{-2} M tartaric acid (1',2') by 0.2M aliquat 336; OH xylene solution as a function of NaOH concentration.

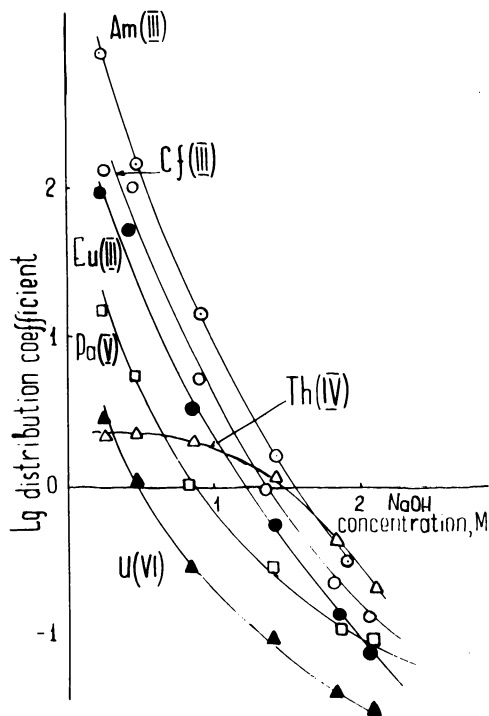


Figure 6. Extraction of actinides and lanthanides from alkaline solutions by 0.2M aliquat 336; OH in the presence of 2.5×10^{-2} M tartaric acid.

genic phase is probably an ionic associate consisting of a metal-complex-forming agent compound as the anion and the extractant as the cation.

Extraction of anionic complexes of elements from alkaline solutions by aliquat may be used for solving some practical problems. Thus in the alkali-DOBTA and alkali-tartaric acid systems it provides for group extraction of trivalent actinides and lanthanides and for separation of elements in different oxidation states. A study on extraction of Ac(III), Am(III), Cf(III), Th(IV), Pu(IV), Np(V), Pa(V) and U(VI) has shown that at NaOH concentration less than 0.5 M most actinides are transferred into the organic phase, the distribution coefficients being high enough (Figure 6) for these systems to be used in concentrating actinides from alkaline solutions. The higher the alkali concentration, the better is the separation coefficient. In the presence of α -oxycarboxylic acids and aminopolycarboxylic acids in 1 M NaOH the elements are extracted in the following order: Ac(III), Am(III), Cf(III) > Th(IV), Pu(IV) > Np(V), Pa(V) > U(VI).

Extraction by alkylpyrocatechol. We have found 4(α , α -dioctylethyl)pyrocatechol (DOP) to be one of the few reagents capable of Am and Eu extraction from very alkaline solutions even in the absence of complex-forming agents. For instance, 30 minutes shaking with 0.04 M DOP toluene solution led to 96-97% extraction from freshly prepared solutions in the NaOH range from 0.5 to 5 M. The extraction decreases with aging because of radiocolloids sorption on the glassware surface; the sorbed particles can not be removed even by long contact with the extractant.

To decrease hydrolysis and to increase selectivity we have employed complex-forming agents such as DTPA and tartaric acid (19). The results show that Am extraction in the NaOH-tartaric acid solution is approximately the same as that of Eu. At low concentrations of the alkali the distribution coefficients are small; as the concentration increases, the extraction of Am and Eu sharply increases to reach a maximum at 2 M NaOH (> 99%) and to stay constant up to 10 M. The $R = f/\text{NaOH}$ dependence by Am and Eu extraction in the form of tartrates by aliquat-336 was different, namely the extraction was high at low alkali concentrations and poor at NaOH concentration greater than 2 M. It may be assumed that DOP forms strong chelates with trivalent actinides and lantha-

nides. Therefore under conditions of profound hydrolysis the substitution of aquo- and hydroxy-groups for tartrate ions results in formation of involved composition ions in the aqueous phase. It is relatively easy to extract these complex ions by a chelate reagent like DOP is, but steric difficulties make the extraction by quaternary ammonium bases hard.

In solution with low alkali concentration, Eu extraction is appreciably dependent on the nature of the diluent. The distribution coefficients decrease with increasing dielectric constant in the order cyclohexane > toluene > chloroform > octyl alcohol. Extraction of Eu from 5 M NaOH is 99% whatever the diluent (except for octyl alcohol). This means that extraction from very alkaline media is favour of coordinatively-saturated compounds.

As DOP concentration in the organic phase increases from 0.01 to 0.05 M, extraction of Am and Eu increases, the best results being obtained with the use of 0.04 M DOP in toluene solutions. Further enhancement in the extractant concentration is not reasonable due to intermolecular hydrogen bonds between DOP molecules. It follows from the slope of the $\log D = f \log /DOP/$ curves, that in the extraction from 1 M NaOH the metal/reagent ratio in the compound being extracted is 1:2. The elements appear to be extracted from 1 M NaOH in the form of hydrated compounds.

Figure 7 shows that Eu distribution coefficients over the range from 0.5 to 4 M NaOH are essentially higher than those of Am. In 2 M NaOH the difference is twenty fold. The extent of Am separation from Eu may be still increased by varying the duration of mixing and the concentration of the reagent. Extraction of the elements is very sensitive to duration of mixing. The Eu-DTPA complex is less stable than Am-DTPA, so its transfer to the organic phase occurs much more rapidly. For instance, after 10 minutes mixing with 10^{-4} M DTPA 96% Eu and just 48% Am is transferred into the organic phase. Since the limiting step of extraction is the decay of DTPA complexes resulting in chelates of the elements with the extractant, at higher concentrations of DTPA the time for the equilibrium to be reached is usually longer.

The extractant concentration also plays a role in the extent of separation. Figure 8 indicates that in the presence of 1×10^{-4} M DTPA 0.01 M DOP toluene solutions extract from 2 M NaOH 60% Eu and

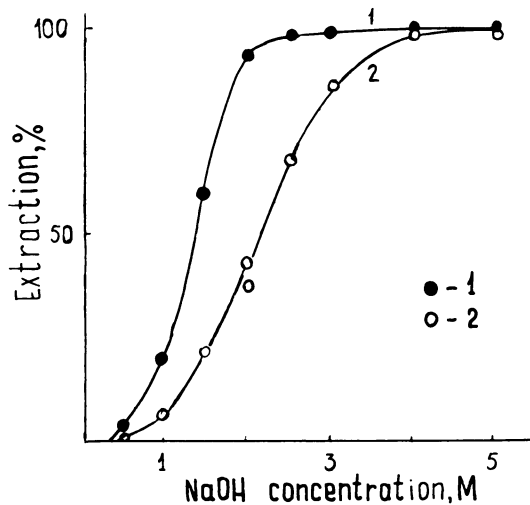


Figure 7. The effect of NaOH concentration on extraction of Eu (III) (1) and Am(III) (2) from 10^{-4} M DTPA by 0.04M DOP toluene solution; extraction time, 10 minutes.

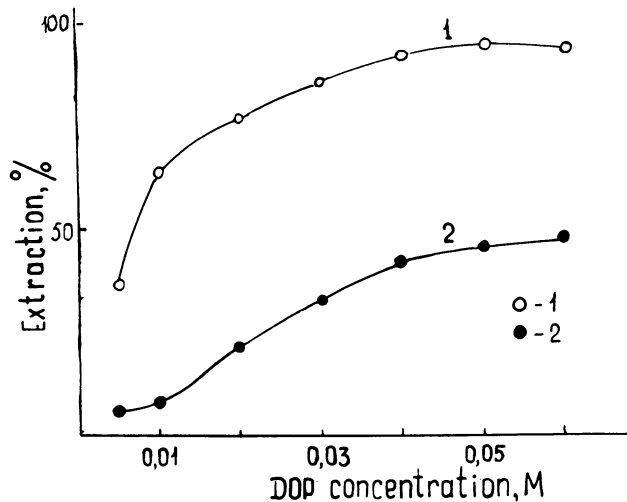


Figure 8. The effect of DOP concentration on extraction of Eu (III) (1) and Am (III) (2) from the solution containing 10^{-4} M DTPA and 2M NaOH; extraction time, 10 minutes.

only 5% Am. Optimum separation of Eu and Am is observed at 2 M NaOH concentration, 10^{-4} M DTPA and 10^{-2} M DOP, the mixing time being 10 minutes. Under these conditions the Eu/Am separation factor is about 30, and triple extraction transfers 97% europium into the organic phase. 90% Am stay in the aqueous phase, where the content of Eu is no higher than 3%. Americium can then be quantitatively extracted by 0.04 M DOP toluene solution, the phases being mixed for 45 minutes.

Conclusions

Thus polydentate organophosphorus compounds appear to be efficient extractants of trivalent TPE from acidic solutions. The full-scale use of these compounds in, for instance, TPE extraction from nuclear acidic waste solutions seems very likely in the future.

Since the structure of the reagents may be widely varied, one may hope that it will be possible to develop highly selective extractants capable of TPE separation from each other as well as from rare earth elements. Some of the reagents described here may be used for extraction chromatography separation of certain TPE whose separation factors are high enough.

Our studies have shown that in the presence of complex-forming agents actinides and lanthanides can be extracted from alkaline solution by using of aliquat 336 and 4(α, α -dioctylethyl)pyrocatechol. The latter reagent is more efficient, as it provides for quantitative extraction of trivalent actinides from very alkaline media and for appreciably better separation of actinides from rare earth elements.

Literature Cited

1. Siddal, T.H. J. Inorg. Nucl. Chem., 1963, 25, 883.
2. Mrochek, J.E.; O'Laughlin, J.W.; Banks, C.V. J. Inorg. Nucl. Chem., 1965, 27, 603.
3. Schulz, W.W.; McIsaac, L.D.; Muller, W.; Lindner, R., Ed. "Transplutonium 1965"; North Holland Publishing Co.: Amsterdam, 1965; p. 433.
4. Kabachnik, M.I.; Medved', T.Ya. Izv. AN SSSR, OKhN, 1962, 11, 2103.
5. Kabachnik, M.I.; Medved', T.Ya.; Polikarpov, Yu.M.; Yudina, K.S. Izv. AN SSSR, OKhN, 1961, 11, 2029.

6. Mitchiner, J.P.; Aquiar, A.M. Organic Preparation and Procedures, 1969, 1, p. 259.
7. Hartmann, H.; Beermann, G.; Czempic, H. Zs. anorg. u. allgem. Chem., 1956, 287, 261.
8. Nesterova, N.P.; Medved', T.Ya.; Polikarpov, Yu. M.; Kabachnik, M.I. Izv. AN SSSR, ser. khim., 1974, 10, 2295.
9. Polikarpov, Yu.M.; Kulumbetova, K.Zh.; Medved', T.Ya.; Kabachnik, M.I. Izv. AN SSSR, ser. khim., 1970, 6, 1326.
10. Kulumbetova, K.Zh.; Medved', T.Ya.; Kabachnik, M.I. Izv. AN SSSR, ser. khim., 1971, 12, 2747.
11. Bodrin, G.V.; Kabachnik, M.I.; Kochetkova, N.E.; Medved', T.Ya.; Myasoedov, B.F.; Polikarpov, Yu. M.; Chmutova, M.K. Izv. AN SSSR, ser. khim., in press (July, 1978).
12. Kabachnik, M.I.; Koiro, O.E.; Medved', T.Ya.; Myasoedov, B.F.; Nesterova, N.P.; Chmutova, M.K. DAN SSSR, 1975, 222, 1346.
13. Chmutova, M.K.; Nesterova, N.P.; Koiro, O.E.; Myasoedov, B.F. Zhurn. analitich. khimii, 1975, 30, 1110.
14. Berkman, Z.A.; Bertina, L.E.; Kabachnik, M.I.; Kossykh, V.G.; Medved', T.Ya.; Nesterova, N.P.; Rozen, A.M.; Yudina, K.S. Radiokhimiya, 1975, 17, 210.
15. Chmutova, M.K.; Kochetkova, N.E.; Myasoedov, B.F. Radiokhimiya, 1978, 20, 713.
16. Palshin, E.S.; Nekrasova, V.V.; Ivanova, L.A.; Karalova, Z.K.; Myasoedov, B.F. Zhurn. analitich. khimii, 1978, 33, 878.
17. Karalova, Z.K.; Nekrasova, V.V.; Rodionova, L.M.; Pyzhova, Z.I.; Myasoedov, B.F. Radiokhimiya, 1978, 20, 845.
18. Karalova, Z.K.; Nekrasova, V.V.; Rodionova, L.M.; Pyzhova, Z.I.; Myasoedov, B.F. Abstracts of the V All-Union Conference on Extraction Chemistry, Novosibirsk, 1978, p. 147.
19. Myasoedov, B.F.; Karalova, Z.K.; Kuznetsova, V. S.; Rodionova, L.M. Radiokhimiya, in press (October, 1978).
20. Kuznetsova, V.S.; Tarnopolski, Yu.I.; Borbat, V. F. Izv. Vysshikh Uchebnykh Zavedeniy, Tsvet. Metallurgiya, 1976, 3, 66.

RECEIVED May 8, 1979.

The Extraction of Uranium (VI) from Sulphuric Acid Solutions by Tri-*n*-Octylphosphine Oxide

TAICHI SATO

Department of Applied Chemistry, Faculty of Engineering, Shizuoka University, Hamamatsu, Japan

We have used tri-*n*-octylphosphine oxide (TOPO) as a solvent extractant of uranium(VI) and thorium(IV) from nitric and hydrochloric acid solutions (1-3). In contrast, the extraction of uranium(VI) and thorium(IV) from nitric and hydrochloric acid solutions has been investigated by tri-*n*-butylphosphate (TBP) (4, 5). However, since TBP reveals a poor efficiency for the extraction of metals from sulphuric acid solutions, this paper extends the work to the extraction of uranium(VI) from sulphuric acid solutions by TOPO.

Experimental

Reagent

TOPO (Hokko Chemical Industry Co. Ltd., Tokyo) was used without further purification and dissolved in kerosene, or benzene. The kerosene was purified by washing with concentrated sulphuric acid (4). The aqueous solutions of uranyl sulphate were prepared by dissolving uranyl sulphate hydrate ($\text{UO}_2\text{SO}_4 \cdot 3\text{H}_2\text{O}$, Yokozawa Chemical Co. Ltd.) in sulphuric acid solutions of the required concentrations. All chemicals were of analytical reagent grade.

Extraction and analytical procedures

Equal volumes (20 ml) of the TOPO solution in the organic solvent and uranyl sulphate solution containing sulphuric acid were shaken for 10 min in 50 ml stoppered conical flasks in a thermostatic water-bath at the required temperature. Preliminary experiments showed that equilibration is complete in 10 min. The mixture was centrifuged and separated, and uranium was stripped from the organic phase with 0.5 M ammonium carbonate solution, and then the distribution coefficient (the ratio of the equilibrium concentration of uranium in the organic phase to that in the aqueous phase, $[\text{U}]_{\text{org}}/[\text{U}]_{\text{aq}}$) was obtained.

Uranium(VI) was determined by titration with EDTA using xylene orange (XO) as indicator (6). The acidity of the organic phase was determined by adding 2 % sodium oxalate solution to the aqueous solution back-washed and titrating with 0.01 M sodium hydroxide

0-8412-0527-2/80/47-117-117\$05.00/0

© 1980 American Chemical Society

solution by using the pH meter. The water content of the organic solution was determined by the Karl Fischer method. The sulphate concentration of the organic phase was determined as follows: the sulphate in the aqueous solution back-extracted from the organic phase was completely precipitated as barium sulphate with barium chloride solution.

Spectrophotometry, infrared and NMR spectral measurements

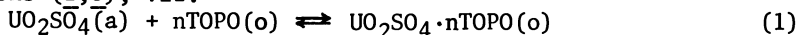
Absorption spectra were obtained on a Shimadzu Model QV-50 spectrophotometer, using 1.00 cm fused silica cells. Infrared spectra were determined on a Japan Spectroscopic Co. Ltd. Model IR-S, equipped with potassium chloride prisms ($4000-550\text{ cm}^{-1}$) using a matched cell with potassium bromide window (a spacer of 0.1 mm) or a capillary film between thallium halide. Nuclear magnetic resonance (NMR) spectra were obtained for samples dissolved in carbon tetrachloride using a Hitachi Perkin-Elmer Model R-20 High Resolution NMR spectrometer utilizing a permanent magnet of 14092 gauss, in the use of tetramethylsilane as an internal reference.

Results and discussion

Extraction isotherm

The extraction of aqueous solutions containing 5 g/l of uranyl sulphate in sulphuric acid at different concentrations was carried out with TOPO in kerosene or benzene at 20 °C. Some representative results are given in Figure 1. The distribution coefficient at first rises with aqueous acidity, passes through a maximum at about 3-4 M acid and then falls at higher acidities. It is also found that the initial aqueous acidity corresponding to the maximum distribution coefficient is not much influenced by varying the TOPO concentration. When benzene is used as a diluent instead of kerosene, the shape of the distribution coefficient curve with the solution in benzene resembles that in kerosene, although the extraction efficiency is in kerosene > benzene, as illustrated in Figure 1.

If we assume that the extraction of uranium(VI) from sulphuric acid solutions with TOPO is governed by solvating reaction as in the case of the extraction from nitric and hydrochloric acid solutions (2,3), viz.



where (a) and (o) represent aqueous and organic phases, respectively, the following relationship would be expected

$$\log E_a^0 = \log K + n \log (C_{\text{TOPO}} - nC_U), \quad (2)$$

in which E_a^0 is the distribution coefficient, K the equilibrium constant, C_{TOPO} the total TOPO concentration and C_U the uranium concentration of the organic phase.

For the extraction of uranyl sulphate solutions (5 g/l) containing sulphuric acid at various concentrations of TOPO in kerosene at 20 °C, the log-log plots of E_a^0 vs. $(C_{\text{TOPO}} - nC_U)$ at constant sulphuric acid concentrations showed that the Eqn. (2) is

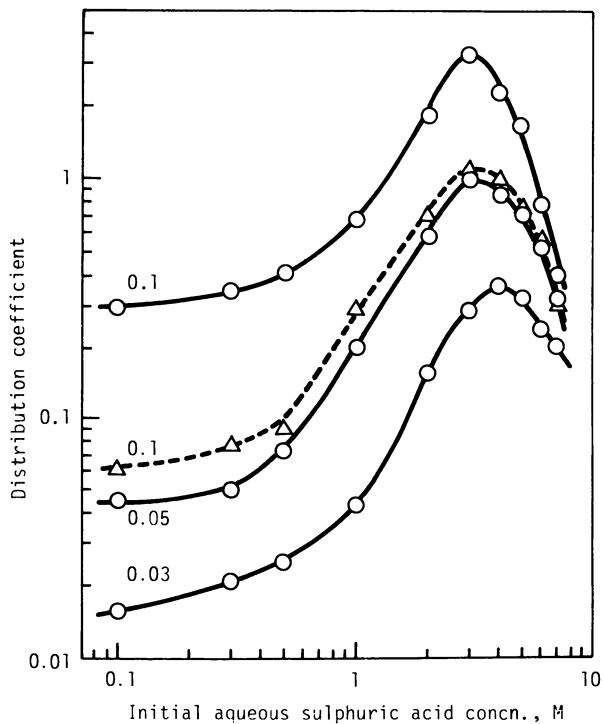
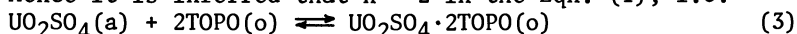


Figure 1. Extraction of U (VI) from sulfuric acid solutions by TOPO in (○) kerosene and (△) benzene; numerals on the curves are TOPO concentrations, M.

satisfied for $n = 2$: the slopes of 2.0, 2.0, 2.3 and 2.3 at 0.5, 1, 2 and 3 M acids respectively. It is thus thought that the value of the distribution coefficient for uranium shows a second-power dependence, indicating the formation of the disolvate $\text{UO}_2\text{SO}_4 \cdot 2\text{TOPO}$. Hence it is inferred that $n = 2$ in the Eqn. (1), i.e.



In the extraction of uranyl sulphate solutions of various concentrations containing 3 M sulphuric acid with 0.03 M TOPO in kerosene at 20 °C, the concentration of uranium in the organic phase as a function of initial aqueous uranium concentration approaches a limiting value (0.015 M) as shown in Table 1, supporting the solvation number of TOPO for uranium obtained from the solvent dependency, although the organic phase is not yet saturated under the present experimental conditions. For those organic phases, the molar ratios of the sulphate concentration and the water content to the concentration of uranium were also determined: the former is nearly unity at the different initial aqueous uranium concentration, based on the fact that the species $\text{H}_2\text{SO}_4 \cdot 2\text{TOPO}$ (7) formed at low acidity is exchanged by the species $\text{UO}_2\text{SO}_4 \cdot 2\text{TOPO}$ arising from the extraction of uranyl sulphate as well as the extraction of uranyl nitrate by TBP (8); the latter decreases to unity as illustrated in Table 1, implying that the uranyl complex formed in the organic phase contains uranium/sulphate/water/TOPO in the molar ratio 1 : 1 : 1 : 2, indicating the stoichiometry to the $\text{UO}_2\text{SO}_4 \cdot \text{H}_2\text{O} \cdot 2\text{TOPO}$.

Absorption spectra

Some representative results for the absorption spectra of both the aqueous and organic phases from the extraction of aqueous solutions containing 5 g/l uranyl sulphate in sulphuric acid at different concentrations with 0.2 M TOPO in kerosene at 20 °C are illustrated in Figures 2 and 3. For the spectra of aqueous uranyl sulphate containing sulphuric acid only (Figure 2), the following results were observed: with increasing up to 5 M H_2SO_4 , the absorption due to uranyl ion UO_2^{2+} (9,10), which exhibits a band center at 420 nm, is accompanied by a progressive increase in the intensity of the absorption at 430 nm by the formation of the species UO_2SO_4 (11-13), the absorption at around 455 nm disappears in above 7 M H_2SO_4 , indicating the formation of the species $\text{UO}_2(\text{SO}_4)_2^{2-}$ (14,15), although Arden et al (16) insist the presence of the complex ion $\text{UO}_2(\text{SO}_4)_3^{4-}$ at pH values below 2.5. In contrast, the spectra of the organic phases (Figure 3) show largely the absorptions due to the species of the $\text{UO}_2(\text{SO}_4)_2^{2-}$ type, even though the spectrum of the aqueous solution at low sulphuric acid concentration does not indicate the presence of $\text{UO}_2(\text{SO}_4)_2^{2-}$. It is thus presumed that the extracted species is an six-coordinated uranium complex ion, although the spectra of the organic phases reveal the fine structure attributed to the ligand field effect.

Infrared spectra

The organic phases from the extraction of uranyl sulphate

Table 1. The concentrations of uranium and sulphate and the water content in the organic phase from the extraction of uranyl sulphate solutions containing 3 M sulphuric acid with 0.03 M TOPO on kerosene at 20 °C.

g/l	Initial [U] _{aq} '		[U] _{org} ' M	[SO ₄] _{org} ' M	[H ₂ O] _{org} ' M	Molar ratio in the organic phase		
	M					[H ₂ O]/[U]	[TOPO]/[U]	[SO ₄]/[U]
1	0.00274		0.00075	0.01370	0.0118	15.7	40.0	18.3
5	0.0137		0.0029	0.01358	0.0116	4.00	10.2	4.62
10	0.0274		0.0045	0.01365	0.0114	2.53	6.67	3.03
25	0.0685		0.0065	0.01345	0.0108	1.66	4.62	2.13
50	0.137		0.0078	0.01476	0.0106	1.36	3.85	1.89
100	0.274		0.0092	0.01480	0.0102	1.11	3.26	1.61
300	0.822		0.0109	0.01535	0.0101	0.93	2.75	1.41

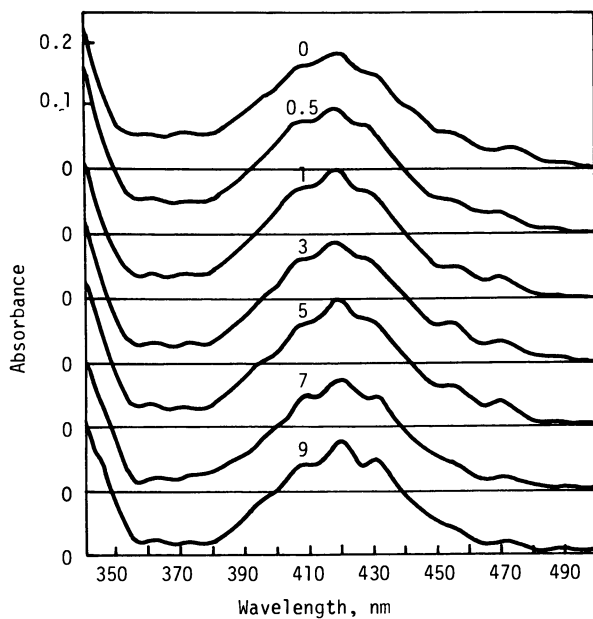


Figure 2. Absorption spectra of aqueous uranyl sulphate solutions containing sulfuric acid at different concentrations; numerals on curves are sulfuric acid concentrations, M.

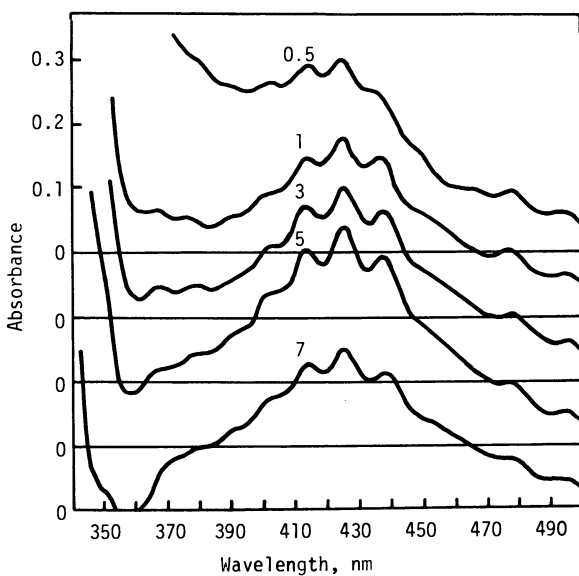


Figure 3. Absorption spectra of the organic solutions from the extraction of aqueous uranyl sulphate solutions containing sulfuric acid at different concentrations with 0.2M TOPO in kerosene; numerals on curves are initial aqueous sulfuric acid concentrations, M.

solutions (0, 1, 5, 25 and 100 g/l) containing 3 M sulphuric acid with 0.1 M TOPO in kerosene were examined in comparison with the aqueous solution of uranyl sulphate at 250 g/l by infrared spectroscopy. The representative spectra of the organic phases are illustrated in Figure 4.

The spectrum of the aqueous uranyl sulphate solution reveals the absorption bands at 1140, 1030 and 970 cm^{-1} , assigned to the vibration of the bisulphate group (point group C_{3v} symmetry) (17, 18), and the asymmetric stretching frequency of the uranyl group (19) at 950 cm^{-1} in addition to the strong absorptions of the OH group due to the OH stretching and bending vibrations at 3320 and 1625 cm^{-1} , respectively, ascribed to the presence of water. This implies that the equilibrium $\text{UO}_2^{2+} + \text{HSO}_4^- \rightleftharpoons \text{UO}_2\text{SO}_4 + \text{H}^+$ exists in the aqueous solution at low acidity, corresponding to the electronic spectral result.

The spectrum of the water-saturated TOPO exhibits the OH vibrations (stretching and bending bands at 3380 and 1620 cm^{-1} , respectively) and the P \rightarrow O stretching band at 1185 cm^{-1} (actually a doublet at 1185 and 1170 cm^{-1}), indicating the presence of a weak hydrogen bond in the compound $\text{TOPO}\cdot\text{H}_2\text{O}$. In the organic solution from the extraction of 3 M sulphuric acid solution, the absorption assigned to the P \rightarrow O stretching band of TOPO shifts to the lower frequency, resulting from the formation of the species $\text{H}_2\text{SO}_4\cdot 2\text{TOPO}$ (7). For the spectra of the organic solutions from the extraction of the aqueous solutions containing uranyl sulphate, the following pattern is observed with increasing the concentration of uranium: the intensity of the OH vibrations caused by the presence of the compound $\text{TOPO}\cdot\text{H}_2\text{O}$ (7) decreases, and simultaneously the OH stretching and bending bands appear at 2800 and 1700 cm^{-1} , respectively, demonstrating that the complex has a coordinated water molecule in agreement with the result of the Karl-Fischer titration (Table 1); the absorption due to the P \rightarrow O stretching band of TOPO bonded with uranium ion, appears at 1090 cm^{-1} ; the absorptions of the sulphate group (point group C_{3v} symmetry) (20) at 1250, 1150 and 1020 cm^{-1} are accompanied by the asymmetric stretching band (19) of the uranyl group at 925 cm^{-1} . Hence the infrared results confirm that uranium extracted into TOPO solution is bonded to the phosphoryl oxygen atom, suggesting that the extracted species exists as a complex $[\text{UO}_2\text{SO}_4(\text{H}_2\text{O})(\text{TOPO})_2]$ in an octahedral arrangement.

NMR spectra

The organic phases from the extraction of uranyl sulphate solutions (0, 5 and 100 g/l) containing sulphuric acid with 0.1 M TOPO in carbon tetrachloride at 20 °C were examined by NMR spectroscopy. The NMR spectrum of water-saturated TOPO solution shows a peak at 9.11 (τ value) in a triplet due to the methyl protons, a sharp peak at 8.68 arising from methylene protons, and a peak at 5.53 from methylenic protons attached to a phosphorus atom, and the water proton signal at 7.58, indicating the formation of the compound $\text{TOPO}\cdot\text{H}_2\text{O}$. In the organic solutions from the extraction of

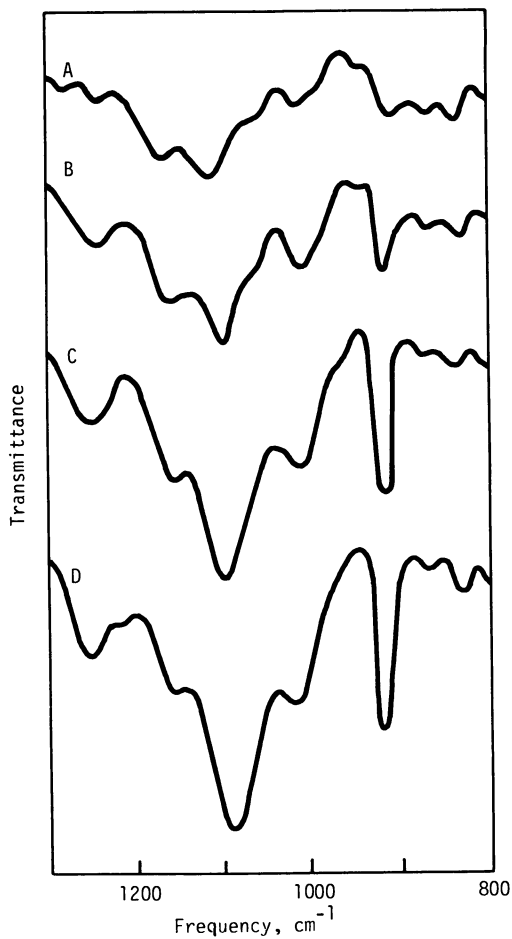


Figure 4. IR spectra of the organic solutions from the extraction of aqueous uranyl sulphate solutions containing 3M sulfuric acid with 0.1M TOPO in kerosene; A, B, C, and D represent uranyl sulphate solutions of 1, 5, 25, and 100 g/L, respectively.

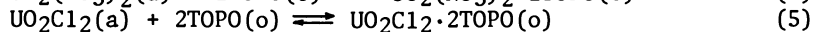
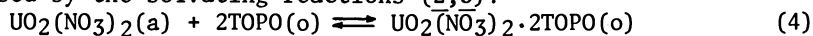
aqueous solutions containing uranyl sulphate at 5 and 100 g/l in 3 M sulphuric acid the methylenic protons attached to the carbon atoms immediately adjacent to a phosphorous atom appear at 8.45, 8.42 and 8.20, respectively, and the water proton resonances at 4.00, 3.85 and 3.70, respectively. The fact that the signals of the methylenic proton and water proton shift to a lower field with increasing initial aqueous concentration of uranyl sulphate is consistent with the infrared data, indicating that the compound $\text{H}_2\text{SO}_4 \cdot 2\text{TOPO}$ is displaced by the species $\text{UO}_2\text{SO}_4 \cdot 2\text{TOPO}$. Also this corresponds to the results for the acidity of the organic phase.

Temperature effect

The extraction of aqueous solutions containing 5 g/l of uranyl sulphate in 3 M sulphuric acid with 0.1 M TOPO in kerosene at the temperatures between 20 and 50 °C gave the data shown in Table 2, indicating that the distribution coefficient decreases with rising temperature. This is analogous to the results for the extraction from nitric and hydrochloric acids (2,3). The heat of reaction (change in enthalpy) for Equation (3) was estimated to be 24.56 and 23.93 kJ/mol in 0.05 and 0.1 M TOPO, respectively (24.25 kJ/mol as average value). Similar results were obtained by varying the TOPO concentration. From this it is found that the heat of reaction is in the order 38.91 > 25.31 > 24.25 (kJ/mol) for the extraction systems from nitric, hydrochloric and sulphuric acids, respectively, corresponding to their extraction efficiencies for uranium(VI).

Comparison of the extraction systems from nitric, hydrochloric and sulphuric acid solutions

Some representative results for the extraction of aqueous solutions containing 5 g/l of uranyl salts in nitric, hydrochloric and sulphuric acids, respectively, at different concentrations with 0.03 M TOPO in kerosene at 20 °C are shown in Figure 5, suggesting their extraction efficiencies of TOPO for uranyl salts are in the order nitrate > chloride > sulphate. The distribution coefficient passes through a maximum although the respective maxima appear at about 0.3 M HNO_3 , 5 M HCl and 4 M H_2SO_4 . Accordingly, as the shape of their extraction curves closely resemble to each other, it is evident that their extraction equilibria are expressed by the solvating reactions (2,3):



and Equation (3). However, since the complexes formed in the organic phases have no coordinated water molecules except the uranyl sulphate complex containing a water molecule, it is thought that extracted species exist as the complexes $[\text{UO}_2(\text{O}_2\text{NO})_2(\text{TOPO})_2]$, $[\text{UO}_2\text{Cl}_2(\text{TOPO})_2]$ and $[\text{UO}_2(\text{OSO}_3)(\text{OH}_2)(\text{TOPO})_2]$ in the coordination numbers of eight, six and six, respectively, on the basis of the results for the absorption and infrared spectra. Additionally, when the respective data (1163, 1110 and 938) for the apparent molecular weights of the uranyl nitrate, chloro and sulphato complexes with TOPO are compared with the theoretical values (1168,

Table 2. Temperature dependence of distribution coefficient on the extraction of uranyl sulphate solutions containing 3 M sulphuric acid with TOPO in kerosene.

Temperature °C	Distribution coefficient	
	0.05 M TOPO	0.1 M TOPO
20	0.977	3.34
30	0.760	2.29
40	0.487	1.78
50	0.388	1.42

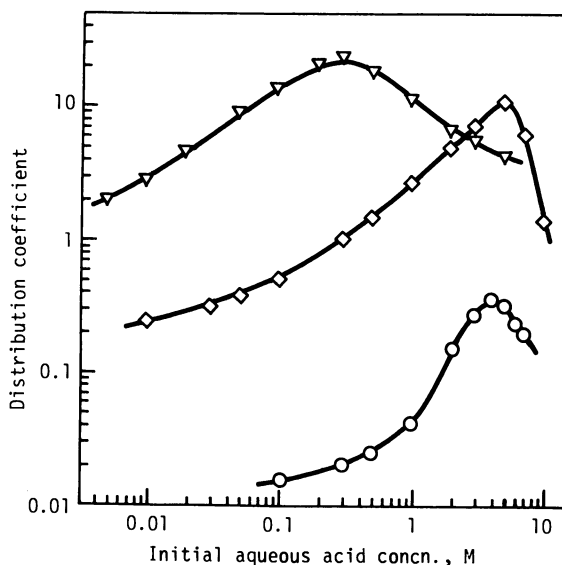


Figure 5. Extraction of U (VI) from aqueous solutions containing nitric, hydrochloric, and sulfuric acids with 0.03M TOPO in kerosene at 20°C; (\diamond), (∇), and (\circ) represent the extractions of uranyl nitrate, chloride, and sulphate, respectively.

Table 3. Extraction of aqueous solutions containing 5 g/l of uranyl salts in nitric and sulphuric acids by TOPO in various organic solvents.

Diluent	Distribution coefficient ^a			
	1 M HNO ₃	0.01 M HNO ₃ +0.99 M NaNO ₃	1 M H ₂ SO ₄	0.1 M H ₂ SO ₄ + 0.9 M Na ₂ SO ₄
Kerosene	10.4	12.6	0.270	0.051
Benzene	15.7	8.62	0.068	0.022
Cyclohexane	15.9	16.7	0.250	0.016
Carbon tetrachloride	9.57	4.37	0.042	0.031
n-Hexane	20.8	21.8	0.325	0.025
Toluene	12.7	10.3	0.072	0.034
Chloroform	1.44	0.236	0.036	0.006
Chlorobenzene	30.1	12.4	0.153	0.042
o-Dichlorobenzene	5.30	6.27	0.195	0.065

^a The values for the extractions of uranyl nitrate and sulphate are the respective TOPO concentrations of 0.03 and 0.05 M.

1114 and 1158) of the molecular weights for their monomeric species, it is considered that the complexes exist as monomer. In this case, the complexes are prepared from the organic solutions in the extraction under the following conditions, but it seems that the organic solution from the extraction of uranyl sulphate is not yet saturated with uranium: the extraction with 0.1 M TOPO in benzene at 20 °C of uranyl nitrate solution (50 g/l) containing 0.01 M nitric acid and 0.29 M sodium nitrate, of uranyl chloride solution (250 g/l) containing 0.1 M hydrochloric acid and 4.9 M lithium chloride and of uranyl sulphate solution (300 g/l) containing 3 M sulphuric acid.

Furthermore when the effect of diluent on the extraction efficiency of TOPO for uranium(VI) is examined in the extraction of aqueous solutions containing 5 g/l of uranyl salts in nitric and sulphuric acids, it is found from some representative data (Table 3) that hydrocarbons such as alkane or cycloalkane enhance the extraction efficiencies in all systems, while halogen-substituted hydrocarbon such as chloroform reduces them.

Conclusions

The distribution of uranium(VI) between sulphuric acid solutions and solutions of tri-n-octylphosphine oxide (TOPO) in organic solvent has been investigated under different conditions. The aqueous and organic phases are examined spectrophotometrically, and the organic phases by infrared and nuclear magnetic resonance spectroscopies. As a result, it is found that the extraction is expressed by the equilibrium equation $UO_2SO_4(aq) + 2TOPO(org) \rightleftharpoons UO_2SO_4 \cdot 2TOPO(org)$, in which the extracted species exists as a complex $[UO_2SO_4(H_2O)(TOPO)_2]$ in an octahedral arrangement. Additionally the obtained results are compared with those for the extraction from nitric and hydrochloric acid solutions.

Acknowledgements

The author wishes to thank Messrs. T.Nishida and F.Ozawa for assistance with experimental work, and the Hokko Chemical Industry Co. Ltd. for the sample of TOPO.

Literature Cited

1. Sato, T., and Yamatake, M., J. Inorg. Nucl. Chem. 1969 31, 3633.
2. Sato, T., Nishida, T., and Yamatake, M., J. Appl. Chem. Biotechnol. 1973 23, 909.
3. Sato, T., and Nishida, T., J. Inorg. Nucl. Chem. 1974 36, 2087.
4. Sato, T., J. Appl. Chem. 1965 15, 489.
5. Sato, T., J. Appl. Chem. 1966 16, 53.
6. Kinnunen, J., and Wennerstrand, B., Chemist-Analyst 1957 46, 92.
7. Sato, T., Watanabe, H., and Yamatake, M., J. Appl. Chem. Biotechnol. 1976 26, 697.
8. Sato, T., J. Inorg. Nucl. Chem. 1959 9, 188.

9. Sutton, J., J.Chem.Soc. 1949 s275.
10. Rabinowitch, E., and Belford, R.L., "Spectroscopy and Photochemistry of Uranyl Compounds", Pergamon Press, Oxford, 1964 p.97.
11. Betts, R.H., and Michels, R.K., J.Chem.Soc. 1949 s286.
12. Ahrlund, S., Acta Chem.Scand. 1951 5, 1151.
13. As reference 10, p.116.
14. Day, Jr., R.A., and Powers, R.M., J.Am.Chem.Soc. 1954 76, 3895.
15. Katz, J.J., and Seaborg, G.T., "The Chemistry of the Actinide Elements", Methuen, London, 1957 p.186.
16. Arden, T.V., and Wilkins, C.H., Anal.Chem. 1952 24, 1253.
18. Walrafen, G.E., and Dodd, D.M., Trans.Faraday Soc. 1961 57, 1286.
19. Gatehouse, B.M., and Comyns, A.E., J.Chem.Soc. 1958 3965.
20. Nakamoto, K., "Infrared Spectra of Inorganic and Coordination Compounds", 2nd ed., John Wiley, New York 1970, p.173.

RECEIVED May 17, 1979.

Properties and Uses of Nitrogen and Sulfur Donors Ligands in Actinide Separations

C. MUSIKAS, G. LE MAROIS, R. FITOUSSI, and C. CUILLERDIER

Division de Chimie, Département de Génie Radioactif, Centre d'Etudes Nucléaires de Fontenay aux Roses, BP N° 6, Fontenay aux Roses, 92260 France

Most of the complexing agents used in actinide separations are oxygen donor ligands (1, 2), because of the hard acceptor character of the *f* series ions. The aqueous complexes of ligands of which the donor atoms are less electronegative than oxygen (Pauling's electronegativity 3.5) are weak because of the competition with water for the coordination sites of the metal. However, unusual actinide separations involving these weak complexes have been performed. For instance, the group of trivalent lanthanide ions has been separated from trivalent actinides by using concentrated aqueous chloride media (electronegativity 3.0) from which trivalent actinide ions are selectively absorbed in anion exchange resins (3) or extracted by organic solutions of tri or tetraalkylammonium chloride salts (4). 4*f* - 5*f* group separation is also possible by using aqueous thiocyanate solutions, where the trivalent actinide ion can be selectively extracted in an organic solution of tetraalkylammonium thiocyanate (5) or fixed on an anion exchange resin (6).

For the thiocyanate complexes of lanthanides or actinides, the coordination occurs via the nitrogen atom (electronegativity 3.0).

For these two cases, there is no obvious explanation of the origin of group separation. Formation constants of weak complexes are difficult to measure and the expected greater covalent effect for actinide has not been clearly established.

This paper reports the results of investigations of the complex formation between actinide or lanthanide ions and azide or orthophenanthroline. The aim of this work was first to confirm whether these relatively soft ligands give complexes of different stabilities with the trivalent lanthanide and actinide ions, as a consequence of the broader extension of 5*f* orbitals as compared with 4*f*. Secondly, we attempted to use the results in actinide chemical separation processes.

Dialkyldithiophosphates are also soft ligands (electronegativity of sulfur 2.5) and as part of a systematic study for their binding properties to the actinides ions we report the results of

0-8412-0527-2/80/47-117-131\$05.00/0
© 1980 American Chemical Society

solvent extraction of U (VI) and Np (IV).

Experimental

Chemicals. All reagents used in this study were analytical grade and were supplied by Prolabo or Merck. Thenoyltrifluoroacetone (TTA) supplied by Koch Light was purified by sublimation. The actinide elements were provided by CEA-SPT (Fontenay aux Roses) as oxide or nitrate solutions. We used the isotopes ^{232}U , ^{237}Np , ^{239}Pu , ^{241}Am , ^{244}Cm , ^{152}Eu , ^{147}Nd , ^{169}Yb used as tracers were supplied by Isotec (Versailles). Bis - (2 ethylhexyl)dithiophosphoric acid (HDEHDP), trioctylphosphine oxide (TOPO) and dihexylmethoxyoctylphosphine oxide (POX 11) were supplied by Ircha (Vert le Petit).

Apparatus. Ultraviolet, visible and near infrared spectra were recorded with a Cary 17 spectrophotometer. γ spectroscopy was carried out with a Ge-Li detector and a Zoomax (Sein) multi-channel analyzer. pH measurements were taken with an Aries 10000 (Tacussel) potentiometer. α spectroscopy was carried with a solid state α detector and a (Intertechnique) multichannel analyzer.

Results and Discussion

Azide complexes. The aqueous trivalent actinide and lanthanide azides complexes were examined by two techniques :

- U.V., visible, near I.R. spectroscopy (Nd, Eu, Er, Pu, Am, Cm),
- Solvent extraction : (Nd, Eu, Yb, Am) using radioactive tracer techniques.

The spectral changes observed on addition of azide ions to trivalent actinide or lanthanide perchlorate solutions are shown in figure 1.

To calculate the formation constants of the complexes we used equation (1), which correlates the molecular extinction coefficient of the various metallic species (ϵ_i) and the measured apparent molecular extinction coefficient (ϵ_M), with the stability constants of the complexes (β_i).

$$\epsilon_M = \epsilon_0 + \sum_{i=1}^{i=i_{\max}} \beta_i \cdot (\text{N}_3^-)^i / 1 + \sum_{i=1}^{i=i_{\max}} \beta_i \cdot (\text{N}_3^-)^i \quad (1)$$

β_i and ϵ_i were calculated by least square adjustment. Good adjustments are obtained when i_{\max} is limited to 2 in the range 0 to 2M in azide. Generally, to minimize the number of coefficients to be found in one adjustment, we used a mathematical program (7) making it possible to fix one or more coefficients found in separate previous experiments or calculations. For the Nd complexes we used also a deconvolution method to obtain the formation constants. The results of the calculation of formation

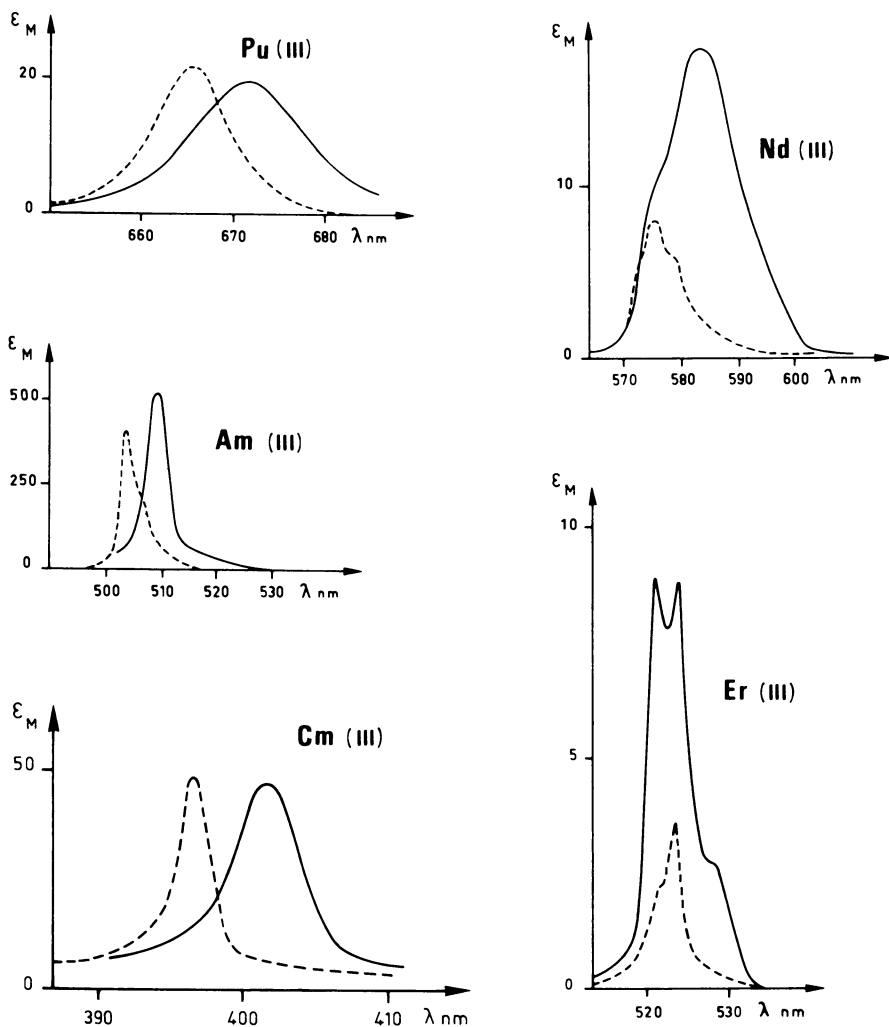
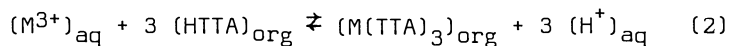


Figure 1. Absorption spectra of trivalent actinide and lanthanide ions in the absence or presence of azide: (---) perchloric media, $\mu = 5$, $\theta = 25^\circ\text{C}$, $\text{pH} = 5.4$; (—) 4M azide, $\mu = 5$, $\theta = 25^\circ\text{C}$, $\text{pH} = 5.4$.

constants are given in Table I. Note that a clear difference in stability is observed between actinide and lanthanide complexes, the first former being more stable. For Eu (III), the formation constants were calculated from the occurrence of an absorption band in the U.V. portion of the spectrum. As this absorption band exists only in the spectra of lanthanide elements, which have rather stable divalent ions, we attributed it to azide to metal charge transfers. Figure 2 shows how this band varies in the serie Eu, Yb, Sm.

The energy of absorption peak tends towards higher values as the stability of the divalent ions decreases, in agreement with the semi-empirical theory postulated by Nugent et al(8).

In order to verify the differences observed in 4f-5f complex stability, we used an additional solvent extraction method based on the competition between a soluble organic chelatant (TTA) and the aqueous soluble azide ions for binding the metal ions. The extraction equilibrium is shown by equation (2) and the distribution coefficients (D) of the metal at constant pH are correlated with the formation constants by equation (3).



$$D = D_0 / \sum_{i=0}^{i=i_{max}} \beta_i \cdot N_3^- \quad (3)$$

where D_0 is the distribution coefficient when no complexing agent is present in the aqueous phase.

i_{max} can be determined by the maximum slope of the curve $D = f(\log N_3^-)$. Its value is closed to three in concentrated azide solutions.

Typical extractions curves are shown in figure 3. By the least square adjustment of experimental D to equation (3), we calculated the coefficients β_1 and β_2 of which value are 2 and 8. It can be seen that the results found by spectrophotometry are confirmed. Figure 4 shows the ratio of Eu (III) to Am (III) distribution coefficients as a function of free azide concentration. This curve shows clearly the higher stability of the aqueous, Am (III) azide complexes. Distribution coefficients of Am (III) and Eu (III), present in the same solutions, were determined by γ spectroscopy. In conclusion, it appears that the azide complexes of actinides are more stable.

As shown by the values of the formation constants found by solvent extraction (overall formation constants) and by spectrophotometry (inner sphere formation constants), it is safe to assume that azide complexes are mostly inner sphere. This is also supported by the values of the formation constant of Eu (III) calculated using the charge transfer band whose appearance must be attributed to close contact between azide and metal ion.

TABLE I : Formation constants of azides complexes of trivalent actinide and lanthanide derived from spectrophotometric data.

Complex	β_i	Electronic transition observed	Calculation method
$\text{Nd}(\text{N}_3)^{2+}$	1,2	f-f (800 nm)	deconvolution
$\text{Eu}(\text{N}_3)^{2+}$	4,0	charge transfer	see ref. [16]
$\text{Er}(\text{N}_3)^{2+}$	1,2	f-f (525 nm)	adjustment to equation (1)
$\text{Pu}(\text{N}_3)^{2+}$	(4) ^x	f-f (665 nm)	deconvolution
$\text{Am}(\text{N}_3)^{2+}$	10	f-f (503 nm)	adjustment to equation (1)
$\text{Am}(\text{N}_3)_2^+$	23	f-f (503 nm)	adjustment to equation (1)
$\text{Cm}(\text{N}_3)^{2+}$	8	f-f (397 nm)	adjustment to equation (1)
$\text{Cm}(\text{N}_3)_2^+$	24	f-f (397 nm)	adjustment to equation (1)

^x At pH 5,4 Pu (III) is partially oxidized and $\text{Pu}(\text{N}_3)^{2+}$, β_1 value is less reliable than $\text{Am}(\text{N}_3)^{2+}$ or $\text{Cm}(\text{N}_3)^{2+}$ value.

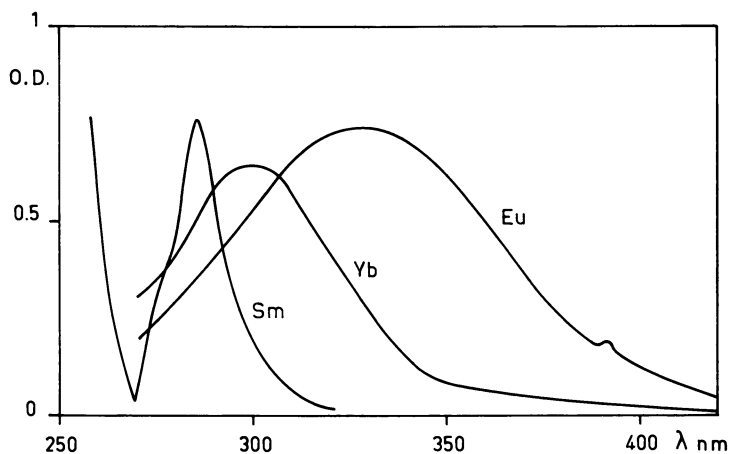


Figure 2. UV absorption band of aqueous mixtures of selected lanthanide ions in the presence of azide (1-mm cell); $C_M = 0.05M$, 2.4M azide, $pH = 5.4$, $\mu = 5$.

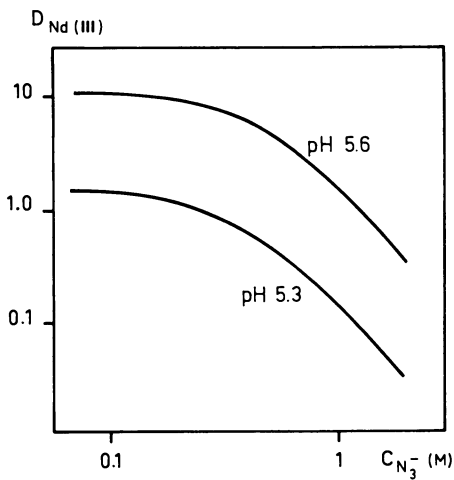
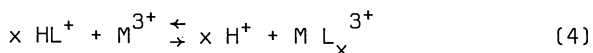


Figure 3. Distribution coefficients of Nd (III) between aqueous azide solutions and 0.0075M HTTA in benzene at 23°C; aqueous phases $\mu = 5$, $Nd \approx 10^{-5}M$.

Orthophenanthroline complexes. As azides exhibit greater chemical affinity for trivalent actinide ions, we tried to check this behavior with a bidentate ligand. We chose 1-10 phenanthroline ($C_{12}H_8N_2$) which has two nitrogen donors at 2.75 Å from each other and give bonds in the first coordination sphere of trivalent lanthanide, as shown by several spectroscopic methods (9). Many solids containing orthophenanthroline (L) and lanthanides have been prepared by precipitation from aqueous solutions (10), but no quantitative measurement of the stability of the aqueous soluble complexes appears in literature.

We studied the complexes of lanthanides and Am (III) by potentiometry. This method is based on pH variations due to the competition between H^+ and the metal ions for the coordination site of orthophenanthroline ($pK_a \approx 5.2$), as shown by equation (4).



The formation constants of the complexes were calculated by using equations (5) and (6).

$$\bar{n} = \frac{C_L}{C_M} \cdot \frac{(H_L - H_M)}{H_L} \quad (5)$$

$$\bar{n} = \frac{\sum_{i=1}^{i=4} i \cdot \beta_i \cdot L^i}{\sum_{i=0}^{i=4} \beta_i \cdot L^i} \quad (6)$$

where

\bar{n} is the average number of ligand molecules bonded to the metal.

C_L and C_M are the ligand and metal concentrations respectively.

H_L and H_M are the abscissae values of the curves in figure 5 and represent the amounts of acid in the presence of metal.

β_i is the formation constant of the complex ML_i^{3+} . We limited i to 4 because of steric hindrance.

The calculation results are shown in table II. We also report formation constants determined from spectrophotometry for Ho and Nd, and by solvent extraction for Er. Without going into detail for these two methods, it may be noted that the results show fair agreement. That fact points out the inner sphere character of orthophenanthroline lanthanous complexes. The main absorption band of Am (III) is modified by the presence of orthophenanthroline. We used these spectral variations to calculate the formation constants of Am (III), as described in the previous paragraph. As for azide complexes, we observed that Am monoorthophenanthroline is more stable than the equivalent lanthanide complex, and for the bis orthophenanthroline species, the difference

Figure 4. Variation in the ratio $D_{Eu(III)}/D_{Am(III)}$ as a function of azide concentration at 25°C; organic phase HTTA in benzene, aqueous phase $\mu = 5$, pH = 5.4.

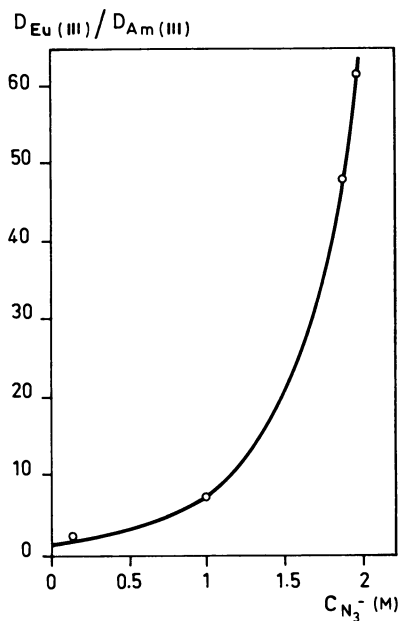


Figure 5. Distribution coefficients of U(VI) between 5M aqueous phosphoric acid and mixture of HDEHDTP and neutral oxygen donors in solution in dodecane as a function of the reagent concentration ratio; (1) 0.5M (HDEHDTP + POX 11), (2) 0.5M (HDEHDTP + TOPO), (3) 0.5M (HDEHDTP + TBP).

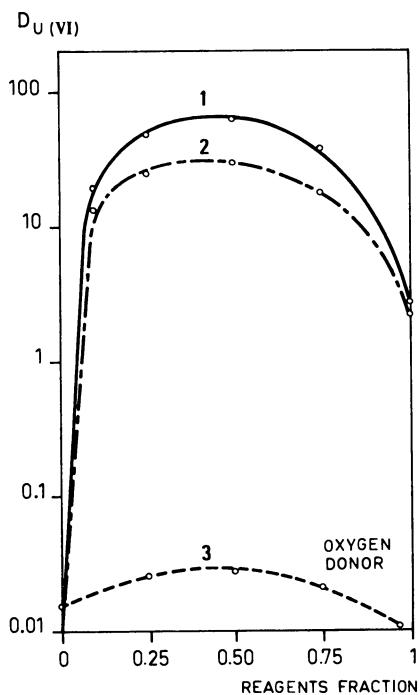


TABLE II : Formation constants of trivalent lanthanide and actinide complexes with orthophenanthroline derived from various investigation techniques data.

Element	Potentiometry		Spectrophotometry		Solvent extraction	
	Log β_1	Log β_2	Log β_1	Log β_2	Log β_1	Log β_2
Nd	1.09	3.99			0.79	3.53
Sm	1.17	3.99				
Eu	1.31	4.02				
Gd	1.22	4.00				
Dy	1.50	4.10				
Ho	1.66	4.16	1.67	3.95		
Er	1.78	4.16			1.99	4.03
Lu	1.88	4.3				
Am	2.68	4.66	2.56	4.03		

between the two series is not as significant.

We attempted to use orthophenanthroline as an extractant. For this purpose it was necessary to have, in the organic phase, a reagent able to neutralize the tripositive charge of the orthophenanthroline metallic species. We chose nonanoic acid which has poor solubility in aqueous phases. Nitrobenzene is suitable as a diluent because it solubilizes orthophenanthroline. The results of Eu (III) and Am (III) extraction in the nitrobenzene/orthophenanthroline/nonanoic acid mixture are given in Table III.

At the working pH orthophenanthroline is present mostly in the organic phase and its higher affinity for Am (III) ions is shown by the higher distribution coefficients. Without orthophenanthroline Am (III) and Eu(III) ions are not extracted in the mixture nonanoic acid, nitrobenzene.

Sulfur donor ligands. Complexes of actinides or lanthanides ions with sulfur donor ligands such as dithiocarbamate (S_2CNR_2) (11) and dialkyldithiophosphates ($(RO)_2 P S_2$) (12) have been obtained in non-aqueous solutions. The uses of dialkyldithiophosphates as extractants for uranium (VI) have been reported (13), (14). Dialkyldithiophosphates are poorer extractants than dialkylphosphates because the soft sulfur atom has less affinity than oxygen for the hard f cations. However, the $P \begin{smallmatrix} \text{O} \\ \text{SH} \end{smallmatrix}$ group has a lower tendency than $P \begin{smallmatrix} \text{O} \\ \text{OH} \end{smallmatrix}$ to dimerize via hydrogen bonds. Furthermore, the distribution coefficients of metallic species between aqueous phases and organic phases containing dialkyldithiophosphates can have higher values despite this lower affinity. We found one example of this effect in U (VI) extraction from concentrated phosphoric acid solutions. We investigated the synergistic extraction of U(VI) by mixtures of di (2 ethylhexyl)dithiophosphoric acid (HDEHDP) and neutral oxygen donors such as tributylphosphate (TBP), trioctylphosphine oxide (TOPO), and dihexylmethoxioctylphosphine oxide (POX 11) in dodecane.

Distribution coefficients of U (VI) as a function of the composition of the organic phase are shown in figure 5. The maximum of the distribution coefficients always occurs for the proportion 1 : 1 of HDEHDP and neutral oxygen donor. This suggests that the extracted species have the formula $UO_2 (DEHDP) (R_3 PO) (H_2 PO_4)$ where $R_3 PO$ represents the neutral oxygen donor. The variation of distribution as a function of HDEHDP or TOPO organic concentrations are shown in logarithmic coordinates in figure 6. The slope 1 for the straight line observed supports the proposed formula of the extracted species. The effect of the aqueous concentration of phosphoric acid on the distribution coefficients of U (VI) is shown in figure 7. They decrease probably because of U(VI) phosphate complex formation in aqueous solutions. The higher values of the distribution coefficients of U (VI) in mixtures of HDEHDP and TOPO as compared with equivalent mixtures of di(2 ethylhexyl)phosphoric acid and TOPO (15) are probably due to the difference in nature of the extracted species as suggested by the position of

TABLE III : Distribution coefficients of Am (III) and Eu (III) between nitrobenzenic mixtures of 0.25 M 1-10 phenanthroline and 0.25 M nonanoic acid as a function of aqueous nitric acid concentration ($\mu = 0.1$)

HNO ₃ aq (M)	pH at equilibrium	D _{Am (III)}	D _{Eu (III)}	$\frac{D_{Am (III)}}{D_{Eu (III)}}$
0.004	5.08	51	2.8	18.3
0.006	4.89	22.8	1.4	16.6
0.008	4.75	10.1	0.6	17.1
0.01	4.64	7.2	0.4	18.5
0.012	4.55	4.9	0.3	16.5

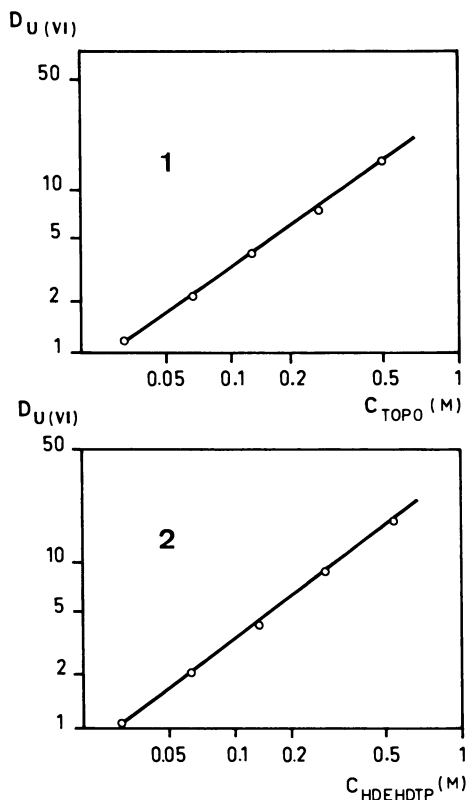
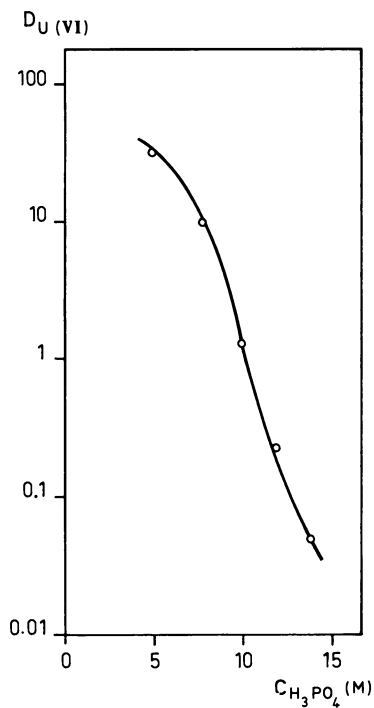


Figure 6. Distribution coefficients of U (VI) between 5M aqueous phosphoric acid and mixtures of HDEHDTP and TOPO in solution in dodecane; (1) 0.01M HDEHDTP, TOPO variable, (2) 0.01M TOPO, HDEHDTP variable.

Figure 7. Distribution coefficients of U (VI) as a function of aqueous phosphoric acid concentration; organic phases 0.25M HDEHDTP + 0.25M TOPO.



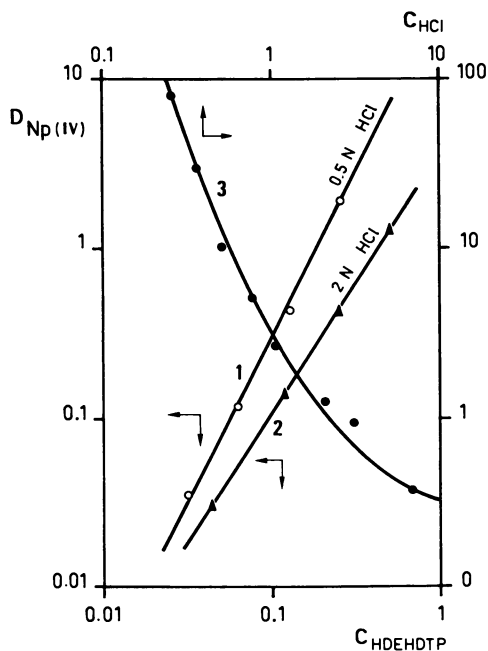


Figure 8. Distribution coefficients of Np (IV) as a function of HDEHDTP organic concentrations [(1), (2)] or aqueous HCl (3)

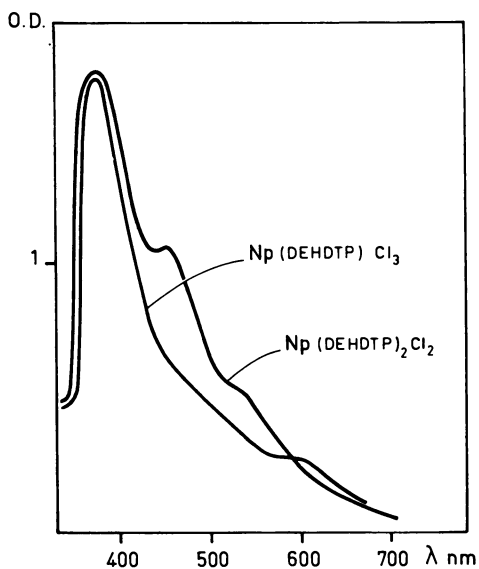
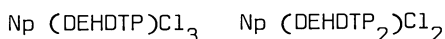


Figure 9. Spectra of Np (IV) extracts in dodecane-HDEHDTP solutions; $C_{Np(DEHDTP)_2Cl_2} = 0.001M$; $C_{Np(DEHDTP)Cl_3} = 0.00033M$.

the distribution coefficients maximum as a function of organic phases composition. The strong hydrogen bonds in HDEHP are probably extraction inhibitors by two effects : lower activity of free ligand, and formation of species which do not easily allow other ligands present in the system to enter the coordination sphere of the metal. Another example of high number of species which can be extracted in organic phase by using HDEHDP as ligand is shown in figure 8, where we can see the distribution coefficients of Np (IV) from chloride solutions as a function of pH and HDEHDP concentration. These curves suggest that the species extracted have the formulas :



Spectrophotometry confirms these changes in the Np (IV) environment as shown in figure 9.

Conclusions

Investigations of complexes of 5f ions and 4f ions with nitrogen donor ligands show that trivalent actinide ions are more strongly complexed than trivalent lanthanide ions, and these properties can be exploited in actinide-lanthanide group separation by the choice of appropriate extraction systems. The higher affinity of nitrogen ligand for 5f trivalent ions is not attributable to the occurrence of different type of complex for the two series (inner vs outer sphere), as shown by the use of several complexation techniques. This difference might be attributed to greater covalent bond contributions in the actinide complexes. Dialkyldithiophosphates can be better extractants than their dialkylphosphate equivalents, as shown by the synergistic extraction of U (VI) from concentrated phosphoric acid. This effect is probably due to the weaker hydrogen bonds of the $\text{P} \begin{matrix} \text{S} \\ \diagdown \\ \text{SH} \end{matrix}$ group which allow the formation of a greater variety of extracted species. In this particular case, we showed that the extracted species has the formula : $\text{UO}_2 (\text{H}_2 \text{PO}_4)$ $(\text{R}_3 \text{PO})$ (DEHDP).

Literature cited

1. Gmelin Handbuch der Anorganischen Chemie Band 21 Transurane Teil 2 von Günter Koch Springer Verlag 1975
2. Comprehensive Inorg. Chem. Bailar J.C., Emeleus H.A., Sir R. Nyholm, Trotman Dickenson A.F. - Vol 5 Actinides Pergamon Press (1973)
3. Hulet E.K., Gutmacher R.G., Coops M.S. J. Inorg. Nucl. Chem. 1961 17, 350
4. Leuze R.E., Lloyd M.H. Process Chemistry 1970 4, 597

5. Gerontopoulos P. Th., Rigali L., Barbano P.G.,
Radiochimica Acta 1965 4, 75
6. Coleman J.S., Asprey L.B., and Chisholm R.C.
J. Inorg. Nucl. Chem. 1969 31, 1167
7. Ngyen-Ngoc H.,
Rapport D.I. n° 465 CEN-S (Mars 1971)
8. Nugent L.J., Baybarz R.D., Burnett J.L., Ryan J.L.,
J. Phys. Chem. 1973 77, 1528
9. Sinka S.P., Butter E.
Mol. Phys. 1969 16, 285
10. Mac Whinnie W.R., Miller J.D., in "Advances in Inorg.
Chem. and Radiochem." - Academic Press 1969 12, 135
11. Bagnall K.W., Brown D., Holah D.G.,
J. Chem. Soc. (A) 1968 1149
12. Pinkerton A.A.,
Inorg. Nucl. Chem. Lett. 1974 10, 495
J. Chem. Soc. Dalton 1978 267
13. Curtui M., Haiduc I., Marcu Gh.,
J. of Radioanal. Chem. 1978 44, 109
14. Marcu G., Curtui M., Haiduc I.,
J. Inorg. Nucl. Chem. 1977 39, 1415
15. Bunus F.T., Domocos V.C., Dimitrescu P.,
J. Inorg. Nucl. Chem. 1978 40, 117
16. Ahrland S.,
Acta Chem. Scand. 1949 3, 783

RECEIVED June 18, 1979.

The "Cleanex" Process: A Versatile Solvent Extraction Process for Recovery and Purification of Lanthanides, Americium, and Curium

JOHN E. BIGELOW, EMORY D. COLLINS, and LESTER J. KING

Oak Ridge National Laboratory, Oak Ridge, TN 37830

The reagent di(2-ethylhexyl) phosphoric acid (HDEHP), a liquid cation exchanger, is used to extract trivalent actinide and lanthanide elements in the "Cleanex" solvent extraction process. The name "Cleanex" was coined because the process was initially developed to "clean up" several batches of rework solutions from a wide variety of contaminants. The process was so effective that it was later incorporated into the mainline operations at the Transuranium Processing Plant (TRU) at the Oak Ridge National Laboratory (ORNL), where it has been in routine use for 12 years. At TRU, the process has been applied to a number of different batch solvent extraction operations at the 50-liter scale. These include purification of solutions of transplutonium elements, transfer of transplutonium elements from nitrate to chloride solutions, and recovery of transplutonium elements from rework and waste streams (1). The transplutonium elements involved are trivalent actinides. The Cleanex process was adapted from the Dapex process (2), which has been used for many years in the uranium milling industry.

The chemistry, reagents, equipment, and basic operations relating to the Cleanex process and typical results obtained with the Cleanex process are covered in the sections below.

Process Chemistry

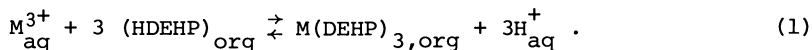
The process consists of liquid-liquid solvent extraction of trivalent actinides and/or lanthanides from a dilute acid or salt solution in which the anion can be either nitrate or chloride. The relatively inextractable impurities can be scrubbed from the pregnant organic phase with dilute acid (0.03 M) and the solutes back-extracted, or stripped, with more-concentrated acid (2-6 M). The process is equally effective with nitric or hydrochloric acid, or mixtures of the acids. Since the extracted species does not contain complexed acid, the solutes may be stripped into an acid different than the one from which they were initially extracted.

American Chemical
Society Library
© 1980 American Chemical Society
1155 16th St. N. W.

In Washington, D. C. 20036

The organic extractant is the ester *bis*-2-ethylhexyl hydrogen phosphate, which has acidic properties because of the replaceable hydrogen ion, and is usually called in the trade di(2-ethylhexyl) phosphoric acid or HDEHP. Since this reagent has a relatively high density and viscosity, it is usually diluted with a nonpolar solvent to a concentration of about 1 M to produce an organic extractant phase with suitable operating characteristics. In the Cleanex process, aliphatic diluents are preferred over aromatic diluents because of about a fivefold higher extraction coefficient for the trivalent actinides.

The HDEHP is a cation exchanger, and its extraction of trivalent metal ions (M^{3+}) can be expressed by the following chemical reaction:



At equilibrium, the concentrations of the reacting species are related as follows (neglecting activity coefficients):

$$K = \frac{[M(DEHP)_3]_{org} [H^+]_{aq}^3}{[HDEHP]_{org}^3 [M^{3+}]_{aq}} \quad (2)$$

where K is the equilibrium constant for the reaction. The equilibrium extraction coefficient (E) for the trivalent metal, defined as the ratio of the concentration in the organic phase to the concentration in the aqueous phase at equilibrium, can be obtained by a rearrangement of Eq. (2):

$$E = \frac{[M(DEHP)_3]_{org}}{[M^{3+}]_{aq}} = \frac{K [HDEHP]_{org}^3}{[H^+]_{aq}^3} \quad (3)$$

Thus, the extraction coefficient, E , varies directly with the third power of the concentration of uncombined HDEHP in the organic phase (neglecting activity coefficients) and inversely with the third power of the aqueous phase acidity (H_{aq}^+).

The acid dependency observed in practice has been only approximately inverse third power. Impurities in Cleanex feed solutions often cause a departure from ideality (e.g., by common-ion effect or by consumption of some of the HDEHP), and we have not been able to control the extraction of the actinide elements solely by monitoring the aqueous-phase acidity. Fortunately, when processing transplutonium elements, the high specific activity of ^{244}Cm facilitates the detection of that isotope in both phases, thus permitting a rapid determination of the degree of extraction. The extraction coefficients of the trivalent actinides and lanthanides are all quite similar, so the ^{244}Cm serves as an excellent marker for all the extracted ions.

Materials

Feed Solutions. The process is applicable to solutions of trivalent actinides or lanthanides in either dilute acid or a variety of salt solutions in either nitrate or chloride or mixed media. Sodium concentrations up to 3 M can be tolerated, but lithium begins to have adverse effects above 2 M and potassium is objectionable even at 0.5 M. Certain special constituents can be tolerated in the feed if specific precautions (described later) are taken.

Extractive Reagent. The extractive reagent is commercial-grade di(2-ethylhexyl) phosphoric acid (HDEHP). Various lots of material obtained from Mobil, from Stauffer, and from Union Carbide, have all appeared equally usable. The commercial material typically contains 1-1.5% of the monoester (which is di-acidic) and a small amount of inert material, probably unreacted 2-ethylhexanol and pyrophosphoric acids. The HDEHP generally titrates about 98% (2.8 M) and is used without treatment other than dilution.

Diluents. An aliphatic diluent with a high flash point is preferred for safety reasons. At TRU, both Amsco 125-82 and NPH (normal paraffin hydrocarbon, supplied by The South Hampton Co., Silsbee, Texas), have given good results. Currently, we are using odorless mineral spirits, which is supplied by Amsco and has a flash point of 52°C, a specific gravity of 0.750, and a boiling range of 144-208°C. All of these diluents have been satisfactory, and no effort has been made to systematically evaluate them for our applications. We generally pretreat the diluent by passing it successively through a packed column of silica gel and alumina to remove traces of surface-active agents that might later contribute to the formation of stable emulsions.

Equipment

The equipment typically used at TRU for carrying out the Cleanex process batchwise is illustrated schematically in Figure 1. The operating technique and design considerations for some of the items in Figure 1 have been more fully described by Chatten (3). The feed is adjusted, and the extraction is carried out batchwise in a tantalum-lined evaporator with a capacity of 60-70 liters. Phase contact is accomplished by air-sparging. A vacuum transfer system is used to raise the aqueous phase from the bottom of the tantalum evaporator, through a phase separator (or bull's-eye), and into a vacuum transfer tank. Replacing the vacuum source with a low-pressure air line, and operating a valve, permits discharge of the accumulated aqueous phase from the vacuum transfer tank into either a waste receiver or a product receiver tank. The raffinate (including scrubs) are eventually transferred to

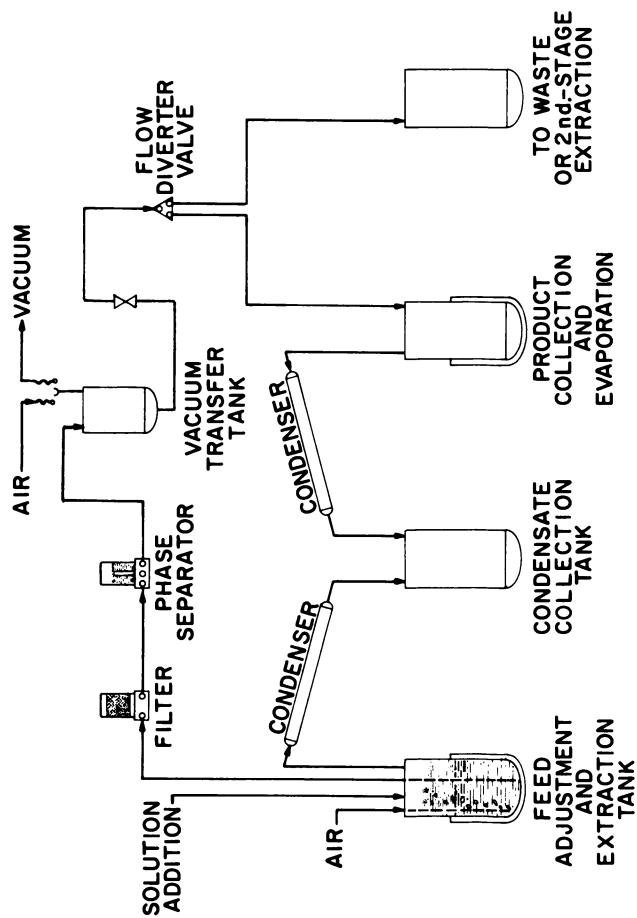


Figure 1. Equipment arrangement for Cleanex process

a waste storage tank. The product receiver is usually another tantalum-lined evaporator so that successive volumes of strip acid can be combined and concentrated prior to their introduction into the next step in the overall process.

Processing Steps

Feed Adjustment. The product from a step prior to Cleanex is transferred and flushed into the tantalum-lined evaporator. Most of the excess acid contained in the composited Cleanex feed is removed by evaporation either to a final volume of 2 liters or, if the salt content is high, to a final boiling temperature of 130°C, whichever occurs first. If the feed is a nitrate solution, hydrolysis of some elements (e.g., zirconium) may have occurred during the evaporation; therefore, about 1 liter of 12 M HCl is added and the feed solution is reheated to 120°C to redissolve any hydrolyzed materials. The feed is then diluted with water to make a total volume of 12 liters and is mixed and sampled. An addition of acid or NaOH is made (if necessary) to adjust the solution acidity into the range of 0.1 to 0.4 N. An oxidant solution (1.5 M LiOCl) is added to make the feed 0.1 M LiOCl, and the feed solution is then heated to 80°C and digested for 20 minutes to remove any gaseous reaction products. This oxidation procedure is carried out to ensure that all molybdenum in the feed is oxidized to the extractable Mo(VI) form (4). Otherwise, unextractable molybdenum may hydrolyze under the relatively low-acid conditions achieved later in the extraction step and result in severe emulsion problems.

Extraction. About 30 liters of the previously prepared organic extractant is added. Adequate mixing of the phases is achieved by air sparging at a superficial air velocity of 1.3 mm/sec (0.25 ft/min); this is the same velocity used to mix a single phase prior to sampling. After mixing is begun, NaOH is added to further reduce the aqueous phase acidity and thereby increase the extractability of the trivalent actinides. The amount of NaOH added is calculated to reduce the acidity to 0.03 N, a limit chosen to minimize the likelihood of hydrolysis and precipitation of unextracted feed components, which might result in emulsification. The mixing is interrupted after 30-60 minutes and the phases allowed to settle. The aqueous phase is sampled and analyzed for free acid and for gross alpha (primarily ^{244}Cm). The free acid is almost always higher than 0.03 N because acid is transferred to the aqueous phase in exchange for the metallic cations which were extracted into the organic phase. A new NaOH addition is calculated, based on the acid results, and the cycle of acid adjustment and sparging is repeated until the amount of unextracted curium remaining in the aqueous phase is less than the specified limit. On some occasions, it may be necessary to terminate the extraction step short of the goal if successive

analyses show the amount of unextracted curium has begun to increase. This latter phenomenon is believed to be due to displacement of the curium by aluminum resulting from a slow, irreversible extraction of aluminum which consumes the reagent, HDEHP. The total time typically consumed in the extraction step of the process is on the order of 2 shifts, or 16 hours. Following extraction, the aqueous raffinate is transferred to a separate tank and the pregnant organic phase is subsequently scrubbed and stripped in the same vessel.

Scrubbing. Since a relatively large amount of NaOH is added during a Cleanex extraction to neutralize excess acidity, sodium is usually the predominant metallic impurity. A very small portion of the sodium is extracted by the HDEHP; this amount can be reduced by scrubbing the pregnant organic with 0.03 N acid. A second function of the scrubs, and probably the most important function, is to flush the residual, unextracted impurities from the aqueous heel underlying the pregnant organic layer.

The pregnant organic phase is usually scrubbed twice with 0.03 N HCl (the first scrub is 0.03 N HNO₃ if the feed solution had been in the nitrate form). The volume of each scrub is one-third of the organic-phase volume. Each scrub is mixed with the organic phase by air-sparging at least 30 minutes. The scrub raffinates are usually combined with the extraction raffinate to provide a composite feed for a second-stage extraction.

Organic Phase Modification and Stripping. Iron is frequently a significant impurity in Cleanex feeds and, if present, will have been oxidized to Fe(III) by radiolysis and by the LiOCl that was added to the feed. The Fe(III) would tend to follow the transplutonium elements through the extraction and stripping steps. In order to retain the Fe(III) in the organic phase while the transplutonium elements are stripped, a solution of 1.6 M Adogen 364-HP (a straight-chain tertiary amine obtained from Archer Daniels Midland Co.) in diethylbenzene (DEB) is added to the pregnant Cleanex organic phase just before stripping. The amount of Adogen added is enough to make the organic phase 0.2 M in amine.

Following this modification of the organic phase, the transplutonium elements are stripped with 6 M HCl--0.5 M H₂O₂. The hydrogen peroxide in this strip solution overcomes the transient oxidizing effect caused by ionizing radiation acting on the HCl medium, thereby preventing oxidation of berkelium to the highly extractable tetravalent state. It is always necessary to strip the organic phase with several batches of strip solution in order to effect transfer of all of the transplutonium elements to the collection tank. Stripping coefficients for the transcurium elements are lower than for curium; thus, the amounts of californium remaining in the organic phase and in the aqueous heel solution (as indicated by gross neutron counts) are monitored to confirm the completeness of the stripping operations.

Additional Operating Considerations

Exposure of the Organic Extractant to Radiation. Radiolytic damage to the organic extractant is quite likely to occur since ^{244}Cm (2.83 watts/g) is present in the organic phase for a significant time. At TRU we generally try to hold planned exposures below 150 watt-hours/liter (6×10^7 rad). Thus, in the case of a feed containing enough ^{244}Cm to generate 5 watts/liter (in the organic phase), the extraction and scrubbing must be completed and stripping begun within 30 hours. We have not experienced any operating difficulties with Cleanex runs made under these conditions, but several samples of curium oxide product have been found that contained 5 to 8% phosphorus, presumably from radiolytic decomposition of the HDEHP. Potentially, the process of decomposition can form extractant species that behave quite differently from HDEHP and cause a variety of deleterious effects. Increasing difficulty in stripping has been observed on occasions when the exposure approached 200 watt-hours/liter.

Organic Phase Entrainment During Aqueous Phase Transfers. One advantage of batch solvent extraction processes is that adequate time can be allowed for the organic and aqueous phases to settle and separate. The aqueous (bottom) phase can then be transferred to a separate tank using a special phase-separator vessel. Although the phase-separator is very effective in preventing bulk transfer of the wrong phase, a small amount of the organic phase is frequently entrained in the aqueous phase. If the next processing step requires evaporation of the Cleanex product solution to a small volume, the entrained HDEHP could be decomposed to a tar which could sorb a significant amount of the actinide elements. When this possibility exists, the transfer of Cleanex product solution to the evaporator is made via a tank containing a few liters of organic diluent (DEB or Amsco) so that a second, cleaner phase separation can be made. Possible entrainment of the pure diluent into the product is of little consequence since the diluent will steam-distill out of the receiving tank during evaporation of the aqueous product.

Results

Typical results of the Cleanex process, as applied to a HFIR target processing campaign, are shown in Table I. Part A shows the quantities of the transplutonium elements found in a typical target campaign, and their behavior in the process. Part B shows the behavior of major fission products, while Part C shows the purification that can be obtained from common macroscopic contaminant ions. Note that the solute ions found in the second stage organic phase are usually stripped and accumulated as a rework fraction to be recycled to subsequent campaigns. The first stage organic phase and the second stage aqueous raffinate are discarded.

Table I. Typical Composition of Cleanex Feed Solutions When Processing Transplutonium Elements During a HFIR Target Campaign

Component	Amounts in Feed Solution	% Distribution to Exit Solutions			
		First Stage Product	Waste Organic	Second Stage Organic	Raffinate
<u>Part A: Transplutonium Elements</u>					
²⁴³ Am	0.1 g	95	<0.1	5	<0.1
²⁴⁴ Cm (Total Cm)	17 (50) g	95	<0.1	5	<0.1
²⁴⁹ Bk	35 mg	97	<0.1	3	<0.1
²⁵² Cf	400 mg	98	<0.1	2	<0.1
²⁵³ Es	2000 μg	99	<0.1	1	<0.1
²⁵⁷ Fm	0.8 pg	99	<0.1	1	<0.1

<u>Part B: Fission Products</u>					
⁹⁵ Nb	900 Ci		~100		
⁹⁵ Zr	900 Ci		~100		
^{103,106} Ru	2500 Ci	4	10	4	82
^{134,136,137} Cs	300 Ci				~100
¹⁴⁰ Ba	800 Ci	~50			~50
¹⁴⁰ La	800 Ci	~100			
^{141,144} Ce	3000 Ci	~100			
¹⁵⁶ Eu	1500 Ci	~100			
Gross Gamma	2 x 10 ¹⁵ c/m	45	10	2	43

<u>Part C: Macroscopic Impurities</u>					
Al	50 g	20	25	15	40
Cr	1 g				~100
Cu	1 g				~100
Fe	10 g		~100		
Na	~500 g ^a	3			97
Ni	10 g				~100
Mo	5 g		~100		
Pd	7 g				~100
Zr	5 g		~100		

^aSeveral hundreds of grams of Na, as NaOH, are added to neutralize the aqueous phase acidity.

Conclusions

The Cleanex process is particularly well suited to be carried out as a batch process. The extraction coefficients are strong functions of the aqueous-phase acidity; thus, for complete extraction, it is important to reduce the acidity to the minimum practical value. However, as the acidity is reduced, more of the solute ions extract into the organic phase, where they undergo a cation exchange reaction with the extraction reagent (HDEHP), thus releasing free acid. This free acid will back-extract into the aqueous phase, where it will strongly affect the extraction coefficient. A stepwise addition of NaOH allows one to "titrate" the free acid, achieving almost any desired degree of extraction. Furthermore, the precision of acid control that this affords allows one to control the reaction pathway so that certain extractable but easily hydrolyzed cations, such as Zr(IV), can be completely removed from the aqueous phase before the acid concentration is decreased to its final value. This significantly reduces the potential of these impurity ions to form interfacial cruds. Even if some crud is formed, and phase separation is thereby retarded, a batch extraction does not require a rapid phase separation and thus is tolerant of a very dirty solution.

In the environment of the TRU Facility at ORNL, the Cleanex process has proved to be extremely valuable and is routinely relied upon to perform a variety of separations and purifications.

Acknowledgment

This research was sponsored by the Office of Basic Energy Sciences, U.S. Department of Energy, under contract W-7405-eng-26 with the Union Carbide Corporation.

Literature Cited

1. Collins, E. D.; Bigelow, J. E. Proc. 24th Conf. Remote Syst. Technol., 1976, 130-139.
2. Brown, K. B.; Coleman, C. F.; Crouse, D. J.; Blake, C. A.; Ryon, A. D. "Solvent Extraction Processing of Uranium and Thorium Ores"; 2nd Int'l. Conf. on the Peaceful Uses of Atomic Energy, A/Conf. 15/P/509, Sept. 1958.
3. Chattin, F. R.; King, L. J.; Peishel, F. L. Proc. 24th Conf. Remote Syst. Technol., 1976, 118-129.
4. Weaver, B. S. Private Communication, May 1967.

RECEIVED May 14, 1979.

Work performed under U.S. Government contract number W-7405-eng-26.

Americium-Curium Separation by Means of Selective Extraction of Hexavalent Americium Using a Centrifugal Contactor

C. MUSIKAS, M. GERMAIN, and A. BATHELLIER

Division de Chimie, Département de Génie Radioactif, Centre d'Etudes Nucléaires de Fontenay-aux-Roses, BP N°6, Fontenay aux Roses, 92260, France

Americium-curium separations have always posed a challenge to chemists, mainly for two reasons :

- In the trivalent state Am and Cm have closely comparable chemical properties, due to the proximity of their ionic radii (0.99 and 0.986 Å).

Americium ions in the higher valency states (IV, V, VI, VII) are powerful oxidizing agents, and the known chemical processes for heterovalent actinide ion separations are not reliable because of the instability of Am ions in all valency states except (III). This paper deals with Am (VI) - Cm (III) separation in nitrate media. Three topics are examined in order to improve the performance of this process.

- The kinetics of oxidation of Am (III) by sodium persulfate in the presence of Ag^+ ions were reinvestigated by studying the effect of additions of small amounts of reagents which do not drastically change the distribution coefficients of Am (VI) or Cm (III) ions.

Organo phosphorus solvents were selected because they are radiation resistant, possess weak reductant properties and that their affinity for hexavalent ion is high.

The operating procedure was selected by consideration of the results of the two previous investigations. This can be done by using a centrifugal contactor enabling it to set organic-aqueous phase contact time in accordance with the kinetics of extraction of Am (VI), oxidation of Am (III) in aqueous phase, and reduction of Am (VI) in organic phase.

EXPERIMENTAL

Reagents

- Extractants and diluent
bis (2 ethylhexyl)phosphoric acid (HDEHP) and tri n octylphosphine oxide (TOPO) were analytical grade
bis (2,6 dimethyl 4 heptyl)phosphoric acid (HD(DIBM)P) was

0-8412-0527-2/80/47-117-157\$05.00/0

© 1980 American Chemical Society

prepared and purified by IRCHA (France)

the alcohol used in this synthesis was provided by Touzard & Matignon.

HDEHP and HD(DIBM)P were determined by titration with standard Na OH solution, TOPO concentration was obtained by nitric extraction.

- Hyfrane 130 was used as diluent (obtainable from Hyfrans a, Boussens 31 France); it is a mixture of n paraffins ranging from C₁₀ to C₁₃ (boiling point 190-230 C; specific gravity 0.755-0.760; viscosity at 20°C 1.96 cS).

The remaining reagents, nitric acid, perchloric acid, phosphoric acid, sodium persulfate, silver nitrate, uranyl nitrate, etc... were analytical grade (Prolabo-NORMAPUR).

Pure²⁴¹Am and ²⁴⁴Cm were obtained from the SPT specialized laboratory (Fontenay aux Roses) and were measured by radiometric methods.

Equipment and Procedures

Kinetic Studies. The oxidation of Am (III) was observed by spectrophotometry by measuring optical densities at 503 nm.

Am (VI) and Am (V) were characterized by their absorption peaks at 990 to 1010 nm, and, 715 to 720 nm respectively.

The following procedures were utilised :

Oxidation of Am (III) : One aliquot of Am (III) nitrate stock solution was dried under an infra red lamp, and the dry solid was dissolved in a measured volume of the appropriate solution and transferred to the thermostatically-controlled spectrophotometric cell. The stability of Am (VI) in organic phases was examined by spectrophotometry by observing the absorption peak of Am (VI) in the region 990-1010 nm. All the spectrophotometric studies were carried out with a Cary 17 spectrophotometer.

Extraction Studies. A centrifugal contactor (EC 8-1) was designed for laboratory scale mass transfer and process purification studies. This is a single stage extractor with rotating plexiglas bowl, designed to allow visual observation of mixing and settling zones.

"Figure 1" shows the two phases paths in the extractor. The mixing chamber has a volume of 1 cm³, while total hold-up of the contactor is 8 cm³. In experiments 3 and 4, the volume of the settling chamber was increased to 10 cm³ to prevent entrainment of the phases.

These contactors can be interconnected by special tubings to allow temperature monitoring and sampling "figure 2". They are pump fed with the phases and flow rates are regulated by passage through a damping out system. Speed of rotation was 3600 rev/min (centrifuge field at the level of interface 200 g) and temperature was 21 ± 2°C. For test runs, several extractors were used in the following conditions :

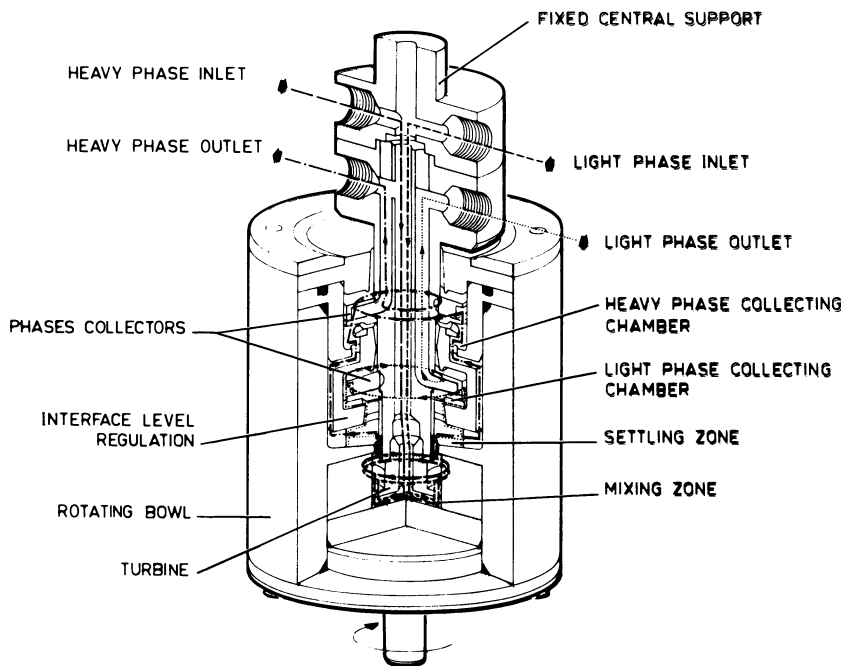


Figure 1. Flow diagram of phases in the EC 8-1 extractor

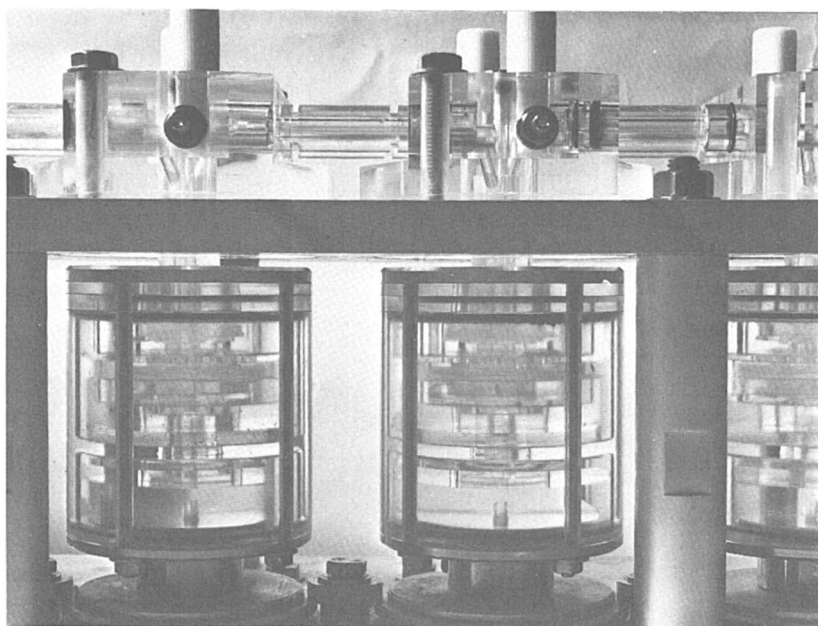


Figure 2. View of 3 centrifugal contactors connected by tubing

Experiments 1 and 2 : Three extractors were used. Runs 1a and 2a used one extraction stage and two scrub stages, flow ratios (O/A) were 1.05 for extraction and 1.37 for scrub. Runs 1b and 2b used three extraction stages and a flow ratio of 4.5. The aqueous phase had the following composition :
 0.2 N HNO_3 , $4.1 \cdot 10^{-3}$ M Am (III), $4 \cdot 10^{-5}$ M Cm (III), 0.1 M $\text{Na}_2\text{S}_2\text{O}_8$, 10^{-2} M AgNO_3 , 10^{-2} M H_3PO_4 .

Experiment 3 : In both runs three extractors were used for extraction and two (3a) or three (3b) were used for scrub. Flow ratios were 2 for extraction and 4 for scrub. Americium and curium concentrations were respectively 0.001 and $8 \cdot 10^{-6}$ M, and all remaining aqueous reagent concentrations were similar to experiments 1 and 2.

Experiment 4 : 3 extraction stages and 3 scrub stages were used. Flow ratios were respectively 4 and 16. All aqueous concentrations were similar to those used in experiment 3, except for the H_3PO_4 concentration, which was $3 \cdot 10^{-2}$ M in experiment 4b.

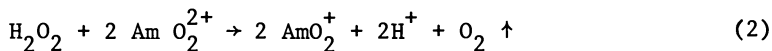
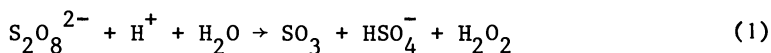
Solvents were pretreated with scrub solution : in experiments 1 and 2 the contact was achieved in a centrifugal contactor (mixing time 4 seconds), while in experiments 3 and 4, it was achieved during 5 min in a separatory funnel.

Before each run, the extractors were rinsed for 30 minutes, with the solutions (without Am and Cm) at nominal flow rates.

RESULTS AND DISCUSSION

Oxidation Kinetics of Am (III)

It is well known (1, 2, 3) that persulfate can oxidize Am (III) to Am (VI). The reaction kinetics are slow and Ag^+ is required as a catalyst. The kinetics depend on different factors and Table I shows the present status of the literature. It must be stressed that for acidities above 0.5 N (4), persulfate reduces Am (VI) according to the mechanisms shown in equations (1) and (2).



In accordance with the suggested interpretations (5) of the effects of silver ions on the kinetics of oxidation by persulfate ions, the oxidation of Am (III) occurs according to equations (3) and (4).

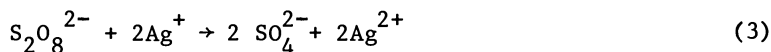
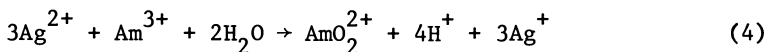


Table I. Factors which influence the Am (III) oxidation rate by mixtures of $S_2O_8^{--}$ and Ag^+ ions.

Factor	Observation	Temperature °C	Medium	Half time of reaction (minutes)	Reference
Am (III)	First order reaction when other reagents concentrations are constant	50	0.02 M $S_2O_8^{--}$ 0.001 M Ag^+ 0.06 N HNO_3 $\mu = 0.5$	70	(3)
$S_2O_8^{--}$	first order reaction	50	0.001 M Ag^+ 0.06 N HNO_3 $\mu = 0.5$	10	(3)
Ag^+	rate constants increase linearly with Ag^+ concentration	50	0.02 M $S_2O_8^{--}$ 0.06 N HNO_3 $\mu = 0.5$	divided by eight going from 0 to 0,001 M $AgNO_3$	(3)
H^+	rates decrease with acidity no oxidation is obtained above 0.5N H^+	60	0.02 M $S_2O_8^{--}$ 0.001 M Ag^+ $\mu = 0.5$		(1), (2), (3).
Temperature	enthalpy and entropy of activation are 18.9 kcal mole ⁻¹ and 2.2 e.u.				(3)



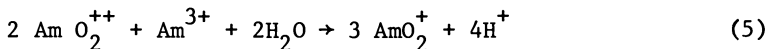
Reaction (4) is rate limiting in most cases, consequently the nature of the silver (II) species is liable to affect the oxidation kinetics considerably.

We examined the effects of non-oxidizable complexing agents on the oxidation kinetics of Am (III). "Figure 3" shows the effect of small additions of phosphoric acid or sodium bisulfate on the oxidation rate of Am (III) at room temperature. The two reagents are effective in accelerating the oxidation of Am (III). Moreover, their presence solubilizes the argentic oxide which begins to precipitate at the acidity used. Solubilization probably results from the known complex formation between Ag^{2+} ions and sulfate (6) or phosphate anions (7). Charge changes in silver (II) complexes are probably responsible for the variations in oxidation rates of Am (III). The additions of phosphoric acid or sodium bisulfate in the concentration range used here has no effect on the absorption spectra of Am (III) and Am (VI), and there is probably no drastic change in the Am species.

This conclusion is supported by calculations of the free Am ion concentrations, taking into account the values of formation constants of sulfate or phosphate complexes given in the review of L.G. Sillen et al. (8).

Contrary to the authors of (3), we found that Am (III) oxidation is not a first order reaction with respect to Am (III) ions. While the oxidation rate does accelerate at low concentrations of Am (III), this acceleration can probably be attributed to reaction (5), which is thermodynamically possible, as it may be calculated from the formal oxidation potentials of Am (VI)/Am (V) and Am (V)/Am (III) couples (9).

The further oxidation of AmO_2^+ ions by Ag^{2+} is a fast reaction at room temperature (10).



The formal kinetics law of equation (6) shows the influence of Am (VI) concentration on the process of oxidation of Am (III)

$$-\frac{d(\text{Am (III)})}{dt} = k_1 (\text{Am (III)}) \cdot (\text{Ag (II)}) + k_2 (\text{Am (III)}) \cdot (\text{Am (VI)})^2 \quad (6)$$

The disagreement with the results of Ohyoshi et al (3) can be ascribed to the differences in concentrations of Am (III) used in the two works (10^{-7} M against 10^{-3} M). The influence of ionic strength on oxidation rate was studied in order to confirm the suggested explanation of phosphate and sulfate effect on the kinetic rates. "Figure 4" shows how the Am (III) oxidation rate varies with the ionic strength with and without phosphoric acid. We attempted to adjust these results to the Bronsted equation (7), which correlates the rate constants of a reaction with the reagent

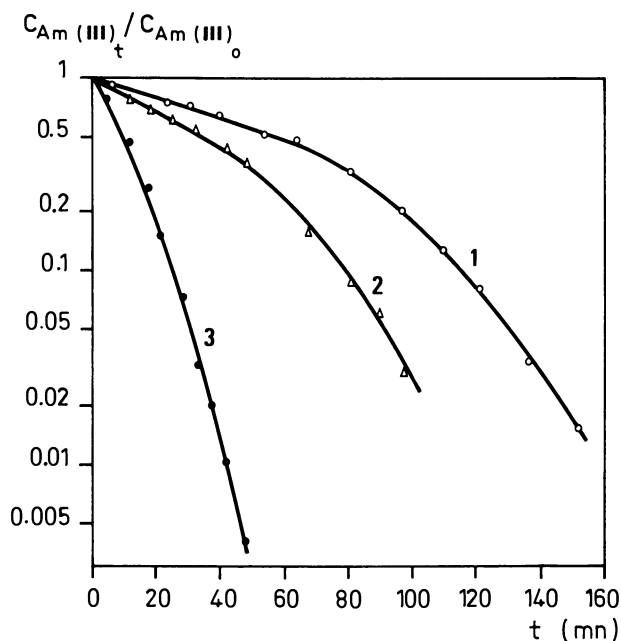


Figure 3. Effect of NaHSO_4 and H_3PO_4 on the oxidation kinetics of Am (III) ions at 25°C : (1) 0.2N HNO_3 , $0.1\text{M Na}_2\text{S}_2\text{O}_8$, 0.01M AgNO_3 , 0.001M Am (III) ; (2) same as 1 + 0.04M NaHSO_4 ; (3) same as 1 + $0.03\text{M H}_3\text{PO}_4$.

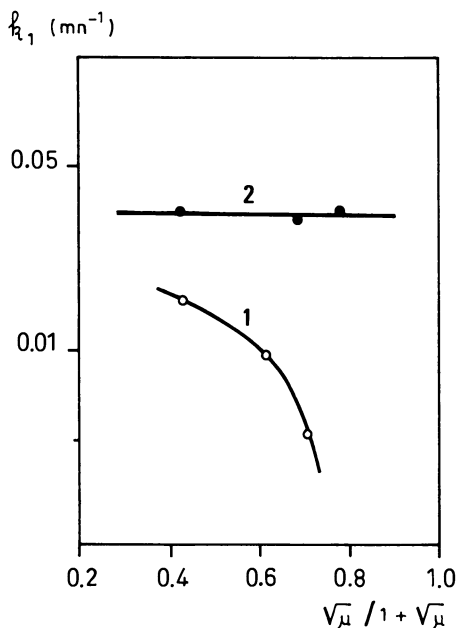


Figure 4. Effect of the ionic strength on oxidation kinetics of Am (III) at 25°C : (1) 0.2N HClO_4 , $0.1\text{M Na}_2\text{S}_2\text{O}_8$, 0.01M AgNO_3 , 0.001M Am (III) , NaClO_4 variable; (2) same as 1 + $0.03\text{M H}_3\text{PO}_4$.

charge and the ionic strength of the solution.

$$\log k_1 = B + 1.08 z_A \cdot z_B \sqrt{\mu} / (1 + \sqrt{\mu}) \quad (7)$$

where k_1 is the rate constant (in the present case we took the pseudo first order constant in Am (III) found at the origin of the curves in figure 4).

B is a constant related to the formation constant of the activated complex.

z_A and z_B are the charges of the ions reacting to give the activated complexes.

μ , the ionic strength is defined as $1/2 \sum z_i^2 \cdot C_i$ where z_i and C_i are the charge and the concentration of the ions present in the solution.

The results show that in the presence of 0.03 M phosphoric acid one is dealing with a reaction between a neutral and a charged species. As Am (III) is positively charged this means that the oxidizing complexes are neutral, and may be $\text{Ag}(\text{H}_2\text{PO}_4)_2$. Without phosphoric acid it seems that one is dealing with a reaction between two species with opposite charges, implying that Ag (II) is probably present as anionic species, at least at high ionic strengths, where AgO is completely dissolved. The spectrophotometric results of Rechnitz et al suggest the existence of such species (10).

In conclusion, we can state that additions of small amounts of phosphoric acid increase the rate of Am (III) oxidation by Ag^{2+} ions without drastically changing the distribution coefficients of the species involved, because no complexation of Am occurs in these solutions, contrary to what occurred in the extensive studies of Myassoeodov et al. (12, 13) in more concentrated phosphoric acid, where the kinetic effects must be attributed to changes in americium and silver (II) ionic species. In our Am-Cm separations we added phosphoric acid, which accelerates the oxidation rates of Am (III), solubilizes argentic oxide, and makes it possible to obtain Am (VI) quantitatively and rapidly at room temperature.

Am (VI)-Cm (III) Separation by Solvent Extraction

The extraction of hexavalent americium has been studied by several authors (14, 15, 16). In order to optimize the Am (VI)-Cm (III) separations, we reinvestigated the extractive properties of four oxidation-inert organo-phosphorus solutions :

- HDEHP in hyfrane 130
- TOPO in hyfrane 130
- mixtures of HDEHP and TOPO in hyfrane 130
- HD(DIBM)P in hyfrane 130

The distribution coefficients of UO_2^{++} and Am^{3+} ions were measured between these solvents and aqueous phases in 0.2 N nitric acid

and the more significant results are given in Table II.

TABLE II
 UO_2^{++} and Am^{3+} distribution coefficients with various solvents

D	Solvent			
	0.05 M TOPO	0.03 M HDEHP	0.0075 M HDEHP 0.0075 M TOPO	0.1 M HD(DIBM)P
$D_{UO_2^{++}}$	40	26	210	17
$D_{Am^{3+}}$	$7 \cdot 10^{-1}$	$1.5 \cdot 10^{-2}$	$1.5 \cdot 10^{-2}$	$3.4 \cdot 10^{-4}$
$\alpha = D_{UO_2^{++}}/D_{Am^{3+}}$	57	1,730	14,000	50,000

It appears that separation factor $\alpha = D_U(VI)/D_{Am}(III)$ is higher using HD(DIBM)P and mixtures of HDEHP, TOPO. The results concerning HD(DIBM)P are in agreement with those of Mason et al. (15) who attribute the increase in separation factors to steric hindrance for the extraction of the trivalent ions. With the mixture HDEHP, TOPO a synergistic effect is observed for U (VI) but not for Am (III). The maximum of $D_U(VI)$ occurs with equimolar mixtures "Figure 5". This fact suggests that the extracted species is $UO_2H(DEHP)_2(TOPO)_2(NO_3)$ or $UO_2(DEHP)(TOPO)NO_3$. Synergistic extractions of U (VI) with HDEHP, TOPO mixtures have been reported by Blake et al. (17) from aqueous sulfuric acid solutions, and by Bunus et al. (18) from phosphoric acid solutions. In these two cases, the maxima of $D_U(VI)$ occur at different proportions of extractant, revealing the effect of the ligands present in aqueous solutions on the nature of the extracted species. The depressive effect of oxidizing reagents on the distribution coefficients of U (VI) is shown in Table III, with the apparent distribution coefficients of Am (VI) obtained in batch experiments. It may be seen that once again the best Am (VI)-Am (III) separation factors are obtained with HD(DIBM)P and the synergistic mixtures. Reduction rates of Am (VI) in the solvents TOPO and HDEHP are shown in "figure 6". The distribution coefficients which correspond to chemical equilibrium, are modified in transient systems involved with the short contact time possible in centrifugal contactor.

Typical extraction curves obtained in our laboratory scale apparatus show that Murphree's efficiency (E) varies with the nature of the solvent and with mixing time "figure 7". From the linear dependence of $E/1-E$ on mixing time, it may be concluded that our centrifugal contactor can be assimilated to a perfectly stirred continuous reactor of which the characteristic equation is (19)

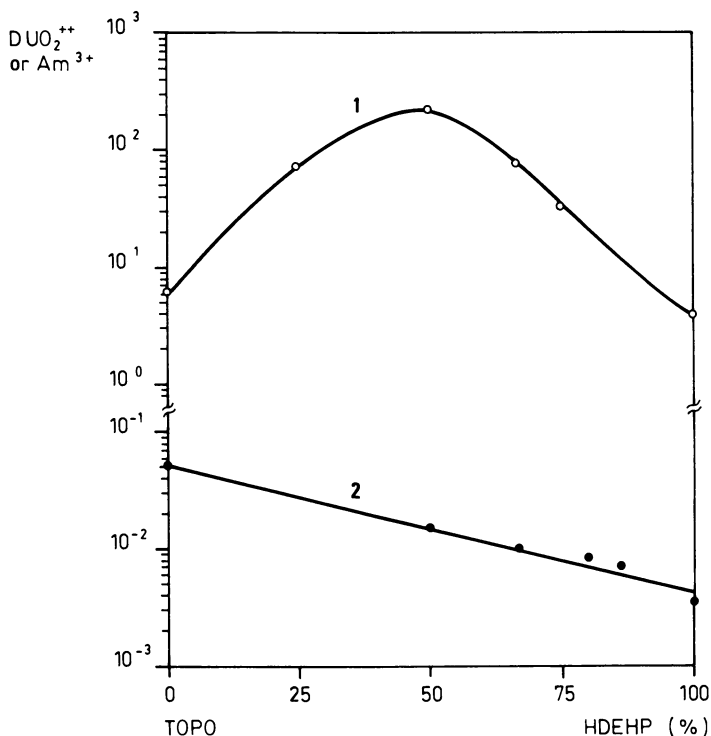


Figure 5. UO_2^{2+} and Am^{3+} extraction with 0.015M (HDEHP + TOPO): (1) aqueous initial concentrations $4.2 \times 10^{-4}M$ UO_2^{2+} , 0.2M HNO_3 , phase ratio O:A = 1, temperature 21°C, (2) aqueous initial concentrations $2 \times 10^{-5}M$ Am^{3+} , 0.2M HNO_3 , phase ratio O:A = 1, temperature 21°C.

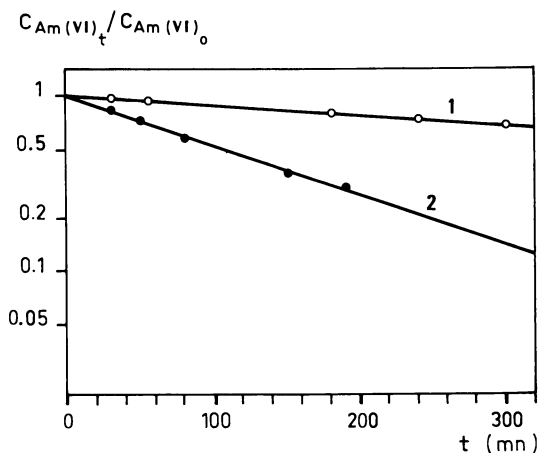


Figure 6. $Am(VI)$ concentration in organic phases as a function of time: (1) 0.15M HDEHP in hyfrane 130; (2) 0.03M TOPO in hyfrane 130.

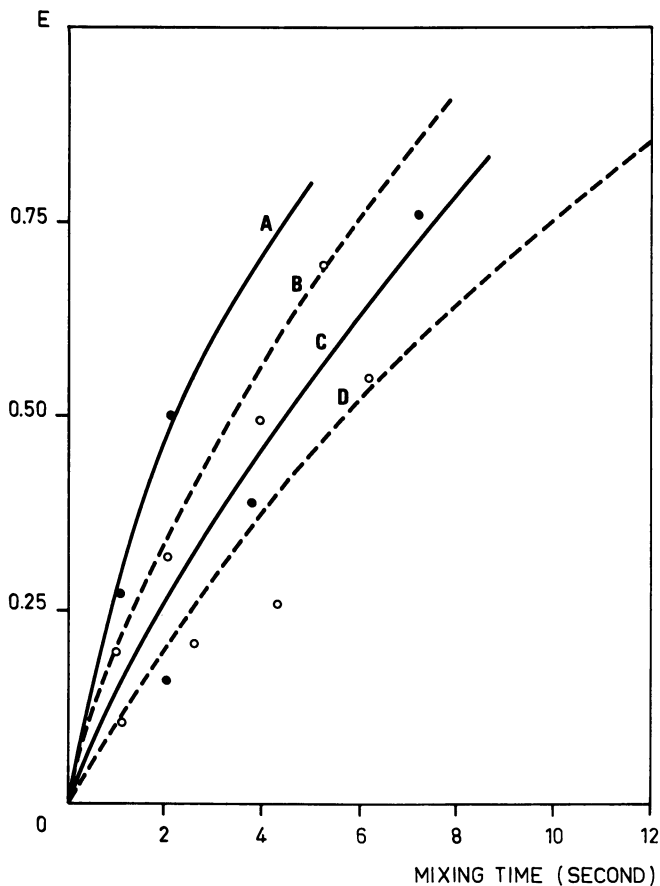


Figure 7. Dependence of Murphree's efficiency on phase contact time; centrifugal contactor EC 8-1, speed of rotation 3600 rpm, temperature 21°C: (A) solvent: 0.0375M HDEHP + 0.0375M TOPO, cation: AmO_2^{++} + oxidizing reagents; (B) solvent: 0.05M TOPO, cation: UO_2^{++} + oxidizing reagents; (C) solvent: 0.05M TOPO, cation: AmO_2^{++} + oxidizing reagents; (D) solvent: 0.05M HDEHP, cation: UO_2^{++} + oxidizing reagents.

TABLE III
Influence of oxidizing reagents on uranium (VI) and americium
distribution coefficients.

	0.05 M TOPO	0.015 M HDEHP + 0.015 M TOPO	0.2 M HD(DIBM)P
$D_{UO_2^{++}}$	40	400	25
$D_{UO_2^{++}}$ + oxidizing reagents	14	27	--
$D_{AmO_2^{++}}$ + oxidizing reagents	7	7	2.10^{-1}
$D_{Am^{3+}}$	7.10^{-1}	7.10^{-2}	$4.6.10^{-4}$
$\alpha = D_{AmO_2^{++}}/D_{Am^{3+}}$	10	100	434

$$(k.a) = \frac{\beta}{T} \frac{E}{1-E}$$

where (k.a) is the apparent overall mass transfer coefficient and β

$$\beta = \frac{FA}{FA + FO} \quad \text{is the flow ratio, } T \text{ mixing time}$$

Apparent overall transfer coefficients were calculated and used to compare the extraction kinetics of the various systems (Table IV). Although some scattering was observed, it appears that all extractions are rapid and that no significant differences can be noted between the solvents.

TABLE IV
Apparent overall transfer coefficients in second⁻¹

aqueous \ organic	0.05 M HDEHP	0.05 M TOPO	0.015 M HDEHP 0.015 M TOPO	0.1 M HD(DIBM)P
UO_2^{++}	----	0.053	----	0.090
UO_2^{++} + oxidizing reagents	0.051	0.15	0.018	0.014
Am^{3+}	----	----	very high	very high
AmO_2^{++} + oxidizing reagents	----	0.13	0.13	----

Americium-Curium Separation Runs

HDEHP, TOPO, (HDEHP + TOPO) and HD(DIBM)P were tested using several contactors installed as indicated in "figure 8". The experimental conditions of the runs are given in the experimental section and the results are summarized in Table V.

In experiment 1 runs (1a and 1b) where 0.03 M TOPO is the solvent, we observe that without scrub section decontamination factors (DF) Am/Cm is 24 and DF Cm/Am is 14.5, while with two scrub stages (1a), DF Am/Cm increases to 230 and DF Cm/Am falls to 1.7.

DF Am/Cm increases as anticipated when scrub stages are used, while the drop in DF Cm/Am is greater than calculated and results mainly from the presence of hexavalent americium in the raffinate, instead of the AmO_2^+ - Am^{3+} mixture prevailing without a scrub section.

In experiment 2 (2a and 2b) with HDEHP, as with TOPO, the replacement of two extraction stages by two scrub stages causes :

DF Am/Cm increase from 5 to 220

DF Cm/Am decrease from 13 to 8

A comparison of runs 1a and 2a shows that DF Am/Cm are nearly equal while DF Cm/Am is higher with HDEHP, although the aqueous raffinate still contains traces of hexavalent americium. Hence to obtain purer americium and to reduce americium losses, it was decided to increase the number of scrub stages and, in the extraction section, the number of stages and the extraction factor ($\text{Ex} = \frac{\text{DxFO}}{\text{F}_A}$)

The synergistic mixture (HDEHP + TOPO) was used in Experiment 3 (runs 3a-3b). The DF Cm/Am values obtained were very similar (7 and 7.5) and not higher than previously, while DF Am/Cm are respectively 1,300 and 6,100 with two and three scrub stages. The aqueous raffinate was found to contain hexavalent and trivalent americium (the apparent distribution coefficient in the final extraction stage was 0.2).

HD(DIBM)P (Experiment 4) permits the best purification of americium (DF Am/Cm 18,750) while DF Cm/Am remains close to 7. An aqueous acidity decrease, which was expected to increase DF Cm/Am, has no effect, but causes a drop in DF Am/Cm, probably due to higher curium extraction.

These results suggest that, whatever the solvent, when scrub stages are used, DF Cm/Am remains unchanged if the number of extraction stages is greater than one ($\text{DF} \approx 7$), DF Am/Cm increases with the selectivity of the solvent and the number of scrub stages. The limited extraction of americium results from the unextractable valency state AmO_2^+ , Am^{3+} formed by chemical and radiochemical reduction. From the data in reference (20) it appears that the latter should be very limited in our conditions, so that it is probable that chemical reduction in the organic phase is responsible for poor americium extraction. Experimental reduction rates estimated from the test runs, given in Table VI, show only slight differences

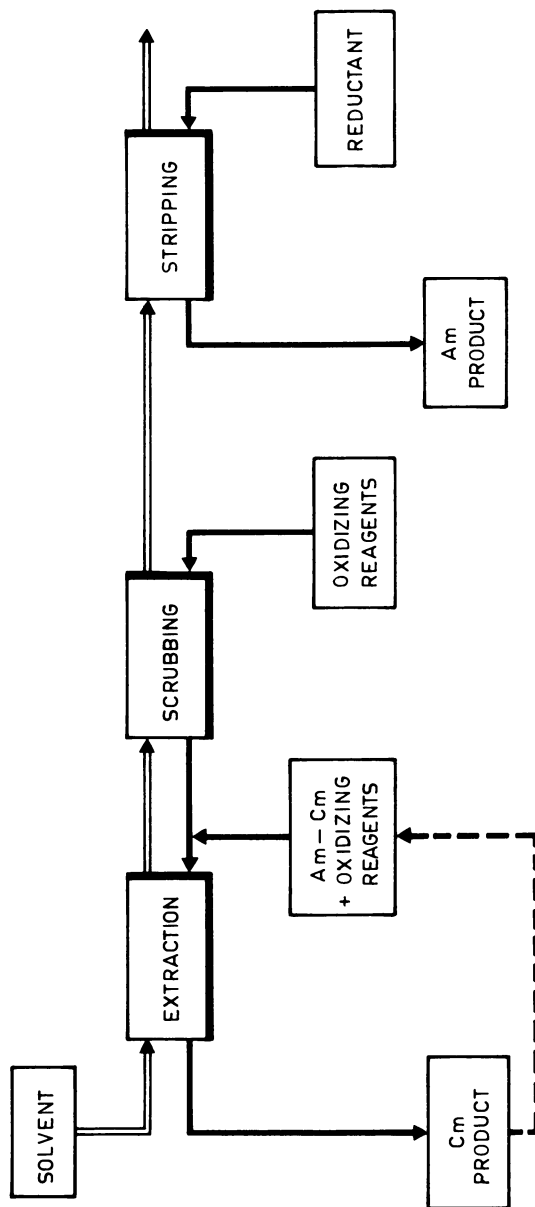


Figure 8. Flowsheet of the process used for Am-Cm separation.

Table V. Results of Am/Cm separation runs in centrifugal contactor.

experiment	solvent	Initial Conditions				Results DF	
		extraction stages	scrub stages	total residence time (s)	H ⁺ feed	Am/Cm	Cm/Am
1	1a	1	2	102 s	0.2 M	230	1.7
	1b	3	----	147 s	0.2 M	24	14.5
2	2a	1	2	102 s	0.2 M	220	8
	2b	3	----	147 s	0.2 M	5	13
3	3a	3	2	216 s	0.3 M	1,300	7
	3b	3	3	244 s	0.3 M	6,100	7.5
4	4a	3	3	208 s	0.26 M	18,750	7.1
	4b	3	3	208 s	0.06 M	3,480	6.7

TABLE VI
Apparent reduction rates of AmO_2^{++}

Experiment	Run	Solvent	Reduction rate in % per min of residence in the organic phase	Observed valency
1	1a	0.03 M TOPO	4.3	AmO_2^+ , Am^{3+}
2	2a	0.15 M HDEHP	4.7	Am^{3+}
3	(3a + 3b)	0.015 M TOPO 0.015 M HDEHP	5.4	Am^{3+}
4	(4a + 4b)	0.2 M H(DIBM)P	6.4	-----

between the solvents, and it may be noted that AmO_2^+ is observed with TOPO. However, curium purification was improved by a second extraction cycle carried out with the aqueous raffinate, which had been stored long enough (1-2 hours) to allow Am^{3+} reoxidation at room temperature. With (HDEHP + TOPO) as solvent, we compared the DF Cm/Am obtained in the first and second extraction cycles.

These values are respectively 7 and 4 (runs 3a and 3a') and 7.5 and 4.6 (runs 3b and 3b'). Although the efficiency of the second cycle is lower than that of the first, the two cycles provided overall DF Cm/Am of 28 (3a-3a') and 34.5 (3b-3b').

Supplementary extraction cycles should increase these DF Cm/Am.

Acknowledgement

We are grateful to Mrs RANARIVÉLO H, MARTEAU M, PLUOT P. and LAMOTTE C. for technical assistance.

Literature Cited

1. Penneman, R.A.; Asprey, L.B. "Proceedings of the International Conference on the Peaceful Uses of Atomic Energy" ; 1955, 7, 359 United Nations New York N.Y., 1956.
2. Ermakov, V.A. ; Rykov, A.G. ; Timofeev, G.A. ; Yakovlev, G.N. Radiokhimiya, 1971, 13, 6, 826
3. Ohyoshi, A. ; Jyo, A. ; Kanaya, T. ; Shinohara, T. Radiochem. Radioanal. Lett. 1971, 7, 1, 7
4. Rykov, A.G. ; Ermakov, V.A.; Timofeev, G.A.; Chistyakov, V.M. ; Yakovlev, G.N. Radiokhimiya 1971, 13, 6, 832.
5. House.D.A. Chemical Review 1962, 62 , 185.
6. Rechnitz, G.A. ; Zamoheick, S.B. Talanta 1964, 11, 1645.
7. Rechnitz, G.A. ; Zamoheick, S.B. Talanta 1965, 12, 479.

8. Sillén, L.G.; Martell, A.E. Stability constants. Special publication n°17 and 25. The Chemical Society. London 1964 and 1971.
9. Musikas, C. in Gmelin Handbuch der Anorganischen Chemie Band 21 Transurane D 1 von Günter Koch Springer-Verlag 1975 chap. 2.
10. Asprey, L.B.; Stephanou, R.A.; Penneman, R.A. J. Am. Chem. Soc. 1951, 73, 5715.
11. Rechnitz, G.A.; Zamochvick, S.B. Talanta 1964, 11, 713.
12. Myasoedov, B.F.; Lebedev, I.A.; Milyukova, M.S. Transplutonium 1975, W. Müller, R. Lindner editors, North-Holland/American Elsevier, 1976, p.311.
13. Milyukova, M.S.; Litvina, M.N.; Myasoedov, B.F. Radiokhimiya, 1977, 19, 3, 349.
14. Hulet, E.K. J. Inorg. Nucl. Chem. 1970, 26, 1721.
15. Mason, G.W., Bollmeier, A.F., Peppard, D.F. J. Inorg. Nucl. Chem. 1970 32, 1011.
16. Myasoedov, B.F. Radiokhimiya, 1974, 16, 5, 716.
17. Blake, C.A.; Horner, D.E.; Schmitt, J.M. 1959 ORNL 2259.
18. Bunus, F.T.; Domocos, V.C.; Dimitrescu, P. J. Inorg. Nucl. Chem. 1978 40, 117.
19. Bergeonneau, Ph.; Jaouen, C.; Germain, M.; Bathellier, A. Int. Solv. Ext. Conf. 1977 Toronto, CEA-CONF 4151.
20. Weaver, B. 1963 ORNL 3496, p.44.

RECEIVED July 13, 1979.

National Program for Pyrochemical and Dry Processing of Spent Reactor Fuel

C. H. BEAN and M. J. STEINDLER

Chemical Engineering Division, Argonne National Laboratory, Argonne, IL 60439

The current national nuclear energy policy makes it important to develop alternative reactor-fuel recycle systems that will reduce the risk of nuclear weapons proliferation. A viable nuclear power system for supplying national energy needs includes the reprocessing of spent fuel. The availability of reprocessing systems that reduce the risk of proliferation of nuclear weapons is, therefore, an integral part of the continued use of nuclear power within the confines of national policy. In June, 1977, the ERDA Division of Waste Management, Production, and Reprocessing outlined a fuel cycle program that supports the national nuclear energy policy. This program included effort to develop pyrochemical and dry processing methods. Argonne National Laboratory was requested to act as the lead laboratory for this development. The program has the objective of demonstrating the feasibility of selected processes applicable to a variety of fuels and reactor fuel cycles in order to ensure availability of technology that is compatible with the need for safe and reliable nuclear power generation. The Pyrochemical and Dry Processing Methods (PDPM) Program is aimed at reprocessing systems that meet this need. The PDPM Program is, therefore, directly in support of the national policy on the use of nuclear energy.

Program Description

Initially, the objective of the PDPM Program was to develop processing technology applicable to converter and fast-reactor fuel-cycle systems which meet nonproliferation criteria and technical, safety, and economic guidelines. Subsequent decisions by DOE have narrowed the scope of the PDPM Program to those fuel cycles that may be applied to fast breeder reactors. The processing technology should be applicable to candidate thorium-uranium and plutonium-containing fuels. The program should be capable of

0-8412-0527-2/80/47-117-177\$05.00/0
© 1980 American Chemical Society

identifying and developing to the stage of demonstrated feasibility those processes that can result in products usable in reconstituted fuel and that meet selected criteria regarding proliferation risks.

Included in the objectives of the PDPM Program is assurance of the availability of materials of construction needed for the processes. Suitable materials for crucibles, vessels, transfer piping, pumps, and other equipment will have to be developed, tested, and selected for use in the processing system.

Aqueous reprocessing methods have been developed to effect an efficient and thorough separation of fissile elements from the contaminating fission products in spent fuel(1). While these processes may be altered to yield a proliferations-resistant product by coprocessing or by the addition of radioactive material that will contaminate the clean fissile material, it still is necessary to safeguard some of the process steps to ensure that material useful in nuclear weapons will not be diverted (3). The safeguard requirements and the ease of subversion of such provisions make many versions of the conventional processes subject to unacceptable proliferation risks.

Some of the pyrochemical processes have more potential for being proliferation resistant because of the great similarity of the chemistry of uranium, plutonium, and some of the fission products in the chosen systems. Ordinary processes are designed to maximize differences in chemical behavior in order to separate constituents. For some of the pyrochemical processes the chemical equilibria are such that partial separations are possible but complete separations are thermodynamically limited. For example, excess uranium can be separated from plutonium by precipitation in a molten metal such as zinc only until both are present in about equal quantities in solution, but no further (3, 4). Likewise, the solubility of fission products is selectively limited. Only a portion of elements such as ruthenium will stay in solution and be removed (5). The majority of the ruthenium precipitates with the actinides. A complete separation is again thermodynamically limited. As a result only a modest dependence needs to be placed on process equipment and facility design for proliferation resistance.

Although the retention of selective fission products in fissile materials may not adversely affect the performance of fuel in a reactor, the intensity of the gamma radiation is such that the fissile material must be handled, transferred, and fabricated remotely. As a result, it is both technically difficult to divert the fissile material and fabricate a weapon, and nearly impossible to do so without detection. The levels of residual radioactivity in the product of some of the pyrochemical or dry processing methods is close to that found in spent unprocessed fuel and hence the reprocessed product presents a risk to proliferation only trivially less than that of spent fuel. Pyrochemical and dry processing methods can be used that will

selectively remove undesirable fission products and still retain sufficient radioactive material that fissile material will be resistant to proliferation whether or not the fissile elements are separated from one another. Little or no safeguards other than what is applied to spent fuel need be provided to pyrochemical processes that are incapable of producing a clean separation of fissile elements without the retention of highly radioactive fission products. This aspect of proliferation resistance of pyrochemical or dry processes permits the export of reprocessing technology that could satisfy the need for closing the fuel cycle in other countries while minimizing the risk that weapons can be immediately produced from materials in the fuel cycle facilities, including the fuel fabrication plant.

Pyrochemical and dry reprocessing methods are relatively easily adapted to modest scale operation and hence are amenable to close-coupling with reactors. This aspect has been demonstrated at EBR-II (6) and is probably most suitable to fast breeder reactors.

The potentially desirable attributes that justify the development and application of PDPM processes to spent fuel reprocessing under current nonproliferation policies are summarized as follows:

1. Nonproliferation Attributes. (a) Processes can accommodate high radiation fields and short-cooled fuel, thereby minimizing the need for extensive inventory of spent fuel in storage; (b) fissile components are contaminated by residual fission products and actinides, reducing access to the material and increasing detectability of diversion; (c) close-coupling of processing, fabrication, and reactor facilities reduces reliance on transportation in the fuel cycle.

2. Processes are Applicable to Various Fuels, Fuel Cycle, and Breeder Reactor Types. (a) Processes may be applied to thorium-uranium, uranium-plutonium, thorium-plutonium, or thorium-uranium-plutonium fuels; (b) the types of fuel that can be processed include metal, oxides, or carbides; (c) fuel from FBR core or blanket can be processed.

3. Favorable Economics. (a) The economics of a small scale reprocessing facility (0.1 to 1.0 Mg/day) favors PDPM because of the concentration of material in process thus minimizing plant size; (b) the capability for processing short-cooled fuel reduces the turn-around time in the fuel cycle with a corresponding reduction in inventory costs; (c) the elimination of conversion steps at the head-end and for the final product may reduce overall processing costs relative to aqueous processes.

4. Minimum Waste Handling. (a) Wastes that are produced are in a solid form, some of which require minimum treatment for packaging, shipment, and storage.

5. Sound Resource Utilization. (a) Plutonium can be safely recycled without risk of proliferation instead of being discarded. (b) Rapid recycle of short-cooled fuel reduces the total demand for fissile material in the fuel cycle.

6. Product Amenable to Fabrication. (a) Products from PDPM may be available to a fabricator as either oxide, carbide, or metal. (b) Process controls may yield products with the characteristics desired for optimum fabricability.

7. Minimum of Safeguards. (a) Processes that are incapable of producing fissile material in a pure form, or with a high enrichment of fissile isotopes, or with a high level of decontamination may require little or no added safeguards except for protection from sabotage.

8. Process is Exportable. (a) The combination of proliferation-resistant processing, compactness of plant, and minimum need for safeguards make PDPM processing attractive for export to other countries.

The implementation of the PDPM Program was planned to provide several successive points at which the future course of the program could be assessed and subjected to potential redirection. This is particularly appropriate during the first few years during which ten processes were picked for initial evaluation.

During the initial phase of the program, all process and materials developments were treated in the same way. A review of pertinent experience and literature to establish technical feasibility was followed by the development of a process outline that included flow sheets, expected behavior of important elements, and available engineering information. The preliminary process outlines focused the chemical ideas for processing on identified fuels, waste, and products. The outlines also identified the uncertainties and information gaps that challenged the feasibility of the process. These deficiencies constituted the basis for initial experimental programs once the decision to pursue a particular flow sheet was made. At the conclusion of the first year's effort, four of the initial processes selected for evaluation were eliminated as a result of program redirection and process difficulties.

In the second (or development) phase, effort in the process types being pursued consists largely of laboratory experimental work and engineering scale-up aimed at providing process information. This activity includes experiments to define the behavior of specific important elements (*e.g.*, uranium, thorium,

plutonium), and broader experiments that establish physical and chemical properties of the processing methods such as reaction rates and solubilities. The process scale-up will include the usual attention to equipment, materials of construction, and unit operations, (*e.g.*, mass transfer, separations of solids from liquids, or distillation of solvent metals) as carried out remotely. Intensive cold laboratory testing should yield products that can be used for fuel fabrication and performance testing in other parts of the fuel-cycle program. Engineering and hot studies are included in the process scale-up plans.

The number of candidate processes to be evaluated in the component and systems development phase should be narrowed to not more than two or three. During this phase equipment for cold and hot (remote) processing should be designed, installed, and tested. At this time, planning and design studies may be initiated for the construction of a ~70 metric ton/year dedicated reprocessing facility based on modification to the EBR-II Fuel Cycle Facility.

Principal constraints that may limit PDPM development or deployment are, (a) the possibility that reagents (*i.e.*, metals or salts) may not be capable of recycle in some processes with the result that material costs and amount of high-level waste produced will be excessive, or (b) the inability of fuel fabricators to accommodate to the hot fuel product from reprocessing.

The time that major decisions will be made that affect the PDPM Program have been identified as follows:

(a) Review Preliminary Flow Sheets	1978-1979
(b) Identify Reference Processes	1981-1982
(c) Define Process Systems	1984-1985
(d) Evaluate Engineering-Scale Equipment	1985-1986

During the first five years of the program the effectiveness, safety, economics, reliability, and major environmental impact of reference processes will be evaluated for full scale application of a selected process. If any impediments to full scale application are identified as a result of these studies, they will be evaluated and further experiments performed to find solutions during the process scale-up phase.

Separations Processes

Six processes that are representative of those initially selected for evaluation in the PDPM Program are summarized below. Several of these processes are described in separate papers that are included in this Actinide Separations Symposium. A seventh process, the Zinc Distillation Process is described in greater detail. This process was selected as a reference process to meet the criteria for a proliferation-resistant exportable technology.

1. Carbide Fuel Processing. Several methods are being evaluated for the reprocessing of (U,Pu)C and (Th,U)C fuel. In principle, carbides can be burned to oxides and then reprocessed like oxide fuel. A direct reduction of the carbides into a metal solvent or an oxidation into a salt phase is more attractive for pyrochemical fuel recovery processes. Two alternatives are being considered. In the first, carbides are dissolved and partially separated from fission product elements and each other in liquid bismuth. In the second, carbides are oxidized into a salt phase using zinc chloride or cadmium chloride. The salt phase is then contacted with a liquid metal such as cadmium-magnesium to partially separate the actinides from fission products and each other. This second alternative is a head-end step for salt transport processes being evaluated for other fuels in the PDPM Program.

Reprocessing in Liquid Bismuth (7). The reaction or dissolution of some of the carbides in bismuth to form bismuthides is the basis for the separation of fission products from the actinides. Some unreacted fission product carbides and some bismuthides are lighter than bismuth and, along with free carbon, float on the bismuth and are physically separated. Uranium carbide dissociates to only a limited degree (dependent upon the solubility of uranium in bismuth). Plutonium is much more soluble in bismuth than is thorium. The solubility of the plutonium is reduced by lowering the temperature, whereupon PuBi₂ precipitates. The compounds PuBi₂ and ThBi₂ are denser than bismuth, are of limited solubility in bismuth, and are expected to settle in the bismuth along with unreacted uranium carbide.

Molten Cadmium/Salt Reprocessing (7). The initial steps involve (a) conversion of the actinide and various fission product carbides to chlorides by reaction with CdCl₂ dissolved in MgCl₂-NaCl-KCl eutectic (mp, 397°C) and (b) reduction of the salt phase with a cadmium-magnesium alloy, thereby partitioning the fissile, fertile, and fission product elements between the salt and metal phases. Cadmium-based rather than zinc-based oxidizing and reducing agents were chosen to allow operation at temperatures below 650°C with readily available container materials such as mild steel and series 400 steels. In essence, this processing concept serves as a head-end step for introducing carbide fuels into various pyroprocesses (*e.g.*, salt transport).

2. Salt Transport Processing (8, 9, 10, 11). The selective transfer of spent fuel constituents between liquid metals and/or molten salts is being studied for both thorium-uranium and uranium-plutonium oxide and metal fuels. The chemical basis for the separation is the selective partitioning of actinide and fission-product elements between molten salt and liquid alloy phases as determined by the values of the standard free energy of formation of the chlorides of actinide elements and the fission products. Elements to be partitioned are dissolved in one alloy (the donor

alloy), are oxidized upon being mixed with a salt, enter the salt, are transported in the salt to a second alloy (the acceptor alloy), are reduced, and dissolve in the acceptor alloy.

For convenience, the fission product elements are divided into four groups, FP-1, FP-2, FP-3, and FP-4, that correspond to the order in which separations occur, Table I. The FP-1 fission products are volatile and do not react with either the salts or metal elements. They are removed during the head-end processing. Elements that are sufficiently active to be oxidized by CaCl_2 are designated as FP-2 fission products. Also designated as FP-2 fission products are iodine, bromine, selenium and tellurium, that are removed with the salt during the oxide reduction step. The FP-3 fission products are oxidized by MgCl_2 or ZnCl_2 , are transferred to the salt phase, and are finally taken up by an acceptor alloy. The FP-4 elements are too inert to be oxidized by MgCl_2 or ZnCl_2 and remain with the donor alloy. The actinide elements are then separated from the FP-4 fission products by salt transport to the acceptor alloy followed by vacuum retorting and conversion of metallic intermediates to suitable products.

Table I. Fission Product Groups Corresponding To The Order In Which Separations Occur

<u>Group</u>	<u>Fission Product Elements</u>
FP-1	Tritium, Xe, Kr
FP-2	Cs, Rb, Sr, Ba, Sm, I, Br, Se, Te
FP-3	Y, La, Ce, Pr, Nd, Pm, Gd, Tb
FP-4	Zr, Nb, Mo, Tc, Ru, Rh, Pd, Ag, Cd, In, Sn, Sb

The degree of decontamination can be controlled by the retention of FP-3 and/or FP-4 fission products with the final product.

Proof-of-principle experiments are being performed to demonstrate the above basic steps. Other experiments include controlled removal of fission products, characterization of salts, salt purification methods, and a proliferation analysis of the process.

3. Dry Processing (AIROX) of LWR (U,Pu) O_2 Fuels (12). The evaluation of the AIROX process is an extension of previous fuel reprocessing technology and consists of gas-solid fuel reactions to (a) release gaseous fission products, (b) pulverize the fuel, and (c) separate the fuel from the cladding. This is a multiple oxidation-reduction cycle for oxide fuel in which the UO_2 is oxidized to U_3O_8 to rupture the cladding and disintegrate the pellets. The U_3O_8 is subsequently reduced with hydrogen to UO_2 for fabrication. Solid radioactive fission products are retained in the fuel and all the uranium and plutonium are coprocessed and returned to the fuel cycle.

4. Molten Nitrate Salt Oxidation Process (10). The reaction of UO_2 with molten nitrate salts to form uranates that are subsequently reduced to effect a separation of the uranium is being evaluated. The actinide behavior and uranate composition in equimolar sodium-potassium nitrate is being studied to determine the uranate stability and forecasting of cation behavior in subsequent process steps.

Optimum conditions are being determined for formation of the uranate. Studies include utilizing 100% nitric acid vapor to determine uranium-plutonium separation and to investigate alternate separation methods, particularly the effects of added anions. Each process step is being investigated for fission product behavior and distribution with respect to the desired actinide recovery. The effect of added constituents on the behavior of actinide and fission-product compounds in molten nitrates will be studied. Soluble species in molten nitrates are to be identified and a determination made as to whether fission product elements are present, either as soluble species or solids, as anionic or cationic species.

5. Extraction of Actinides from Bismuth into Ammonium Chloroaluminate (13, 14, 15). Experiments are being performed to demonstrate the oxidative extraction of the actinides from bismuth into ammonium chloroaluminate (NH_4AlCl_4) and product recovery from the latter salt. Initial experiments with uranium dissolved in bismuth showed essentially complete extraction of the uranium into the salt with only a minimum of contact time at 330°C . Extraction of thorium from bismuth took appreciably longer and the solubility of ThCl_4 in NH_4AlCl_4 at 375°C was appreciably less than that of UCl_4 at the same temperature, (1.1 wt % ThCl_4 vs. 7.0 wt % UCl_4).

The recovery of actinide chlorides from ammonium chloroaluminate by distillation of the solvent at 400°C resulted in very little of the uranium or thorium being carried over with the distillate. The aluminum/nitrogen ratios in the bottoms indicated a non-volatile compound that contained aluminum but not nitrogen. This latter compound may have been aluminum oxychloride.

6. Molten-Tin Process for Reactor Fuels (16). Liquid tin is being evaluated as a reaction medium for the processing of thorium- and uranium-based oxide, carbide, and metal fuels. The process is based on the carbothermic reduction of UO_2 , nitriding of uranium and fission product elements, and a mechanical separation of the actinide nitrides from the molten tin. Volatile fission products can be removed during the head-end steps and by distilling off a small portion of the tin. The heavier actinide nitrides are expected to sink to the bottom of the tin bath. Lighter fission product nitrides should float to the top. Other fission products may remain in solution or form compounds with

the tin. The retention of some fission product nitrides with the actinides should improve the proliferation resistance of the product.

Initial experiments have demonstrated the feasibility of carbothermic reduction of UO_2 and nitriding of uranium in molten tin. Nitriding of the product of carbothermic reduction of mixed UO_2 - PuO_2 and added fission product elements is one of the steps to be confirmed for this process to be deemed potentially useful.

Ultimately, the potential for recovery and recycle of tin by filtration to remove solids and by the decomposition of intermetallics from decladding steps also must be evaluated.

7. Zinc Distillation Process (3, 4). A zinc distillation process was selected as a reference pyrochemical process that would have a sufficient degree of proliferation resistance that it could be used by nonweapons nations to reprocess spent fuel without significantly increasing their weapons production capability. The process has the inherent proliferation-resistant advantages of being a low decontamination process with limited plutonium enrichment in uranium-plutonium-zinc mixtures. The process chemistry flow sheet for this process is shown in Figure 1.

The zinc distillation process consists of four basic operations to coprocess and recover uranium and plutonium containing fission products from spent FBR mixed-oxide fuels. These operations are:

- (a) decladding,
- (b) oxide reduction,
- (c) plutonium enrichment, and
- (d) final fission product decontamination and heavy metals concentration.

a. Decladding. In the decladding operation, the stainless steel cladding and shroud are dissolved in liquid zinc at $800^\circ C$. The uranium and plutonium oxides do not react with the zinc. A molten $CaCl_2$ - KCl - $ZnCl_2$ - CaF_2 cover salt is maintained on top of the zinc to inhibit the vaporization of zinc. When the cladding is breached, the FP-1 fission products, Table I, are vented and are collected in the argon cover gas which is confined for decay and further processing. Iodine, released from the fuel, reacts with zinc to form ZnI_2 which subsequently complexes with KCl in the cover salt. Some of the more noble FP-4 fission products (ruthenium, rhodium, palladium, silver, etc.) may be leached from the oxide fuel by zinc.

After decladding is completed, the zinc-cladding alloy is separated from the oxide fuel and cover salt. The zinc is recovered by distillation for recycle.

The $ZnCl_2$ also reacts with any sodium metal associated with the FBR fuel subassembly; the $NaCl$ is dissolved in the cover salt.

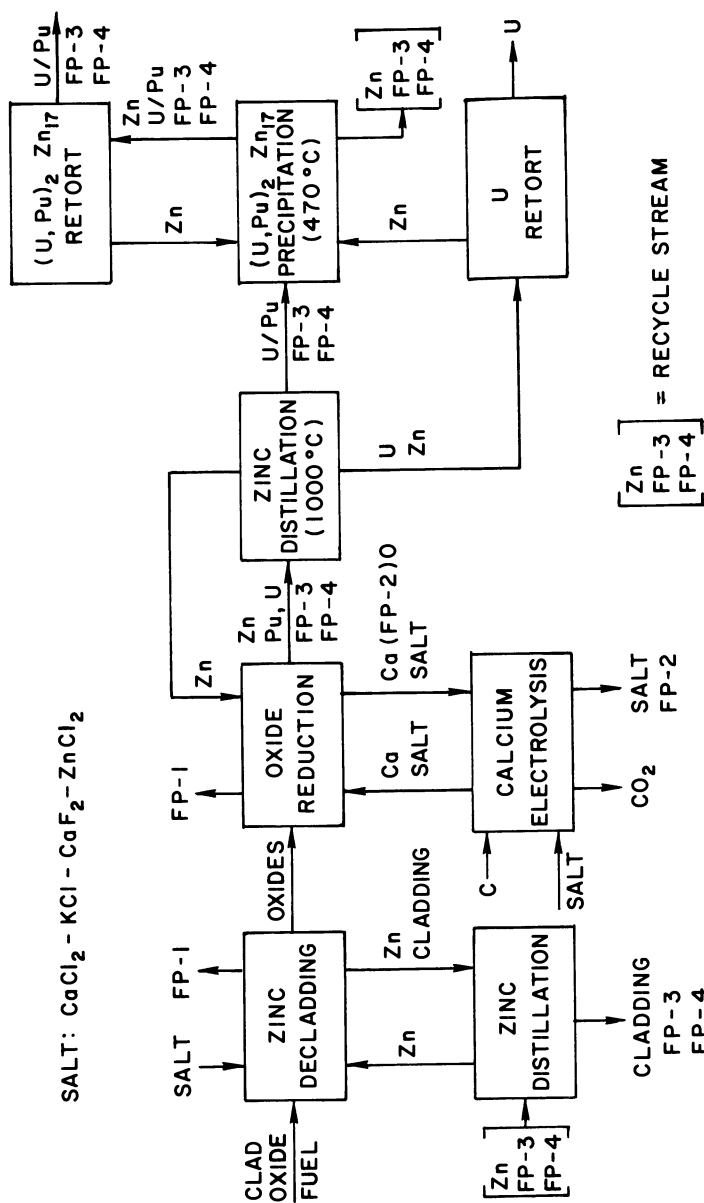


Figure 1. Zinc distillation CO-processing of $(\text{U}, \text{Pu})\text{O}_2$ FBR fuel

b. Oxide Reduction. The oxide reduction is performed in the same vessel as the decladding. Additional salt as well as molten zinc and calcium metal are added to the vessel and vigorously contacted with the oxide fuel at about 800°C. The uranium, plutonium, and FP-3 fission product oxides are reduced by the calcium. The CaO byproduct and the chloride salts of the FP-2 fission products are taken up by the salt. The remaining FP-1 gaseous elements are released during the reduction reaction and are taken up by the argon cover gas that is handled in the same manner as in the decladding step. The uranium, plutonium, FP-3 fission products, and FP-4 fission products are dissolved by the zinc.

The CaO must be removed from the salt so that the salt can be recycled. To accomplish this, the CaO is electrolyzed in a cell wherein graphite is a consumable anode and the reduced calcium collects at the cathode as molten metal. Oxygen formed at the anode reacts with graphite and the resultant CO and CO₂ are vented from the cell. At the end of the electrolysis, a small salt stream carrying FP-2 elements is bled to waste; the remainder of the salt is transferred back to the reduction vessel.

c. Plutonium Enrichment. The plutonium content in the uranium/plutonium product stream must be about 20 percent for recycle back to the reactor. Because the core and the associated axial blankets are processed together, a step is required that removes uranium and, thus, enriches the plutonium content. This enrichment is achieved by distilling the partially decontaminated reduction alloy at 1000°C. In accordance with the zinc-uranium phase diagram, gamma-uranium precipitates from the zinc solution at 1000°C when the uranium concentration exceeds 18 atom percent. The zinc distillation is continued until about 50 percent of the uranium that was initially present has precipitated. The precipitate is washed with zinc, recovered, and, ultimately, converted to oxide for blanket fuels.

The ratio of plutonium to uranium in the zinc solution remaining after distillation is dependent on how much zinc is distilled away. At the nominal end-point of the distillation the plutonium/uranium ratio is 1:4.

d. Final Fission Product Decontamination and Heavy Metal Concentration. The zinc solution, which contains the plutonium and the unprecipitated uranium, is transferred from the 1000°C distillation vessel, combined with the wash, diluted with additional zinc until the zinc content is 96 atom percent, and then cooled to 470°C. At this temperature, the uranium in solution precipitates as the U₂Zn₁₇ intermetallic with 99.8 percent efficiency. Plutonium and the fission products that form similar isostructural compounds with zinc coprecipitate with the U₂Zn₁₇. The coprecipitate coefficients, as defined by the Doerner-Hoskins equation, are 0.66 for plutonium and 0.57 to 0.66 for the FP-4 elements; a coefficient of 0.66 amounts to 98 percent

coprecipitation. Individual FP-4 fission products are distributed between the intermetallic compound and the liquid zinc with nearly all of the ruthenium and technetium remaining with the plutonium while rhodium, zirconium, and palladium remain with the residual zinc solution and eventually are sent to waste.

The solid $(U,Pu)_2Zn_{17}$ intermetallic compound, containing FP-3 and selective FP-4 fission products for proliferation resistance is vacuum distilled to remove the zinc, which is recycled. The uranium/plutonium concentrate is injection cast into rods suitable as feed to the refabrication process.

The plutonium/uranium ratio may be adjusted to the desired plutonium enrichment by the addition of the appropriate amount of uranium.

Conclusions

Pyrochemical processing methods may offer unique advantages over more conventional aqueous methods with respect to meeting nonproliferation goals. Some pyrochemical processes are intrinsically proliferation resistant because the process is incapable of producing a weapons-usable product without significant alterations. The product also can be sufficiently radioactive that it is physically difficult to divert. These features warrant the examination of pyrochemical and dry processing methods under current nonproliferation policies.

Literature Cited

1. Starks, J. B., U. S. Department of Energy Report DPSPU-77-11-1, Savannah River Laboratory, Aiken, S. C., 1977.
2. Levenson, M.; Zebroski, E., A Fast Breeder System Concept, A Diversion Resistant Fuel Cycle, Presented at the 5'th Energy Technology Conference, Washington, D.C., (February 25, 1978).
3. Chiotti, P.; Mason, J. T., Phase Diagram and Thermodynamic Properties of the Uranium-Zinc System, J. Less Common Metals, 1975, 40, 39.
4. Cramer, E. M.; Wood, D. H., Phase Relations in the Zinc-Rich Portion of the Plutonium-Zinc System, J. Less Common Metals, 1967, 13, 112.
5. Knighton, J. B.; Burris, L. Jr.; Feder, H. M., U. S. Atomic Energy Commission Report ANL 6.223, Argonne, IL, 1961.
6. Steunenber, R. K.; Pierce, R. D.; Burris, L., "Progress in Nuclear Energy, Series III, Process Chemistry" Pergamon Press: Oxford & New York, 1969; p. 465.

7. Steindler, M. J., U. S. Department of Energy Report ANL-78-76, Argonne, IL, 1978.
8. Steunenbergh, R. K.; Pierce, R. D.; Johnson, I., "Status of the Salt Transport Process for Fast Breeder Reactor Fuels," in "Symposium on Reprocessing of Nuclear Fuels, The Metallurgical Society of AIME, Ames, IA, August 1969," *Nucl. Metallurgy*, Vol. 15.
9. Knighton, J. B.; Johnson, I.; Steunenbergh, R. K., "Uranium and Plutonium Purification by the Salt Transport Method," in "Symposium on Reprocessing of Nuclear Fuels, The Metallurgical Society of AIME, Ames, IA, August 1979," *Nucl. Metallurgy*, Vol. 15.
10. Steindler, M. J., U. S. Department of Energy Report ANL-79-6, Argonne, IL, 1978.
11. Bates, J. K.; Jardine, L.; Krumpelt, M., This vol. p.
12. Brand, G. E.; Murbach, E. W., U. S. Atomic Energy Commission Report NAA SR 11389, 1965.
13. Ross, R. G.; Grimes, W. R.; Barton, C. J.; Bamberger, C. E.; Baes, C. F. Jr., "The Reductive Extraction of Protactinium and Uranium from Molten LiF-BeF₂-ThF₄ Mixture Into Bismuth," in "Symposium on Reprocessing of Nuclear Fuels, The Metallurgical Society of AIME, Ames, IA, August 1969," *Nucl. Metallurgy*, Vol. 15.
14. Shaffer, J. H.; Molton, D. M.; Grimes, W. R., "The Reductive Extraction of Rare Earths from Molten LiF-BeF₂-ThF₄ Mixtures Into Bismuth" in "Symposium on Reprocessing of Nuclear Fuels, The Metallurgical Society of AIME, Ames, IA, August 1969," *Nucl. Metallurgy*, Vol. 15.
15. Ferris, L. M.; Smith, F. J.; Mailen, J. C.; Bell, M. J., *J. Inorg. Nucl. Chem.*, 1972, 34, 2921.
16. Anderson, R. N.; Parlee, N. A. D.; Gallagher, J. M., *Nucl. Tech.*, 1972, 13, 29.

RECEIVED May 14, 1979.

Pyrochemical Coprocessing of Uranium Dioxide-Plutonium Dioxide LMFBR Fuel by the Salt Transport Method

JAMES B. KNIGHTON and CHARLES E. BALDWIN

Rockwell International, Box 464, Golden, CO 80401

The Salt Transport Process is being developed for coprocessing uranium and plutonium in spent LMFBR fuels as part of the Pyrochemical and Dry Processing Methods (PDDM) program. The PDDM program is administered by Argonne National Laboratory for the Department of Energy. The major objectives of this work are: (1) develop a pyrochemical process for spent LMFBR fuel that gives a uranium-plutonium-fission product oxide suitable for fabrication into new fuel, and (2) produce a product from which recovery of plutonium for subsequent use in weapons would require a major detectable effort by a foreign nation. Under current non-proliferation policies, fission product retention with coprocessed plutonium and uranium is desirable to enhance resistance to diversion of fissile material and proliferation of nuclear weapons.

Commencing during the early 1950's and extending through the 1960's, research and development work on pyrochemical and pyrometallurgical processes was conducted at various sites. The processes studied may be grouped into the following general categories: melt refining, zone melting, electrorefining, vacuum distillation, fractional crystallization, gas-solid reactions, and liquid-liquid extraction using either immiscible molten metal phases or immiscible molten salt-metal phases. Various survey papers have been published describing the above methods for processing irradiated nuclear reactor fuels (1-8). The term "Salt Transport" has been applied to a purification technique whereby a metallic solute is transferred selectively from one liquid alloy (donor) to another liquid alloy (acceptor) by circulating a molten salt between the two alloys. Mass transfer takes place by oxidation of a solute by the salt at the donor alloy and reduction of the solute by the acceptor alloy.

Salt Transport processes were investigated at Brookhaven National Laboratory (9,10,11,12), Ames Laboratory (13,14), and Argonne National Laboratory (15,16,17,18,19). Because of the funding restraints, the work at Argonne National Laboratory was terminated in 1969. At that time, most of the laboratory studies needed to define appropriate solvent systems were completed, the

0-8412-0527-2/80/47-117-191\$05.00/0
© 1980 American Chemical Society

chemical feasibility of all the major separations was established in laboratory scale experiments, engineering investigations were in progress on pyrochemical unit operations, and material of construction were being evaluated (20).

The present work at Rocky Flats is an extension of the Argonne work and is directed to development of a proliferation resistant pyrochemical process for LMFBR fuels. This article describes a conceptual pyrochemical process and preliminary engineering concepts for coprocessing uranium and plutonium in spent LMFBR core-axial blanket and radial blanket fuels using the Salt Transport Process.

Description of Process Chemistry

The chemical basis for the various separations used in this pyrochemical process is the differences in the partitioning of uranium, plutonium, and the fission product elements between molten salt and liquid alloy phases. This difference in partitioning is largely determined by the values of the standard free energy of formation (ΔG_f°) of the chlorides of uranium, plutonium, and the fission product elements.

For convenience purposes, the fission product elements are divided into four groups: FP-1, FP-2, FP-3, and FP-4. FP-1 fission products are volatile and consist of ^3H , Xe, and Kr. FP-2 fission products are I, Br, Cs, Rb, Ba, Sr, Sm, Eu, Se, and Te. FP-3 fission products are Y, La, Ce, Pr, Nd, Pm, Gd, and Tb. FP-4 fission products are Zr, Nb, Mo, Tc, Ru, Rh, Pd, Ag, Cd, In, Sn, and Sb.

Table I lists the chlorides of selected elements in the order of decreasing values of the free energy of formation at 1000°K. Two separate oxidation-reduction couples ($\text{CaCl}_2\text{-Ca}$ and $\text{MgCl}_2\text{-Mg}$) are used to "buffer" the partitioning of elements between molten salt and liquid metal phases. The FP-2 elements lie above CaCl_2 in the free energy scale. The FP-3 elements lie between CaCl_2 and MgCl_2 and the FP-4 elements lie below MgCl_2 . In structuring the process, the separations occur in the numerical sequence of the above fission product groups.

Figure 1 gives the distribution coefficients for cerium, plutonium, and uranium partitioning between molten MgCl_2 and liquid Cu-Mg and Zn-Mg alloys of varying magnesium content at 800°C. As shown in Figure 1, the distribution coefficients fall in the same general order as the values of the free energies of formation for the chlorides of cerium, plutonium, and uranium. However, as also shown in Figure 1, large differences in the value of the distribution coefficients occur because of solvent effects as the alloy system and magnesium content in the alloy is varied. These solvent effects provide the basis for salt transport separations. For example, Cu-low Mg alloys are donor alloys and cerium, plutonium, and uranium partition to the salt while Zn-low Mg alloys are acceptor alloys and cerium, plutonium, and uranium partition to

TABLE I

Standard Free Energies of Formation
of Chlorides at 1000°K

MCl_n	$-\Delta G_f$ (KCal/g equiv. Cl)	Fission Product Group
BaCl ₂	*	83.6
CsCl	*	82.6
RbCl	*	82.5
LiCl		78.8
KCl		81.6
SrCl ₂	*	80.8
SmCl ₂	*	80.0
EuCl ₂	*	79.0
CaCl ₂		76.7
NaCl		76.2
LaCl ₃	*	67.0
PrCl ₃	*	66.3
CeCl ₃	*	66.3
NdCl ₃	*	64.2
YCl ₃	*	61.2
PuCl ₃		58.4
MgCl ₂		57.7
UCl ₃		54.0
ZrCl ₂	*	34.2
ZnCl ₂		34.1
CrCl ₂		32.8
CdCl ₂	*	30.4
FeCl ₂		26.3
CuCl		22.0
NiCl ₂		18.6
NbCl ₅	*	11.4
MoCl ₂	*	8.0
TcCl ₃	*	7.4
PdCl ₂	*	5.3
RhCl	*	1.4
RuCl ₃	*	0.3

*Fission Products

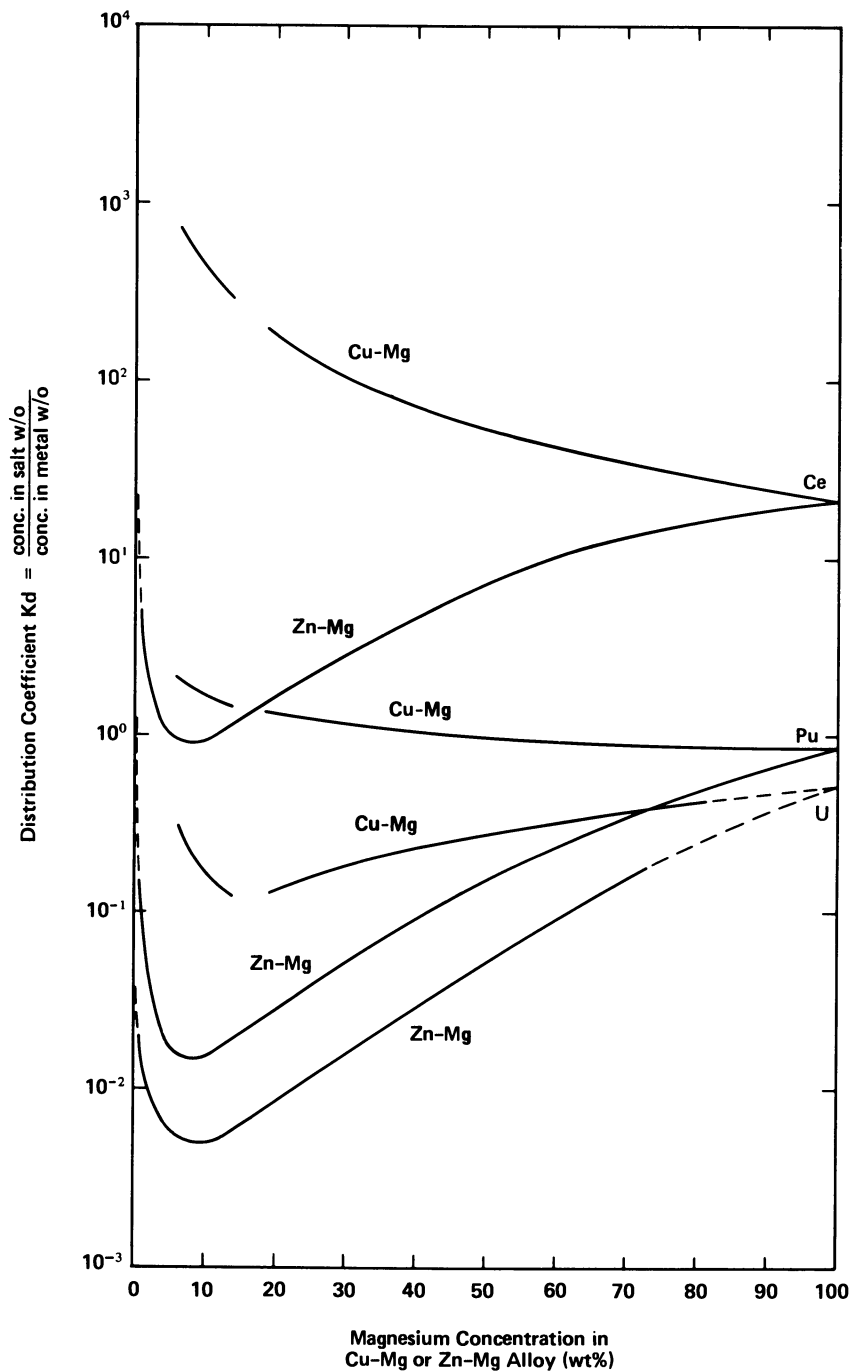
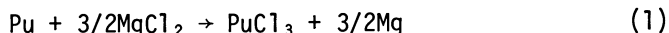


Figure 1. Distribution of Ce, Pu, and U between magnesium chloride salt and Cu-Mg or Zn-Mg alloy at 800°C

the metal. A typical donor reaction is given for plutonium:



A typical acceptor reaction is given for plutonium:



The acceptor reaction is the reverse of the donor reaction. The MgCl_2 consumed by the donor reaction is regenerated by the acceptor reaction. Thus, the salt is not consumed and may be reused indefinitely. For each mole of plutonium transferred from the donor alloy to the acceptor alloy, there is a reverse transfer of 1.5 moles of magnesium from the acceptor alloy to the donor alloy.

Other variables that affect the partitioning of solutes between molten salt and liquid metal phases include: temperature, salt system, MgCl_2 content of the salt, and solubility of the solutes in the alloy systems. A detailed description of the chemistry for each process step is beyond the scope of this paper.

Preliminary Design Criteria

Criteria used to develop the conceptual pyrochemical process for coprocessing uranium and plutonium from spent LMFBR fuel include the following:

1. Uranium and plutonium will be coprocessed for proliferation and diversion resistance.
2. Fission product removal will be incomplete.
3. Plutonium recovery will exceed 99%.
4. Plutonium enrichment in mixed oxide product must be sufficient for recycle to the reactor.
5. All process operations must be simple and reliable.
6. All process operations must be remotable.
7. Types of process operations will be minimized.
8. All fission products must be contained.
9. The amount of process waste must be minimized.
10. The mixed UO_2 - PuO_2 product must be fabricable.
11. The recycle fuel must be compatible with reactor operations.
12. The process must be tamper-proof.

Process Flow Sheet

The block flow diagram presented in Figure 2 gives the major operations of the conceptual process. Feed to the process is one core-axial blanket or radial blanket fuel assembly. The fuel assembly hardware below the active section is removed prior to processing. The hardware above the active section is not introduced into the process. In this low decontamination process, the active section of the spent fuel is selectively dissolved into molten metals and molten salts from which coprocessing of uranium and

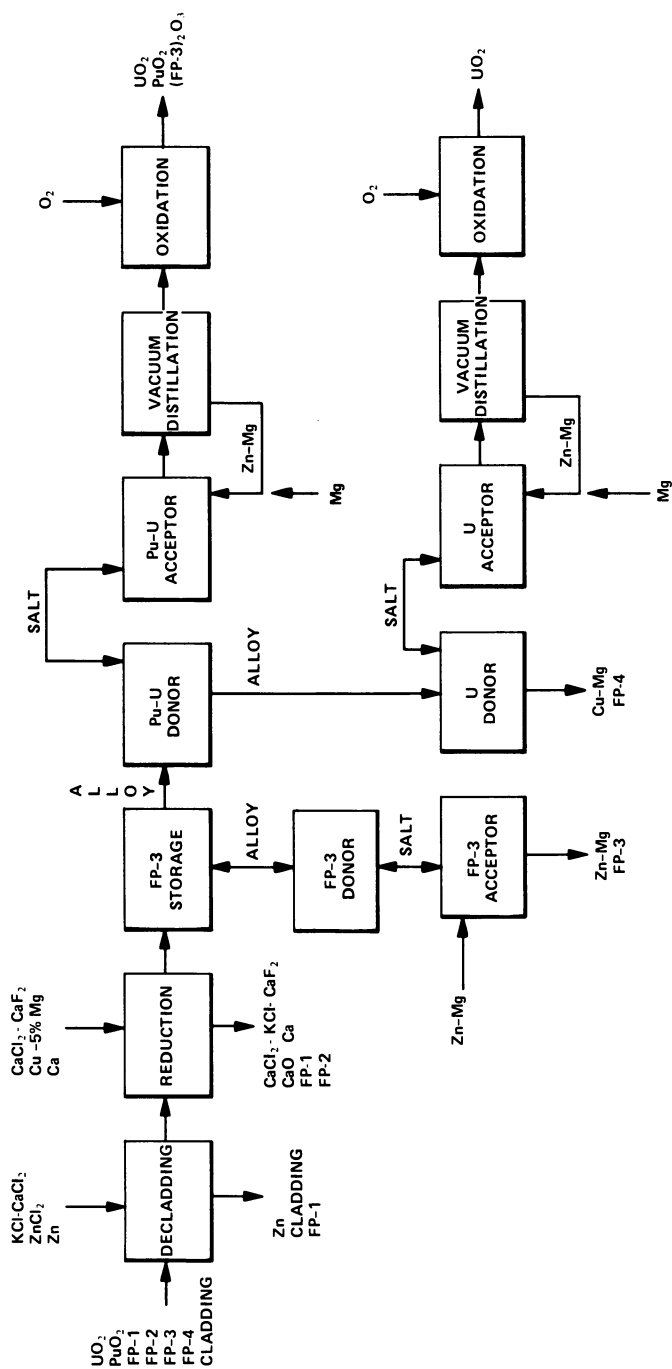


Figure 2. Conceptual salt transport process for UO_2 - PuO_2 fuel

plutonium and separation from fission products is achieved.

In the first step of the process, stainless steel cladding is separated from the mixed oxide fuel by selective dissolution in molten zinc at about 800°C. When the cladding is breached, the FP-1 gaseous fission products are vented and are contained in the furnace cover gas. After decladding is completed, the zinc-stainless steel liquid alloy is separated from the mixed oxide fuel.

The fuel is dissolved during reduction of the mixed oxides by calcium. This oxide reduction operation is done in the presence of a CaCl_2 - CaF_2 salt and a Cu-Mg alloy. The FP-2 elements and the CaO reaction product are taken up by the salt and the reduced uranium, plutonium, FP-3, and FP-4 elements are taken up by the alloy. Uranium is present in excess of its solubility limit and precipitates as the UCu_5 intermetallic compound.

Removal of FP-3 elements is by a salt transport process in which FP-3 elements are transferred from a donor alloy to an acceptor alloy by circulating a KCl - CaCl_2 - MgCl_2 salt between the alloys. To assure that only a limited FP-3 removal can be made, the process is designed so that only about 10% of the donor alloy is involved in the FP-3 removal salt transport process. The remaining alloy containing FP-3 elements, uranium, plutonium, and FP-4 elements is not available for FP-3 removal. The FP-3 elements not removed follow plutonium through the process.

Uranium, plutonium, and the remaining FP-3 elements are separated from the FP-4 elements and the donor alloy by a second salt transport process using a MgCl_2 - MgF_2 salt. The Cu-Mg reduction alloy is the donor alloy. A zinc-magnesium alloy is the acceptor alloy.

Uranium transfers at a slower rate than plutonium because uranium has a lower solubility than plutonium in the donor alloy and uranium has a lower distribution coefficient than plutonium in the donor alloy-salt system. This difference in the rate of transfer is very desirable because it provides a means for enriching the plutonium content of the product to required concentrations for recycle to the reactor core. This enrichment is obtained by terminating the circulation of the transport salt between donor and acceptor alloys before complete uranium transfer has occurred. As uranium transfers, the solid UCu_5 compound dissolves into the donor alloy. After plutonium and the desired amount of uranium are separated from FP-4 elements, the remaining uranium may be separated by diverting the transport salt to a second zinc-magnesium acceptor alloy.

Because both zinc and magnesium are volatile, these acceptor alloy elements are separated from the actinides by vacuum distillation. The zinc-magnesium overhead product from vacuum distillation is recycled. After the volatile solvent metals are removed, the resultant distillation bottom products (U-Pu for core fuel and U for blanket fuel) are converted to suitable oxides by reaction with oxygen. The oxide products are available for refabrication into new fuel. The FP-3 elements that follow plutonium and the

presence of uranium make the core oxide fuel unattractive for weapons use.

To minimize waste streams, ancillary processes not shown in Figure 2 may be used to treat used process solvents for recycle.

Process Size

To determine the process size, material balances were calculated for each process operation. Feed to the process was one core-axial blanket fuel assembly.

TABLE II

AI Reference Oxide LMFBR Core-Axial Blanket Fuel Assembly (21)

8% Burnup of Core Fuel
59,519 MWD/Ton (Core/Axial Blanket)
90-Day Cooling

<u>Component</u>	<u>Kg</u>	<u>Thermal Watts</u>
UO ₂	73.1	0.005
PuO ₂	11.5	50.7
FP-1	0.6	2.04
FP-2	1.0	307
FP-3	1.1	1600
FP-4	1.7	3520
Cladding	56.7	344

Table III gives the quantity, volume of salt and metal present, and design volume at each major process operation.

TABLE III

Process Volumes

<u>Operation</u>	<u>Kg</u>			<u>Liters</u>			<u>Design Volume</u>
	<u>Salt</u>	<u>Metal</u>	<u>Total</u>	<u>Salt</u>	<u>Metal</u>	<u>Total</u>	
Decladding	15.0	581.9	596.9	7.0	78.4	85.4	250
Reduction	202.1	378.0	580.1	89.4	45.6	135.0	250
FP-3 Donor	30.0	49.6	79.6	16.7	5.6	22.3	30
FP-3 Acceptor	30.0	22.0	52.0	16.7	4.6	21.3	30
U-Pu Donor	270.0	371.9	641.9	150.0	42.4	192.4	250
U-Pu Acceptor	270.0	224.3	494.3	150.0	32.6	182.6	250
U Donor	270.0	331.5	601.5	150.0	42.8	192.8	250
U Acceptor	270.0	265.8	535.8	150.0	45.5	195.5	250

In the practical operation of the process, decladding, reduction, FP-3 storage, and U-Pu donor operations will be conducted sequentially in the same crucible. A design volume of 250 liters was selected for these four operations and also for U-Pu acceptor, U donor, and U acceptor operations. A design volume of 30 liters was selected for the FP-3 donor and FP-3 acceptor operations. The small volume of the FP-3 donor and acceptor crucible builds in a tamper-proof feature to prevent higher than designed removals of FP-3 elements.

Preliminary Engineering Concepts

Because of the relatively high operating temperatures ($\sim 800^{\circ}\text{C}$), it is important that simple process operations are used and that the various types of operations are kept to a minimum. Process operations must be removable and process equipment must be fabricable. The basic unit operation used in this process is liquid-liquid extraction using molten salts and liquid metals as the immiscible process solvents. The simplest option to equilibrate the immiscible solvents is to use a crucible and intermix the molten salt and liquid metal phases with a mixing paddle. The process has been structured around this simple concept. Mixing of phases, phase disengagement, and phase separation are done sequentially in the same crucible. Molten salt and liquid metal phases are pressure transferred between crucibles through heated tubes.

In the proposed operation of the process, four types of transfer are envisioned: (1) separate salt from the top of the metal, leaving a small salt heel, (2) transfer all of the salt, taking a small metal heel, (3) transfer the metal only, leaving a small metal heel with the salt, and (4) transfer both salt and metal. These four modes of transfer are accomplished by proper positioning of the transfer tube inlet and by use of an underflow weir when transfer of only metal is required.

Remote transfer of solids between crucibles is not practical. In the conceptual flow sheet, Figure 2, solids (mixed oxide fuel or UCu_5 intermetallic compound) are present in the first four operations. To avoid transferring of solids, a turntable, Figure 3, with four operating positions is proposed to facilitate moving the solids through the process.

The primary process operations are conducted sequentially in the same tungsten crucible. These primary operations are conducted in a circular processing assembly with operating stations dedicated for each operation. Decladding is conducted at the first station, oxide reduction is conducted at the second station, FP-3 donor is conducted at the third station, and U-Pu donor is conducted at the fourth station. Each station has the necessary apparatus to conduct the desired operations (introduction of fuel assembly, stirring, and transfer of molten salt and metal phases into and out of the crucible). Figure 4 gives a cross section view of the turntable.

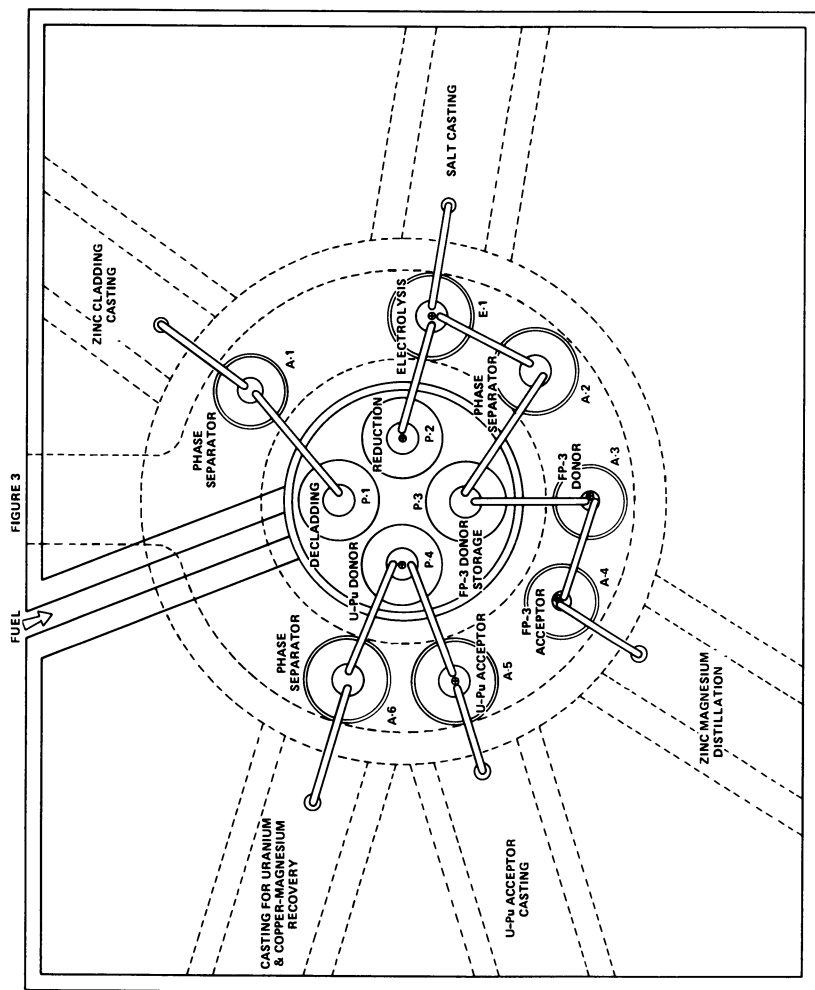


Figure 3. Crucible turntable

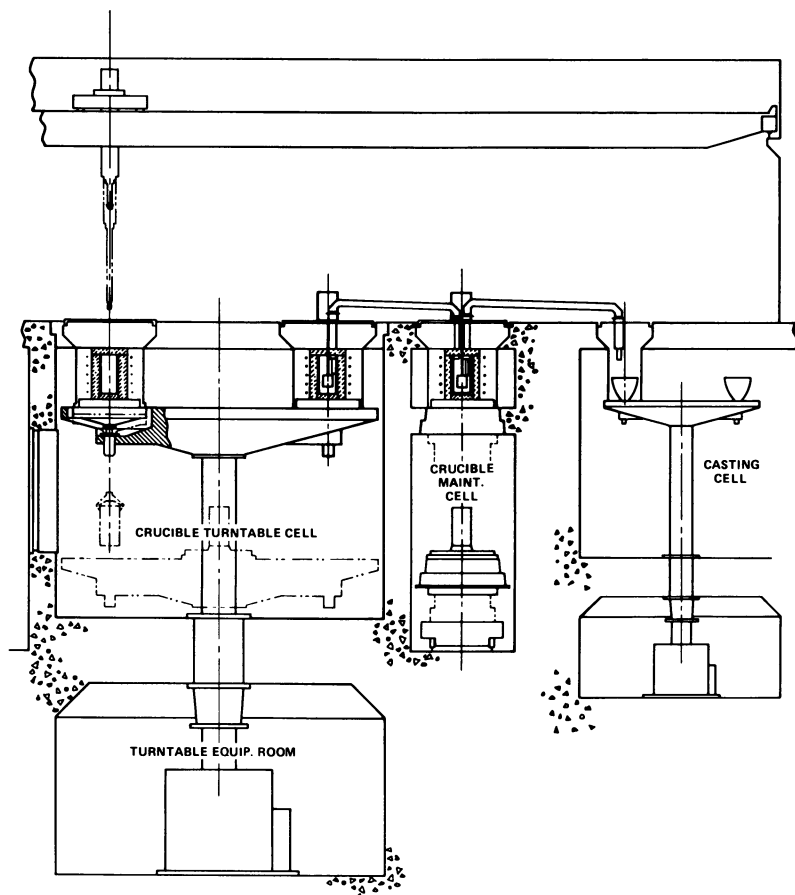


Figure 4. Pyrochemical fuel processing facility

At each of these operating stations, a furnace (with an open bottom) is suspended from the cover of the processing assembly. At each of the operating stations a tungsten crucible is located on the turntable. After each operation is completed, the turntable is rotated for the next operation. Prior to rotation, the turntable (and crucibles) must be lowered so that the stirrers and transfer tubes will not obstruct the rotation of the crucibles. After rotation, the crucibles are raised back to the operating level at the new operating position. The mechanisms and seals for raising, lowering, and rotating the turntable are located below the heated zone of the furnace.

To facilitate the flow of molten material into and out of the main process vessels, auxiliary furnaces are positioned around the turntable. These auxiliary furnaces are stationary. The auxiliary furnaces are used to: (1) premelt feed to the process, (2) provide storage of molten process solvents, (3) provide a means of effecting clean salt-metal phase separations, (4) provide containment of various donor and acceptor alloys, and (5) conduct electrowinning of CaO for recycle of calcium metal and reduction salt.

At the tail end of a solvent extraction process, the solvents are separated from the solutes for recycle. In this application of solvent extraction, vacuum distillation is used to separate volatile zinc and magnesium from coprocessed uranium and plutonium and from the uranium product. Feed to vacuum distillation is solid alloy. Overhead and bottom products are likewise cast into a solid alloy. These vacuum distillation operations are conducted in separate cells. The actinide products are converted to oxide for fuel fabrication.

Process Waste Streams

The process has five waste streams: Cladding; FP-1 fission gas; Reduction salt containing FP-2; FP-3 acceptor alloy; and spent donor alloy. The amount, volume, and fission product decay heat for each stream are given in Table IV.

TABLE IV
Process Waste Streams

Stream	Weight (Kg)	Volume (Liter)	Thermal Watts*		Total
			Per Kg	Per Liter	
Cladding	56.7	7.1	6.1	48.5	344
Fission Gas	0.6	-	3.4	-	2
Reduction Salt	20.2	8.9	15.2	34.5	307
FP-3 Acceptor	1.1	0.2	1455	8000	1600
Spent Donor	33.2	4.3	106	818.6	3520
	<u>163.8</u>	<u>27.0</u>			

*8% Burnup of Core Fuel, 59,519 MWD/Ton (Core/Axial Blanket) 90-Day Cooling.

The zinc-cladding stream, FP-3 acceptor alloy, and spent donor alloy are fed to a single vacuum distillation operation to separate the volatile solvent zinc and magnesium for recycle. The resultant distillation bottom product is an alloy sponge of stainless steel, FP-3 elements, copper, and the FP-4 elements. The stainless steel cladding is the disposal matrix for the FP-3 and FP-4 elements. Reduction salt containing FP-2 elements may be cast into the stainless steel sponge. This compact waste is solid and may be sealed in high-integrity steel containers for interim and long-term storage. The adequacy of this disposal method has not been verified.

Plant Capacity

The plant processing capacity has been scaled to process one reference fuel assembly as shown in Table V. It is estimated that the maximum limiting process residence time at any one operating position may range from three to six hours, which will determine the actual plant feed rate.

Changes in fuel assembly size will increase or decrease plant throughput. Processing more than one fuel assembly per batch will require an increase in vessel size. Additional capacity also can be achieved by establishing parallel operations. The single fuel assembly per batch operation can process up to 200 tons per year of mixed oxide LMFBR fuel or up to eight fuel assemblies per day.

Materials of Construction

Because of the high temperature and corrosive environment in which the various pyrochemical operations will be conducted, a limited variety of construction materials are available. Tungsten and tungsten-alloys are the primary candidates where containment of alloys is required. Ferritic alloys may be used where only salt containment is required. Auxiliary hardware such as transfer tubes and agitators may require either tungsten, tungsten alloys, or ferritic alloys depending on their application.

Studies are currently underway at Rocky Flats and Argonne National Laboratory to investigate the corrosion resistance and fabricability of the various candidate materials. Some effort is also being expended in examining alternate, limited life materials, such as coated or impregnated ceramics.

Conclusions

The pyrochemical coprocessing of spent nuclear fuel by the Salt Transport Process appears to be a potentially viable reprocessing method, not only as an "exportable proliferation resistant technology," but as a domestic reprocessing operation. All operations are nonaqueous and waste generation is in solid form, thus requiring no conversion from aqueous solutions to solids.

TABLE V

Plant Capacity

Batches Per Day	Hours ^a Per Batch	Fuel Assemblies Per Batch	Fuel Rate Assemblies Per Day	Kg Mixed Oxide ^b Per Day	Tons of Mixed Oxide	
					100%	80%
					Plant Factor	Plant Factor
4	6	1	4	355.6	129.8	103.8
4	6	2	8	711.3	259.6	207.7
4	6	3	12	1066.9	389.4	311.5
6	4	1	6	533.45	194.7	155.8
6	4	2	12	1066.9	389.4	311.5
6	4	3	18	1600.4	584.1	467.3
8	3	1	8	711.3	259.6	207.7
8	3	2	16	1422.5	519.2	415.4
8	3	3	24	2133.8	778.8	623.1

^aMaximum operating time for any operation.

^bBased on 88.9 kg mixed oxides/fuel assembly.

Though considerable development effort was conducted in the 50's and 60's on pyrochemical processes, further development is required before Salt Transport can be performed on a production scale.

Literature Cited

1. Feder, H. M.; Dillon, I. G. in Stöller, S. M.; Richards, R. B., Eds., "Reactor Handbook, Vol. II, Fuel Reprocessing"; 2nd ed., Interscience Publishers, Inc.: New York, 1961; p. 313.
2. Motta, E.; Sinizel, D.; Brank, G.; Foltz, J.; Gardner, W.; Ballif, J.; Guca, J.; Kendall, G.; Luebben, T.; Mittern, K. TID-7534, 1957, 2, p. 719.
3. Schraidt, J. H.; Levenson, M. in Bruce, F. R.; Fletcher, J. M.; Hyman, H. H., Eds., "Progress in Nuclear Energy, Series II, Process Chemistry, Vol. III"; Pergamon Press: New York, 1961; p. 329.
4. Martin, F. S.; Myles, G. L. "Progress in Nuclear Energy, Series III, Process Chemistry, Vol. I"; Pergamon Press: New York, 1956; p. 291.
5. Burris, Jr., L.; Levenson, M.; Schraidt, J. H.; Steunenberg, R. K. Trans. Amer. Nucl. Soc., 1961, 4 (2), p. 192.
6. Lawroski, S.; Burris, Jr., L. At. Energy Rev., October 1964, 2 (3), p. 3.
7. Pierce, R. D.; Burris, Jr., L. in Link, L. E., Ed. "Reactor Technology, Selected Reviews"; TID-8540, 1964; p. 711.
8. Burris, Jr., L.; Harmon, K. M.; Brank, G. E.; Murbach, E. W.; Steunenberg, R. K. "Proceedings of 3rd International Conference on Peaceful Uses of Atomic Energy"; IAEA, Geneva, 1965, Vol. X, p. 501.
9. Dwyer, O. E. J. AICHE, 1956, 2, p. 163.
10. Bareis, D. W.; Wiswall, R. H.; Winsche, W. E. Chem. Eng. Progr. Symp. Ser. 50, 1956, p. 228.
11. Dwyer, O. W.; Teitel, R. J.; Wiswall, R. H. "Proceedings of International Conference on Peaceful Uses of Atomic Energy"; IAEA, Geneva, 1955, Vol. IX; p. 604.
12. Wiswall, R. H.; Egan, J. J.; Ginell, W. S.; Miles, F. T.; Powell, J. R. "Proceedings of 2nd International Conference on Peaceful Uses of Atomic Energy"; IAEA, Geneva, 1958, Vol. 17; p. 421.
13. Chiotti, P. U.S. Patent 3, Feb. 4, 1964; 120, p. 435.
14. Chiotti, P.; Klepfer, J. S. Ind. Eng. Chem. Process Design Develop., 1965, 4 (2), p. 232.
15. Knighton, J. B.; Johnson, I.; Steunenberg, R. K. ANL-7524, March 1969.
16. Knighton, J. B.; Johnson, I.; Steunenberg, R. K. "Symposium on Reprocessing of Nuclear Fuels"; Nuclear Metallurgy, Conf. 690801, August 1969; 15, p. 337.
17. Steunenberg, R. K.; Pierce, R. D.; Johnson, I. "Symposium on Reprocessing of Nuclear Fuels"; Nuclear Metallurgy, Conf.

- 690801, August 1969; 15, p. 325.
18. Pierce, R. D.; Miller, W. E.; Knighton, J. B.; Bernstein, G. J. "Symposium on Reprocessing of Nuclear Fuels"; Nuclear Metallurgy, Conf. 690801, August 1969; 15, p. 511.
 19. Johnson, I. in Fitterer, G. R., Ed., "Applications of Fundamental Thermodynamics to Metallurgical Processes"; Breach Science Publ., New York, 1969; p. 153.
 20. Kyle, M. L.; Pierce, R. D.; Kolba, V. M. "Symposium on Reprocessing of Nuclear Fuels"; Nuclear Metallurgy, Conf. 690801, August 1969; 15, p. 443.
 21. "Aqueous Processing of LMFBR Fuels, Technical Assessment and Experimental Program"; ORNL-4436, June 1970.

RECEIVED September 14, 1979.

Work performed under Argonne National Laboratory contract number 31-109-38-4149.

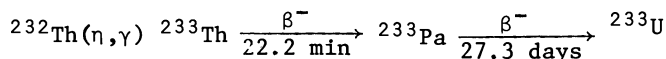
A Nonaqueous Reprocessing Method for Thorium-Based Fuels

J. K. BATES, L. J. JARDINE, and M. KRUMPELT

Chemical Engineering Division, Argonne National Laboratory, Argonne, IL 60439

Programs have been active periodically to develop a thorium-based fuel cycle for increasing the nation's resource of fissile material. Part of the effort has been the investigation of nonaqueous reprocessing methods for separating thorium from uranium and the behavior of these elements in the presence of fission products and other impurities (1). Interest in such pyrometallurgical methods and the entire thorium fuel cycle declined in the early 1970s, primarily due to the lower breeding ratio of the Th-²³³U cycle compared to that of the ²³⁸U-²³⁹Pu cycle, and the consequent effort placed on developing the PuO₂-UO₂ fuel cycle for fast breeder reactors. The recent advent of proliferation concerns has renewed the interest in the thorium fuel cycle and associated pyrometallurgical reprocessing. One reprocessing scheme which addresses the current problem is described below.

The effect of proliferation concerns on the acceptability of a fuel cycle, and the development of aqueous Civex processes designed to meet these concerns have been outlined previously (2). One new criterion imposed on reprocessing by proliferation issues is that the process streams be diversion and proliferation resistant. For thorium-based fuel cycles, this means that those products containing fissile material, ²³³U or ²³⁹Pu, must be co-processed with thorium or be denatured with ²³⁸U. In addition, reprocessing schemes must take into account special features of the thorium fuel cycle, such as the buildup of ²³³Pa which decays to ²³³U. The breeding chain for ²³³U is as follows:



Since ²³³Pa is a neutron poison, (3) a significant waiting period may be necessary before the reprocessed fuel would be returned to the reactor. Separation of the ²³³Pa would allow a quick return to the reactor, but would lead to a pure ²³³U product, and thus increase the proliferation risk.

Another feature of the thorium fuel cycle which affects reprocessing is the buildup of ²³²U in the irradiated fuel.

0-8412-0527-2/80/47-117-207\$05.00/0

© 1980 American Chemical Society

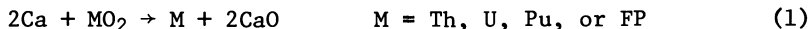
Equilibrium concentrations of ^{232}U may be reached in a few years during fuel irradiation but even 100 day irradiations may produce substantial concentrations of ^{232}U (4). The decay of the short half life of ^{232}U leads to a long decay chain of nuclides which include a penetrating 2.6 MeV gamma ray. This will likely require shielding and remote handling of the fuel during all phases of reprocessing and refabrication.

A desirable feature for the reprocessing method is that it should be adaptable to various thorium fuel cycles and to several fuel types, and it must be able to produce a product with a high enough fissile content for core fuel specifications. As an example, a fuel cycle that includes different needs is a symbiotic cycle where ^{239}Pu which is produced in existing light water reactors (LWR) is combined with thorium and burned in FBRs. The irradiated core fuel from the FBR would contain plutonium, uranium, and thorium while the blanket contains ^{233}U and thorium. The process for the FBR fuel must therefore meet two demands: one product stream must be suitable for HTGR or LWR fuels and the other for return to the FBR core. The actinides in the spent FBR fuel should therefore be separated into a uranium-thorium portion (for HTGR or LWR) and a plutonium-thorium portion (for FBR core).

Process Description

A conceptual pyrometallurgical method for the reprocessing of thorium-based fuels is presented in Fig. 1. It is responsive to the constraints described previously, being operable with either oxide or metal alloy fuel, and producing product streams consisting of enriched uranium/thorium and plutonium/thorium. The process can be divided into three main steps: (1) oxide reduction or metal dissolution, (2) uranium/plutonium separation and thorium partition, and (3) product recovery. Each step is described below.

1. Reduction. Assuming the fuel to be declad using a method compatible with subsequent process steps, it must then be converted to metallic form. For an oxide fuel, this involves a reduction of the type



Carbides can be converted to oxides and reduced as above. Metal alloy fuels are already in suitable form and can be processed directly. Calcium is used as the reducing agent as the free energy of Reaction 1 is -6.6 kcal/mole at 1000°C . The other fuel and fission product oxides are reduced more easily than ThO_2 , thus the reduction should be complete once the thoria is reduced.

The reduction proceeds via the addition of calcium to a magnesium based alloy which is covered with a fused salt

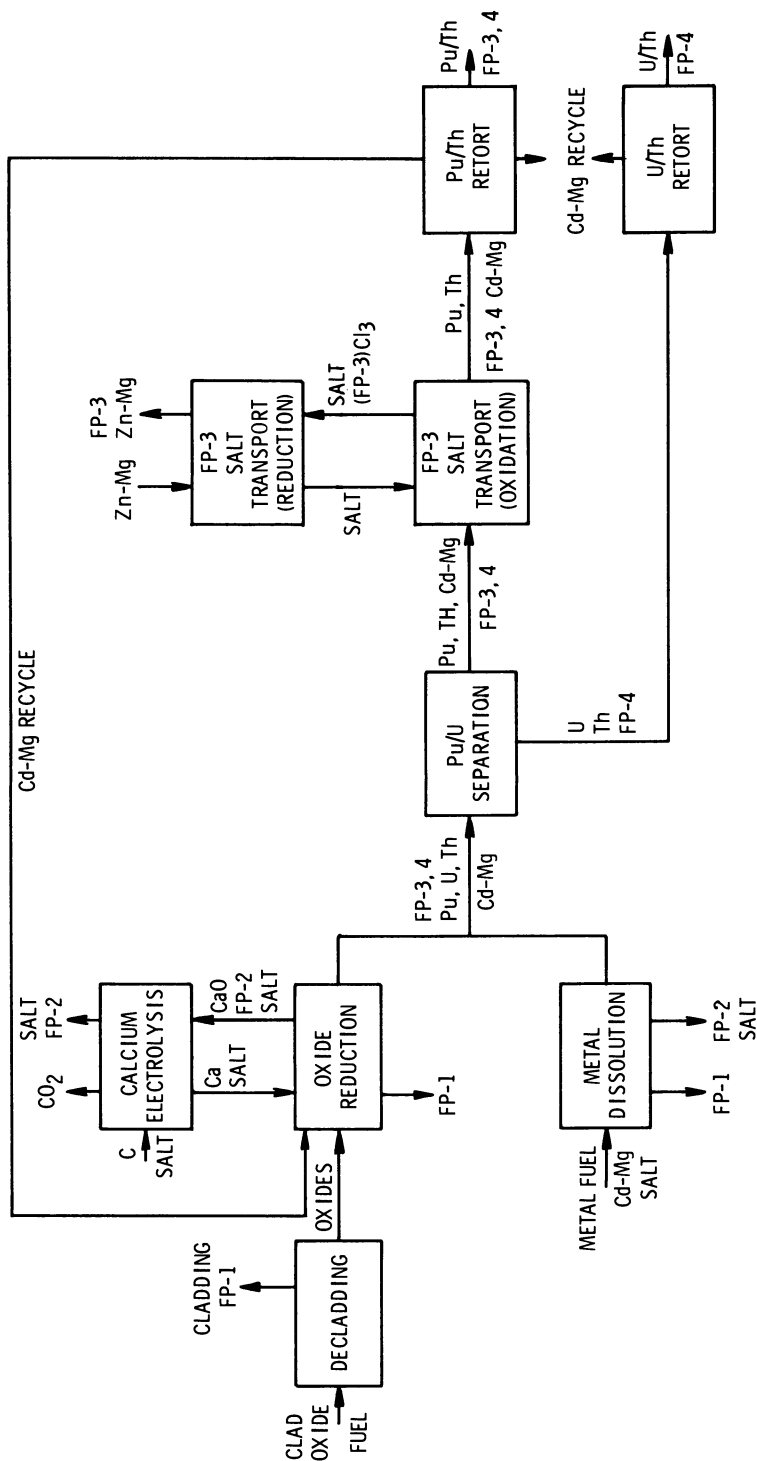


Figure 1. A conceptual flow sheet for Th-based oxide and metal fuels

(CaCl_2 , CaF_2). The salt wets the oxide fuel and serves as a medium for the reduction. It also dissolves the CaO produced during the reduction and takes up the alkali and alkaline earth fission products (FP-2) and also the iodine (5). The salt represents the major waste stream in the process and needs to be bled off because of a buildup of FP-2. High salt discard rates are not necessary because the CaO is removed by electrolysis and the calcium is recycled. The variables controlling reduction are discussed more fully later.

2. Uranium/Plutonium/Thorium Partition. After the reduction step, the metals partition according to their solubility in the magnesium alloy. Magnesium is used as the focus metal because it provides a means of separating uranium from plutonium.

The solubilities of uranium, plutonium, and thorium in magnesium at 650°C are 0.002 wt %, 55 wt %, and 44 wt %, respectively. Thus, assuming no solute interaction, uranium is essentially insoluble in magnesium, while plutonium is quite soluble and good separation may be effected. While precipitation of an insoluble phase from solution would appear to be a straightforward process, the behavior of a solute in a given metal or alloy may differ from its behavior when influenced by the inclusion of other solutes. One element may increase or suppress the solubility of another through coprecipitation or intermetallic compound formation. Such effects must be determined experimentally.

Under proposed process conditions the amount of thorium far exceeds other elements. To obtain the necessary division of thorium between the minor uranium and plutonium constituents, only a method of controlling the quantity of thorium in solution is needed. This can be achieved by controlling the amount of liquid magnesium solvent. By limiting the volume of the liquid magnesium, thorium can be divided into a soluble and insoluble fraction. Even more control can be gained by alloying cadmium with magnesium. This alloy solvent retains the low solubility of uranium and complete solubility of plutonium but allows the thorium solubility to be varied between 5 and 42 wt % (Fig. 2). It is also compatible with the reduction and retorting operations.

As an example, for one metric ton of plutonium/thorium (1:4) fuel with a burnup of 55 000 MWD the resulting core composition (wt %) is Th-75.5, Pu-14.6, FP-5.9, U-3.7, and Pa-0.3 (6). Thus to produce product streams plutonium/thorium (1:4) and uranium/thorium (1:4.5) the process requires 1600 kg of Cd-50 wt % Mg alloy at 600°C .

The necessary nonproliferation constraints are provided by the high radioactivity of each product stream, and the remote handling requirement of each process step. In addition, both the fissile uranium and plutonium are coprocessed with thorium. Pure plutonium cannot be obtained because both thorium and plutonium have a large solubility in the solvent alloy. Pure uranium could in principle be obtained by repeatedly washing the uranium-

thorium precipitate with fresh liquid magnesium. However, in practice such separations have proven difficult (7). Finally, the protactinium, which decays to ^{233}U , remains with the uranium and does not provide a source of clean fissile material (8).

3. Product Recovery. After the uranium/thorium precipitate has settled a solid liquid separation is effected. The remaining uranium/thorium is retorted to remove entrained solvent and the product is recovered.

The alloy in which the plutonium/thorium is dissolved also contains the soluble rare earth fission products (FP-3). A fraction of these radioactive products are selectively extracted from the alloy using a "salt-transport" process (9). The remainder of the FP-3 fission products stays with the plutonium/thorium stream to provide diversion resistance. The plutonium/thorium remaining in the original alloy is then recovered by retorting the alloy. The solvent in both retorting steps is recycled to the beginning of the process.

Process Chemistry

The direction of each fuel constituent and the control which can be exercised over it during the process is summarized below.

FP-1 (krypton, xenon, hydrogen)--are removed during de-cladding and reduction and are treated as off gases.

FP-2 (iodine, cesium, rubidium, strontium, barium, europium, samarium)--are removed during the reduction step by extraction into the salt phase. There will be an accumulation of FP-2 fission products in the salt which is controlled by a continuous salt bleed. For 1000 kg of fuel, 2000 kg of salt are required. To keep a constant level of 10% FP-2 in the salt a bleed of 200 kg of salt/batch is necessary.

FP-3 (yttrium, lanthanum, cerium, praseodymium, neodymium, promethium, gadolinium, terbium)--are soluble (~15 wt %) in the process alloy and are removed by selective extraction into the salt after the reduction. This is a salt-transport step and is used as the method of controlling the FP-3 concentration in the process stream and of consolidating the FP-3 for waste handling. A nominal amount of FP-3 remains in the plutonium/thorium stream for diversion resistance.

FP-4 (zirconium, niobium, molybdenum, technetium, ruthenium, rhodium, palladium, silver, cadmium, indium, tin, antimony)--are only slightly soluble (<1 wt %) in the process alloy, thus will partition between both product streams. The process, as presented, offers no method of FP-4 removal and possibly an unwanted increase in these products would occur if the fuel were to be recycled. However, it would be possible to separate the FP-4 from the plutonium/thorium stream by recovering the plutonium/thorium by hydriding. The FP-4 do not form stable hydrides and would remain in solution.

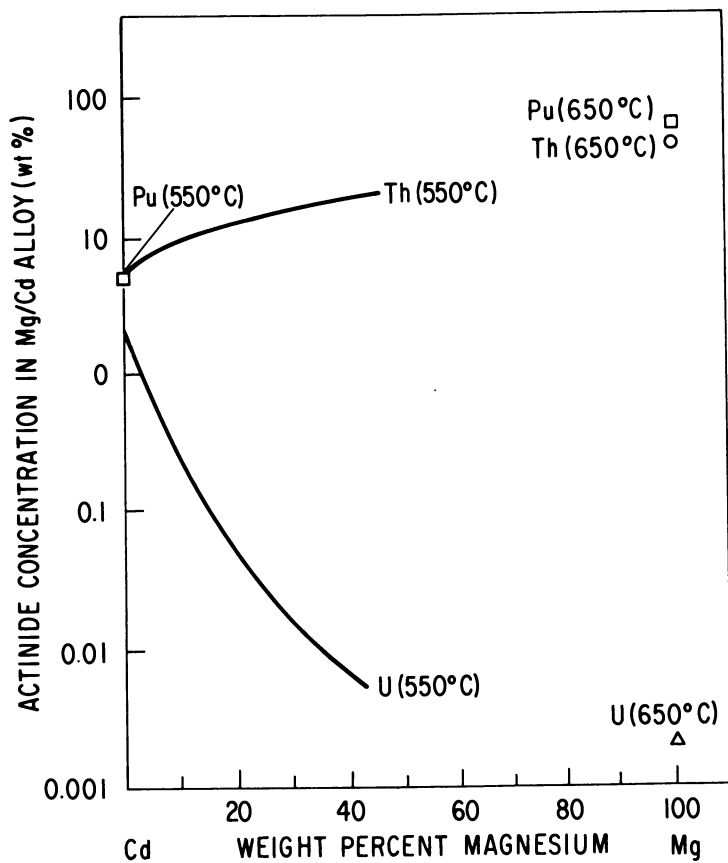


Figure 2. The solubility of U, Pu, and Th in Cd-Mg alloys

Uranium--is very insoluble in the alloy chosen for reduction and <0.1% of the uranium in the fuel will be in the plutonium stream. Also uranium does not transfer into the salt during the FP-3 removal to a significant extent so total uranium losses should be negligible.

Plutonium--is very soluble in the process alloy so only through coprecipitation will any follow the uranium stream. There will be some plutonium loss during the FP-3 extraction but should be <0.4% with proper choice of alloy and salt.

Thorium--will not go into the salt at all and is partitioned by solubility as desired between the plutonium and uranium streams.

Protactinium--precipitates with the uranium and after about 300 days will have decayed completely into ^{233}U .

Solubility of Thorium in Cadmium/Magnesium Alloys

The key to the partitioning of thorium in the described conceptual flow sheet is the solubility in cadmium-magnesium. Experimental data associated with this problem have been obtained. The weight percent thorium in solution was determined by taking samples of the equilibrated liquid at varying temperatures and alloy compositions. The samples were analyzed for thorium, magnesium, and cadmium using atomic absorption spectroscopy and the results are estimated to have a relative accuracy of $\pm 3\%$. Samples were taken in tantalum sampling tubes having a porous tantalum filter (35 μ pore) at the end. An explanation of the sampling technique has been reported previously(10). The melts were contained in tantalum crucibles and equilibrated by stirring for 1-1/2 hours between samples. The temperatures were measured by means of a calibrated chromel-alumel thermocouple with an estimated accuracy of $\pm 1^\circ\text{C}$.

The results are shown in Fig. 3. The thorium solubility decreases uniformly as the cadmium concentration of the melt is increased or as the temperature is decreased. Samples were not taken below 550°C as melts with higher magnesium concentration are solidified.

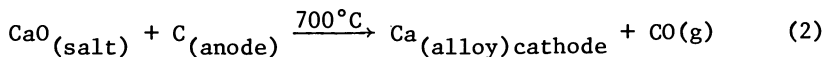
These results compare favorably with previous data obtained for the solubility of thorium in cadmium(11) but indicate a much larger thorium solubility at high magnesium concentrations than had previously been reported(12). The present results are reasonable in that the solubility of thorium in magnesium is 42 wt % at 582°C .

Electrolysis

During the reduction process, calcium oxide is generated which is collected in the salt phase. The amount of CaO in the salt can reach about 30 atom percent before the reduction rate substantially decreases. The salt can be either discarded as

high level waste or processed to remove the CaO. The volume of waste salt generated for each metric ton of fuel processed would be ~850 L. This amount can be decreased to 8 L by using the calcium recycle process presented in Fig. 4.

This concept is based on electrolysis of CaO in a fused salt (CaCl₂ · CaF₂). The net cell reaction is



The cathode reaction generates calcium metal for recycle and the anode reaction yields oxygen which combines *in situ* with the carbon anode to produce a mixture of CO and CO₂. (For simplicity only CO is considered in the mass balances.) Thus, the oxygen is removed from the oxidic fuel not as a large volume solid waste but as a common gas which can be scrubbed for release into the atmosphere.

Electrolysis of CaO has been achieved in previous studies(13) where gram quantities of calcium metal were produced from the fused salt electrolysis of CaCl₂ containing ≤2 wt % CaO at ~800°C. No chlorine was detected at the anode which indicated CaO rather than CaCl₂ was electrolyzed, which is consistent with thermodynamics.

To establish the feasibility of Equation 2, experiments utilizing a cell design employing a liquid metal cathode and a graphite anode are being conducted. The metal cathode serves as the collector for the calcium metal. The selected cathode metal should be more dense than the fused salt electrolyte and be compatible with the oxide reduction reaction so that the regenerated calcium can be recycled directly to the reduction step. Graphite immersed in the salt electrolyte is used as an anode. The entire cell is operated in a dry argon atmosphere.

Initial experiments utilized cadmium as the cathode and CaCl₂, 15 wt % CaF₂, 5 wt % CaO as the salt. The cell was run at 700°C and a current density of about 0.5 amp/cm². The cell potential was 2 volts. The reaction was monitored by taking filtered samples of the metal and salt phases and samples of the gas stream directly above the cell. The results indicate that during the electrolysis the calcium metal concentration in the cathode metal increased from 0 to 3 wt %. The CaO in the salt decreased from 5 to 1 wt % and CO₂ and CO were found in the off gas. These results indicate the electrolysis proceeds as expected and, with optimization of the operating conditions, will serve as a means of recycling calcium metal thus reducing the waste volume from the reduction step.

Reduction

As indicated in the reference flow sheet for oxide fuels (Fig. 1) the processing of the fuel constituents requires a reduction step. Pyrochemical reduction of UO₂, (14) PuO₂, (15) and

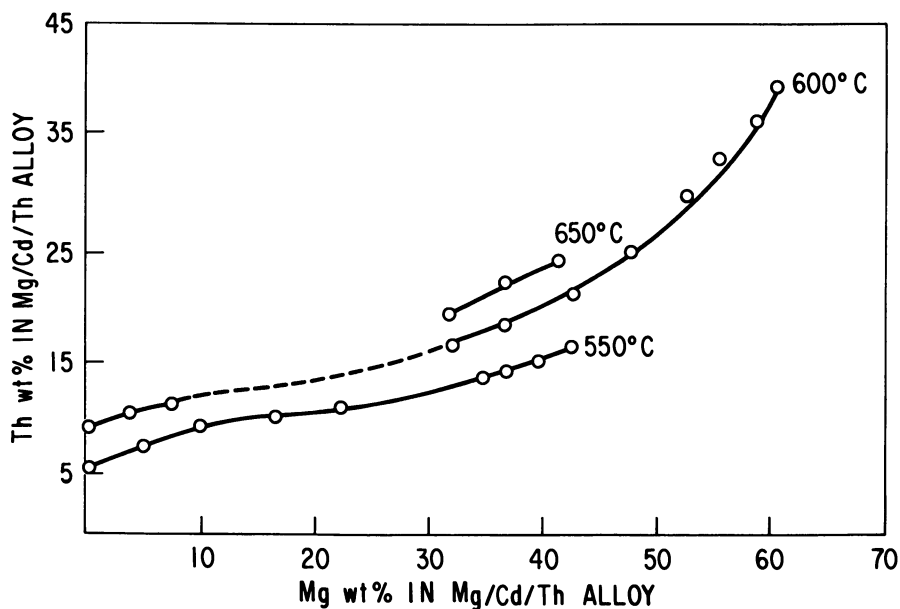


Figure 3. The solubility of Th in Cd-Mg alloys

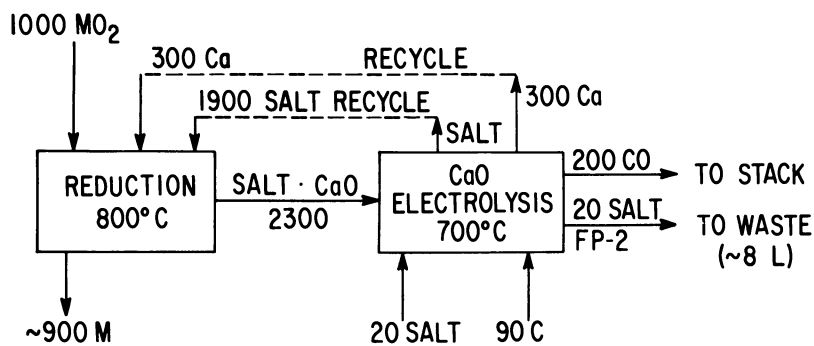


Figure 4. Schematic of the Ca recycle process designed for the reduction of oxide fuels

ThO_2 (12) has been demonstrated, but the process parameters have not been optimized for calcium reduction. These parameters include alloy and salt composition, temperature, effect of mixing, CaO and metal loading in the salt and alloy respectively, and type of oxide being reduced. Importantly, only the reduction of powdered ThO_2 has been demonstrated. Reduction of high fired ThO_2 , as might be obtained from a reactor, has not been attempted. Preliminary experiments designed to demonstrate this reduction are reported.

Two types of high fired thoria (1700°C) were used, 200 mesh microspheres and 1/4 in. pieces of irregular shape (Cerac, 99.9% pure). The other process variables were chosen to be compatible with the flow sheet and to optimize conditions for reduction. A Cd-45 wt % Mg, 10 wt % Ca alloy was covered with premelted salt (CaCl_2 , 20 at. % CaF_2) and equilibrated at 675°C. Enough ThO_2 was added so that with complete reduction the resulting alloy would contain 5 wt % thorium. Upon addition of the ThO_2 the melt was mixed by stirring with a flat impeller located at the salt-metal interface. The stirring rate was 800 rpm. The salt and alloy were sampled at the beginning of the experiment and at timed intervals up to four hours. For both types of starting material there was a decrease in the calcium concentration and an increase in the thorium concentration in the alloy indicating the reduction went to about 5% completion. A change in the CaO concentration in the salt, larger than experimental error, could not be detected.

These results indicate the reduction of high fired thoria is difficult and that an understanding of the reaction mechanism is likely to be necessary so that the optimum conditions can be identified.

Conclusions

A conceptual flow sheet for the pyrometallurgical reprocessing of thorium-based fuels has been presented which meets current concerns about nonproliferation and waste control. Preliminary results indicate the desired process streams, uranium/thorium and plutonium/thorium, can be obtained using actinide solubility differences in cadmium-magnesium alloys and that salt waste can be minimized by electrolyzing CaO produced during the reduction process and recycling the calcium. However, further optimization of conditions controlling the reduction rate must be achieved before the process can be used for oxide fuels.

Acknowledgement

The technical support of D. Kroeck, and J. Meisenhelder and the interest and encouragement of C. H. Bean, M. J. Steindler, D. S. Webster, and L. Burris, Jr. are gratefully acknowledged.

Literature Cited

1. P. Chiotti, *J. Nucl. Mat.* 51, 178(1974).
2. R. V. Laney and P. R. Huebotter, *Amer. Nucl. Soc. Trans.* 28, 320(1978)
3. H. L. Scherff, *Euratom-Revue* 1, 74(1968).
4. F. M. Mann and R. E. Schenter, *Nucl. Sci. and Eng.* 65, 544(1978).
5. M. Krumpelt, *et al.*, *Nucl. Tech.* 15, 391(1972).
6. K. M. Myles, ANL, private communication.
7. J. D. Chilton, *et al.*, "Separation of Uranium from Thorium by Liquid Metal Extraction, Thorium Recovery, and Fission Product Distribution," NAA-SR-6666, AI(1962).
8. P. Chiotti, P. F. Woerner, and K. L. Malaby, *J. Chem. and Eng. Data* 5, 435(1960).
9. I. Johnson, "Partition of Metals between Liquid Metal Solutions and Fused Salts," in *Applications of Fundamental Thermodynamics to Metallurgical Processes*, G. R. Fitterer, ed., Gordon and Breach, New York, 153-179(1967).
10. I. O. Wansch, *et al.*, "Sampling of Liquid Alloys," ANL-7088 (1965).
11. A. E. Martin, ANL, private communication.
12. B. Amecke, "Contributions to the Reprocessing of Thorium-Uranium Nuclear Fuels with the Salt-Transport Method," Dissertation Technical University of Carolo-Wilhelmina at Braunschweig, ANL-TRANS-1141 (1978).
13. W. Threadgill, *J. Electrochem. Soc.* 111, 1408(1964).
14. R. A. Sharma and I. Johnson, *Metallurgical Trans.* 1, 291 (1970).
15. W. Z. Wade and T. Wolf, UCRL-50403 (1968).

RECEIVED May 15, 1979.

AIROX Dry Pyrochemical Processing of Oxide Fuels

A Proliferation-Resistant Reprocessing Method

L. F. GRANTHAM, R. G. CLARK, R. C. HOYT, and J. R. MILLER

Rockwell International, Energy Systems Group, 8900 De Soto Avenue,
Canoga Park, CA 91304

During the early developmental phases of nuclear power, several low-decontamination methods of recycling spent fuel were investigated. Continued development of these low-decontamination methods was abandoned in favor of high-decontamination methods of recycling spent nuclear fuel. However, recent concern over potential diversion by national or subnational groups of highly decontaminated fissile material from power production has brought about a reevaluation of low-decontamination fuel cycles. The AIROX process (1,2,3) is a dry, pyrochemical, low-decontamination method of recycling spent fuel. The AIROX process simultaneously declads and pulverizes spent fuel by simple gas-solid reactions; the pulverized fuel is reenriched, repelletized, and recycled to the reactor. A discussion of proliferation resistance is given first; this is followed by a description of the AIROX processing method. Fuel cycles that could utilize this method are then suggested; this is followed by decladding and pulverization data. This paper is concluded with a discussion of the status of AIROX reprocessing including advantages and disadvantages of this reprocessing method.

Proliferation Resistance

Spent fuel is generally regarded as proliferation-resistant due to the high level of radioactivity and the low concentration of fissile material in the fuel removed from a reactor. High levels of radioactivity promote proliferation resistance because special, easily monitored facilities are required to process the fuel and the high level of radioactivity makes removal of fuel without detection extremely difficult. Spent fuel is also proliferation-resistant because the concentration of fissile material is below that required to achieve a nuclear detonation.

0-8412-0527-2/80/47-117-219\$05.00/0
© 1980 American Chemical Society

This discharged fuel can be recycled back to the LWR or the FBR after reprocessing and refabrication. The reprocessing step, if conducted by conventional methods for recycle, would separate the fissile material (plutonium) from the spent fuel. Potential diversion of a portion of this separated fissile material to nuclear weapons by national or terrorist groups has caused the Federal Government to postpone all fuel reprocessing and to re-evaluate proliferation-resistant methods of recycling the spent fuel. Several proliferation-resistant reprocessing methods have been proposed, such as CIVEX(4,5), PYRO-CIVEX(6,7), and AIROX(1), the process that will be discussed in this paper. All of these reprocessing methods recycle fuel containing fission products and avoid complete fissile-fertile separation to enhance proliferation resistance. Fuel cycles utilizing AIROX reprocessing are proliferation-resistant because (1) the fission product content is 30-60% that of spent fuel, (2) no fissile-fertile material separations are made, and (3) the process cannot be easily modified to effect fertile-fissile separation.

AIROX Process

The AIROX (Atomics International Reduction Oxidation) process is being developed to reprocess spent uranium oxide-based fuel. It is a cyclic oxidation-reduction process that employs only gaseous and solid materials; no liquids are used. Hence, this process is often referred to as a dry process which simultaneously de-clads and pulverizes the fuel. Pulverization permits release of volatile fission products and comminutes the fuel for re-enrichment and recycle. It also provides gaseous access to unreacted fuel in the center of the pellet.

Pulverization takes place by oxidation of the uranium dioxide (UO_2) with air at elevated temperatures ($\sim 400^\circ C$) which expands the fuel volume; if the oxidation is continued until U_3O_8 is obtained, a 30% volume expansion is achieved. The volume increase ruptures the cladding and pulverizes the fuel. Complete oxidation of UO_2 to U_3O_8 is not required to obtain sufficient volume expansion for pulverization.

The oxidized UO_2 is reduced back to UO_2 by reaction with dilute hydrogen (10-20%) in nitrogen at about $600^\circ C$. After reduction, the fuel can be reoxidized to achieve further pulverization if desired. Ultimately, the fuel is reduced back to UO_2 for enrichment and pelletization prior to recycle to the reactor.

In the AIROX processing system, the hardware is sheared off the ends of the fuel assembly and individual fuel pins are fed into a continuous rotary punch, which is essentially a V-belt pulley with punch dies extended from the center of the groove. This provides small holes in the fuel pins spaced at an optimum distance (2.5 to 4.0 cm apart) to permit gaseous reactant (O_2 and H_2) access to the fuel. The cladding after AIROX processing is shown in Figure 1. A typical-size distribution of fuel particles

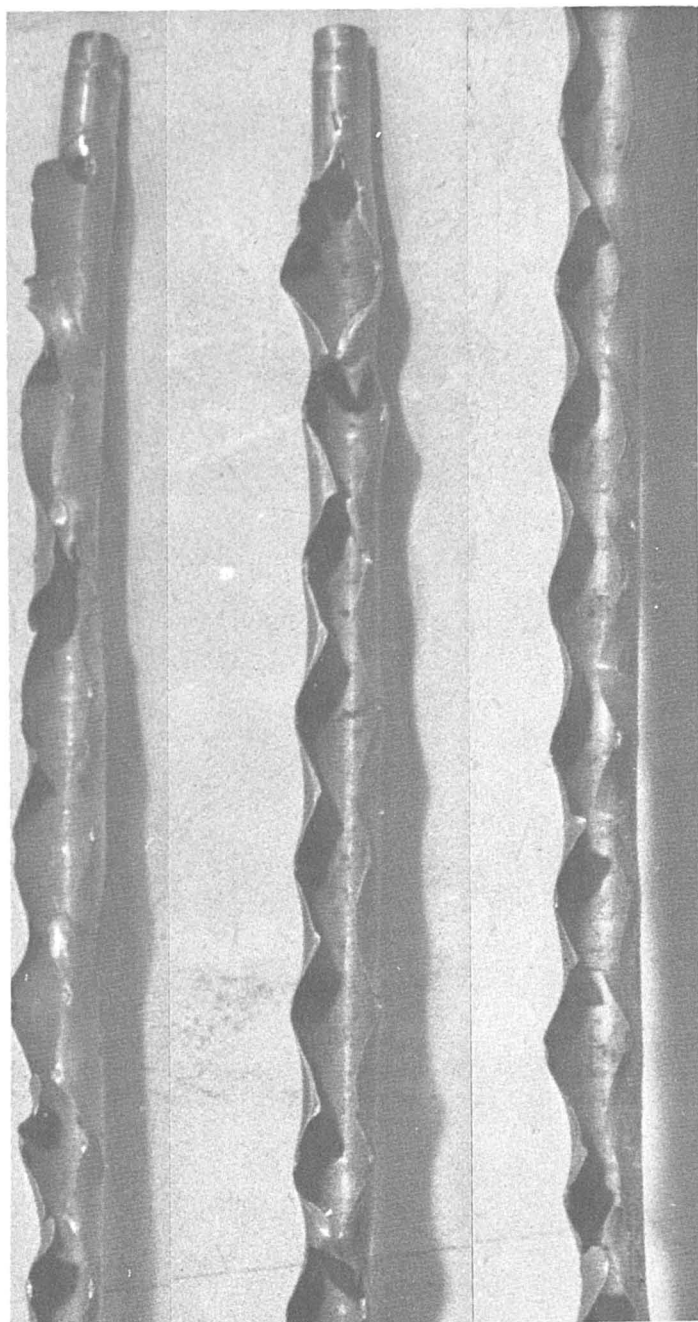


Figure 1. Cladding after AIROX processing

after different processing conditions is shown in Table I. After a single oxidation, the fuel is readily pulverized to a size suitable for repelletization (i.e., 2-10 microns) by ball milling for a few minutes. The fact that the fuel does not pulverize to micron size during the first oxidation is advantageous. Submicron and micron-sized particulates of fuel would tend to cling to the ruptured cladding and to be dispersed by air currents in the process vessels. Pulverization to about 10 mesh (2000 microns) is all that is required to assure decladding and complete (> 99.9%) fuel-cladding separation. Note also in Figure 1 that the cladding ruptures up to the end plugs; it is not necessary to shear the end plugs to assure complete removal of the fuel from the fuel pin.

Possible Fuel Cycles

AIROX processed spent fuel must be enriched in fissile content prior to reactor recycle.

LWR Cycle. The source of this enrichment material for an LWR can be either virgin uranium(1) or FBR blanket material containing the required amount of fissile material. The fuel cycle is proliferation resistant because of the high radioactivity of the product and the low concentration of fissile material in all process steps. Between 50-85% of the spent LWR fuel can be recycled to the LWR that produced the fuel; the remaining 15 to 50% of the spent fuel can be used to startup a new light-water reactor, processed by a proliferation-resistant method to recover the fissile material or disposed of at a Federal repository. Only about 80% as much virgin uranium would be required to refuel the reactor using recycled fuel after AIROX processing as would be necessary to refuel the reactor if no spent fuel were recycled. The fraction of the fuel that can be recycled to the LWR that produced the spent fuel can be varied from 50-85%, but as the fraction of recycled fuel increases, the concentration of U^{235} in the enrichment stream must also be increased from approximately 5 to 20%. In order for this enrichment stream to be proliferation-resistant, the maximum concentration of U^{235} in the enrichment stream should be limited to ~20%.

The penalty for recycling fission products back to an LWR is that the concentration of the fissile material in the fuel must be slightly higher (3.5 vs 3.2% for a pressurized-water reactor, PWR) to make up for the neutrons that will be absorbed by the fission products(8). The neutron cross section varies with each isotope of each fission product; therefore, the importance of removing each fission product depends on the neutron spectrum and on the concentration and half life of each fission product. The importance of removing the various fission products for uranium and plutonium recycle in the PWR neutron spectrum is given in Table II. The volatile fission products removed during AIROX processing decrease the parasitic neutron absorption about 25%.

TABLE I
TYPICAL SIZE DISTRIBUTION OF AIROX PROCESSED FUEL

Particle Size (μ)	Percent of Pulverized Material			Second Oxidation Reduction Cycle
	Partial Oxidation ($UO_{2.4}$)	Partial Oxidation* ($UO_{2.6}$)	First Oxidation Reduction Cycle	
2000	0	0	0	0
297 to 2000	27.8	23.2	10.5	0.6
210 to 297	0.1	1.7	3.2	0.3
125 to 210	0.2	3.1	6.8	1.0
74 to 125	0.1	4.9	4.5	2.4
37 to 74	0.3	9.2	10.5	13.0
20 to 37	13.4	37.3	17.6	72.3
10 to 20	56.0	19.4	26.7	8.6
5 to 10	2.0	1.3	18.5	1.8
<5	0.0	0.0	1.7	0.0

*50% oxygen in oxidizing gas; remaining test performed with air (21% O_2).

TABLE II
FISSION PRODUCT ELEMENT RELATIVE
REMOVAL IMPORTANCE

Element	Fission Product Neutron Absorption (% of Total)*		
	Uranium Recycle		Plutonium Recycle
	180 day cooling	10 year cooling	180 day cooling
Samarium	21.7%	23.3%	18.2%
Neodymium	16.8	17.3	11.3
Cesium**	13.5	13.2	12.9
Europium	8.2	8.1	9.5
Rhodium	7.6	7.8	12.2
Xenon**	6.6	6.7	7.8
Molybdenum	4.6	4.8	3.7
Technetium	3.9	4.0	3.2
Palladium	3.3	3.4	5.4
Promethium	3.2	0.3	4.9
Ruthenium**	3.1	3.2	3.1
Silver	1.4	1.4	3.0
Praseodymium	1.2	1.2	0.7
Zirconium	1.2	1.2	0.8
Lanthanum	0.9	0.9	0.6
Iodine**	0.8	0.9	0.9
Krypton**	0.8	0.8	0.5
Cerium	0.3	0.2	0.2
Gadolinium	0.3	0.7	0.3
All Others	0.7	0.7	0.8

*Percent of neutrons absorbed by a specific fission product element compared to the neutrons absorbed by all the fission products in a PWR neutron spectrum.

**Elements removed during AIROX processing.

FBR Cycle. The AIROX process is also applicable to FBR fuel recycle. The FBR driver fuel must be enriched in fissile content before recycle by transferring fissile material from the spent FBR blanket. Since the concentration of fissile material is too low and since the AIROX process does not separate fertile and fissile material, the AIROX process must be used in conjunction with a process which does separate fissile material. To obtain the enrichment material, the spent FBR driver fuel and a portion (20-30%) of the spent blanket fuel must be processed by the proliferation-resistant CIVEX or PYROCIVEX methods. The remainder of the spent fuel, 70-80% of the blanket can be recycled after AIROX processing only(1). The portions of the spent blanket fuel with the highest fissile content (such as the spent internal and axial blankets) as well as a portion of the remaining external blanket would be recycled without further processing. The simplicity of the AIROX process provides an economic incentive for development of this dual-reprocessing system.

The Atomic International Bullseye or Parfait Core FBR(9) fuel cycle was analyzed to determine the maximum amount of blanket fuel which comprises 78% of the spent fuel that could be recycled after AIROX processing only. In this analysis, it was assumed that the enrichment stream from the Civex or Pyrocivex reprocessing plant was about 48% fissile material, 42% fertile material, and 10 wt % fission products. In one fuel management scheme, about 70 wt % of the blanket fuel can be recycled after AIROX processing only. About 51% of the spent blanket fuel is refabricated into LWR fuel and about 21% is used to dilute the fissile material from the Civex or Pyrocivex reprocessing plant to the required FBR fissile content before it is refabricated into driver fuel. Only 28% of the spent blanket fuel requires processing by aqueous or pyrochemical means. In another fuel management scheme which recycles 25% of the spent blanket fuel back to the axial blanket to increase subsequent blanket fissile content, the amount of the blanket fuel which can be recycled after AIROX processing only is over 80% and less than 20% must be processed by aqueous or pyrochemical methods. About 21% of the spent driver fuel is refabricated into driver fuel while 40% of the spent blanket fuel is refabricated into LWR fuel.

In the FBR fuel cycles, the fraction (i.e., 21% in the examples above) of the blanket fuel recycled for use in refabricating driver fuel after AIROX processing only depends on the concentration of fissile material in the Civex or Pyrocivex product. As the fissile content of the Civex or Pyrocivex product is decreased, the amount of blanket fuel recycled for driver fuel fabrication must also be decreased proportionately and the amount of spent blanket fuel processed by the Civex or Pyrocivex process must be increased.

Experimental Results

Several tests were run to determine oxidation and reduction reaction rates of UO_2 pellets at various processing conditions. The rate of reaction was followed by measuring the amount of gaseous reactant consumed and confirmed by weighing and analyzing the product at the end of a test. The product from several of the tests was sieved to determine the size distribution.

The oxidation of UO_2 appears to proceed in three distinct steps, i.e., (1) induction period; (2) rapid oxidation; and (3) moderate oxidation. This is shown in Figure 2. During the induction period, essentially no oxygen is removed from the surrounding gas; this time probably corresponds to that required for the fuel to reach processing temperature, diffusion of air into the microcracks in the fuel and the initiation of surface oxidation. The rapid oxidation corresponds to the formation of intermediate uranium oxide phases, such as U_4O_9 or $UO_{2.6}$, as the crystal structure changes from cubic to the less dense tetragonal phase. The oxygen-to-uranium ratio at the transition varies from 2.5 to 2.6 at oxidation temperatures of 400-500°C. The upper boundary of the third oxidation step is the formation of U_3O_8 (O:U ratio of 2.67). Examination of Figure 2 indicates that the time required to perform the first two oxidation steps is markedly reduced as the oxidation temperature approaches 480°C. Essentially, all of the fuel has decomposed to fine particles after the first oxidation step where the UO_2 is oxidized only as far as the intermediate phase; complete oxidation to U_3O_8 is unnecessary. These results, along with previous results(2,3,10) indicate that the decladding can be accomplished on the first oxidation.

During the first oxidation in AIROX processing, factors such as temperature and oxygen partial pressure control the amount of time required to pulverize the spent fuel. With air as the oxidizing gas, a minimum reaction time was found at 480°C. As the oxygen partial pressure was increased at about 435°C, the minimum reaction time occurs with about 50% oxygen. These data indicate that if one tries to oxidize too rapidly by increasing the temperature and oxygen content, the oxidation rate can actually decrease. This is probably because rapid oxidation expands the surface oxide so that microcracks in the fuel are blocked and the oxygen must diffuse through an oxide film whereas if the oxidation is conducted more slowly, the oxygen can diffuse through microcracks in the film.

The degree of pulverization does vary with the pulverization conditions as shown in Tables I and III. Three general observations can be reached from examining the pulverization data. First, over 70% of the product was less than 297 microns in size after the first partial oxidation (all of the fuel was less than 2 millimeter in size). Second, there is little product that is less than 297 microns and greater than 74 microns. In other words, once pulverization of a fragment begins, the fragment pulverizes

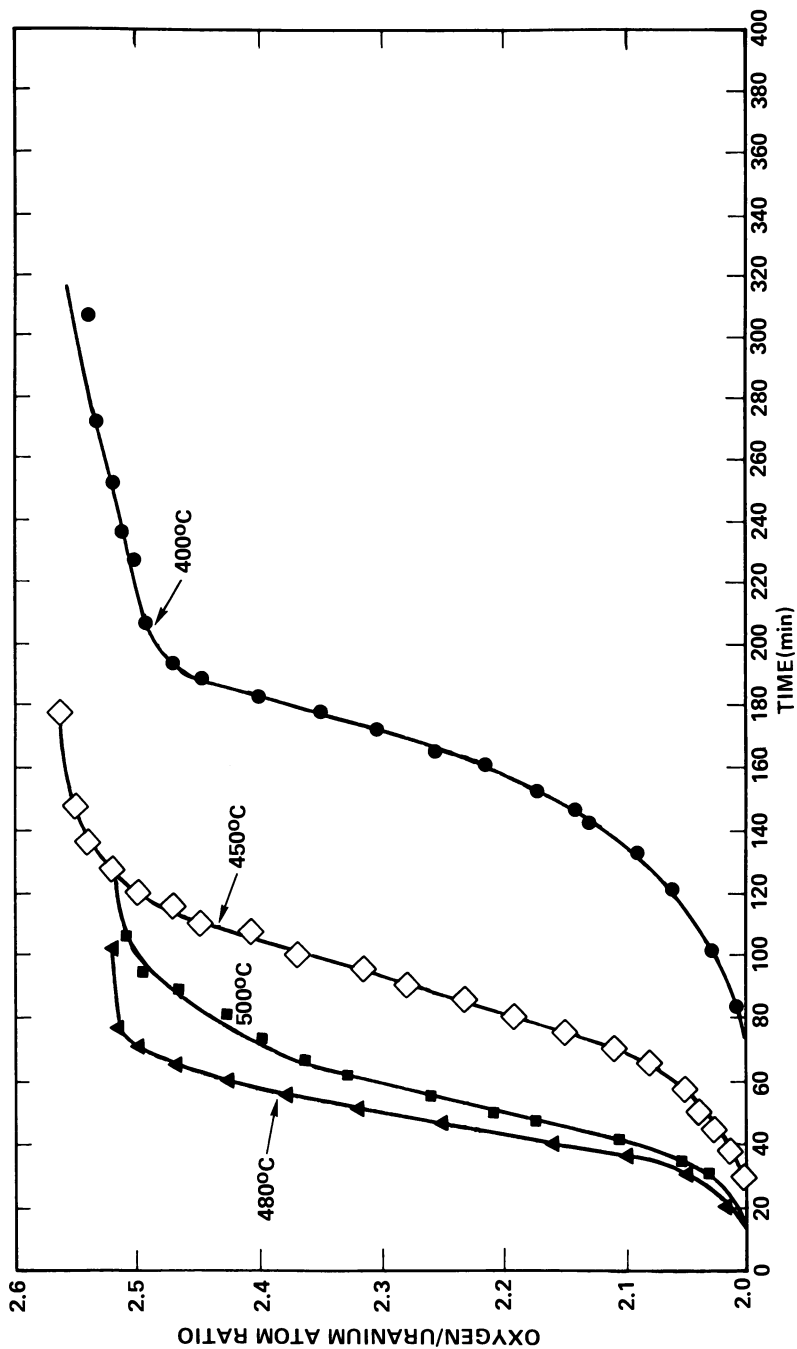


Figure 2. Reaction rate of UO_2 fuel

TABLE III
PULVERIZATION OF UO₂ PELLETS

Test No.	Processing Conditions									
	Oxidation		Reduction		Size distribution of AIROX Product (%)					
	Temp. (°C)	% O ₂	Temp. (°C)	% H ₂	>297μ	297 to 37μ	37 to 20μ	<20μ		
5	400	21	625	21	5	<1	21	94		
6	400	21	-	-	28	<1	13	58		
7	400	21	625	21	<1	11	25	63		
8	450	21	625	21	<1	19	29	53		
9	480	21	625	21	2	27	32	38		
10	500	21	625	21	5	25	38	32		
11	425	50	-	-	27	18	26	28		
12	430	100	-	-	21	31	16	36		
13	480	50	-	-	23	23	30	23		
14	480	50	625	21	20	19	17	45		
18	486	50	-	-	23	19	37	21		
19	370	21	-	-	17	5	36	41		
20	370	21	625	21	6	2	18	73		

readily to a power less than 74 microns in size. Third, the amount of material less than 5 microns in size is negligible, and, therefore, particulate control or dusting in a commercial process may not be a problem.

The interrelationship between the various processing parameters and the size distribution is quite complex, and there may be synergistic effects not elucidated at the present state of development. However, some tentative effects of the various parameters are illustrated in the data in Table III. During the first oxidation, the enhancement of pulverization at lower temperatures and vol % oxygen is shown in Tests 13, 18, and 19 and 12, 11, and 6. These data indicate that although the amount of material greater than 297 microns in size may increase slightly (~6%), the amount of material pulverized to less than 20 microns is significantly greater (20%) as the oxidation temperature and oxygen partial pressure is decreased.

The degree of pulverization is enhanced by a reduction following the initial oxidation as shown in Tests 13 and 14, as well as Tests 19 and 20. These data indicate that pulverization is improved markedly by reduction of the oxidized product back to UO_2 . Note that both the amount of material greater than 297 microns is reduced, and the amount of material less than 20 microns is increased during the reduction portion of the first redox cycle.

Increased oxidizing temperature during the first oxidation-reduction cycle appears to reduce the degree of pulverization. These data are shown in Tests 20, 5, 7, 8, 9, and 10. The amount of material greater than 297 microns appears to pass through a minimum between 400 and 450°C. However, the amount of material 297 μ to >37 μ size and 37 μ to >20 μ sizes increases markedly while the amount of material less than 20 microns decreases markedly as the initial oxidation temperature is increased.

The improved pulverization with a second oxidation-reduction cycle is shown in Table I. These data show a marked reduction in the amount of material greater than 297 microns and a marked increase in the amount of material less than 37 microns after a second oxidation-reduction cycle.

The maximum pulverization does not occur at the maximum oxidation rate. With 21% oxygen, the maximum oxidation rate occurs at 480°C, but the maximum pulverization occurs at the lower temperatures (see Tests 20, 5, 7, 8, 9, and 10). This observation appears to support the theory that if the oxidation is carried out too rapidly, the U_3O_8 on the surface of the fragments inhibits further oxidation and pulverization. Therefore, if maximum pulverization is desired, the oxidation should be carried out at a temperature less than that where the maximum oxidation rate occurs.

To obtain maximum pulverization at minimum time, the oxidation temperature should be decreased as the material is oxidized. To minimize the induction period, the oxidation should begin at

~480°C, and then be decreased to ~425°C to optimize pulverization. Under these conditions, decladding and pulverization can be accomplished in less than 1 hour.

No induction period was found during the second oxidation and the second oxidation occurs much more rapidly than the initial oxidation. The reduction reaction increases with increasing reduction temperature and hydrogen content of the reducing gas. A hydrogen concentration of 10-20% will produce satisfactory reduction times (<30 min). Unlike oxidation, the reduction rate does not appear to decrease with successive cycles. The reduction conditions do not appear to affect the degree of pulverization.

Status of Development

Pellets of UO₂ have been pressed, sintered, and reprocessed several times via the AIROX process(10,11,12). In one series of tests, stable fission products equivalent to 20,000 Mwd/MTU burnup were added during each of five cycles until the fission products content of the UO₂ was equivalent to 100,000 Mwd/MTU burnup. No difference in behavior of the fuel was detected as the material was repeatedly processed. During these tests, it was found that tap density was a better index of sinterability than sieve-size distribution. In some of these tests, AIROX processed UO₂ that contained stable fission products equivalent to 100,000 Mwd/MTU was refabricated and irradiated to 5,000 Mwd/MTU; excellent reactor stability of these pellets was obtained.

Several capsules were filled with UO₂ pellets that had undergone various irradiation levels up to 21,000 Mwd/MTU prior to AIROX processing, enrichment up to 7.4 wt % U²³⁵, and repelletization. Irradiations up to 10,000 Mwd/MTU were performed, and the fuel was subsequently AIROX-processed. Up to 58% of the volatile fission products were removed when the capsule was ruptured. The remainder of the volatile fission products were removed during AIROX processing. The uranium and plutonium isotopic distribution in the as-received, reprocessed, and refabricated material was determined; no significant loss of plutonium during reprocessing and refabrication was found. Although these irradiation tests show the feasibility of recycling AIROX processed fuel, more extensive recycling experience must be obtained before this method of fuel recycle can be used in a commercial reactor.

Process Advantages and Disadvantages

The disadvantage of using AIROX processing or any processing method that recycles fission products is that a slightly higher fissile content of the fuel is required for the LWR and that a slight decrease in breeding ratio is obtained in the FBR.

Besides being proliferation resistant, the other advantages of fuel cycles using AIROX reprocessing are (1) extension of uranium reserve by recycling the fissile material in spent fuel,

(2) decreased amount of spent fuel requiring prolonged storage, and (3) decreased amount of nuclear waste requiring environmental isolation. When all portions of the nuclear fuel cycle are considered, the proliferation-resistant AIROX process for recycling LWR fuel may be even more economical than the postponed conventional reprocessing method for recycling spent fuel. Clearly reprocessing, fuel storage, and waste management costs should be less using AIROX reprocessing. However, further development of remote refabrication facilities which will increase fuel cycle costs when AIROX reprocessing is used is required to verify the AIROX process economics. This development is required for all other low-decontamination processed fuel.

Abstract

Potential diversion of nuclear material from power production to weapons production by national or subnational groups has resulted in a reevaluation of the proliferation resistance of various fuel cycles. The low-contamination fuel cycle, utilizing AIROX dry processing, is proliferation resistant due to the retention of fission products with the fuel and to the low concentration of fissile material in all process steps. In the AIROX process, UO_2 is oxidized with air to U_3O_8 to expand the fuel volume which simultaneously declads and pulverizes the fuel; the fuel is subsequently reenriched, repelletized, and recycled to the reactor.

Fuel cycles utilizing this method of reprocessing will extend our uranium reserves, decrease the spent fuel storage requirements, and decrease the amount of waste requiring storage in a Federal Repository for environmental isolation. AIROX reprocessing is applicable to both light-water reactor fuel cycles as well as fast-breeder fuel cycles.

Literature Cited

1. Asquith, J. G.; Grantham, L. F., *Nucl. Tech.*, 1978, **41**, 137.
2. Brand, G. E.; Murbach, E. W., U. S. Atomic Energy Commission Report NAA-SR-11389, North American Aviation, Downey, CA, 1965.
3. Brand, G. E.; Murbach, E. W., "Experiments on Pyrochemical Reprocessing of Uranium Carbide Fuel" in "Symposium on Reprocessing of Nuclear Fuels, The Metallurgical Society of AIME, Ames, Iowa, August, 1969", *Nucl. Metallurgy*, Vol. 15, 1969.
4. "Civex: A Diversion-Proof Plutonium Fuel Cycle," *EPRI Journal*, 1978, April, 11.
5. "An Assessment of the Civex Concept", paper presented at Atomic Industrial Forum, Washington, D.C., 1978.

6. Miles, K. M., Argonne National Laboratory, "The Pyrocivex Processes are Proliferation Resistant Pyrochemical Reprocessing Methods such as the Zinc Distillation or Modified Salt Transport Process," Private Communication, 1979.
7. Knighton, J. B.; Johnson, I.; Steunenberg, R. K., "Uranium and Plutonium Purification by the Salt Transport Method," in "Symposium on Reprocessing of Nuclear Fuels, The Metallurgical Society of AIME, Ames, Iowa, August 1969," *Nucl. Metallurgy*, Vol. 15, 1969, p. 337.
8. Colby, L. J. Jr.; Mattern, K. L.; Pearlman, H.; Murbach, E. W.; Brand, G. E., U. S. Atomic Energy Commission Report NAA-SR-8036, North American Aviation, Downey, CA, 1963.
9. Vitti, J. A.; Felton, L. D.; Galluzzo, N. G.; Otter, J. M.; Brittingham, J. C., "Nuclear Design and Economic Comparison of a Conventional and Bullseye LMFBR Core," *Nucl. Tech.*, In press.
10. Bodine, J. E.; Guon, J.; Sullivan, R. J., U. S. Atomic Energy Commission Report NAA-SR-11375, North American Aviation, Downey, CA, 1964.
11. Guon, J.; Bodine, J. E.; Sullivan, R. J., U. S. Atomic Energy Commission Report NAA-SR-8213, North American Aviation, Downey, CA, 1964.
12. Strausberg, S., U. S. Atomic Energy Commission Report NAA-SR-7138, Downey, CA, 1962.

RECEIVED May 14, 1979.

Work performed under U.S. Government contract number EY-76-C-03-0701.

Molten Salt Oxidation-Reduction Processes for Fuel Processing

L. G. MORGAN, L. L. BURGER, and R. D. SCHEELE

Pacific Northwest Laboratory, Richland, WA 99352

Pyrochemical and dry processing methods for nuclear fuel processing may meet nonproliferation criteria more easily than aqueous processing methods. One promising pyrochemical approach is the use of molten nitrate systems as oxidants for irradiated nuclear fuel components. This paper is a progress report of work initiated at the Pacific Northwest Laboratory (PNL) for the Department of Energy in FY1978 under the Pyrochemical and Dry Processing Methods Program, Consolidated Fuel Recycle Program. The specific goals of our project are to: critically evaluate the existing literature; experimentally study the basic chemistry of nitrate melts and their reactions with irradiated fuel materials; investigate volatilization phenomena and separation of fission products from actinides; and determine the compatibility of the process with other nonaqueous steps. This project is continuing, and the results of additional studies will be published at a later date.

Review of Previous Studies

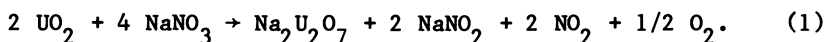
The use of molten nitrates as oxidants for nuclear fuel components has not been studied as much as other pyrochemical or pyrometallurgical processes. Previous studies of molten nitrate systems were primarily conducted in European laboratories, although some research was done in Japan and the United States.

A large body of information exists on molten nitrates. Most of the research concerns the physical properties and theoretical aspects of molten nitrate systems. Very little information exists on the behavior of the various elements and their compounds in molten nitrate systems.

Actinide Oxides in Molten Alkali Metal Nitrates. The chemical behavior of actinide oxides in molten alkali metal nitrates is an area with little available experimental data. Most investigations (1, 2, 3, 4), including our own, have shown that molten

0-8412-0527-2/80/47-117-233\$05.00/0
© 1980 American Chemical Society

alkali metal nitrates do not dissolve uranium dioxide but rather convert it to a diuranate according to the reaction proposed below:



Avogadro and DePlano reported that the composition of the uranate formed varied with the composition of the alkali metal nitrate melt, while Yamagishi and Kamemoto reported that only the diuranate species was produced (1, 7). Unfortunately, analyses of the uranate product were not reported by some authors (3, 4). Although the evidence is sparse, some authors have assumed that plutonium dioxide would form a plutonate by a similar reaction (1, 2, 3, 5, 6). Wurm, however, predicted that plutonium dioxide would be unaffected by contact with molten nitrates (4).

In contrast to the direct formation of a uranate species, there is evidence that both uranium and plutonium dioxide form a soluble species in molten alkali metal nitrates in the presence of nitric acid vapor (8, 9, 10) or ammonium nitrate (7). However, the soluble species was converted to an insoluble actinide species when the temperature was increased over that used for dissolution. The soluble species was not identified and only one report (7) analyzed the insoluble material produced. Cohen reported similar results for neptunium (IV) oxide (11).

Thorium oxide would not be expected to react with molten alkali metal nitrates. Brambilla claims, however, that a soluble thorium species is produced in the molten phase when nitric acid vapor is combined with fluoride ion in molten nitrates (10).

Fission Products in Molten Alkali Metal Nitrates. The behavior of fission products in molten alkali metal nitrates is also an area with little available experimental data.

The reaction of the irradiated oxide fuel with the molten nitrate melt destroys the existing crystalline lattice. Several authors have claimed the complete or partial release of the rare gases (1, 4, 5, 6, 9, 10, 12, 13) and tritium (1, 4, 6, 9, 10, 13) to the off-gas stream as a result of this change in crystalline lattice.

In addition, Brambilla has claimed that both iodine and ruthenium are volatilized when the molten nitrate reacts with the oxide fuel (9). In contrast to this volatilization, other literature claims that both iodine and ruthenium will be found in the molten phase (6, 13). Avogadro and Wurm state that most of the fission products, other than the noble metals, are either volatile or soluble in the nitrate melt, even without addition of nitric acid vapor (12). In a later paper, however, Avogadro reports that iodine is stable as iodide in molten nitrates, and that ruthenium is partially soluble in the molten phase, and partially volatilizes, while the majority remains with the

solids produced (1). He expects to find most of the other fission products, such as the rare earths, barium, strontium, and zirconium, in the solids (1).

Chemistry in Molten Alkali Metal Nitrates. The chemical behavior of actinide oxides and fission products reported in the previous sections appear to be based mainly on predicted behavior; little experimental data has been provided to support the various claims. This, in part, may be because several of the claims are reported in the patent literature, rather than in technical documents or in journal literature.

The chemical behavior of various elements and their compounds is best described by Plambeck and Kerridge (14, 15, 16). However, as their articles recognize, much remains unknown or incomplete. Two major areas, in which studies are both controversial and incomplete, are: 1) identification of the acidic and basic species in nitrate melts, and 2) the thermal decomposition of molten nitrates. Both of these areas are, of course, directly related to the chemistry of molten nitrates. This lack of information on chemical reaction, as well as the complexity of irradiated-oxide fuel compositions results in a situation requiring thorough experimental studies. Such studies will explain the chemistry of various actinide oxides and fission products in molten alkali metal nitrates.

Current PNL Studies

The goals of our laboratory studies were to: 1) investigate the behavior of uranium dioxide and plutonium dioxide in molten alkali metal nitrates, determining the significant experimental parameters; 2) verify the claims that soluble actinide species could be obtained in the molten phase through addition of nitric acid vapor; 3) determine the thermal stability of these species; 4) determine the composition of the uranates and/or plutonates and study their conversion to dioxides; 5) determine the behavior of significant fission products and their distribution for each stage of any proposed process; and 6) study the effects of selected anion additives on the chemistry of actinide and fission-product species.

Uranium Dioxide in Molten Lithium Nitrate/Potassium Nitrate Eutectic. The behavior of uranium dioxide in a molten lithium nitrate/potassium nitrate eutectic was investigated. Our goal was to determine whether a soluble uranium species could be produced using a nitric-acid vapor sparge. The materials used were a lithium nitrate/potassium nitrate eutectic mixture, pure nitric acid (100% HNO_3), and powdered uranium dioxide. The mass ratio of uranium dioxide to the nitrate melt was 1:100. The experiments were performed using a Pyrex reaction tube

equipped with a gas-sparge tube and exit vent. The reaction tube and contents were placed in a pot-type furnace equipped with viewing ports so that visual observation of the melt was possible.

The results of the test showed that the uranium dioxide produced a vigorous reaction with the nitrate melt, beginning at approximately 400°C. At this time the melt was open to the atmosphere, and no nitric acid was being added. Nitrogen dioxide was evolved as a gaseous product of the reaction, but there was no visual indication of any uranium solubility in the molten nitrate eutectic. Complete reaction, indicated by the cessation of gas evolution, required approximately 2.5 hours at 500°C. The product of this reaction appeared to have smaller particles than the original uranium dioxide, which settled rapidly to the bottom of the reaction tube. These particles were recovered by aqueous dissolution of the solidified eutectic and filtration of the insoluble uranium-containing species. No hydrolysis of the insoluble uranium-containing species is believed to occur with aqueous dissolution of the salt matrix. To preclude hydrolysis in experiments where it was more likely, the nitrate salts were dissolved in 0.5 M HNO₃.

A second test was conducted under the above conditions. Reaction of the uranium dioxide was assumed to be complete when gas evolution ceased. At that point, the temperature of the melt was reduced to 200°C, and nitric acid vapor was added to the melt. The nitric acid vapor was carried from a heated vessel containing 100% nitric acid with the inert gas sparge. Transfer lines were heated to minimize condensation. The quantity and transfer rate of the nitric acid were not determined. Addition of the nitric acid produced a reaction with the solids present, shown by gas evolution from the solid's surface, which yielded a soluble uranium species in the nitrate melt. The total solids were dissolved, which produced a characteristic uranyl color in the melt. After complete dissolution of the uranium species, the nitric acid sparge was removed, and the melt was open to the atmosphere.

The soluble uranium species produced was stable at 200°C for at least three hours, at which time the temperature was gradually increased from 200°C to 300°C over a period of one hour. Suspended solids were first noted at 300°C. The temperature was increased to 350°C for one hour, then to 400°C for 0.5 hour. The solids produced through the thermal decomposition of the soluble uranium species were accompanied by gas evolution. We did not determine if this gas evolution was simply removal of excess nitric acid from the melt or a decomposition product. The solids were formed uniformly throughout the melt and had a gelatinous appearance. These solids settled very slowly to the bottom of the reaction tube. The final product of this second test was also recovered by aqueous dissolution of

the nitrate eutectic and filtration of the insoluble uranium species.

We have not completed identifying the final products produced in the two experiments. However, these preliminary experiments verified claims (8, 9, 10) that a soluble uranium species can be formed in molten alkali metal nitrates through the addition of nitric acid vapor.

Uranium Dioxide in Molten Equimolar Sodium-Potassium Nitrate. After completing the above experiments, we decided to use an equimolar sodium-potassium nitrate melt to preclude the rapid attack of our Pyrex reaction vessels that we noted when lithium nitrate was used. Uranium dioxide reacted with the equimolar $\text{NaNO}_3\text{-KNO}_3$ melt at approximately 350°C . The reaction was fairly vigorous, but at no time was it excessive. During this portion of the experiment, an inert gas (argon) sparge was maintained to agitate the melt and to sweep out the NO_2 produced. Complete reaction required about 2.5 hours at a maximum temperature of 420°C .

After reaction was complete and the inert gas sparge had removed the remaining NO_2 , the supernate was clear and colorless. The melt temperature was then lowered to 275°C , and nitric acid vapor was added to the melt as previously described. The uranium completely dissolved. The temperature was slowly increased to 420°C over one hour. The formation of solids was first apparent at 300°C to 320°C . Formation of the solids produced a large quantity of NO_2 ; sparging removed this gaseous product. When the thermal decomposition was complete, the melt was again clear and colorless.

Plutonium Dioxide in Molten Equimolar Sodium-Potassium Nitrate. The behavior of plutonium dioxide in molten alkali metal nitrates is an area of major concern. Claims that alkali metal plutonates are formed (1, 2, 3, 5, 6) are not substantiated by definitive analytical results. In some cases (5, 6), sodium peroxide was added as an oxidant to either an alkali metal nitrate melt (6) or to an alkali metal hydroxide melt (5). If the temperature is great enough, for example above 700°C , thermal decomposition of the nitrate melt produces peroxide species. Other studies (4, 9, 12, 17) do not claim formation of a plutonate species, but only state that an insoluble plutonium-containing compound exists. However, in all the references cited, the results were given for mixed uranium-plutonium dioxide; definitive analytical results were not given.

Our studies of the behavior of plutonium dioxide in molten alkali metal nitrates were conducted in equimolar sodium-potassium nitrate without addition of peroxide. Melt temperatures were low enough so that thermal decomposition was not expected to produce peroxide species. In addition, we studied

both the behavior of plutonium dioxide and mixed uranium-plutonium dioxide.

The behavior of plutonium dioxide is highly dependent upon the history of the material. Thus, although irradiated plutonium dioxide may differ from laboratory samples, it is essential that the samples be well documented. The plutonium dioxide used in our studies was prepared in the following manner: 1) A plutonium (IV) nitrate solution was purified by ion exchange. 2) The Pu (IV) was reduced to Pu (III) with ascorbic acid. 3) Plutonium (III) oxalate was precipitated with oxalic acid and air dried. 4) The oxalate was calcined at 750°C. Typical calcination temperatures for plutonium dioxide prepared for fuels manufacture are 650°C to 850°C. Our material was not sintered at higher temperatures, although this is normally done, in the preparation of mixed oxide fuels following blending and pellet formation.

For this study we chose a mass ratio of 1:100, plutonium dioxide-to-nitrate melt. The experiments were performed in a glove box, designed for containment of high alpha-activity materials. Plutonium dioxide and equimolar $\text{NaNO}_3\text{-KNO}_3$ were added to the reaction vessel, and the temperature was increased to 525°C. The temperature exceeded 350°C approximately three hours, and 500°C for at least one hour. No reaction of plutonium dioxide was noted at any time. The melt remained clear and colorless throughout the entire period. It therefore appears that plutonium dioxide does not react with the alkali metal nitrate melt to produce a plutonate within the temperature range cited ($\leq 525^\circ\text{C}$). The temperature of the melt was then reduced to 275°C, and nitric acid vapor was added. At no time were there any visual indications of solubility or reaction of the plutonium dioxide in the melt.

Analytical results of the study of the behavior of plutonium dioxide in equimolar sodium-potassium nitrate show that, under the conditions cited, plutonium dioxide did not react and did not form a soluble species either with the original melt or with the addition of 100% nitric acid vapor. The analytical results were based on alpha-energy analysis of samples of the molten phase taken throughout the experiment. All molten phase samples were dissolved in 0.5 M HNO_3 .

Mixed Uranium-Plutonium Dioxide in Equimolar Sodium-Potassium Nitrate. The behavior of two compositions of mixed uranium-plutonium dioxide has been investigated thus far at PNL. The first composition, designated material A, consists of 5.44% $\text{PuO}_2/94.56\%$ UO_2 . The second composition, designated material B, consists of 27.56% $\text{PuO}_2/72.44\%$ UO_2 . Both materials were acquired as pellets that had been sintered at 1700°C. The behavior of both mixed-oxide materials was studied under the same conditions used in the previous experiments.

Reaction of material A was similar to that of powdered uranium dioxide, although a higher temperature, 400°C, was required to initiate the reaction. Reaction of material A was completed at 450°C. The temperature of the melt was reduced to 275°C following the completion of the oxidation reaction, and nitric acid vapor was added as in previous experiments. Most of the solids dissolved in the melt, producing the characteristic uranyl color, but not all of the solids could be dissolved with this treatment. Preliminary analyses of the molten phase taken throughout the experiment indicated that plutonium dioxide remained insoluble at all times. All molten phase samples were dissolved in 0.5 M HNO₃ before they were analyzed.

Material B required an even greater melt temperature than material A to initiate and complete the oxidative reaction, 500°C to 550°C. The reaction rate also appeared to be less than that in previous studies, even at this higher temperature. Reduction of the melt temperature to 275°C and addition of nitric acid vapor produced the same results as for material A.

Although these studies are not complete, it appears that molten alkali metal nitrates will react with mixed uranium-plutonium dioxide material of varying composition. Higher melt temperatures and longer reaction times are required, however, as the plutonium enrichment is increased. The insolubility of plutonium dioxide must certainly be investigated further since its solubility in the molten phase upon addition of nitric acid vapor has been claimed in various patents (8, 9, 10). It should also be noted that the behavior of irradiated uranium-plutonium dioxide may differ from the material used in our experiments.

Alkali Metal Uranate. Preliminary studies to determine the composition of the alkali metal uranates formed in the various alkali metal nitrate melts have also been conducted at PNL. Uranium dioxide was reacted with the following melts: sodium nitrate; equimolar sodium-potassium nitrate; and lithium-potassium nitrate eutectic, 42.2 mole% lithium nitrate. A 20:1 mole ratio of nitrate to uranium dioxide was used in each case. The reaction was conducted in a muffle furnace at 425°C for 4.5 hours. The solidified and cooled salt cake from the reaction was dissolved by addition of distilled water. Hydrolysis of the insoluble uranium reaction product is not expected to occur. The remaining solids were filtered and thoroughly washed with distilled water on a fritted glass filter. The filter plus the solids were dried in a vacuum oven at 120°C for two days.

The alkali metal species and content were determined by atomic absorption. The uranium content was determined by x-ray fluorescence; strontium was used as an internal standard. X-ray

powder diffraction patterns were also obtained for comparison to known compounds. Table I lists typical analyses.

Empirical formulas for the products from each melt system were obtained; we assumed that oxygen was the other constituent of the compounds. The elemental ratios are subject to some variation because of uncertainties in the analytical data. The uranium analyses are estimated to be valid within $\pm 2\%$. Independent analytical determinations have shown that the original uranium dioxide contained approximately 0.5% iron, plus a trace of silica. Adjustment of the analytical data for these minor impurities was not done.

Products of both the sodium nitrate and equimolar sodium-potassium nitrate melts indicated that a diuranate species, $U_2O_7^{2-}$, had been formed. The product obtained from equimolar sodium-potassium nitrate indicated that sodium was the favored cation in the compound; less than 10% of the alkali metal was potassium. X-ray powder diffraction data support the evidence that the diuranate species is formed in both of these melt systems.

The product obtained from the lithium nitrate-potassium nitrate eutectic is neither identifiable as the diuranate ($U_2O_7^{2-}$) or uranate (UO_4^{2-}) species, nor as a mixture composed of each of these species. To date, the x-ray powder diffraction pattern has not been identified with any known compound. It is interesting to note the ratios of the alkali metals for this system, however: approximately a 2:1 atomic ratio of lithium to potassium, indicating lithium is the preferred cation.

No change in composition of the uranate product was found in the equimolar sodium-potassium nitrate following dissolution of the original uranate with nitric acid vapor and subsequent thermal decomposition of that soluble species. Analyses of the uranate produced over 300°C to 450°C indicated that only the diuranate species is formed. There was, however, a trend toward a decreasing potassium content as the reaction temperature increased.

Based on the above data, it appears that the stability of the uranate product formed is in the order of: $Na \gg K < Li$.

Table I. Alkali Metal Uranate Composition

Constituent, %	Alkali Metal Nitrate System		
	$NaNO_3$	$NaNO_3-KNO_3$	$LiNO_3-KNO_3$
Li	--	--	1.07
Na	6.68	6.18	--
K	--	0.71	3.17
U	76.1	75.2	75.0

Additional studies and determinations of the uranate composition from various nitrate melts are planned.

Fission Products in Equimolar Sodium-Potassium Nitrate. Fission-product behavior in molten alkali metal nitrates is largely unknown. Information on the behavior of various elements and their compounds is incomplete. In addition, the complexity of the composition and chemical nature of irradiated fuel material makes prediction of individual fission-product behavior even more difficult.

Our own studies to date have been mainly qualitative. Three methods have been utilized thus far: 1) A synthetic fission-product mixture was prepared and added with uranium dioxide to the molten nitrate. 2) Individual fission-product compounds were added to nitrate melts and their behavior was observed. 3) Fission-product compounds were spiked with radioactive tracers and studied in a nitrate melt.

In our first approach, a nonradioactive, representative fission-product mixture was prepared, consisting of equal masses of the desired elements. An ammonium hydroxide solution was used to dissolve molybdenum trioxide, MoO_3 ; this solution was added to an aqueous solution containing the nitrates of cerium, palladium, and rhodium. The resulting mixture was calcined at 500°C for 17 hours, then at 550°C for an additional seven hours. The solids from the calcination were powdered and added to a blended mixture consisting of the oxides of antimony, ruthenium, samarium, strontium, yttrium, and zirconium. Cesium was then added as cesium iodide; niobium was added as potassium hexaniobate, $\text{K}_8\text{Nb}_6\text{O}_{19}\cdot 16\text{H}_2\text{O}$.

The final representative fission-product mixture is therefore believed to consist of the oxides of: antimony, cerium, molybdenum, palladium, rhodium, samarium, strontium, yttrium, and zirconium; cesium iodide; and potassium hexaniobate. Current analytical tests in progress will provide the exact concentrations of the elements of concern.

The behavior of uranium dioxide, containing the addition of the synthetic fission-product mixture, was investigated in equimolar $\text{NaNO}_3\text{-KNO}_3$. The mass ratio of the fission product mixture to uranium dioxide was 1:10; the mass ratio of uranium dioxide to total alkali metal nitrate was 1:100. A complete experimental cycle was conducted, testing the: reaction with the molten nitrate; reduction of melt temperature and addition of nitric acid vapor; and thermal decomposition of the soluble uranium species.

Samples were taken of the molten phase throughout the experiment, and the final solids were recovered by aqueous dissolution of the nitrate melt after solidification. Analyses were conducted on the samples for uranium and the various elements in the added fission-product mixture. Samples were analyzed by Spark Source Mass Spectrometry for the elements of interest. Results

are semiquantitative, but the detection level was approximately one part per million on an atomic basis.

Analysis of the molten phase sample taken after reaction with the molten nitrate indicated that only cesium and cerium were present in concentrations greater than the detection limit. Samples taken after dissolution of the solids with nitric acid vapor indicated that, besides uranium, only cesium and cerium were present in concentrations exceeding the detection limit. Following the thermal decomposition of the soluble uranium species, cesium, cerium, and molybdenum were present in the molten phase at levels above the detection limit.

Analyses of the final solids indicated that all fission product elements of concern were present: antimony, cerium, cesium, iodine, molybdenum, niobium, palladium, rhodium, ruthenium, samarium, strontium, yttrium, and zirconium. Both iodine and ruthenium were found in the solids, indicating that if these formed volatile species, release was not complete over the period of the experiment.

In our second method, elements of interest were added as a compound to the sodium-potassium nitrate, which was then melted. Visual observation was the only test in these qualitative experiments.

The individual elements produced various results. Additions of antimony oxide, tin(II) oxide, and samarium oxide gave no evidence of reactions with the nitrate melt or solubility. The addition of zirconyl nitrate resulted in the evolution of nitrogen dioxide from the melt and the formation of a white insoluble precipitate. Addition of palladium nitrate to the melt produced a black melt and black insoluble solids. Dissolution of the cooled and solidified salt cake with distilled water indicated that a palladium mirror had formed at the meniscus of the melt. Niobium was added as potassium hexaniobate, $K_8Nb_6O_{19} \cdot 16H_2O$. There was no visual evidence of reaction or solubility. Cesium iodide added to the nitrate system appeared to completely dissolve, as did molybdenum trioxide.

A potassium ruthenium nitrite compound, whose exact composition is unknown, was added to the nitrate melt. The original compound was an amber color. Observation of the melt indicated the formation of black solids, which settled to the bottom of the reaction vessel, leaving a green, molten supernate. Distilled water dissolved the solidified and cooled melt and appeared to dissolve nearly all the ruthenium present.

Antimony oxide was dissolved in concentrated hydrochloric acid, and the resulting solution completely evaporated. The product of this treatment is probably either $SbCl_3$ or $SbOCl$. These solids were added to the nitrate melt; evolution of nitrogen dioxide was observed, after which a white precipitate was observed. There was no evidence of solubility at any time.

The results of these qualitative tests and those obtained by Spark Source Mass Spectroscopy in the first experiment, indicate that of the elements tested thus far, we may expect to find cerium, cesium, iodine, molybdenum, and possibly ruthenium as soluble species present to some extent in the equimolar sodium-potassium nitrate melt.

As our third technique, we have begun studies on tracer quantities of selected fission products, and preliminary results indicate some solubility in the melt for both europium and strontium. Material balances or decontamination factors are not available at this time. Both qualitative and quantitative studies of fission product behavior are continuing. The results of these studies will be reported as the data become available.

Effects of Additives. Selected additives to molten nitrate systems offer possibilities of specific acid-base reactions or formation of specific complexes with the various chemical species. Acids and bases are conveniently denoted in oxyanionic molten salt systems by the Lux-Flood definition (18, 19). Acids are defined as compounds capable of removing oxide ions from the melt, while bases are defined as compounds capable of donating oxide ions to the melt. Examples of various acidic and basic species may be found in the general review articles (14, 15, 16). We may be able to change the chemistry of uranium, plutonium, and fission-product elements reported in this paper with specific additives.

For example, halide ions may form soluble actinide complexes without addition of nitric acid vapor. Preliminary tests have shown, however, that uranyl chloride, UO_2Cl_2 , is not soluble in either a 6-mole% potassium chloride/94-mole% potassium nitrate melt, or a 5-mole% sodium chloride/95-mole% sodium nitrate melt. Uranyl fluoride, UO_2F_2 , was slightly soluble in a 9-mole% potassium fluoride/91-mole% potassium nitrate system. There was no evidence of solubility of uranyl fluoride in 3.5 mole% sodium fluoride/96.5-mole% sodium nitrate.

In addition, precipitation of fission-product elements has been demonstrated. The addition of sodium carbonate or sodium sulfate to molten equimolar sodium-potassium nitrate containing soluble strontium nitrate results in precipitation of strontium carbonate or strontium sulfate, respectively. Molybdenum trioxide, MoO_3 , added to an equimolar sodium-potassium nitrate melt resulted in evolution of nitrogen dioxide and dissolution of the molybdenum, presumably as the molybdate anion, $\text{Mo}_2\text{O}_7^{2-}$ (14). Addition of soluble strontium nitrate to this nitrate melt produced an insoluble precipitate that was also insoluble in water. The existence of an aqueous insoluble strontium molybdate is known, and it is believed that a similar species is formed in the melt.

Thus, the addition of selected reagents to molten nitrate systems offers the possibility of using molten nitrates not only

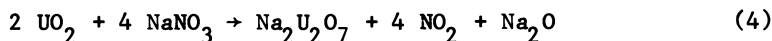
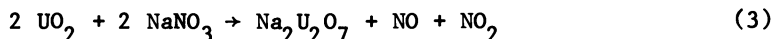
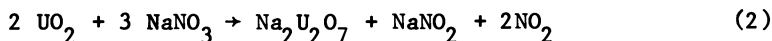
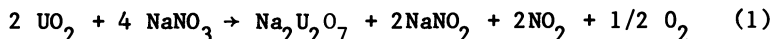
as an oxidative medium but also as a solvent for specific chemical reactions. Fission-product interactions, as demonstrated by the behavior given for strontium and molybdenum, must be carefully considered and determined.

Proposed Conceptual Process Flowsheet

Figure 1 represents a proposed conceptual process flowsheet based upon the existing literature and our studies conducted thus far.

Decladding. Our conceptual process does not use chemical decladding. The initial oxidation step is compatible with either stainless steel or Zircaloy cladding; that is, the nitrate melt does not react to any significant extent with the cladding. This allows either chopping or shearing the fuel rods into pieces before introducing them into the molten nitrate. The oxidation should separate the oxidized fuel from the cladding because the density of the product is less than that of the original MO_2 . A basket can be used to introduce the fuel element pieces into the nitrate melt and withdraw the cladding hulls following the disaggregation of the fuel material.

Redox Reactions. The initial chemical reaction is oxidation of uranium dioxide. In the equimolar sodium-potassium nitrate system the product is sodium diuranate. The following reactions are believed to be the only valid oxidation reactions that are possible.



Reactions (1) and (2) are essentially equivalent if one considers the equilibrium of



Reaction (4) is not likely since pH measurements of the solidified nitrate salt dissolved in water, following reaction with UO_2 , do not indicate a basic solution.

Exactly which reaction predominates is presently unknown. All those listed may occur to some extent and may be dependent upon reaction temperature, removal of gaseous products through sparging, or other as yet unidentified factors. Plutonium

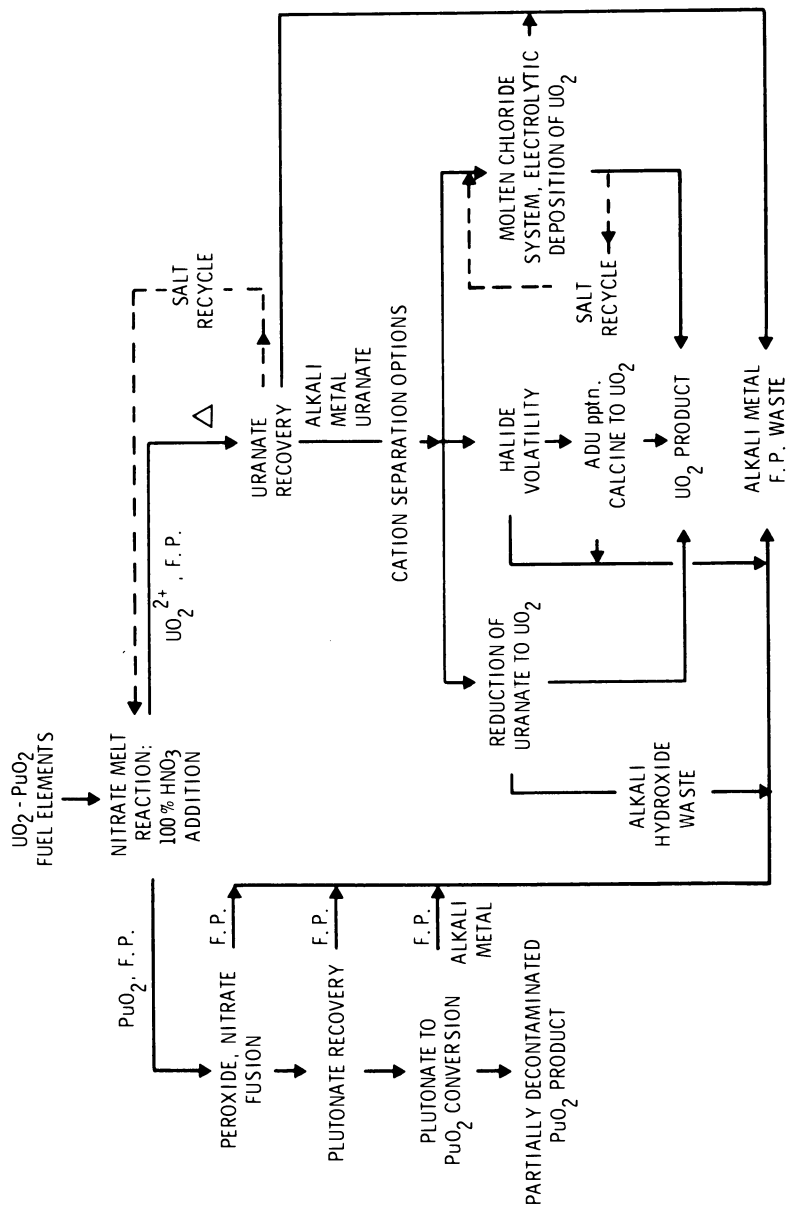
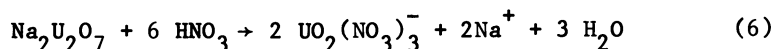


Figure 1. Conceptual process flowsheet; F.P. represents "fission products"

dioxide has been shown in our studies to be unaffected in molten sodium-potassium nitrate. Thorium oxide would not be oxidized in the nitrate melt.

Dissolution. The second step of our proposed process is the dissolution in the nitrate melt ($T < 300^\circ\text{C}$) of the sodium diuranate through addition of nitric acid vapor in the sparge gas. Initial studies used 100% HNO_3 , but recent tests have demonstrated that commercial white-fuming nitric acid is equally effective. Concentrated nitric acid does not completely dissolve the sodium diuranate.

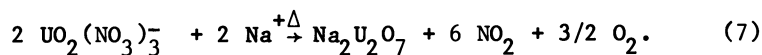
The postulated dissolution reaction is



Once in solution, the uranium species is stable at temperatures less than 300°C without further addition of HNO_3 and is not destroyed by continued sparging of the melt with an inert gas. Our studies indicate that plutonium dioxide is not dissolved in the melt by the addition of the nitric acid vapor.

Separations. **Uranium:** Our process separates uranium and plutonium by dissolving the sodium diuranate with nitric-acid vapor. Once the uranium is in solution, a solid (PuO_2 and insoluble fission products) - liquid (nitrate melt containing uranium and soluble fission products) phase separation is required at a temperature of approximately 275°C . Filtration is presently envisioned as the phase separation method, but no studies have been conducted or alternatives investigated.

Once sodium diuranate is separated from PuO_2 and the insoluble fission products, it is recovered from the nitrate melt as an insoluble phase by an increase in temperature ($T > 300^\circ\text{C}$). The following reaction is postulated for this step.



Our preliminary studies of fission-product behavior show that those fission products that are soluble in the melt remain so during precipitation of the sodium diuranate. Hence, a relatively "clean" uranium product should be obtained. Again, a liquid (nitrate melt containing soluble fission products) - solid (sodium diuranate) phase separation is required. The melt temperature may be lowered to approximately 275°C for this separation once the diuranate has precipitated.

It appears that whatever the behavior of uranium is in molten nitrates, the end product is most likely to be an alkali metal uranate. Separation of the alkali metal cation and uranium is perhaps the greatest unknown in the development of a

conceptual process. We have not conducted any laboratory studies to date on the conversion of sodium diuranate to uranium dioxide.

Plutonium: In the most optimistic scheme, the PuO_2 and insoluble fission products would be recycled for fuel manufacture without further treatment, except for either aqueous removal or volatilization of adhering nitrate salts. Because of their high level of radioactivity, the fission products that accompany the PuO_2 would provide the desired nuclear deterrence of the fissile material.

More realistically, this material (PuO_2 plus fission products) would require either some further decontamination from deleterious fission products or further treatment to obtain a product having the necessary characteristics for fuel recycle (particle size, chemical form of fission products, other?). This further treatment has not been investigated to date and probably will not be until we have a better knowledge of the fission-product distribution and chemical form.

Our conceptual flowsheet for further decontamination of plutonium dioxide indicates oxidation of PuO_2 with a nitrate melt containing peroxide. A plutonate species should form with this treatment. If formed, we expect the plutonate to be soluble in the melt upon addition of nitric-acid vapor. If this supposition is correct, then the plutonium could probably be recovered similar to uranium. Whether a plutonate or PuO_2 would be obtained from the thermal decomposition of a soluble plutonate species is unknown for this system.

Fission Products: Knowledge of fission-product behavior in our system is still qualitative and incomplete. Several of the elements tested appear in both the soluble and insoluble phases, but their distribution ratio is not yet accurately known. In addition, elemental iodine has been observed in the off-gas lines when cesium iodide is present in the melt. None of the fission-product species that are soluble have been identified or even investigated to date. In fact, without use of actual irradiated fuel, correctly identifying fission-product behavior is believed to be a major uncertainty in any process.

It has been observed, however, that those fission products that are initially soluble in the nitrate melt remain so throughout addition of nitric-acid vapor and subsequent recovery of sodium diuranate. Those fission products that are initially insoluble in the nitrate appear to remain so, although it is expected that the addition of the nitric-acid vapor will shift the distribution ratio.

Future Studies

Additional research is required for each proposed process step so that accurate feasibility determinations can be made. The identity and quantity of the various actinide and fission-product species in the molten, solid, and gaseous phases are

American Chemical
Society Library

1155 16th St. N. W.

Washington, D. C. 20036

necessary if we are to determine partition factors and calculate material balances. Thermodynamic and kinetic data are required to define process parameters.

Process Requirements and Problems. Overall process considerations raise other questions which must be addressed: construction materials; the control of volatile fission products; waste management, including recycle of process chemicals; and solid-liquid phase separations at elevated temperatures are included.

At the reaction temperatures involved, molten nitrate systems are not particularly corrosive and conventional materials, such as stainless steels, are probably adequate for the reaction, dissolution, and separation steps. If high-temperature volatilization or transfer to a halide system is necessary, then other materials will be required.

The behavior of volatile fission products is largely unknown. Brief literature references to iodine and ruthenium are contradictory. It is likely that elemental iodine is the stable species in the melt (16), and that some will be volatilized. Possible process modifications to guarantee a unique path for ruthenium have not been considered. The rare gases should escape because of the elevated temperature crystal modification. However, experience with the voloxidation process suggests that this release may not be complete. The behavior of both Kr-85 and tritium must thus be investigated.

Pyrochemical processes have the potential for low waste volume, but only if materials are recycled. No major problems are foreseen for recycle of the greatest bulk component, sodium nitrate. Regeneration will be required, but the presence of a considerable amount of nitrite is not a problem since nitrite also oxidizes uranium dioxide. Removal of the highly soluble fission products, such as cesium and iodine, will eventually require either a separation step or a bleed-off of the nitrate stream.

Solid-liquid phase separations at elevated temperatures are unit operations that we have not investigated. The efficiency of this type of separation, the design and material requirements, and the reliability of the phase separation must be studied.

Fuel Recycle Requirements. We assume that the final product returned for fuel fabrication and recycle is a mixed uranium-plutonium dioxide material, partially decontaminated from fission products. The questions of fissile material enrichment, radiation levels, and required handling facilities are not addressed.

Fission-product decontamination is restricted by the requirement that gamma-emitting nuclides must remain with uranium-plutonium to provide nuclear deterrence. Various nuclides have been considered, including Co-60, which would be added to

the fuel. Nuclides from fission that are candidates are Cs-137, Ce-144, Ru-106, and Zr-95. Selle has identified possible criteria based on both nuclear properties and chemical and physical properties of the metal and its oxide (20). Based on these criteria the potential fission nuclides are limited to Ce-144 and Ru-106.

Preliminary experiments have shown that for these four nuclei, nearly all the zirconium, cerium, ruthenium, and approximately 40% of the cesium stayed with the uranate during a simple treatment of the oxide fuel with sodium nitrate (21).

Conclusions

Several specific items were identified as crucial to the development of any conceptual processes utilizing molten nitrates.

1. Will the uranates always precipitate, or can UO_2^{2+} be kept in solution?

We have verified that a soluble uranium species is produced by the addition of 100% nitric acid vapor to a nitrate melt containing uranates formed by reaction of the melt with uranium dioxide. The temperature range of dissolution and the thermal stability of the soluble species have been approximately defined. Neither the identity nor the solubility limit of the uranium species has been determined.

2. How does plutonium behave under conditions similar to those for uranium?

We have determined that plutonium dioxide does not react with molten nitrates under the same conditions that uranium dioxide does. We have also determined that plutonium dioxide is not soluble in molten nitrates with the addition of 100% nitric acid vapor under conditions which did produce soluble uranium. This observation must be further verified under the various conditions which can produce the soluble uranium species.

3. How can ThO_2 be handled in these systems?

Although ThO_2 will not be oxidized by the melt, it may be possible to produce a soluble thorium species. This has not been investigated in experiments to date.

4. What subsequent steps can be used to separate the sodium or other cations from the uranate, e.g., transfer to another salt system?

It appears that whatever the behavior of uranium is in molten nitrates, the end product is most likely to be an alkali

metal uranate. Separation of the alkali metal cation and uranium is perhaps the greatest unknown in the development of a conceptual process. We believe that the following offer promising solutions to this separation: reduction of the uranate to UO_2 and volatilization of the alkali metal hydroxide; conversion of the uranate to a halide species with separation by volatility; and dissolution of the uranate in an alkali metal chloride melt, followed by electrolytic deposition of UO_2 from the melt.

Based on available information, we believe that transfer of the uranate to a molten chloride system with electrolytic reduction is the most feasible method. Electrolytic deposition from molten alkali metal chlorides was an integral step in the pyrochemical process known as the Hanford Salt Cycle. Documentation of this phase of the process was extensive and also represents one of the very few pyrochemical processes that has been carried through pilot-plant scale on irradiated fuel. Unknowns exist, such as the rate and conditions of uranate dissolution, but considerable use could be made of previously documented results.

5. How can fission-product distribution be controlled during uranate precipitation and on subsequent dissolution or other treatment?

Sufficient knowledge of fission-product behavior in molten nitrate systems is not available in the literature. Laboratory investigations must define the behavior of the three types of fission products of concern: volatile fission products, high energy gamma emitters, and high neutron cross-section members.

Preliminary investigation has shown that most fission products are not soluble in alkali metal nitrate melts and that they are not dissolved by addition of 100% nitric acid vapor. If these characteristics are verified by further experiments, a fission product separation is easily envisioned. One could react the fuel with the molten nitrate, dissolve the uranate with the addition of 100% nitric acid, and separate the uranium from the remaining solids, which should consist of both plutonium dioxide and fission products.

Acknowledgements

Work supported by the U.S. Department of Energy under Contract EY-76-06-1830. The laboratory assistance of A. D. Peoples and C. W. Pollack is gratefully acknowledged.

Literature Cited

1. Avogadro, A.; DePlano, A. "Pyrochemical Pretreatment of Fuels Derived from Fast Power Reactors: Oxidation with Fused Alkaline Nitrates", EUR-4784, 1972.
2. Henrion, P.N.J.; Johannes, W.F.; Claes, L. Belgian Patent 815 189.
3. Heylen, P.R.; Claes, W.; Henrion, P.; Baetsle, L.H.; Lecerf, H.; Van Impe, J.; DeBeukelaer, R.C. "Nuclear Energy Maturity, Proceedings of the European Nuclear Conference, Paris, Vol. 8: Reprocessing, Transport and Waste Disposal"; Pergamon Press: Oxford, 1975; pp. 60-79.
4. Wurm, J.G.; Heylen, P.R.; DeBeukelaer, R.C.; DeConinck, A. "Pyrochemical Head-End Conception for Fast Breeder Fuel Processing", EUR-4614e, 1970.
5. Wurm, J.G.; Avogadro, A. "Process for Reprocessing Nuclear Fuels", British Patent Specification 1 108 042, 1968.
6. Centre d'Etude de l'Energie Nucleaire 'C.E.N.' at Brussels. "Process for the Conditioning of Irradiated Nuclear Fuel", Netherlands Patent No. 7 500 663, 1975. Available also as BNWL-TR-319, 1978.
7. Yamagishi, S; Kamemoto, Y. J. Nucl. Sci. Tech., 1965, 2, 457.
8. Brambilla, G.; Caporali, G.; Zambianchi, M. "Process for the Dissolution of Ceramic Nuclear Fuels", Ger. Offen. 2 319 717, 1973.
9. Brambilla, G.; Caporali, G. "Process for the Pyrochemical Separation of Plutonium from Irradiated Nuclear Fuels", Ger. Offen. 2 611 333, 1976.
10. Brambilla, G.; Caporali, G.; Zambianchi, M. "Reprocessing Method of Ceramic Nuclear Fuels in Low-Melting Nitrate Molten Salts", U.S. Patent 3 981 960, 1976.
11. Cohen, D. J. Amer. Chem. Soc., 1961, 83, 4094.
12. Avogadro, A.; Wurm, J. "A Method of Processing Nuclear Fuels", British Patent Specification 1 221 604, 1971.
13. Heylen, P.R.; Wurm, J.G.; Etienne, J.C.; Lecerf, H.; Rombaux, J.P.; Van Impe, J.; DeBeukelaer, R.; Dubois, G.; Glibert, R. "Fast Reactor Program, Reprocess Project--Pyrochemical Head-End, Preliminary Technical and Economic Evaluation", BLG-478, 1973. Available also as PNL-TR-356, 1979.
14. Plambeck, J.A. "Encyclopedia of Electrochemistry of the Elements, Vol. X, Fused Salt Systems"; Marcel Dekker, Inc.: New York, 1976; pp. 165-232.
15. Addison, C.C.; Sowerby, D.B., Ed. "MTP Int. Rev. Sci., Inorg. Chem. Ser. 1, Vol. 2, Main Group Elements, Groups V and VI"; H.J. Emeleus, Consultant Ed. Butterworths: London, 1972; pp. 29-61.
16. Kerridge, D.H. "Molten Salts as Nonaqueous Solvents", in "The Chemistry of Nonaqueous Solvents, Vol. VB, Acidic and

- Aprotic Solvents"; Lagowski, J.J., Ed., Academic Press: New York, 1978; pp 298-329.
17. Baehr, W.; Vogg, H.; Ochsenfeld, W. "Method of Separating Nuclear Fuels", Ger. Offen. 1 197 630, 1965.
 18. Lux. H. Z. Electrochem., 1939, 45, 303.
 19. Flood, H.; Forland, T. Acta Chem. Scand., 1947, 1, 592.
 20. Selle, J.E. "Chemical and Physical Considerations of the Use of Nuclear Fuel Spikants for Deterrence", ORNL/TM-6412, 1978.
 21. Burger, L.L.; Scheele, R.D. "Tritium Removal Alternatives for the Purex Process", PNL-2080-14, 1978.

RECEIVED September 4, 1979.

Photochemistry of the Actinides

L. M. TOTH, J. T. BELL, and H. A. FRIEDMAN

Chemistry Division, Oak Ridge National Laboratory, Oak Ridge, TN 37830

Prior to the advent of the laser, photo-induced reactions sat, for the most part, in the chemical background. Photochemists of that time typically gave little thought to actinide elements other than uranium which was known for years to be a very excellent chemical actinometer when present as the uranyl ion. The expertise and specialized equipment required in the handling of the other actinides, coupled with their very limited supply, served to discourage photochemists from fundamental investigations of these elements. As a result, no report of actinide photochemistry (save that of uranium) is to be found in the open literature prior to 1969.

With no supporting fundamental data, reactor technologists concerned with the chemistry of reactor fuels could merely speculate on the behavior of the actinide solutions should they be exposed to electromagnetic radiation. Then as fuel reprocessing became a topic of much interest during the past decade, the concern of possible photochemical activity began to occupy the thoughts of some researchers.

The first attention given to actinide photochemistry was for the purpose of identifying any photochemical activity which might alter the efficiency of the extraction or exchange processes. Subsequently, the identification of photochemically active species of uranium and plutonium gave some indication that the photo-reactions could be turned to a useful end and, perhaps, offer a cleaner way to separate actinides from each other and from the other elements accompanying them in nuclear fuel elements.

Since that time, laser photochemistry has become a popular subject and with it have come the laser photochemists looking for a photon 'target'. Obviously, the first laser photons would be aimed toward isotope separations which required the narrow bandwidths which the laser so uniquely provided; but spin-off targets have since included the separations of reactor fuel components in reprocessing and/or waste isolation systems. Although much has been promised from the application of lasers to the reprocessing of nuclear fuels, there has been very little evidence that would

0-8412-0527-2/80/47-117-253\$05.00/0

© 1980 American Chemical Society

suggest their usage is essential. Consequently, most of the pertinent photochemical work has been performed with conventional light sources.

A relatively small amount of energy is required to do the job in a typical reprocessing plant. We estimate, under the most ideal circumstances, that 2000 Watts of absorbed light for a typical 5 ton/day plant would be necessary to achieve the reductive stripping of plutonium. (This is based on the assumption that the dominant photo-reaction will be UO_2^{2+} reduction with a Quantum Yield, $QY, = 0.5$. The two-fold excess of U^{4+} is then used to reduce Pu^{4+} which is present as 1 percent of the spent LWR fuel (1). Neptunium, occurring as 0.05 percent of the spent fuel, has been neglected for this estimate.) This is indeed an attractive alternative to some chemical reagents, but presently, for want of more data, no photochemical process has been seriously considered even though several interesting suggestions have been offered and some patents have been obtained.

This report shall review the basic photochemistry of uranium, plutonium, and neptunium which has been studied during the past several years, shall suggest where a photochemical process might be most efficiently applied and then shall assess the general applicability of photochemistry to fuel reprocessing. We shall assume that the attractive features of photochemical separations are appreciated and that the reader is able to perform the simple conversion of Watts input power to moles of resulting product provided the quantum efficiencies to the photochemical reactions are known. Most elementary texts on physical chemistry (2) or photochemistry (3) provide ample background that need not be repeated here. The focus of this report will be on the photochemistry of the actinides themselves and the promise which this gives to the possibility of separating them.

Historically, the study of actinide photochemistry at both Oak Ridge and elsewhere has proceeded along the sequence shown in Table I, moving from a spectroscopic study of uranyl species to photochemical reduction thereof and ultimately to the photochemistry of the more radioactive actinides. The fundamental photochemistry of plutonium and neptunium has been probed only during the past ten years and by only two laboratories (9-14), due largely to the difficulty of handling and their limited supply. The Russian workers were truly first to investigate plutonium and neptunium, but their reports are brief and do not mention essential factors such as quantum efficiencies and wavelength effects on the photo-induced reactions. For these reasons, the research which followed at Oak Ridge was performed to answer some of the essential questions.

Ultimately, a number of photochemistry groups turned their interests to reprocessing using the fundamental information thus far gathered and the realization of the benefits which photochemical processes had to offer. All of these investigators followed a similar path - that of photo-reducing uranyl to $U(IV)$ and using the resulting uranium as the chemical reductant for $Pu(IV)$ in

Table I. Actinide Photochemistry and Related Spectroscopy

(I) URANIUM		
(A) Spectroscopy		Bell and Biggers [1965-68] (4) Bell, Friedman, Billings [1974] (5)
(B) Photoreduction of UO_2^{2+}		Nemodruk et al. [1967] (6) Bell et al. [1974-75] (7)
(II) PLUTONIUM		
(A) Photoredox		Palei, Nemodruk, Bezrogova [1969] (8)
(B) Polymer degradation	}	{ Bell and Friedman [1976] (9) Friedman, Toth, Bell [1977] (10)
(C) Equilibrium photoshift		
(III) NEPTUNIUM		
(A) Photoredox in $HClO_4$, HCl , HNO_3 , H_2SO_4		Nemodruk et al. [1972-73] (11,12,13,14)
(B) Photoredox in $HClO_4$, HNO_3		Friedman and Toth [1979] (15,16)
(IV) REPROCESSING		
(A) Pu(IV) reduction with U(IV)		Carroll, Burns, Warren [1961] (17) Wilson [1971] (18) Friedman, Toth, Bell [1977] (19) Goldstein et al. [1977] (20) DePoorter, Rofer-DePoorter [1978] (21)

order to achieve the reductive extraction of plutonium. The first known report of such work was by Carroll and coworkers (17) at Hanford in 1961 followed by a patent by Wilson (18) in 1971 from the same laboratory suggesting the organic phase reduction of UO_2^{2+} using tributyl phosphite and phosphoric acid.

Later, an aqueous phase photochemical process which would produce reductive extraction of plutonium from a TBP organic phase containing both uranium and plutonium was patented (19) at Oak Ridge. Goldstein and coworkers (20), although they could do no experimental work, were quick to see the merits of uranyl reduction using photochemistry and have written several reports suggesting its usage as a means of separating plutonium from uranium. Since that time the group at Los Alamos has performed some experiments on organic phase reductions of uranyl ion (21) similar to that of the Hanford work in 1971; but, instead of using tributyl phosphite and phosphoric acid as the reductants for uranium, they proposed the usage of the TBP itself. This has already been treated in a previous report (22) and the details shall not be discussed any further here.

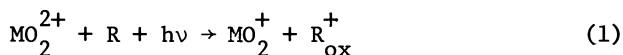
It may seem strange at first that all of the groups involved in the reprocessing chemistry chose to look at the same basic idea - uranyl photochemical reduction to U(IV). However, realizing that the early workers were not aware of the plutonium and neptunium photochemistry and that they knew U(IV) was an acceptable chemical reductant for Pu(IV), the common course of action is not so difficult to understand. The later groups had the advantage of knowing that the quantum efficiency for direct reduction of Pu(IV) to Pu(III) was much less than that for photo-reduction of uranyl to U(IV). In addition, there was the realization that uranyl could be photolyzed with light of wavelengths (7) well out in the visible while plutonium required the usage of ultraviolet radiation (<350 nm).

All of the photochemistry presented here will be with respect to aqueous solutions. Although others have considered photochemical reactions in organic media, the accompanying photo-degradation of organic molecules such as TBP (or oxidation of the organic molecules as a result of participation in photo-redox reactions) makes the organic phase an unattractive region for practical photochemical reprocessing.

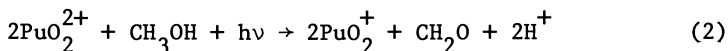
Photochemical reactions of the actinides (and fission products) in the very radioactive dissolver solution have not been considered because the radioactive and otherwise-complex nature of the solution is such that controlled photo-reactions would be most difficult therein. Downstream, however, in the aqueous stripping solution, conditions are much more amenable to the level of development presently achieved.

Uranium and Plutonium Reactions

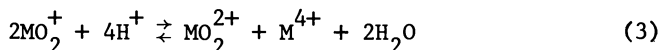
The photochemical reduction of the VI oxidation state:



(where M can be either uranium or plutonium) has been found to occur (8,9,10) using a variety of reductants, R, such as alcohols, aldehydes, hydrazine and hydroxylamine. The product of the reaction is the pentavalent actinide ion and the oxidized form of the reductant, R_{ox}^+ . For example:

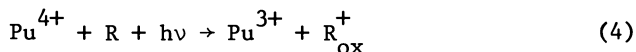


The MO_2^+ species of uranium and plutonium is ordinarily unstable and undergoes rapid disproportionation via:

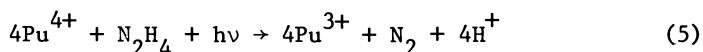


with the resulting formation of tetra- and hexa-valent actinide ions. A comparison of the quantum efficiencies for these reactions, listed in Table II, reveals one reason why the photo-reprocessing proposals rely so heavily on the uranyl photoreduction; it is simply a matter of higher efficiency.

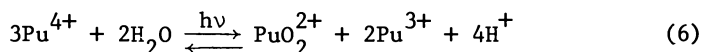
Other reactions observed for plutonium have been (1) the direct photochemical reduction of Pu(IV) using reductants such as formic acid, ethanol and hydrazine (8,9,10) in perchloric acid:



For example:



where quantum efficiencies as shown in Table II have been measured; (2) Photo-equilibrium shift of the Pu(IV) disproportionation reaction (9,10):



which, in reality, is a two-step equilibrium that involves the PuO_2^+ intermediate; and (3) Photo-assisted depolymerization of Pu(IV) hydrous polymers (9,10). None of these will be further discussed because they have already been presented in detail and space here is limited. Instead, attention shall be focused on photo-reprocessing related chemistry and, in particular, neptunium which has not been previously considered.

Neptunium Reactions

Neptunium, like its plutonium neighbor, can exist in oxidation states that vary from +3 to +6 (disregarding the +7 state which is not pertinent to reprocessing-related solutions). In

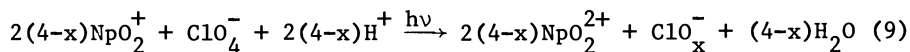
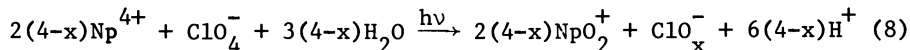
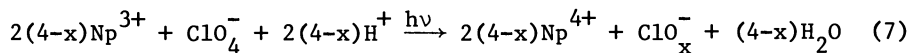
Table II. Quantum efficiencies for the redox reactions of the actinides shown as a function of acid concentration, when known. Redox agents marked with * are associated directly with the solvent medium.

Reaction	Wavelength	Redox agent	Medium	Quantum efficiencies for acid concentration (mole/liter)			
				0.1	0.5	1.0	4.0
U(VI) → U(IV)	250-600 nm	C ₂ H ₅ OH	H ₂ SO ₄ , HNO ₃	0.5	0.5	0.5	0.5
Pu(VI) → Pu(IV)	<350 nm	C ₂ H ₅ OH	HClO ₄ , HNO ₃			0.01	
Pu(IV) → Pu(III)	<350	C ₂ H ₅ OH, N ₂ H ₄	HClO ₄ , HNO ₃			0.03	
Np(VI) → Np(V)	254	C ₂ H ₅ OH	HClO ₄	.07	.068	.068	.040
	300	C ₂ H ₅ OH	HClO ₄			.068	
	254	*NO ₂ ⁻	HNO ₃	.04		.03	.002
	300	*NO ₂	HNO ₃	.001		.002	
Np(V) → Np(IV)	254	C ₂ H ₅ OH	HClO ₄	.006	.006	.008	.011
	300	C ₂ H ₅ OH	HClO ₄			.004	
Np(IV) → Np(III)	254	C ₂ H ₅ OH	HClO ₄	.03	.02	.02	.02
	300	C ₂ H ₅ OH	HClO ₄			.01	
Np(IV) → Np(V)	254	*ClO ₄ ⁻	HClO ₄	.02	.011	.010	.005
Np(V) → Np(VI)	254	*ClO ₄ ⁻	HClO ₄	.004	.005	.010	>.010

contrast to its uranium and plutonium analogs, neptunium has a very stable +5 oxidation state which tends to dominate the chemistry of inorganic acid solutions. Nemodruk and coworkers were the first to study the photo-redox reactions of Np and they looked separately at perchloric acid (11), hydrochloric acid (12), nitric acid (13) and sulfuric acid (14) media. However, noticeably absent in their work was any consideration of quantum efficiencies and wavelengths effects for the various photoredox reactions.

The recent photochemistry interests at Oak Ridge have been turned to an examination of these aspects for neptunium in perchloric (15) and nitric acid (16) solutions. A perchloric acid medium provides a much simpler starting point because the ClO_4^- ion is not subject to photolysis as is the NO_3^- ion when exposed to light of 250-360 nm wavelength. Nevertheless, nitric acid media were ultimately examined because of their obvious practical importance.

Perchloric Acid Media. In perchloric acid, solutions of Np(III), (IV), and (V) are oxidized after the absorption of 254 or 300 nm radiation in a stepwise fashion according to the following general reactions (15):



where the by-product ion is suspected to be either ClO_2^- or ClO^- . The change in species concentration for Np(IV) photo-oxidation is shown in Fig. 1 while that for Np(V) photo-oxidation is shown in Fig. 2. Quantum efficiencies for these and other reactions are given in Table II. The complex changes which occur when Np(IV) is photo-oxidized (cf., Fig. 1) demonstrate that several phenomena take place simultaneously. These include: (1) the retarding effects from the product ion ClO_x^- as seen at 250 minutes for the Np(V) species in 0.1 N H^+ ; (2) the acceleration of the Np(V) formation rate in 4.0 N acid as Np(V) accumulates and is, in turn, photo-oxidized at a higher quantum efficiency to Np(VI) which then combines rapidly with the residual Np(IV) to form Np(V); and (3) the build-up of Np(VI) in the low acid media prior to complete conversion of Np(IV) to Np(V), which is in contrast to the observation of the previous workers (11).

The photo-oxidation of Np(V) is more straight-forward since there are only two species possible. Figure 2 shows the effect of acid as expected from the reaction given in Eq. 9.

The photochemical reduction of neptunium in aqueous perchloric acid is complicated because it must compete at times with the oxidation processes caused by the HClO_4 . In contrast to the

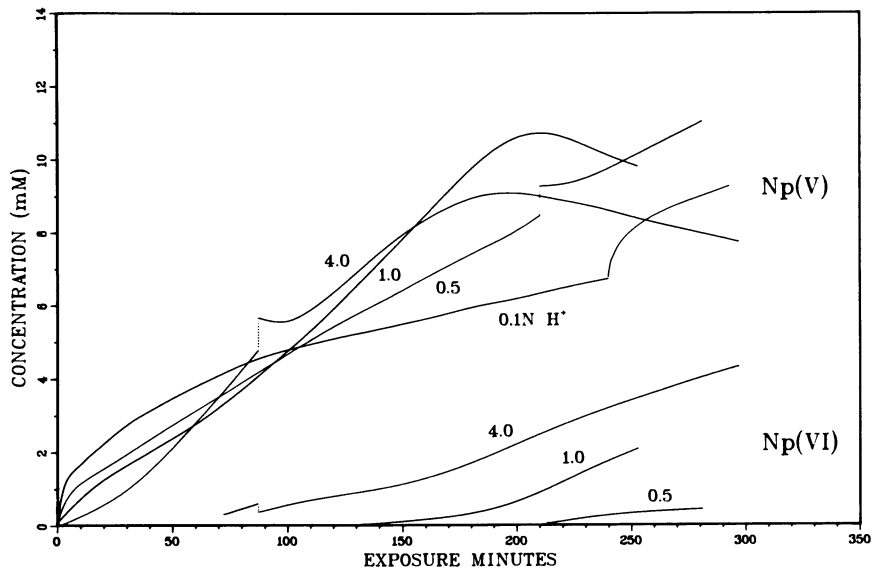


Figure 1. Photooxidation of Np (IV) with 254-nm radiation at 22°C; formation of Np (V) and Np (VI) products shown; total [Np] = 12mM for each solution photolyzed; dotted portions on curves represent dark period interruptions during the photolysis run.

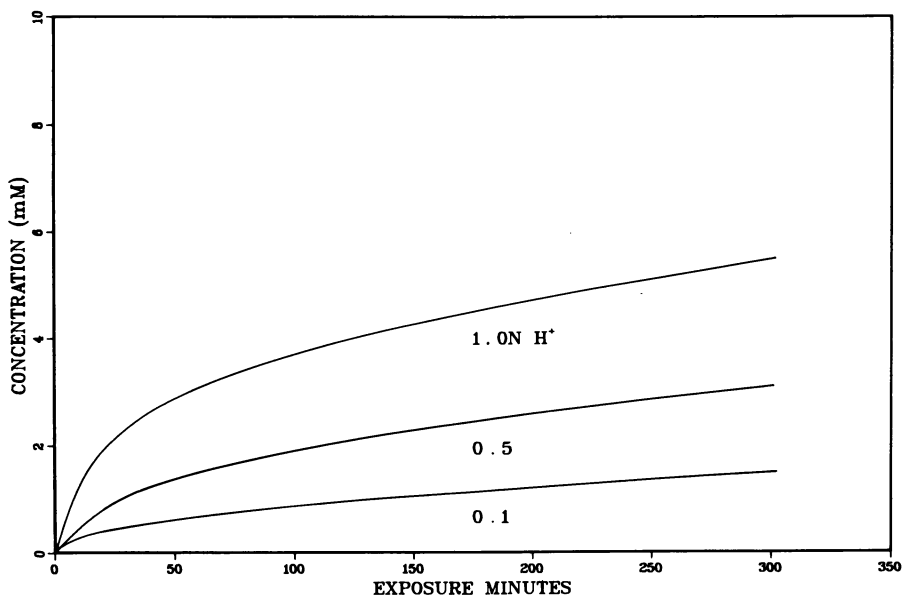
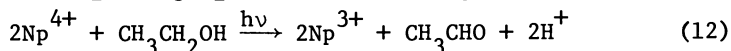
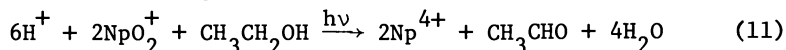
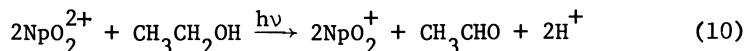


Figure 2. Photooxidation of Np (V) with 254-nm radiation at 22°C; total [Np] = 12mM for each solution photolyzed, Np (VI) concentration as a function of time shown.

previous study (11), the current results show that even the Np(III) state can be photochemically generated. The overall photoreduction reactions using ethanol have been identified as:

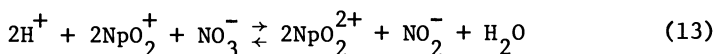


and the quantum efficiencies are given in Table II for each of these reactions. For more detail on this chemistry, the reader is referred to an earlier publication (15).

Nitric Acid Media. The photo-redox reactions of neptunium in nitric acid are, as stated earlier, complicated by the NO_3^- photo-reduction which prevents the complete photo-oxidation of neptunium to the (VI) state. At first this might seem to pose a dilemma which ought to be avoided, but recent results have shown how this apparent complication is essential to a photo-separation process. Two photochemical reactions working together will be shown to be necessary in order to reach what we have accepted as a practical result.

When photolyzed in the absence of any added reductants, nitric acid solutions of Np(VI) and Np(IV) are converted to Np(V). The photochemistry of Np in nitric acid differs from that in HClO_4 solutions since in the former, complete reduction of $\text{Np(VI)} \rightarrow \text{Np(V)}$ ultimately occurs, while in the latter, oxidation of $\text{Np(V)} \rightarrow \text{Np(VI)}$ is observed (cf., Fig. 2 and Eq. 9). The difference is obviously due to the presence of photochemically produced NO_2^- which serves as the reductant for Np(VI). The quantum efficiencies for Np in Table II show that the reactions occur best when irradiated with 254 rather than 300 nm light in agreement with the increased QY for NO_3^- photo-reduction at shorter wavelengths (23) but in opposition to the difference in NO_3^- light absorption as shown in Fig. 3. The Np(VI) reduction probably involves an excited state of Np, but the evidence in support of this is not conclusive. Although the quantum efficiency for Np(VI) reduction is not as great as that for the reduction of UO_2^{2+} with ethanol or hydrazine, it is not so prohibitively low that it cannot be useful.

Exposure of Np(V) solutions to 254 nm radiation produces a steady-state conversion of about 10 percent $\text{Np(V)} \rightarrow \text{Np(VI)}$ which returns to Np(V) in the dark. [There is therefore no net effect of UV light on Np(V)]. These observations can be explained by the shift of the equilibrium:



upon photo-excitation of NpO_2^+ .

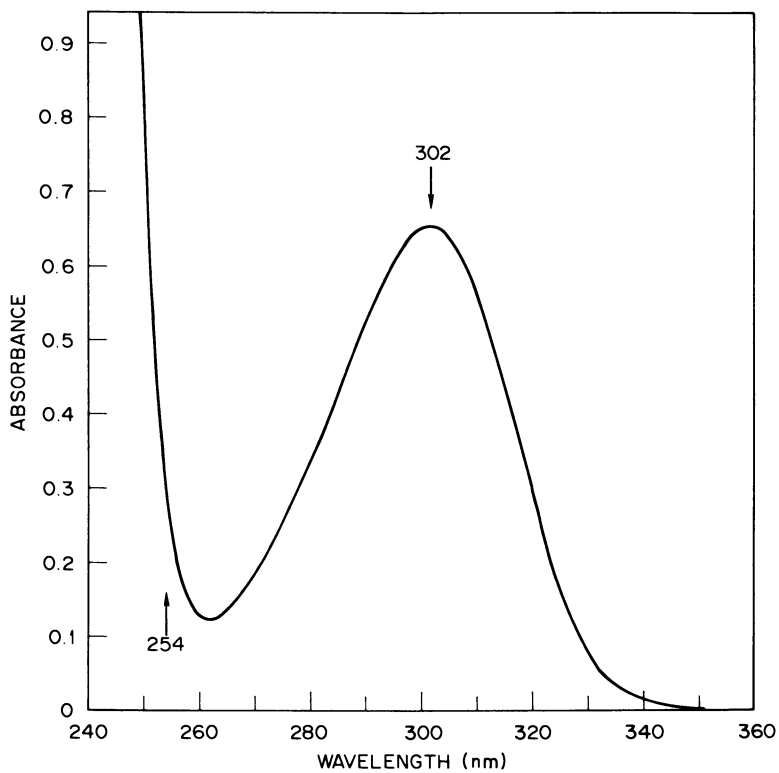


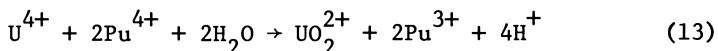
Figure 3. Absorption spectrum of HNO_3 ; $[\text{HNO}_3] = 0.1\text{N}$, cell pathlength = 1.0 cm .

Exposure of Np(IV) nitric acid solutions produces a simple photo-oxidation of Np(IV) \rightarrow Np(V) similar to the forward reaction of Eq. 13.

The addition of hydrazine has little effect on the neptunium photo-reactions in nitric acid. There is some evidence that it serves as a reductant, but it is not enough to be significant. Experiments are still in progress which should further define the Np redox chemistry in the presence of added reductants; but the competition between the various redox reactions involving both solvent and added reagents limits the potential for application to process conditions.

Actinide Separation Processes

Taking the foregoing neptunium photochemistry into account, it would be useful to apply it to the development of a more complex photo-separation scheme than has been mentioned previously (19,24), one which includes Np, U and Pu. Since Np(VI) can be photochemically reduced in the absence of any intentionally added reductants, it might be possible to photolyze a nitric acid solution containing the three actinides, reducing the Np(VI) while leaving the Pu(IV) and U(VI) unchanged. After the Np(V) has been removed by an extraction process, hydrazine could then be added and the solution photolyzed to achieve the simultaneous reduction (as was described previously) of UO_2^{2+} to U^{4+} and Pu^{4+} to Pu^{3+} with the accompanying assistance of the reaction:



The separation of Np from U and Pu was actually accomplished in a 0.5 N HNO_3 starting solution containing approximately 0.005 M, each, of Np(VI), U(VI) and Pu(IV). Previously, it was demonstrated that Pu and Np could be individually separated from U (19,24). The results of these separation processes are shown in Table III, thus demonstrating photo-separations of these ions are feasible.

Summary

To summarize the promise of actinide photochemistry briefly, it has been found that all three major actinides have a useful variety of photochemical reactions which could be arranged in a sequence to achieve a separations process that requires fewer reagents, and, understandably, a reduced volume of waste solutions. Most of the impact of photochemistry on reprocessing is admittedly speculative since only the chemical feasibility has been demonstrated.

Nevertheless, the attractive characteristics of photochemical reactions will continue to be stated (and sometimes overstated) as laser-related research interests grow. During the past years, we

Table III. Effect of light on the reductive extraction of Np-Pu-U solutions.

Solutions (approx 10 ml) typically contained approx 0.005 M of each actinide in question. Wavelength, exposure time, absorbed intensity, starting acidity, and final adjusted acidity were as follows: A, 254 nm, 20 min, 1W, 0.5 N, 2.0 N; B, 200 nm, 30 min, 1W, 1.4 N, 2.6 N (contained also 0.5 M hydrazine nitrate); C, 254 nm, 10 min, 1W, 0.5 N, 2.0 N. Acidification was followed by extraction into an equivalent volume of 30% TBP in dodecane. Part B taken from previous results (19,24).

		Dark		Light	
		Sample		Sample	
A Separation of Neptunium from Np-U Mixture					
Aqueous		14% Np		93.8% Np	
Layer		12.4% U		12.3% U	
TBP		86% Np		6.2% Np	
Layer		87.6% U		87.7% U	
B Separation of Plutonium from Pu-U Mixture					
Aqueous		33% Pu		90% Pu	
Layer		3% U		3% U	
TBP		67% Pu		10% Pu	
Layer		97% U		97% U	
C Separation of Neptunium from Np-U-Pu Mixture					
Aqueous		22% Np		82.3% Np	
Layer		18.1% U		13% U	
		16% Pu		20% Pu	
TBP		78% Np		17.7% Np	
Layer		81.4% U		86% U	
		84% Pu		80% Pu	

have realized several features which merit enumerating in conclusion: (1) Laser photochemistry is not, at the moment, as uniquely important in fuel reprocessing as it is in isotopic enrichment. The photochemistry presently at hand can be successfully accomplished with conventional light sources. (2) The easiest place to apply photo-reprocessing is on the three actinides discussed here. The solutions are potentially cleaner and more amenable to photo-reactions. (3) Organic-phase photo-reactions are probably not worth much attention because of the troublesome solvent redox chemistry associated with the photochemical reaction. (4) Upstream process treatment on the raffinate (dissolver solution) may never be too attractive since the radiation intensity precludes the usage of many optical materials and the nature of the solution is such that light transmission into it might be totally impossible.

Acknowledgment

Research sponsored by the Office of Basic Energy Sciences, U.S. Department of Energy under contract W-7405-eng-26 with the Union Carbide Corporation.

Literature Cited

1. Croff, A. G.; Tedder, D. W.; Drago, J. P.; Blomeke, J. O.; Perona, J. J. "A Preliminary Assessment of Partitioning and Transmutation as a Radioactive Waste Management Concept"; ORNL/TM-5808, Sept. 1977.
2. See for example: Moore, W. J. "Physical Chemistry"; 4th ed., Prentice Hall Inc.; New Jersey, 1972; p. 792.
3. Calvert, J. G.; Pitts, J. N. Jr. "Photochemistry"; John Wiley & Sons Inc., New York, 1966.
4. Bell, J. T.; Biggers, R. E. J. Mol. Spectry., 1968, 25, 312.
5. Bell, J. T.; Friedman, H. A., Billings, M. R. J. Inorg. Nucl. Chem., 1974, 36, 2563.
6. Nemodruk, A. A.; Bezrogova, E. V. Zh. Anal. Khim., 1968, 23, 388.
7. Bell, J. T.; Buxton, S. R. J. Inorg. Nucl. Chem., 1974, 36, 1575.
8. Palei, P. N.; Nemodruk, A. A.; Bezrogova, E. V. Radiokhimiya, 1969, 11, 300.
9. Bell, J. T.; Friedman, H. A. J. Inorg. Nucl. Chem., 1976, 38, 831.
10. Friedman, H. A.; Toth, L. M.; Bell, J. T. J. Inorg. Nucl. Chem., 1977, 39, 123.
11. Nemodruk, A. A.; Bezrogova, E. V.; Ivanova, S. A.; Novikov, Yu. P. Zh. Anal. Khim. 1972, 27, 73.
12. Nemodruk, A. A.; Bezrogova, E. V.; Ivanova, S. A.; Novikov, Yu. P. Zh. Anal. Khim. 1972, 27, 1270.

13. Nemodruk, A. A.; Bezrogova, E. V.; Ivanova, S. A.; Novikov, Yu. P. Zh. Anal. Khim. 1972, 27, 2414.
14. Nemodruk, A. A.; Bezrogova, E. V.; Ivanova, S. A.; Novikov, Yu. P. Zh. Anal. Khim. 1973, 28, 379.
15. Friedman, H. A.; Toth, L. M.; Osborne, M. M. J. Inorg. Nucl. Chem. 1979, in press.
16. Toth, L. M.; Friedman, H. A. (results to be published).
17. Carroll, J. L.; Burns, R. E.; Warren, H. D. "The Photo-activated Reduction of Uranium (VI) to Uranium (IV) Nitrate" HW-70543, 1961.
18. Wilson, A. S. "Organic Phase Reduction of Plutonium in a Purex-Type Process", U.S. Patent 3,620,687 (1971).
19. Friedman, H. A.; Toth, L. M.; Bell, J. T. "Method for Selectively Reducing Plutonium Values by a Photochemical Process", U.S. Patent 4,131,527 (12/26/78).
20. Goldstein, M.; Barker, J. J.; Gangwer, T. "A Photochemical Technique for Reduction of Uranium and Subsequently Plutonium in the Purex Process", BNL-22443 (1976).
21. Rofer-DePoorter, C. K.; DePoorter, G. L.; Hayter, S. W. "Photochemically Produced Uranium (IV) as a Reductant for Plutonium (IV) and Applications in LWR Fuel Reprocessing", LA-UR-78-383 (1978).
22. DePoorter, G. L.; Rofer-DePoorter, C. K. "Application of Photochemical Techniques to Actinide Separation Processes", Preceding paper in this symposium.
23. Kistiakowsky, G. B. "Photochemical Processes", ACS Monograph Series, 1928, p. 225.
24. Toth, L. M.; Friedman, H. A.; Bell, J. T. "Photochemical Separation of Actinides in the Purex Process" CONF-770506-1 (1977).

RECEIVED May 14, 1979.

Research sponsored by the Office of Basic Energy Sciences, U.S. Department of Energy under contract W-7405-eng-26 with the Union Carbide Corporation.

Application of Photochemical Techniques to Actinide Separation Processes

G. L. DEPOORTER and C. K. ROFER-DEPOORTER

Los Alamos Scientific Laboratory, University of California, Los Alamos, NM 87545

Photochemical techniques offer a potential for selectivity in systems where chemical methods offer little selectivity. Although thermal chemical properties of species to be separated may be similar, spectral differences can be exploited in photochemical separations. A further advantage of photochemical methods is the substitution of light energy for quantities of reagents. Both of these characteristics suggest the applicability of photochemical techniques to the actinides, whose separation and purification is often difficult, and whose radioactivity causes problems in the handling of waste reagents from their processing. In this paper, we review the application of photochemical techniques to actinide separations and related photochemical processes. The advent of the laser has brought about renewed interest in this field. Thus, these studies are in research stages and have not been developed to plant-scale processes.

The use of photochemistry in separation processes is fairly recent. An attempt was made in 1922 to separate chlorine isotopes by irradiating a mixture of H_2 and Cl_2 with light filtered through Cl_2 enriched in ^{35}Cl (1), but the first successful attempt was by irradiation of $COCl_2$ with an aluminum arc in 1932 (2). Although the photochemical reactions of the uranyl ion (UO_2^{2+}) were known since 1833 (3), they were not applied to separations until the early part of the Manhattan Project, when the spectra and photochemical reactions of uranyl compounds and UF_6 were investigated for their potential in isotope separation (4). No photochemical process was found that could compete with gaseous diffusion in efficiency and rapid development to large scale.

All of the basic requirements for photochemical separations were recognized in this early work:

1. The absorptions of the species to be separated must be significantly different.
2. A photochemical reaction must take place in one species to change its chemical form so that it can be separated from the mixture.

0-8412-0527-2/80/47-117-267\$05.00/0

© 1980 American Chemical Society

3. There must be no other interfering reactions that will cause a loss of the selectivity.
4. A light source must be available with a sufficiently narrow wavelength distribution to discriminate among spectral features, and it must have sufficient intensity to cause photochemical reaction in a reasonable time.

The first three requirements relate to the inherent chemical properties of the mixture to be separated. The requirements for the light source depend on the properties of the mixture, but its availability is a technological variable. Lasers, with their narrow wavelength ranges and high intensities, have generated new interest in photochemical separations. Infrared lasers have also made possible the completely new field of infrared-induced chemistry, in which some significant isotope separations have been reported.

The four principles of photochemical separation apply to the separation of other chemical entities, elements and compounds, as much as they do to the separation of isotopes. Since the spectra of elements and compounds differ to a much greater degree than the spectra of isotopes, the problem is simpler.

Several types of application of photochemistry to separations can be distinguished: separation of a chemical species that undergoes photochemical reaction from species that do not; selective irradiation and photochemical reaction of one of several photochemically active species; changes in conventional separations resulting from irradiation; and photochemical generation of separation reagents. This list does not cover all possibilities, but it serves to categorize the available literature.

The solution photochemistry of the actinides begins with uranium; none has been reported for actinium, thorium, and protactinium. Spectra have been obtained for most of the actinide ions through curium in solution (5). Most studies in actinide photochemistry have been done on uranyl compounds, largely to elucidate the nature of the excited electronic states of the uranyl ion and the details of the mechanisms of its photochemical reactions (5a). Some studies have also been done on the photochemistry of neptunium (6) and plutonium (7). Although not all of these studies are directed specifically toward separations, the chemistry they describe may be applicable.

The spectra and chemical properties of the actinides vary greatly. For example, the spectra of UO_2^{2+} and U^{4+} are shown in Fig. 1. In the presence of fluoride, UO_2^{2+} remains in solution, but UF_4 precipitates. Thus, combination of photochemical and thermal chemical properties can be used in their separations. Both oxidation and reduction have been reported in the literature as photochemical reactions of actinides. The reported reactions are summarized in Fig. 2.

The problem of the light source is simplest for separating a compound that undergoes a photochemical reaction from compounds that do not. In this case, a broadband light source, such as the

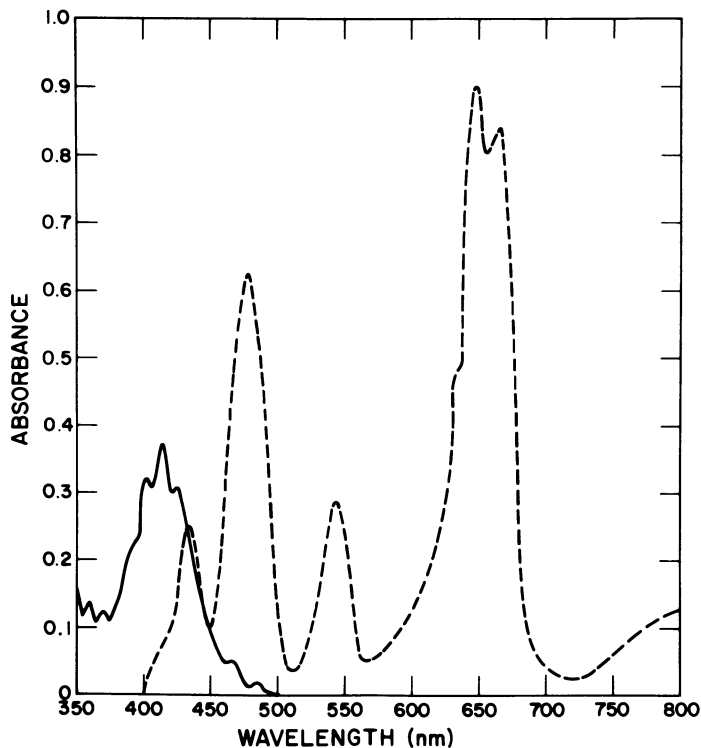


Figure 1. UV-visible absorption spectra of U (IV) and U (VI) at equal concentrations in nitric acid: (—) 0.042M UO_2^{2+} , 1N HNO_3 ; (---) 0.042M U (IV), 4N HNO_3 . U (IV) spectrum from Ref. 28.

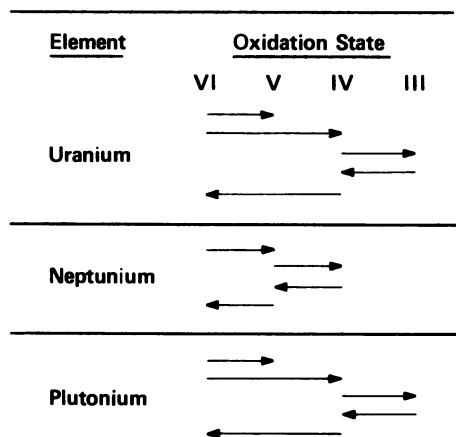


Figure 2. Reported photochemical actinide oxidations and reductions from Ref. 5, 6, and 7.

sun, can be used. Processes of this sort can be both simple and cheap. This principle has been applied to wet refining of uranium oxide (8) and to separation of uranium from some of its fission products, as a potential step in nuclear fuel reprocessing (9). Good separations were reported in these experiments (Table I), but no large-scale applications have been reported.

With a single-line source, two photochemically active components can be separated in solution by irradiation and subsequent reaction of one of the components. This technique has been applied to the separation of the transition metals cobalt and iron (10) and of europium from the other lanthanides (11). Although no separation of this type has been reported for the actinides, there is nothing in principle that prevents it. This method could prove particularly useful in separating actinides from lanthanides, where thermal chemical methods are particularly difficult.

Irradiation also affects the course of more conventional separation processes. Visible and ultraviolet light have been found to affect plutonium solvent extraction by photochemical reduction of the plutonium (12). Although the results vary somewhat with the conditions, generally plutonium(VI) can be reduced to plutonium(IV), and plutonium(IV) to plutonium(III). The reduction appears to take place more readily if the uranyl ion is also present, possibly as a result of photochemical reduction of the uranyl ion and subsequent reduction of plutonium by uranium(IV). Light has also been found to break up the unextractable plutonium polymer that forms in solvent extraction systems (7b,c). The effect of vibrational excitation resulting from infrared laser irradiation has been studied for a number of heterogeneous processes, including solvent extraction (13).

In particular, when a solvent extraction system of uranyl nitrate, aqueous nitric acid, and tri-n-butyl phosphate (TBP) in a hydrocarbon diluent was irradiated with a CO₂ laser, a change was observed in the equilibrium distribution of uranyl nitrate between the phases (14). When the solution was irradiated at 944 cm⁻¹, close to the uranyl asymmetric stretching frequency, the effect was observed. When a nonresonant frequency was used or the energy was absorbed in the solvent, no effect was observed. Little heating could be expected, and, in any case, heating effects should have been in the opposite direction from that observed.

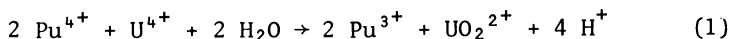
Since we had proposed a similar experiment with irradiation in the ultraviolet-visible absorption band of the uranyl ion (15), we tried to reproduce these results, but without success (16). Collisions in the liquid phase occur so rapidly (about 10¹² s⁻¹) that vibrational excitation of the uranyl ions would be dissipated long before any significant fraction of excited uranyl ions could reach the interface and therefore change the distribution between the two phases. Rapid loss of vibrational excitation in relation to other processes is a generic problem for infrared laser effects in any system of condensed phases. However, differences between experimental setups may account for the differences in results,

Table I. Solar Uranium Separations

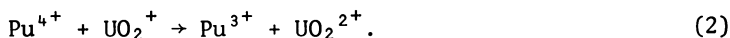
<u>Starting Solution</u>	<u>Additions</u>	<u>pH</u>	<u>Product</u>	<u>Separated From</u>	<u>% Recovery</u>	<u>% Purity</u>
Aqueous $\text{UO}_2(\text{NO}_3)_2$	$\text{NH}_4\text{F}\cdot\text{HF}$ Alcohol	4.7	$\text{NH}_4\text{F}\cdot\text{UF}_4\cdot\text{H}_2\text{O}$	Al Th, Ce, La	99 95	100 100
Aqueous $\text{UO}_2(\text{NO}_3)_2$	$\text{NH}_4\text{F}\cdot\text{HF}$ Alcohol	2.5	$\text{NH}_4\text{F}\cdot\text{UF}_4\cdot\text{H}_2\text{O}$	Fe V Be Zr	88 90 97 97	99.9 99.9 Not Given Not Given
Spanish Yellow Cake dissolved in Sulfuric Acid.	Ethyl Alcohol Hydrazine Sulfate	5	Hydrated Uranous Oxide	Cd, B, P, Cu, Cr, Fe, Pb, Mg, Zn, Na, Sn		

although possible reasons are obscure. Further experiments have shown no other extractants that behave in this way upon infrared irradiation (17).

Photochemistry can also be used in the generation of reagents for actinide separations. In the first step of solvent-extraction reprocessing methods, uranium and plutonium are extracted into the organic phase from most of the other actinides and the fission products, which remain in the aqueous phase. In subsequent steps of reprocessing, plutonium and uranium are separated and purified. The reprocessing schemes vary in the degrees of separation achieved in these steps. For example, Civex proposes that a much higher concentration of fission products be carried with the uranium and plutonium than in the Purex process (18); in co-processing, the uranium and plutonium are to be incompletely separated from each other (19). A plutonium reductant is needed for the complete or partial separation of uranium and plutonium. Plutonium(IV) extracts more readily into the organic phase, and plutonium(III), into the aqueous phase of the typical solvent extraction system (20). Uranium(IV) is a good reductant for tetravalent plutonium (21), and it can be produced by the photochemical reduction of uranyl by organic compounds, including several compounds that are used in normal reprocessing operations (22). Photochemical methods can produce solutions of uranium(IV) in either the aqueous or the organic phase (22,23). TBP is a good photochemical reductant for the uranyl ion, the reaction product being either uranium(IV) or uranium(V), depending on the experimental conditions (22c,d,e). Uranium(V), by its redox potential, should also be a plutonium reductant (24). The reaction for reduction of plutonium(IV) by uranium(IV) is



or, for reduction by uranium(V),



Although the redox potentials for aqueous solution indicate that uranium(IV) should reduce plutonium(IV), anions and other complexing agents can change the potentials sufficiently that uranium(IV) and plutonium(IV) can coexist in solution (25). Since one of the products of photochemical reduction of uranyl by TBP is dibutyl phosphate (DBP), which complexes plutonium(IV) strongly, experiments were done to test the photochemically produced uranium(IV) solutions as plutonium(IV) reductants (26). Bench-scale stationary tests showed these solutions to be equivalent to hydroxylamine nitrate solutions stabilized with hydrazine (27). The results of these experiments are shown in Table II. For these experiments, the uranium(IV) was in the organic phase and the plutonium(IV) was in the aqueous phase. Although large amounts of nitrite were present in the aqueous phase, no nitrite suppressors were necessary. In reductions in which both the uranium(IV) and

Table II. Organic U (IV)-Aqueous Pu (IV) Reductions Experiments

<u>Aqueous</u> <u>Organic</u>	<u>U(IV)</u> <u>Pu(IV)</u>	<u>Pu After Reduction</u>			
		<u>Aqueous</u>	<u>Organic</u>	<u>Pu(o)</u> <u>Pu(a)</u>	<u>Pu(a)</u> <u>Pu(o)</u>
0.73	2.34	1.93 g/l	0.0544	0.0282	35.48
0.29	5.86	1.90	0.0408	0.0215	46.57
0.15	11.72	1.84	0.0245	0.0133	75.10

Initial Solution Concentrations

Aqueous: 2.04 g/l Pu (0.0085 M), 1.5 N HNO₃

Organic: U(IV) 0.0147 M, U(VI) 0.0187 M, 33 v% TBP in CCl₄

No Nitrite suppressors used in either phase

plutonium(IV) were initially in the organic phase, the photochemically produced uranium(IV) was also effective in reducing the plutonium(IV) and allowing it to be stripped into the aqueous phase. We conclude that the amount of DBP produced in the photolysis was not sufficient to interfere in the stripping of plutonium(III) from the organic phase. Further experiments should be done to determine the amounts of DBP and other potentially deleterious byproducts generated by the various photochemical uranyl reductions.

The photochemical reduction of a solution containing both uranium(VI) and plutonium(IV) is also of interest for reprocessing applications. Early experiments (12a) showed a significant reduction of plutonium(IV) by light in Purex-type process solutions. Since the quantum yield for plutonium redox reactions is about one-tenth that for uranyl reduction (7b,c) the most likely path of plutonium(IV) reduction in these experiments appears to have been by uranium(IV) or uranium(V) generated by photochemical reduction of uranyl by other components of the solutions. Further experiments in this area would be useful.

Photochemical separation, with the new capabilities of lasers as light sources, provides many new areas of investigation. Application of photochemical techniques to actinide separations alone has an enormous potential. As lasers become more reliable and economical, photochemical separation should become an attractive technique for many systems.

Acknowledgement

We thank D. T. Vier and E. L. Zebroski (Electric Power Research Institute) for helpful discussions of early photochemical actinide research. The skill of J. M. Furnish in locating some of the older references was invaluable.

Literature Cited

1. Hartley, H.; Ponder, A. O.; Bowen, E. J.; Merton, T. R. Phil. Mag. (1922) 43(6), 430.
2. (a) Kuhn, W.; Martin, H. Naturwiss. (1932) 20, 772. (b) Kuhn, W.; Martin, H. Z. Physik. Chem. (1932) B21, 93.
3. Brewster, D. Trans. Roy. Soc. Edinburgh (1833), 12.
4. (a) Lipkin, D.; Weissman, S. I. Jan 1943, Columbia University Report 100XR-79. (b) Urey, H. C. Jul 1943, Columbia University Report 2C-R-135. (c) Crist, R. H. Feb 1944, Columbia University Report 2R-1241. (d) Dieke, G. H. Mar 1945, Manhattan District Report A-3227. (e) Dieke, G. H.; Duncan, A. B. F. "Spectroscopic Properties of Uranium Compounds"; McGraw-Hill: New York, 1949.
5. For example: (a) Uranyl ion. Rabinowitch, E.; Belford, R. L. "Spectroscopy and Photochemistry of Uranyl Compounds"; Macmillan: New York, 1964. Burrows, H. D.; Kemp, T. J. Chem. Soc. Rev. (1974), 139. (b) Uranium(V). Newton, T. W.;

- Baker, F. B. Inorg. Chem. (1965) 4(8), 1166. Ekstrom, A. Inorg. Chem. (1974) 13(9), 2237. (c) Uranous. Ahrlund, S.; Liljenzin, J. O.; Rydberg, J. In "Comprehensive Inorganic Chemistry", Bailar, J. C., Ed.; Pergamon Press: New York, 1973; Vol. 5. (d) Trivalent uranium. Drozdzyński, J. J. Inorg. Nucl. Chem. (1973) 40, 319. (e) Plutonium III, IV, V, and VI. Costanzo, D. A.; Biggers, R. E.; Bell, J. T. J. Inorg. Nucl. Chem. (1973) 35, 609. (f) Neptunium IV, V, and VI. Hindman, J. C.; Magnusson, L. B.; LaChapelle, T. J. In "The Transuranium Elements", Seaborg, G. T.; Katz, J. J.; Manning, W. M., Eds., McGraw-Hill: New York, 1949. (g) Americium III and Curium III. Penneman, R. A.; Keenan, T. K. "The Radiochemistry of Americium and Curium", Nuclear Science Series 1960 NAS-NS-3006.
6. (a) Nemodruk, A. A.; Bezrogova, E. V.; Ivanova, S. A.; Novikov, Yu. P. Zh. Anal. Khim. (1972) 27(1), 73; 27(7), 1270; 27(12), 2414; (1973) 28(2), 379. (b) Toth, L. M.; Friedman, H. A.; Bell, J. T. private communication.
 7. (a) Palei, P. N.; Nemodruk, A. A.; Bezrogova, E. V. Radio-khimiya (1969) 11(3), 300. (b) Bell, J. T.; Friedman, H. A. J. Inorg. Nucl. Chem. (1976) 38, 831. (c) Friedman, H. A.; Toth, L. M.; Bell, J. T. J. Inorg. Nucl. Chem. (1977) 39, 123.
 8. Zaki, M. R.; Farah, M. Y.; El-Fekey, S. A., Acta Chim. (Budapest) (1974) 80(2), 167.
 9. (a) Singh, K.; Sahoo, B.; Patnaik, D. Proc. Indian Acad. Sci. (1959) 50A, 129. (b) Singh, K.; Patnaik, D. Proc. Indian Acad. Sci. (1959) 50A, 358. (c) Singh, K.; Sahoo, B.; Patnaik, D. J. Sci. Ind. Res. (1960) 19B, 31.
 10. Donohue, T. Chem. Phys. Lett. (1977) 48(1), 119.
 11. Donohue, T. J. Chem. Phys. (1977) 67(II), 5402.
 12. (a) Haas, W. O.; Zebroski, E. L. Aug 1950, General Electric Report KAPL-375. (b) Burger, L. L.; Rehn, I. M.; Slansky, C. M. Feb 1952, General Electric Report HW-19949. (c) Ghosh Mazumdar, A. S.; Sivaramkrishnan, C. K. J. Inorg. Nucl. Chem. (1965) 27, 2423.
 13. Karlov, N. V.; Prokhorov, A. M. Usp. Fiz. Nauk (1977) 123(1), 57.
 14. Karlova, E. K.; Karlov, N. V.; Kuz'min, G. P.; Laskorin, B. N.; Prokhorov, A. M.; Stupin, N. P.; Shurmel', L. B. Pis'ma Zh. Eksp. Teor. Fiz. (1975) 22, 459.
 15. DePoorter, G. L.; Rofer-DePoorter, C. K. Jan 1976, Los Alamos Scientific Laboratory Report LA-5630-MS, Vol. II.
 16. DePoorter, G. L.; Rofer-DePoorter, C. K., J. Inorg. Nucl. Chem. (1977) 39, 2061.
 17. Karlov, N. V., private communication, June 1978.
 18. For example, Levenson, M.; Zebroski, E. "A Fast Breeder System Concept: A Diversion Resistant Fuel Cycle", presented at the Fifth Energy Technology Conference, Washington, D. C., Feb 1978.

19. For example, Okamoto, M. S.; Thompson, M. C. Nucl. Tech. (1979) 43, 126.
20. Best, G. F.; McKay, H. A. C.; Woodgate, P. R., J. Inorg. Nucl. Chem. (1957) 4, 315.
21. For example, Jenkins, E. N.; Streeton, R. J. W. 1959 Report AERE-R-3158.
22. (a) Carroll, J. L.; Burns, R. E.; Warren, H. D. 1961 General Electric Report HW-70543. (b) Toth, L. M.; Friedman, H. A.; Bell, J. T. In "Proceedings of the ANS Topical Meeting on the Plutonium Fuel Cycle", 1977 CONF-7705061. (c) Rofer-DePoorter, C. K.; DePoorter, G. L. J. Inorg. Nucl. Chem. (1977) 39, 631. (d) DePoorter, G. L.; Rofer-DePoorter, C. K. J. Inorg. Nucl. Chem. (1978) 40, 1895. (e) Rofer-DePoorter, C. K.; DePoorter, G. L. J. Inorg. Nucl. Chem. (1979) 41, 215. (f) DePoorter, G. L.; Rofer-DePoorter, C. K. U. S. Patent 4 080 273, 1978.
23. Bhat, T. R.; Mathur, B. S. Indian J. Technol. (1963) 1, 14.
24. Fuger, J.; Oetting, F. L. "The Chemical Thermodynamics of Actinide Elements and Compounds", part 2, "The Actinide Aqueous Ions"; International Atomic Energy Agency: Vienna, 1976.
25. (a) Marcus, Y. J. Phys. Chem. (1958) 62, 1314. (b) Yanir, E.; Givon, M.; Marcus, Y. J. Inorg. Nucl. Chem. (1968) 32, 1322.
26. DePoorter, G. L.; Rofer-DePoorter, C. K.; Hayter, S. W. Nucl. Tech. (1979) 43, 132.
27. (a) Richardson, G. L.; Swanson, J. L. 1975 Report HEDL-TME-75-31. (b) Barney, G. S. 1971 Report ARH-SA-100.
28. Keder, W. E.; Ryan, J. L.; Wilson, A. S. J. Inorg. Nucl. Chem. (1961) 20, 131.

RECEIVED August 31, 1979.

Work performed under the auspices of U.S. Energy Research and Development Administration under contract number W-7405-eng-36.

Plutonium Partitioning Methods in Power Reactor Fuel Reprocessing

ALFRED SCHNEIDER and BARRY G. WAHLIG

School of Nuclear Engineering, Georgia Institute of Technology, Atlanta, GA 30332

The bismuth phosphate process, developed and used during World War II for the isolation and purification of plutonium, did not provide for the recovery of uranium. Furthermore, this was inherently a batch process and thus not amenable to improvements in chemical processing which can be obtained with continuous operation. In the immediate postwar period, attention was devoted to solvent extraction methods which promised to overcome the shortcomings of the bismuth phosphate process. The Redox process, employing methyl isobutyl ketone (hexone) as the organic solvent and aluminum nitrate as the "salting agent" to promote the extraction of uranium and plutonium, was developed at the Argonne National Laboratory. Pilot-plant testing of the Redox process was done at the Oak Ridge National Laboratory (ORNL) in 1948 and 1949 and its large-scale use started at Hanford in 1952. In the Purex process, tributyl phosphate (TBP) in a hydrocarbon diluent is the organic solvent, while nitric acid is used as the "salting agent." This process, developed at about the same time as the Redox process by the Knolls Atomic Power Laboratory and ORNL, was put into large-scale operation at the Savannah River Plant in 1954 and at Hanford in 1956. Over two decades later and after numerous studies of alternate reprocessing methods and intensive searches for better solvents, the Purex process remains the prime reprocessing method for spent nuclear fuels throughout the world.

Uranium-Plutonium Partitioning in the Purex Process

The U-Pu separation is based on the much lower extractability of Pu^{3+} ions by TBP than of Pu^{4+} ions and the relative ease of oxidation and reduction of plutonium in solutions. The original Purex process utilized Fe^{2+} to achieve the reduction of Pu^{4+} to Pu^{3+} . Since nitrite ions, which are generally present in nitric acid solutions, reoxidize Pu^{3+} and thus affect the net reduction rate, a "holding reductant" is added to scavenge nitrite ions. Sulfamate ion, NH_2SO_3^- , is an effective holding reductant and this led to the selection of ferrous sulfamate, $\text{Fe}(\text{NH}_2\text{SO}_3)_2$, as the

0-8412-0527-2/80/47-117-279\$05.00/0

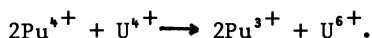
© 1980 American Chemical Society

reducing agent in the original Purex process (1,2). The U-Pu partitioning is done in countercurrent solvent extraction contactors (Fig. 1). Several incentives arose for modifying the original partitioning method with ferrous sulfamate: the corrosive action of both iron and sulfate (the eventual degradation product of sulfamate ions) on process equipment, particularly the high-level liquid waste tanks; the desire to avoid the introduction of additional salts in the waste; the much higher plutonium content of power reactor fuels, especially Pu breeder fuel, compared with that in the irradiated uranium from Pu production reactors; and the much greater burnup and consequently fission product content of power reactor fuels. The modifications were generally aimed at replacement of Fe^{2+} and NH_2SO_3^- with other reagents but, more recently, there have been more radical developments involving novel equipment concepts and flowsheet modifications.

Alternate Reducing Agents and Holding Reductants

Hydrazine (N_2H_4) was found to be an effective scavenger of NO_2^- ions and thus a promising holding reductant. Production scale tests at Hanford in 1968 with hydrazine-stabilized ferrous nitrate were plagued by problems associated with the carryover of nitrite, though the soundness of this method was demonstrated (3).

U^{4+} reduces Pu^{4+} to Pu^{3+} and was shown to be an effective reductant for U-Pu partitioning (4). The net reaction is:



While the use of U^{4+} avoids the introduction of extraneous metal ions, the holding reductant must be retained to prevent not only the reoxidation of Pu^{3+} , but also the autocatalytic oxidation of U^{4+} to U^{6+} . Hydrazine has been the preferred holding reductant. Several methods are available for the production of $\text{U}(\text{NO}_3)_4$: catalytic or electrolytic reduction of $\text{UO}_2(\text{NO}_3)_2$; dissolution of the hydrated oxide of U^{4+} in nitric acid; aluminum powder reduction of $\text{UO}_2(\text{NO}_3)_2$; etc. The partitioning method using $\text{U}(\text{NO}_3)_4$ -hydrazine was tried at Hanford in 1970 and has been employed in reprocessing plants in Western Europe, Japan, and the Soviet Union. While partitioning with U^{4+} is generally satisfactory, the need to introduce additional uranium into the process streams has two drawbacks: fuels with high plutonium content (e.g. breeder fuel) may require a substantial increase in throughput capacity to accommodate the large excess of uranium; and, unless the ^{235}U enrichment of the uranium reductant matches that of the uranium in the fuel, there is a loss in the value of the recovered uranium. This led to the development of in situ U^{4+} production, such as the electrochemical methods described below. The in situ photochemical production of U^{4+} contained in the organic phase has also been studied (34,35).

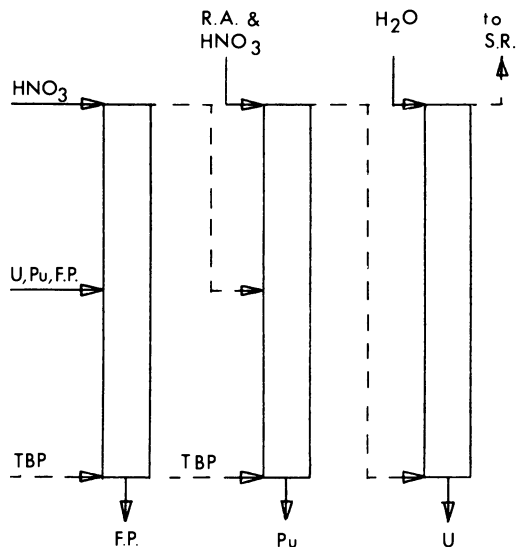


Figure 1a. Classical Purex partitioning schemes—early partitioning; (—) aqueous streams, (---) organic streams; R. A., reducing agent; TBP, n-tributyl phosphate in an aliphatic diluent; S. R., solvent recovery.

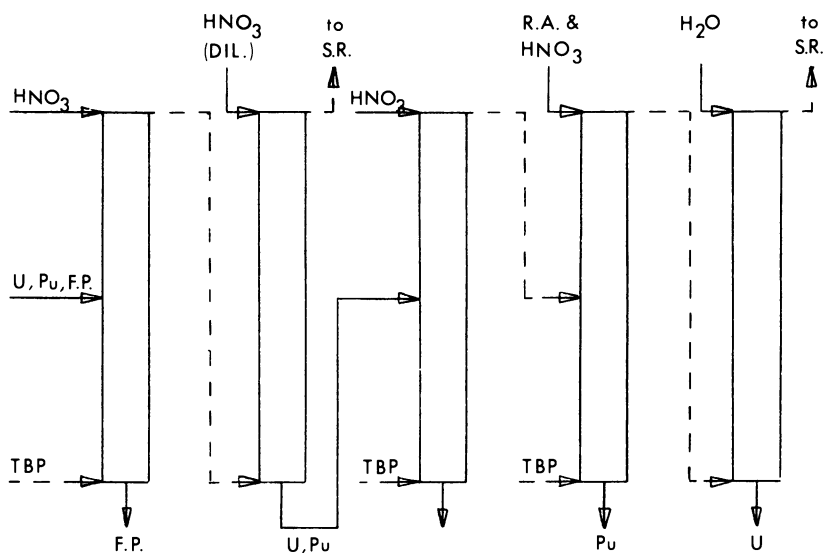


Figure 1b. Classical Purex partitioning schemes—late partitioning

Hydroxylamine salts were found to be good reductants of plutonium, under certain conditions (5). Interest in these reducing agents stemmed from the desire to avoid the introduction of metallic cations in the separated plutonium product. Hydroxylamine sulfate was used on a large scale at the Savannah River Plant (6). While partitioning was satisfactory, the objectionable presence of sulfate ions led to the adoption of hydroxylamine nitrate (HAN). The reaction mechanism and kinetics of the HAN reduction of plutonium have been studied extensively (7,8). The major problem with HAN has been the slow reduction rate with increasing HNO₃ concentrations. Barney derived the following equation which relates the Pu reduction rate with the reciprocal of $[H^+]^b$:

$$\frac{-d[\text{Pu(IV)}]}{dt} = k' \frac{[\text{Pu(IV)}]^2 [\text{NH}_2\text{OH}^+]^2}{[\text{Pu(III)}]^2 [H^+]^b (K_d + [\text{NO}_3^-]^2)} \quad (8)$$

While a low HNO₃ concentration is possible in plutonium purification cycles, a higher HNO₃ concentration is necessary to retain the uranium in the organic phase during the primary U-Pu partitioning. Plant-scale experience was obtained at Hanford with HAN in the second Pu and U cycles (3), and at Savannah River in the primary partitioning cycle, where HAN was particularly effective when used with Fe(NO₃)₂, as well as in the second plutonium cycle (6,9).

Two approaches were proposed to alleviate the aforementioned problem with unfavorable kinetics when HAN is used in the primary U-Pu partitioning: A low acid scrub containing HAN and N₂H₄ is introduced at the top of the partitioning column which reduces all of the Pu⁴⁺ and causes it to strip into the aqueous phase along with some of the U⁶⁺, while a high acid stream is introduced in the lower part of the column which causes the uranium to transfer back into the organic phase. The internal refluxing of uranium eventually leads to near saturation of the solvent, which further enhances the stripping of the plutonium.

The second approach, which represents a departure from previous Purex partitioning, provides for the quantitative reduction of Pu⁴⁺ to Pu³⁺ with HAN and N₂H₄ (as the holding reductant) prior to the introduction of the U- and Pu-containing feed into a second cycle extraction column (Fig. 2). This method was proposed for both the EXXON reprocessing plant in Tennessee (10) and the ORNL Reprocessing Facility for LMFBR fuel (11). HAN will continue to be an attractive reductant because, not only is the introduction of metallic cations avoided, but HAN is decomposed safely by heating at temperatures above 60°C, which simplifies the reoxidation of Pu³⁺ to Pu⁴⁺ prior to subsequent extraction cycles.

Hydrogen in the presence of a reduction catalyst will also reduce Pu⁴⁺ to Pu³⁺ and can thus be used as a reductant for U-Pu partitioning. The feasibility of this concept was demonstrated in 1965 (38,39).

Electrochemical Partitioning

The search for an *in situ* reduction of U^{6+} and Pu^{4+} to avoid the need for the introduction of extraneous U^{4+} into a partitioning column, led Schneider and coworkers to investigate, in 1967, the electrolytic reduction of uranium in a heterogeneous dispersion of the TBP-containing solvent in the continuous aqueous phase (12). These studies progressed rapidly from small-scale cell experiments with uranium and plutonium to the successful development of several types of large-scale "electropulse columns" (13) (Fig. 3). A full-scale unit with a nominal plutonium partitioning capacity in excess of 75 kilograms per day was installed at the Barnwell Nuclear Fuel Plant in South Carolina. Plant checkouts of this unit, using only uranium, have been in progress since 1977. In these tests, the fraction of U^{6+} reduced to U^{4+} was determined for a wide range of operating conditions.

Baumgärtner and coworkers at Karlsruhe have, since 1968, done numerous studies on the application of electrolytic reduction-oxidation methods to Purex reprocessing schemes (15,16) (Fig. 4). The utility of the *in situ* electrolytic reduction method was demonstrated with good results on a small scale for a breeder reactor fuel containing 15% Pu (17). Electrolytic reduction studies were reported in France (18), the Soviet Union (19,20), the United Kingdom (27), and China (37).

Non-Reductive Partitioning Methods

Several methods were proposed for Pu-U partitioning which are not based on a reduction of plutonium to the less extractable trivalent state. The separation is achieved by either forming aqueous Pu^{4+} complexes which have a low solubility in the TBP-hydrocarbon solvent or by saturating the organic solvent with uranium, which depresses the extractability of plutonium.

Complexing with H_2SO_4 has been used for some time to promote the stripping of plutonium from TBP solutions. The U-Pu partitioning in small-scale reprocessing trials of highly irradiated fast reactor fuel was done at Windscale by scrubbing with dilute H_2SO_4 (21). Though the Pu-U partitioning achieved was satisfactory, continued use of H_2SO_4 is not foreseen because of its corrosiveness and incompatibility with eventual waste solidification processes.

The utility of carboxylic acids (formic, acetic), which also form Pu^{4+} complexes sparsely soluble in TBP solutions, was investigated by Germain (22) and McKay (23). The results were not encouraging.

A partitioning method which does not require any additives was proposed by Weech (24). The plutonium separation is accomplished by recycling part of the separated uranium to a reflux column in which a high saturation of uranium is maintained in the organic phase. The plutonium extraction is thus greatly

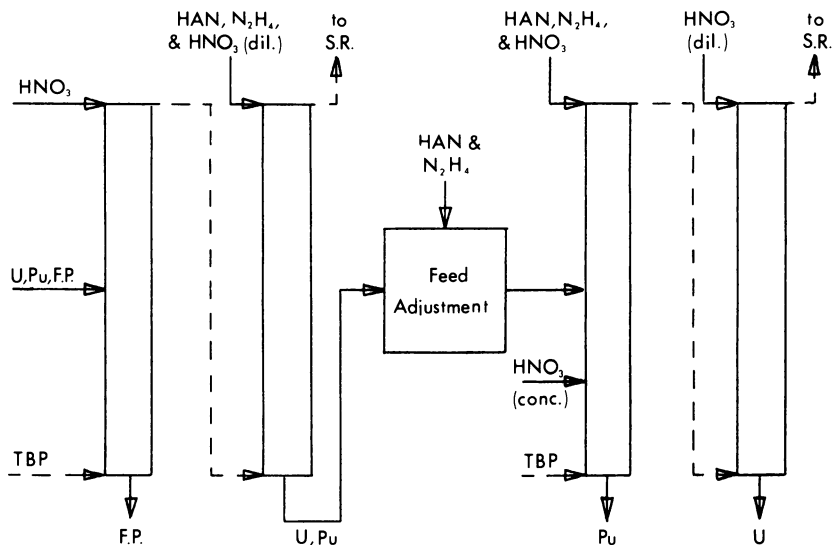


Figure 2. Prereduction partitioning scheme; HAN, hydroxylamine nitrate; N_2H_4 , hydrazine.

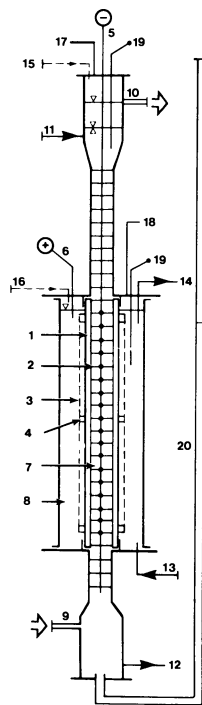


Figure 3. AGNS laboratory-scale electropulse column: 1, diaphragm; 2, cathode; 3, anode; 4, spacers; 5, cathode bus bar; 6, anode bus bar; 7, cathode chamber; 8, anode chamber; 9, organic feed; 10, organic effluent; 11, aqueous feed; 12, aqueous effluent; 13, anolyte effluent; 15, air purge; 16, air purge; 17, vent; 18, vent; 19, thermocouple; 20, pulse leg.

Allied-General
Nuclear Services

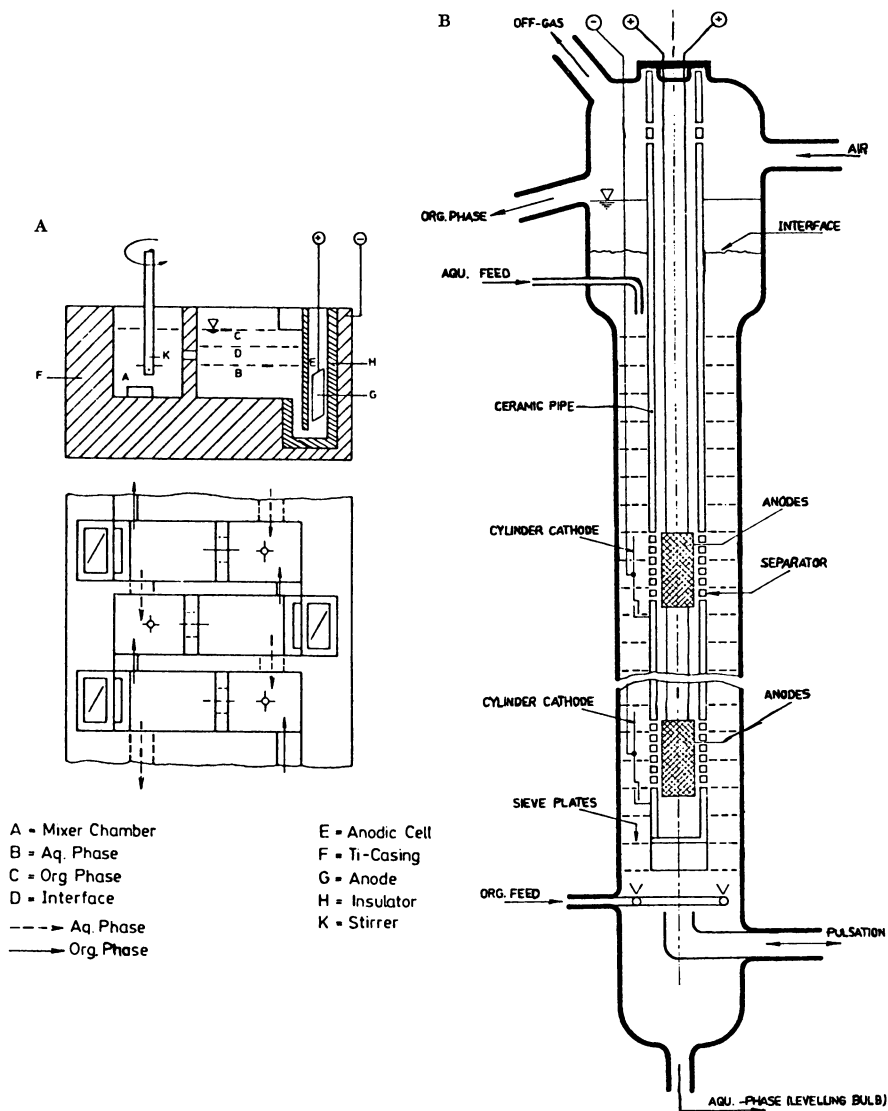


Figure 4. KFK electrolytic contactors; a. mixer settler, b. pulsed column.

depressed. It is claimed that by suitable control of the HNO_3 content in the lower part of the reflux column, that acceptable decontaminations were obtained from Pu in the organic stream containing U and from U in the aqueous stream containing Pu and Np.

A more radical modification of the Purex process, the Aquafleur process, developed by General Electric for its Midwest Fuel Recovery Plant, retained only a single TBP co-decontamination cycle followed by a continuous anion exchange contactor in which plutonium was to be removed from the U-Pu nitrate solution. The performance of this plant was never tested with plutonium, since General Electric decided to forego operation of the plant after technical difficulties developed during the "cold" check-out trials.

Equipment

Conventional solvent extraction contactors, mixer-settlers or pulsed columns, have been used exclusively until now for the Pu-U partitioning step. Centrifugal contactors have been considered, but there has been some concern about the compatibility of short residence time with the kinetics of plutonium reduction.

The development of in situ electrolytic methods by Allied Chemical resulted in a novel unit, the electropulse column, in which mass transfer and electrolytic reduction are carried out simultaneously (25). The basic feature of the electropulse column, (Fig. 3), is the dual function of the horizontal perforated plates, acting as cathodes as well as pulse plates, and the introduction of vertical anode screens contained in porous ceramic sleeves. This design was found particularly suitable for Pu-U partitioning, since it permits operation with an aqueous-continuous phase, which is needed to maintain adequate electrical conductivity, while the organic to aqueous flow ratio is kept quite large to obtain a high plutonium concentration in the exiting aqueous stream.

The parallel electrolytic reduction developments at Karlsruhe appear to have concentrated initially more on the reduction of Pu and U in electrode-equipped mixer-settlers in which the reduction occurred largely in the settled aqueous phase rather than in a heterogeneous mixture. It was determined that a separating membrane may not be necessary because of the redox potentials in the U^{4+} - U^{5+} - U^{6+} system and the absence of gaseous products at the electrodes which could lead to explosive mixtures. A pulsed column, with internals quite different from those of Allied Chemical's electropulse column, was eventually developed and successfully tested (15,26) (Fig. 4).

A combined electrochemical cell and pulsed solvent extraction column in which one of the electrodes consists of a bed of electrically conducting particles was developed at the U.K. Atomic Energy Authority (27).

Flowsheet Modifications

The location of the Pu-U partitioning step in Purex flowsheets and the selection of specific operating variables (flow rates, concentrations, temperature) were generally determined by the type of fuel to be reprocessed, the subsequent waste management schemes, and the desired characteristics of the products. The Purex Process has been used either with "early" or with "late" Pu-U partitioning (Fig. 1). The early split in the first cycle avoids the co-stripping of uranium and plutonium which may result in higher plutonium losses. In other flowsheets, the partitioning is delayed until the second cycle. While no particular trend has been obvious, some of the recent flowsheets in which the plutonium is reduced prior to re-extraction (10,11) will necessarily require a second cycle partitioning.

Considerable effort has been devoted in recent years to flowsheets which are more "proliferation resistant." This generally consists of avoiding the separation of pure plutonium, by either providing for co-processing (i.e. a partial Pu-U partitioning) or incomplete removal of fission products ("spiking"), to complicate the subsequent manipulations with plutonium. There are no fundamental reasons why any of the partitioning methods described could not be adapted to co-processing and partial decontamination and the results of several studies were published (28, 29,30,31,32). A. Moccia and coworkers reported good results with the use of long-chain aliphatic amides for the selective extraction of U^{6+} from HNO_3 solutions of U^{6+} and Pu^{4+} (36). This is believed to be useful in co-processing flowsheets where the Pu-U partitioning is limited to the removal of a small fraction of excess uranium. Interest has also developed in so-called "denatured fuel cycles," usually based on U-Th reactors, in which the ^{233}U produced is diluted with natural uranium to a fissile content below 12%. Since appreciable amounts of plutonium will be produced in such fuel, the reprocessing flowsheets must provide for some Pu-Th-U separations. Conceptual flowsheets have been developed for several cases (33) (Fig. 5). Typically, U, Pu, and Th are co-extracted into a TBP solution and Pu is partitioned by reductive stripping in the first cycle. Partial or complete partitioning of U and Th is obtained by a Th-limiting extraction in a second cycle. Additional purification cycles are foreseen for the Pu, Th, and U (or Th-U) products.

Conclusions

The Purex process will continue to be the main method for the reprocessing of nuclear reactor fuels. The inherent flexibility of this process allows for modifications needed to accommodate a large range of fuel compositions and product specifications. Among the several plutonium partitioning methods developed, those avoiding the introduction of extraneous metal ions

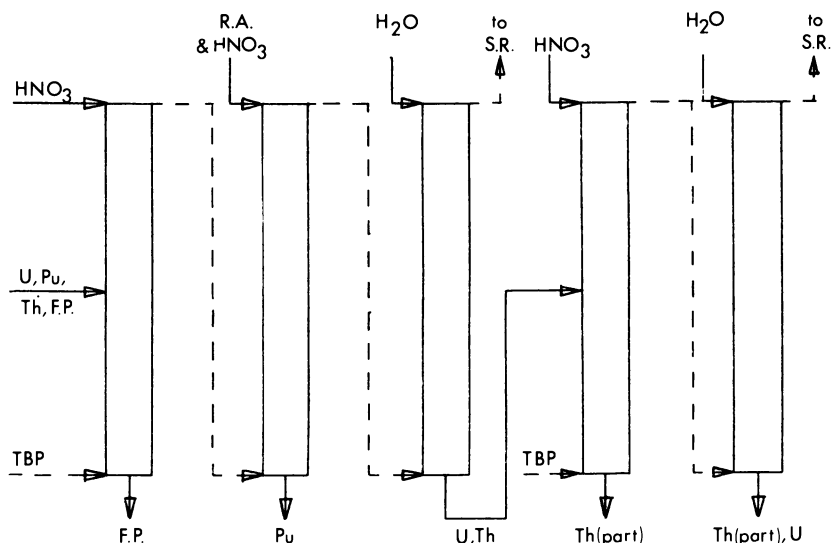


Figure 5. Partitioning scheme for U-Pu-Th fuel

(e.g. U^{4+} , HAN, electrolytic) are likely to be favored. In situ reduction methods have introduced new equipment concepts which may be particularly well suited for the processing of breeder fuel with high plutonium content.

Literature Cited

1. Irish, E. R., and Reas, W. H., "Symposium on the Reprocessing of Irradiated Fuels, Held at Brussels," USAEC Report TID-7534 (Bk. 1), 1976; pp. 83-106.
2. Cooper, V. R., and Walling, Jr., M. T., "Proceedings of the Second International Conference on the Peaceful Uses of Atomic Energy, Geneva, 1958," United Nations, N.Y., 1959; pp. 291-323.
3. Walser, R. L., "The Hanford Purex Plant Experience with Reductants," USAEC Report ARH-SA-69, Atlantic Richfield Hanford Co., Richland, WA, 1970.
4. Schlea, C. S., Caverly, M. R., Henry, H. E., and Jenkins, W. J., "Uranium (IV) Nitrate as a Reducing Agent for Plutonium (IV) in the Purex Process," USAEC Report DP-808, E. I. du Pont de Nemours & Co., Aiken, S.C. 1963.
5. Seaborg, G. T., Ed., "The Actinide Elements," McGraw-Hill Book Co., Inc., New York, 1954; pp. 274-276.
6. Orth, D. A., McKibben, J. M., and Scotten, W. C., "Proceedings of the International Solvent Extraction Conference I.S.E.C. 71," Soc. of Chemical Industry, London, 1971; pp. 514-533.

7. Richardson, G. L., and Swanson, J. L., "Plutonium Partitioning in the Purex Process with Hydrazine-Stabilized Hydroxylamine Nitrate," Report HEDL-TME-75-31, Hanford Engineering Development Lab., Richland, WA, 1975.
8. Barney, G. S., "Kinetic Study of the Reaction of Pu(IV) with Hydroxylamine," Report ARH-SA-207, Atlantic Richfield Hanford Co., Richland, WA, 1975.
9. Thompson M. C., Burney, G. A., and McKibben, J. M., "Recent Savannah River Experience with Actinide Separations," Paper presented at this Conf. (INDE #142).
10. Exxon Nuclear Co., "PSAR Nuclear Fuel Recovery and Recycling Center," Vol. 4, US NRC, Docket-50564-7; 1976.
11. Irvine, A. R., and Jones, F. J., "LMFBR Spent Fuel Reprocessing: A Study of an Industrial-Scale Facility," Report ORNL/TM-5723, Oak Ridge National Lab., 1977.
12. Schneider, A., and Ayers, A. L., (to Allied Chemical Corp.), "Electrochemical Concentration of Metallic Solutions," and "Electrochemical Oxidation or Reduction," U.S. Patents 3,616,275 and 3,616,276; 1971.
13. Cermak, A. F., Gray, J. H., Murbach, E. W., Neace, J. C., and Spaunburgh, R. G., "Development of the Electropulse Column for the BNFP," in Back End of the LWR Fuel Cycle Conf. held in Savannah, GA, 1978 (CONF-780304), p. V-11.
14. Cermak, A. F., and Spaunburgh, R. G., "Development of the Electropulse Column for Uranium-Plutonium Partitioning in the AGNS Reprocessing Plant," Paper presented at this Conf. (INDE #162).
15. Schmieder, H., Baumgärtner, F., Goldacker, H., and Hausberger, H., "Electrolytic Methods in the Purex Process," Report KFK-2082 (in German) Kernforschungszentrum Karlsruhe, 1974.
16. Baumgärtner, F., Goldacker, H., and Schmieder, H., "Electro-redox Procedures for Plutonium in Power Reactor Fuel Reprocessing," Paper presented at this Conf. (INDE #163).
17. Ochsenfeld, W., "Versuche zur Aufarbeitung von Schnell-Brüter Brennstoffen in der Anlage MILLI," Report KFK-2396 (in German), Kernforschungszentrum Karlsruhe, 1977.
18. Miquel, P., and Boudry, J. C., "First Experiments on the Reprocessing of Fast Reactor Fuels in France," Paper presented at 82nd AIChE Mtg., Atlantic City, N.J., 1976.
19. Fomin, V. V., *Atomnaya Energia*, 1977, 43, 481.
20. Dem'ianovich, M. A., *Atomnaya Energia*, 1977, 43, 486.
21. Warner, B. F., Naylor, A., Duncan, A., and Wilson, P. D., "Proceedings of the International Solvent Extraction Conf. I.S.E.C. 74," Soc. of Chem. Industry, London, 1974, pp. 1481-1497.
22. Germain, M., Bathellier, A., and Berard, P., "Proceedings of the International Solvent Extraction Conf. I.S.E.C. 74," Soc. of Chem. Industry, London, 1974, pp. 2075-2092.
23. McKay, H. A. C., Miles, J. H., and Park, H. S., "Possible Use of Carboxylic Acids for U/Pu Separation in Nuclear Fuel Reprocessing," Report AERE-R-8509, Harwell, U.K., 1976.

24. Weech, M. E. (to General Electric Co.), "Irradiated Fuel Recovery System," U.S. Patent 3,714,324; 1973.
25. Cermak, A. F., Ayers, A. L., Gray, J. H., and Schneider, A. (to Allied Chemical Corp.), "Apparatus for Electrolytic Oxidation or Reduction, Concentration, and Separation of Elements in Solution," U.S. Patent 3,770,612; 1973.
26. Baumgartner, F., Ochsenfeld, W., and Schmieder, H., "Development Work on Reprocessing of Oxidic LMFBR Fuel by the Purex Process," Paper presented at 82nd AIChE Mtg., Atlantic City, N.J., 1976.
27. "Electrochemical Processes and Apparatus for the Execution Thereof," (to U.K.A.E.A.) Belgian Patent 775,718, 1972.
28. Okamoto, M. S., and Thompson, M. C., "Coproducting Solvent Extraction Studies," Report DP-MS-77-76, E. I. du Pont de Nemours & Co., Aiken, S.C., 1978.
29. Hall, J. C., "Evaluation of Alternatives for Processing Uranium-Based LWR Fuels," Report AGNS-1040-3.1-15, Allied-General Nuclear Services, Barnwell, S.C., 1978.
30. Levenson, M., and Zebroski, E., "CIVEX," Paper presented at the 5th Energy Technology Conf., Washington, D.C., 1978.
31. Flowers, R. H., Johnson, K. D. B., Miles, J. H., and Webster, R. K., "Possible Long Term Options for the Fast Reactor Plutonium Fuel Cycle," Paper presented at the 5th Energy Technology Conf., Washington, D. C., 1978.
32. Cermak, A. F., Neace, J. C., and Spaunburgh, R. G., "Adaptation of the Electropulse Column to Coprocessing Flow-sheets," Report AGNS-1040-3.2-56, Allied-General Nuclear Services, Barnwell, S.C., 1978.
33. Schneider, A., and Massey, J. V., "Reprocessing Plants in International Fuel Service Centers," Paper to be presented at the ANS Annual Meeting in Atlanta, GA, June 1979.
34. DePoorter, G. L., Rofer-DePoorter, C. K., and Hayter, S. W., "Photochemically Produced Uranium (IV) and Application in LWR Fuel Reprocessing," Back End of the LWR Fuel Cycle Conf. held in Savannah, GA, 1978 (CONF-780304), p. V-15.
35. Toth, L. M., Friedman, H. A., and Bell, J. T., "Photochemical Separation of Actinides in the Purex Process," Paper presented at the Plutonium Fuel Cycle Mtg., Bal Harbour, FL., 1977.
36. Moccia, A., Cao, S., Abita, M., Gasparini, G. M., and Grossi, G., "The Search for Alternate Fuel Recycling Technologies in LWR-FBR Systems," Paper to be presented at the second ENC, Hamburg, May 1979.
37. He, J., Zhang, Q., and Lo, L., "The Separation of Uranium and Plutonium by Electrolytic Reduction in the Purex Process," Paper presented at this Conference (INDE).
38. Rainey, R. H., Nuclear Applications, 1965, 1, 310.
39. Rainey, R. H., (to U.S. A.E.C.), "Method of Selectively Reducing Plutonium Values," U.S. Patent 3,276,850; 1966.

RECEIVED May 14, 1979.

Development of the Electropulse Column for Uranium-Plutonium Partition in the AGNS Reprocessing Plant

A. F. CERMAK and R. G. SPAUNBURGH

Allied-General Nuclear Services, Post Office Box 847, Barnwell, SC 29812

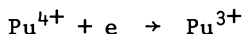
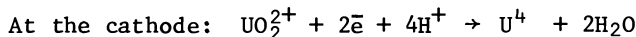
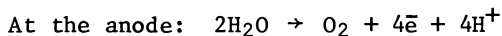
In the Purex process, plutonium and uranium are coextracted into an organic phase and partitioned by reducing plutonium(IV) to the aqueous-favoring plutonium(III). This has been achieved chemically by use of a suitable reductant such as ferrous sulfamate (1) or uranium(IV). (2, 3, 4, 5) The use of ferrous sulfamate results in accelerated corrosion of the stainless steel, due to the presence of ferric ions and sulfuric acid, and in an increase in the volume of wastes. The use of natural uranium(IV) can cause dilution of the ^{235}U in slightly enriched uranium, thus lowering the value of the recovered uranium.

In 1968, an electrolytic reduction process was proposed by A. Schneider and A. L. Ayers (6) to circumvent the above disadvantages. A research program was carried out in the Allied Chemical Corporation's laboratories during the years 1968 to 1972 to develop the process and equipment. The work resulted in the development of the Electropulse Column (7) for the continuous (differential) electrolytic uranium-plutonium partition process, which was later scaled up, fabricated, and installed in the Allied-General Nuclear Services reprocessing plant at Barnwell, South Carolina. About the same time, a stagewise electrolytic uranium-plutonium partition process was tested on a mini mixer-settler unit in Germany. (8)

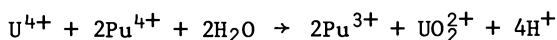
0-8412-0527-2/80/47-117-291\$05.00/0

© 1980 American Chemical Society

In the Electropulse Column, plutonium reduction is achieved both through the redox reaction of plutonium(IV) with uranium(IV), produced electrolytically from uranium(VI) in the cathode chamber, and by direct reduction of the plutonium(IV) at the cathode. The basic reactions involved in the electrolytic method are as follows:



Redox reaction in the cathode chamber:



Initial experiments were performed to verify and demonstrate the feasibility of the electrolytic reduction method with uranium, followed by experiments with a mixture of uranium and plutonium. Experiments were conducted batchwise in a small electrolytic cell. Basic parameters, such as concentration of solutes and type of holding agents (in the aqueous phase) for removal of any nitrite which would reoxidize the reduced heavy metal, electrode material and geometry, off-gas composition and type of diaphragm, were also determined. These data were valuable in the conceptual design of the first continuously operating column for the electrolytic reduction process.

Experimental

Two laboratory units, a 2.54-cm and a 12.7-cm diameter Electropulse Column, shown in Figures 1 and 2, respectively, were designed and fabricated for electrolytic experiments. The electrode configuration of both columns was the same, i.e., internal cathode-external anode. The electroactive part of the column consisted of a cylindrical porous ceramic diaphragm, about 60 cm long, provided with cathode perforated plates (Figure 1) or screens (Figure 2). It was located within a tubular anode chamber made of a glass pipe provided with a cylindrical platinum screen serving as the anode. The cathode in the 2.54-cm diameter column was made first of gold and later, during experiments with the uranium-plutonium mixture, of titanium perforated plates with a spacing of 1.9 cm. The cathode screens in the 12.7-cm diameter column were made of copper plated with silver. Sieve (perforated) plates, made of teflon or stainless steel (electrically insulated), were located and placed alternately with the cathode screens within the cylindrical ceramic diaphragm. The plate and cathode

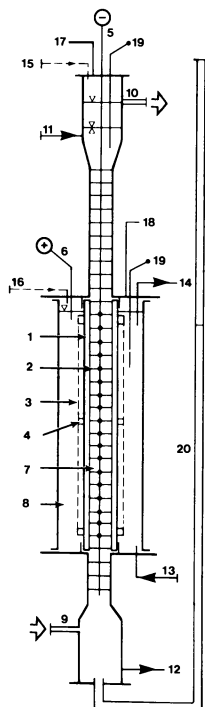


Figure 1. 2.54-cm diameter electro-pulse column: 1, diaphragm; 2, cathode; 3, anode; 4, spacers; 5, cathode bus bar; 6, anode bus bar; 7, cathode chamber; 8, anode chamber; 9, organic feed; 10, organic effluent; 11, aqueous feed; 12, aqueous effluent; 13, anolyte feed; 14, anolyte effluent; 15, air purge; 16, air purge; 17, 18, vent; 19, thermocouple; 20, pulse leg.

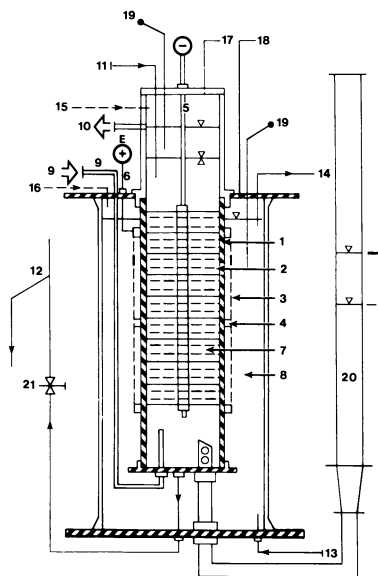


Figure 2. 12.7-cm diameter electro-pulse column: 1, diaphragm; 2, cathode; 3, anode; 4, spacers; 5, cathode bus bar; 6, anode bus bar; 7, cathode chamber; 8, anode chamber; 9, organic feed; 10, organic effluent; 11, aqueous feed; 12, aqueous effluent; 13, anolyte feed; 14, anolyte effluent; 15, air purge; 16, air purge; 17, 18, vent; 19, thermocouple; 20, pulse leg; 21, control valve.

screen spacing was varied from 2.5 to 7.5 cm during tests. Both columns were provided with an air pulser and a rectifier as the direct current power supply. The basic material for column construction was glass. Stainless steel was used for covers, piping, and the electrically insulated plates in both columns.

Both the 2.54-cm and 12.7-cm diameter Electropulse Columns were tested for uranium reduction. The feed to the columns consisted of a solution of uranyl nitrate in 30 v/o tributyl phosphate in a normal paraffin hydrocarbon diluent (organic feed) and a nitric acid solution (aqueous feed) containing hydrazine as the holding agent for the produced uranium(IV). Electrolytic experiments started after completion of hydrodynamic tests to determine the pulse column optimal operating conditions. Uranium(VI) concentration in the organic feed was tested in the range of 45 to 95 grams uranium/L. Nitric acid concentration in the aqueous feed was varied during tests in a range of 0.8 to 3 M and hydrazine in a range of 0.15 to 0.25 M. Anolyte acidity was about the same as that of the aqueous feed. Nitric acid concentration in the organic feed was within a range of 0.1 to 0.2 M. The run duration on the 2.54-cm diameter Electropulse Column varied with experimental requirements. The shortest electrolytic run lasted about 2 hours, the longest 32 hours. Electrolytic runs on the 12.7 cm diameter Electropulse Column lasted approximately 1.5 to 2 hours. Both the organic and aqueous phase were sampled periodically at the inlet and outlet of the column and analyzed for U(IV), U(VI), HNO₃ and N₂H₄. The runs on the 12.7-cm diameter column were made with the organic phase recirculating. In this case, the organic feed tank was also the receiver. Generally, when it was observed that the U(IV) concentration in both phases did not change, the run was considered completed and the column was shut down. Final evaluation of each run was made after completion of chemical analyses.

A total of about 80 electrolytic runs for uranium reduction was performed on both columns. The main objectives for runs on the 12.7-cm diameter Electropulse Column were to determine the best plate and cathode screen geometry and arrangement, and to define optimal operating conditions for uranium reduction with regard to mass-transfer and hydrodynamics. A total of 27 electrolytic runs were made in the 12.7-cm diameter column. During these runs, the organic flow rate was tested in a range of $L_{(o)} = 0.8 - 3$ L/min. The organic feed rate was tested during uranium runs in the 2.54-cm column in a range of $L_{(o)} = 16 - 120$ mL/min. In both columns, the volumetric flow rate ratio was tested in a range of $P_a = \text{aqueous/organic} = 1/2 - 1/8$ and current density in a range of $i = 0.02 - 0.08$ A/cm².

Results

Resultant data have shown that within the experimental range tested the uranium reduction efficiency $R(U)$, expressed as

$$R(U) = \frac{U(IV) \text{ produced per unit time}}{\text{Total } U(VI) \text{ in feed per unit time}} \times 100(\%),$$

increases with an increase in uranium concentration in the organic feed, cathode surface area, flow rate ratio ($P_a = \text{aqueous/organic}$), pulse velocity and current density. However, it decreases with an increase in the organic feed flow rate and aqueous feed acidity. For illustration, some data are presented in Table I. The current efficiency in the 2.54-cm diameter column was within a range of 25 to 90%, and in the 12.7-cm diameter column within a range of 20 to 75%, depending on the run conditions (Table I). Current efficiency is the percentage of $U(IV)$ produced per unit time of that calculated from Faraday's law.

With respect to the resultant data from uranium runs on both Electropulse Columns, the following correlation was derived for the uranium reduction efficiency:

$$R(U) = H \cdot C_{(o)} \cdot E_R \cdot (\log i + 2.55) \dots \quad (1)$$

where:

$$E_R = \frac{S_c}{L_{(o)}} \cdot (1 + P_a) \cdot f \cdot A_o \quad (2)$$

is a dimensionless number, which includes hydrodynamic and geometric parameters affecting the reduction efficiency within the Electropulse Column.

Experiments have shown that H in equation (1) is a function of the nitric acid concentration $[C(a)]$ in the aqueous phase. Its experimental values are:

$$\begin{array}{ll} H \approx 1.56 \times 10^{-4} & \text{at } C(a) \approx 3.0 \text{ M HNO}_3 \\ 2.17 \times 10^{-4} & \text{at } 1.4 \text{ M HNO}_3 \\ 2.75 \times 10^{-4} & \text{at } 1.0 \text{ M HNO}_3 \\ 3.50 \times 10^{-4} & \text{at } 0.8 \text{ M HNO}_3 \end{array}$$

The correlation derived from these data is:

$$H = 0.000116 \exp \left[\frac{0.883}{C(a)} \right] \dots \quad (3)$$

Equation (1) can then be rewritten in the form

$$R(U) = 0.000116 \frac{S_c \cdot f \cdot A_o}{L_{(o)}} (1 + P_a) \cdot (\log i + 2.55) \cdot C_{(o)} \cdot \exp \left[\frac{0.883}{C(a)} \right] \dots \quad (4)$$

TABLE I
URANIUM ELECTROLYTIC REDUCTION, RUN DATA

Run:	Column Diameter: (cm)	C(o) (g U/L)	C(a) (M HNO ₃)	I _(o) (ml/min)	S _c /L(o) (min/cm)	l + P a	Pulse Velocity: f x A _o (cm/min)	Current Density i (A/cm ²)	Reduction Efficiency		Current Efficiency nc %
									R(U) exp. %	R(U) calc. %	
PE-9	12.8	84.0	2.9	3000	0.69	1.125	142-145	0.081	2.15	2.15-2.20	44.5
PE-10	12.8	85.6	2.97	3000	1.33	1.125	127-130	0.0425	3.0	3.0-3.07	61.2
PE-15	12.8	95.0	2.88	3000	1.33	1.125	127-130	0.05	3.8	3.6-3.95	73.2
PE-17	12.8	93.4	2.88	3000	0.44	1.125	130-142	0.05	1.3	1.2-1.3	74.0
PE-23	12.8	52.7	0.81	2000	2.0	1.50	68-73	0.05	4.7	4.6-4.9	33.5
PE-27	12.8	44.0	0.84	2000	2.0	1.63	63.5-73	0.05	3.5	3.45-3.95	20.8
PE-1-7	2.5	53.5	1.0	24	9.33	1.125	123-130	0.08	28.1	28.0-29.6	27.0
PE-1-8	2.5	53.5	0.99	24	9.33	1.50	120-126	0.08	37.8	36.8-38.7	36.5
PE-1-9	2.5	53.5	0.99	80	2.8	1.5	136-142	0.08	12.8	12.5-13.0	41.2
PE-1-24	2.5	50.0	1.08	50	4.48	1.67	142-146	0.02	12.0	11.8-12.1	90.1
PE-1-26	2.5	50.0	1.08	80	2.8	1.5	110-120	0.05	7.6	7.55-8.2	36.7
PE-1-28	2.5	50.0	1.08	110	2.04	1.5	105-110	0.02	3.6	3.6-3.75	59.5
PE-1-48	2.5	45.5	1.07	110	2.04	1.13	142-146	0.08	6.0	5.7-5.9	24.0
PE-1-53	2.5	79.5	3.12	120	1.87	1.125	110-120	0.02	2.5	2.4-2.6	71.6

Verification of the validity of equation (4) was made during subsequent uranium runs on the 2.54-cm diameter Electropulse Column. The calculated uranium reduction efficiency for each run [from equation (4)] was compared with its experimental value. In all cases, the predicted value of the reduction efficiency correlated well with the corresponding experimental value, as shown in Figure 3.

Discussion

The Electropulse Column can be considered as a scrubbing contactor, with regard to uranium transfer from the organic into the aqueous phase. In such a contactor, the uranium transfer rate to the aqueous phase increases with an increase in the aqueous phase (scrubbing agent) flow rate and uranium concentration in the organic feed. However, it decreases with an increase in the organic phase flow rate and acidity of the aqueous scrubbing stream. This can be verified through the basic mass balance equation for scrubbing contactors. In a pulse column, operating under given concentration and flow conditions, the pulse velocity ($f \times A_0$ product) affects considerably the mass-transfer process. The higher the pulse velocity, the higher is the number of theoretical stages within the column and also the uranium transfer rate to the aqueous phase. With an increase in the rate of uranium in the aqueous phase entering in contact with the cathode of a given surface area, the uranium reduction efficiency increases. All these effects, proven during the electrolytic runs, are summarized in empirical equation (4).

The above equation was used for scale-up calculations and design of both the pilot plant and full-scale Electropulse Column. A total of 18 experimental runs for uranium(VI) electrolytic reduction was performed on the 20-cm diameter pilot-scale column. (10) As shown in Figure 4, the predicted reduction efficiency calculated from equation (4) correlated well with the experimental values obtained during these runs. The same good correlation between the predicted and experimental $R(U)$ values was achieved later during cold uranium tests in the full-scale unit (Figure 4). The accuracy of correlation was within the range of $\pm 6\%$.

The 2.54-cm diameter Electropulse Column shown in Figure 1, after completion of uranium runs, was installed at Battelle Memorial Institute (Columbus, Ohio) for uranium-plutonium partition tests. Six electrolytic runs were made under conditions corresponding to partitioning in the first process cycle to determine the effect of uranium reduction efficiency $R(U)$ on the separation process. The organic feed contained 80 to 83 grams/L of uranium and 0.71 to 0.82 grams/L of plutonium. The nitric acid concentration in the aqueous feed was 2.5 to 2.8 M and in the organic feed 0.2 to 0.3 M.

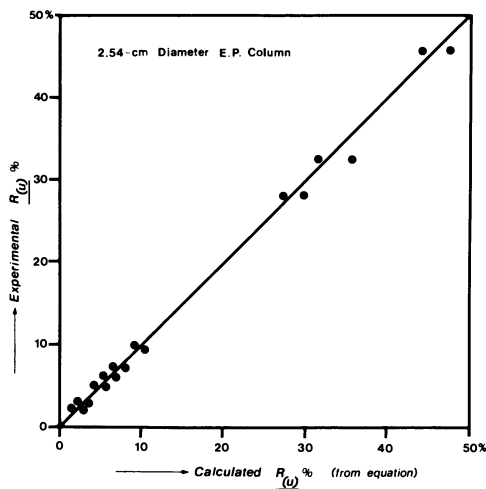


Figure 3. Comparisons of experimental U reduction efficiencies with calculated (predicted) values from the derived equation; 2.54-cm diameter E. P. column.

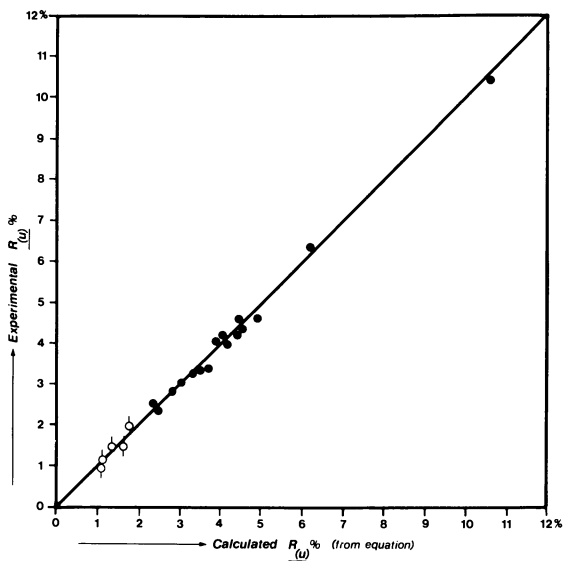


Figure 4. Comparison of experimental U reduction efficiencies with those calculated (predicted) from the derived equation; (●) pilot plant column, (○) full-size column.

As expected, the higher uranium reduction efficiency resulted in a higher percentage of plutonium transferred to the aqueous phase (Figure 5). At a uranium reduction efficiency higher than about 2.4%, over 99% of the plutonium in the organic feed is transferred to the aqueous phase, which indicates an efficient partition process.

The equation indicates high flexibility for the uranium reduction process control. For example, in a given Electropulse Column operating under constant flow conditions and at a given uranium concentration in the organic feed, the reduction efficiency can be affected by either acidity of feed streams, current input, or pulse velocity. Any combination of these variables is also possible.

The equation provides the means for determining the conditions necessary to obtain a desired uranium concentration in the aqueous effluent stream through the electrolytic reduction process. Any change in variables and parameters included in the equation will change the uranium transfer rate to the aqueous phase. The higher the transfer rate, the higher the reduction efficiency and the content of uranium in the aqueous phase leaving the column (9). This will affect the uranium-plutonium partition with respect to process requirements.

Notations

- R_(U) uranium reduction efficiency (%)
- C_(o) uranium(VI) concentration in the organic feed (grams uranium/L)
- C_(a) nitric acid concentration in the aqueous feed (M)
- S_c cathode surface area (cm²)
- L_(o) organic feed flow rate (mL/min)
- P_a flow rate ratio (aqueous/organic)
- f pulse frequency (cycles/minute)
- A_o pulse amplitude (centimeter/cycle)
- i cathode current density (A/cm²)

Acknowledgement

The authors wish to express their appreciation to Dr. A. Schneider and Mr. A. L. Ayers for the initial idea and support during the research and development work, as well as to Mr. J. C. Neace who performed the chemical analyses.

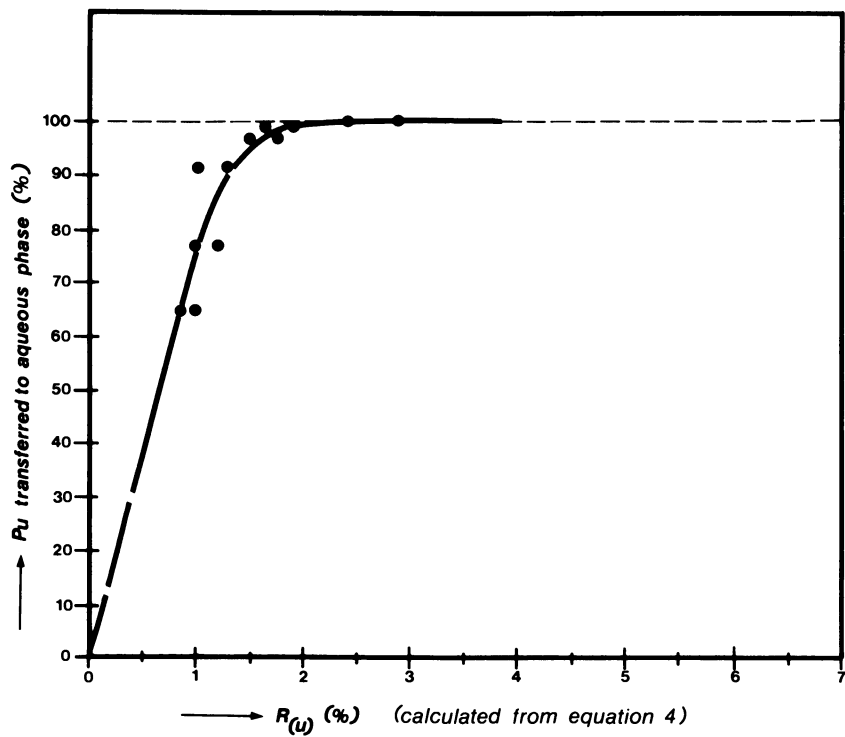


Figure 5. Effect of U reduction efficiency $R_{(U)}$ on the Pu transfer to the aqueous phase (for conditions in the first process cycle)

Literature Cited

1. Culler, F. L.; Bruce, F. R.; and Flanary, J. R., International Conference on Peaceful Uses of Atomic Energy, Vol. 8, Paper 822 (1955).
2. Newton, T. W., J. Phys. Chem., **63**, 1493 (1959).
3. Biddle, R., J. Inorg. Nuclear Chem., **28**, 736 (1966).
4. Srinivassan, N., Report BARC-375, Bhaba Atomic Research Center, Bombay, India (1968).
5. Solamon, L.; Lopez-Menchero, E., Ind. Eng. Chem., Vol. 9, No. 3, pp 345-358 (1970).
6. Schneider, A.; Ayers, A. L., U. S. Patents 3,616,275 and 3,616,276 (October 1971).
7. Cermak, A. F.; Gray, J. H.; Schneider, A.; Ayers, A. L., U. S. Patent 3,770,612 (November 1973).
8. German Patent 1,905,519 (August 1970).
9. Cermak, A. F.; Neace, J. C.; Spaunburgh, R. G., Adaptation of the Electropulse Column to Coprocessing Flow-sheets, AGNS-1040-3.2-56 (October 1978).
10. Cermak, A. F.; Gray, J. H.; Murbach, E. W.; Neace, J. C.; Spaunburgh, R. G., Development of the Electropulse Column for BNFP, ANS Topical Meeting, Savannah, Georgia; CONF-780304, pp V-11, March 19-23, 1978.

RECEIVED May 15, 1979.

Electroredox Procedures for Plutonium in Power Reactor Fuel Reprocessing

FRANZ BAUMGÄRTNER, HUBERT GOLDACKER, and HELMUT SCHMIEDER

Kernforschungszentrum Karlsruhe GmbH, Institut für Heisse Chemie, Postfach 36 40, 7500 Karlsruhe 1, West Germany

Reduction and oxidation (redox) steps are major process steps in the Purex process. Use is made of redox reactions to alter the valency of plutonium, uranium or neptunium with the object of producing these metals with a high degree of purity.

Electro-reduction and -oxidation processes are easy to operate and control remotely. Unlike the use of redox chemicals, they do not give rise to waste salts. Convenient remote control and operation and avoidance of waste salts are especially attractive features for commercial processing of any type of power reactor fuel. Accordingly, the electrode reactions were introduced quite early as intermediate steps in reprocessing. The electrochemical decladding of spent fuels was the first process in this field to be advanced up to the technical scale in the USA (1,2,3,4).

In the sixties hydrazine stabilized U(IV) solutions, electrochemically produced, successfully substituted the traditional corrosive and salt generating ferrous sulfamate (5) reducing agent for the U/Pu separation (e.g. Eurochemic in Mol, Karlsruhe Reprocessing Plant WAK).

Further development work on electrochemical methods started again both in the USA and in Germany also in the sixties (6,7). The objectives were to make the U/Pu separation more effective and to improve the product quality by electro-reduction taking place in the extraction apparatus itself (in-situ processing).

Today there exist technically mature apparatuses: an electro-reduction column (17) for the U/Pu separation in the AGNS Plant, Barnwell and an in-situ electro-reduction mixer settler, installed in the 2nd Pu-cycle in the German WAK Plant, Karlsruhe.

Parallel to in-situ reduction, electro-oxidation of products has been developed at Karlsruhe (8).

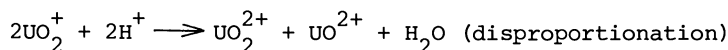
The following part describes the development of electro-redox processes at KfK, Karlsruhe.

Main Electrode Reactions and Side Reactions

The cathodic reduction of the uranyl ion is described by the following equation:



At nitric acid concentrations 0,2 to 2,0 M HNO_3 usually applied in the separation step the primary reduction product is U(V) and U(IV) is formed by disproportionation.



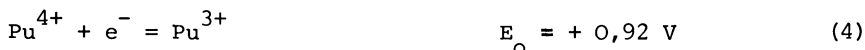
Oxidation experiments showed that U(IV) cannot be oxidized below the oxygen generation potential, therefore the disproportionation step can be considered as irreversible below this limit (8,19,20).

Oxidation of the stabilizer hydrazine, usually applied in the Purex process takes place as the preferred anodic reaction, so that practically no or only little oxygen generation occurs under the process conditions.

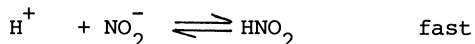
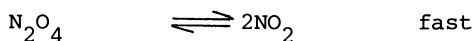
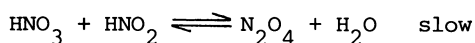
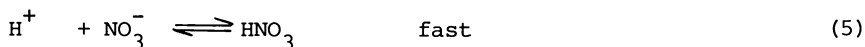


Consequently the in-situ process needs principally no diaphragms.

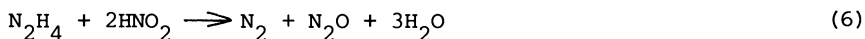
Plutonium is reduced directly at the cathode or by the electrochemically produced U(IV):



For the cathodic nitric acid reduction the following mechanism is proposed by Vetter (9):



Hydrazine reacts finally with nitrite in excess as follows:



Since hydrazine reacts quickly with HNO_2 the reaction preceding the electron transfer step is hindered. This interruption of

nitrate reduction (eqn. 5) has been confirmed in practice (8).

The preferred hydrazine oxidation at the anode far below the oxygen generation potential is the reason why Pu(III) is not or only in small amounts oxidized to Pu(IV) under these conditions. The complete conversion of Pu(III) to Pu(IV) is only possible after the hydrazine has been destroyed.

Pu(VI) is formed in minor amounts at the anode, depending on the current densities and on the nitric acid concentration, because a similar mechanism like in the U(VI)-U(IV)-couple can be assumed.

Electro-reduction in Mixer Settlers (8)

A 16 stage mixer settler (MILLI-EMMA) made from titanium has been operated for a total of about 2000 hours coupled to the MILLI facility (Hot Pilot Plant of the KfK, throughput about 1 kg of fuel per day). Figure 1 shows the basic layout. The titanium casing serves as cathode. In the settling section, the platinum anode has been placed in the anodic chamber lined with ceramic isolating material. The electrically conducting connection to the titanium casing is provided by the opening below the base level, thus preventing macroamounts of organic phase penetrating into the anode space in case of operational failure. A detailed description of the mixer settler with construction and operation data is given in KfK-report no. 2082 (8).

U/Pu split

Table 1 is a compilation of some characteristic test results for the U/Pu separation. With about 5 theoretical stages (only 30 to 50 % stage efficiency for U(VI) extraction was realized with the miniature mixer-settler) residual Pu contents in the 1BU flow of 1 mg/l were obtained. These values are influenced by the HDBP concentration in the organic phase and by the excess of U(IV) in the aqueous phase at the 1BU discharge point. The U(IV) is necessary to strip the residual Pu complexed by HDBP.

Figure 2 shows the concentration profile in the battery measured in test number 33 of table 1.

The separation efficiency is also decisively influenced by the aqueous acid, a profile of which can be seen in figure 2. In the BX part of the separation battery concentrations of 0,2 to 1,2 M HNO_3 and in the BS part of 1,2 to 1,5 M HNO_3 must be considered as optimum acidities. In spite of that quite low acid conditions plutonium colloid formation have never been observed because plutonium exists mainly in the trivalent state.

The behaviour of neptunium has been studied in the same contactor in quite a number of experiments, resulting in residual Np concentrations in the U product of about 1 %. Nearly 99 % of the Np went with the Pu product stream under optimized process conditions, e.g. 0,2 M HNO_3 in the BXS_a flow and a maximum phase

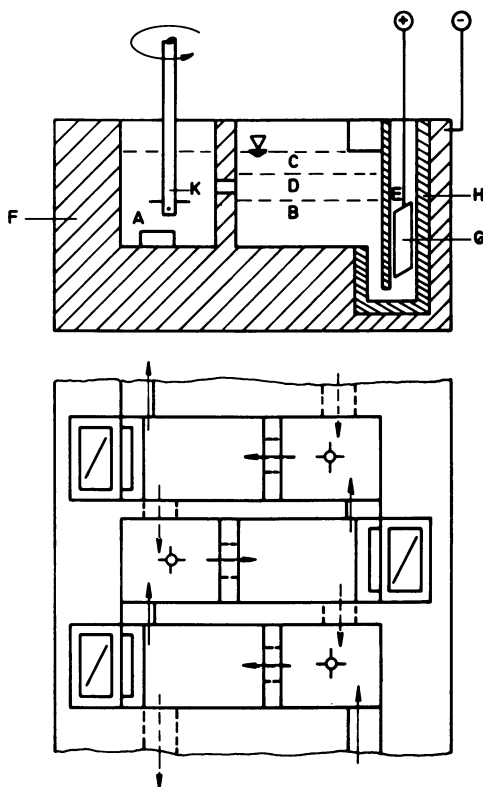


Figure 1. Principle of the electroreduction mixer settler MILLI-EMMA (8): A, mixing chamber; B, aqueous phase; C, organic phase; D, interface; E, anode cell; F, Ti containment; G, anode; H, insulator; K, stirrer; (---) aqueous phase; (—) organic phase.

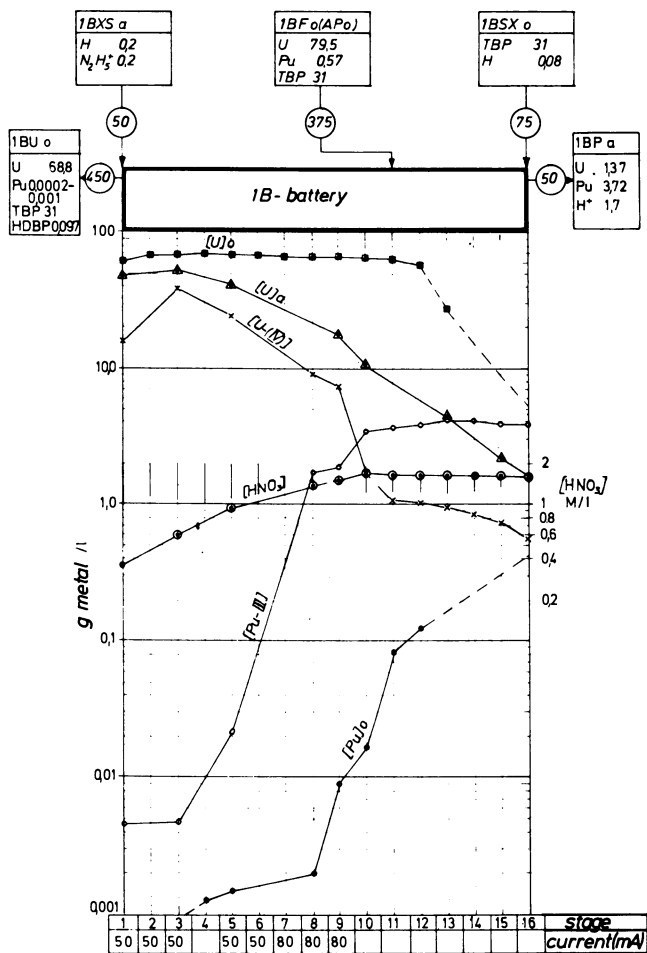


Figure 2. U-Pu separation (Experiment no. 33); concentration profile in the 16-stage electroreduction mixer settler, MILLI-EMMA (8): [HNO₃], [N₂H₅NO₃] in mol/L; [U], [Pu] in g/L; [TBP] in vol %; flows in mL/hr.

ratio AP_0/BXS_a of 5 (14).

Pu backextraction (purification cycles)

Acid concentration and HDBP content are also essential parameters for the electrolytic Pu backextraction in the Pu purification cycles. As shown experimentally the maximum acid concentration should be less than 1,0 M HNO_3 in the Pu product. The small amount of U entrained from the U/Pu separation battery markedly reduces the Pu losses. Characteristic results shown in table 2 demonstrate this effect. Figure 3 gives the corresponding concentration profiles of test number 18. Again a certain amount of U(IV) has to be kept in the discharge stage for the BW flow by a suitable distribution of anodes over the 16 stage battery.

A special advantage of the electrolytic technique for the Pu purification cycles is in the use of high Pu product concentration, which in subsequent tests was increased up to 60 g/l. The decontamination factors achieved in the experiments surpassed the results obtained with the conventional backextraction relying on diluted nitric acid by a factor of at least 10. At the WAK Plant (Demonstration Plant at Karlsruhe, throughput about 40 tons of fuel per year) the 2BW stream is returned to the first cycle on account of the high residual Pu content (≥ 100 mg/l).

The development of in-situ reduction in mixer settlers started in 1969 and was finalised quite recently in a 6 week long test using a 12 stage electro-reduction mixer settler on the WAK level in a Pu test cycle installed in the Institut für Heisse Chemie (15).

Using this technical titanium contactor, the design principles of which are similar to that shown in figure 1, residual Pu concentrations in the 2BW of 0,0002 to 0,005 g Pu/l have been achieved at product concentrations up to 45 g Pu/l and a maximum throughput of 1,5 kg Pu per day. The mixer settler is now installed in the second Pu cycle of the WAK Plant.

The corrosion rates of the titanium casing under cathodical conditions were smaller than that of stainless steel in nitric acid ($\sim 0,05$ mm Ti/y). This value as well as the corrosion rate of the platinized tantalum anode is within the expected order of magnitude ($< 0,005$ mm/y).

Electro-reduction in Pulsed Columns (16)

Parallel with the electro-reduction mixer settler an electro-reduction column with a 10 cm diameter has been developed at Karlsruhe.

The most simple design of such a column is shown in figure 4. The column wall and the sieve plates are made of titanium and work as cathodes. The central rod made of platinized tantalum and separated electrically from the sieve plates by means of ceramic rings, serves as the anode. Additional cylindrical metal sheets

Table 1. Typical Results of U-Pu Separation in the 16-Stage Electroreduction Mixer Settler MILLI-EMMA (8)

Experiment no.	Feed LAP ₀			IBXS _a			U product IBU ₀			Pu product IBP _a			Total current A	Current efficiency %	U (IV) in settling chamber No. 1
	TBP vol% 70	Flow cm ³ /hr	U g/L	HNO ₃ M	LAP ₀ / IBX _a	U g/L	Pu g/L	DFPu	U g/L	Pu g/L	U g/L	DF U			
7	20	750	68	0.5	6	49	0.0005	2000	0.0005	19	0.13	2800	1.68	19	3.9
11	20	750	49.1	0.4	5	41	0.0013	1700	0.0013	21	0.13	1900	2.08	20	3.5
30	30	750	73.7	0.20	7.1	61	0.0008	430	0.0008	3	1.5	1000	0.54	7	10.5
33	30	375	79.5	0.20	7.5	69	0.0002	1600	0.0002	3.7	1.5	800	0.49	5	16.6

Table 2. Typical Results of Pu Backextraction in the 16-Stage Electroreduction Mixer Settler MILLI-EMMA (8)

Experiment no.	2BP _a			2AP ₀			2BW ₀			Total current A	Current efficiency %
	Pu g/L	U g/L	HNO ₃ M	2BP _a	Pu g/L	Pu loss %	U g/L	HDBP mg/L			
18	10	0.3	0.5	1	0.00015	0.0015	1.5	80	0.73	31	
28	12.5	0.1	0.4	1	0.33	0.25	0.1	170	1.2	20	
37	48	0.6	0.6	3.5	0.003	0.02	2.9	70	1.2	22	
38	40	1.3	0.5	2.5	0.0008	0.005	2.5	400	0.84	43	

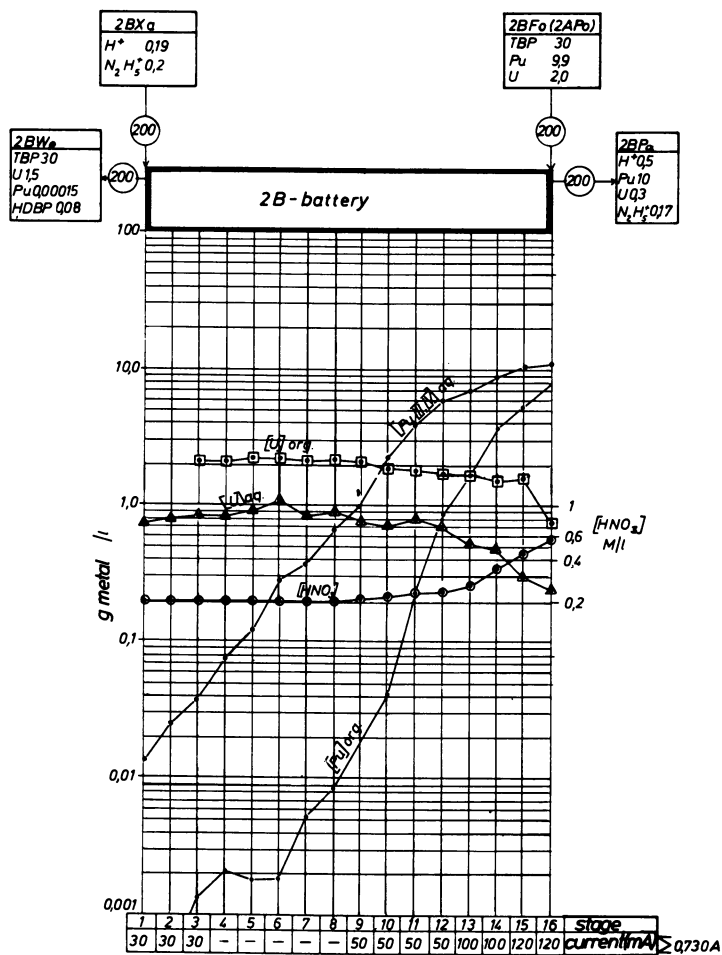
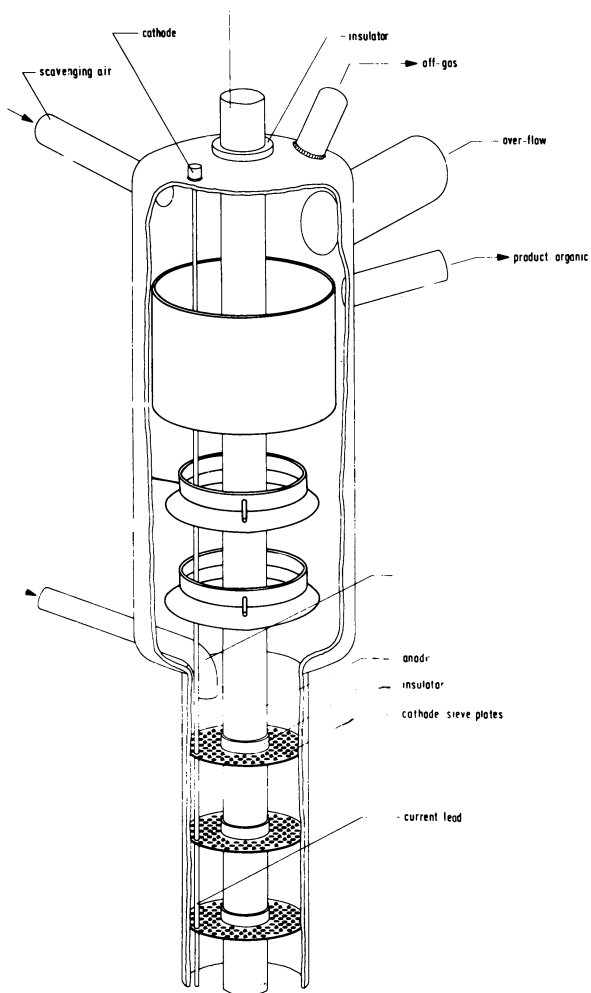


Figure 3. Pu backextraction (Experiment no. 18); concentration profile in the 16-stage electroreduction mixer settler, MILLI-EMMA (8); concentrations and flows, see Figure 2.



Verlag Karl Thieme

Figure 4. Pulsed extraction column for in-situ electroreduction (16)

are installed in the top decanter in order to remove entrained continuous aqueous phase and to separate the electrode gas generated in the column.

Extraction tests with U showed that the extraction efficiency is very little affected by internal electrodes. For example an HTS value of 0,8 m was obtained for the U extraction. This value is similar to that of normal pulsed columns of these dimensions.

The conversion rate of about 1,3 g U(IV) per Ah, calculated by means of the column concentration profile, hold-up and operating current corresponds to the value found for the electro-reduction mixer settler.

Figure 5 shows a comparison of U(IV) concentration profiles realized experimentally for the mixer settler and the pulsed column. The U(IV) profile in the columns shows an inventory of about a tenfold stoichiometric excess for the aqueous phase, relative to the Pu profile to be expected from LWR fuel. The U(IV) production rate in the column can easily be increased to an extent higher than the feed rates of externally produced U(IV) normally required in the conventional reduction column. Therefore one can at least expect equally good results for the U/Pu separation with the electro-reduction column as with the normal procedures. This is also confirmed by experiments in the USA which resulted in the installation of an electro-reduction column in the AGNS Plant at Barnwell. In these experiments even with high acid concentrations (2 M HNO₃ in the aqueous strip, BXS) high plutonium decontamination factors have been achieved (17).

At the present time the titanium column shown in figure 4 is installed in a Pu-test cycle at Karlsruhe with a throughput of about 400 g Pu/h, where the electro-reductive Pu backextraction can be tested and compared with the competitive procedure using hydroxylamine nitrate (HAN) as reducing agent.

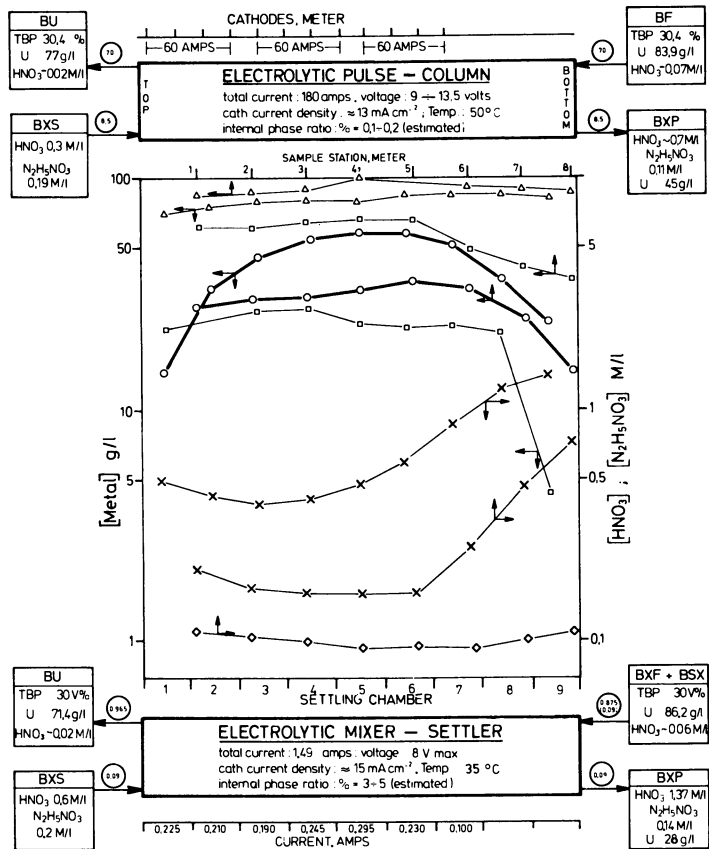
Electro-oxidation of the Pu(III) Product (8,16)

After each extraction cycle, the Pu(III) product solution has to be oxidized to the extractable Pu(IV). At the same time the hydrazine stabilizer has to be destroyed.

This process step is carried out in existing facilities by sodium nitrite or by NO₂ gas as oxidizing agent. NaNO₂ gives rise to sodium salts in the waste. NO₂ is needed in great stoichiometric excess due to low reaction efficiency. Since nitrite is quite extractable in the organic phase it has to be removed by purging with air prior to each extraction. The desorption produces a gaseous NO_x effluent loaded with α/β aerosoles.

This oxidation step can also be made by electro-oxidation at the anode without additional chemicals and waste production.

Equations 3 and 4 show that hydrazine is oxidized at the anode prior to Pu(III). Equation 6 is a possible side reaction increasing the efficiency for the hydrazine destruction.



Verlag Karl Thiemeig

Figure 5. Concentration profiles in the electroreduction column and the electroreduction mixer settler (16): (Δ) $[U]_{org}$; (\square) $[U(VI)]_{org}$; (\circ) $[U(IV)]_{aq}$; (\times) $[HNO_3]_{aq}$; (\diamond) $[N_2H_5NO_3]$.

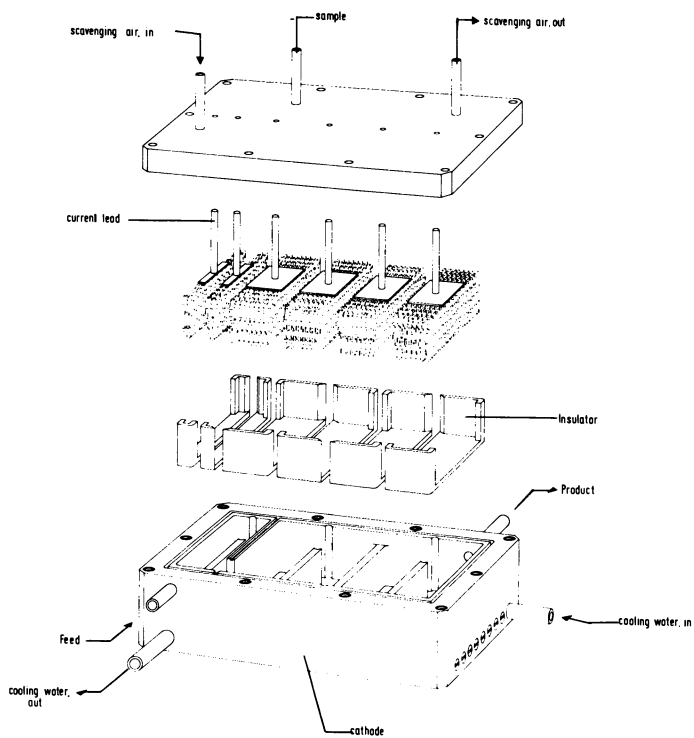


Figure 6. Electrooxidation cell (8, 16)

For technical purposes the oxidation cell is divided into a hydrazine destruction part and a Pu oxidation part. For the hydrazine oxidation high anodic current densities are applied. The reaction is following formally a zero order law. In the second part, at lower current densities only Pu(IV) is produced in the hydrazine-free electrolyte. Furthermore the production of Pu(VI) can be avoided by increasing the nitric acid concentration ($\geq 1,0$ M HNO_3) (18).

Figure 6 shows schematically a flat titanium cell with four parallel channels. The anodes are made of platinized tantalum nets and are isolated from the cathode by ceramic plates.

Together with the long-running test of the electro-reduction mixer settler, an electro-oxidation cell at a Pu throughput of 1,5 kg per day was operated over 6 weeks without any interruption (15). The average feed concentrations were 0,1 to 0,15 M $\text{N}_2\text{H}_5\text{NO}_3$ and 25 to 45 g Pu(III) per liter. The average energy requirement was 38 Ah/l. The design principles correspond to that of figure 6. The cell is now installed in the 2nd Pu cycle of WAK Plant directly after the electro-reduction mixer settler.

Further Development Steps

To prove the suitability of the electro-redox methods for the industrial application the electrode behaviour e.g. with respect to corrosion or coating by impurities has to be investigated in long-running tests under real process conditions. This is the aim of the tests in the WAK Plant.

A Pu test cycle (PUTE) in KfK Karlsruhe will give the possibility to test electrolytical pulsed columns in technical scale and design. The construction will be finished in 1979.

In parallel a full scale electro-reduction column will be installed in an U test cycle for 4 tons of U per day in KfK and set in operation by the German industry.

Literature cited

1. Progress in Nuclear Energy, Ser. III, Process Chemistry, Vol. 4, p. 82, Pergamon Press, 1970
2. Caracciolo, V.P., Kishbaugh, A.A., USAEC-Report, DP-896, 1964
3. Kerr, W.B., Lakey, L.T., Denney, R.G., USAEC-Report, IDO-14643, 1965
4. Bjorklund, W.J., USAEC-Report, ICP-1028, 1974
5. Schlea, C.S., USAEC-Report, DP-808, 1963
6. Newman, R.I., Nuclear Engineering International, p. 938/941, Nov. 1972
7. Baumgärtner, F., Schwind, E., Schlosser, P., Deutsches Pat. Nr. OS 1965519 (6.8.1970), US Pat. 3730851
8. Schmieder, H., Baumgärtner, F., Goldacker, H., Hausberger, H., Gesellschaft für Kernforschung Karlsruhe, Report KfK 2082, 1974

9. Vetter, K.J., *Elektrochemische Kinetik*, Springer Verlag, 1961, S. 409/910
10. Kolthoff, I.M., Harris, W.E., *J. Am. Chem. Soc.* 68, 1175 (1946)
11. Pitzer, E.C., USAEC-Report KAPL 653, Dec. 1951
12. Hartland, S., Spencer, A.J.M., *Trans. Inst. Chem. Engrs.* 41 (1963), p. 328/335
13. Chemical Engineering Division, ANL, Summary Report July, August, Sept. 1953, USAEC-Report ANL-5169
14. Warnecke, E., Dissertation, Universität Heidelberg, 1975
15. in preparation, H. Schmieder, Goldacker, H., Finsterwalder, L., Hausberger, H., Kernforschungszentrum Karlsruhe
16. Schmieder, H., Huppert, K.C., Goldacker, H., in "Chemie der Nuklearen Entsorgung", von F. Baumgärtner, Verlag Karl Thieme, München (1978), Part II, p. 50-87
17. Cermak, A.E., Gray, J.H., Murbach, E.W., Neace, J.C., Spaunburgh, R.G., Proc. of the American Nuclear Soc. Topical Meeting, March 1978, Savannah Georgia p. V-11
18. Schmieder, H., Goldacker, H., Interner Bericht Kernforschungszentrum Karlsruhe, 1975
19. Kolthoff, I.M., Harris, W.E., *J. Am. Chem. Soc.* 68, 1175 (1946)
20. McDuffie, B., Reilley, C.N., *Anal. Chem.* 38, 1881 (1966)

RECEIVED May 11, 1979.

The Separation of Uranium and Plutonium by Electrolytic Reduction in the Purex Process

HE JIAN-YU, ZHANG QING-XUAN, and LO LONG-JUN

Institute of Atomic Energy, Academic Sinica, Beijing, People's Republic of China

In the partitioning of U and Pu in the first cycle of the purex solvent extraction process for reprocessing spent nuclear fuel from production reactors, ferrous sulfamate is still being used as the reducing agent for Pu(IV). Its use seriously impairs the economy in the treatment of medium active waste because of the introduction of scale-forming and corrosive ions to the effluent. This drawback is more serious in the reprocessing of spent fuel from power reactor, where the Pu-content would be so high that a tenfold increase in the amount of undesirable salts introduced to the process stream would result.

Therefore, many alternatives for the ferrous sulfamate reduction method have been studied(1,2,3); besides, the use of U(IV) as the reductant has actually found some practical application. Since U(IV) is being prepared by means of electrolytic reduction of U(VI), it is natural to go a step further, namely, to introduce electrolytic reduction to the process stream itself. In such an in-situ electrolytic process, not only P(IV) would be expected to be directly reducible to Pu(III), but any U(IV) formed would also be expected to serve as the reductant for Pu(IV).

In fact, such a method has been investigated and developed both in the Federal Republic of Germany(4,5) and in the United States(6,7). This process has also been studied in the People's Republic of China for some time and here are presented some of our experimental results.

DETERMINATION OF CURRENT-POTENTIAL CURVES

In order to help selecting a suitable current or potential for controlling the course of electrolysis, current-potential curves for solutions containing one or more constituents of the substances present in the 1B battery were determined, with no stirring in the cell. The solution of Pu(IV) was prepared from its stock containing 3M/L HNO₃. Results on Pt-cathode were shown in Fig.1 and 2, those on Ti-cathode shown in Fig.3, from

0-8412-0527-2/80/47-117-317\$05.00/0

© 1980 American Chemical Society

In Actinide Separations; Navratil, J., et al.;

ACS Symposium Series; American Chemical Society: Washington, DC, 1980.

Figure 1. Current-potential curves for Pt cathode: $S_{Pt} = 0.28 \text{ cm}^2$; $V = 20 \text{ mL}$; (○) 1.6M HNO_3 , 10 mg/mL Pu (IV); (△) 1.6M HNO_3 , 10 mg/mL Pu (IV), 70 mg/mL U (VI).

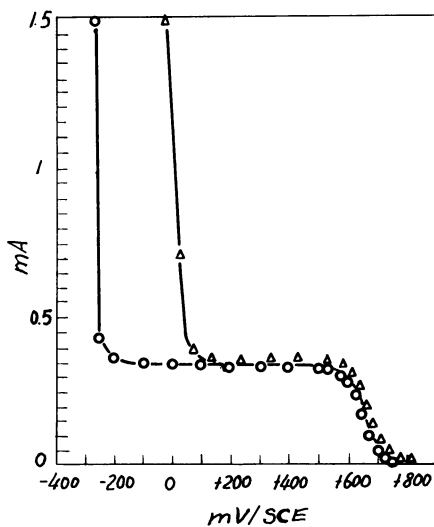
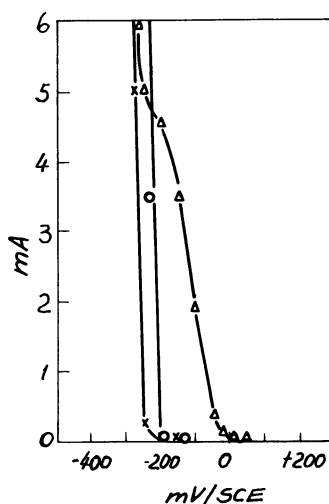


Figure 2. Current-potential curves for Pt cathode: $S_{Pt} = 0.28 \text{ cm}^2$; $V = 40 \text{ mL}$; (○) 1.6M HNO_3 ; (×) 1.6M HNO_3 , 0.2M N_2H_5^+ ; (△) 1.6M HNO_3 , 0.2M N_2H_5^+ , 70 mg/mL U (VI).



which the following observations could be made:

1. The overpotentials of U(VI)-U(IV), Pu(IV)-Pu(III) and hydrogen on the Ti-cathode are larger than those on the Pt-cathode, especially for the Pu(IV)-Pu(III) couple. A diffusion-controlled region is clearly indicated by the S-shaped curve of the Pu(IV)-Pu(III) couple.

2. The difference between the overpotential for U(VI)-U(IV) and that for hydrogen is small on the Pt-cathode as well as on the Ti-cathode. Therefore the reduction of U(VI), which is desirable because the U(IV) formed will serve to reduce Pu(IV), would cause an unavoidable evolution of hydrogen.

Ti was chosen as the cathode material for all of the following experiments except when otherwise indicated. This material is much cheaper than Pt and, when properly pretreated, has an electrolytic property good enough for our purpose.

ELECTROLYTIC REDUCTION IN THE MONOCELL WITH A DIAPHRAGM IN THE AQUEOUS PHASE

The monocell consists of two compartments separated by a sintered-glass diaphragm, with Ti wire screen as the cathode and Pt coil as the anode. All experiments with this monocell were carried out with stirring at constant cathode potential.

NITRIC ACID REDUCTION. As is well known, HNO_2 is detrimental to the reduction of Pu(IV), because it could reoxidize the Pu(III) and this reduction is autocatalytic as indicated by the following reactions:



So it would be of interest to study the reduction of HNO_3 under the conditions employed for the electrolytic reduction of Pu(IV).

The formal potential for the Pu(IV)-Pu(III) couple is 0.93 V/SHE in 1N HNO_3 while the potential of NO_3^- - NO_2^- couple is 0.94 V/SHE. Theoretically, therefore, the reduction of HNO_3 simultaneously with the reduction of Pu(IV) is to be expected.

However, there have been different opinions about the mechanism for reduction of HNO_3 on the cathode. Ellingham(8) suggested that HNO_3 could be reduced by active hydrogen atom generated on the cathode and HNO_2 has catalytic action for the reduction of HNO_3 . Most other authors(9,10,11) think that in the absence of HNO_2 , nitric acid could not be reduced electrically. Krumpelt and others(7) did electrolytic reduction experiments with 0.5 M/L HNO_3 in the presence and absence of hydrazine and found that HNO_3 could not be reduced.

We have conducted a series of electrolytic reduction expe-

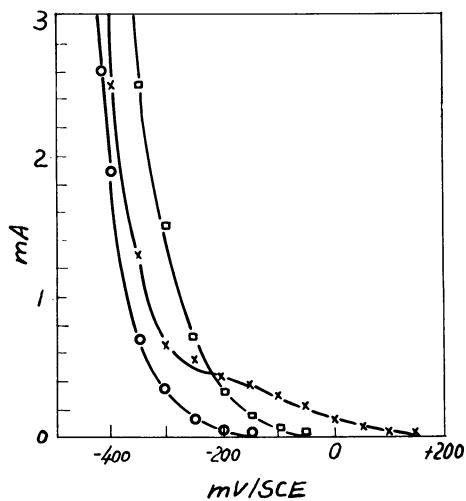


Figure 3. Current-potential curves for Ti cathode: $S_{Ti} = 0.28 \text{ cm}^2$; $V = 20 \text{ mL}$; (○) 1.6 M HNO_3 ; (×) 1.6 M HNO_3 , 10 mg/mL Pu (IV) ; (□) 1.6 M HNO_3 , 70 mg/mL U (VI) .

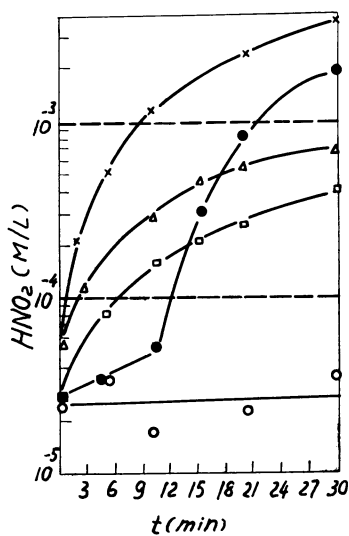


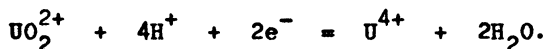
Figure 4. Electrolytic reduction of HNO_3 ; $S_{Ti} = 36 \text{ cm}^2$; $V = 20 \text{ mL}$; $E = 400 \text{ mV/SCE}$; with stirring; (○) 0.47 M HNO_3 ; (□) 0.98 M HNO_3 ; (△) 1.52 M HNO_3 ; (×) 2.0 M HNO_3 ; (●) 2.0 M HNO_3 , $2.8 \times 10^{-4} \text{ M N}_2\text{H}_5^+$.

periments with HNO_3 solutions of 0.5 M/L to 2 M/L which contains an initial HNO_2 concentration of around 10^{-4} - 10^{-5} M/L. The results, as shown by Fig.4, indicated that, whereas HNO_3 is difficult to reduce at 0.5 M/L, its reduction becomes more and more easy as its concentration goes from 1 M/L to 2 M/L. Besides, for the 2 M/L HNO_3 in the presence of hydrazine, the rate of formation of HNO_2 , while being depressed at the beginning of the electrolysis, rises sharply after a while. This last experiment also proves that on Ti-cathode HNO_3 could be reduced to HNO_2 even when there is no HNO_2 present in the initial HNO_3 solution.

Therefore, for the separation of Pu and U by electrolytic reduction in HNO_3 solutions (as being practised in the Purex Process), enough hydrazine should be added as the supporting reducing agent.

ELECTROLYTIC REDUCTION OF U(VI). Since U(VI) in the form of UO_2^{2+} is present in large amount in the 1B battery in the first cycle of the purex process, its successful electrolytic reduction to U(IV) would create a most favorable condition for the reduction of Pu(IV).

Both Heal(12) and Finlayson(13) have shown that H^+ ion is involved in the electrolytic reduction of U(VI) to U(IV) as summarized by the following reaction:



The object of our work is to measure the rate of reduction of UO_2^{2+} as a function of typical operating parameters such as the applied cathode potential, HNO_3 concentration and the amount of hydrazine added.

As shown in Fig.5 and Fig.6, the reduction rate of U(VI) increases with increasing applied cathode potential and HNO_3 concentration. Fig.7 indicated that the addition of hydrazine effectively promotes the rate of reduction of U(VI) but this effect becomes very small beyond 0.1 M/L hydrazine.

We have decided to add 0.2 M/L hydrazine in our experiments for the reduction of Pu(IV) to make sure that the detrimental effect of HNO_2 could be counteracted.

ELECTROLYTIC REDUCTION OF Pu(IV). Cohen(14) had studied systematically the electrolytic oxidation and reduction of Pu. His results showed that the overpotentials of Pu(IV)-Pu(III) and Pu(VI)-Pu(V) couples are low, but it is high for Pu(V)-Pu(IV) on Pt electrode. Our experiments showed that the overpotential of Pu(IV)-Pu(III) on Ti-electrode is also high. However, in the partitioning step of the first cycle in the purex process, the large excess of U present would be expected to be beneficial for the reduction of Pu(IV).

In our work, the effect of acidity and U-content on the

Figure 5. Electrolytic reduction of U (VI) as a function of cathode potential: $S_{Ti} = 20 \text{ cm}^2$; $V = 20 \text{ mL}$; with stirring; composition: 1M HNO_3 , $0.2\text{M N}_2\text{H}_5^+$, 70 mg/mL U (VI) ; (\circ) $E = -300 \text{ mV/SCE}$; (\triangle) $E = -500 \text{ mV/SCE}$; (∇) $E = -600 \text{ mV/SCE}$; (\times) $E = -700 \text{ mV/SCE}$; (\bullet) $E = -1000 \text{ mV/SCE}$.

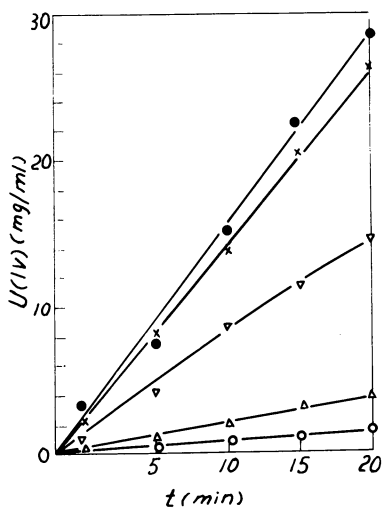


Figure 6. Electrolytic reduction of U (VI) as a function of nitric acid concentration: $S_{Ti} = 20 \text{ cm}^2$; $V = 10 \text{ mL}$; with stirring; $E = -700 \text{ mV/SCE}$; (\square) 0.5M HNO_3 ; (\triangle) 1.0M HNO_3 ; (\times) 1.5M HNO_3 .

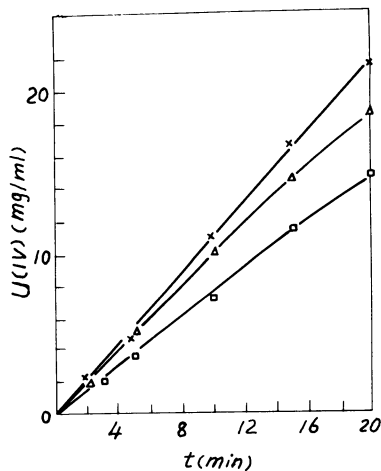
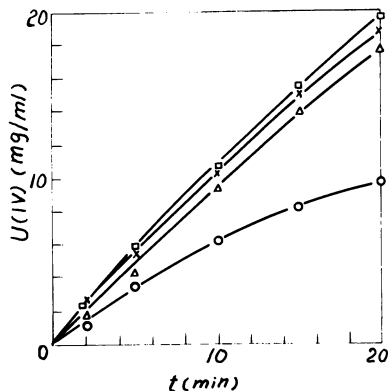


Figure 7. Electrolytic reduction of U (VI) as a function of N_2H_5^+ concentration; $S_{Ti} = 20 \text{ cm}^2$; $V = 10 \text{ mL}$; $E = -700 \text{ mV/SCE}$; with stirring; (\circ) 1M HNO_3 , 70 mg/mL U (VI) , $0\text{M N}_2\text{H}_5^+$; (\triangle) 1M HNO_3 , 70 mg/mL U (VI) , $0.05\text{M N}_2\text{H}_5^+$; (\times) 1M HNO_3 , 70 mg/mL U (VI) , $0.1\text{M N}_2\text{H}_5^+$; (\square) 1M HNO_3 , 70 mg/mL U (VI) , $0.5\text{M N}_2\text{H}_5^+$.



Pu(IV) reduction rate were studied. Fig.8 shows that at large excess of U and low concentration of Pu, no effect of acid concentration on Pu(IV) reduction rate could be observed. After a period of electrolysis of less than 30 seconds, nearly all of the Pu(IV) could be converted to Pu(III). This fact corresponds to the change of the potential of the electrolyte solution with time, which drops very rapidly after the start of the electrolysis. The effect of U-concentration on the reduction rate of Pu(IV) is shown in Fig.9, from which it is clearly shown that the reduction rate of Pu(IV) depends very much on the amount of U relative to that of Pu in the electrolyte solution. The upper two curves showed that if the weight ratio of U/Pu is near or more than one, the reduction rate of Pu(IV) could be greatly accelerated. This fact indicates clearly that here U(IV) plays an important role in the reduction of Pu(IV). On the other hand, if the U-content in the solution is small compared to that of Pu, the rate of reduction of Pu(IV) is determined chiefly by the electrolytic reduction of Pu(IV) itself which is rather slow. This fact should be borne in mind in designing electrolytic reduction equipments in the purex process.

ELECTROLYTIC REDUCTION OF U(VI) IN A MONOCELL WITHOUT A DIAPHRAGM

Schmieder(5) said that in the presence of hydrazine in a common cathode-anode space, there happens only the formation of U(IV) on the cathode without any reoxidation of it on the anode until the course of electrolysis reaches the stage of oxygen evolution on the anode. He said that this is due to the fact that oxidation of U(IV) has a high overpotential on the anode. Then it should be possible to construct an electrolytic reduction apparatus without a diaphragm.

We have conducted several experiments in such a set-up and the results were shown in Fig.10. From this figure it could be seen that after 30 minutes of electrolysis, appreciable amount of U(IV) is formed even when the area of anode is larger than that of cathode and the hydrazine remaining in the cell is 70% of the initial amount added.

In Fig.11 the current-potential curves of $N_2H_5^+$, U^{4+} and HNO_3 on Pt-anode are represented. It could be seen that for the curve of U(IV) oxidation, there appear two waves, the first representing U(IV) oxidation and the second having not yet been identified. Fig.12 shows the oxidation of U(IV) in HNO_3 acid solution in the presence of large excess of hydrazine. The results of these experiments indicate that U^{4+} and hydrazine could be simultaneously oxidized on the Pt-electrode before oxygen evolution.

ELECTROLYTIC REDUCTION IN A MILLI TYPE MIXER-SETTLER FOR THE SEPARATION OF U AND Pu

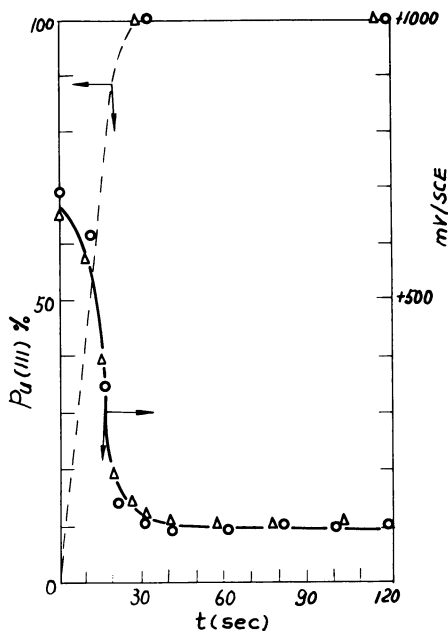


Figure 8. Electrolytic Pu (IV) reduction as a function of nitric acid concentration at low Pu (IV) concentration: $S_{Ti} = 20 \text{ cm}^2$; $V = 10 \text{ mL}$; $E = -700 \text{ mV/SCE}$; (○) 0.5 M HNO_3 , $0.56 \text{ mg/mL Pu (IV)}$, 70 mg/mL U (VI) ; (△) 1 M HNO_3 , $0.56 \text{ mg/mL Pu (IV)}$, 70 mg/mL U (VI) .

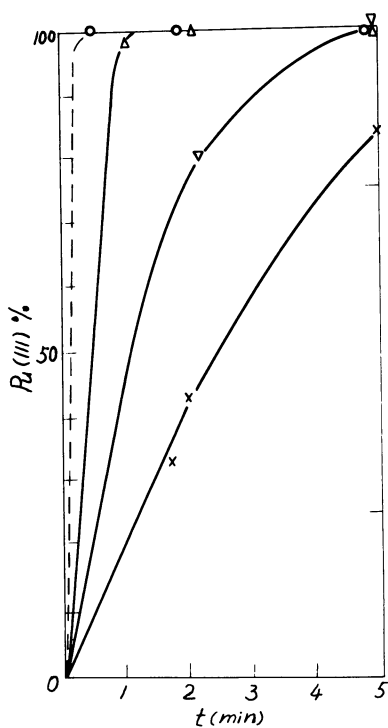


Figure 9. Electrolytic Pu (IV) reduction as a function of U (VI) concentration: $S_{Ti} = 20 \text{ cm}^2$; $V = 10 \text{ mL}$; $E = -700 \text{ mV/SCE}$; with stirring; (○) 1 M HNO_3 , $0.2 \text{ M N}_2\text{H}_5^+$, 70 mg/mL U (VI) , $0.56 \text{ mg/mL Pu (IV)}$; (△) 1 M HNO_3 , $0.2 \text{ M N}_2\text{H}_5^+$, $0.06 \text{ mg/mL U (VI)}$, $0.1 \text{ mg/mL Pu (IV)}$; (▽) 1 M HNO_3 , $0.2 \text{ M N}_2\text{H}_5^+$, $0.06 \text{ mg/mL U (VI)}$, 1 mg/mL Pu (IV) ; (×) 1 M HNO_3 , $0.2 \text{ M N}_2\text{H}_5^+$, $0.06 \text{ mg/mL U (VI)}$, 8 mg/mL Pu (IV) .

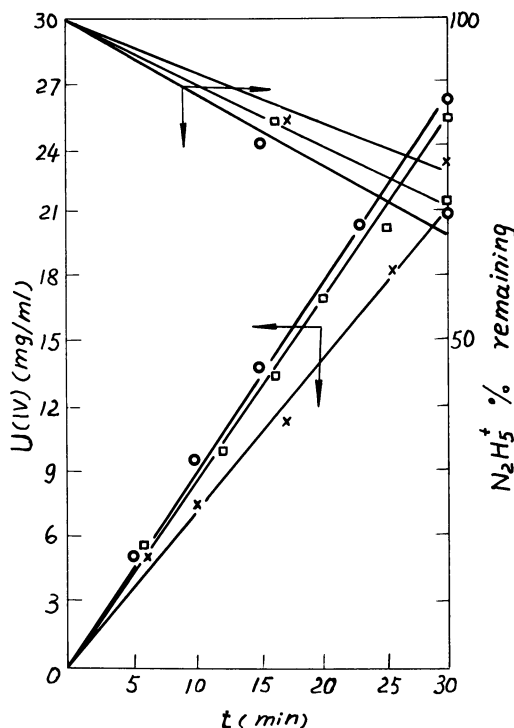


Figure 10. Electrolytic reduction of U (VI) as a function of ratio of anode and cathode area in common space: $S_{Pt} = 22 \text{ cm}^2$ (cathode area); $V = 40 \text{ mL}$; $E = -350 \text{ mV/SCE}$; with stirring; composition: 1.5M HNO_3 , $0.2\text{M N}_2\text{H}_5^+$, 70 mg/mL U (VI) ; (O) $R = 2$, $i = 440 \text{ mA}$; (□) $R = 1$, $i = 420 \text{ mA}$; (X) $R = .2$, $i = 400 \text{ mA}$; $R = S_{anode}/S_{cathode}$.

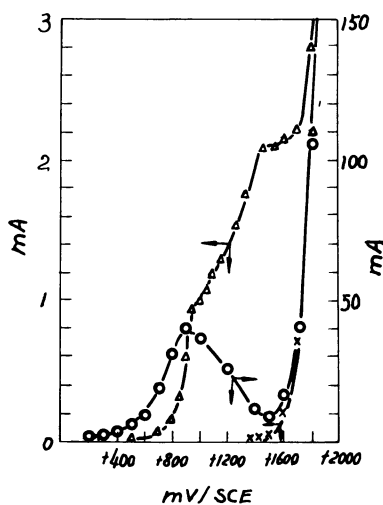


Figure 11. Current-potential curves for Pt anode: $S_{Pt} = 0.28 \text{ cm}^2$; $V = 30 \text{ mL}$; (X) 2M HNO_3 ; (O) 1.5M HNO_3 , $0.2\text{M N}_2\text{H}_5^+$; (Δ) 1M HNO_3 , 24 mg/mL U (IV) ; $95\% \text{ U (IV)}$.

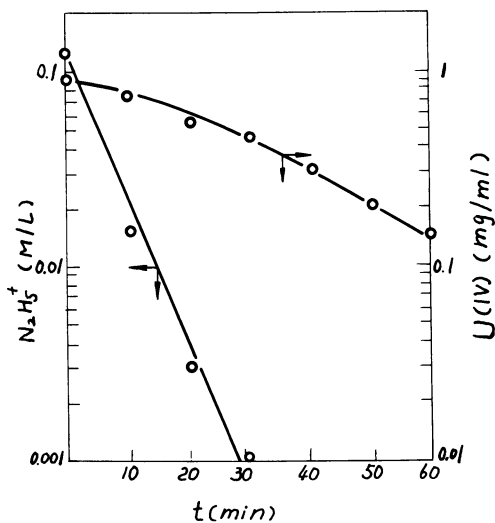


Figure 12. Cycle electrolytic oxidation of $N_2H_5^+-U(IV)$ solution: $S_{Pt} = 280 \text{ cm}^2$; $V = 55 \text{ mL}$; $E_{anode} = +900 \text{ mV/SCE}$; throughput, 10 mL/min .

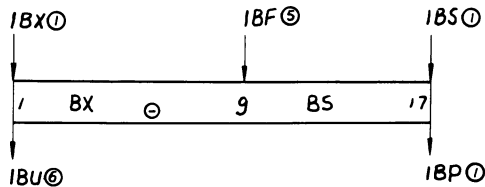


Figure 13. Flowsheet for partitioning of U and Pu: (\oplus) electrolytic part, (\odot) flow ratio.

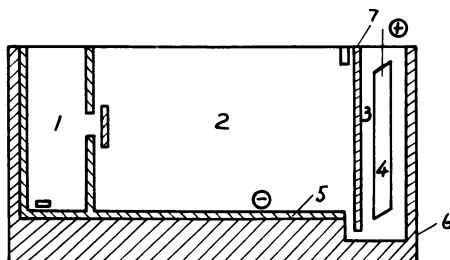


Figure 14. Schematic of electrolytic mixer settler: 1, mixing chamber; 2, settling chamber; 3, anode cell; 4, Pt anode; 5, Ti cathode plate; 6, insulator; 7, separator.

The construction of the Milli-type counter-current mixer-settler extraction equipment is similar to that employed in the Federal Republic of Germany. A flow diagram and a sketch of the cell construction used in our experiments are shown in Fig.13 and Fig.14. In the apparatus there are 17 stages, 9 of which for extraction(the BX part) and the remaining ones for organic washing(the BS part). The housing of the mixer-settler itself serves as the cathode which is made of Ti-metal. Pt-wire wrapped on a hollow insulated plate serves as the anode. The volume is about 8.4cm^3 for each mixing chamber and 25.2cm^3 for each settling chamber. Residence time of more than one minute is maintained in each mixing chamber and air pulse is used for mixing the organic and aqueous phases. The throughput of organic feed solution is 5ml per minute and the flow ratio of feed solution 1BF to aqueous extraction stream 1BX and to organic wash stream 1BS is 5/1/1. Reduction is carried out mainly in the settling chamber and constant current is used for controlling the electrolytic process. Operation of the mixer-settler has been found satisfactory, U and Pu products achieve acceptable level of quality.

Data and results of the experiments are given in table I and the concentration profile in the mixer-settler shown in Fig.15. From these the following points could be noted:

1. The acid concentration profile in the mixer-settler plays an important role for removing U from Pu. With the proper current strength satisfactory results could be achieved when the concentration of HNO_3 in the Pu product ranges from 1.4 M/L to 2 M/L. Increasing the acid concentration by acidifying the organic wash stream and increasing HNO_3 in 1BF in the BS part could increase the SF_{Pu} substantially, as shown by comparing the results of experiments No. 2 and 3. The effect of acid concentration in the BX part on SF_{Pu} is not so important, as could be seen by comparing the results of experiments No. 2 to 4, where a change in the acid concentration of the BX part gives almost the same SF_{Pu} .

2. It seems that current density plays a definite role for obtaining a good separation of U and Pu. As shown in table I, low values of SF_{Pu} are obtained in experiments No. 1 and 6, for which the current strength is 10 to 30% lower than that used in experiments 2 through 5, for which high values of SF_{Pu} (10^4) are obtained.

3. The influence of radiolytic decomposition product dibutyl phosphate, which could form a strong complex with Pu(IV), has been examined in experiments 5 and 6. In each case 9×10^{-4} more per liter of HDBP has been added to the organic feed solution. No significant difference could be seen, when a current strength of 100mA is used. Experiment No.6 gives a somewhat lower value of SF_{Pu} but here a lower current strength, namely, 90mA has been used.

To summarize, under the conditions of our experiments, sa-

Table I. Results of U and Pu Separation in the Mixer-settler

No.	g. H ₂ O + g. HNO ₃	1BP			1BX			1BS		1BU			1BP			SP Pu x 10 ³	SP U x 10 ³	SP Pu x 10 ³	η %	Cur- rent mA
		U mg/ml	Pu mg/ml	HNO ₃ M/L	HNO ₃ M/L	HNO ₃ M/L	HNO ₃ M/L	HNO ₃ M/L	U mg/ml	Pu μg/ml	Pu μg/ml	HNO ₃ M/L	U mg/ml	Pu mg/ml	U mg/ml					
1	12	90.0	0.303	0.20	0.43	0.20	0.33	0.06	64.0	1.07	1.71	0.1	1.58	≥5	0.2	15.0	70			
2	16	84.6	0.343	0.24	0.49	0.18	0.52	0.04	72.0	0.008	2.00	0.03	1.38	11	36	9.3	100			
3	16	88.5	0.307	0.17	0.49	0.18	0.52	0.04	71.0	0.009	1.70	0.24	1.60	1.9	28	10.8	100			
4	15	87.4	0.277	0.18	0.61	0.21	0.46	0.04	82.1	0.007	1.78	0.10	1.27	4.0	37	8.6	100			
**5	15	91.4	0.312	0.18	0.47	0.22	0.51	0.05	80.5	0.024	1.42	0.19	1.42	2.2	11	9.6	100			
**6	14	91.4	0.312	0.18	0.47	0.22	0.51	0.04	68.8	0.037	1.42	0.35	1.24	1.0	6.4	9.3	90			

1BP throughput: 5ml/min.; flow ratio: 1BP/1BX/1BS=5/1/1.

* Current efficiency based on Pu. ** 9x10⁻⁴M/L HDBP added.

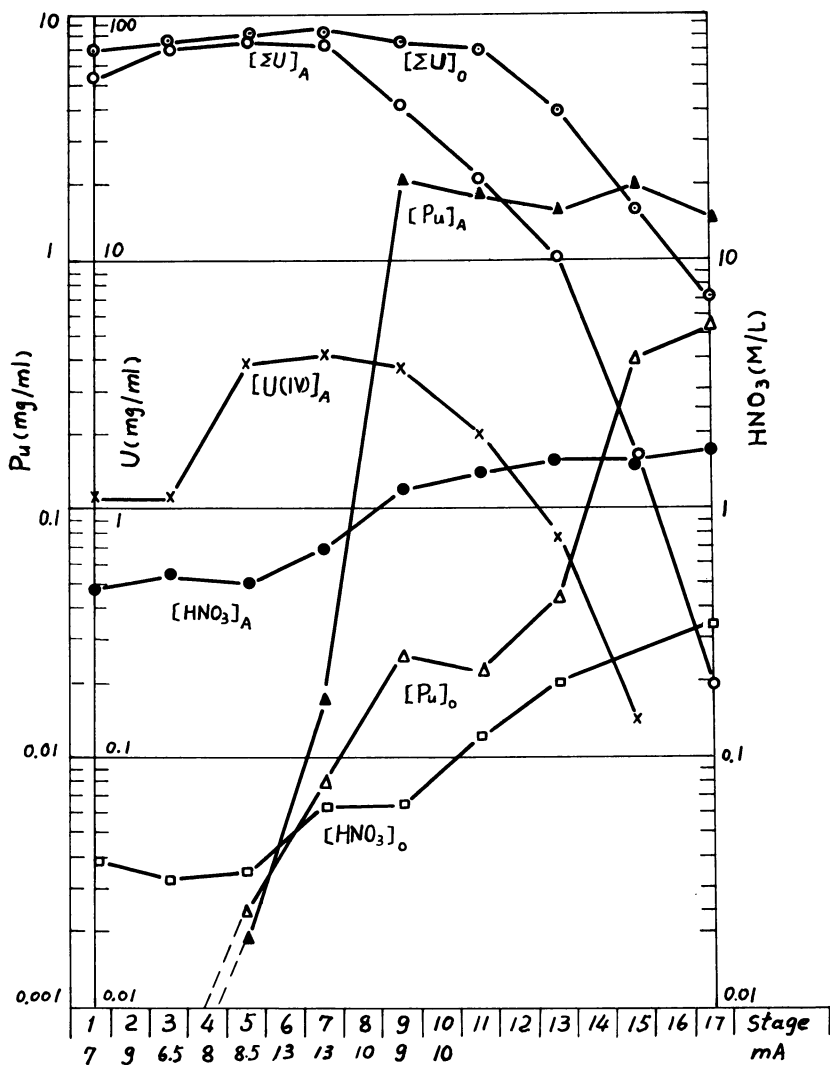


Figure 15. Concentration profile in the mixer settler: O, organic phase; A, aqueous phase.

tisfactory results have been obtained for the separation of U and Pu by means of electrolytic reduction.

SUMMARY

Experiments on the electrolytic reduction of U and Pu in the aqueous phase in presence of hydrazine were carried out to investigate the effect of various factors influencing the rate of reduction. The potentials of the aqueous solution, which can serve to indicate the course of the reduction process, were measured and operating parameters such as acid concentration, hydrazine concentration, applied potential on the cathode, etc., were investigated. Experimental results indicated that, on Ti-cathode nitric acid could be reduced to nitrous even when there is no HNO_2 in the initial HNO_3 solution; and, with a U/Pu ratio ranging from 10^{-2} to 10^2 , Pu(IV) can be reduced readily when the U/Pu ratio is near or more than 1 at low concentration of Pu. In this case, obviously U(IV) formed in the process plays an important role in the reduction of Pu(IV).

To investigate the feasibility for applying this method in the partitioning of U and Pu in the first cycle of the purex process, electrolytic reduction experiments have been carried out in a Milli-type mixer-settler counter-current extraction apparatus, with the first 9 stages serving as the electrolysis cells and the remaining ones for the back washing of uranium. With a flow rate of 1BF/1BX/1BS of 5/1/1, a separation factor SF_u varying from 10^3 to 10^4 was obtained, depending on the current density as well as the acid concentration in the BS part of the battery 1B. The organic wash stream was acidified to increase the acid concentration in the BS part so as to obtain a high SF_u . Under the conditions employed in our experiments satisfactory results for the separation on U and Pu have been obtained.

ACKNOWLEDGEMENT

The authors are indebted to prof. Wang De-Xi for consultation and advice during the work.

Li Zhao-Yi, Jiang Dong-Liang, Tian Bao-Sheng, Zhu Zhu-Zhong, Zhang Jia-Jiun, Zhan Yi-Zhu and Wu De-Zhu also took part in this work.

REFERENCES

1. Mckibben, J. M.; Bercaw, J. E. DP-1248, 1970.
2. Richardson, G. L. HEDL-TME-75-31, 1975.
3. Goldstein, M. AEC-BNL-22443, 1976.
4. Koch,; Ochsenfeld, W.; Schwind, E. KFK-990, 1969.
5. Schmieder, H.; Baumgartner, F.; Goldacker, H.; Hausberger, H. ORNL-tr-2999; Report KFK-2082, 1975.

6. Krumpelt, M.; Heiberger, J.; Steindler, M. J. ANL-7799, 1971.
7. Krumpelt, M.; Heiberger, J.; Steindler, M. J. ANL-7871, 1972.
8. Ellingham, H. J. T. J. Chem. Soc., 1932, 1565.
9. Miroljubov, E. N. J. Appl. Chem. (Russian), 1962, 35, 132.
10. Schmidt, G.; Bunsenges, B. J. Phys. Chem., 1961, 65, 531.
Schmidt, G.; Krichel, G., *ibid.*, 1964, 68, 531.
11. Vetter, K. J. "Electrochemical Kinetics"; Academic Press, New York, 1967, p.493.
12. Heal, H. G. Trans. Faraday Soc., 1949, 45, 1.
13. Finlanyson, M. B.; Mowat, J. A. Electrochem. Tech., 1965, 3, 148.
14. Cohen, D. J. Inorg. Nucl. Chem., 1961, 18, 207.

RECEIVED July 10, 1979.

Studies on Actinides Separation in JAERI

TOMITARO ISHIMORI

Japan Atomic Energy Research Institute, 1-1, Shinbashi, Minato-ku, Tokyo 105

The separation of actinides has been studied for various purposes in Japan Atomic Energy Research Institute (JAERI). The works which have been carried out so far, are classified into four categories; preparation studies of actinides nuclides, separation chemistry for chemical analysis, separation of actinides from radioactive waste, and studies on reprocessing of spent nuclear fuels. The present work is to review studies of actinide separation performed in JAERI, emphasizing the need of the separation for the main purpose of individual. Concern is focussed on the separation of transuranium elements and studies on thorium and uranium are put aside.

Preparation of Actinides Nuclides

Since 1958, more than 20 nuclides of actinides ranging from neptunium to einsteinium were identified and prepared for tracer studies. From neutron-irradiated uranium samples ^{239}Np was adjusted to the pentavalent state and separated by TBP extraction from perchloric acid media. Plutonium-239 was separated by TBP extraction from nitric acid solution followed by anion exchange in a system of Dowex-1 resin and nitric acid. Neptunium-237 was separated from a spent fuel solution of JRR-1 (Japan Research Reactor -1) using anion exchange and TBP extraction. The TBP extraction in the hydrochloric acid medium is a simple and effective technique to purify neptunium from plutonium contamination. On the other hand, both anion exchange and solvent extraction with HDEHP could be used to separate tracer scale plutonium from irradiated neptunium targets.

Curium, berkelium, californium and einsteinium were separated from the americium samples irradiated by neutrons. For preliminary separation the anion exchange in hydrochloric acid and lithium chloride solutions was used as well as the HDEHP extraction. Mutual separation of the transamericium elements was made by using DIAION CK08Y cation exchange resin. Nuclides prepared and separation methods adopted are summarized in Table 1 (1-15).

0-8412-0527-2/80/47-117-333\$05.00/0

© 1980 American Chemical Society

Table 1 Preparation of actinides nuclides in JAERI

Nuclide	Reactor/ Accelerator	Formation process/ Source material	Separation techniques	Detection/ Identification	Year	Ref.
^{239}Np	JRR-1	$^{238}\text{U}(n, \gamma) \xrightarrow{\beta^-} ^{239}\text{U} \xrightarrow{\beta^-} ^{239}\text{Np}$	TBP - HClO_4 solvent extraction	γ -ray spectrometry	1959	1
^{239}Pu	JRR-1	$^{238}\text{U}(n, \gamma) \xrightarrow{\beta^-} ^{239}\text{U} \xrightarrow{\beta^-} ^{239}\text{Np} \xrightarrow{\beta^-} ^{239}\text{Pu}$	TBP - HNO_3 solvent extraction (Separation from U and FP) Dowex 1 X-8 - HNO_3 ion-exchange (Pu purification)	α -ray spectrometry	1959	2
^{237}Np		JRR-1 spent fuel	Dowex 1 X-8 - HNO_3 ion-exchange (Extraction of ^{237}Np and ^{239}Pu) TBP - HCl solvent extraction (^{237}Np purification)	α -ray spectrometry	1960	3
^{242}Cm	JRR-1	$^{241}\text{Am}(n, \gamma) \xrightarrow{\beta^-} ^{242}\text{Am} \xrightarrow{\beta^-} ^{242}\text{Cm}$	Dowex 50 X-8 - 2-methyl lactate ion-exchange	α -ray spectrometry, $T_{1/2}$	1962	4
^{238}Np	JRR-1	$^{237}\text{Np}(n, \gamma) \xrightarrow{\beta^-} ^{238}\text{Np}$	TBP - HCl solvent extraction	γ, β, α -rays spectrometry, $T_{1/2}$	1961	5
^{239}Pu		JRR-3 spent fuel	Purex process	Mass spectrometry	1968	6
^{236}Pu	20MW LINAC	$^{237}\text{Np}(\gamma, n) \xrightarrow{\beta^-} ^{236}\text{Np} \xrightarrow{\beta^-} ^{236}\text{Pu}$	Dowex 1 X-8 - HNO_3 ion-exchange	α -ray spectrometry	1970	7

Table 1 (cont'd)

Nuclide	Reactor/ Accelerator	Formation process/ Source material	Separation techniques	Detection/ Identification	Year	Ref.
^{243}Cm	JRR-2	$^{241}\text{Am}(n, \gamma) \xrightarrow{\beta^-} ^{242}\text{Am} \xrightarrow{\beta^-} ^{242}\text{Cm}(n, \gamma) \xrightarrow{\beta^-} ^{243}\text{Cm}$	HDEHP - HNO_3 solvent extraction (Preliminary separation) CK08Y - 2-methyl lactate (Cm purification)	γ -ray spectrometry	1971	8
^{241}Am		Pu tablets	$\sim 7\text{M } \text{HNO}_3$ solution $\xrightarrow{\text{Ca(OH)}_2}$ precipitation $\xrightarrow{\text{HNO}_3, \text{H}_2\text{C}_2\text{O}_4}$ precipitation $\xrightarrow{\text{HNO}_3}$	α -ray spectrometry	1972	9
$^{238}\text{-}^{242}\text{Pu}$	JRR-2	Long irradiated ^{241}Am sample	anion-exchange (Pu, ^{241}Am separation)	Mass spectrometry	1972	10
^{238}Pu	JRR-2	$^{237}\text{Np}(n, \gamma) \xrightarrow{\beta^-} ^{238}\text{Np} \xrightarrow{\beta^-} ^{238}\text{Pu}$	Dowex 1 X-8 - HCl ion-exchange (Preliminary separation) Dowex 1 X-8 - HNO_3 ion-exchange (Pu purification) HDEHP - HNO_3 solvent extraction	α -ray spectrometry	1972	11

Table 1 (cont'd)

Nuclide	Reactor/ Accelerator	Formation process/ Source material	Separation techniques	Detection/ Identification	Year	Ref.
$^{242m, 243}\text{Am}$	JMTR	Long irradiated	Dowex 1 X-8 - HCl, LiCl	Am, Cm: Mass spectrometry	1972~3	12
$^{242\sim 245}\text{Cm}$		^{241}Am sample	ion-exchange (Preliminary separation)	Cf: α -ray spectrometry, SF		
$^{250, 252}\text{Cf}$			CK08Y - 2-methyl lactate			
$^{242\sim 246}\text{Cm}$	JMTR	Long irradiated	Dowex 1 X-8 - HCl, LiCl	Cm: Mass spectrometry	1974	13
^{249}Bk		^{241}Am sample	ion-exchange (Preliminary separation)	Bk: β -ray spectrometry, $T_{1/2}$		
$^{249, 250}\text{Cf}$,			CK08Y - 2-methyl lactate	Cf: α -ray spectrometry		
^{252}Cf			HDEHP - HNO_3 solvent extraction (Bk separation)			
$^{242\sim 247}\text{Cm}$	JRR-2	$^{242\sim 245}\text{Cm}(n, \gamma)^n, ^{242\sim 247}\text{Cm}$	do.	Mass spectrometry	1974	14
^{253}Es	JRR-2	$^{249, 250, 252}\text{Cf}(n, \gamma)^{253}\text{Cf}$ $\beta^- \text{ } ^{253}\text{Es}$	Dowex 1 X-8 - HCl ion-exchange CK08Y - 2-methyl lactate (^{253}Es purification)	α -ray spectrometry	1976	15

Separation for Chemical Analysis

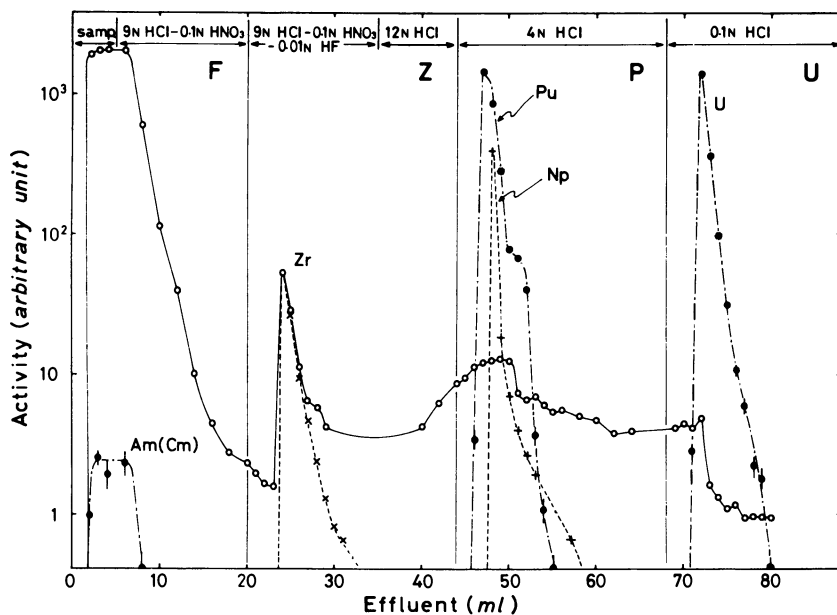
Separation of Actinides from the Samples of Irradiated Nuclear Fuels. For the purpose of chemical measurements of burnup and other parameters such as accumulation of transuranium nuclides in irradiated nuclear fuels, an ion-exchange method has been developed to separate systematically the transuranium elements and some fission products selected for burnup monitors (16). Anion exchange was used in hydrochloric acid media to separate the groups of uranium, of neptunium and plutonium, and of the transplutonium elements. Then, cation and anion exchange are combined and applied to each of those groups for further separation and purification. Uranium, neptunium, plutonium, americium and curium can be separated quantitatively and systematically from a spent fuel specimen, as well as cesium and neodymium fission products.

Figure 1 shows a typical elution curve of the first anion-exchange process for group separation. Plutonium is strongly adsorbed on the anion-exchange resin from hydrochloric acid solutions of concentrations higher than 6 M, in either the tetra- or hexavalent state. The plutonium adsorbed is reduced to the trivalent state in the resin phase, and is loosened and removed from the resin column as the elution with hydrochloric acid solutions proceed. The rate of removal of the plutonium depends on the concentration of hydrochloric acid and also on elution time. Addition of 0.1 M nitric acid into the hydrochloric acid solution is effective in preventing the reduction of plutonium in the resin phase. On the other hand, the presence of nitric acid disturbs the rapid elution of light lanthanide elements due to the formation of complex compound with nitrate ions. After elution with two column volumes of 9 M hydrochloric acid containing 0.1 M nitric acid, about 1 % of cerium still remains in the anion-exchange column, while cesium has been completely eluted. Three column volumes of the eluent are necessary to reduce the loss of cerium to less than 0.1 %.

The presence of nitrate ions in the resin phase also disturbs the elution of plutonium. Washing with concentrated hydrochloric acid in the latter part of the fraction Z is to remove the remaining nitric acid and hydrofluoric acid from the resin.

For the mutual separation of plutonium and neptunium, both of those are adsorbed on an anion-exchange resin column and the resin converted to chloride form by washing with concentrated hydrochloric acid. Then the plutonium is reduced to the trivalent state and eluted with 9 M hydrochloric acid solution containing 0.1 M hydroiodic acid.

Various gel- and porous-type resins have been examined for use in the cation-exchange chromatographic separation of the transplutonium elements from the fission-product lanthanides with an eluent of 11.7 M hydrochloric acid (17). In the case of gel-type resins, very fine ones such as colloidal aggregate, are needed to perform good separation. The number of theoretical plate obtained



Atomic Energy Society of Japan

Figure 1. A typical elution curve of group separation by anion exchange: (○) $\beta(\gamma)$ activity by GM counter; (●) α activity by proportional counter; (×) Zr elution curve by γ spectrometry; (+) Np elution curve by γ spectrometry; volume of resin column, 5 mL (0.7 cm \times 13 cm). (16)

from a given column increases with decreasing cross-linkage of resin, but both the distribution coefficients of relevant ions between the resin and hydrochloric acid and the ratio of the distribution coefficients of the actinides and the lanthanides become smaller.

While those coefficients obtained from the porous-type resins are similar to those from the gel-type ones, the number of theoretical plates increases by a factor of about 3 and the tailing of elution curve decreases remarkably. Three groups, of americium and curium, of yttrium and of europium to cerium, can be well separated with 11.7 *M* hydrochloric acid which is a commercially available chemical reagent, as shown in Figure 2.

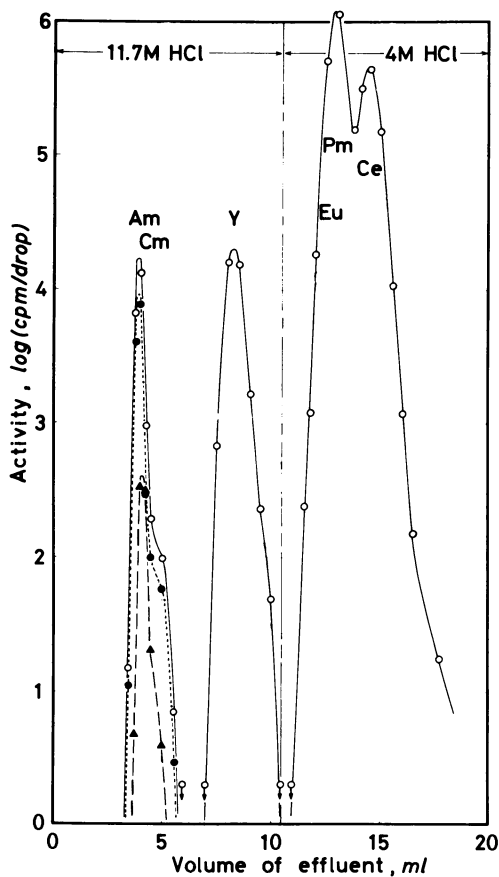
Separation of Plutonium from Air-monitoring Samples. Plutonium-238, ^{239}Pu and ^{240}Pu have been introduced into environment because of the experiments of nuclear explosion in air and of some accidents of the artificial satellites. Analysis of the plutonium is needed to elucidate the distribution of the plutonium in air and the rate of descent to the surface. For this purpose analytical procedures have been developed and utilized for routine measurements of the air-borne plutonium (18).

Air-borne plutonium is collected by passing air continuously through a long strip of filter paper. The filter is composed of 87 % cellulose - 12 % asbestos or 80 % cellulose - 19 % glass fibre and is 76 mm wide and 60 m long. The filter moves 2.5 cm/h while 200 ~ 250 l air/min passes through. After 1 month operation, plutonium on the filter is separated for counting as follows:

Filter paper recovered from the monitoring station monthly is ashed completely at 450 °C. The ash thus obtained is placed in a 2-l beaker and ^{236}Pu is added as spike (7). Sixhundred millilitres of 8 *N* nitric acid is added and the mixture is heated on a hot plate with occasional stirring. After allowing to stand for about one hour, leached solution and residue are separated with a centrifuge. The residue is leached again with 400 ml of 6 *N* hydrochloric acid for 3 hours under heating. The recovery of plutonium is about 75 %.

The nitric and hydrochloric solutions are combined. Plutonium in the solution is coprecipitated with ferric hydroxide. The precipitate collected both by decantation and centrifuge is dissolved with 10 ml of nitric acid. The solution is evaporated and the residue is dissolved with 30 ml of 8 *N* nitric acid. Insoluble residue is removed with a centrifuge.

The supernatant is shaken with 15ml of 10 % tri-n-octyl amine in xylene pre-equilibrated with 8 *N* nitric acid. The extraction is repeated twice. Since plutonium is extracted into the organic phase together with thorium and uranium, the solvent is washed in turn with 2 portions of 15 ml of 8 *N* nitric acid and with 2 portions of 15 ml of 10 *N* hydrochloric acid in order to remove most of thorium and uranium. Then plutonium is back-extracted with 15 ml of 6 *N* hydrochloric acid containing 0.2 *N* hydrofluoric acid or



Japan Atomic Research Institute

Figure 2. Elution curve of the chromatographic separation of the Am, Cm, Y, and Eu-Ce groups: (●) α activity of Am; (▲) α activity of Cm; (○) $\alpha + \beta$ activity (17).

0.5 N hydrochloric acid containing 0.02 N hydrofluoric acid in a polyethylene vessel. The resulted aqueous phase is washed with an about 20-ml portion of xylene and heated with 5 ml of nitric acid and 0.5 ml of perchloric acid in order to decompose organic substances.

The residue is dissolved in a mixture of 0.5 ml of 0.1 N hydrochloric acid, 0.5 ml of 0.5 M oxalic acid, 0.15 ml of 2 M ammonium formate, 5 ml of 4 M sodium chloride and 3 ml of water and plutonium is electrodeposited on a stainless-steel disc (19).

Activities of ^{238}Pu and of ^{239}Pu - ^{240}Pu are measured by α -spectrometry in reference to the activity of ^{236}Pu spiked. Figure 3 shows the flow-sheet of the procedures.

Separation from Radioactive Waste

Treatment of α -bearing Aqueous Waste from a Plutonium Handling Laboratory. The Tokai Establishment of JAERI has a plutonium handling laboratory for basic research. Alpha-bearing aqueous waste from the laboratory has amounted to several hundred litres every year. Since the regulations do not permit transportation of plutonium bearing waste in liquid form to the waste management facility of JAERI, much liquid waste containing α emitters is accumulated in the laboratory. Recovery of plutonium from the waste is desired to keep the α -activities minimum in the final waste.

At the same time, americium had not been readily available in Japan and it was desired to prepare a weighable amount of ^{241}Am for chemical studies. Under the circumstances, a process (9, 20) was developed both for the volume reduction of the aqueous waste and for the recovery of plutonium and americium (21).

Alpha radioactive aqueous waste from the laboratory is of a wide variety. It is, however, bottled and classified according to its occurrence: Washings of glass wares are almost water. The purification of large amounts of plutonium gives liquid waste containing nitric acid, sodium nitrate, weighable amounts of americium and about 0.1 g/l of plutonium. The waste solution from the analytical work contains sulphuric acid, perchloric acid and chelating agents such as Arsenazo III.

The waste solutions are neutralized with calcium or sodium hydroxide in order to avoid explosion in the following evaporation procedure. Calcium hydroxide is inexpensive and suitable for use in the treatment of a large amount of waste, whereas sodium hydroxide is preferred for neutralizing the waste containing sulphate.

Then 20 ml of 30 % hydrogen peroxide and 20 ml of 0.01 M ferric chloride are added into one litre of the neutralized solution. Hydrogen peroxide keeps plutonium in the tetravalent state in alkaline medium and ferric hydroxide formed carries actinides down. This coprecipitation gives decontamination factors of $\sim 10^4$ both for Pu (IV) and Am (III). Figure 4 shows the flow-sheet for the procedure mentioned above.

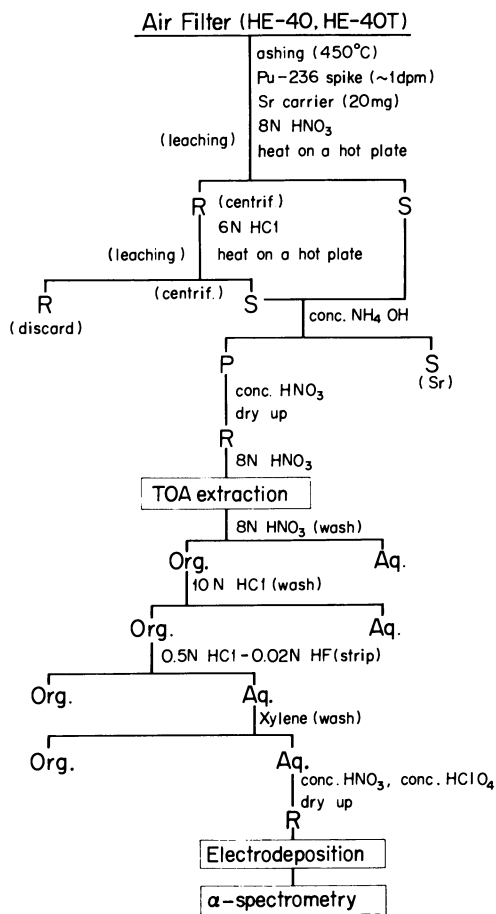


Figure 3. Analytical procedures of ²³⁹Pu in an air-monitoring sample

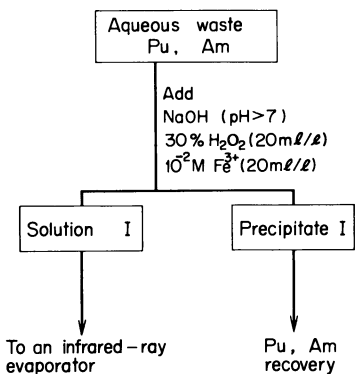


Figure 4. Flowsheet for Pu and Am recovery from α-radioactive aqueous waste (20)

Radiochemical and Radioanalytical Letters

The ferric hydroxide precipitate obtained is dissolved with nitric acid and is made to about 7 M nitric acid solution. This is poured on an anion-exchange resin column (3 ϕ \times 40 cm) in order to adsorb plutonium. The effluent from the column is almost neutralized and americium is extracted with 30% dibutylphosphate-dodecane solution keeping the volume ratio of organic to aqueous phases 1 : 2. Americium is back-extracted with 1 M nitric acid. About 15 g of plutonium and 160 mg americium were recovered from about 200 l of the aqueous waste from the plutonium laboratory.

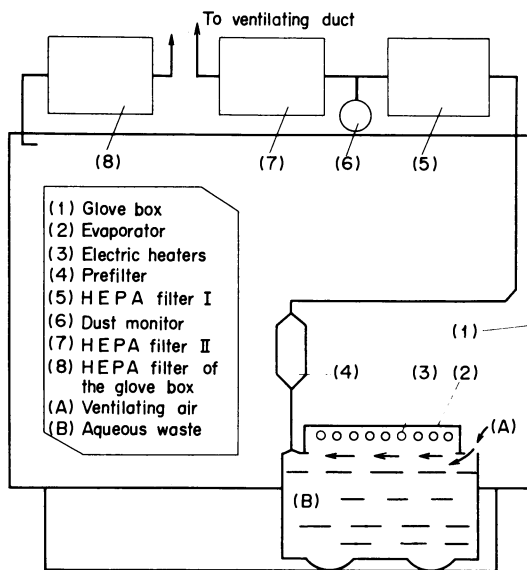
The α -activity of the supernatant solutions was about 3 μ Ci/l. This is too high to discard to the environment. Therefore, it is evaporated to a pasty state using a simple evaporator which is shown schematically in Figure 5. The device is made of steel and installed in a glove box. Thirty litres of the alkalized aqueous waste is fed in the evaporator and heated with six 1/6-kW electric resistance heaters which are sheathed in quartz tubes and set under the whole ceiling of the evaporator. Water vapor generated is carried on the ventilating air of the glove box. The air is filtered through a set of filters. About 30 m³/hr of air passes through this route. The evaporation rate in this system was found to be about 0.6 l/hr. As the air is heated to about 50 °C at the outlet of the glove box, no condensed water was found in the air-filter boxes during evaporation. Solutions are made alkaline in advance and there is neither possibility of explosion nor formation of acidic fumes.

After evaporation, the highly concentrated salt solution containing solid salts remains in evaporator. The residue is transferred and solidified with anhydrous gypsum. The solid has 1/5 - 1/10 volume of the original solution.

Separation of Actinides from High-level Waste (HLW). From the point of view of seeking a possible approach to the ultimate disposal of the HLW from the reprocessing of spent nuclear fuels, processes of solvent extraction and ion-exchange techniques have been studied to recover both americium and lanthanides from the HLW and to separate those subsequently.

In early studies, di-(2-ethylhexyl) phosphoric acid (DEHPA) had been chosen as the extractant (22). DEHPA extracts americium from the solutions of low acid concentrations such as 0.1 M, while a small percentage of americium is carried with the precipitate formed by denitration of the HLW with formic acid for acidity adjustment. At the end of the denitration, the pH of solution has to be kept lower than 0.5 to avoid the loss of americium more than 0.1 % due to coprecipitation with zirconium, molybdenum and tellurium.

As shown in Figure 6, diisodecylphosphoric acid (DIDPA) gives higher distribution ratios compared with those of DEHPA, being more suitable for using as extractant at higher acid concentrations. One M DIDPA diluted with normal paraffins can be used to recover americium and lanthanides from the HLW of PUREX process.



Radiochemical and Radioanalytical Letters

Figure 5. IR evaporating system for the treatment of α -radioactive waste (21)

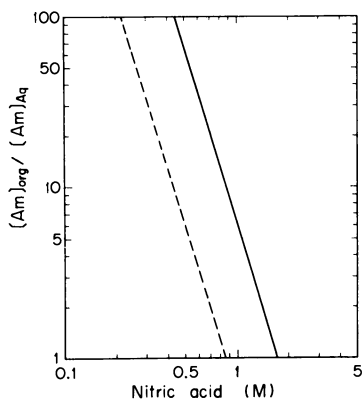


Figure 6. Distribution ratio of Am on extraction with DIDPA and DEHPA: (—) 1M DIDPA-NPH, (---) 1M DEHPA-NPH.

The separation of americium from the lanthanides is feasible by either solvent extraction or ion-exchange process. For the solvent extraction, 0.25 M DIDPA diluted with diisopropylbenzene (DIPB) provides appropriate distribution ratios of americium between the organic phase and the aqueous phase composed of 0.05 M Na₅DTPA and 1 M lactic acid.

The effect of radiation damage has been studied of the solvents using γ rays from ⁶⁰Co. The results show that the solvents are not degraded by exposing to the γ radiations up to 1×10^8 rad, which is more than 100 times of the dose resulted from the treatment of the HLW.

Wheelwright has developed a cation exchange separation of americium from the lanthanides using DTPA as eluent (24). Nakamura et al. have improved the process by incorporating a porous-type cation-exchange resin and a pressurized column (25). The effect of radiation damage of the resin has been also investigated on operation modes.

A conceptual flow-sheet is proposed as shown in Figure 7. The apparatus of those processes have been prepared and the experiments using 1 kCi of real waste solutions are scheduled in 1980.

Studies on the Reprocessing of Nuclear Fuel

Aqueous Process. In 1967-68, a hot reprocessing test had been conducted using the spent fuel (ca. 600 MWD/T) from JRR-3 (Japan Research Reactor-3) (6). About 200 g of purified plutonium was recovered by a modified PUREX process from aluminum-clad uranium fuels of natural isotopic composition.

In order to support this hot test, chemical processes have been studied with the view improving aqueous separation process.

Effects of γ irradiation on the plutonium extraction characteristics were studied of tributylphosphate (TBP) and alkylamines (26). In irradiation to the extent of 10^8 R, marked change was observed with TBP system tending to bring losses of plutonium, while little change was found with the extraction systems of trin-octyl amine and of cyclohexyl dilauryl amine.

As for the Pu purification process, a modified method is proposed for the effective stripping of plutonium from TBP (27). The nitrous acid acts as "redox reagent" for Pu (IV) in the stripping and in the extraction feeds. The addition of 0.1 mol/l of nitrous acid to the extraction feed is sufficient to the effective stripping of plutonium up to 99.9 %. This modified flow-sheet was demonstrated through the process studies with miniature mixer-settlers.

In order to evaluate the plutonium purification process with TBP, a calculation code has been developed for the system composed of TBP, nitric acid and plutonium on the basis of a batchwise counter-current extraction cascade (28). The code computes not only number of theoretical stages required, but also concentration profile for steady or transient state. The profiles of calculated

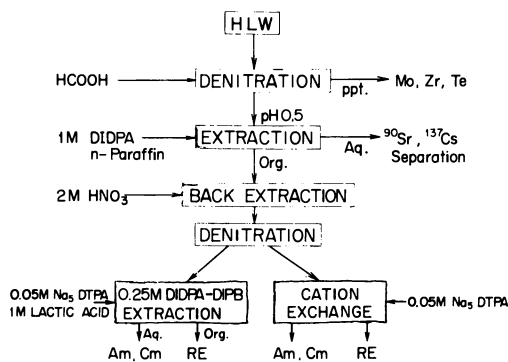


Figure 7. Flowsheet of actinide separation from Purex high-level waste with DIDPA

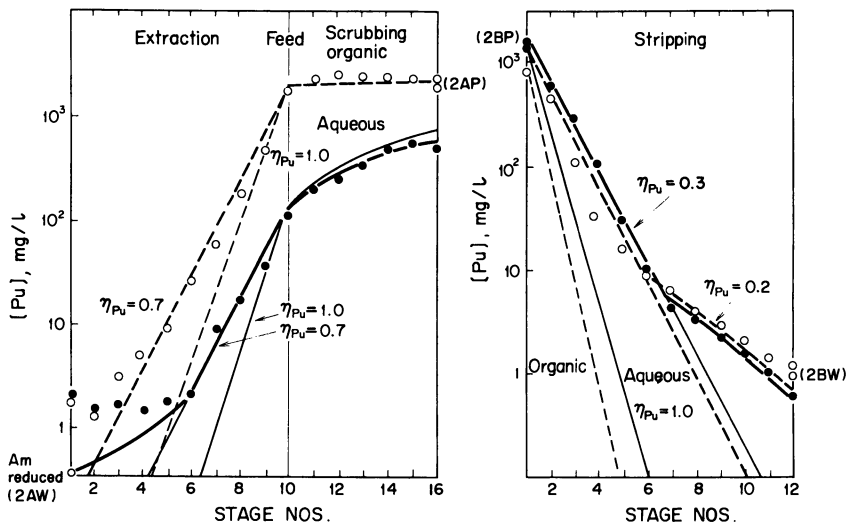


Figure 8. Concentration profiles for Pu in the process studies: (●, ○) experimental values; (—, ---) calculated values.

plutonium concentration were well agreed with those obtained from experimental process data as shown in Figure 8. Actual flow-sheet calculation was undertaken in accordance with the pilot plant test (29).

For the purpose of improving the decontamination factor (DF) of FPs from U or Pu in the reprocessing of highly irradiated fuels such as those from FBR, a modified method adding inactive zirconium or hafnium ion is proposed. The feasibility of this concept has been experimentally demonstrated by both batchwise extraction and process studies with miniature mixer-settlers.

The addition of inactive zirconium has resulted in improving DF by a factor of about 4 in the simulated FBR fuel reprocessing flow-sheets (30).

Process studies were also performed on the ion-exchange and precipitation methods for the recovery of plutonium and americium from the aqueous or organic waste discharged from the above mentioned process (31).

Non-aqueous Process. A halide volatility process has been extensively studied among the dry reprocessing processes. The chloride distillation using carbon tetrachloride has been studied in applying to the treatment of irradiated uranium dioxide (32). In a proposed flow-sheet, chlorination and distillation processes are followed by the sorption and desorption process of uranium chloride on a barium chloride bed. Fundamental data of decontamination for the fission products have been accumulated, showing that excellent purification of uranium is achieved.

Process studies on fluoride volatility method have been carried out for the purpose of evaluating feasibility for the reprocessing of FBR fuels (33). Process concept investigated is shown in Figure 9. It aimed at a simple and advanced process for continuous operation. Experiments are mainly made on the fluorination and purification using bench-scale fluid-beds and traps.

The two step-fluorination process shown in Figure 9 has been proved to provide a stable recovery of plutonium more than 99 % (34). The retention mechanism of plutonium on alumina fluidizing media is interpreted in terms of the elutriation characteristics of plutonium fluorides (35).

Effective purification of plutonium hexafluoride is proved through the selective adsorption of FPs on NaAlF_4 . A rather high decontamination factor (more than 5×10^3) is attained for ruthenium fluoride (36). A new separation process of PuF_6 from UF_6 by the selective adsorption onto UO_2F_2 is proposed (37).

Although promising data have been acquired for the fluoride volatility process, the technical feasibility has not been demonstrated yet. Aside from chemical problems, many technological problems such as process stability due to powder handling and remote maintenance, are still remained unsolved. In order to solve these problems, head-end process studies as voloxidation have been started. Here, stress is put on the environmental protection of

American Chemical
Society Library
1155 16th St. N. W.

Washington, D. C. 20036

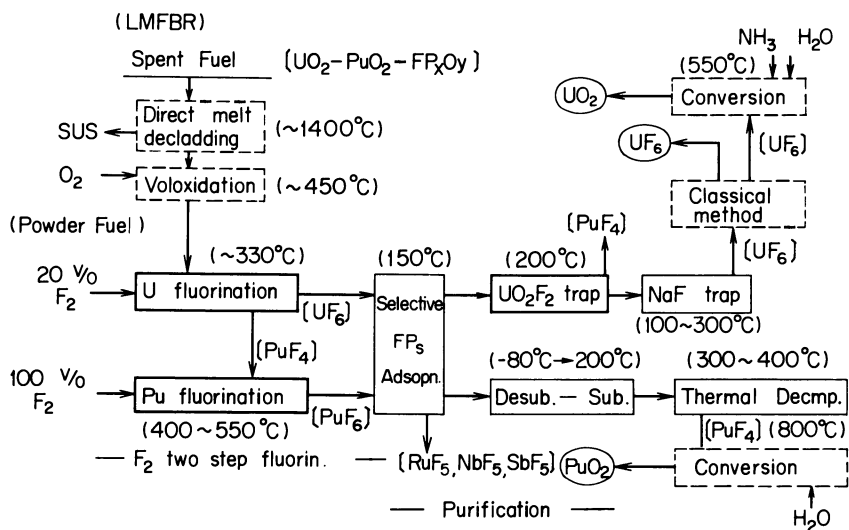


Figure 9. Conceptual process diagram of the reprocessing of FBR fuels

reprocessing. The above proposed concept has recently been reoriented for the proliferation resistant process (38).

Literature Cited

1. Ishimori, T.; Nakamura, E. Bull. Chem. Soc. Japan, 1959, 32, 713.
2. Kimura, K.; Ishimori, T.; Naito, K.; Umezawa, H.; Watanabe, K. J. Atomic Energy Soc. Japan, 1960, 2, 328.
3. Nakamura, E. ibid., 1961, 3, 502.
4. Fujino, T. ibid., 1963, 5, 640.
5. Nakamura, E. ibid., 1962, 4, 585.
6. Aochi, T. Nucl. Eng. [Genshiryokugogyo], 1969, 15, 45; 1970, 16, 81.
7. Ishimori, T.; Akatsu, E. J. Nucl. Sci. Technol., 1969, 6, 480.
8. Ueno, K.; Watanabe, K.; Sagawa, C. ibid., 1972, 9, 45.
9. Akatsu, J.; Ishimori, T. ibid., 1972, 9, 237.
10. Watanabe, K.; Sagawa, C.; Ueno, K. ibid., 1973, 10, 62.
11. Akatsu, J. ibid., 1973, 10, 696.
12. Ueno, K.; Watanabe, K.; Sagawa, C.; Ishimori, T. ibid., 1974, 11, 8.
13. Ueno, K.; Watanabe, K.; Sagawa, C.; Ishimori, T. ibid., 1975, 12, 356.
14. Watanabe, K.; Sagawa, C.; Ueno, K. The 1974 Annual Meeting of the Atomic Energy Soc. Japan, 1974.
15. Ueno, K.; Watanabe, K.; Sagawa, C. J. Nucl. Sci. Technol., 1977, 14, 532.
16. Natsume, H.; Umezawa, H.; Okazaki, S.; Suzuki, T.; Sonobe, T.; Usuda, S. ibid., 1972, 9, 737.
17. Umezawa, H.; Ichikawa, S.; Natsume, H. JAERI-M 5785, 1974.
18. Imai, T.; Kasai, A. Private communication.
19. Sakanoue, M.; Nakaura, M.; Imai, T. IAEA-SM-148/54, 1971, 171.
20. Akatsu, J. Radiochem. Radioanal. Lett., 1974, 19, 25 and 33.
21. Akatsu, J. ibid., 1974, 18, 51.
22. Nakamura, H.; Kubota, M.; Tachimori, S.; Yamaguchi, I.; Sato, A.; Aoyama, S.; Amano, H. JAERI-M 6958, 1977.
23. Tachimori, S.; Sato, A.; Nakamura, H. J. Nucl. Sci. Technol., 1978, 15, 421.
24. Wheelwright, E. J.; Roberts, F. P. BNWL-1072, 1969.
25. Kubota, M.; Konami, Y.; Nakamura, H.; Amano, H. J. Radioanal. Chem., 1978, 45, 73.
26. Tsujino, T.; Ishihara, T. J. Nucl. Sci. Technol., 1966, 3, 320.
27. Tsujino, T.; Aochi, T.; Hoshino, T. ibid., 1976, 13, 321.
28. Tsujino, T.; Kohsaka, A.; Aochi, T. JAERI-M 6284, 1975.
29. Aochi, T.; Tsujino, T.; Kohsaka, A.; Hoshino, T. Solvent Extraction 1971, 1971, 1, 138.
30. Tsujino, T.; Hoshino, T.; Aochi, T. Ind. Eng. Chem. Process Des. Dev., 1976, 15, 396.
31. Tsujino, T.; Hoshino, T.; Yasu, S.; Kawashima, Y. JAERI-M 6106, 1975.

32. Hirano, K. JAERI-M 5878, 1974.
33. Tsujino, T. Advisory Group Meeting on Reprocessing of LMFBR fuels (Leningrad, USSR, 1976).
34. Fuel Rep. Lab. JAERI-M 6392/6393, 1976.
35. Tsujino, T.; Nishimura, M.; Yamazaki, K.; Sugikawa, S.; Yagi, E. The 8th International Symposium on Fluorine Chemistry (Kyoto, 1976).
36. Tsujino, T.; Nishimura, M.; Yamazaki, K.; Miyajima, K. The 1977 Annual Meeting of the Atomic Energy Soc. Japan (Osaka, 1977).
37. Tsujino, T.; Nishimura, M.; Yamazaki, K.; Sugikawa, S. French patent 75-02790, 1975.
38. Tsujino, T.; Aochi, T. Private communication.

RECEIVED July 27, 1979.

Heavy Element Separation for Thorium-Uranium-Plutonium Fuels

G. R. GRANT, W. W. MORGAN, K. K. MEHTA, and F. P. SARGENT

Atomic Energy of Canada Limited, Whiteshell Nuclear Research Establishment,
Pinawa, Manitoba

A large potential exists for resource conservation through introduction of thorium fuel cycles in CANDU (CANada Deuterium Uranium) reactors (1). While a number of fuel cycles have been suggested (2), this paper deals with one using thorium dioxide fuel topped with plutonium, and a processing scheme in which all fissile and fertile materials are separated and recycled. Although not discussed here, other cycles not involving complete separation are also being studied as part of the International Nuclear Fuel Cycle Evaluation.

To test the separation of the three actinides (Th, U and Pu) from each other, a modified Thorex solvent extraction flow sheet using 30% tributylphosphate (TBP) has been developed. Considerable work has already been reported in the literature for separations in Th-U systems (3, 4), but inclusion of Pu in the fuel cycle adds additional complexities (5). The flow sheet adopted is that in Figure 1, which also shows the relative flows (FL) of the inlet streams and concentrations (M or mol/L) of the major components. The flow ratios and acidities for each contactor were initially derived by constructing McCabe-Thiele operating diagrams based on unpublished distribution measurements made in our laboratories (6).

Contactors I and II are used as a decontamination cycle to remove most of the fission products from the actinides. After intercycle concentration and Pu valency adjustment (to Pu(III)), the next three contactors make up the primary separation system and are used to recover Pu(III), Th and ^{233}U . In this work, natural U was used in place of ^{233}U .

Experimental

Laboratory Scale Contactor Tests. The feasibility of each part of the flow sheet was tested in small, commercially available mixer-settler units which had 12 or 16 stages with individual mixer and settler volumes of 15 mL and 49 mL, respectively. Total volume through-puts up to 600 mL/h were attainable with

0-8412-0527-2/80/47-117-351\$05.00/0

© 1980 American Chemical Society

good hydrodynamic performance.

The general procedure was to prepare a typical synthetic feed solution and run the contactor at constant inlet conditions until steady state was achieved, as indicated by mass balances.

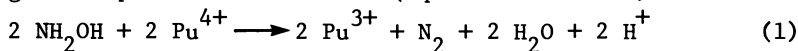
The tendency for the Th-TBP complex to form a third phase at high concentrations when kerosene-type diluents are used is well known (7). To counteract this phenomenon, the diluents used were either pure diethyl benzene (DEB) or a commercial isoparaffinic kerosene to which sufficient DEB was added as modifier.

Since much of the flow sheet is similar to that of a standard Thorex processing scheme, only those areas where changes were required because of the inclusion of Pu will be discussed in detail.

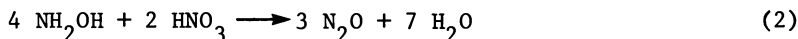
Feed solutions for Contactor I tests were prepared with the approximate composition shown as the IAF stream in Figure 1. The heavy element concentrations are representative of those which would be obtained from dissolving irradiated Th-Pu fuel. Fluoride and aluminum were also included in the feed because they would be needed in an actual dissolution step for ThO₂ (fluoride catalyzes the dissolution, and aluminum counteracts the corrosiveness of the fluoride). For efficient Th extraction, the acidity of the feed solution should be in the range of 2 to 3 mol/L in HNO₃. This is a significant departure from the acid Thorex process which uses an acid-deficient feed solution and is reported to achieve improved decontamination from fission products (8). However, acid-deficient feed solutions were considered undesirable in our flow sheet because Pu hydrolyzes and tends to polymerize at low acidity (9). The effect of the higher feed acidity used here on fission product decontamination has not yet been established but will be assessed in later experiments.

Feed preparation also included Pu valency adjustment where NaNO₂ or NO + O₂ gas was used to convert all Pu to the readily extractable Pu(IV) state.

Before being fed to Contactor III, the aqueous feed solution was treated to reduce Pu to the Pu(III) state, to prevent its extraction and ensure its recovery in the aqueous Pu product stream (3PP). The reference reductant for the flow sheet was hydroxylamine nitrate (HAN) at 0.3 mol/L with hydrazine nitrate (0.1 mol/L) as a holding agent or HNO₂ scavenger (10). Use of HAN as Pu reductant was considered desirable because in reaction with Pu, as well as in subsequent reactions where the reductant is destroyed, only gaseous products are formed (equations 1 and 2).



and



HAN does not contribute any solids to the waste streams which must ultimately be treated for disposal. As will be shown later, however, complete recovery of Pu with the aqueous product stream was not achieved using HAN as reductant and substantial losses of

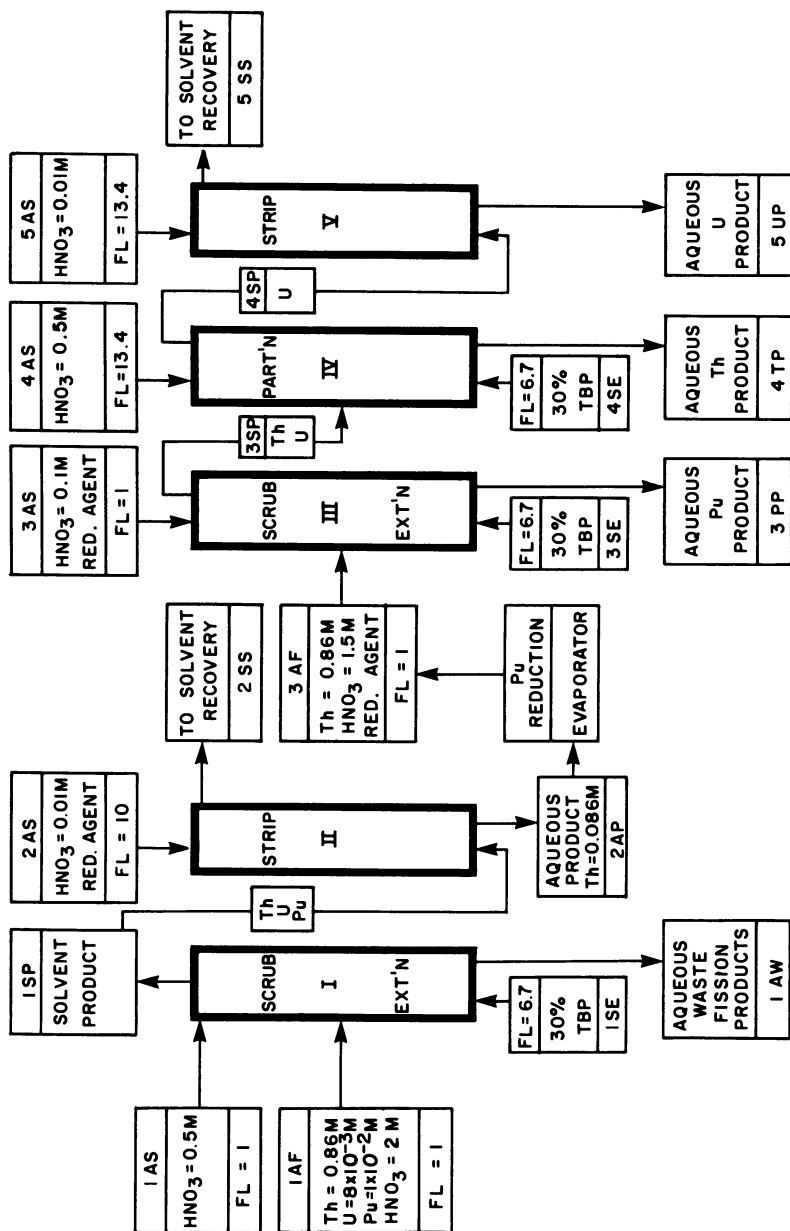


Figure 1. Modified Thorex flowsheet for Th-U-Pu fuel

Publication Date: April 16, 1980 | doi: 10.1021/bk-1980-0117.ch025

Pu with the solvent invariably occurred. This loss was attributed to oxidation of Pu(III) to Pu(IV) in the organic phase as has also been observed in Purex-related tests (10, 11).

Two additional Contactor III tests were performed as follows:

- Plutonium was reduced in the feed solution with hydrazine-stabilized HAN and an organic-soluble reducing agent, 2, 5 di-tert-amylhydroquinone (DAH₂Q) (12), dissolved in the solvent (0.03 mol/L) was used to reduce any Pu(IV) formed in the contactor.

- The feed solution (3AF) was treated with ferrous sulfamate (FeSA) to reduce Pu to Pu(III) and FeSA was also added with the scrub stream (3AS) to reduce any Pu(IV) formed in the scrub section. The concentration of FeSA in both solutions was 0.05 mol/L and both were stabilized with 0.05 mol/L sulfamic acid.

Solvent Extraction Computer Code. For modelling the extraction behaviour of the actinides and nitric acid in the five contactors of our flow sheet, a solvent extraction computer code called SECTOR has been developed. It is a modification of SEPHIS (13), a code developed at Oak Ridge National Laboratories (ORNL) for the reprocessing of fuel by the Purex process. Attempts to develop SECTOR based on a chemical model to describe the experimental distribution data had some limited success, however, the current version relies on a mathematical description of the distribution data. The variables used in deriving the correlations for the various distribution ratios, D_{Th} , D_U , D_{HNO_3} , etc., are the concentrations of Th and HNO₃ in the aqueous phase. It was assumed that U and Pu, being present at low concentrations only, would not affect D_{Th} or D_{HNO_3} . Because of its empirical nature, any change in the parameters describing the aqueous phase cannot be accommodated by the current model, e.g., addition of a salting agent such as NaNO₃, or HAN, or a change in operating temperature requires remeasurement of distribution data and derivation of new correlations. Nevertheless, this version of SECTOR has been extremely useful in interpreting some of the experimental contactor data obtained.

Additional changes incorporated into SECTOR to account for the oxidation-reduction reactions occurring with Pu included:

- Simultaneous reduction of Pu(IV) (when a reductant was present) in the aqueous phase of a mixer, and redistribution of both Pu(III) and Pu(IV) between the two phases, for a time equal to the average residence time in the mixer.

- Further reduction in the aqueous phase of any remaining Pu(IV) in the settler, for a time equal to the average residence time in the settler. No further redistribution of Pu species was assumed to occur in the settler.

- Oxidation of Pu(III) to Pu(IV) in the organic phase of a settler to an extent assumed to be proportional to the Pu(III) and HNO₃ concentrations of the organic phase, i.e.,

$$\Delta[\text{Pu(IV)}]_o = A [\text{HNO}_3]_o \cdot [\text{Pu(III)}]_o \quad (3)$$

where A is an empirically defined proportionality constant, and []_o represents concentrations of the species (mol/L) in the organic phase.

Results and Discussion

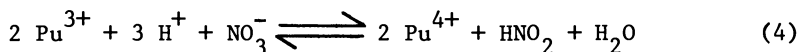
Contactor I Data. Typical experimental concentration profiles for Th, HNO₃ and Pu are shown in Figures 2, 3 and 4 respectively, together with the profiles calculated using SECTOR. Also shown in the figures are schematic diagrams of the contactor and the actual feed concentrations used.

The thorium profile (Figure 2) shows that Th is extracted efficiently and that loss to the aqueous waste stream is reduced to < 0.1% in five extraction stages (i.e., stages 7 to 11).

The profile for HNO₃ (Figure 3) shows that this solute refluxes considerably at the chosen operating conditions. This is due to appreciable extraction of the HNO₃ over stages 10 to 16 where the Th concentration is low, and somewhat poorer extractability over stages 1 to 9 where the Th concentration is higher. This gives a peak aqueous acidity of more than 4 mol/L compared to an average acidity of ~ 2 mol/L based on the two inlet streams (HNO₃ is 3 mol/L and 0.5 mol/L in 3AF and 3AS respectively).

The experimental Pu concentration profile shown in Figure 4 indicates that Pu is extracted efficiently over only the first few extraction stages, and then is extracted quite inefficiently over the remaining stages. This poorer extractability may be due in part to hydrolysis of Pu(IV), but it is believed to be mainly due to the presence of a small amount of Pu(III) in the feed solution.

In nitric acid solutions, Pu(III) is oxidized according to the following equation (14):



Nitrous acid is not only a product of the reaction but it also catalyzes this oxidation. However, its use for Pu valency adjustment inevitably shifts the equilibrium to the left and results in some Pu(III) remaining in the feed solution. The equilibrium for the reaction is described by:

$$K = \frac{[\text{Pu(III)}] \cdot [\text{H}^+]^{1.5} \cdot [\text{NO}_3^-]^{0.5}}{[\text{Pu(IV)}] \cdot [\text{HNO}_2]^{0.5}} \quad (5)$$

Using a value of $K = 0.93 \text{ (mol/L)}^{1.5}$ (14), we estimate that in the typical feed solutions used in these tests up to 2% of the Pu may be present as Pu(III).

In Contactor I, Pu(IV) is readily extracted but the Pu(III)

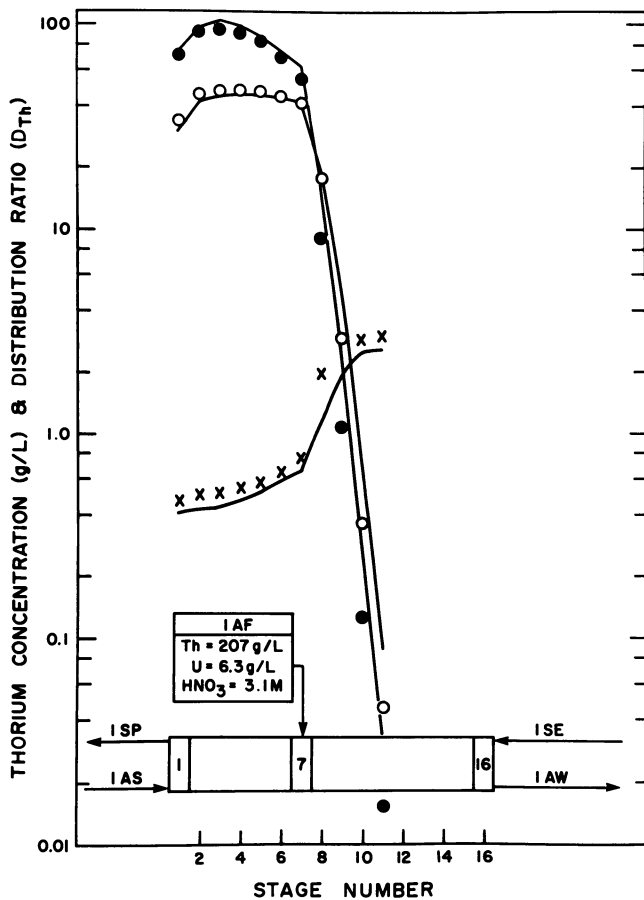


Figure 2. Thorium concentration profile and distribution ratio for Contactor I: (●) aqueous phase; (○) solvent phase; (×) distribution ratio (D_{Th}); (—) calculated.

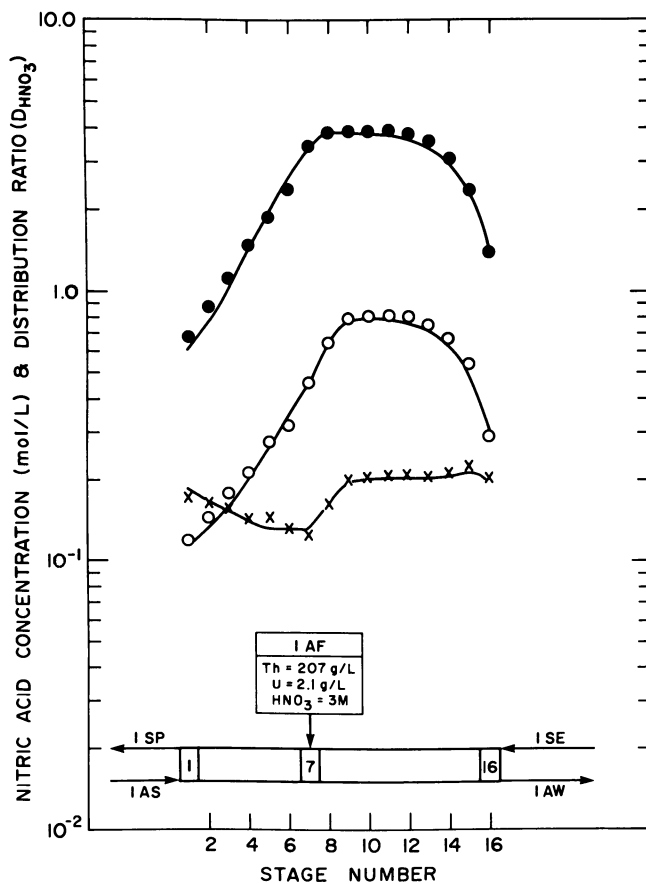


Figure 3. Nitric acid concentration profile and distribution ratio for Contactor I: (●) aqueous phase; (○) solvent phase; (×) distribution ratio (D_{HNO_3}); (—), calculated.

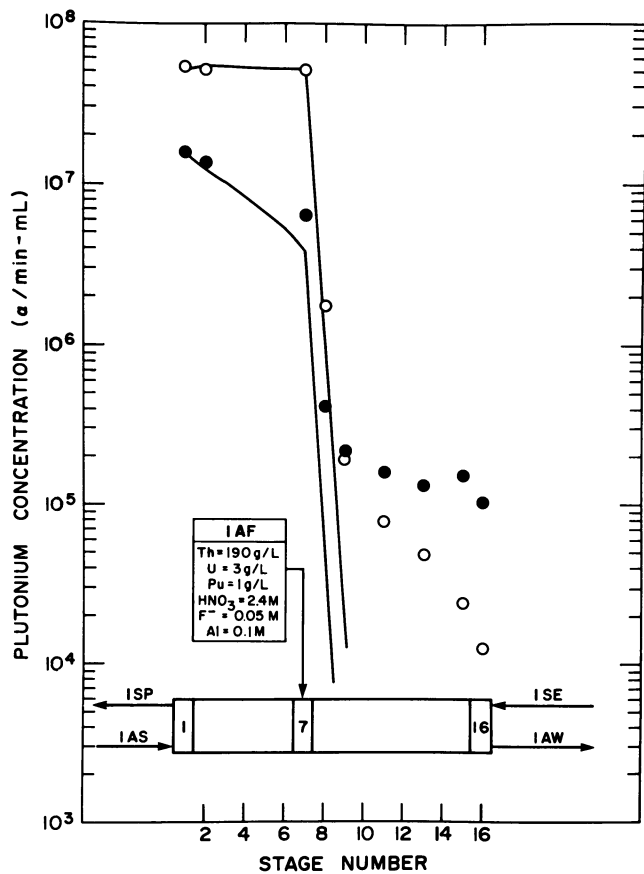


Figure 4. Plutonium concentration profile for Contactor I: (●) aqueous phase; (○) solvent phase; (—) calculated.

tends to remain with the aqueous phase. Nitrous acid is also extracted by the solvent (15), so that the equilibrium should shift to the right. However, the oxidation of Pu(III) by nitric acid takes place only slowly when HNO_2 is no longer available in the aqueous phase to catalyze the reaction, and the result is a small loss of Pu with the aqueous waste stream ($\sim 0.1\%$ in the case shown).

Contactor II. Results for Contactor II were exactly as expected, i.e., all actinides were easily stripped from the organic phase in about five stages. With the low acidity used in the 2AS stream, HAN reduced Pu easily and prevented any polymerization of Pu(IV). The relatively high flow ratio used here (aqueous to organic, A/O = 1.5) was necessary to prevent refluxing of U. Although not a problem in this work, where natural U was used, refluxing could be of concern for separations involving fissile U isotopes.

Contactor III Data. A typical experimental Pu concentration profile for Contactor III where hydrazine-stabilized HAN was used as reductant is shown in Figure 5. Plutonium in the feed solution was initially reduced to Pu(III) using HAN. At acidities of less than 1.5 mol/L HNO_3 , more than 99% of the Pu is reduced, and it should be inextractable. The calculated profile for both phases for Pu(III) is shown as dashed lines on the plot. For stage numbers less than 10, the Pu is predicted to be easily scrubbed from the solvent. Experimentally, the behaviour was very different and substantial amounts of Pu were extracted and carried with the solvent, leading to a loss of $\sim 12\%$ with the 3SP stream. This behaviour is attributed to the oxidation of some of the Pu(III) in the organic phase and an excessively low reduction rate of Pu(IV) by HAN which operates only on the aqueous phase. To account for this in the computer calculations, an oxidation step was incorporated into the SECTOR code as described earlier. The proportionality constant A of equation (3) was determined empirically to be that which gave the best fit for a number of experimentally determined profiles obtained under various conditions of acidity and heavy element concentration. When using HAN as reductant, a value of $A = 1.5$ L/mol per unit of setting time appears to be most appropriate. The calculated profile incorporating the oxidation step is also shown in Figure 5 as solid lines. Note that the shape of the experimental profile is reproduced extremely well, using only this single adjustable parameter in the pseudo kinetic expression for the Pu(III) oxidation.

In contrast to this, McCutcheon et al (16) have used kinetic expressions for up to five aqueous phase reactions involving HAN, N_2H_4 , HNO_2 , HNO_3 and Pu in their simulation model and have obtained similarly shaped concentration profiles for Pu. However, the oxidation of Pu(III) in the organic phase was not included in

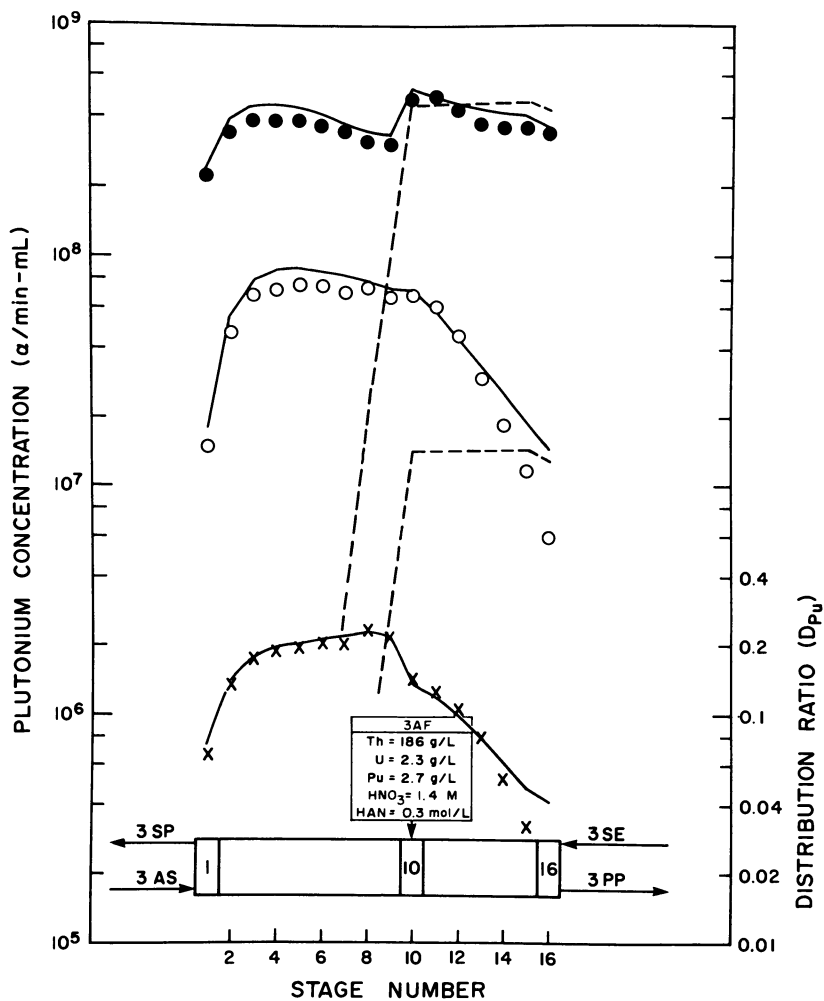


Figure 5. Plutonium concentration profile and distribution ratio in Contactor III using HAN as reductant: (●) aqueous phase; (○) solvent phase; (×) distribution ratio (D_{Pu}); (---) calculated profile for Pu(III); (—) calculated; $A = 1.5$ (see text).

their model.

Barney has shown that the reduction rate of Pu(IV) by HAN is retarded very severely at higher acidities, being inversely proportional to the fourth power of $[H^+]$ (17) as shown in equation (6):

$$-\frac{d [Pu(IV)]}{dt} = k \cdot \frac{[NH_3OH^+]^2 \cdot [Pu(IV)]^2}{[H^+]^4 \cdot (1 + [NO_3^-])^2 \cdot [Pu(III)]^2} \quad (6)$$

Therefore, if the feed acidity is decreased, the reduction rate should be enhanced and lower Pu losses should be achieved. This was confirmed by experiment where the loss was decreased to $\sim 2\%$ Pu at a feed acidity of 0.8 mol/L. The calculated effect of feed acidity on Th and Pu losses from Contactor III is shown in Figure 6. The Pu oxidation model was used in deriving these results. An acidity of less than 0.6 mol/L would apparently be required to limit Pu losses to $\sim 0.1\%$. At the same time, Th losses to the Pu product stream would be over 10%. Experimentally thorium loss was reduced to acceptable levels by adding a salting agent ($NaNO_3$) to the 3AF and 3AS streams, but this solution unfortunately eliminates one of the major advantages of using HAN as reductant, viz, a decrease in the amount of solid wastes which must be treated.

Similar calculations for a U-Pu separation using HAN as reductant and the flow ratios of our modified Thorex flow sheet indicate that about the same Pu loss behaviour should be expected. However, for flow conditions more appropriate to the Purex process, negligible Pu losses are predicted. Uranium losses are predicted to be negligible for both sets of conditions. These predictions were also confirmed in contactor tests.

Because the Pu oxidation appeared to be taking place in the organic phase and the reductants usually employed operate only in the aqueous phase, it was felt that Pu losses could be diminished by using an organic-soluble reductant, e.g., 2,5 di-tert-amylhydroquinone (DAH₂Q) (12) dissolved in the extractant. Plutonium in the feed solution was initially reduced to Pu(III) with hydrazine-stabilized HAN, but, in the one run which was completed, the reduction did not go to completion and the feed solution actually contained $\sim 12\%$ Pu(IV). However, since there was a large molar excess of reductant over Pu(IV), very little Pu loss was expected. During the first several hours of the run, the reductant appeared to be functioning satisfactorily, however, Pu losses with the 3SP stream slowly increased until they reached about 5% after 14 hours of operation.

The reduction of Pu(IV) with DAH₂Q proceeds according to the reaction:

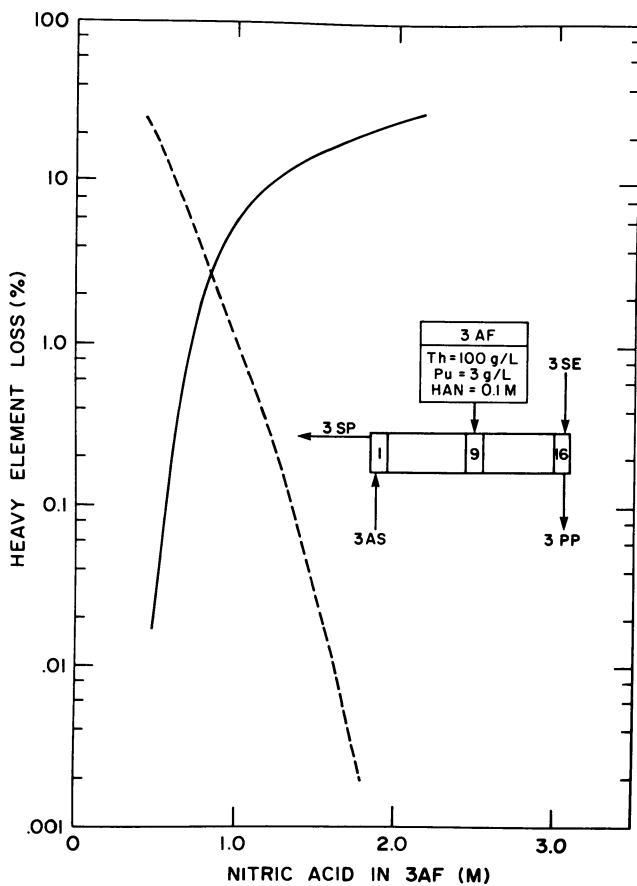
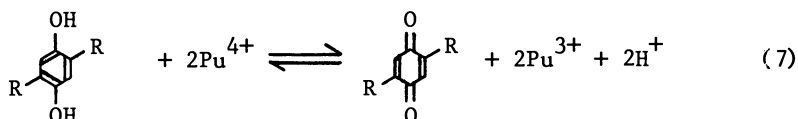
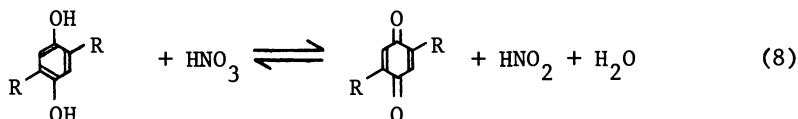


Figure 6. Calculated Pu and Th loss from Contactor III as function of feed acidity: $A = 1.5$ (see text); (—) Pu loss with 3SP stream; (---) Th loss with 3PP stream.



where R represents the tertiary amyl group.

This indicates that as acidity increases in this contactor (e.g., due to refluxing, in the same manner as seen for Contactor I) reduction is impeded. A competing reaction with DAH₂Q is then postulated to become more important:



We have identified HNO₂ as a reaction product in HNO₃-DAH₂Q-TBP systems by the characteristic spectrum of the HNO₂·TBP complex in the organic phase (18). We have also obtained evidence that DAH₂Q can react with HNO₂ and therefore might also be considered for use as a holding reductant under certain conditions. Although the reaction product was not identified, nitrosation of the ring seems plausible. However, at high acidity, reaction (8) appears to become predominant and the resulting HNO₂ probably leads to the autocatalytic oxidation of Pu(III) and the loss of Pu(IV). Other possible undesirable side reactions may also have taken place in this contactor run involving HAN or hydrazine and the quinone, e.g., oximes or hydrazones could have been produced (19).

Because of the problems encountered with the other reductants, some Contactor III tests were conducted with ferrous sulfamate, the most commonly used Pu reductant. These tests were successful and very low Pu losses were achieved as shown by the data in Figure 7. Two sets of SECTOR-calculated profiles are also shown in the figure; the dashed lines were obtained when an oxidation step was included, whereas the solid lines are the result of assuming zero oxidation. For the oxidation case it was assumed that any Pu(IV) produced is reduced rapidly in the aqueous phase by Fe(II) according to equation 9:



the kinetics of which have been shown by Rozen et al. (20) to be described by:

$$- \frac{d[\text{Pu(IV)}]}{dt} = k_1 \cdot [\text{Pu(IV)}] - k_2 \cdot [\text{Pu(III)}] \quad (10)$$

Because of the large molar excess of Fe²⁺ over any Pu⁴⁺ in the system, we have assumed that the second term (which Rozen included because of the back reaction) could be neglected. The constant k₁ was evaluated from:

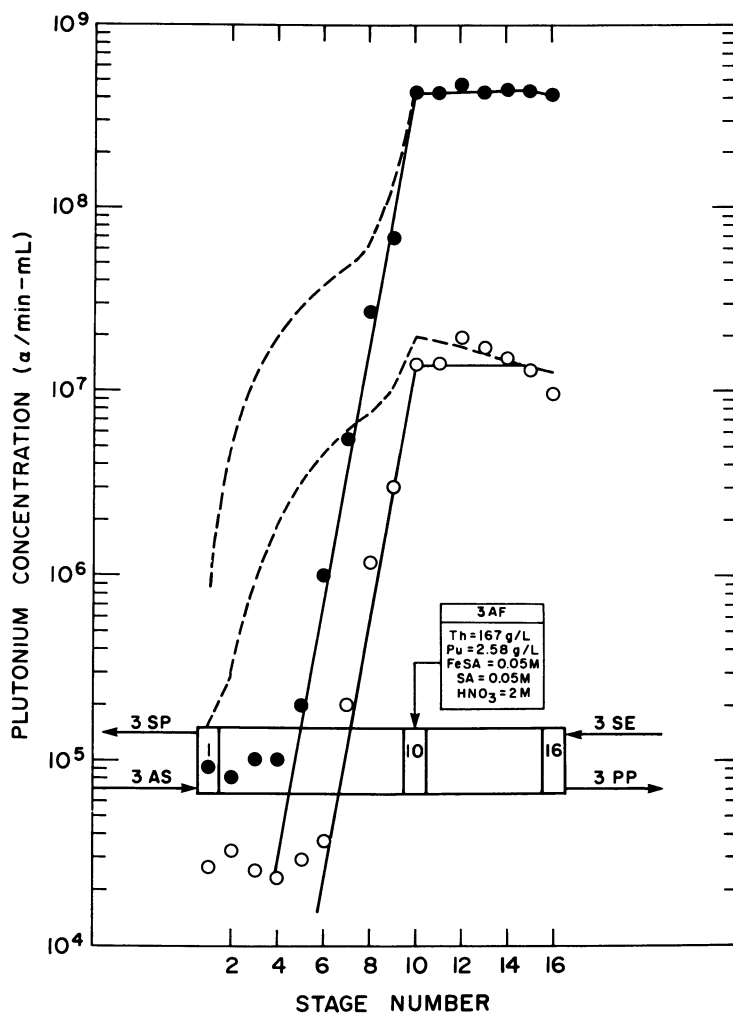


Figure 7. Plutonium concentration profile for Contactor III using ferrous sulfate as reductant: (●) aqueous phase; (○) solvent phase; (---) calculated, $A = 0.25$ (see text); (—) calculated, $A = 0.0$ (see text).

$$k_1 = \frac{1620 [\text{Fe(II)}]}{(1 + 2.9[\text{NO}_3^-])[\text{H}^+]} \quad (11)$$

It is apparent that if oxidation of Pu(III) in the organic phase does occur, the extent of oxidation is much less than when HAN is used as reductant. For the case plotted, the oxidation was assumed to be only $\sim 1/6$ of that which gave the best fit to the HAN data, (i.e., $A = 0.25$) and even this amount of oxidation appears to be excessive when compared with the experimental data. In fact the data indicate that oxidation of Pu may be inhibited completely in this system.

The success of FeSA may be due in part to the fact that sulfamic acid is soluble in the organic phase to a small extent ($D \sim 10^{-2}$) and therefore may operate as an HNO_2 scavenger in both phases. We have determined spectrophotometrically that HNO_2 in the organic phase is consumed at a faster rate when it is mixed with solvent previously contacted with sulfamic acid (see Figure 8), although the concentrations at which the effect was observed are higher than those applicable to typical process solutions. The constants (k) given for the three curves are the apparent first order rate constants for HNO_2 destruction.

Oxidation of Pu in Organic Phase. Two sets of shaker-tube experiments were designed to obtain additional information on the oxidation of Pu(III) in the organic phase.

In the first, typical 3AF feed solution containing Pu(III) and hydrazine-stabilized HAN was extracted with 30% TBP solution. The organic phase containing the extracted Pu(III) was then re-equilibrated after various standing times with an aqueous phase containing 1.5 mol/L HNO_3 and 0.1 mol/L hydrazine (the latter was added to minimize any effect due to HNO_2), and the distribution ratio of Pu was measured. The results are shown in Figure 9. After an induction period of 15-20 minutes, D_{Pu} rose sharply indicating rapid oxidation of the extracted Pu(III) to Pu(IV). The S-shaped curve also suggests that the organic-phase oxidation, like that in the aqueous phase, may be autocatalytic and therefore far more complicated than that assumed by the simple oxidation step used in SECTOR.

The effect of nitrous acid on oxidation of Pu(III) in the organic phase was assessed in the second series of experiments. Portions of aqueous feed solution containing Pu(III) as above were shaken with 30% TBP solutions which contained increasing amounts of nitrous acid. The measured Pu distribution ratios are shown as a function of shaking time in Figure 10. They indicate that quite small concentrations of HNO_2 can affect D_{Pu} significantly and the threshold for enhanced oxidation of Pu in these tests was between 10 and 100 $\mu\text{mol/L}$ of HNO_2 .

These observations on oxidation of Pu(III) in the organic phase are consistent with those in reference (11) where U(IV)

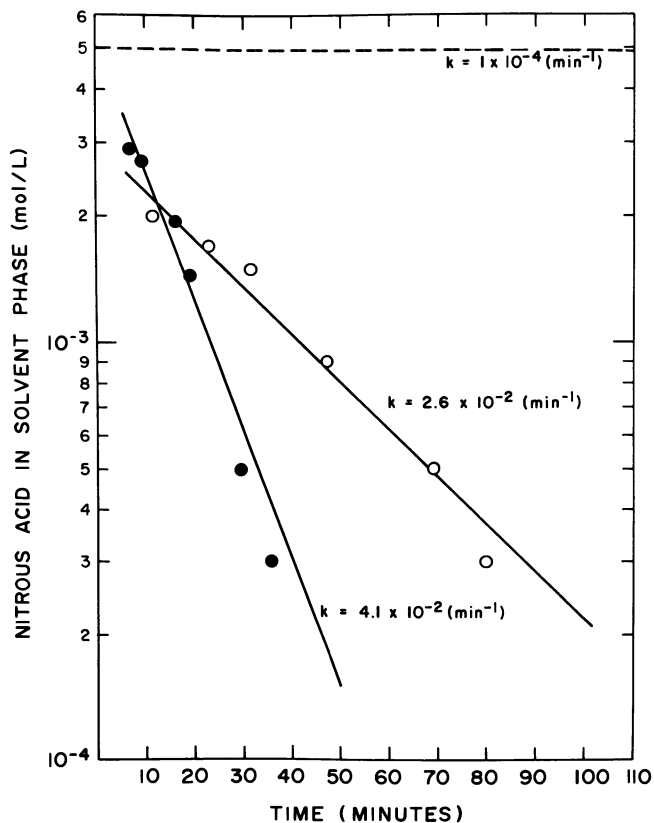


Figure 8. Effect of sulfamic acid (SA) on HNO_2 destruction in solvent phase: (---) no SA present; (O) solvent preequilibrated with 0.5 mol/L SA and 0.5 mol/L HNO_3 ; (●) solvent preequilibrated with 1.0 mol/L SA and 0.5 mol/L HNO_3 .

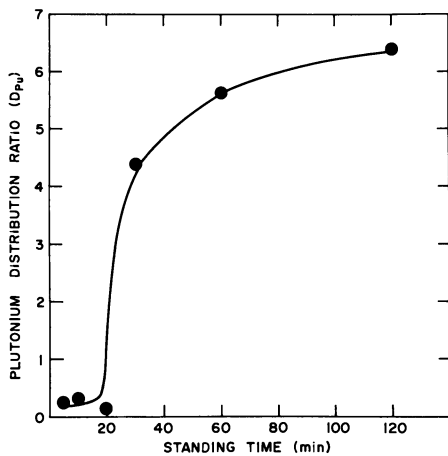


Figure 9. Distribution ratio of Pu as function of standing time in solvent phase

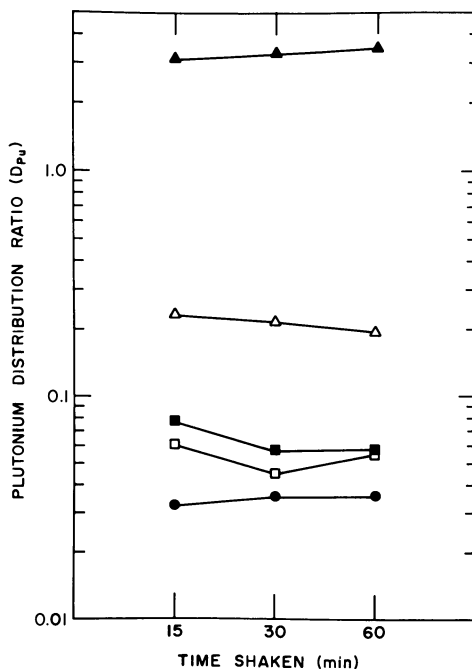


Figure 10. Effect of nitrous acid in solvent on distribution ratio of Pu; solvent preequilibrated with 0.1 mol/L HNO_3 and NaNO_2 at the following concentrations (mol/L): (●) 10^{-5} , (□) 10^{-4} , (■) 10^{-3} , (△) 10^{-2} , (▲) 10^{-1} .

rather than HAN was used as the reductant. Evidence of Pu(III) oxidation in contactor tests of the Purex partitioning step using HAN was also obtained by Richardson (10).

Contactors IV and V. The partitioning of Th from U in Contactor IV was achieved relatively easily although the solvent product (4SP) contained somewhat more Th than desired. The flow ratios and acidities used here were different from those used in the standard Thorex process and were chosen to ensure that U refluxing would not occur. Optimization of the flow sheet which has not been attempted to any extent may well lead to changes in operating conditions and improved separation.

Stripping of U from Contactor V was easily achieved.

Summary of Results

- The flow sheet presented here has been shown, in laboratory tests using mixer-settlers, to be suitable for separating the the three actinides, Th, U and Pu from each other.
- Successful partitioning of Pu(III) from Th was achieved when ferrous sulfamate was used as the Pu-holding reductant.
- The flows and acidities required for recovery of Th with the solvent stream from Contactor III are such that hydroxylamine nitrate cannot prevent the oxidation of Pu(III) which occurs predominantly in the organic phase in the settlers, and Pu losses are sustained.
- The oxidation of Pu(III) in the organic phase and its enhancement by the presence of HNO_2 in the organic phase was confirmed.
- SECTOR, a modification of the computer code SEPHIS, has been used successfully to calculate solute behaviour in mixer-settler experiments. It also accounts for the oxidation of Pu(III) in the organic phase although improvements to this part of the code could be made when the kinetics of the oxidation are established.

Acknowledgements

We wish to thank L.J. Clegg, R.J. Porth, D.G. Juhnke of the Chemical Technology Branch, and R.W. Dyck, C. Murphy and their colleagues in the Analytical Science Branch for their contributions to the above work.

Literature Cited

1. Critoph, E., Banerjee, S., Barclay, F.W., Hamel, D., Milgram, M.S., Veeder, J.I., Atomic Energy of Canada Limited Report, AECL-5501 (1976).
2. Critoph, E., Atomic Energy of Canada Limited Report, AECL-5705 (1977).

3. Morgan, W.W., Atomic Energy of Canada Limited Report, AECL-508 (1958).
4. Ryon, A.D., Oak Ridge National Laboratory Report, ORNL-3045 (1961).
5. Schulz, W.W., Pacific Northwest Laboratory Report, BNWL-57 (1965).
6. Smee, J.L., Clegg, L.J. Juhnke, D.G., and Porth, R.J., unpublished data.
7. Farrell, M.S. and Goldrick, J.D., AAEC/E26 (1958).
8. Rainey, R.H. and Moore, J.G., Nucl. Sci. & Eng., 1961, 10, 367.
9. Schuelein, V.L. ARH-SA-233 (1975).
10. Richardson, G.L. and Swanson, J.L., Hanford Engineering Development Laboratory Report, HEDL-TME-75-31 (1975).
11. Biddle, P., McKay, H.A.C. and Miles, J.H., in "Solvent Extraction Chemistry of Metals", MacMillan, London, 1965.
12. Grossi, G., International Solvent Extraction Conf., Toronto, 1977.
13. Groenier, W.S. Oak Ridge National Laboratory Report, ORNL-4746 (1972).
14. Koltunov, V.S. and Marchenko, V.I., Soviet Radiochem., 1973, 15, 754.
15. Gourisse, D., Paper 106, "Proc. Int. Solv. Extr. Conf.", The Hague, 1971, Soc. of Chemical Industry, London, 1971.
16. McCutcheon, E.B., Burkhart, L.E., and Felt, R.E., Advances in Instrum., 1975, 30, 716.
17. Barney, G.S., J. Inorg. and Nuc. Chem., 1976, 38, 1677.
18. Woodhead, J., AERE-R-3432 (1960).
19. Fuson, R.C., "Reactions of Organic Compounds", John Wiley & Sons, 1966.
20. Rozen, A.M., Zel'Venskii, M. Ya., Shilin, I.V., Translated from Atomnaya Energiya, 1975, 38, 367.

RECEIVED May 11, 1979.

Improvements in Thorium-Uranium Separation in the Acid-Thorex Process

GLEN E. BENEDICT

General Atomic Company, San Diego, CA 92138

The Acid-Thorex process has been used in recent years to recover ^{233}U from neutron irradiated thoria targets.⁽¹⁻⁴⁾ This process uses n-tributyl-phosphate (TBP) in normal paraffin hydrocarbon (NPH) as the extractant and the relative uranium and thorium solubilities in each phase are adjusted by control of the nitric acid concentration. The Acid-Thorex process is the primary candidate for use in proposed aqueous thorium fuel cycles. In this process, uranium is separated from thorium through exploitation of the difference in equilibrium distributions since no usable valence change is available to aid in this separation.

This report describes some of the flowsheet development work done in the General Atomic Company pilot plant pulse column equipment in support of the High Temperature Gas Cooled Reactor (HTGR) Fuel Recycle Development Program. Data are presented showing the beneficial effect of adding low concentrations of fluoride ion to the thorium partitioning solution. These data also show the results of tests where dibutylphosphate (DBP) was added to simulate solvent degradation and cold zirconium and ^{95}Zr tracer to simulate fission product zirconium.

Fluoride addition not only improves the thorium-uranium separation, but also minimizes the precipitation of thorium dibutylphosphate in the uranium stripping column which has been a major problem in processing thorium based nuclear fuel materials using this process.^(3,4)

Experimental

Flowsheet testing and data collection were performed using the General Atomic Company solvent extraction pilot plant equipment shown in Figure 1. Included in this equipment are several 5.1 to 7.6 cm (2 to 3 in.) diameter cylindrical glass pulse columns, a 15.2 cm (6 in.) diameter annular pulse column, a centrifugal contactor (Robatel Co.) and associated tanks, feed systems and concentrators.

0-8412-0527-2/80/47-117-371\$05.00/0

© 1980 American Chemical Society

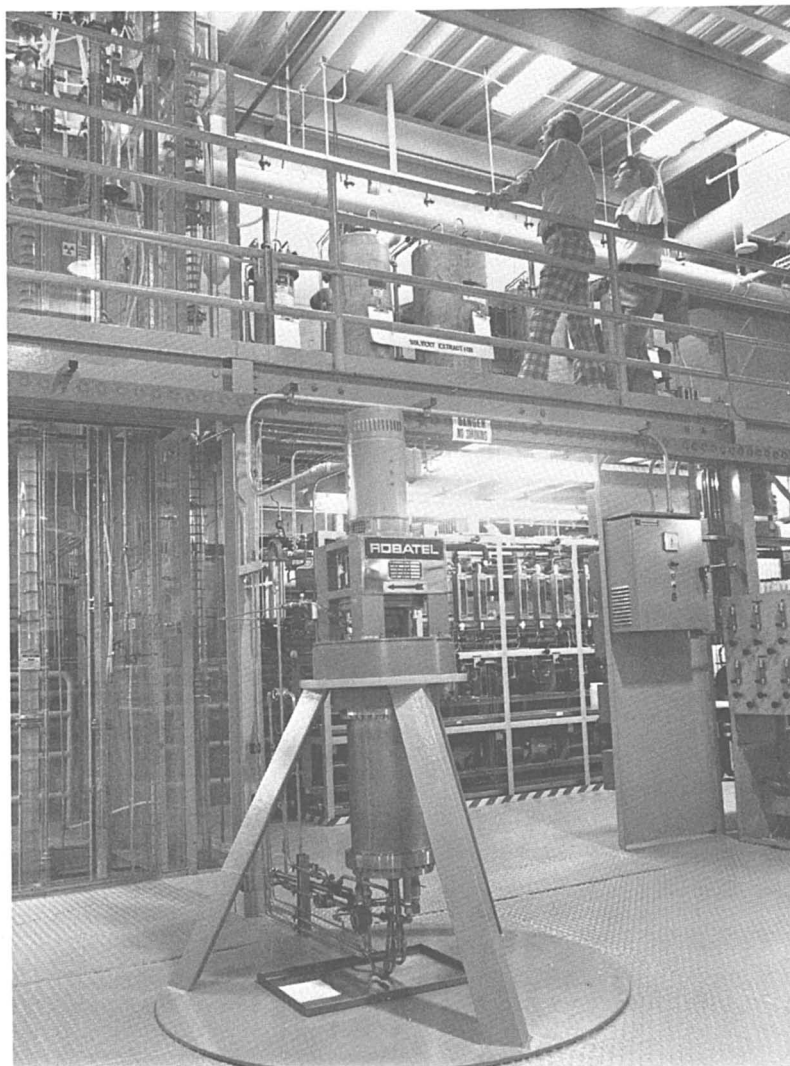


Figure 1. Solvent extraction pilot plant

The flowsheet used in these studies is shown in Figure 2 and illustrates the path of thorium through the partition cycle. The thorium, uranium, and fission products enter at the center of the extraction-scrub (1A) column and the uranium and thorium are extracted into the rising solvent with the fission products being largely rejected with the nitric acid. The loaded solvent is transferred to the bottom of the partition column (4.6 m (15 feet) long, about 4 to 5 theoretical stages) where it rises through the thorium partition solution (1BX). A change in flow rate and nitric acid concentration allows most of the thorium and very little uranium to be stripped from the solvent. The fluoride additions were made into the thorium partition solution (1BX) stream.

The partition cycle columns were operated on flowsheet values and then a DBP solution was pumped to the extraction feed point in increasing amounts. The thorium content of the uranium product stream from the thorium partition column was monitored. The runs were then repeated using increasing increments of fluoride in the thorium partition solution and the thorium content again monitored in the uranium product from the partition column.

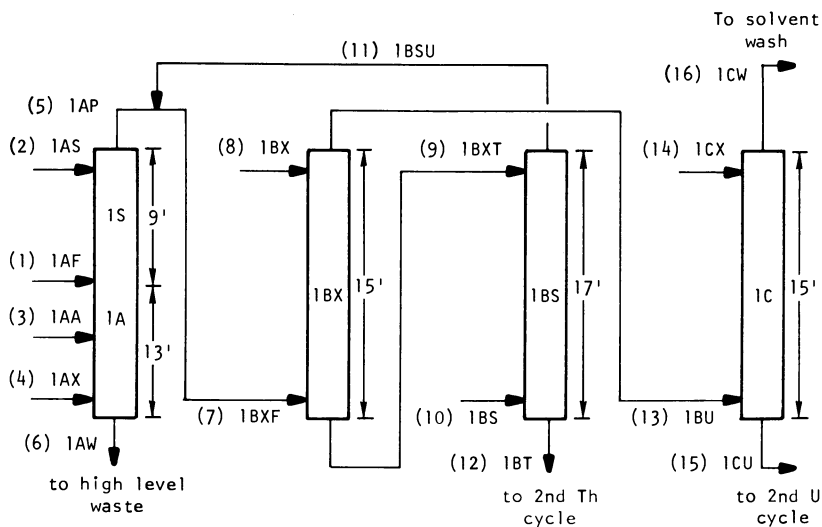
Residual small amounts of thorium in the uranium stream after thorium partitioning were analyzed by ion exchange chromatography from a chloride medium followed by Thorin colorimetry.

Results and Discussion

Fluoride is known to separate zirconium fission product and plutonium from solvent degradation products.⁽⁵⁾ Since fluoride is used to speed dissolution of thoria in nitric acid, and is already present in thorium solvent extraction process feed solutions, it was the first choice as an agent to use to improve thorium-DPB separation.

The results of adding no fluoride and 0.001 and 0.005 M fluoride to the thorium partition solution are shown in Figure 3. An improvement of a factor of 10 in thorium separation from uranium is obtained with the 0.005 M fluoride, a concentration recommended for process use. This amount of fluoride increases the total fluoride concentration in the high level waste by 40%. Furthermore, this amount of fluoride addition increased the operability of the downstream uranium strip column by lowering the precipitation of thorium-DBP in that column where the acidity is lower. The thorium-DBP precipitation caused problems in the processing of thorium target elements⁽⁴⁾ where this column periodically required cleaning to remove the sticky precipitate. The decrease of the thorium-DBP precipitation is probably the more significant result of the fluoride addition. The effect of DBP on uranium carry over to the solvent wash system in the ICW stream is also shown in Figure 3.

Early solvent extraction flowsheets for HTGR fuels recycle developed at the General Atomic Company contained a coextraction costrip cycle for thorium and uranium prior to the partitioning



Stream	Stream No.	Relative Flow Rate	U (g/l)	Th (g/l)	HNO ₃ (M)
1AF	1	100	35	348	1.0
1AS	2	130	--	--	1.0
1AA	3	40	--	--	13.0
1AX	4	1000	--	(30% TBP)	--
1AP	5	1000	3.5	35	0.2
1AW	6	270	0.005	0.05	2.0
1BXF	7	1180	--	--	--
1BX	8	600	(F 0.001 to 0.005 M)	--	0.2
1BXT	9	600	--	--	--
1BS	10	180	--	(30% TBP)	--
1BSU	11	180	2.5	20	0.1
1BT	12	600	0.001 to 0.005	58	0.5
1BU	13	1180	2.98	(See Fig. 3)	0.02
1CX	14	593	--	--	0.01
1CU	15	593	5.93	Trace	0.03
1CW	16	1180	0.003	(30% TBP)	0.001

Figure 2. Acid-Thorex partition cycle flowsheet

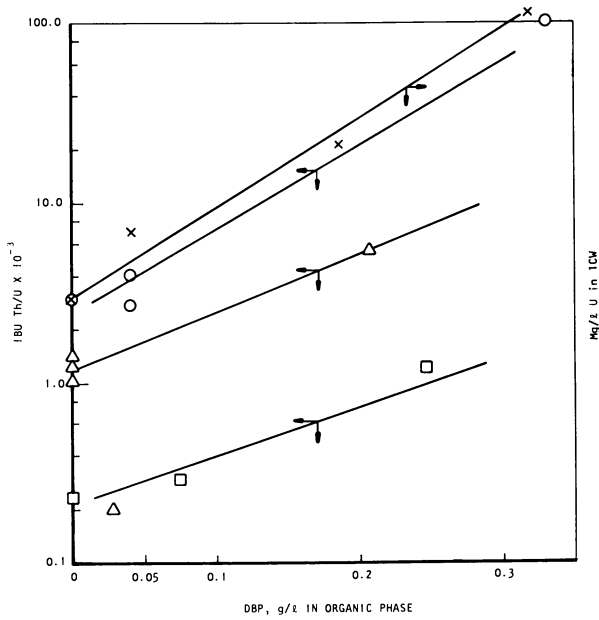


Figure 3. Effects of fluoride in 1BX stream: (O) no F^- in 1BX; (Δ) 0.001M F^- in 1BX; (\square) 0.005M F^- in 1BX; (\times) 0.001M F^- in 1BX.

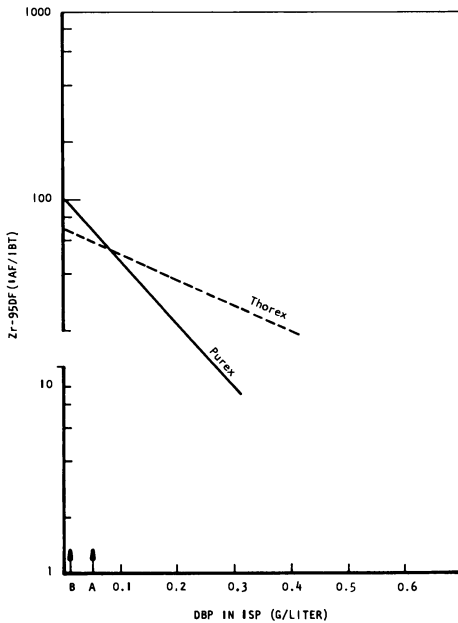


Figure 4. Measured ^{95}Zr decontamination factors: (A) estimated DBP level in processing 180-day cooled reference fertile particles in pulsed column; (B) same as above with Robatel centrifugal contactor.

cycle. Since most radiation damage to the solvent occurs in the first solvent extraction cycle, most of the DBP will be formed there. In a coextraction cycle, the thorium-DBP precipitates in the co-strip column in a manner which is very deleterious to process operation. That fact, coupled with the above observations using fluoride to aid separation of thorium and DBP, led to the recommendation that the uranium thorium partition cycle be the first cycle in any Acid-Thorex flowsheet arrangement on spent thorium fuels.

It is of interest to note that addition of 0.001 M fluoride to the extraction scrub solution did not improve the zirconium-thorium separation significantly in the scrub section. A large improvement in zirconium-uranium separation has been observed by addition of fluoride to scrub streams in the Purex process. This difference is probably due to the thorium complexing the fluoride and lowering the free fluoride to a level which is ineffective in altering zirconium distribution.

It is also of interest to note that the effect of DBP on zirconium separation from thorium in the Acid-Thorex system is different than zirconium separation from uranium in the Purex system. (Figure 4) The Purex data are from reference 6 and the Acid-Thorex data are from General Atomic Company pilot plant studies. The thorium probably forms a stronger DBP complex than does uranyl ion and, therefore, the amount of uncomplexed DBP available for raising the equilibrium distribution of zirconium would be less in the Acid-Thorex process.

Conclusions

In the Acid-Thorex process, fluoride ion should be added to the thorium partitioning solution (IBX) to decrease thorium transfer to the uranium stripping column, particularly where highly radioactive feeds are used. This fluoride ion addition then decreases the precipitation of thorium-DBP in the uranium stripping column. Also, the partition cycle should be the first cycle in the Acid-Thorex process to allow separation of thorium from DBP.

Acknowledgments

The author acknowledges the contributions of G. W. Reddick, R. G. Wilbourn and L. E. Jolley to the study reported here. Additional data from their reports are contained in references 7 and 8.

Literature Cited

1. Rainey, R. H.; Moore, J. G., Nuc. Sci. and Eng., 1961, 10, No. 4, 367.
2. Haas, W. O., Jr.; Smith, D. J., U.S. Atomic Energy Commission

- Report KAPL-1306, General Electric Co., Schenectady, New York, 1956.
3. Rathvon, J.C.; Blasewitz, A. G.; Maher, R.; Eargle, J. C., Jr.; Wible, A. E., Recovery of ^{233}U from Irradiated Thoria in "Thorium Fuel Cycle-Proceedings of Second International Thorium Fuel Cycle Symposium, Gatlinburg, Tennessee, May 3-6, 1966," U.S. Atomic Energy Commission Report CONF-660524, Oak Ridge National Laboratory, Oak Ridge, Tennessee, 1968; pp. 765-824.
 4. Jackson, R. R.; Walser, R. L., Eds., U.S. Energy Research and Development Administration Report ARH-2127, Atlantic Richfield Hanford Company, Richland, Washington, 1977.
 5. Swanson, J. L., U.S. Atomic Energy Commission Report BNWL-1588, Pacific Northwest Laboratory, Richland, Washington, 1971.
 6. Richardson, G. L., U.S. Atomic Energy Commission Report HEDL-TME-73-51, Westinghouse Hanford Company, Richland, Washington, 1973.
 7. Reddick, G. W., U.S. Energy Research and Development Administration Report GA-A13835, General Atomic Company, San Diego, California, 1976.
 8. Wilbourn, R. G., U.S. Department of Energy Report GA-A15030, General Atomic Company, San Diego, California, 1978.

RECEIVED July 2, 1979

Work performed under U.S. Government contract number DE-AT03-76SF1053.

Actinide Partitioning Flowsheets

D. D. TEDDER¹, B. C. FINNEY, and J. O. BLOMEKE

Oak Ridge National Laboratory, Oak Ridge, TN 37830

During the past three years, the Department of Energy has funded an R&D program (1,2,3,4,5) to study actinide partitioning for waste management purposes. A large part of this effort has been related to the development of credible, chemical processing flowsheets for removing actinides from fuel reprocessing and refabrication wastes. The result is a concept of waste treatment facilities (WTFs) that are adjacent to, but not integral with, either conventional or safeguarded reprocessing and refabrication plants. These WTFs treat wastes as they are generated during spent fuel recycle operations, remove residual actinide contamination from the wastes, recycle a mixture of concentrated actinide nitrates to the main processing facilities, and discharge treated wastes to the on-site waste treatment facilities for final packaging and terminal storage.

The operation of the WTFs for actinide partitioning does not exclude any particular safeguard strategy, since the concentrated actinides recovered from the wastes are returned to the on-site facility that produced them via a shielded, underground pipeline. Moreover, the operation of the WTF is largely independent of the flowsheet operated in the main processing plant insofar as the same generic wastes are produced from a Purex plant regardless of whether or not the actinides are coprocessed or processed separately. Generically, the wastes will have the same compositions, although there may be differences in the quantities of waste.

A primary objective of the DOE program has been to develop actinide partitioning flowsheets that are defensible from the standpoint of chemical feasibility. A four-point strategy was adopted in order to meet this objective:

1. Utilize only demonstrated technology that is readily applicable to commercial recycle operations.

¹Present address: Georgia Institute of Technology, School of Chemical Engineering, Atlanta, GA 30332.

0-8412-0527-2/80/47-117-381\$05.00/0

© 1980 American Chemical Society

2. Develop generic capabilities to deal with all types of wastes.
3. Choose processing systems that complement each other and provide actinide recovery opportunities in depth.
4. Experimentally evaluate the proposed treatment concepts.

The first of these points greatly reduced the scope of the study, since many possible separation schemes (e.g., pyrochemical) were excluded on this basis. The second point tended to expand the scope of the study, since work prior to this program had focused almost exclusively on removing actinides from the high-level liquid wastes. However, it is well known that significant actinide losses occur to other wastes as well (e.g., HEPA filters, incinerator ashes, chemical salt wastes, dissolver solids, etc.) and, as far as waste management is concerned, it is essentially meaningless to ignore these wastes.

Point three is important with respect to providing additional assurance that the required levels of actinide decontamination can be routinely met in a large-scale operation. Unfavorable interactions between processes within the WTF can make the system unworkable, even if the separated processes operate well alone. On the other hand, complementary systems provide recovery backup that can be exploited by considering the consequences of various recycle strategies within the WTF under conditions of maloperation.

The experimental assessments so far have yielded favorable results as far as achieving the partitioning objectives. Of course, these tests are not conclusive, since they have been performed on only a very small scale and only separate subsystems have been examined. However, there does not appear to be any fundamental reason that precludes achieving the stated partitioning goals and, in fact, it may be possible to exceed them. Rather, the question appears to be one of cost and diminishing returns on incremental investment.

Actinide Partitioning Goals

The partitioning of actinides from waste has been viewed as a means to reduce or mitigate the long-term biological hazard of nuclear waste (after 1000 years of storage) by achieving higher removal of all actinides from the waste than has been attained in the past (6,7,8,9). After 1000 years in geologic isolation, it is the actinide concentrations in the stored wastes which dominate its radiotoxicity. With these elements more completely removed before isolation the waste may be less harmful, even if released to the environment in the distant future. Therefore, the actinide partitioning goals were set at levels such that the radiotoxicity of the resulting waste forms after 1000 years would be comparable to that of natural bodies of radioactive ores.

In summary, these goals would be largely achieved if the actinide losses to all reprocessing wastes can be kept below 0.1% of the main plant feed and if the losses to refabrication wastes can be kept below 0.15% of the actinides refabricated.

Waste Treatment Systems

The subsystems for a WTF supporting a fuel reprocessing plant have been subdivided into the following treatment areas: (1) High-Level Solid Waste Treatment, (2) High-Level Liquid Waste Treatment, (3) Solid Alpha Waste Treatment, (4) Cation Exchange Chromatography, (5) Salt Waste Treatment, (6) Actinide Recovery, (7) Solvent Cleanup and Recycle, (8) Off-Gas Treatment, (9) Product Concentration, and (10) Acid and Water Recycle. Each of these areas has major design problems; the WTF supporting a fuel fabrication facility is similar, but without areas 1 and 2. In both cases, all subsystems are integrated so as to operate together in a single, on-site processing building.

High-Level Solid Waste Treatment. Cladding hulls and dissolver solids are generated as wastes from reprocessing LWR fuels. The alpha activity associated with these head-end wastes is normally low, but as a precautionary measure the WTF provides an area where these wastes may be given an extended tertiary $\text{HNO}_3/\text{KF}/\text{HCl}$ leach. Experimental studies with mixed-oxide reactor fuels (10,11,12) suggest that actinide losses can be held to 0.01% or less if fluoride and chloride are present in the leachant.

High-Level Liquid Waste (HLLW) Treatment. The high-level liquid waste is produced as a raffinate from the HA solvent extraction cycle in Purex. After generation, the HLLW is immediately transferred to the WTF via an underground pipeline without concentration or interim storage. This strategy minimizes the problems associated with solids precipitation.

Upon entry into the WTF, the HLLW is contacted (see Figure 1) with the bidentate extractant dihexyl-N,N-diethylcarbamylnmethylene phosphonate (CMP) which is diluted to 30 vol % with di-isopropylbenzene. Under high acid conditions (13,14), this extractant will remove all trivalent and tetravalent actinides to some degree from the HLLW. Of the fission products, only Zr, Tc, Ru, Mo, Nb, Y, and Pd extract to any significant extent. These species can be controlled either by subsequent scrubbing of the organic phase or by adjusting extraction conditions so as to reject those fission products that exist as anions to the raffinate.

After scrubbing, the coextracted actinides and lanthanides are removed from the organic phase by two separate strip columns (a reductant and dilute nitric acid strip, followed by a dilute oxalic acid strip). After destruction of the excess oxalic acid, the two strips are combined with other recycle streams that are

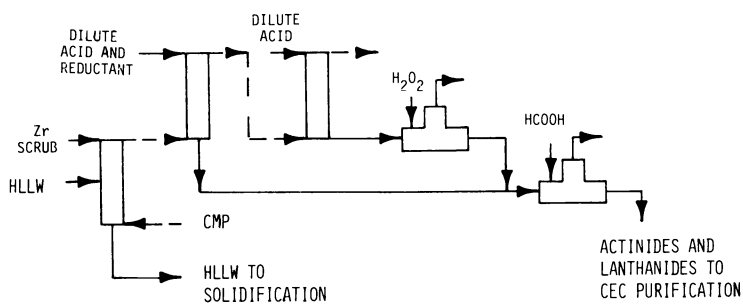


Figure 1. The high-level liquid waste can be adequately partitioned by solvent extraction with 30% CMP.

produced in the WTF, concentrated, partially denitrated and sent to cation exchange chromatography for lanthanide removal.

Experimental results to date (13), using actual HLLW generated from dissolving H. B. Robinson reactor fuel that had a burnup of $\sim 27,000$ MW days/MT and had been cooled for about 2 years, suggest that greater than 99.99% of the tetravalent actinides and greater than 99.9% of the trivalent actinides may be removed using CMP extraction subsequent to Purex. Also, by adding small amounts of fluoride to the HLLW before CMP extraction, it may be possible to convert this stream into a non-transuranic waste (i.e., <10 nCi α /g of HL glass). However, without fluoride this goal does not seem possible due to the presence of small amounts of inextractable tetravalent actinides.

Solid Alpha Waste Treatment. Solid Alpha Waste Treatment consists of those processing steps that have been developed to remove actinides from contaminated HEPA filters and incinerator ashes. These wastes are generated from the nitrate-to-oxide conversion step in reprocessing, comminution steps during pellet fabrication, and the incineration of alpha-contaminated combustibles that result from cell cleanup and glove box operations. Generally, from 0.5 to 2.5% of the actinide feed to the fuel reprocessing and refabrication plants may be lost to these wastes. Actinide recovery from them is complicated by mechanical handling problems that result from the waste bulk, possible chemical interferences from the bulk wastes, and the intractability of refractory actinide oxides.

As conceived, much of the initial mechanical handling of these wastes occurs in the feed preparation area of the on-site, radwaste incinerator. HEPA filters are initially disassembled in the preparation area of the on-site incinerator which is assumed to exist as a separate entity from the WTF. The HEPA frames are burned in the incinerator; the HEPA media are shredded and placed in 55-gal drums which are then placed into on-site transfer containers and sent to the receiving area of the WTF. Incinerator ashes are similarly placed in 55-gal drums and transferred on-site to the WTF.

Because of the handling problems associated with these wastes, the Alpha Waste Treatment Area in the WTF is more correctly designated as a mechanical, rather than a chemical, hot cell. Upon receipt of the shredded HEPA filters, they are dumped into a hopper and metered through a low-temperature (300°C) asher with a screw. This step partially oxidizes any high-molecular-weight glues or binding materials that may have been used to fabricate the HEPA filters. Subsequently, the HEPA waste is metered into an accumulation hopper for eventual loading into the HEPA leaching equipment. Hoppers are used in this fashion to permit the low-temperature asher to operate continuously, while the leaching step is a batch operation.

Actinides are removed from the HEPA waste by leaching them with a mixture of nitric acid and ceric nitrates. Intimate contact is achieved through the use of a specially designed thermosiphon/oxidizer apparatus consisting of a vertical cylinder that is connected at the top and bottom to a smaller, stirred oxidizer tank that contains the electrodes. The HEPA waste is charged to the top of the cylinder which becomes a fixed HEPA bed. Leachant is circulated upward through the cylindrical fixed bed, horizontally to the oxidizer tank where it is cooled slightly and electrolytically reoxidized, then downward into the thermosiphon leg until it is reintroduced into the bottom of the fixed bed cylinder. The thermosiphon effect is induced by steam jacketing the cylindrical fixed bed and a portion of the leg feeding into it, while cooling the leachant slightly in the stirred oxidizer tank that also receives cold reflux from the off-gas condenser.

A leaching cycle begins by screw metering a batch of waste from the accumulation hopper into the top of the cylindrical bed. Next, a mixture of nitric acid, cerous nitrate and gadolinium nitrate is charged to the thermosiphon. Fluid circulation is induced by steam heating the HEPA bed and the thermosiphon leg. As the leachant circulates and approaches reflux temperature, an electrical potential is applied across the electrodes in the oxidizer tank that converts the cerous nitrate into a mixture of cerous and ceric nitrates. Since the latter species are either neutral or anions in solution, it is not necessary to separate the electrodes with a diaphragm in the electrolytic oxidation tank. However, the cathode is partly shielded with a cylindrical finger that surrounds it and air-sparged to remove nitrous acid which does reduce the ceric species.

After several hours of oxidative leaching at reflux temperatures, the leachant is cooled and reduced by the addition of oxalic acid. (The oxalic acid converts the ceric nitrates back to cerous nitrate, which is compatible with stainless steel; the leaching equipment must be constructed of titanium.) The solution is then transferred to a holding tank for subsequent centrifugation and actinide removal. The HEPA filter residue is washed several times with nitric acid and water, compacted to about its original volume by expressing the entrained water with a slight air pressure at the top of the leaching cylinder, and discharged as a slug into a hopper below the leaching apparatus. Subsequently, the HEPA waste is screw metered back into 55-gal drums which are then sent to the on-site solid waste treatment facilities where the waste is immobilized with concrete and eventually transported off-site to a terminal waste storage facility.

Incinerator ashes are decontaminated simply by loading them into a separate, stirred electrolytic oxidizer tank. The cathode in this tank is partly shielded from the anode and air-sparged to remove nitrous acid. After several hours of leaching at reflux, the excess ceric nitrates may be reduced with oxalic acid, the

solution cooled, and then sent to a holding tank for centrifugation to remove the ash residue.

Clearly these operations are complex, especially for a remote operation, but the experimental studies (2,3,4,5,15,16) suggest that they are probably technically feasible, although very expensive. The ceric nitrate leaching has several important features, relative to fluoride, that should be mentioned. First of all, it is about as effective as fluoride in accelerating the dissolution of all transuranic actinides. Secondly, the ceric nitrates do not dissolve or greatly soften the HEPA filter waste, whereas fluoride converts the HEPA fiberglass into an intractable, gooey mess that cannot be pumped or filtered. Similarly, fluoride totally dissolves incinerator ashes, whereas this latter waste is only partly dissolved (~50%) by the ceric nitrate leach. Also, the ash residue resulting from cerium treatment is readily centrifuged. After treatment, the HEPA waste retains much of its fibrous, pulpy character and can be screw metered into 55-gal drums.

In terms of decontamination, the ceric leaching appears adequate for HEPA filters. The experimental studies (5,15,16) have achieved 99.99% dissolution of the most refractory of the tetravalent actinides. However, the leaching of the incinerator ashes (5,16) has been less successful, since as much as 5% of the alpha activity initially in this waste does not dissolve with ceric treatment alone. However, this last 5% may be recovered by dissolving the ash residuum entirely with fluoride. (This 5% loss would represent about 0.05% of the actinide feed to the main plant.)

For waste management, cerium-promoted dissolution has another important characteristic relative to fluoride dissolution. Fluoride dissolves these wastes totally and is not readily recycled, since it is consumed by the formation of silicon fluorides. In this case, the fluoride reagent becomes a waste that must be disposed of at greater expense, since this fluoride addition increases the weight and bulk of the chemical wastes that must be converted to immobile solids (i.e., a concrete or glass waste). Cerium, on the other hand, can be recycled within the WTF by coextracting it with the trivalent actinides using the CMP extractant in the Actinide Recovery Area. Gadolinium can also be recycled with the cerium and used as a neutron poison in the Solid Alpha Waste Treatment equipment, thereby eliminating the need for critically safe geometry. Although some increase in waste quantities results from this strategy (primarily from the solvent cleanup scrub wastes), these increases are modest compared to the consequences of fluoride-promoted dissolution.

Cation Exchange Chromatography (CEC). This process is identical to that described elsewhere (17), except that a number of small batches must be run in parallel in order to deal with the large quantities of curium that build up due to the recycle of the

transuranics. This problem is dealt with by a modular approach in designing the cation exchange racks. Each rack (or module) consists of a single feed column and two elution columns mounted on a balanced frame that has overall dimensions about the size of an office file cabinet. In this manner, the watts per batch of radioactive material loaded onto the module are kept small.

The experimental work relating to this processing area has focused on identifying any interactions between the cation exchange chromatography (CEC) area of the WTF and the HLLW Treatment Area that produces the CEC feed, and in determining the elution sequence for the tetravalent actinides. Both studies (5,18) gave favorable results. The expected impurities in the feed to the CEC will not significantly affect system performance. No evidence for CEC feed adjustment beyond the control of acidity level appears to be necessary. Also, it was verified that the tetravalent actinides will elute ahead of the barrier ion in CEC; therefore, these elements will report to the Salt Waste Treatment system as desired.

Salt Waste Treatment. Alkaline and acidic salt wastes are produced from a variety of sources during fuel reprocessing and refabrication. The most important of these wastes, with respect to actinide losses, is the alkaline sodium carbonate scrub waste that is generated during TBP recycle and cleanup. This waste may contain up to 0.5% of the actinide feed, along with the solvent degradation products (sodium salts of monobutyl and dibutyl phosphoric acids). These acidic degradation products prevent actinide stripping from a neutral extractant such as TBP and, therefore, they must be removed from the waste before the actinides can be recovered by TBP solvent extraction. Additional troublesome salt wastes are the alkaline detergent wastes containing surfactants that extract into TBP and, in the WTF, the sodium carbonate scrub wastes resulting from CMP recycle and cleanup.

These potential losses are unacceptable during actinide partitioning, but recent developments at Argonne National Laboratory have led to an effective chemical treatment using 2-ethylhexanol. Detergent wastes may also be treated.

The Argonne process (5,19), designated as "alcohol extraction," (see Figure 2) consists of acidifying the alkaline wastes and then contacting them with 2-ethylhexanol. This alcohol is a very effective extractant for those acidic degradation products like dibutyl and monobutyl phosphoric acids, but only weakly extracts the actinides which remain in the raffinate. Consequently the raffinate may be subsequently treated with 30% TBP and CMP for actinide recovery since it no longer contains those acidic degradation products that would otherwise extract and prevent stripping. The alcohol extractant which contains the degradation products (and any detergents as well) is then recycled by washing out these acidic species with sodium carbonate.

Recent test results (19) appear very favorable for this system. Although it is relatively robust, a further improvement has been identified through the addition of small amounts of diethylenetriaminepentaacetic acid (DTPA) to the sodium carbonate scrub before it is contacted with used TBP or CMP. Under these conditions, the actinide loadings in the carbonate scrub can be increased significantly before interfacial cruds appear. Also, when the resulting alkaline waste is acidified, neither interfacial cruds nor actinide polymers are formed. Actinides are then easily recovered by TBP solvent extraction from the alcohol extraction column raffinate, and can be stripped from TBP and CMP in the usual fashion.

Actinide Recovery Area. Both WTFs require an Actinide Recovery Area where actinides are recovered from the liquors being produced in the above-mentioned treatment areas. The WTF supporting the fuel reprocessing plant (see Figure 3) requires both a TBP and CMP extraction cycle, but the WTF supporting the fuel refabrication plant can be operated with a CMP extraction cycle alone and by utilizing the existing, on-site TBP scrap recovery system.

In both cases, the various actinide-bearing liquors are concentrated, acidified, and clarified by centrifugation as needed. Subsequently, the concentrate is contacted with TBP and then with CMP. The raffinate, now essentially actinide-free, is further concentrated, denitrated with formic acid, and the resulting slurry converted to a concrete waste that is packaged in 55-gal drums. The TBP organic is stripped in the usual manner, with the recovered actinides being sent back to the main processing facility. The CMP organic is stripped in two columns, similar to the operation of the HLLW treatment strip columns (see Figure 1), to recover the stable cerium and gadolinium for recycle to the Solid Alpha Waste Treatment Area. Low concentrations of trivalent actinides are maintained in the cerium recycle stream by bleeding a fraction of this stream to the CEC system. Thus, the major differences between the Actinide Recovery Area and the HLLW Treatment Area are the anticipated higher levels of radioactivity in the latter system.

Solvent Cleanup and Recycle. Both TBP and CMP solvents can be cleaned up with simple water and dilute sodium carbonate washes. The conceptual flowsheets also include preequilibration of the solvents with acid before they are recycled to the extraction columns. This treatment helps to maintain high acid concentrations in the extraction column raffinates. For the CMP extractant, equilibration with high acid also helps to strip the ruthenate and pertechnetate anions from the solvent. Activity levels in the Actinide Recovery Area are further controlled by bleeding a fraction of its CMP solvent to the CMP Solvent Recycle

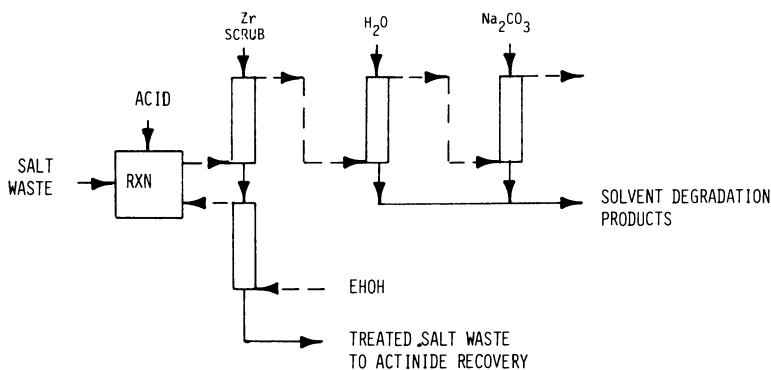


Figure 2. Actinides may be recovered from acidified salt wastes by TBP extraction after the degradation products have been removed using 2-ethylhexanol extraction.

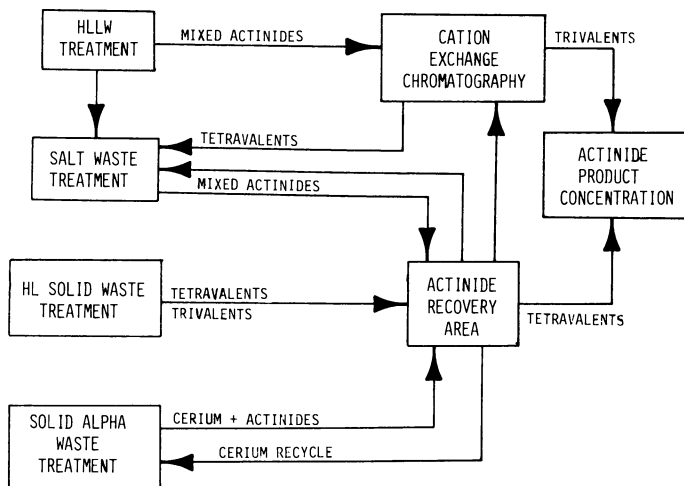


Figure 3. Actinide recycle occurs between the subsystems within the WTF. Wastes enter the subsystems in the left column. Actual recovery occurs in the central column subsystems. A mixture of actinide nitrates is sent from Actinide Product Concentration to the fuel reprocessing plant for codenitration.

Area for HLLW Treatment. Also, a small fraction of the CMP extractant from the HLLW Treatment Area is continuously sent to the on-site solvent burner.

Off-Gas Treatment. Both WTFs require extensive off-gas treatment. The adequate removal of nitrogen oxides appears especially troublesome for the WTF supporting the fuel reprocessing plant, since considerable amounts of acid denitration occur in the flowsheets. Also, ruthenium volatilization is problematic in the Solid Alpha Waste Treatment Area, so ruthenium adsorption beds are provided to treat these off-gases. The design strategy is to air-sparge the electrolytic oxidizer tanks and adsorb any oxidized ruthenium on silica gel beds, rather than allowing it to reflux in the oxidizers. The fuel reprocessing plant WTF will also require iodine retention systems; both WTFs utilize extensive HEPA filtration and catalytic NO_x destruction as a polishing step.

Acid and Water Recycle. Acid and water recycle is a significant problem, especially in the fuel reprocessing WTF. The streams generated internally by the WTFs are characteristically voluminous, with low levels of alpha activity, but containing large amounts of dissolved solids. This condition results in a need to recycle large quantities of dilute acid and water as evaporator overheads. However, the high levels of dissolved solids in the WTF waste evaporator feeds severely limit the extent to which solvent extraction feeds to the Actinide Recovery Area can be concentrated without precipitating chemical solids and thereby running the risk of additional actinide losses by coprecipitation. Because of the dissolved solids constraint, the pulse columns required for use in the Actinide Recovery Area of the WTF are about the same size as those required in the HLLW Treatment Area, although the actinide concentrations in the Actinide Recovery Area feeds are about an order of magnitude lower than in the HLLW. Thus, the dissolved solids result in less efficient operation in the Actinide Recovery Area than is possible in the HLLW Treatment Area.

Conclusions

The actinide partitioning program will show (20) that alpha-bearing wastes can probably be partitioned to a level that would significantly reduce the actinide concentrations in the resulting wastes. Also, the waste quantities would not be greatly increased because of WTF operation. No increase in HL glass quantities is anticipated. The LL and IL fuel reprocessing concrete wastes would increase about 25% in volume while the fuel fabrication waste volumes would increase about 16% with these flowsheets. However, the WTF that partitions fuel reprocessing wastes may actually be larger in size than the main reprocessing plant

itself. It appears technically feasible to develop chemical systems for dealing with all types of alpha wastes, but these treatment systems are themselves highly complex. A simple Purex plant only uses one solvent (i.e. TBP); a WTF would utilize at least three different solvents (i.e. TBP, CMP, and 2-ethylhexanol). In addition, the WTF would require complex mechanical hot cells to treat HEPA filter wastes and incinerator ashes, as well as operate a bank of cation exchange chromatography columns. Although the CEC system might be replaced with an equivalent solvent extraction cycle, this improvement would be small since the resulting WTF would then be utilizing four different solvents.

Acknowledgments

This research was sponsored by the Office of Nuclear Waste Management, U.S. Department of Energy under contract W-7405-eng-26 with the Union Carbide Corporation.

Literature Cited

1. Croff, A. G., Tedder, D. W., Drago, J. P., Blomeke, J. O., and Perona, J. J., "A Preliminary Assessment of Partitioning and Transmutation as a Radioactive Waste Management Concept," ORNL/TM-5808, Oak Ridge National Laboratory, Oak Ridge, TN (1977).
2. Tedder, D. W. and Blomeke, J. O. (ed.), "Actinide Partitioning and Transmutation Program Progress Report for Period October 1, 1976 to March 31, 1977," ORNL/TM-5888, Oak Ridge National Laboratory, Oak Ridge, TN (1977).
3. Tedder, D. W. and Blomeke, J. O. (ed.), "Actinide Partitioning and Transmutation Program Progress Report for Period April 1 to June 30, 1977," ORNL/TM-6056, Oak Ridge National Laboratory, Oak Ridge, TN (1977).
4. Tedder, D. W. and Blomeke, J. O. (ed.), "Actinide Partitioning and Transmutation Program Progress Report for Period July 1 to September 30, 1977," ORNL/TM-6174, Oak Ridge National Laboratory, Oak Ridge, TN (1978).
5. Tedder, D. W. and Blomeke, J. O. (ed.), "Actinide Partitioning and Transmutation Program Progress Report for Period October 1, 1977 to March 31, 1978," ORNL/TM-6480, Oak Ridge National Laboratory, Oak Ridge, TN (1978).
6. Beaman, S. L., *Trans. Am. Nucl. Soc.* (1975) 22, 346.
7. Claiborne, H. C., "Effect of Actinide Removal on the Long-Term Hazard of High-Level Waste," ORNL/TM-4724, Oak Ridge National Laboratory, Oak Ridge, TN (1975).
8. Gasteiger, R., "Development of an Irradiation Technology for the Recycling of Am-241 in Nuclear Reactors - A Contribution to the Possibilities for the Reduction of the Hazard Potential of α -Bearing Wastes," (in German), KFK-2431, Nuclear Research Center, Karlsruhe, Federal Republic of Germany (1977).

9. Haug, H. O., "Production, Disposal, and Relative Toxicity of Long-Lived Fission Products and Actinides in the Radioactive Wastes from Nuclear Fuel Cycles," (in German), KFK-2022, translated as ORNL-tr-4302, Oak Ridge National Laboratory, Oak Ridge, TN (1975).
10. Goode, J. H. and Stacy, R. G., "Head-End Reprocessing Studies with H. B. Robinson-2 Fuel," ORNL/TM-6037, Oak Ridge National Laboratory, Oak Ridge, TN (1978).
11. Goode, J. H. and Stacy, R. G., "Head-End Processing Studies with Mechanically Blended (U,Pu)₂O₂ Reactor Fuels," ORNL/TM-6266, Oak Ridge National Laboratory, Oak Ridge, TN (1978).
12. Goode, J. H. and Stacy, R. G., "Comparative Studies of Head-End Processing Using Irradiated, Mechanically Blended and Coprecipitated (U,Pu)₂O₂ Reactor Fuels," ORNL/TM-6370, Oak Ridge National Laboratory, Oak Ridge, TN (1978).
13. McIsaac, L. D., Baker, J. D., Krupa, J. F., LaPointe, R. E., Meikrantz, D. H., and Schroeder, N. C., "Study of Bidentate Compounds for Separation of Actinides from Commercial LWR Reprocessing Wastes," ICP-1180, Idaho National Engineering Laboratory, Idaho Falls, ID (in press).
14. McIsaac, L. D., Baker, J. D., Krupa, J. F., Meikrantz, D. H., and Schroeder, N. C., "Flowsheet Development Work at the Idaho Chemical Processing Plant for the Partitioning of Actinides from Acidic Nuclear Waste," Actinide Separations Symposium, ACS Pacific Chemical Conference, Honolulu, April 3-5, 1979.
15. Scheitlin, F. M. and Bond, W. D., "Recovery of Plutonium from HEPA Filter Media by Continuously Leaching in a Packed Column with Electrolytically Produced Ce(IV) Nitrate and Nitric Acid," ORNL/TM-6802, Oak Ridge National Laboratory, Oak Ridge, TN (in press).
16. Thompson, G. H., Childs, E. L., Kochen, R. L., Schmunk, R. H., and Smith, C. M., "Actinide Recovery from Combustible Waste: The Ce(IV)-HNO₃ System," RFP-2907 (in press).
17. Wheelwright, E. J., Bray, L. A., Van Tuyl, H. H. and Fullam, H. T., "Flowsheet for Recovery of Curium from Power Reactor Fuel Reprocessing Plant Waste," BNWL-1831, Battelle Pacific Northwest Laboratory, Richland, WA (1974).
18. Forsberg, C. W., personal communication to D. W. Tedder, Oak Ridge National Laboratory (June 1978).
19. Horwitz, E. P., Mason, G. W., Bloomquist, C. A. A., Leonard, R. A., and Bernstein, G. J., "The Extraction of DBP and MBP from Actinides: Applications to the Recovery of Actinides from TBP-Na₂CO₃ Scrub Solutions," Actinide Separations Symposium, ACS Pacific Chemical Conference, Honolulu, HA April 3-5, 1979.
20. Tedder, D. W., Finney, B. C., and Blomeke, J. O., "Waste Treatment Facilities for the Partitioning of Actinides from LWR Reprocessing and Refabrication Plant Wastes," ORNL/TM-6881 (in press).

RECEIVED May 4, 1979.

Flowsheet Development Work at the Idaho Chemical Processing Plant for the Partitioning of Actinides from Acidic Nuclear Waste

L. D. McISAAC, J. D. BAKER, J. F. KRUPA, D. H. MEIKRANTZ,
and N. C. SCHROEDER

Allied Chemical Corporation—Idaho Chemical Programs, Idaho National Engineering Laboratory, Idaho Falls, ID 83401

The Idaho Chemical Processing Plant (ICPP) located at the Idaho National Engineering Laboratory near Idaho Falls, Idaho is a multipurpose reprocessing facility for DOE fuels containing highly enriched uranium. Fuels routinely processed at ICPP include stainless-steel-clad fast-reactor fuels, aluminum-clad test-reactor fuels, and zirconium-clad fuels for which the ^{235}U enrichments before burnup vary from 50 to 93%. The stainless-steel-clad fuel is electrolytically dissolved in HNO_3 , the aluminum-clad fuels are dissolved in $\text{HNO}_3\text{-Hg}(\text{NO}_3)_2$, and zirconium-clad fuels are dissolved in HF and HNO_3 . These multi-headend dissolver solutions provide the feed for a single solvent extraction system which is comprised of a first cycle of TBP extraction followed by two cycles of methyl-isobutyl ketone extraction. The uranyl nitrate product from the extraction system is denitrated in a fluidized bed denitrator to UO_3 for shipment.

The aqueous fission product wastes resulting from the ICPP solvent extraction operations contain small amounts of uranium and transuranium elements; primarily neptunium, plutonium, and americium with traces of curium and transcurium isotopes. The safe and effective management of these nuclear wastes has been a primary goal of the ICPP operation for the past 27 years. The major technique for management of this waste has been to store the liquid waste safely for a period not to exceed 5 years, followed by solidification of the waste into a granular oxide and storage in stainless steel bins inside a concrete vault. Prior to calcination, the high- and intermediate-level liquid wastes (HLLW and ILLW) are stored in doubly-contained, cooled, stainless steel tanks. To date, there is no evidence of corrosion from the acidic wastes stored in these tanks. The HLLW have been solidified on a routine basis in the Waste Calcining Facility (WCF) since December 1963, with a resultant eight- to ten-fold volume reduction factor. To date, this pioneering effort has resulted in approximately 55% of the liquid wastes being converted to solids, with approximately 50,000 cubic feet in storage. Although the projected life of the solids storage bins is at least 500 years, the bins are designed

0-8412-0527-2/80/47-117-395\$05.00/0

© 1980 American Chemical Society

such that retrieval of the wastes for further treatment or transport to a Federal repository might be accomplished whenever desired.

The waste generated at ICPP is different with respect to anticipated commercial processing plant waste for two reasons. First, all of the multi-headend processes result in complete dissolution of the cladding and matrix as well as the fission products and actinide elements; second, the production of transuranium elements in highly enriched fuels is less than in low enrichment/high burnup power fuels. Additionally, the total fission product inventory in the fuel is substantially lower at ICPP as compared to power reactor fuels and consequently, the radioactivity of the resulting waste solutions are very different for these two cases. Thus, the ratio of actinides to total solids in the ICPP waste is significantly less than in currently anticipated commercial wastes. The bulk of the raffinate stored at ICPP has been generated from the processing of zircaloy- and aluminum-clad fuel elements. The uranium recovery process for zircaloy-clad elements requires the addition of aluminum nitrate as both a salting agent and a complexant for the free fluoride present in the dissolution process. When available, the dissolver solution from aluminum-clad elements is coprocessed with zircaloy-clad elements, thus serving the same purpose. Raffinates generated from these campaigns are, therefore, similar. The chemical analyses of a major first-cycle raffinate storage tank at ICPP are shown in Table I. Actinide analyses are also given in Table I.

TABLE I

TYPICAL COMPOSITION OF ICPP Zr-Al FIRST-CYCLE WASTE

<u>Bulk Chemical (M)</u>		<u>Actinides (g/L)</u>	
Acidity (H ⁺)	1.5	²³⁷ Np	1.2x10 ⁻⁵
Nitrate	2.36	²³⁸ Pu	~ 5x10 ⁻⁴
Fluoride	3.12	²³⁹ Pu	1.4x10 ⁻³
Aluminum	0.68	²⁴⁰ Pu	3.4x10 ⁻⁴
Zirconium	0.44	²⁴¹ Pu	1.5x10 ⁻⁴
Iron	0.005	²⁴² Pu	4.8x10 ⁻⁵
Boron	0.22	²⁴¹ Am	4.4x10 ⁻⁵
Mercury	~ 0.002	²⁴³ Am	1.2x10 ⁻⁵

A litre of waste shown in Table I, when calcined, results in the production of ~250 g of total solids. The plot shown in Figure 1 describes significant actinide concentrations in ICPP calcine from a typical raffinate as a function of time. Though uranium and neptunium are present in the calcine, their contribution to alpha activity is not significant. It is apparent that separation factors of ~100 must be attained for the Pu and Am to

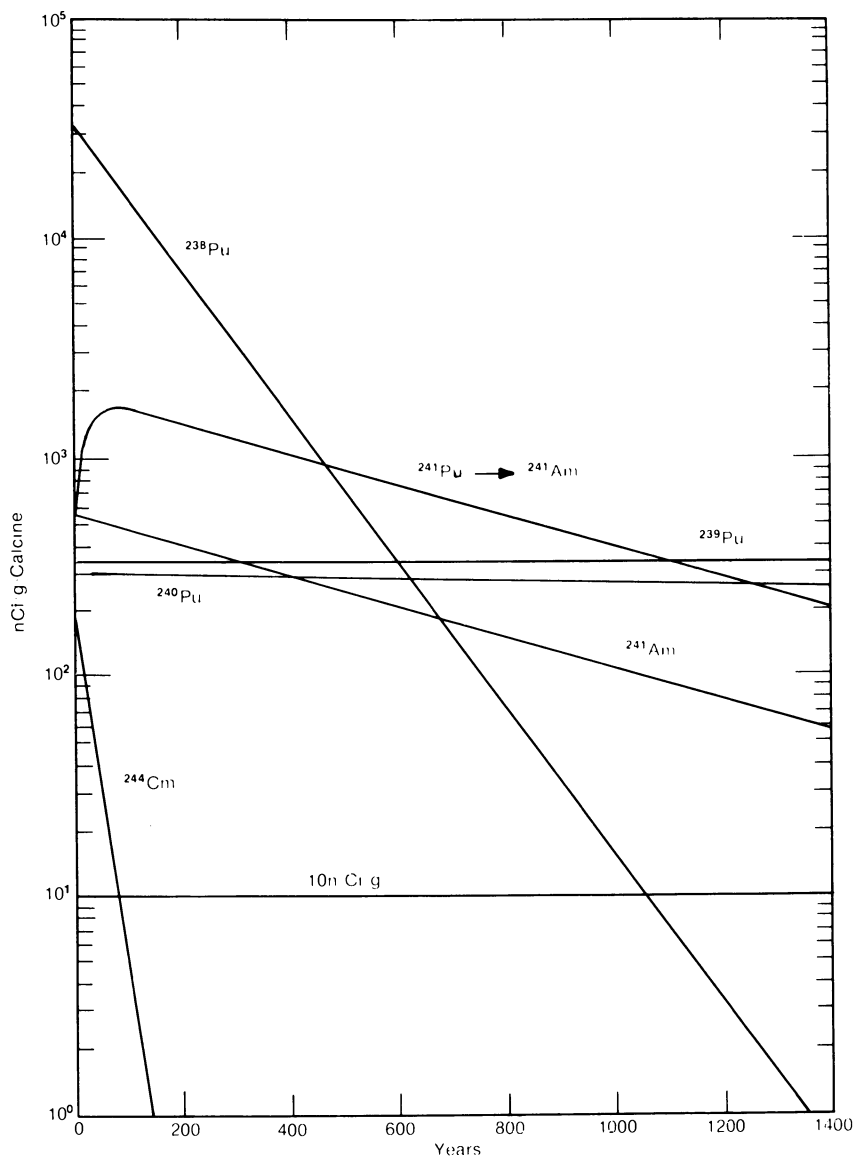


Figure 1. Significant actinides in ICPP calcine as a function of storage time

reach the desired alpha-free guideline of <10 nCi of alpha-emission per gram of solids after 1000 years of storage. A removal by a factor of ~250 would allow the calcine to decay to <10 nCi/g after 500 years of storage.

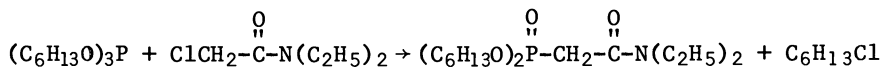
This paper reviews our actinide partitioning program and summarizes our latest findings.

Separation Requirements

The thrust of the experimental program at ICPP was to find a separation procedure that would separate plutonium, americium, and curium from high-level first-cycle raffinate (see Table I) and leave behind the cladding elements, salting agents, and the bulk of the fission products. Fission-product lanthanides, because of their similar valence and ionic size, would be expected to follow americium in nearly any simple separation scheme. Americium and curium are present in ICPP waste as trivalent ions while plutonium is most likely present as both Pu(IV) and Pu(VI). Any separation scheme must be applicable to all these ionic actinide species. Due to an instability of dissolver solution toward the formation of zirconium and aluminum fluorohydrates at lower acid levels, decreasing the acidity before actinide separation is impractical.

A literature survey was made for procedures or technical information that would be applicable to the removal of (III) as well as (IV) and (VI) valence actinides from high fluoride, highly acidic ICPP first-cycle raffinate. A synthetic Zr-Al dissolver solution, having a bulk chemical composition similar to that given in Table I with added lanthanum (0.2 mg/L) and tagged with ^{241}Am and ^{239}Pu tracers, was used to evaluate promising procedures. Plutonium solutions were stabilized as Pu(IV) and Pu(VI) with nitrite and chromate, respectively. Common monodentate neutral organophosphorus extractants such as TBP (tri-n-butylphosphate) and DBBP (dibutyl-butylphosphonate) were found to extract Pu(VI) very well, but not trivalent americium. These monodentate reagents will, however, extract trivalent americium reasonably well from low-acid, highly salted solutions. Solvent extraction processes which use HDEHP [bis(2-ethylhexylphosphoric acid)] as the extractant have been used in the United States (1) and in Germany (2) for recovery of americium from nuclear waste solutions previously adjusted to a pH ≥ 1 .

Of the many solvent systems we studied for removing actinides from ICPP high-level waste, extraction with the bidentate organophosphorus reagents, dibutyl-N,N-diethylcarbamylmethylenephosphonate (DBDECMP) and the dihexyl homologue, DHDECMP, are the most promising. This class of compounds was first synthesized by Siddall in the 1960's (3,4) using the Arbuzov rearrangement. Shown below is the preparation of DHDECMP.



Siddall investigated the ability of these compounds to extract Am(III), Ce(III), Pm(III), and HNO_3 from 0.1 to 12M HNO_3 solutions. His favorable results led him to suggest such bidentate extractants could be used to remove trivalent actinides from high-level TBP extraction process waste. This idea was later patented (5). Schulz demonstrated in 1973 that DHDECMP was an effective extractant for americium and plutonium from radioactive Hanford generated wastes (6).

We have evaluated both DHDECMP and DBDECMP as actinide extractants from the ICPP wastes. Both reagents were purchased from Wateree Chemical Company, Inc., Lugoff, S.C. on a "custom-synthesis" basis. Due to the ease of purifying the "as-received" DBDECMP, much of our early experimental work was with this compound (7,8). When aqueous solubility measurements indicated DBDECMP to be appreciably soluble (60 g/L) in 0.1M HNO_3 our attention was directed to the use of DHDECMP which exhibits an aqueous solubility similar to TBP (0.4 to 0.5 g/L) (7,9).

DHDECMP Purification

Technical grade DHDECMP (50% pure) contains unreacted starting materials and many impurities. This grade of DHDECMP is unsuitable for direct application as an extractant because actinides, once extracted, are poorly stripped. The identification of impurities has been reported previously (10).

We purify litre quantities of DHDECMP by vacuum distillation using a centrifugal molecular still. The fraction distilling at ~ 0.5 Pa and 120°C is $\sim 86\%$ pure DHDECMP and can be used without further treatment for actinide extraction and stripping studies. Impurities present in this product appear to be innocuous. For the sake of simplicity in making volume percent DHDECMP-solvent dilutions, the stock DHDECMP (86%) was considered to be pure.

Starting with 86% DHDECMP, we have prepared 25 mL of $>99\%$ pure DHDECMP by preparative liquid chromatography. The liquid chromatograph used was a Jobin Yvon "Chromatospac-Prep 100", Instruments SA, Inc., Mutechen, N.J. Physical properties studied with purified DHDECMP were density, refractive index, viscosity, U-V, IR and NMR spectra. A mutagenic test was also conducted and found to be negative. A detailed description of this work and the resultant physical properties of DHDECMP have recently been published (11). A limited number of extractions have been made using this high purity DHDECMP to demonstrate that DHDECMP is the dominant extracting component in our extraction studies.

Diluent Effects

Our earlier studies have shown that the extraction of americium from synthetic Zr-Al waste solutions is strongly dependent upon the particular carrier solvent used to dilute the DHDECMP (10). Aromatic solvents proved to be good diluents, the best of the aromatics being branched alkane derivatives. A second

organic phase forms when solutions of DHDECMP dissolved in straight chain aliphatic hydrocarbons are contacted with aqueous HNO_3 solutions. Decalin, decahydronaphthalene, proved to be a superior diluent when compared to aromatics; however, when DHDECMP-decalin extractants are contacted with $\geq 3\text{M}$ HNO_3 solutions, a second organic phase forms. Addition of an aromatic modifier such as diisopropyl benzene (DIPB) to a DHDECMP-decalin extractant prevents second organic phase formation even at acidities as high as 6M HNO_3 . Much of our early work was with xylene and with diisopropyl benzene diluents. Later, with large quantities of extractant being required for cold pilot-plant testing, we focused on the use of a decalin-DIPB diluent.

Reaction Kinetics

Batch contact studies have shown that both Am(III) and Pu(IV) transfer rapidly at 23 to 25°C between DHDECMP-diluent solutions and aqueous HNO_3 . In all tests conducted, equilibrium was reached in <30 seconds.

Radiolytic Effects

We have contacted DHDECMP-decalin-diisopropyl benzene solvents with high-level Zr-Al waste for periods up to 16 hours (12). The only deleterious effect attributed to radiolysis was that a small percent ($\sim 0.1\%$) of extracted plutonium was not readily strippable by dilute HNO_3 -hydroxylamine nitrate (HAN). However, subsequent strips with dilute HNO_3 - $\text{H}_2\text{C}_2\text{O}_4$ readily removes the residual plutonium from the extractant. The DHDECMP solvent is readily returned to "as new" condition by washing with dilute aqueous Na_2CO_3 solution. An earlier study was performed (13) where DBDECMP was irradiated in our fuel storage basin. The solvent received doses up to 50 Watt hr/L. Plutonium extracted into solvents receiving >4 Watt hr/L was not readily stripped. Carbonate washing of irradiated solvent before extraction use eliminated stripping problems.

Typical Actinide vs. HNO_3 Distribution Data

The distribution coefficients have been determined for Cm(III), Am(III), Cf(III), Pu(IV), Pu(VI), Np(IV), Np(VI), and U(VI) between 30 volume % DHDECMP in DIPB and various nitric acid concentrations. Results are shown in Figure 2. Tracers were taken to incipient dryness in concentrated nitric acid several times, then dissolved with the particular nitric acid concentration being studied. After setting the oxidation state, extractions were done using equal volumes of aqueous and organic phases. Contact times were 5 minutes at 23°C. Extractions were done in 10 mL tubes which were agitated with a mechanical wrist shaker. Each data point was obtained by a separate extraction.

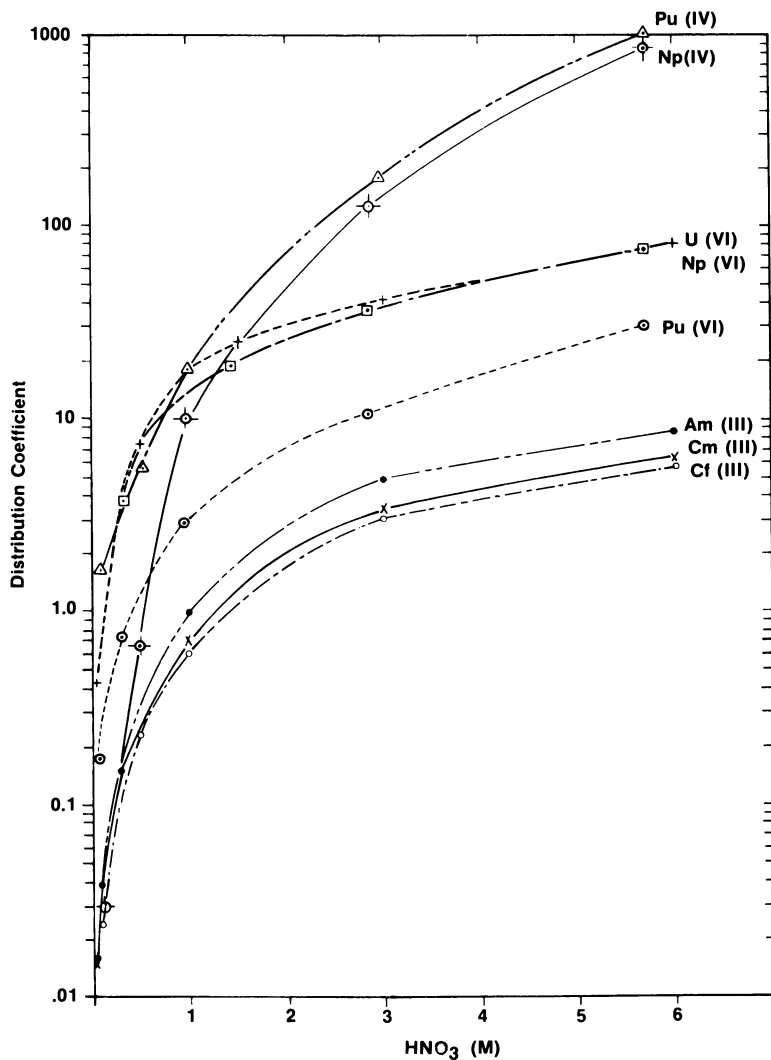


Figure 2. Actinide distribution between 30 vol % DHDECMP in DIPB and HNO₃ as a function of initial HNO₃ concentration

The Pu(VI) oxidation state was set by making the solution 0.025M NaBrO₃ - 0.001M Ce(NH₄)₂(NO₃)₆. Pu(IV) was set by adding one drop of 30% H₂O₂ before taking to incipient dryness. After dissolution, the nitric acid solutions were made 0.025M in nitric, then capped to prevent nitric oxides from escaping. Np(IV) and Np(VI) states were set by making the solutions 0.025M Fe(SO₃NH₂)₂ and 0.025M NaBrO₃ - 0.001M Ce(NH₄)₂(NO₃)₆, respectively. Americium, curium and californium are normally in the trivalent state and therefore required no redox treatment. Several hours at 60°C were required to complete the oxidation to Pu(VI) at the highest acidity. One hour at 60°C was required to complete other oxidations to Pu(VI) and Np(VI). All other samples were equilibrated for at least one hour at 23°C prior to extraction.

Efforts to determine distribution coefficients for Pu(III) using 0.025M Fe(SO₃NH₂)₂ or 0.025M sodium formaldehyde sulfoxylate (NaCH₂OSO₂) were successful up to 1.0M nitric acid. Above that concentration, oxidation to Pu(IV) readily occurred.

Figure 2 shows conclusively that DHDECMP can extract trivalent as well as tetravalent and hexavalent actinides from moderately concentrated nitric acid solutions. The valence (III) actinides, Am, Cm, and Cf, have distribution coefficients greater than one above 1.5M HNO₃, while valence (IV) and (VI) actinides have values greater than one above 0.5M HNO₃. In addition, DHDECMP shows very favorable back extraction or stripping characteristics below 0.3M HNO₃. Pu(IV) polymer formation undoubtedly occurred in low-acid measurements and may account for the low distribution coefficients.

Extraction Studies with Zr-Al High-Level Waste

Comprehensive data for the distribution of actinides, fission products, and inert constituents of ICPP Zr-Al high-level waste into 30 volume % DHDECMP-xylene solvent have been previously reported (10). We have focused our attention recently on a more efficient use of DHDECMP where the diluent is a mixture (2:1) of decalin and DIPB.

Batch distribution data have been obtained for the extraction of actinides and key elements between synthetic Zr-Al coprocess first-cycle raffinate and 20 volume % DHDECMP in 2:1 decalin-DIPB. The effect of scrubbing and stripping of the pregnant extractant has also been studied. All contacts were for five minutes using a wrist action shaker at 23°C. The major constituents present in synthetic dissolver solution have been described elsewhere (7). Except for acidity, tracer techniques were used for the determination of distribution coefficients. Each feed component was investigated separately. Gamma-ray emitters were analyzed by NaI(Tl) and Ge(Li) spectrometry and alpha emitters by liquid scintillation counting. With the exception of ^{99m}Tc, which was carrier-free, macro-quantity amounts of elements studied were present in the µg/mL range. Fission product element concentrations were at ~0.1 mg/L. Other constituents were as shown in

Table I. Tracers plus carriers, where appropriate, were taken to near dryness several times with concentrated nitric acid then equilibrated with the synthetic waste for at least one hour before extraction contact. Each constituent was studied separately. All measurements were made in duplicate. Results from these studies are presented in Table II. Distribution ratios, except where noted, have an estimated accuracy of $\pm 10\%$.

For those runs where the element under study was extracted significantly but was poorly stripped, the effect of an additional equal volume contact with $0.5M$ Na_2CO_3 - $0.025M$ KCN was measured. These results are reported in Table III. The use of KCN in the $0.5M$ Na_2CO_3 wash solution has been suggested (14) as a possible procedure for removing mercury from the solvent before recycle. From these results, it appears that palladium and ruthenium are also effectively removed.

Chemical analyses of aluminum in the aqueous phase before and after extraction contact confirmed our earlier results with 30 volume % DHDECMP in xylene which indicated low extraction ($D_{Al} = 0.0025$) (10). To obtain an accurate value for aluminum would have required activation analysis. This was not felt to be warranted. A measurement of Pu(VI) was not included here because previous studies with other diluents have shown higher distribution for Pu(VI) than for Pu(IV).

From the data in Table II, it is apparent that we should be able to partition actinides from the major constituents present in high-level Zr-Al waste. Scrubbing, stripping, and solvent regeneration also appear feasible.

Extraction Studies on ICPP High Sodium Waste

Low-level wastes high in sodium content have been collecting at the ICPP for years. Though these wastes represent but a small fraction of the total wastes produced, their cumulative volume is considerable (10^6 gal). The typical composition of high sodium concentration waste is shown in Table IV.

We have made equal volume batch extraction measurements on synthetic high sodium concentration waste using 20 volume% DHDECMP in 2:1 decalin-DIPB. Only actinides and a few chemical constituents were examined. Techniques were as described in the above section. Extraction data are shown in Table V.

Actinides are readily extracted from synthetic high sodium concentration waste. With the exception of mercury, no other macro constituent would be expected to follow the actinides in a DHDECMP flowsheet. The high distribution for Pu(IV) is most likely due both to the high $NaNO_3$ concentration and the low fluoride concentration.

TABLE II
DHDECMP EXTRACTION-SCRUB-STRIP STUDIES WITH
SYNTHETIC Zr-Al COPROCESS WASTE

Feed Component	DISTRIBUTION COEFFICIENTS					
	Extraction ^a Contact	Scrub ^b Contact	Strip Contacts ^c			
			1	2	3	4
Am(III)	7.6	3.7	0.21	0.015	0.013	--
Pu(IV)	7.6	3.9	0.20	0.004	0.05	--
Np(V)	0.55	0.16	0.010	--	--	--
U(VI)	55.	34.	2.7	0.22	0.25	0.010
Hg(II)	16.	10.	84.	130.	>200.	>200.
Ce(III)	4.8	4.1	0.28	0.017	0.023	--
Ba(II)	0.015	0.011	--	--	--	--
Cs(I)	0.00040	--	--	--	--	--
Cd(II)	0.014	< 0.01	--	--	--	--
Pd(II)	1.9	0.62	0.82	1.4	7.2	17.0
Ru(III, IV)	1.2	0.81	7.4	8.2	14.0	8.4
Tc(VII)	1.4	0.93	2.7	1.0	0.68	0.84
Mo(VI)	0.26	0.20	--	--	--	--
Nb(V)	0.079	0.055	--	--	--	--
Zr(IV)	0.0095	0.016	--	--	--	--
Y(III)	0.36	0.41	0.015	--	--	--
Sr(II)	0.018	0.015	--	--	--	--
H ⁺	0.2	--	--	--	--	--

a Equal vol (o/a=1) contact with 20 vol% DHDECMP in 2:1 Decalin-DIPB

b Scrub: 3M HNO₃, o/a=5

c Strips 1-3: 0.015M HNO₃-0.05M HAN, o/a=1
Strip 4: 0.005M HNO₃-0.05M H₂C₂O₄, o/a=1

TABLE III20% DHDECMP WASH WITH 0.5M Na₂CO₃ - 0.025M KCN

<u>Element Loaded</u>	<u>Distribution Coefficient</u>
Hg(II)	0.014
Pd(II)	0.067
Ru(III, IV)	0.013
TC(VII)	0.23

TABLE IV

TYPICAL COMPOSITION OF HIGH SODIUM CONCENTRATION WASTE

<u>Bulk Chemical</u>	<u>(M)</u>	<u>Actinides (g/L)</u>
Acidity (H ⁺)	1.4	U ~2 x 10 ⁻²
Nitrate	4.4	Pu ~1 x 10 ⁻³
Aluminum	0.50	Am ~1 x 10 ⁻⁵
Zirconium	~1 x 10 ⁻⁴	
Mercury	0.0050	
Fluoride	~6 x 10 ⁻⁴	
Sodium	1.7	
Chloride	0.030	
Phosphate	0.020	

TABLE V

DISTRIBUTION DATA FOR DHDECMP AND HIGH SODIUM CONCENTRATION WASTE

<u>Feed Component</u>	<u>Distribution Coefficient</u>
Am(III)	9.5
Pu(IV)	190.0
U(VI)	140.0
Hg(II)	7.7
Zr(IV)	0.05
H ⁺	0.43

Mercury Extraction and Stripping

Mercury coextracts with actinides into DHDECMP and is not stripped by conventional means. The bulk of our future waste will be mercury free; however, our tanks contain so much mercury from past campaigns that mercury removal from pregnant DHDECMP must be dealt with.

We have just completed a study of the effects of mercury loading in DHDECMP on extraction and stripping of actinides and alternative mercury stripping techniques (14). Mercury can be removed from DHDECMP by direct electrolysis or electrolytic replacement by another metal such as copper. Removal of mercury in the carbonate wash was found to be feasible if either cyanide or thioglycolate were present. The use of thioglycolate was abandoned because of its instability with time in sodium carbonate solutions. Because of the problems associated with scaling up an electrolytic method, we prefer the use of cyanide complexation for mercury removal. The wealth of information generated on the use of carbonate-cyanide solutions by the electroplating industry should be readily applicable to our waste management needs.

We have found that mercury can be readily removed from carbonate-cyanide solutions by electrodeposition, thus making mercury recycle possible.

Flowsheet

Based on batch extraction, scrub and strip data (Table II), the flowsheet shown in Figure 3 has been developed. Relative flows are shown in parentheses. Six stages of extraction and two stages of scrubbing should produce waste of <10 nCi/g after calcination and storage for 500 years. The number of stages for stripping was not determined, but we expect at least six stages would be necessary in each column. The second strip column is felt necessary to remove plutonium not stripped in the preceding strip column. This flowsheet does not include a specific mercury removal step. The addition of KCN to the carbonate used in the solvent wash column would cause mercury to report to the solvent wash waste.

Though this flowsheet was developed for Zr-Al high-level waste, it should be adaptable to other waste generated at ICPP.

Mixer-Settler Test

Flowsheet parameters have been tested with actual ICPP waste in a multi-stage miniature mixer settler. The results of these tests and a complete description of the equipment used have recently been reported (12). Tables VI and VII summarize the results of hot runs using Zr-Al coprocess waste and high sodium waste. Both runs involved continuous countercurrent operation using six stages of extraction with 20 volume % DHDECMP in 2:1 decalin-DIPB and two stages of scrubbing with 3M HNO₃. For the

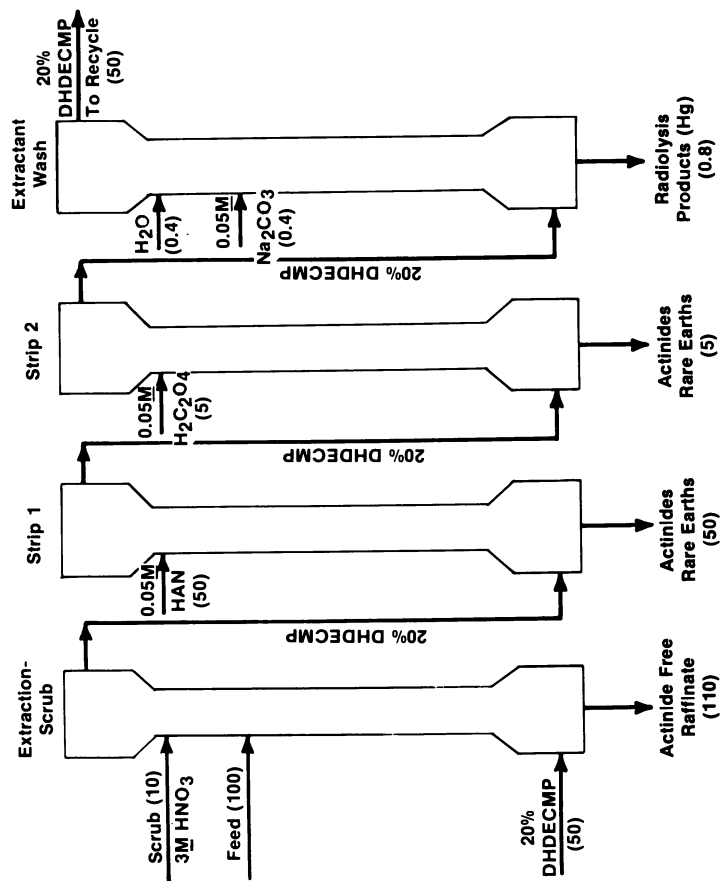


Figure 3. Conceptual flowsheet for actinide partitioning from ICPP acidic waste

TABLE VI
ACTINIDE REMOVAL FROM ICPP Zr-Al COPROCESS
HIGH-LEVEL WASTE: MINIMIXER-SETTLER RUN

	<u>Am(ng/mL)*</u>	<u>Pu(ng/mL)*</u>
Feed	56.6 ± 0.2	2228 ± 5
Raffinate	0.333 ± 0.001	0.864 ± 0.017
DF	170	2580

*Isotopic Content (%): ^{241}Am - 87.11; ^{243}Am - 12.89;
 ^{238}Pu - 20.15; ^{239}Pu - 56.56; ^{240}Pu - 14.05;
 ^{241}Pu - 6.93; ^{242}Pu - 2.31

TABLE VII
ACTINIDE REMOVAL FROM ICPP HIGH SODIUM CONCENTRATION
WASTE: MINIMIXER-SETTLER RUN

	<u>Am(ng/mL)*</u>	<u>Pu(ng/mL)*</u>
Feed	15.20 ± 0.05	907 ± 3
Raffinate	~ 0.01	~ 0.07
DF	~ 1500	~ 13000

*Isotopic Content (%): ^{241}Am - 92.36; ^{243}Am - 7.64;
 ^{238}Pu - 5.61; ^{239}Pu - 82.85; ^{240}Pu - 8.63;
 ^{241}Pu - 2.15; ^{242}Pu - 0.76

Zr-Al coprocess waste test, the feed, extractant, and scrub flows were 1, 0.5, and 0.1 mL/min, respectively. For the high sodium concentration waste, the feed, extractant, and scrub flows were 0.75, 1, and 0.25 mL/min, respectively. Samples of raffinate were drawn for analytical analysis approximately five hours after equilibrium had been reached. The resultant decontamination factors agreed reasonably well with our calculations. For the coprocess waste run, we expected an americium decontamination factor of ~200. We purposely built in a large "overkill" in the sodium waste run by increasing the organic to aqueous flow rates. The sodium waste run produced a raffinate that, when calcined, would be well below the guideline for alpha-free waste with no allowance for decay. Analytical analysis of feeds and raffinates confirmed our batch results in that actinides were fractionated from major waste constituents such as aluminum, zirconium, sodium, and fluoride.

We have not yet demonstrated the stripping sections of the flowsheet during hot operations. We have, however, recently completed a mixer-settler test for Oak Ridge National Laboratory (11) where six stages were used for extraction (30 volume % DHDECMP in DIPB), two for scrubbing and four for stripping. The feed was raffinate from a TBP extraction performed in our laboratory from a high burnup LWR fuel element. In this test, we ran hot for ten continuous hours without any problems. The level of radiation was at least a factor of ten higher than we would expect for any waste generated at ICPP, so we are optimistic that the flowsheet (Figure 3) can be run successfully.

Cold Pilot-Plant Tests

Cold pilot-plant tests are presently in progress using 2-inch diameter pulsed plate columns in continuous countercurrent flow. Synthetic Zr-Al high-level waste loaded with 0.2 g/L Ce(III) is being used as feed and 20 volume % DHDECMP in 2:1 decalin-DIPB as extractant. Cerium is being used as an americium simulant. To date, three complete cycles have been run including a solvent recycle wash with Na_2CO_3 . No major problems have been encountered.

These pilot-plant tests require large quantities of good quality solvent. We had 50L of distilled DHDECMP prepared by Bray Oil Company (1925 N. Mariana Avenue, Los Angeles, Calif., 90032) starting with Wateree Chemical Company crude DHDECMP. Bray used their CVC Pilot-15 centrifugal molecular still for the distillation. Bray has just recently produced 200L of distilled DHDECMP from a batch of crude that they manufactured. This is the first time we have been able to purchase DHDECMP that is ready for extraction use.

Literature Cited

1. Bond, W. D. and Leuze, R. E., U.S.ERDA Report, ORNL-5012, 1975.
2. Koch, G.; Kolarik, Z.; Hang, H.; Hild, W.; Drobnik, S., "Recovery of Transplutonium Elements from Fuel Reprocessing High-Level Waste Solutions"; Proceedings of Symposium on the Management of Radioactive Wastes from Fuel Reprocessing: Paris, France, November 27-December 1, 1971; p. 1081; Organization for Economic Cooperation and Development; Paris, France; 1973.
3. Siddall, T. H.; 111, J. Inorg. Nucl. Chem., 1963, 25, 883.
4. Siddall, T. H.; 111, J. Inorg. Nucl. Chem., 1964, 26, 1991.
5. Siddall, T. H., 111, U.S. Patent 3,243,254, March 1966.

6. Schulz, W. W., U.S. ERDA Report, ARH-2901, 1973.
7. McIsaac, L. D.; Baker, J. D.; Tkachyk, J. W. U.S. ERDA Report, ICP-1080, 1975.
8. Schulz, W. W.; McIsaac, L. D. "Removal of Actinides from Nuclear Fuel Reprocessing Wastes Solutions with Bidentate Organophosphorus Extractants", Transplutonium 1975; Müller, W., and Lindner, R, Eds.; North Holland Publ. Co., Amsterdam, 1976; p. 433.
9. Burger, L. L.; Forsman, R. C. U.S. AEC Report, HW-20936, 1951.
10. Schulz, W. W.; McIsaac, L. D. U.S. ERDA Report, ARH-SA-263, 1977.
11. McIsaac, L. D.; Baker, J. D.; Krupa, J. F.; LaPointe, R. E.; Meikrantz, D. H.; Schroeder, N. C. U.S. DOE Report, ICP-1180, 1979.
12. Baker, J. D.; McIsaac, L. D.; Krupa, J. F.; Meikrantz, D. H.; Schroeder, N. C. U.S. DOE Report, ICP-1182, 1979.
13. McIsaac, L. D.; Baker, J. D.; Tkachyk, J. W. U.S. ERDA Report, ICP-1086, 1976; p. 100.
14. Krupa, J. F.; McIsaac, L. D.; Baker, J. D.; Meikrantz, D. H.; Schroeder, N. C. U.S. DOE Report ICP-1181, 1979.

RECEIVED April 27, 1979.

Recovery of By-Product Actinides from Power Reactor Fuels and Production of Heat Source Isotopes

G. KOCH

Kernforschungszentrum Karlsruhe, Postfach 3640, D 7500 Karlsruhe 1
Federal Republic of Germany

R+D work at Karlsruhe on the recovery of by-product actinides from power reactor fuels was initiated by Institut für Heiße Chemie (IHCH) in 1967. In that year, construction of the WAK pilot reprocessing plant at Karlsruhe had been started, and a R+D cooperation program between KfK (owner of WAK) and GWK (operator of WAK) was established, with the goal to keep the technology to be used in WAK in pace with future demands and developments. One of the five R+D areas of this so-called "Development Program for Fuel Reprocessing", as published in the first status report (1), was the recovery and processing of useful transuranium and fission product isotopes. In the same year, construction of IHCH's laboratory reprocessing facility "Milli" (2), with a cycle capacity of 1 kg fuel per day, was started. This offered the possibility to have available, in the early seventies, both a semi-commercial scale LWR fuel reprocessing plant (WAK), and a flexible, laboratory-scale multi-purpose reprocessing facility (Milli).

In 1971, the "Actinides Project" (PACT) was founded at KfK, with the goal to promote the production and application of transuranium isotopes (3). R+D work devoted to the recovery of raw-material transuranium isotopes was incorporated into this project which for some years led to a considerable extension of the activities in this field. However, due to the fact that a satisfactory commercial market for these products did not develop in Germany, the decision was reached in 1973 to terminate the PACT activities.

The present paper reviews the processes which were designed by IHCH for the recovery of raw-material actinides from power reactor fuels and for the production of heat-source isotopes, and describes the state of development which has been reached.

0-8412-0527-2/80/47-117-411\$05.00/0

© 1980 American Chemical Society

1. Recovery of Neptunium-237

A laboratory study was undertaken to determine the behaviour of neptunium in the WAK flowsheet, and to devise a procedure for its recovery. Based on static (4) and counter-current experiments (5), the conclusion was reached that about half of the Np is co-extracted with the U and Pu in the HA-HS mixer-settlers of WAK while the other half is rejected to the HAW, see Fig.1. It could also be shown that an increase of the aqueous acidity, or the addition of pentavalent vanadium as an oxidant into the lower stages of the HA mixer-settler (6), would increase the Np yield in the organic solvent. In the 1BX-1BS mixer-settlers where the partitioning of U and Pu is carried out by use of uranium (IV)nitrate - hydrazine nitrate, a splitting of the co-extracted Np between the two product streams was observed; the proportions of the (co-extracted) Np which ended up in the 1CU (uranium product) stream fluctuated from 30 to 93 % while the difference amount (from 7 to 70 %) ended up in the 1BP (plutonium product) stream. No definite reason for these fluctuations could be identified, but it is known that neptunium, due to its complicated redox chemistry, reacts in a very sensitive way to even minor process variations (7,8). Based on these results the proposal was made (5) to recover the "co-extracted" portion of the neptunium by running the second plutonium and uranium purification cycles under conditions where the Np is directed into the aqueous raffinate (2AW and 2DW streams). In the Pu purification cycle, this can be done by adding sufficient nitrous acid to keep the Np pentavalent, while in the U purification cycle (which is run under slightly reducing conditions) a low acidity and a high loading help to reject Np into the aqueous 2DW stream. The two raffinate streams are combined in WAK in the 3W evaporator, and the Np is thus collected in the concentrate from this unit (3WW stream). Consequently the proposal was made to recover the Np from this 3WW stream by use of the well-known anion exchange process (9,10).

Based on these proposals, a neptunium production unit called NEPP was designed and installed in WAK for the anion exchange recovery of Np from the 3WW stream. However, NEPP had not gone into operation when the PACT project was terminated in 1973.

It is interesting to note that the 1979 attitude regarding neptunium is quite different from what it was ten years ago. In those years, Np was considered to be a potentially valuable material worth to be recovered; today, Np has more the touch of an unwanted contaminant

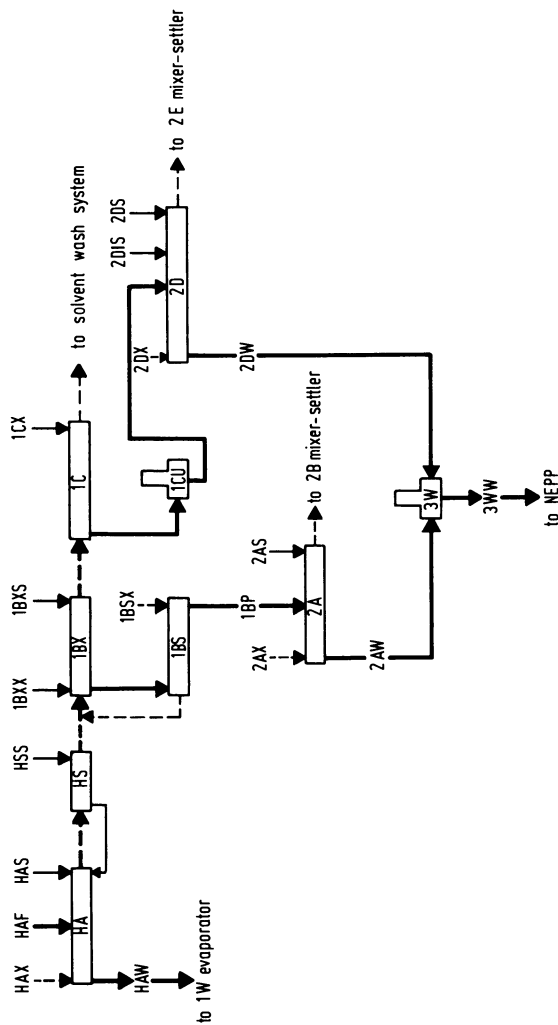


Figure 1. Simplified solvent extraction flowsheet of the WAK plant showing the path of Np: Np-bearing streams are indicated by fat lines; (—) aqueous streams; (---) organic streams.

requiring some cumbersome treatment for it to be removed. Ironically enough, tests of a Purex flowsheet (11) developed for large-scale processing of high-burn-up LWR fuels resulted in about 90 % co-extraction of the Np in the HA-HS extractor system (12). Partitioning of the co-extracted Np into the 1BP and 1CU first-cycle product streams was found to be similar as with the WAK flowsheet, i.e. between 50 and 85 % going into the 1CU uranium stream and the remainder into the 1BP plutonium stream. Methods to decontaminate the products from Np in the second and third purification cycles have been devised and tested (12).

2. Recovery of Am-241/243 and Cm-244 from High-Level Waste

The americium and curium isotopes formed during irradiation of nuclear reactor fuels are diverted into the high-level waste (HLW) stream during fuel reprocessing. The HLW is thus the biggest potential source for these elements, and R+D activities to develop a process for the recovery of Am and Cm from HLW were started in 1967. A major condition was that the process to be developed must not essentially increase the waste amount to be processed further, must not use strongly corrosive reagents, and must be compatible with the final waste solidification procedure.

The separation process chosen was based on HDEHP extraction of a lanthanides - actinides fraction (13, 14) and a TALSPEAK-type (15,16) separation of Am/Cm from the rare earths. In its first version (17), the extraction was made from a citrate-complexed and buffered HLW as the feed, and the actinides/lanthanides partitioning was done in what we called the "reverse-TALSPEAK" mode, i.e. by backwashing the Am + Cm from the loaded organic extractant by an aqueous lactic acid / diethylene triamine pentaacetate (DTPA) solution. Citrate complexing of the feed served for suppression of extraction of certain fission and corrosion products, e.g. Zr, Nb, Ru, and Fe; and the "reverse"-mode of the TALSPEAK process resulted in the saving of a separate extraction cycle. However, studies of the solidification behaviour of the high-level waste produced with this process showed that the presence of organic material (citric acid) would lead to vigorous exothermic reactions during calcination; therefore the process was later substantially modified.

In its final version (18-20), see Fig. 2, the process started with a conditioning of the HLW by formic acid denitration, with the goal (a) to reduce

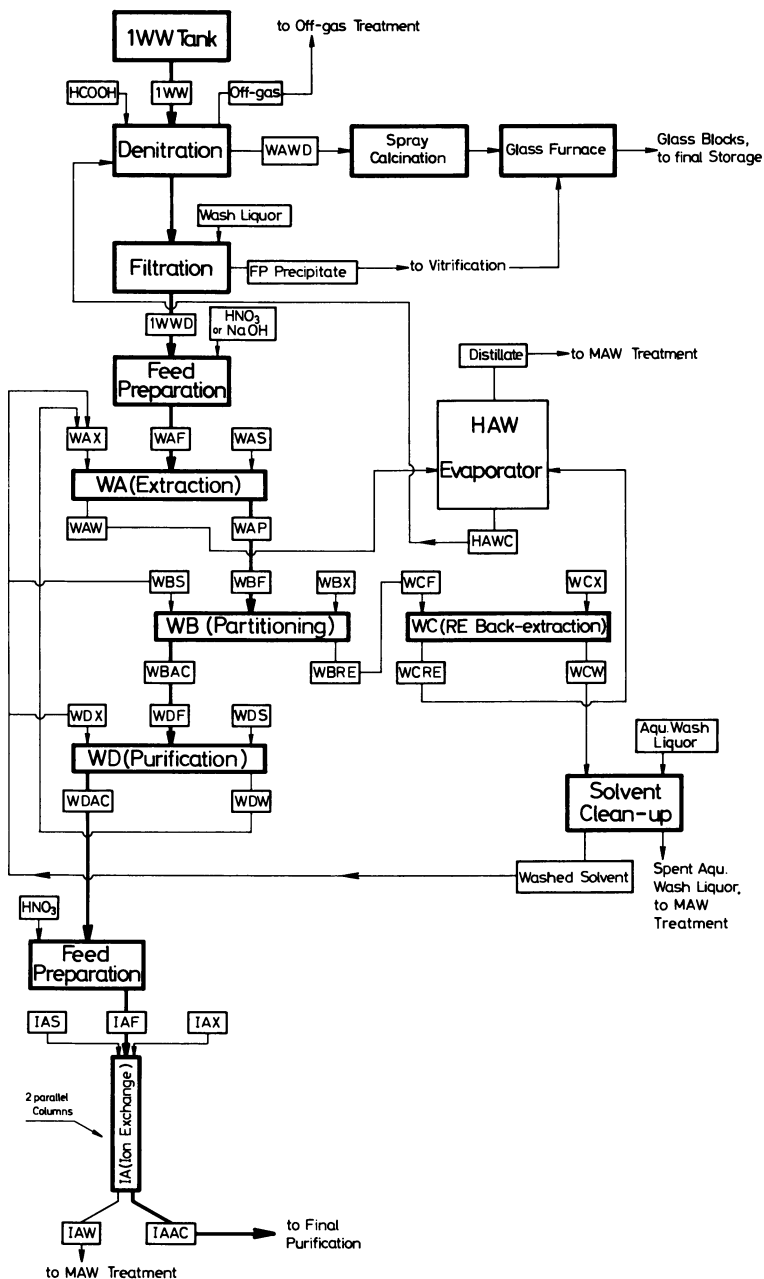


Figure 2. Flowsheet for Am + Cm recovery from high-level waste solutions (18)

Publication Date: April 16, 1980 | doi: 10.1021/bk-1980-0117.ch029

the acidity of the HLW down to a value suitable for the HDEHP extraction, and (b) to remove "trouble-making" fission and corrosion products by precipitation, thus eliminating the need to complex the extraction feed with organic complexants. Conditions were chosen such that Am, Cm, and rare earths (R.E.) remained in solution while most of the Zr, Nb, Mo, noble metals, and Fe were precipitated. The solid sludge could be filtered off and sent for solidification. The liquid supernate was adjusted to extraction conditions and fed to the solvent extraction cycle, using 0,3 moles/l HDEHP (extractant) + 0,2 moles/l TBP (modifier) in a n-alkane diluent as the solvent. Am, Cm, and R.E.s were extracted in the WA contactor from the non-complexed feed, Am and Cm were partitioned from the R.E.s in the WB contactor into 0,05 molar DTPA / 1 molar lactic acid, R.E.s were re-extracted from the solvent in WC by 5 molar nitric acid, and the Am/Cm product solution from WB was further purified from R.E.s by an additional organic solvent scrub stream in WD. In the latter step, extraction kinetics of the R.E.s from the strongly complexed aqueous phase was shown to play an important role to the purification effect (21). For the final purification and concentration of the Am + Cm product a cation exchange process was developed (19,20,22). Separation of the Am from Cm, if necessary, might be performed by the Hanford cation exchange process (23, 24), by high-pressure cation exchange (25-27), or else by potassium americium(V) carbonate precipitation (28); for a review, see (29).

"Cold" laboratory tests of the single steps of the flowsheet were made using simulated HLW solutions spiked with fission product tracers, Am, and Cm. The denitration step turned out to be a sensitive process but Am/Cm recoveries of ca. 90 % in the aqueous supernate could be realized under optimized conditions while $DF > 1000$ for Zr, Nb, and Mo, and $DF \approx 100$ for Ru and Fe, were obtained with the precipitation (19). The solvent extraction₃ cycle gave > 98 % recovery of Am/Cm, and $DF > ca. 10^3$ for the individual rare earths, Sr, and Cs (18). Appreciable decontamination was also obtained for Zr/Nb ($DF = 20$), Ru (50), U (> 650), Pu (250), Np (800), and Fe (420). The ion exchange cycle served mainly for Am+Cm concentration and for removal of DTPA and lactic acid; based on simulated tests with europium, concentration factors of about 50 could be expected under optimized conditions (22).

Planning work was started for the construction of a pilot plant for the recovery of Am + Cm to which the name ISAAC (from the German "Isolierungs-Anlage für

Americium und Curium") was given (18). These plans were abandoned when the PACT project was terminated in 1973. Thus, high-active demonstration of the separation process is lacking, and no judgement can be made on its performance.

3. Recovery of Americium-241 from Plutonium Scrap

The scraps which arise during the fabrication of plutonium-containing nuclear fuels are collected and stored for some time before they are processed to recover the plutonium. Due to the decay of Pu-241, considerable amounts of Am-241 may build up in the stored material. At the Alkem company, plutonium is recovered from the scrap by anion exchange; the americium which is not sorbed on the resin is collected in the combined effluents from the loading and wash steps. The effluents are concentrated by evaporation; besides americium, the concentrated effluents contain major amounts of uranium, plutonium, corrosion products, and residues from chemical reagents. A typical composition is given below:

Am,	8,2 g/l	Mn,	48,7 g/l	Ca,	4,1 g/l
Pu,	12,0 g/l	Ni,	48,5 g/l	Si,	0,5 g/l
U,	140,0 g/l	Pb,	23,0 g/l	Co,	0,4 g/l
Al,	22,5 g/l	Cu,	15,6 g/l	Mg,	0,2 g/l
Na,	10,5 g/l	Cr,	8,0 g/l	Mo,	0,2 g/l
Fe,	82,0 g/l	Ti,	4,8 g/l		

A process for the recovery of Am (and Pu) from these concentrates, based on solvent extraction with tricapryl methyl ammonium nitrate, TCMAN (Aliquat-336, nitrate form), was developed (30), and was operated for some time in a small-scale facility equipped with pulsed glass columns at the Alkem company to produce multi-gram amounts of americium dioxide. In its final version (31) the process worked as follows: The concentrated effluents were made up to 6 to 7 moles/l nitric acid, and the U and Pu were extracted in the first column by 0,5 moles/l TCMAN dissolved in Solveso-100, a high-boiling aromatic diluent. U and Pu were back-extracted in a second column into acetic acid - hydroxyl amine sulfate solution. The effluent from the first column was saturated with oxalic acid, and was neutralized with ammonia to pH = 2,5. This precipitated a nearly white precipitate of Am and Ca oxalates while most of the metallic contaminants (e.g., Fe, Cr, Al) remained in solution as stable oxalato complexes. The precipitate was filtered off, dissolved

in concentrated nitric acid, neutralized with ammonia to pH = 2,5 to 3, and the Am was extracted from the strongly salted aqueous ammonium nitrate solution by 0,5 molar TCMA/Solvesso. The loaded organic solvent was scrubbed with concentrated ammonium nitrate solution, and the americium was back-extracted with dilute nitric acid. Americium was precipitated from this solution as the oxalate, and was converted into AmO_2 by calcination at 800 °C. The Am recovery was > 90 %, the product purity > 99 %.

4. Recovery of Pu-238 from irradiated Np-237

In the frame of the PACT project, irradiation of several kilograms of Np-237 to produce Pu-238 was planned for the years after 1973. A test irradiation of ca. 180 g Np-237 was initiated by the Alkem company in 1970. The neptunium was fabricated by Alkem into target rods containing pellets of a 10 % NpO_2 -iron-cermet. The targets were irradiated in the BR-2 reactor at Mol, Belgium, for about 2 months, and were then cooled for 9 months before processing in the Milli.

Early in 1971, construction of the solvent extraction plant Milli had been finished, and she was the only highly-shielded chemical facility which we had available to process the material. Milli did not incorporate shielded ion exchange equipment, only a non-shielded ion exchange column was available which could be used for final product purification. This meant that a solvent extraction process was to be used for primary recovery of Pu-238 and Np-237. Another restriction was that, according to its original destination as a PUREX test facility, processing of a series of high-burn-up power reactor fuels was planned in the Milli after the Pu-238 campaign. It was therefore decided to use a TBP process for the Pu-238 campaign, in order not to contaminate the plant with a foreign organic solvent, although we were aware that TBP could not be considered a "first choice" for Pu-238 processing (32). Thus, a TBP flowsheet was developed (33,34), and processing of the irradiated Np-237 targets started in the last quarter of 1971 using the scheme shown in Fig. 3.

The irradiated target rods were cut open, the $(\text{Np,Pu})\text{O}_2$ -Fe cermet pellets were removed from the hull and dissolved in two stages. First, the iron matrix was dissolved with 2 molar nitric acid below 60 °C. Tests with unirradiated pellets had shown that NpO_2 is practically undissolved with this procedure; however, with the irradiated pellets losses of Np and Pu occurred during matrix dissolution which necessitated

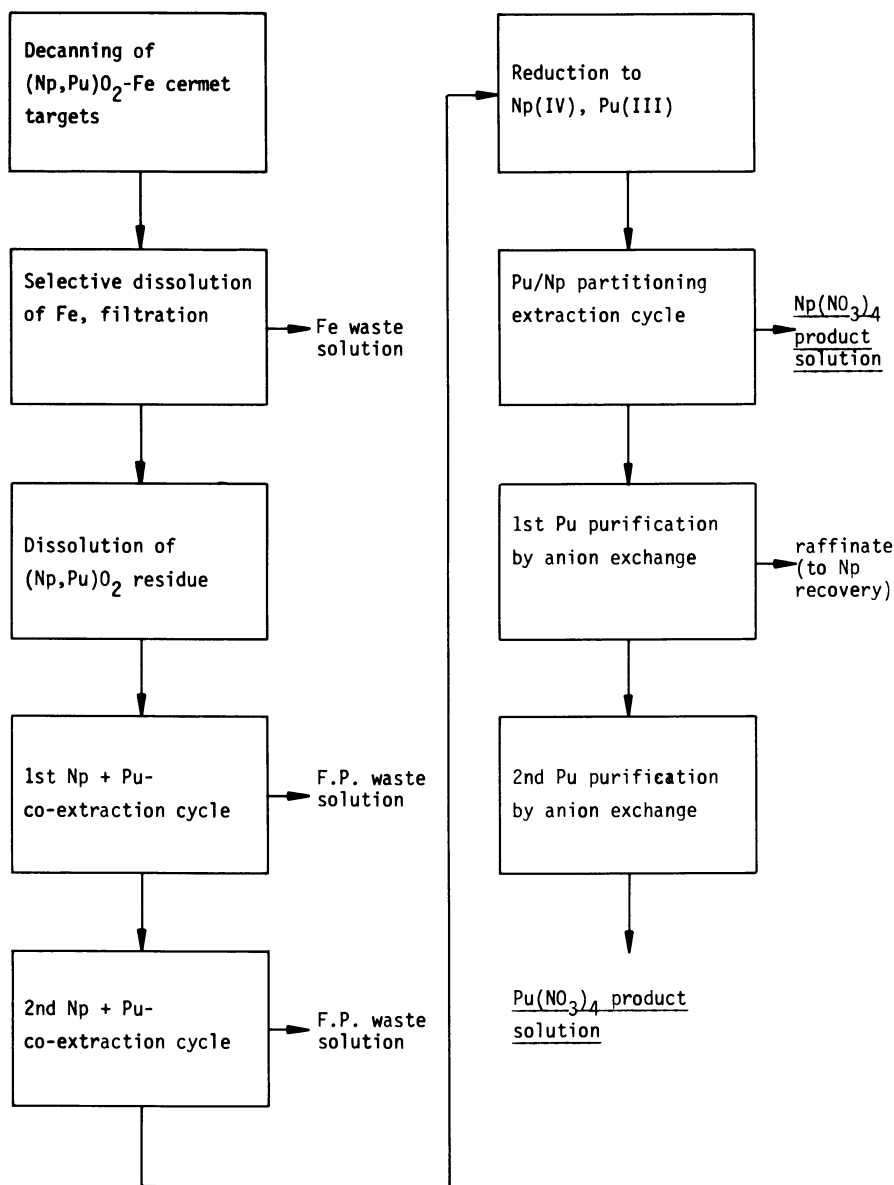


Figure 3. Block scheme for the processing of irradiated $\text{NpO}_2\text{-Fe}$ targets in the Milli facility (37)

a separate processing of this stream. Undissolved (Np, Pu) O_2 residues were filtered off, and were then dissolved with boiling 10 molar nitric acid. The solubility of this material was lower than expected from unirradiated Np O_2 , and after 3 days an undissolved residue of ca. 2 g Np O_2 remained which was filtered off, and was finally dissolved within 20 hours using boiling 10 molar nitric / 0,02 molar hydrofluoric acid. The dissolver solution was made 3 molar in nitric acid, and was fed to the HA mixer-settler of the first TBP co-decontamination cycle. Due to the prolonged boiling of the dissolver solution, most of the Np (86 %) was hexavalent in the extraction feed solution, while > 80 % of the Pu was present as Pu(IV) and < 20 % as Pu(VI). The solvent used was 10 vol.% TBP in n-alcane C₁₀-C₁₃. 0,3 moles/l vanadate was introduced with the 3 molar nitric acid scrub (HAS) solution to oxidise residual Np(V) to extractable Np(VI) (6). Pu and Np were back-extracted in the HC mixer-settler by 0,2 molar nitric acid. A gross-gamma decontamination factor (DF) of only 9 was obtained by this extraction cycle, with single-isotope DFs of 3,5 for Zr-95, 35 for Np-95, and 70 for Ru-103. The residual gamma activity of the product solution was mainly due to Zr-95 (61 %), Pa-233 (17 %), Nb-95 (4 %), and Ru-103 (0,5 %). The Pu/Np product solution was stored in a catch tank for several days during which about half of the Pu-238 "vanished" from the solution. The explanation for this "mysterious" effect was found when it was detected that a few liters of organic solvent had incidentally run with the product solution into the catch tank, probably because of insufficient phase separation in the HC mixer-settler. Sufficient dibutyl phosphoric acid was formed by radiolysis of this solvent over the days to extract a major part of the plutonium. This radiolized solvent was then separated from the aqueous phase, and the Pu-238 recovered by a special treatment (see below). The aqueous product, after concentration by evaporation, was fed to the second co-decontamination cycle which was run under similar conditions as the first cycle; however, the HA-1AS-1B-1C mixer settlers of Milli were used for this cycle, and 0,2 moles/l chromate was introduced as the oxidant with the scrub instead of the vanadate. This cycle gave a gross-gamma DF of 14; of the residual gamma activity of the product solution, 39 % were due to Ce-144 and 23 % to Pa-233. The product solution was concentrated by evaporation, and a pre-reduction using 0,2 moles/l hydrazine nitrate plus 0,001 moles/l ferrous nitrate catalyst was carried out during 4 hours at 50°C. Then the solution was made up

to 0,2 moles/l ferrous nitrate, 0,45 moles/l (nominal) hydrazine nitrate, and 3,4 moles/l HNO_3 , and was fed to the partitioning cycle which was carried out in the 2A-2B mixer-settlers of Milli. The Np(IV) was extracted by 10 vol.% TBP/n-alcane while the Pu(III) remained in the aqueous raffinate. The loaded solvent was scrubbed with 2 molar nitric acid containing 0,1 moles/l ferrous nitrate and 0,2 moles/l hydrazine nitrate, and the Np was back-extracted by 0,2 molar nitric acid. The Np product contained 17 ppm Pu-238, the total gross gamma DF over the three cycles was ca. 800, and the residual gamma activity was mainly due to the Np-237 daughter, Pa-233 (81 %); the Np product thus corresponded to specifications. The Pu product solution contained 55,2 mg/l Pu and 119 mg/l Np; Pu-238 and Np-237 were separated and further purified by anion exchange using Dowex 1X2 resin und applying essentially the procedure developed at Savannah River Laboratory (38).

Recovery of Pu-238 from the strongly radiolized solvent mentioned above was performed (35) by repeated treatment with an aqueous solution containing 0,1 to 0,2 moles/l ferrous nitrate, 0,2 moles/l hydrazine nitrate, and 0,2 moles/l nitric acid, followed by a final wash with 0,1 moles/l uranium(IV) nitrate, 0,2 moles/l hydrazine nitrate, and 0,5 moles/l nitric acid which was the most effective. Pu-238 was recovered and further purified from the combined wash solutions by anion exchange (36).

A balance of this campaign (36) had the following results: 4,4 g Pu-238 were in total analyzed in the dissolver solutions. Of these, 2,5 g Pu-238 were recovered as the purified product. Major losses arose during selective iron dissolution and filtration (ca. 0,4 g), during anion exchange processing (ca. 0,5 g), and in the different aqueous and organic raffinate streams of the solvent extraction cycles. The principal conclusion to be drawn from this cumbersome campaign was that TBP solvent extraction, as we had expected, is not a well-suited method for recovery of Pu-238 from irradiated Np-237. Another conclusion was that iron is not a well-suited target matrix material. Consequently, the design of a shielded ion-exchange facility was envisaged for the planned routine processing of irradiated Np-237 targets. Also, a study on a solvent extraction process using the secondary amine Amberlite LA-2 as the extractant to recover Pu and Np was initiated (43) in case that the Milli would have to be used on an intermittent basis for further Pu-238 campaigns. However, no further Np-237 irradiations were carried out after termination of the PACT project.

5. Production of Medical-grade Pu-238 from irradiated Am-241

Plutonium-238 produced from neutron-irradiated Np-237 is not isotopically pure; usually, the material contains > 80 % Pu-238 and < 20 % of heavier Pu isotopes, and in addition a few ppm of Pu-236. While the presence of other Pu isotopes generally does not seriously affect the applicability of Pu-238 as a heat source, its use for medical applications (heart pacemakers etc.) is limited by Pu-236 because of the intense gamma radiation of some of the Pu-236 daughters. Pu-238 which is practically free from Pu-236 can be made by irradiation of Am-241, and alpha decay of the Cm-242 thus produced. There are in principal two ways for producing such material:

- either, the irradiated Am-241 target is processed after a short cooling time to separate the plutonium formed in the target (mainly a mixture of Pu-238 and Pu-242) from the curium-242 and the fission products. After storage for Cm-242 decay, the mixture is processed to recover isotopically pure Pu-238 and not-consumed Am-241. Alternately, the Cm-242 and Am-241 may be separated from fission products and from one another immediately after primary separation of the Pu-238/242 mixture, and the isolated Cm-242 may be stored for decay and then processed for Pu-238 purification. By both these options two plutonium fractions are produced, one low-assay Pu-238 fraction and one isotopically pure Pu-238 fraction. Either of these options involves the processing of short-cooled material with very high specific activities.
- or, the target is processed after decay of the Cm-242 to recover a single Pu-238 fraction containing about 20 % of heavier Pu isotopes but essentially no Pu-236. Evidently this option involves the processing of long-cooled material with much decreased specific activities.

A study on the different production options (39) showed that the latter has an economic advantage against the former one, and probably also against the Np-237 route in case that a very low ($\leq 0,1$ ppm) Pu-236 assay would be demanded. (Such extremely low Pu-236 assays may be demanded for large medical power sources, e.g. for an artificial heart). The chemical process which was worked out for the processing of irradiated americium dioxide - aluminium cermet targets consisted of the following steps (40,41): (a) Aluminium is dissolved with 8 molar NaOH. (b) The caustic solu-

tion is filtered off, and the AmO_2 residue is dissolved with 9 molar nitric acid. (c) Pu is adjusted to Pu(IV), and is sorbed on Dowex 1X4 (< 400 mesh) resin on a high-pressure ion-exchange column. The column is washed with 7 molar nitric acid, and the Pu is eluted with 0,5 molar nitric acid. (d) Pu is further purified by a second high-pressure anion exchange cycle. (e) For Americium recovery, the effluent of the first anion exchange cycle is denitrated by formic acid to $\leq 0,5$ moles/l hydrogen ion. (f) Am is sorbed together with rare earths (R.E.) and residual Cm on a high-pressure cation exchange column using AG 50X12 resin (21 to 29 μm grain size). The adsorption column is washed free from other fission products by 0,5 molar ammonium nitrate solution. (g) Am is separated from Cm and R.E.s by chromatographic elution with α -hydroxy isobutyric acid (pH = 3,45) through a high-pressure separation column loaded with AG 50X12 resin (21 to 29 μm).

The process was tested in 1973 on a small scale in a lead-shielded box with single irradiated AmO_2 -Al targets (41,42). Dissolution of Al was slower than with unirradiated pellets, and the tendency to foaming was stronger. Losses of plutonium with the caustic increased strongly with increasing contact time of the americium oxide with the NaOH solution, raising from 3,3 % loss after 2 h contact to 16,1 % loss after 28 h contact. In contrast, losses of Am and Cm with the caustic were usually $\leq 0,5$ % and not time-dependent. In the anion exchange separation, Pu losses occurred when the Pu valency was not properly adjusted; losses increased with increasing Cm-242 concentration and, hence, irradiation dose. However, with valency adjustment by addition of hydrogen peroxide followed by 1 h boiling and by immediate processing through the anion exchange column, losses could be kept at about 5 % even with relatively high Cm-242 concentrations. In the cation exchange step, Am recoveries of 90 to 98 % and Cm-242 recoveries of 85 to 95 % were observed; decontamination factors were 100 to 300 for Zr/Nb-95, > 2000 for Ru-103/106, and > 10000 for other fission products.

References

1. Ramdohr, H.; Knoch, W.; Koch, G.; Krause, H.; Roth, B.; "Entwicklungsprogramm Brennstoffaufarbeitung, erster Statusbericht 1968" (development program fuel reprocessing, first status report 1968), May 1969
2. Ochsenfeld, W.; Diefenbacher, W.; Leichsenring, C.H.; Proceedings "Design of and Equipment for Hot

- Laboratories" (Otaniemie, Finland), IAEA, Vienna 1976
3. Höhlelein, G.; Gasteiger, R.; "Das Actiniden-Projekt der Gesellschaft für Kernforschung mbH, Karlsruhe", in: Proceedings "Radiation Protection Problems related to Transuranium Elements", EUR 4612 (1971), p. 69-84
 4. Bähr, W.; German Rept. KFK-797 (1968)
 5. Ochsenfeld, W.; Bähr, W.; Koch, G.; Reaktortagung, Berlin 1970, Proceedings p. 530
 6. Bähr, W.; Koch, G.; German Pat. 1.919.400 (1969/1974)
 7. Koch, G.; "Recovery of Neptunium-237, Plutonium-238, and Plutonium-242", in Koch, G. (ed.), "Transuranium Elements", Part A1 II, System No. 71 of "Gmelin Handbook of Inorganic Chemistry", Supplement Vol. 7b, p. 288-315, Berlin-Heidelberg-New York 1974
 8. Schulz, W.W.; Benedict, G.E.; USA report TID-25955 (1972)
 9. Ryan, J.L.; USA report HW-59193 REV (1959)
 10. Isaacson, R.E.; Judson, B.F.; Ind. Eng. Chem. Process Design Devel. 3 (1964) 296
 11. Koch, G.; Baumgärtner, F.; Goldacker, H.; Ochsenfeld, W.; Schmieder, H.; German report KFK-2557 (1977)
 12. Ochsenfeld, W.; Baumgärtner, F.; Bauder, U.; Bleyl, H.J.; Ertel, D.; Koch, G.; German report KFK-2558 (1977)
 13. Burns, R.E.; Schulz, W.W.; Bray, L.A.; Nucl. Sci. Engng. 17 (1963) 566
 14. Moore, R.L.; Bray, L.A.; Roberts, F.P.; in: McKay, H.A.C.; Healy, T.V.; Jenkins, I.L.; Naylor, A. (eds.), "Solvent Extraction Chemistry of Metals", Macmillan, London 1965, p. 401
 15. Weaver, B.; Kappelmann, F.A.; USA report ORNL-3559 (1964)
 16. Weaver, B.; Kappelmann, F.A.; J. Inorg. Nucl. Chem. 30 (1968) 263
 17. Koch, G.; in: Kertes, A.S.; Marcus, Y. (eds.), "Solvent Extraction Research", Wiley-Interscience, New York - London - Sydney - Toronto 1969, p. 349
 18. Koch, G.; German report KFK-1656 (1972) p. 1-10
 19. Koch, G.; Kolarik, Z.; Haug, H.; Hild, W.; Drobnik, S.; German report KFK-1651 (1972)
 20. Koch, G.; Kolarik, Z.; Haug, H.; Radiochimica (USSR) 17 (1975) 601; J. Inorg. Nucl. Chem., Suppl. 1976, 165
 21. Kolarik, Z.; Koch, G.; Kuhn, W.; J. Inorg. Nucl. Chem. 36 (1974) 905

22. Haug, H.O.; *J. Radioanal. Chem.* 21 (1974) 187
23. Wheelwright, E.J.; Roberts, F.P.; Bray, L.A.; USA report BNWL-SA-1492 (1968)
24. Wheelwright, E.J.; Roberts, F.P.; USA report BNWL-1072 (1969)
25. Campbell, D.O.; *Ind. Eng. Chem. Process Design Develop.* 9 (1970) 95
26. Hale, W.H.; Lowe, J.T.; *Inorg. Nucl. Chem. Letters* 5 (1969) 363
27. Lowe, J.T.; Hale, W.H.; Hallmann, D.F.; *Ind. Eng. Chem. Process Design Develop.* 10 (1971) 131
28. Burney, G.A.; *Nucl. App.* 4 (1968) 217
29. Vaughen, V.C.A.; "Recovery of Americium and Curium", in: Koch, G. (ed.), "Transuranium Elements", Part A1 II, System No. 71 of "Gmelin Handbook of Inorganic Chemistry", Supplement Vol. 7b, p. 315-326, Springer, Berlin - Heidelberg - New York 1974
30. Koch, G.; Schön, J.; German report KFK-783 (1968)
31. Scheffler, K.; Kuhn, K.D.; Koch, G.; Schön, J.; Reaktortagung, Berlin 1970, Proceedings p. 534
32. Jenkins, I.L.; *Actinide Revs.* 1 (1969) 187
33. Koch, G.; Ochsenfeld, W.; Schön, J.; Hamburger, E.; Schwab, P.; Majchrzak, K.; Franz, G.; German report KFK-1456 (1971), p. 62-91
34. Koch, G.; Schön, J.; Majchrzak, K.; Hamburger, E.; Franz, G.; German report KFK-1544 (1972), p. 65-70
35. Ochsenfeld, W.; Bier, K.; Höffle, G.; Riffel, W.; Schön, J.; Schwab, P.; Hamburger, E.; Kuhn, E.; Ertel, D.; Theis, W.; Knittel, G.; Wettstein, W.; German report KFK-1544 (1972), p. 73-95
36. Ochsenfeld, W.; Höffle, G.; Hamburger, E.; Schön, J.; Schwab, P.; Riffel, W.; Ertel, D.; Theis, W.; Wettstein, W.; Knittel, G.; German report KFK-1656 (1972), p. 63-72
37. Koch, G.; Ochsenfeld, W.; *KFK-Nachrichten* 3 (1972) No. 1, p. 9
38. Burney, G.A.; *Ind. Eng. Chem. Process des. Dev.* 3 (1964) 328
39. Gasteiger, R.; German report PACT-36 (1973)
40. Höhle, G.; Weinländer, W.; German report KFK-1456 (1971) p. 94
41. Weinländer, W.; Bumiller, W.; German report KFK-1849 (1974) p. 54
42. Weinländer, W.; Bumiller, W.; unpublished
43. Koch, G.; Ochsenfeld, W.; Schön, J.; Franz, G.; Tullius, E.; German report KFK-1788 (1973) p. 24-30

RECEIVED June 28, 1979.

Separation of Actinides from Purex-Type High Active Waste Raffinates

Development of Experimental Studies at JRC-ISPRA Establishment

L. CECILLE, H. DWORSCHAK, F. GIRARDI, B. A. HUNT, F. MANNONE, and F. MOUSTY

JRC-ISPRA Establishment, 21020 ISPRA (Varese), Italy

The reduction of the potential long term hazard of radioactive wastes generated by the nuclear fuel cycle has been the objective of European and USA R&D programmes. Several conceptual and experimental studies on the feasibility of the actinide separation from radioactive wastes (waste partitioning) have been developed at various national (USA, Sweden) laboratories (1-4). Experimental investigations in this field were also carried out until 1977 in France, at the CEA laboratories (5).

Various separation techniques currently applied for actinide recovery processes (precipitation, solvent extraction and ion exchange) were regarded as potentially promising for partitioning purposes. The aim of the waste partitioning is however quite different from that of existing actinide recovery processes, which mainly serve to purify actinides from fission products (FP). Consequently, existing actinide recovery processes need to be suitably adapted in order to meet the new requirements of waste partitioning.

If the separation of actinides from HAW is demonstrated to be feasible, a number of alternative waste management options could open up, due to large differences in the radiation properties of the two waste fractions.

HAW Partitioning Studies

Partitioning studies at the Joint Research Centre - Ispra Establishment of the Commission of the European Communities were oriented towards highly radioactive wastes generated by the 1st TBP extraction cycle of the Purex process (HAW raffinates) and towards actinide separation techniques operating under low acidity conditions such as solvent extraction by TBP or HDEHP and oxalate precipitation (6-11). The HAW partitioning was deemed to be the first stage of an advanced waste management strategy based on the continuous recycling of separate actinide wastes within the fuel cycle. Other alternative waste management options based on separate storage and disposal of the two waste fractions, will be studied at a later stage. It was, in fact, considered that, while a decision on waste partitioning or not must be reached within a few years, a final decision on a separated actinide management can be deferred for much longer times.

0-8412-0527-2/80/47-117-427\$05.00/0

© 1980 American Chemical Society

The main objectives of HAW partitioning studies are:

- (1) to demonstrate on a laboratory scale the technical feasibility of the actinide separation from HAW raffinates. Laboratory experiments at tracer and full activity level are performed in order to obtain fundamental data and other information needed to develop on a laboratory scale complete HAW partitioning flow-sheets;
- (2) to evaluate the engineering implications of the partitioning flow-sheets developed on laboratory scale. The engineering assessment is performed assuming that only established technologies and equipment will be utilized;
- (3) to prepare reference conceptual designs for preliminary cost evaluations.

Experimental

To integrate the HAW partitioning into a waste management scheme including concentration, intermediate storage and conditioning steps, two options can be envisaged. The HAW may in fact be partitioned:

- (1) either immediately after being generated by the 1st Purex extraction cycle (DIRECT partitioning);
- (2) or after a suitable period of intermediate storage in concentrated form (DELAYED partitioning).

Experimental studies were therefore directed to investigate the removal of actinides from both diluted (5000 l/t) and concentrated (about 500 l/t) HAW solutions. Three alternative processes have been selected for this purpose. They all rely upon actinide separation at low acidity conditions requiring a preliminary denitration step. Two of them (TBP and HDEHP processes) are based on solvent extraction techniques using as extractants a neutral (TBP) and an acidic (HDEHP) organophosphorus compound respectively. The third process (OXAL) applies as the first step the precipitation of actinides and lanthanides FP as oxalates.

It is assumed that:

- (1) the HAW raffinate to be partitioned is generated by reprocessing of LWR spent fuels irradiated at 33,000 MWd/t, and cooled for 150 days before reprocessing;
- (2) 99.5% of U and Pu originally present in the spent fuel is removed by the Purex reprocessing operations;
- (3) the separation of Np is attained either by co-extraction with U and Pu during the Purex process or, without affecting conventional reprocessing operations, during an additional extraction cycle of acidic HAW aimed at removing residual Pu before the acidity reduction step.

Even though the degree of the actinide removal still needs to be more precisely defined, actinide decontamination factors (DF) of 10^3 for Pu, Am and Cm are taken as target values to be attained (12) by a specific partitioning process on HAW raffinates. A DF of about 10 for Np appears to be sufficient; higher values would indeed yield only an insignificant advantage (12).

The TBP extraction process. The extraction of trivalent actinides by TBP may succeed, as well known, at low acidity conditions, provided a sufficient nitrate salt content is reached in the feed solution (13,14). However, the large amount of salting agents to be added to the HAW (tons of Na and Al nitrate per ton of spent

fuel) would lead to an unacceptable volume increase of the vitrified waste. On the contrary, if about ten-fold concentrated HAW is processed, the amounts of Na and Al nitrate to be added per ton of spent fuel will remain comparable with the proportions of the additives required for the glass making process. This means on the other side that the TBP process can be applied only for a DELAYED partitioning, i.e. after an adequate additional cooling period of the HAW. After 5-years cooling, the activity level will decrease by a factor of 10 approximately with respect to that at 150-days cooling. A still higher benefit may, moreover, come from the virtually total decay of ^{95}Zr and ^{95}Nb , the most detrimental isotopes to solvent integrity.

The concentration of HAW raffinates and the addition of suitable amounts of nitrate salts are therefore the key steps on which the applicability of the TBP process for partitioning purposes is based.

The main steps of this process are illustrated in Fig. 1. The HAW is assumed to be concentrated at the reprocessing plant to about 500 l/ton and will have at the end of the 5-years storage period a nitric acid concentration of about 4 M. Concentrated and stored HAW solutions are expected to contain a considerable amount of precipitates that may have been formed freshly during the foregoing steps and may include also solids from reprocessing operations. After separation, these precipitates are expected to need further treatment for actinide removal. However, laboratory results obtained with simulated HAW solutions showed that maintaining the acidity above 4 M during the HAW concentration, the fraction of Pu adsorbed on the precipitates may be significantly reduced. Therefore, provided the acidity may be kept at the same level also during the storage period, the treatment of these precipitates could eventually be limited to a simple washing.

Two options are proposed for this process. In the case of option 1, after removal of precipitates (clarification), an additional extraction cycle of acidic HAW is introduced before the denitration step. The purpose of this cycle is to get acidic HAW virtually free from extractable Pu (and also from Np and U) so that, during the successive HAW denitration, the formation of Pu-bearing precipitates should be substantially minimized. A conventional Purex type co-decontamination cycle is proposed for the selective removal of Pu, U (and Np, if the latter has not been previously co-extracted during the Purex reprocessing operations). According to option 2, the denitration of concentrated HAW is carried out without any previous Pu extraction. During denitration, as the acidity of the HAW solution decreases, hydrolysis and polymerisation of extractable Pu is expected, together with precipitation of hydrolysable FP still remaining in the solution. It appears, however, at least from results obtained on simulated HAW solutions that by carrying out the denitration under suitably selected process conditions, it should be possible to reduce the retention of Pu on the precipitate to less than 1% of its initial amount. A detailed study on the denitration process and reaction mechanisms involved is presently under way.

The TBP countercurrent extraction step will provide for the separation of Am, Cm and Lanthanides from other FP. From the latter, the most part of extractable Mo and Zr could have been already eliminated in the foregoing steps (Pu, Np, U extraction and precipitation at low acidity) whereas the Ru remaining from the foregoing precipitation (about 50%) should distribute nearly equally between the organic and aqueous phases.

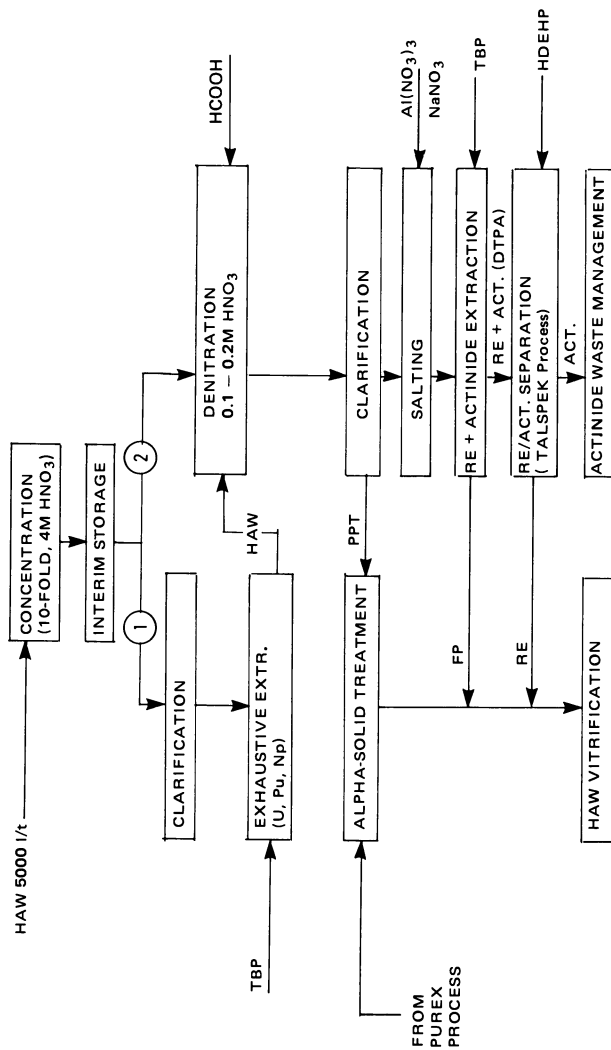


Figure 1. Process scheme for the delayed HAW partitioning based on the actinide extraction by TBP (TBP Process)

Actinides and RE will be back-extracted from TBP by a complexing 0.1 M pentasodium diethylenetriaminepentaacetate (Na_5 DTPA) solution in 1 M glycolic acid at $\text{pH} = 3$.

The aqueous strip solution will form directly the feed solution of the Am, Cm/RE countercurrent separation step, to be performed according to the operating conditions of the TALSPEAK process (15). The presence of a complexing agent like DTPA will prevent the extraction of Am and Cm whereas the RE will be more easily extracted by di(2-ethylhexyl)phosphoric acid (HDEHP) in *n*-dodecane ($\text{pH} = 3$).

By a separate scrubbing of the loaded solvent with a fresh aqueous DTPA solution, the Am-Cm fraction lost to the organic phase should be completely removed. The two DTPA aqueous phases will constitute the starting solution for final actinide conditioning processes.

The HDEHP extraction process. The proposed HDEHP flow-sheet is illustrated in Fig. 2. In this flow-sheet the only extractant used through the whole process is HDEHP. It is a well known acidic organophosphorus compound with extraction capacities for metal-ions highly dependent on the hydrogen-ion concentration. This extractant has not been used in fuel reprocessing plants but in many actinides separation processes such as DAPEX (16), PUBEX and CLEANEX (17). Its properties (extractive capacity, radiation stability, etc...) are therefore reasonably well known (17,18). The use of this extractant has created some problems deriving from the reduced loading capacity of the solvent as well as from its strong complexing properties, causing difficulties for the back-extraction of some elements (Zr, Mo) and for its clean-up.

The solutions so far experimented to solve these problems, namely:

- 1) the use of large volumes of solvent to balance its reduced loading capacity,
- 2) the use of suitable chemicals and operating conditions in order to improve the back-extraction efficiency,
- 3) the addition of TBP to the HDEHP/*n*-dodecane mixture in order to avoid the third phase formation during the alkaline washing,

appear to be effective from the chemical and hydraulic points of view but unsatisfactory from that of the overall waste balance, due to the generation of non-recyclable waste streams in which the absence of alpha-contaminants cannot be guaranteed.

Also for the HDEHP process, two options are proposed that are quite similar to those already proposed for the TBP flow-sheet, i.e. an additional U, Pu and Np extraction cycle to be performed before denitration (option 1) or alternatively a denitration step without any previous HAW treatment (option 2). The operating conditions of the denitration process are similar to those indicated for the TBP flow-sheet. Results obtained using simulated HAW solution showed also in this case the possibility of minimizing the Pu adsorption on precipitates, if suitable process conditions are applied in carrying out the denitration step ($\text{HCOOH}/\text{HNO}_3 = 2$; $\text{pH} = 2$).

After the denitration, the process steps sequence of option 2 is similar to the "Reverse Talspeak Process" already developed on a cold laboratory scale at the KfK laboratories of Karlsruhe (19) for the recovery of actinides from HAW. It involves the coextraction of actinides with RE by HDEHP/TBP in *n*-dodecane at about $\text{pH}2$, the selective stripping of actinides by a Na_5 DTPA-glycolic acid solution and the stripping of RE by 4 M HNO_3 . In the case of option 2, the stripping of co-extracted

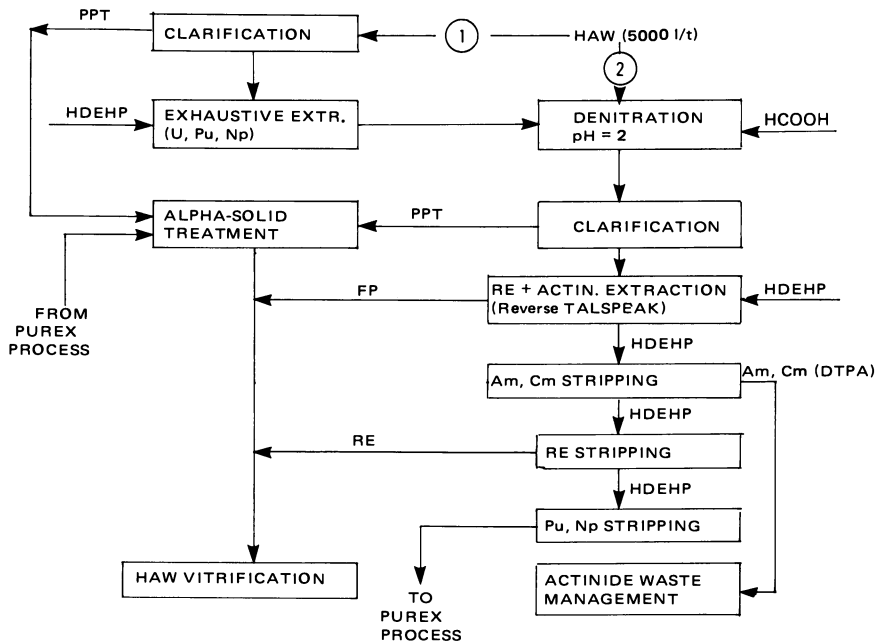


Figure 2. Process scheme for the direct HAW partitioning based on the actinide extraction by HDEHP (HDEHP Process)

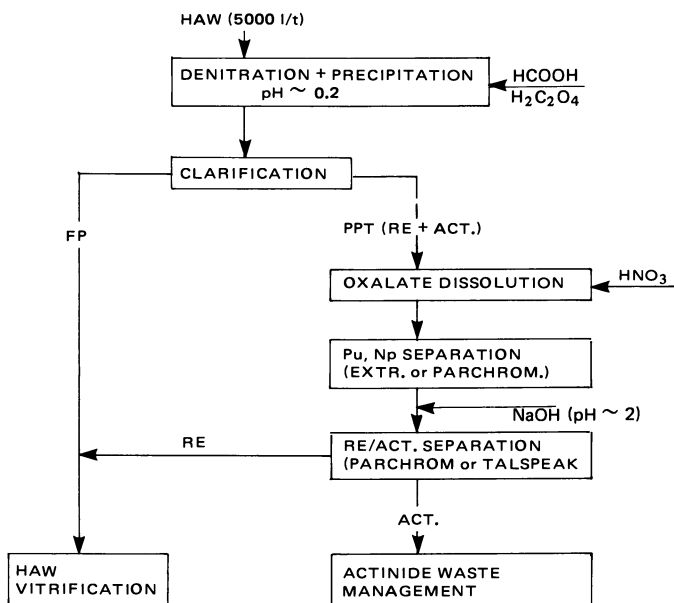


Figure 3. Process scheme for the direct HAW partitioning based on actinide oxalate precipitation (OXAL Process)

Pu and Np is carried out by a 0.8 M $\text{H}_2\text{C}_2\text{O}_4$ solution.

The OXAL process. The flow-sheet of the Oxal process is shown in Fig. 3. The denitration is carried out by slow addition of the waste solution to the boiling mixture of formic and oxalic acid. The presence of the oxalic acid during the denitration prevents the polymerisation and precipitation of hydrolysable ions such as Zr and Mo ions, and assures the precipitation of the RE and actinide oxalates from homogeneous solutions in a well-crystallized form. After clarification, the supernatant is sent to vitrification and the oxalates are dissolved and destroyed by nitric acid so that a final solution (3M HNO_3) is obtained.

The final separation of Am and Cm from RE can be done by applying the solvent extraction techniques developed in the HDEHP and TBP flow-sheets. As an alternative, partitioning techniques based on column extraction chromatography (LEVEXTREL-TBP and LEVEXTREL-HDEHP) are being experimentally studied on fully active HAW solutions. A final decision on the techniques for the actinide/RE separation will be reached at a later stage of the programme.

Results and Discussion

A synthetic waste solution simulating chemically a 150-day decayed HAW raffinate (Table I) was used to carry out tracer laboratory experiments on TBP, HDEHP and OXAL processes.

Fully active laboratory scale experiments were started using firstly a Windscale HAW solution (5000 l/t) generated by the reprocessing of Magnox fuel elements with a burn-up value of 3500 MWd/t. The overall decay time was about 10 months and as the composition was not known, only relative activity measurements were performed. Other fully active HAW solutions were subsequently prepared in Ispra hot cells by dissolving UO_2 samples irradiated at 26 – 36,000 MWd/t and cooled for about 4 years. Successive TBP batch-extraction steps were carried out under the 1st extraction cycle conditions of the Purex process to remove the bulk of U and Pu.

Denitration experiments. Results reported in Table II are relating to the denitration tests performed on the unconcentrated HAW solutions (5000 l/t) as proposed in the HDEHP process scheme (option 2).

By operating the denitration of simulated HAW with a $\text{HCOOH}/\text{HNO}_3$ molar ratio of about 2, it seems possible to maintain almost quantitatively the Pu in the extractable form. The following mechanism is tentatively proposed to explain the Pu behaviour during denitration: the lower retention of Pu into denitration precipitates at pH2 is probably due to the reduction of Pu (IV) to Pu (III), even if Pu is initially present under polymeric form. This reduction is probably promoted by the formic acid decomposition in the presence of the Pd and Rh black acting as catalysts (20,21). Preliminary results of fully active runs (Table II) are quite comparable although some Pu was lost to the precipitate. The higher Pu fraction adsorbed on the precipitate separated in the active run nr. 3 was probably due to the incomplete dissolution of Pu formate by the 4M HNO_3 wash.

TABLE I : Composition of simulated HAW solution calculated from ref. 22 & 23 assuming a value of 5000 l/ton U, (burn-up = 33,000 MWD/ton; initial ^{235}U enrichment = 3.3%; decay time = 150 days)

Element	g/l	Element	g/l
Ge(IV)	$7 \cdot 10^{-5}$	La(III)	0.254
As(III)	$1.75 \cdot 10^{-5}$	Ce(III)	0.576
Se(IV)	0.01	Pr(III)	0.24
Br(V)	$3 \cdot 10^{-3}$	Nd(III)	0.78
Rb(I)	0.066	Pm(III)	0.021
Sr(II)	0.18	Sm(III)	0.16
Y(III)	0.094	Eu(III)	0.036
Zr(IV)	0.73	Gd(III)	0.021
Mo(VI)	0.69	Al(III)	0.0021
RuNO(III)	0.45	Cr(III)	0.096
Rh(III)	0.08	Ni(II)	0.047
Pd(II)	0.26	Cu(II)	0.02
Ag(I)	$1.2 \cdot 10^{-2}$	Zn(II)	0.024
Cd(II)	0.017	Na(I)	1.61
In(III)	$2.4 \cdot 10^{-4}$	Fe(III)	1.88
Sn(IV)	0.011	U(VI)	0.95
Sb(III)	$3.5 \cdot 10^{-3}$	Np	$\geq 15.2 \cdot 10^{-3}$
Te(IV)	0.113	Pu	$9.08 \cdot 10^{-3}$
I(V)	0.054	Am	$30.6 \cdot 10^{-3}$
Cs(I)	0.544	Cm	$7.06 \cdot 10^{-3}$
Ba(II)	0.278		

TABLE II : Behaviour of Pu during denitration of unconcentrated HAW solutions by formic acid

Run nr.	1	2	3	4
HAW solution (5000 l/t)	simulated	simulated	fully active	fully active
chemical form of Pu	ionic	polymeric*	probably ionic	probably ionic
HCOOH/HNO ₃ molar ratio	2	2	~ 2	2.2
% Pu left in the supernatant solution	86	61	70	56
% Pu recovered by formic and nitric washings	14	39	28	43.4
% Pu left in the precipitate	< 0.1	< 0.1	2	0.6

* prepared according to reference 24

The behaviour of Am and Cm was quite similar to that observed for Pu. Experiments are still in progress to optimize the operating conditions.

Results obtained from denitration tests performed on a concentrated synthetic HAW solution (500 l/ton U) as proposed in the TBP process scheme (option 2), were comparable to those discussed above. The experiments were so far done on simulated HAW solutions. Active runs are scheduled for the second half of 1979.

Solvent extraction experiments. Until now all extraction and back-extraction tests were performed batchwise. Typical results obtained for the HDEHP process (Table III) do not show significant differences between extraction tests performed on simulated and fully active HAW solutions.

TABLE III : Percent separation yields obtained from HDEHP batch extraction tests on simulated and fully active HAW solutions

Option	Elem.	Solvent	Simulated HAW		Fully active HAW	
			Acidity	% Extr. yield ¹	Acidity	% Extr. yield ¹
1	Pu	0.25 M HDEHP in mesitylene	4 M HNO ₃	> 99.8	4 M HNO ₃	> 99 ⁴
	U			> 99.9		
	Np			80 ²		³
	Mo			92		
	Zr			99.5		
2	Pu	0.3 M HDEHP	pH=2.11	> 99	pH=2.76	≥ 99.5 ³
	Np	0.2 M TBP		≥ 98		~ 1.0
	Ru	in		~ 0.5		~ 99.5
	Am	n-dodecane		≥ 98		≥ 99.5
	Cm			≥ 99		≥ 99.5
	Ce			≥ 98		≥ 99.5
	Eu			> 99		≥ 99.9

¹ after a single extraction stage

² cumulative, after 4 extraction stages

³ not measured

⁴ solvent: 0.3M HDEHP - 0.2M TBP in n-dodecane

Pu, Am and Cm separation yields appear to be sufficiently high considering that the indicated values correspond to a single extraction stage.

According to the preliminary results of a single back-extraction test performed on fully active laboratory scale, after three successive back-extraction stages, the overall Pu stripped from the loaded HDEHP/TBP solvent originated by the exhaustive extraction step (option 1) was nearly quantitative.

As far as the back-extraction of loaded HDEHP/TBP solvent is concerned (option 2), only simulated HAW solutions have been so far tested. Results reported elsewhere (10) indicated that Pu, Mo, Zr and U may be almost quantitatively removed from the loaded HDEHP/TBP solvent by an oxalate solution at pH 2.5 and confirmed that this organic mixture, employed according to the "Reverse Talspeak

Process", is able to attain a well satisfactory separation of trivalent actinides from RE. Hot cell extraction tests are in progress.

Also in the case of the TBP process, only simulated HAW solutions have been until now used to study the process feasibility. Results have already been reported (9), which indicated that separation yields of about 99.9% can be obtained for Am after three successive extraction stages operating with a concentrated HAW solution adjusted to 0.1 – 0.2 M HNO_3 , 0.65 M $\text{Al}(\text{NO}_3)_3$ and 1.3 M NaNO_3 . The back-extraction of all the actinides and RE from loaded TBP (30% in n-dodecane) was carried out by means of Na_5 DTPA-glycolic acid solution which can be then used directly to separate Am and Cm from RE according to the Talspeak process (15).

Oxalate precipitation experiments. Simulated and fully active HAW solutions have been utilized to carry out experimental tests on the separation of actinides by oxalates precipitation and on the actinide/RE separation steps.

The Oxal process was initially tested by carrying out separately the HAW denitration and the oxalate precipitation. Results obtained from simulated and Windscale HAW solutions are in good agreement. The best DF for Am and Cm ($\sim 2 \times 10^3$) were obtained, however, on the Windscale solution, operating at about pH 2.

To prevent during the denitration step the formation of precipitates on which Pu and Am were partially and irreversibly adsorbed, denitration and oxalate precipitation were carried out in a single step by addition of the waste solution to the formic and oxalic acid mixture, the latter acid acting as a metal complexant during the denitration step. By experimental tests performed on simulated HAW according to this modified process scheme, separation yields of about 99.5% for Pu and 99.8% for Am were measured. A further reduction of the actinide content was reached by flowing the clarified HAW solution through a Dowex 50 resin column. The oxalate precipitation experiments on fully active HAW solutions have practically been completed. The results obtained from five runs (Table IV) confirmed the previous results obtained on simulated solutions.

TABLE IV : Percent distribution of actinides and RE measured after denitration-oxalate precipitation tests on fully active HAW solutions

Streams \ Elements	% Distribution		
	Am, Cm	Pu	RE
Initial HAW solution (5000 l/t)	100	100	100
Supernatant after denitration + oxalate precipitation	0.1 – 0.8	≤ 0.6	≤ 0.5
HAW effluent from DOWEX 50 column	≤ 0.05	≤ 0.1	≤ 0.05
Solution of re-dissolved oxalates ¹	≥ 99.95	≥ 99.9	≥ 99.95

¹ including the resin column wash

LEVEXTREL resin in the HDEHP form (Bayer, Leverkusen, FRG) was used as stationary phase and two columns were utilized to remove Pu and Am-Cm-RE from the respective acidic and low-acidity feed solutions. More than 99% of Pu was adsorbed and eluted from the first chromatographic column by oxalic acid, whereas less satisfactory results were obtained for the Am, Cm/RE separation tests, fractions of Am and Cm as high as a few percent being carried over into the RE fraction.

Process Engineering Assessment Studies

The scope of these assessment studies is the identification of the process engineering and technical solutions suitable to realize the single process steps and relying completely on systems and equipment that have already been successfully employed by the nuclear fuel cycle technology.

The TBP process. Going through option 1 of Fig. 1 a clarification of the concentrated HAW is necessary to take out solids that might have been in the HAW initially or might have been formed during its interim storage. They could, in fact, carry the Pu contamination through the following exhaustive extraction cycle, independently from hydraulic troubles that their presence would provide. Solids can be separated either by filtration or by centrifugation. Since their actinide content is too high for direct vitrification, they can be transferred without any particular washing to a common treatment system with the solids separated in the reprocessing operations from the dissolver product.

The exhaustive U, Pu extraction step is best achieved in pulsed columns rather than in mixer settlers in order to keep the contact time lower at the very high radiation level. This operation is expected to produce as its main product a HAW raffinate that is virtually free of Pu (and Np, U); a scrub appears therefore superfluous and would dilute only the HAW. In order to attain still a good extraction efficiency within a few stages, A/O phase ratios < 3 should be avoided. This ratio corresponds to a TBP saturation by heavy metals of about 18%. Considerable amounts of Zr are therefore co-extracted, being however present essentially as inactive isotope. Either a complexing or a reductive stripping is advisable in order to keep the aqueous flow small and the acidity sufficiently high to avoid hydrolysis of Zr.

The organic waste stream can be regenerated by the usual procedures applied in a Purex scheme and the (rather small) amounts of salted aqueous wash wastes can be treated together with those of the Purex plant in case some alpha contamination is carried over by incomplete stripping due to retention phenomena.

The principal actinides separation step is performed at low acidity, at pH of about 2. Denitration of HAW is therefore a crucial operation step on which little information is available. The operational margin is rather restricted. A too high pH would lead to heavy precipitate formation with actinides adsorbed on them. Only a batch-wise operation mode can satisfy the chemical and operational requirements and furthermore the utilisation of boiling formic acid raises material corrosion problems.

In any case there will be precipitates and the solution needs therefore to be clarified. This operation should be performed just before feeding the solution into the counter-current extraction step. The adjustment by sodium and aluminium nitrate must therefore be performed first. The addition of an acid deficient Na-Al nitrate solution on the other side would allow stopping the denitration at a higher residual free nitric acid concentration, i.e. at less critical process control conditions. As to the precipitates, uncontrolled actinide amounts may be entrained by them. To avoid time consuming control measures, it seems advisable to treat them "a priori" as alpha contaminated. A simple separation without any washing will therefore be sufficient before joining them to the other alpha solids, as mentioned above.

The following extraction-stripping operation provides for complete Am and Cm extraction, together however with the RE fraction of the FP and substantial amounts of Ru. It acts in the 1st option as a back-up cycle for Pu and Np separation, otherwise these elements too must be separated here completely (option 2). The utilisation of pulsed columns remains the first choice also for this operation and the aqueous raffinate must meet the final specifications for "alpha free" HAW. Again it is therefore of highest importance to run the extraction section at convenient conditions, i.e. at a sufficient stage number and phase ratio. To an A/O ratio of 0.33 corresponds 33% TBP saturation (RE). Only experimental counter-current tests may be able to show if this phase ratio can be increased and if perhaps a scrub could provide for a better separation mainly from Ru, without compromising the complete Am-Cm extraction.

The main purpose of the separation of Am-Cm from RE by the well known Talspeak process is to liberate the RE fraction from actinides. The acceptable residual RE content in the actinide stream on the contrary will depend widely on the further destination of the latter. It is in any way not a critical point. Therefore, high A/O ratios and an efficient aqueous scrub section must provide for an as low as possible extraction of Am and Cm. For these operations mixer-settler batteries seem to offer the most convenient approach, taking into account radiation levels, flow rates and extraction (and back-extraction) kinetics.

The HDEHP process. Conceptually this process is very similar to the TBP process as Fig. 2 shows. Therefore only the main differences are pointed out here. They concern:

- 1) the flow rates. The treatment of unconcentrated HAW means about 10-fold higher aqueous flow rates. The factor for the organic extractant is still more unfavourable taking into account the limited loading capacity of the HDEHP with respect to TBP. The consequences on equipment dimensions and plant layout appear evident;
- 2) this process is foreseen for DIRECT HAW partitioning, i.e. for potentially short cooled HAW containing still considerable levels of ^{95}Zr and ^{95}Nb . Both elements are strongly extracted by HDEHP, a fact that will lead to heavy radiation damage with resulting operational difficulties and separation efficiencies reduction;
- 3) no salting is required. Therefore any possibility of a less extended denitration with a final pH adjustment is excluded.
- 4) a simple back-extraction operation on the loaded organic phase is required in the last step. In order to remove the RE in the second stripping section to the re-

quired specifications for residual alpha contaminants, it is essential that in the first stripping section Am-Cm have been back-extracted quantitatively and that residual Pu and Np are kept also quantitatively in the organic layer. Retention and/or entrainment phenomena would seriously compromise the feasibility of this process.

The OXAL process. The most significant difference of this process with respect to the foregoing processes is the possibility of separating from actinides an important fraction of FP (mainly the couples Zr-Nb and Ru-Rh) without requiring solvent extraction operations. This makes the process highly attractive for the early DIRECT partitioning. On the other side, the handling of highly active solids in sludge form is considered one of the most difficult problems in the reprocessing field. A thorough analysis of the problem shows, however, that by operating batchwise, the denitration-precipitation as well as the dissolution of the precipitates could be performed in the same reactor, avoiding any solids transfer and counter-washing operations. After the dissolution of the precipitates, a small insoluble fraction might require clarification. The further separation of the actinides from residual FP mainly RE, or vice versa, can be performed in the most appropriate way by one of the processes described above.

Conclusions

On the basis of the laboratory indications presently available, all three proposed partitioning processes appear to be feasible and to have the potential for removing actinides from HAW up to the necessary level.

Additional data on the actinide losses to the various secondary waste streams, on the radiation stability of the chemicals used for stripping operations, as well as on their recycle or removal as wastes still need to be obtained on laboratory scale for fully active HAW. The obtained results will provide the basis for deciding whether to proceed or not to a pilot plant scale experimentation. Until such experiments are performed it will be impossible to demonstrate the overall feasibility of the selected partitioning process with an acceptable degree of reliability.

Literature cited

- 1 Bartlett J.W., Bray L.A., Burger L.L., Burns R.E., Ryan J.L., BNWL-1776, 1973
- 2 Bond W.D., Leuze R.E., ORNL-5012, 1975
- 3 Croff A.G., Tedder D.H., Drago J.P., Blomeke J.O.B., Perona J.L., ORNL/TM-5808, 1977
- 4 Lieljenzin J.O., Svantesson I., Hagström I., Proc. of the Conf. on Waste Management, Tucson, Arizona 1976 (1977) 303
- 5 Bathellier A., Guillaume B., Moulin J.P., Proc. of First Tech. Meeting on the Nuclear Transmutation of Actinides, Ispra-JRC, 1977, EUR-5897e,f (1977) 129 - 144

- 6 Mannone F., Cecille L., EUR 5816e, 1977
- 7 Cecille L., Landat D., Lestang M., Mannone F., Proc. of First Tech. Meeting on the Nuclear Transmutation of Actinides, Ispra-JRC, 1977, EUR-5897e,f (1977) 145 - 162
- 8 Mousty F., Toussaint J., Godfrin J., Girardi F., Proc. of First Tech. Meeting on the Nuclear Transmutation of Actinides, Ispra-JRC, 1977, EUR-5897e,f (1977) 163 - 168
- 9 Cecille L., Landat D., Mannone F., Radiochem. Radioanal. Letters, 1977, 31 19 - 28
- 10 Cecille L., Le Stang M., Mannone F., Radiochem. Radioanal. Letters, 1977, 31 29 - 38
- 11 Mousty F., Toussaint J., Godfrin J., Radiochem. Radioanal. Letters, 1977, 31 9 - 18
- 12 Girardi F., Bertozzi G., EUR-5214e, 1974
- 13 Orth D.A., McKibben J.M., Prout W.E., Scotten W.D., Proc. of the Int. Solvent Extraction Conf. 1971, the Hague, 1971, 534 - 555
- 14 Thompson M.C., DP-1336, 1973
- 15 Weaver Boyd, Kappelmann F.A., ORNL-3559, 1964
- 16 Leuze R.E., Lloyd M.H., Process Chemistry, 1970, 4, 549
- 17 Bigelow J.E., Chattin F.R., Waughen W.C.A., Proc. of Int. Solvent Extraction Conf. 1971, The Hague, 1971, 507 - 513
- 18 Schulz W.W., Nuclear Technology, 1972, 13, 159 - 167
- 19 Kock G., Kolarik Z., Haug H., Hild W., Drobnik S., KFK-1651, 1972
- 20 Grignard V., "Traité de Chimie Organique", Masson, Paris, 1948, Tome IX, p. 164 - 165
- 21 Pascal P., "Nouveau Traité de Chimie Minérale", Masson, Paris, 1958, Tome XIX', p. 297 - 304 and 594
- 22 Oak Ridge Nat. Lab. Staff, ORNL-445, 1971
- 23 Schneider K.J., BNWL-820, 1968
- 24 Costanzo D.A., J. Inorg. Nucl. Chem., 1973, 35, 609 - 622

RECEIVED May 22, 1979.

Removal of Americium and Curium from High-Level Wastes

W. D. BOND and R. E. LEUZE

Chemical Technology Division, Oak Ridge National Laboratory, Oak Ridge, TN 37830

A number of potential methods for removing americium and curium from high-level liquid waste have been investigated at Oak Ridge National Laboratory for their applicability to waste partitioning (1, 2, 3, 4). Processes acceptable for americium-curium removal must give a high-degree of recovery and produce a semi-pure, concentrated product of these actinides. All separations methods investigated consisted of two general process steps. First, the trivalent actinide and lanthanide elements are separated from the other elements in the waste. In the second step, americium and curium are then separated from the lanthanide elements. Experimental studies have largely been laboratory-scale in which synthetic waste solutions and tracer levels of radioactivity were utilized. A few laboratory-scale experiments were made in hot cells on the coextraction of trivalent actinides and lanthanides. The two most promising methods investigated for co-removal of trivalent actinides and lanthanides are:

1. A solvent extraction process (4, 5) utilizing dihexyl-[(diethylcarbamoyl)methyl]phosphonate (DHDECMP) as the extractant. This extractant is also called dihexyl-N,N-diethylcarbamoylethylphosphonate.

2. The OPIX process (6, 7), which is based on an oxalate precipitation coupled with a cation exchange treatment of the supernatant liquid.

Studies (1, 2, 3, 4) on the separation of americium-curium from lanthanide elements indicate that both cation exchange chromatography (8, 9) and the Talspeak solvent extraction process (10, 11) are promising methods. Only the most recent work at Oak Ridge National Laboratory is reported in this paper. Potential chemical processes for americium-curium removal and evaluations of their feasibility have been reported previously (1, 2, 3, 4). The most recent experimental work carried out includes the following:

1. Hot-cell studies of the DHDECMP extraction process.
2. Feasibility studies of continuous precipitation of oxalates in the OPIX process.
3. Studies of Talspeak process flowsheets in continuous,

0-8412-0527-2/80/47-117-441\$05.00/0

© 1980 American Chemical Society

countercurrent, mixer-settler equipment and in batch extraction tests.

4. Effects of impurities derived from DHDECMP degradation on the ion exchange loading step of the cation exchange chromatography process.

Hot-Cell Studies of the DHDECMP Solvent Extraction Process

The extraction and stripping of trivalent actinides and lanthanides were studied using high-level liquid waste (HLLW) derived from spent LWR fuel (31,000 MWd/MT burnup and decayed for 4 years). After seven batch extraction stages, the Am-Cm remaining in the waste was <0.01% with indications of continuing decrease with additional extraction (Figure 1). In these extractions, the nitric acid concentration of the HLLW was 3 M and the HLLW was successively contacted with an equal volume of 30% DHDECMP in diisopropylbenzene in seven stages of batch, cross-current extraction. The combined extract phases were subsequently stripped in a succession of contacts with 0.05 M HNO₃ using an organic-to-aqueous phase ratio of 0.5. More than 99% of the Am-Cm was stripped in the first 3 stages (Figure 2); however, little, if any, was stripped in subsequent stages. The Am-Cm and lanthanides which remained in the organic phase after the stripping tests with 0.05 M HNO₃ were removed in a single equal-volume contact with 0.2 M Na₂CO₃. The ease of removal of the trivalent elements with sodium carbonate indicates that the degradation products responsible for their retention are acidic in nature. The lanthanide elements, cerium and europium, showed behavior that was essentially identical to Am-Cm in both extraction and stripping. No emulsions or third phases were observed in any of the equilibrations of organic and aqueous phases.

Continuous Precipitation of Actinide-Lanthanide Oxalates from HLLW

The feasibility of recovering >99.9% of the trivalent actinides and lanthanides using the OPIX process had previously been demonstrated by Campbell (6, 7) in small, batch tests in the laboratory and in hot cells. About 90-95% of the trivalent elements were removed in the precipitation step, and the small amount remaining in the supernatant liquid was removed by a cation exchange column. It was therefore of interest to determine whether the oxalate precipitation step could be performed continuously since continuous methods afford many advantages with respect to both process scale-up and operability. Since it was first necessary to demonstrate a continuous precipitation concept that was basically sound, studies were conducted with synthetic wastes. Synthetic wastes were prepared to correspond chemically to HLLW derived from LWR fuel having a burnup of 33,000 MWd/MT. Methods of preparation of this synthetic solution were described previously (2). Elemental compositions are given in Table I. These initial tests

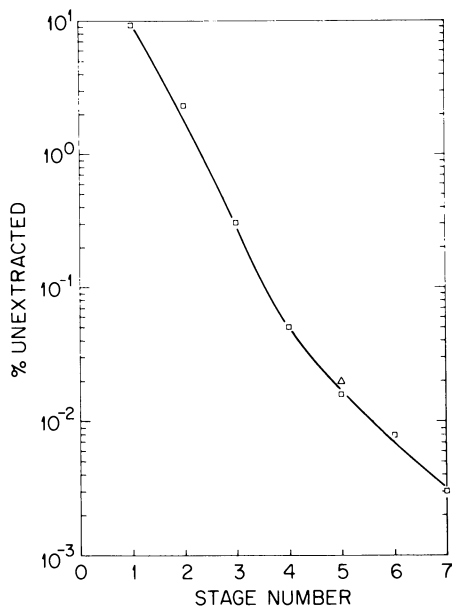


Figure 1. Batch cross current extraction of Am-Cm from high-level liquid waste with 30% DHDECMP: 3M HNO_3 ; 25°C; organic-to-aqueous phase ratio = 1.

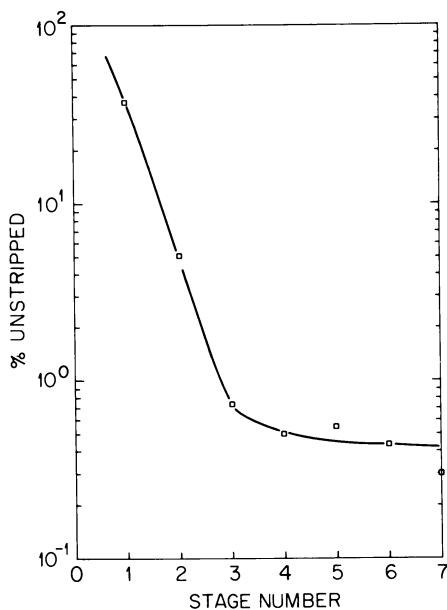


Figure 2. Batch cross current stripping of Am-Cm from 30% DHDECMP with 0.05M HNO_3 ; 25°C; organic-to-aqueous phase ratio = 0.5.

Table I. Synthetic Waste Solution Composition

$$\text{HNO}_3 = 2.5 \text{ M}$$

Elements	g/l
<u>Rare earths</u>	
Lanthanum	0.205
Cerium	0.398
Praseodymium	0.196
Neodymium	0.660
Samarium	0.143
Europium	0.0275
Gadolinium	0.019
Dysprosium	0.0002
Holmium	0.000015
Erbium	0.000005
<u>Group VIII metals</u>	
Ruthenium	0.344
Rhodium	0.0625
Palladium	0.228
<u>Group I A alkali earths</u>	
Rubidium	0.0535
Cesium	0.390
<u>Group II alkaline earths</u>	
Strontium	0.1315
Barium	0.268
<u>Other elements</u>	
Zirconium	0.585
Indium	0.0002
Yttrium	0.0755
Silver	0.0095
Cadmium	0.0185
Arsenic	0.000015
Antimony	0.002
Molybdenum	0.55
Selenium	0.008
Tellurium	0.0905
Tin	0.008

made only with non-radioactive synthetic waste solutions indicate that continuous precipitation of trivalent actinide and lanthanide oxalates appears feasible. Important effects that can be expected by the intense radiation associated with high-level waste are generation of heat within the oxalate precipitate and conversion of oxalate ions to gaseous CO_2 and H_2O .

The experimental equipment used in studying the continuous oxalate precipitation and the separation of the precipitate from the liquid is depicted schematically in Figure 3. The equipment allowed for options of filtering or settling the precipitate and the use of either one or two stirred tank reactors. The following variables were studied:

1. Oxalic acid concentration (0.2 to 0.3 M).
2. Temperature (25 to 50°C).
3. Degree of mixing (125 to 250 rpm).
4. Residence time (15 to 40 min.).

The rotational speeds of the six-bladed stirrers that were used corresponded to power inputs of 0.02 and 0.18 watt/liter at speeds of 125 and 250 rpm, respectively. Concentrations of oxalic acid during precipitation and crystal growth in the stirred tank reactors were varied by changing the flow ratio of oxalic acid-to-waste solution while maintaining the nitric acid concentration constant at 0.9 M. Permissible nitric acid concentrations for the OPIX process (4, 6, 7) are 0.5 to about 1.0 M HNO_3 . Yields of precipitate were determined on the basis of praseodymium recovery. Tracer ^{142}Pr (half-life = 19.2 day, 1.6-MeV γ -ray) was used to measure yields.

The best operating conditions over the range of variables investigated were (12):

1. Two stirred tank reactors in series.
2. An oxalic acid concentration of 0.3 M.
3. Temperature of 25°C.
4. Residence time of 40 min.

Stirrer speeds were not significant in the first stirred tank reactor, but the highest speed (250 rpm, 0.18 watt/liter) gave slightly better performance in the second reactor under some of the test conditions (12). Collection of the precipitate by the gravity settler was not nearly as effective as the series of 12, 5, and 1- μ -diameter Millipore filters. Typical results obtained using two stirred tank reactors in series are shown in Table II. Since a significant fraction of the precipitate particles is $<12 \mu$ in diameter, it is probable that centrifugation would be a good method of separating the precipitate from the supernatant liquid.

Talspeak Process Studies

In the Talspeak process, the separation of trivalent actinides and lanthanides is accomplished by coextracting the two groups of elements into di(2-ethylhexyl)phosphoric acid (HDEHP) from a carboxylic acid solution and then partitioning the acti-

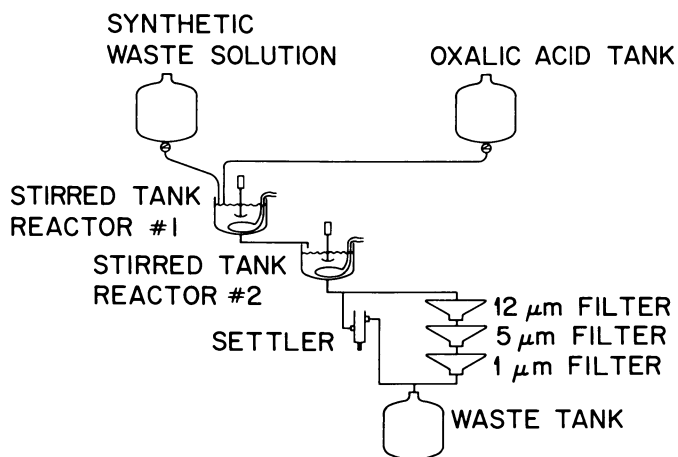


Figure 3. Equipment flowsheet for continuous precipitation of lanthanide oxalates

Table II. Experimental Conditions and Results of Continuous Precipitation of Lanthanide Oxalates from Synthetic High-Level Waste at 350C

	Experiment number										
	27	28	29	30	31	32	33	34	35	36	37
<u>Experimental Conditions</u>											
Residence time per reactor, min	20	40	40	20	40	20	20	40	30	30	30
Stirrer speed in stirred tank reactor 1, rpm	125	250	125	250	125	250	125	250	187.5	187.5	187.5
Stirrer speed in stirred tank reactor 2, rpm	125	125	250	250	125	125	250	250	187.5	187.5	187.5
Oxalic acid concentration, M	0.20	0.20	0.20	0.20	0.29	0.29	0.29	0.29	0.25	0.25	0.25
<u>Product Yield</u>											
Settler	46.2	77.7	76.3	62.5	85.0	68.7	81.8	84.0	79.3	82.6	78.7
Filtration											
12- μ m filter	58.8	81.9	84.1	74.4	90.8	75.8	86.7	89.5	86.0	88.5	86.5
5- μ m filter	65.8	83.1	84.6	78.4	91.0	78.1	88.9	91.3	88.0	88.6	87.1
1- μ m filter	71.1	84.3	87.5	81.6	92.2	77.9	91.3	91.7	89.1	90.2	88.4

American Chemical Society Library
1155 16th St. N. W.

Washington, D. C. 20036

nides into an aqueous phase by stripping the HDEHP with a partially neutralized ($\text{pH} = 3$), aqueous solution containing carboxylic acid and the complexing agent diethylenetriaminepentaacetic acid (DTPA). The aqueous actinide product is acidified (to $\text{pH} 1.5$), and the trivalent actinides are extracted into HDEHP to free them of carboxylic acid and DTPA. They are subsequently back-extracted into 3 M HNO_3 . The effects of impurities on process performance have received little study. Zirconium is known to form highly insoluble compounds with alkylphosphoric acids, but no information was available on the effect of H_2MEHP on the separation factors for trivalent actinides and lanthanides. Performance with respect to zirconium impurity and the expected radiolytic product of HDEHP, mono(2-ethylhexyl)phosphoric acid (H_2MEHP), was of particular interest and was investigated in the studies reported here (13).

The effects of zirconium on phase separations were studied in continuous mixer-settler equipment at reference flowsheet conditions (Figure 4). In these runs neodymium was used to simulate the 0.05 M concentrations of trivalent elements in the feed. Initial batch extraction tests showed that 10^{-4} M Zr had little or no effect on phase separations whereas at 10^{-3} M Zr interfacial emulsions or third phases were formed, making phase separations difficult. Subsequently, three flowsheet runs were carried out in mixer-settlers using 10^{-4} M Zr in the feed solutions and the conditions in Figure 4. No emulsions or interfacial accumulations (sometimes called cruds) were observed in the extraction-partitioning (1A) bank. In the stripping (2A) bank, emulsion formation was noted in stages 10 through 16, and some crud accumulated at the interface of stage 16. Thus, the phase separation was somewhat affected by the presence of 10^{-4} M Zr . (This amount is equivalent to 0.5% of the Zr in HLLW; however, the actinide-lanthanide products obtained from either the DHDECMP extraction process or the OPIX process are not expected to contain this much zirconium.) Nevertheless, the process was operated successfully for scheduled 9-hour periods. The amount of interfacial crud did not appear to increase with time. On the basis of these non-radioactive tests using neodymium, it appears that the process can tolerate zirconium impurity concentrations of about 10^{-4} M without seriously impairing phase separation.

Batch extraction tests showed that H_2MEHP concentrations up to about 0.006 M did not seriously affect separation factors (Table III). The separation factor is defined as the ratio of the distribution coefficient of Am to that of Eu. The distribution coefficient for H_2MEHP between 1 M glycolic acid - 0.05 M DTPA ($\text{pH} = 3$) and 0.7 M HDEHP in diethyl benzene was determined to be about 0.7 and shows that this impurity favors the aqueous phase. Thus, the partitioning step of the Talspeak process is essentially "self-cleaning" with respect to H_2MEHP . The concentration of H_2MEHP on persistent recycle of the solvent within this step would be expected to increase by only a factor of 3 greater than that

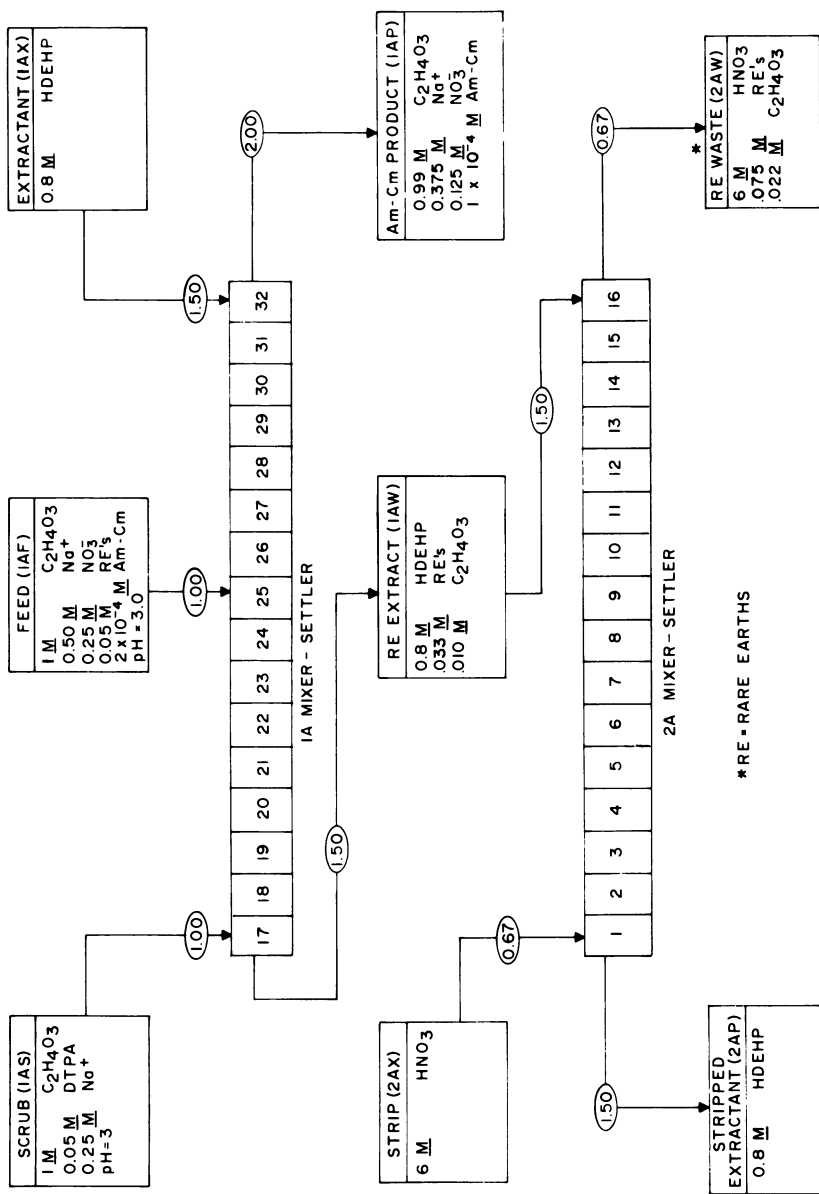


Figure 4. Flowsheet for experimental runs on the first tailpeak cycle in 16-stage mixer settlers

Publication Date: April 16, 1980 | doi: 10.1021/bk-1980-0117.ch031

Table III. Effect of H₂MEHP Concentration on the Separation Factor for Americium and Europium in Talspeak Partitioning

H ₂ MEHP, M	Distribution coefficients		Separation factor
	Am	Eu	
0	1.53	86	56
0.002	1.64	83	50
0.006	1.88	110	59
0.02	2.56	110	43
0.06	5.41	169	31

formed during a single pass using virgin solvent. However, the H₂MEHP formed in the actinide purification step would remain in the organic phase since the distribution coefficient for H₂MEHP at the acidity used for actinide purification (pH = 1.5) is approximately 5. It is expected that the purification step could tolerate significant amounts of H₂MEHP, and solvent purification could be conducted on a campaign basis as needed.

Effects of DHDECMP Degradation Products in Cation Exchange Chromatography

The purpose of this study was to determine if any soluble DHDECMP or impurities derived from DHDECMP by thermal, chemical, or radiolytic degradation might affect the loading step of a cation exchange chromatography (CEC) process. The CEC process has been demonstrated to be technically feasible for trivalent actinide and lanthanide separations (8, 9). Of particular interest was the possible existence of complexing agents among the degradation products that could decrease loading of the trivalent elements. The DHDECMP-derived impurities used in this study were generated by thermal treatment with nitric acid (14, 15). In some cases, the solutions were further treated thermally or with chemical reagents. The principal species formed in the thermal degradation of solvents is generally about the same as with radiation, although the thermal reactions occur more slowly. However, it has been pointed out that there can be important differences (15, 16). Compounds such as hydrogen peroxide and ozone (when air is present) are produced during irradiation and can have an effect.

Table IV. Effects of Dissolved and Degraded DHDECMP Impurities and Oxidative Treatments of These Impurities on the Distribution Coefficient of Tracer Pr-3^+ Between Cation Resin and an Aqueous Solution of $9.7 \times 10^{-4} \text{ M Eu}(\text{NO}_3)_3 - 0.5 \text{ M HNO}_3$

Run no.	Bidentate-derived impurities present	Total phosphorus, ^a mM	Oxidative treatment of initial solution	K
B-1	Yes	2.52	None	348
B-2	Yes	2.52	None	353
B-3	Yes	2.52	Solution refluxed for 3 hours	490
B-4	Yes	2.44	0.3 M H_2O_2 , aged 24 hr. before resin contact	368
B-5	Yes	2.52	Ozone sparging, 10 mg O_3/ml of solution, aged 24 hr.	345
B-6	No	0.00	None	344
B-7	No	0.00	None	328

^aTotal phosphorus concentration is a measure of the amounts of dissolved and degraded DHDECMP present.

Effects of thermal and chemical degradation products were determined by measuring the distribution coefficients, K , between cation resin (Dowex 50-X8) and lanthanide nitrate solutions containing ^{142}Pr (14). In no case did we observe a decrease in K values because of the presence of impurities. Typical experimental results are given in Table IV. The bidentate impurities were prepared by refluxing DHDECMP with 4 M HNO_3 for 9 hours. We generally observed a relatively small increase (10 to 20%) in K values when bidentate-derived impurities were present. It is not known whether the increase is due to sorption of organophosphorus compounds of the lanthanide elements. It may be important to determine the effects of bidentate impurities in the chromatographic elution. However, only a small fraction of the total elements would be expected to be affected.

Summary

The DHDECMP process was demonstrated to give a 99.5% removal of actinides from actual HLLW in small-scale, batch extraction tests. Results from cold tests indicate that it may be possible to carry out the oxalate precipitation step of the OPIX process continuously. About 90% recovery of the trivalent actinides and lanthanides can be achieved in the continuous precipitation. The presence of zirconium impurity in feed solutions to Talspeak process at concentrations of 10^{-4} M (0.5% of the Zr in the original waste) affected phase separations, but equipment could be operated satisfactorily in cold tests. Zirconium concentrations of 10^{-3} M seriously affected phase separations, and substantial quantities of interfacial cruds were formed. Modest concentrations (0.006 M or less) of H_2MEHP , a suspected degradation product of HDEHP, did not affect separation factors. The presence of impurities derived from the thermal degradation of DHDECMP did not inhibit the loading of the trivalent actinide and lanthanide elements in the cation exchange chromatographic process for their separation.

On the basis of our studies to date, it appears that the bidentate (DHDECMP) solvent extraction process and the OPIX process are the leading candidate processes for the co-removal of trivalent actinide and lanthanide elements from HLLW. The cation exchange chromatography and the Talspeak processes are the leading candidate processes for the subsequent separation of actinides and lanthanides. The bidentate and cation exchange processes are further along in their development than the other processes and are currently (17) considered the reference processes for the partitioning of Am-Cm from HLLW.

Literature Cited

1. Bond, W. D., Claiborne, H. C., and Leuze, R. E., Nucl. Technol. (1974) 24, 362.
2. Bond, W. D. and Leuze, R. E., Oak Ridge, TN (1975) ORNL-5012.

3. Bond, W. D. and Leuze, R. E., in *Transplutonium 1975*, Muller, W. and Lindner, R., Eds., North-Holland, Amsterdam, 1976, p. 423.
4. Croff, A. G., Tedder, D. W., Drago, J. P., Blomeke, J. O., Perona, J. J., Oak Ridge, TN (1977) ORNL/TM-5808.
5. Schulz, W. W. and McIsaac, L. D., in *Transplutonium 1975*, Muller, W. and Lindner, R., Eds., North-Holland, Amsterdam, 1976, p. 433.
6. Campbell, D. O. and Buxton, S. R., U.S. Patent 4,025,602.
7. Ferguson, D. E., Oak Ridge, TN (1975) ORNL-5050, pp. 6-11, 30-31.
8. Wheelwright, E. J. and Roberts, F. P., Richland, WA (1968) BNWL-1072.
9. Kelley, J. A., Aiken, SC (1972) DP-1308.
10. Weaver, B. and Kappelmann, F. A., J. Inorg. Nucl. Chem. (1968) 30, 263.
11. Weaver, B. and Kappelmann, F. A., Oak Ridge, TN (1964) ORNL-3559.
12. Forsberg, C. W. and Bond, W. D., Oak Ridge, TN (1977) ORNL/TM-6174, Tedder, D. W. and Blomeke, J. O., compilers, pp. 40-63.
13. Kappelmann, F. A., Katz, S., Scheitlin, F. M., and Bond, W. D., Oak Ridge, TN (1978) ORNL/TM-6174, Tedder, D. W. and Blomeke, J. O., compilers, pp. 63-82.
14. Forsberg, C. W. and Bond, W. D., Oak Ridge, TN (1978) ORNL/TM-6480, Tedder, D. W. and Blomeke, J. O., compilers, pp. 1-15.
15. Bahner, C. T., Shoun, R. R., and McDowell, W. J., Oak Ridge, TN (1977) ORNL/TM-5878.
16. Huggard, A. J. and Warner, B. F., Nucl. Sci. Eng. (1963) 1, 638.
17. Tedder, D. W., Finney, B. C., and Blomeke, J. O., This Symposium.

RECEIVED April 22, 1979.

Americium Recovery and Purification at Rocky Flats

JAMES D. NAVRATIL, LARRY L. MARTELLA, and GARY H. THOMPSON

Rockwell International, Rocky Flats Plant, P.O. Box 464, Golden, CO 80401

The Rocky Flats Plant (RFP) has a large recovery facility to recover plutonium from miscellaneous scraps and residues; a by-product in the plutonium recovery stream is americium from the decay of plutonium-241. Currently a NaCl-KCl-MgCl₂ eutectic salt is used at Rocky Flats to separate americium from plutonium in a molten salt extraction (MSE) process.

As a consequence of experimental runs and changes in process salt mixtures, a variety of waste salts and alloys have been produced, and much of this material is in storage. These waste products contain varying quantities of magnesium, sodium, potassium, calcium, and aluminum as well as plutonium and americium.

Although alloys produced during metallothermic reduction clean-up of waste salts are not being processed, processing of waste salts (except those containing aluminum) is being done by the process shown in Figure 1. The process includes (1) dilute hydrochloric acid dissolution of residues; (2) cation exchange to convert from the chloride to the nitrate system and to remove gross amounts of monovalent impurities; (3) anion precipitation; and (5) calcination at 600°C to yield AmO₂. AmO₂ which meets specifications ($\geq 95\%$ AmO₂, $< 1\%$ individual contaminant elements) is sent to the Department of Energy Isotope Pool.

Americium recovery development at Rocky Flats comprises work to improve the existing process as well as to introduce new methods, especially those that can partition americium and aluminum since the present cation exchange process can not do this.

This report describes attempts to improve the recovery of americium. The first part of the report deals with evaluation of cation exchange resins used for the concentration of americium from low level solutions and for separating americium from major impurities. The second part of the report describes development of a process that will recover americium from residues containing aluminum as well as other common impurities. Results of

0-8412-0527-2/80/47-117-455\$05.00/0

© 1980 American Chemical Society

In Actinide Separations; Navratil, J., et al.;

ACS Symposium Series; American Chemical Society: Washington, DC, 1980.

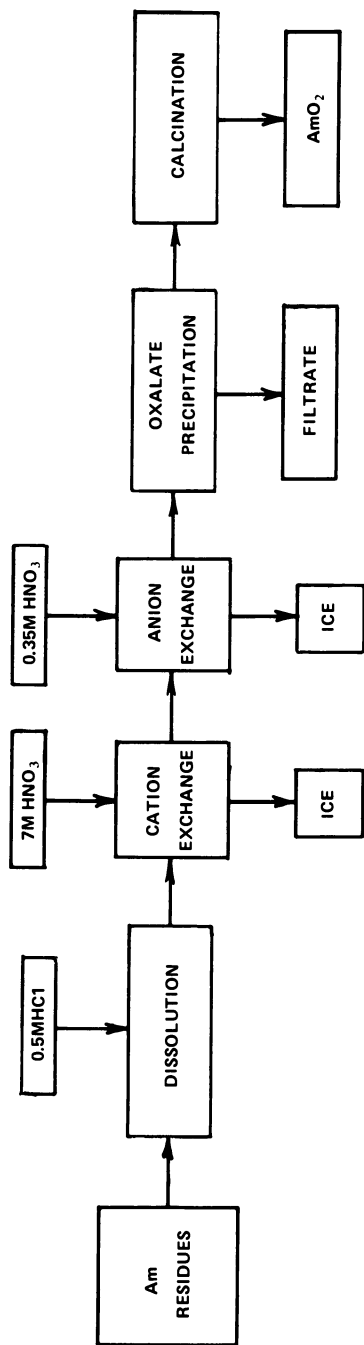


Figure 1. Rocky Flats Am recovery process

preliminary laboratory demonstration tests of both approaches will be described.

Ion Exchange

In the cation exchange process plutonium and americium are cosorbed on the resin with mono- and divalent cations from the MSE process (1). After actinide breakthrough the column is washed with water to remove nonadsorbed ions remaining (e.g. chloride), then eluted with 7M HNO₃. Plutonium is oxidized to Pu(IV) and forms the hexanitrate complex Pu(NO₃)₆²⁻. Although this anionic complex is not adsorbed on the resin it still does not elute very rapidly. We attribute this slow recovery to the difficulty the bulky complex has in diffusing through the resin matrix, as well as the high selectivity of the resin for Pu(IV). The process should be made easier by using a gel-type resin of lower crosslinkage or a macroporous resin. The more open or porous structure of these resins decreases the distance an ion must travel through the matrix until an open channel is reached. In addition it should also be easier to selectively elute contaminant ions from more porous resins by using acid washes or chelating agents for the same reason.

Gel-type cation exchange resins were therefore compared with a macroporous resin for the recovery of plutonium and americium from molten salt residues. The effects on actinide recovery of loading and eluting in the downflow mode, and loading in the upflow, eluting in the downflow mode were also determined.

Experimental

Materials. Two MSE residues were used. These were Na-K-Mg chloride and Ca-K-Mg chloride waste salts containing Pu and Am. The procedure for preparing the solutions is to solubilize the salt in 0.5M HCl at 90°C and filter to remove insolubles. The solutions are diluted to a chloride concentration of 50 g/l. Analysis of these solutions gave the results listed in Table 1.

Three resins were tested during this preliminary program. The first was the conventional gel-type resin currently used at Rocky Flats Plant, Dowex 50W-X8, with 8% crosslinkage. The second was also a gel-type resin, but with only 4% crosslinkage, Dowex 50W-X4. The third resin was Bio-Rad AG MP-50, a macroporous resin. All three cation exchange resins were in the 50 to 100 mesh particle size range.

Chemicals used were reagent grade.

Procedure. Plutonium was adjusted to Pu(III) by addition of 2.5 g/l hydroxylamine hydrochloride one-half hour before the column test. Seven tests were made in the downflow loading and elution mode. Solutions were fed to the column (3.0 cm dia., 150 ml column volume) at 6 ml/min. The ion column effluent (ICE)

TABLE I
Composition of MSE Waste Solutions

$H^+ = 0.5 \text{ M}$

$Cl^- = 50 \text{ g/l}$

<u>Component</u>	<u>Concentration, mg/l</u>	
	<u>Na-K-Mg-Cl System</u>	<u>Ca-K-Mg-Cl System</u>
Al	<10	<10
Ca	15	20000
Fe	11	<10
K	15000	6200
Mg	1700	650
Na	12000	420
Pb	<10	<10
Si	10	10
Pu	3830	10400
Am	180	430

was collected in fractions and sampled to determine actinide content. After actinide breakthrough (0.1 g actinide/l determined by radiometric monitoring of the column effluent) loading was stopped and the column was washed with water at 13 ml/min (total volume = 1 liter). Elution with 7M HNO₃ followed. In the first two tests 4.2 column volumes of ICE were collected. This volume is the average volume required for product recovery in production columns; it should be noted, however, that in production runs loading is upflow, elution is downflow, so this comparison is not appropriate. In the subsequent five tests, product fractions were collected to determine the rate of elution and elution was continued until recovery was more complete. After the product fractions were collected the column was washed with water to remove the 7M HNO₃.

Four additional tests were made in the upflow loading, downflow elution mode. There were no changes in procedure, flow rates, etc., other than the change in direction of flows. Only the Dowex 50W-X8 and Bio-Rad AG MP-50 resins were tested in this test series.

When it became evident that not all plutonium was being removed from the resins, additional washes with 6M HCl or 0.1M diethylenetriaminepentaacetic acid (pH = 8.0) were used to strip the column before the next test.

Samples of all ICE were submitted for analysis. Plutonium and americium were determined by radiometric techniques; and other elements were determined by atomic absorption.

Results and Discussion

Seven ion exchange tests were made in the downflow loading and elution mode. The amount of actinides fed to the column and the percent actinide recovery obtained with 4.2 column volumes of 7M HNO₃ elutriant are shown in Table II.

The capacity of the resins for actinide is less when calcium is present; this is because the divalent calcium competes more effectively for ion exchange sites than does monovalent sodium. The capacities of the resins for individual actinides were not determined in these experiments. The relative capacities for both Pu and Am from the MSE residues are discernible from the actinide adsorbed (the actinide in the feed).

The ideal resin would have high actinide capacity and give complete recovery of plutonium and americium in a small volume of elutriant. Each of the resins tested has apparent advantages and disadvantages, which can best be compared by referring to Table II and Figures 2 and 3. (Figures 2 and 3 show the percent recovery as a function of column volumes for plutonium and americium, respectively.)

Dowex 50W-X4 gives the best recovery of both plutonium and americium, 99.6 and 99.4% respectively in 3.9 column volumes of elutriant. However, the capacity of this resin is inadequate,

TABLE II

ACTINIDE ELUTION FROM CATION EXCHANGE RESIN - DOWNFLOW MODE

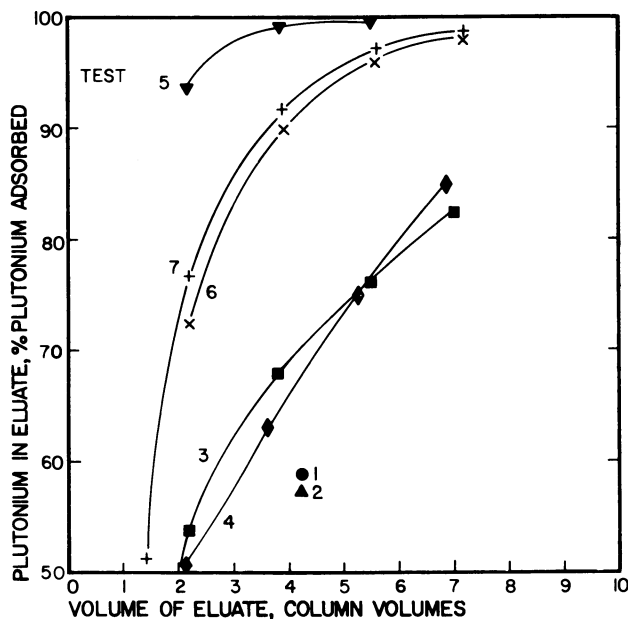
Column Volume (CV): 150 ml Volume of Elutriant: 630 ml (4.2CV)
 Elutriant: 7M HNO₃ Temperature: 23°C
 Flow Rate: 0.85 ml/min-cm² Mode: Downflow for loading and elution

Resin*	Type of MSE Waste**	Actinide in Feed		Actinide Recovery+	
		Pu, g	Am, g	Pu, %	Am, %
Dowex 50W-X8	Na-K-Mg	4.60	0.220	58.2±1.5	94.6±0.1
Dowex 50W-X8	Ca-K-Mg	3.44	0.143	68.8±1.1	88.7±0.1
Dowex 50W-X4	Na-K-Mg	2.19	0.105	99.6	99.4
Bio-Rad AG MP-50	Na-K-Mg	5.94	0.284	91	66
Bio-Rad AG MP-50	Ca-K-Mg	4.21	0.217	93	80

* Dowex 50W-X8 and -X4 are gel-type resins; Bio-Rad AG MP-50 is a macroporous resin

** Waste chloride solutions containing either Na or Ca and K, Mg.

+ Mean % ± standard deviation on duplicate samples, or single determination



Resin: 150 ml (Column Volume), 50 to 100 mesh

Elutriant: 7M HNO_3

Flow Rate: 0.85 ml/min-cm² Feed, Elution (6ml/min)
1.84 ml/min-cm² Wash (13 ml/min)

Tests 1, 2: Na-K-Mg Chloride Solution; 4.6 g Pu; Dowex 50W-X8 Resin

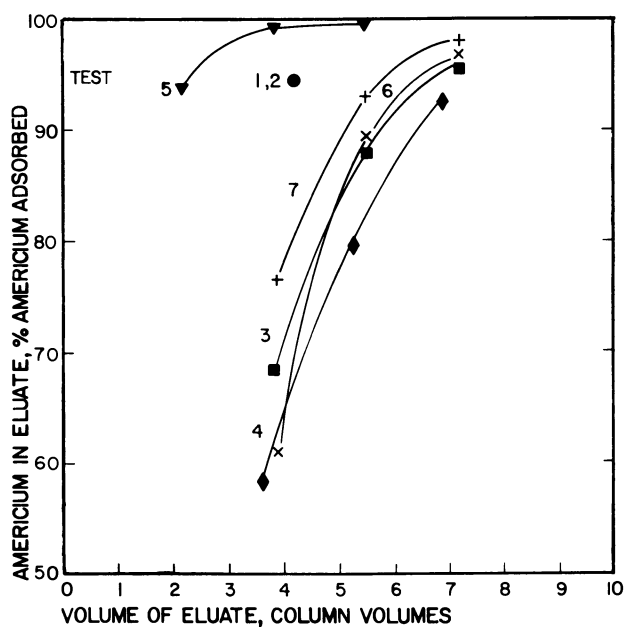
Tests 3, 4: Ca-K-Mg Chloride Solution; 3.44 g Pu; Dowex 50W-X8 Resin

Test 5: Na-K-Mg Chloride Solution; 2.19 g Pu; Dowex 50W-X4 Resin

Test 6: Na-K-Mg Chloride Solution; 5.94 g Pu; Bio-Rad AG MP-50 Resin

Test 7: Ca-K-Mg Chloride Solution; 5.21 g Pu; Bio-Rad AG MP-50 Resin

Figure 2. Recovery of Pu from MSE salt residues by cation exchange—downflow mode



Resin: 150 ml (Column Volume), 50 to 100 mesh

Elutriant: 7M HNO_3

Flow Rate: 0.85 ml/min-cm² Feed, Elution (6 ml/min)
1.84 ml/min-cm² Wash (13 ml/min)

Tests 1, 2: Na-K-Mg Chloride Solution; 0.122 g Am; Dowex 50W-X8 Resin

Tests 3, 4: Ca-K-Mg Chloride Solution; 0.143 g Am; Dowex 50W-X8 Resin

Test 5: Na-K-Mg Chloride Solution; 0.105 g Am; Dowex 50W-X4 Resin

Test 6: Na-K-Mg Chloride Solution; 0.284 g Am; Bio-Rad AG MP-50 Resin

Test 7: Ca-K-Mg Chloride Solution; 0.217 g Am; Bio-Rad AG MP-50 Resin

Figure 3. Recovery of Am from MSE salt residues by cation exchange—down-flow mode

being only 48% of that of Dowex 50W-X8 resin.

The problem with Dowex 50W-X8 is the slow recovery of plutonium. Again, it is suggested that this is because of the oxidation of Pu(III) to Pu(IV) and formation of the hexanitrate plutonium complex; Pu(IV) is more tightly held than Pu(III) and the bulky hexanitrate complex has difficulty diffusing through the polymer matrix. We cannot explain why plutonium recovery is poorer from the Na-K-Mg residue than from the Ca-K-Mg residue whereas americium recovery is better from the Na-K-Mg system and worse from the Ca-K-Mg system. The mean \pm standard deviation for the duplicate tests suggests the effect is real.

The macroporous Bio-Rad AG MP-50 resin has approximately 30% more capacity than the Dowex 50W-X8 for the Na-K-Mg solution and 50% more capacity for the Ca-K-Mg solution. This suggests that trivalent plutonium and americium can displace calcium from the macroporous resin more effectively than from the gel-type Dowex 50W-X8 resin. Another way to look at this effect is to consider the two resins individually. For Dowex 50W-X8, only 74% as much actinide can be adsorbed from the Ca-K-Mg system as from the Na-K-Mg system. With Bio-Rad AG MP-50, 87% as much actinide can be adsorbed from the Ca-K-Mg system; calcium is therefore more effectively displaced.

Plutonium elution from Bio-Rad AG MP-50 is faster than from Dowex 50W-X8; as noted previously, this can be explained as the result of a shorter distance for the bulky hexanitrate anion to diffuse through the matrix before reaching a channel. For plutonium, Bio-Rad AG MP-50 macroporous resin gave the best capacity, calcium decontamination, and elution characteristics.

We have no explanation for the slower elution of americium from macroporous resin. Americium recovery from macroporous resin should be no worse than from gel-type resin; one would expect it to be better.

Because of the poor recovery of americium and because RFP operating procedures involve loading and elution in the upflow and downflow modes, respectively, four additional tests were done in this mode with Dowex 50W-X8 and Bio-Rad AG MP-50 resins and the Na-K-Mg and Ca-K-Mg systems. The results are tabulated in Table III and plutonium and americium elution curves are shown in Figures 4 and 5 respectively.

The analytical results for plutonium in these runs varied, so the overall actinide capacities for the resins in Table II are considered more precise. Less variation was noted in duplicate americium samples. Basing the amount of actinide sorbed on americium, the Dowex 50W-X8 adsorbed 73% as much americium from the Ca-K-Mg system as it did from the Na-K-Mg system; the Bio-Rad AG MP-50 adsorbed 83% as much americium from the Ca-K-Mg system. The results based on americium are similar to those found during the downflow experiments.

The percent recovery of actinide during elution was calculated based on actinide fed to the column and recovered in

TABLE III
 ACTINIDE ELUTION FROM CATION EXCHANGE RESIN -
 UPFLOW AND DOWNFLOW MODE

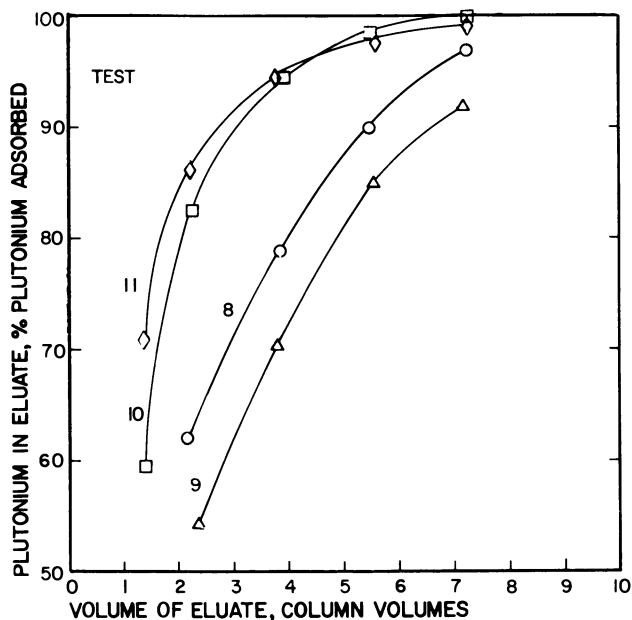
Column Volume (CV): 150 ml Volume of Elutriant: 630 ml (4.2CV)
 Elutriant: 7M HNO₃ Temperature: 23°C
 Flow Rate: 0.85 ml/min-cm² Mode: Load upflow; elute downflow

Resin*	Type of MSE Waste**	Actinide in Feed		Actinide Recovery ⁺	
		Pu, g	Am, g	Pu, %	Am, %
Dowex 50W-X8	Na-K-Mg	4.05	0.194	82	95
Dowex 50W-X8	Ca-K-Mg	3.43	0.142	75	93
Bio-Rad AG MP-50	Na-K-Mg	5.43	0.260	96	98
Bio-Rad AG MP-50	Ca-K-Mg	5.21	0.215	96	97

* Dowex 50W-X8 is a gel-type resin; Bio-Rad AG MP-50 is a macroporous resin.

** Waste chloride solutions containing either Na or Ca and K, Mg.

+ Single determination



Resin: 150 ml (Column Volume) 50 to 100 mesh

Elutriant: 7M HNO_3

Flow Rate: 0.85 ml/min-cm² Feed, Elution (6 ml/min)
1.84 ml/min-cm² Wash (13 ml/min)

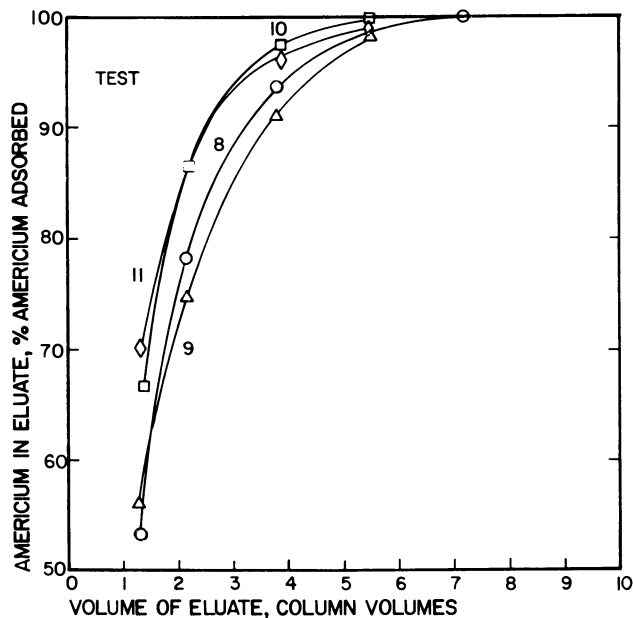
Test 8: Na-K-Mg Chloride Solution; 4.05 g Pu; Dowex 50W-X8 Resin

Test 9: Ca-K-Mg Chloride Solution; 3.43 g Pu; Dowex 50W-X8 Resin

Test 10: Na-K-Mg Chloride Solution; 5.43 g Pu; Bio-Rad AG MP-50 Resin

Test 11: Ca-K-Mg Chloride Solution; 5.21 g Pu; Bio-Rad AG MP-50 Resin

Figure 4. Recovery of Pu from MSE salt residues by cation exchange—feed up-flow, elute downflow



Resin: 150 ml (Column Volume), 50 to 100 mesh

Elutriant: 7M HNO_3

Flow Rate: 0.85 ml/min-cm² Feed, Elution (6 ml/min)
1.84 ml/min-cm² Wash (13 ml/min)

Test 8: Na-K-Mg Chloride Solution; 0.194 g Am; Dowex 50W-X8 Resin

Test 9: Ca-K-Mg Chloride Solution; 0.142 g Am; Dowex 50W-X8 Resin

Test 10: Na-K-Mg Chloride Solution; 0.260 g Am; Bio-Rad AG MP-50 Resin

Test 11: Ca-K-Mg Chloride Solution; 0.215 g Am; Bio-Rad AG MP-50 Resin

Figure 5. Recovery of Am from MSE salt residues by cation exchange—feed up-flow, elute downflow

eluate fractions. Both plutonium and americium recoveries were significantly improved by upflow loading and downflow elution. This shows that americium has an appreciable affinity for the resin even in 7M HNO_3 , and that plutonium may also be retained as cationic Pu(IV) within the resin matrix even though it forms the anionic hexanitrate complex in 7M HNO_3 . (The mechanism for this could be both the stabilization of Pu(IV) adsorbed on the ion exchange sites and the difficulty of getting six nitrate ions around the Pu(IV) ion in the matrix. Complexation with individual nitrate ions probably occurs simultaneously with diffusion through the matrix and bead channels.) Whatever the elution mechanism, it is evident that back-elution is more effective than attempting to force the actinide on through the column.

These results also suggest that (since plutonium and americium are tightly held) it might be possible to wash impurities loaded with plutonium and americium (e.g. calcium and magnesium) off the column with dilute acid (1 to 3M) before eluting plutonium and americium with 7M HNO_3 .

Conclusions and Future Work

As a result of this preliminary work it was concluded that the increased actinide capacity, faster elution kinetics, and better decontamination properties of macroporous resins justify additional work to further evaluate Bio-Rad AG MP-50 and other macroporous resins for the MSE cation process; macroporous resins do appear to be better for actinide recovery from molten salt residues than gel-type resins.

Only three of many commercially available resins were tested in this preliminary work. Other macroporous resins will be tested. Loading and elution kinetics, breakthrough capacities, actinide recovery and radiation stability will be evaluated for candidate resins.

Of particular interest is the possibility of decontaminating actinides from impurities by washing the loaded column with dilute acid or monovalent salts to elute the divalent impurities before stripping the column with 7M HNO_3 . This method is presently being evaluated for lead removal from americium using Bio-Rad AG MP-50.

Bidentate Extraction

Recovery of actinides at RFP with an organophosphorus bidentate has been proposed. The conceptual flow sheet is shown in Figure 6. The bidentate, dihexyl-N,N-diethylcarbamoylmethylenephosphonate (DHDECMP), is especially attractive since it can recover actinides from MSE residues containing aluminum. The cation exchange process is unable to effect actinide purification when aluminum is present. (DHDECMP extracts actinides and lanthanides, but does not extract common RFP contaminants, e.g.

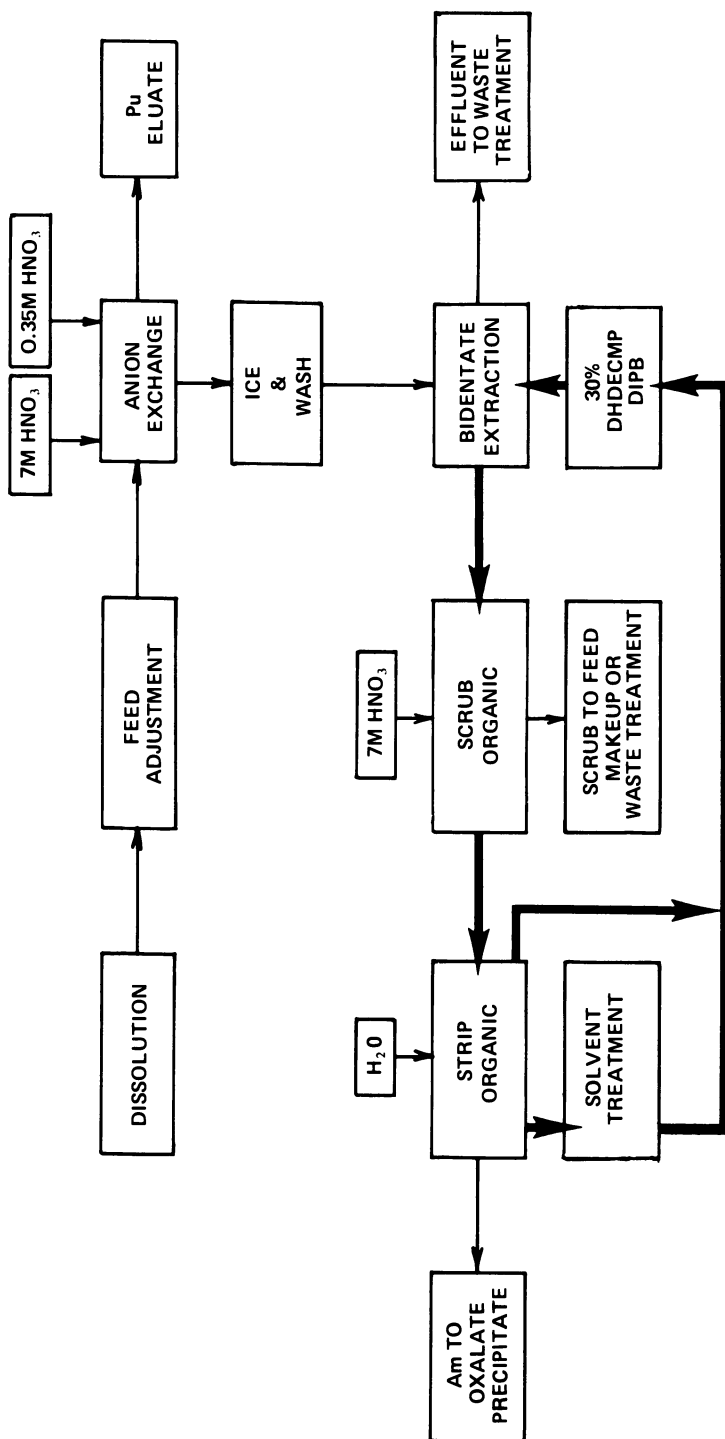


Figure 6. Conceptual flowsheet for processing aluminum residues

aluminum. No lanthanides are used in process streams at RFP.)

The actinides are extracted from high acid (e.g. 7M HNO₃) solutions and can be back-extracted with dilute acid. The method is therefore easily used with the ion column effluent from the anion exchange plutonium recovery step.

Two techniques appear to be useful for the bidentate extraction of actinides. The first is liquid-liquid solvent extraction, a method which has several advantages. Currently, however, the type of equipment needed (mixer-settlers, centrifugal contactors, etc.) is not available at RFP. We are better equipped to use a column technique. This can be done by sorbing the bidentate extractant on an inert solid support, loading ion exchange columns with the sorbent, and proceeding with column runs (extraction chromatography).

Both liquid-liquid extraction and extraction chromatography were tested in this work. Lab and pilot scale recovery tests were done using liquid-liquid extraction, and laboratory scale tests were done using extraction chromatography; results of these preliminary tests are described.

Experimental

Materials. The alloy residue contains approximately 15% Al, 44% Mg, 29% Pu, 2% Am, and other impurities. The residues are dissolved by placing the alloy metal in 0.35M HNO₃ and slowly adding concentrated HNO₃. Time is allowed between additions of concentrated HNO₃ for the dissolution reaction to subside. The solution is adjusted to 0.1M F⁻ with concentrated HF to remove any polymeric or residual plutonium. After filtration through Whatman 42 filter paper, the solution is adjusted to 7M HNO₃.

Plutonium in this feed solution is removed by an anion exchange column process. The anion exchange resin is Dowex 1-X4, 50 to 80 mesh nitrate form, obtained from Bio-Rad Laboratories. Ferrous sulfamate is added to the solution to eliminate hexavalent plutonium, and the feed is passed through the column. The ion column effluent (ICE) contains the americium and impurities. Residual americium and impurities are washed from the column with 7M HNO₃ and the wash is combined with the ICE; this is the feed to the bidentate process. A typical composition in g/l is: Am, 0.15; Pu, 8.2 x 10⁻³, Al, 0.385; and Mg, 1.02. Plutonium is eluted with dilute nitric acid and returned to the production stream.

The DHDECMP is obtained from Wateree Chemical Company, Lugoff, South Carolina, and is purified by an ion exchange method to approximately 67% pure; the method and extractant impurities have been described elsewhere. Diisopropylbenzene (DiPB) was obtained from Pfaltz and Bauer, Inc. The extractant is 30% DHDECMP in DiPB.

The extraction chromatography method used DHDECMP adsorbed

on 20-50 mesh Amberlite XAD-4. The adsorbent was prepared using a column method. The column was loaded with Amberlite XAD-4, washed with acetone, and a mixture of 50 vol% CCl_4 - 50 vol% bidentate was recycled through the column to cause swelling of the beads. The CCl_4 -bidentate mixture was then vacuumed from the column and the column was filled with bidentate and permitted to stand overnight. The excess bidentate was vacuumed from the column and the adsorbent was conditioned by washing with 7M HNO_3 .

Procedure. Americium in the combined wash and ICE is removed by liquid-liquid extraction or extraction chromatography using bidentate.

For liquid-liquid extraction, 2.5 l of feed was contacted with 0.5 l of bidentate ($A/O = 5$) for 15 minutes. This batch process is repeated with fresh batches of extractant until the americium concentration is $<1.9 \times 10^{-2}$ g/l; three contacts were required.

Residual amounts of extracted impurities are removed from the loaded extractant by 7M HNO_3 washing. Three to five contacts are made using an $A/O = 0.2$. The wash is either sent to feed acid adjustment or discarded depending upon americium content. The americium is then stripped from the organic with water (five to seven contacts) using an $A/O = 0.2$. The americium in the strip solution is precipitated with oxalic acid, and the americium oxalate is calcined to AmO_2 . In the lab scale extraction chromatography method, the DHDECMF-impregnated Amberlite XAD-4 was loaded into a column 1.8 cm dia. x 23.5 cm and conditioned with 7M HNO_3 . The americium feed was fed to the column at 1.5 ml/min until a total of 300 ml had been fed. The column was washed with 200 ml of 7M HNO_3 at 1.7 ml/min, then eluted with deionized water until elution was complete (determined radiometrically). Five to seven 50 ml fractions were required for elution. Samples were submitted for analysis.

Results and Discussion

Table IV shows the results of three laboratory runs of the solvent extraction step (after the plutonium was removed by anion exchange). The major elements are shown before solvent extraction, after solvent extraction, in the 7M HNO_3 wash, and in the final strip product. The americium remaining in the organic after stripping is also shown. Although there were some analytical discrepancies, the data show that americium was effectively recovered (except in Test 1, for which we have no explanation). Americium was decontaminated from aluminum and magnesium in all three runs.

Results of the pilot plant test of the liquid-liquid solvent extraction test are shown in Table V. Only 4 l of approximately 17 l of americium strip product were used in the precipitation step. Decontamination from Al and Mg was excel-

TABLE IV
 Recovery and Purification of Am from Al-Mg
 MSE Residue by Solvent Extraction

<u>Test</u>	<u>Stream</u>	<u>Am, mg</u>	<u>Pu, mg</u>	<u>Al, mg</u>	<u>Mg, mg</u>
1	Feed	21	0.39	149	432
	Raffinate	1	<0.001	143	405
	Wash*	4	<0.001	3	8
	Product*	8	0.06	<0.001	<0.001
	Organic ⁺	2	++	++	++
2	Feed	23	0.04	158	459
	Raffinate	1	++	160	470
	Wash*	1	++	2	6
	Product**	18	0.004	<0.113	<0.113
	Organic ⁺	0.4	++	++	++
3	Feed	44	0.07	211	713
	Raffinate	1	0.01	242	634
	Wash*	1	0.05	<2	8
	Product**	42	0.03	<2	1
	Organic ⁺	2	0.36	++	++

*7M HNO₃

**Strip

⁺After Strip⁺⁺Not Available

TABLE V

Results of Pilot Scale Recovery of Americium
from Dissolved Al-Mg Alloy from MSE Process

<u>Stream</u>	<u>Concentration, g/l *</u>			
	<u>Am</u>	<u>Pu</u>	<u>Al</u>	<u>Mg</u>
Feed	0.15	8.17×10^{-3}	0.385	1.02
Strip	0.14	7.5×10^{-4}	0.005	0.002

*Single Determination

TABLE VI

Impurities in Americium Oxide Product*

<u>Impurity Concentrations, ppm**</u>		
<u>Plutonium</u>	<u>Aluminum</u>	<u>Magnesium</u>
3240	<100	<50

* Specifications require >95% AmO₂ with less than 1% of any individual impurity and less than 0.5% Pu

** Single determination

TABLE VII
 Recovery and Purification of Am from Al-Mg
 MSE Residue by Extraction Chromatography

<u>Test</u>	<u>Stream</u>	<u>Am, mg</u>	<u>Pu, mg</u>	<u>Al, mg</u>	<u>Mg, mg</u>
1	Feed	35	0.04	81	204
	Effluent	2	3×10^{-4}	89	200
	Wash*	4	+	+	+
	Product**	22	0.3	0.4	0.18
2	Feed	17	0.02	39	97
	Effluent	0.037	0.0015	25	65
	Wash*	+	+	+	+
	Product**	16	0.2	<0.2	0.2
3	Feed	29	0.04	68	170
	Effluent	0.4	0.003	57	+
	Wash*	3.5	0.0012	+	+
	Product**	25	0.2	<0.45	<0.23

* 7M HNO₃

** Strip

+ Not available

lent with decontamination factors (DF) of 72 and 444, respectively. The corresponding DF for plutonium was 10. (DF is the ratio of impurity in the feed to impurity in the strip product.)

Analysis of the final AmO₂ product is shown in Table VI. Al and Mg were below the detectable limits for these elements. The product met specifications of >95% AmO₂ with less than 0.5% Pu and less than 1% of any other single contaminant. The results of the preliminary lab scale extraction chromatography tests are shown in Table VII. Again, in spite of some analytical problems, it is evident that americium was decontaminated from aluminum and magnesium. A 7M HNO₃ wash step is assumed to account for the americium loss.

Conclusions and Future Work

Laboratory results have shown that americium can be recovered and purified by both solvent extraction and extraction chromatography using the bidentate DHDECMP. Solvent extraction recovery of americium was demonstrated on a pilot plant scale. The americium oxide product prepared from this strip solution met specifications.

Pilot plant scale testing of the extraction chromatography process is currently in progress at Rocky Flats Plant. When adequate testing of both the solvent extraction and extraction chromatography methods has been accomplished, the methods will be compared to see which has the greatest promise for recovering the americium from special MSE residues.

Acknowledgment

The authors wish to thank C. M. Smith for his help and the Analytical Labs personnel for analyses. This work was performed under a contract with the U. S. Department of Energy.

Literature Cited

1. Proctor, S. G., USERDA Report RFP-2347, 1975.
2. Hagan, P. G., Navratil, J. D., presented at the 175th National Meeting of the American Chemical Society, March 12-17, 1978, Anaheim, California.
3. Navratil, J. D., Martella, L. L., Smith, C. M., Thompson, G. H., Cash, D. L., Childs, E. L., Meile, L. J., USDOE Report RFP-2749, 1978.
4. Navratil, J. D., Thompson, G. H., Nucl. Technol., 1979, 43, 136.

RECEIVED September 14, 1979.

Work performed under U.S. Government contract number DE-AC04-76DP03533.

The Extraction of DBP and MBP from Actinides: Application to the Recovery of Actinides from TBP- Sodium Carbonate Scrub Solutions¹

E. P. HORWITZ, G. W. MASON, C. A. A. BLOOMQUIST,
R. A. LEONARD, and G. J. BERNSTEIN

Argonne National Laboratory, 9700 South Cass Avenue, Argonne, IL 60439

Significant amounts of actinides are present in nuclear wastes other than high-level liquid waste produced in spent nuclear fuel reprocessing (1). One such waste stream is produced by scrubbing the radiolytic and hydrolytic degradation products from extractant solutions with Na_2CO_3 . Actinide concentrations in the range of 0.5 to 5 Kg of actinides may be present in the Na_2CO_3 scrub solutions used to "clean-up" TBP-nDD solutions from the reprocessing of one metric ton of spent nuclear fuel (1,2). In addition, Na_2CO_3 scrub waste will be generated in the clean-up of the dihexyl-N,N-diethyl carbamoylmethylene phosphonate (DHDECMP) extractant which is to be used to extract all of the actinides from high-level liquid waste (HLLW) in the proposed waste treatment facility described by Tedder, Finney, and Blomeke (3).

Na_2CO_3 scrub solutions from TBP-nDD consist essentially of a NaHCO_3 - NaNO_3 solution containing varying amounts of the sodium salts of dibutylphosphoric and monobutyl phosphoric acids (HDBP and H_2MBP , respectively) and carbonato- and hydroxo-complexes of the tetra- and hexavalent actinides and zirconium. The actual quantities of DBP, MBP, and actinides depend on the extent of hydrolysis and radiolysis. Analogous waste from DHDECMP-DIPB processing would be similar in composition but would contain mono- and diacidic salts of phosphonic acids and degradation products of DHDECMP (4).

The efficient removal of actinides from the Na_2CO_3 scrub waste solution presents several problems. Acidification of the carbonate solution with excess HNO_3 followed by extraction with TBP (or, preferably, DHDECMP) (3) results in the rapid build-up of acidic degradation products (HDBP and H_2MBP in the case of TBP) which prevent efficient back extraction. In addition, acidification of Na_2CO_3 scrub waste results in the precipitation of actinide-DBP and -MBP complexes which are difficult to dissolve

¹Work performed under the auspices of the Office of Basic Energy Sciences and the Office of Nuclear Waste Management of the U.S. Department of Energy.

and make subsequent processing difficult. Cation and anion exchange methods are also not feasible because of precipitate formation and/or poor actinide recoveries. Thus, any method for processing the Na_2CO_3 scrub waste must address the problem of the interaction and partitioning of the hydrolytic and radiolytic degradation products that are present, as well as the recovery of the actinides.

This paper describes a process for the recovery of actinides from Na_2CO_3 scrub waste solutions which involves the extraction of the HDBP and H_2MBP from acidified solutions using a water-immiscible aliphatic alcohol. All the actinides remain in the aqueous phase, which may then be processed using conventional TBP or DHDECMP procedures (3). We refer to this process as the ARALEX (Argonne alcohol extraction) process. This paper also describes the extraction equilibria measurements performed in the development of the process.

Experimental

Reagents and Labeled Compounds. The sources of all solvents and reagents and the preparation and purification of ^{32}P labeled HDBP, H_2MBP , and TBP were described by the authors in a previous publication (5). ^{32}P -labeled phosphoric acid (H_3PO_4), ^{35}S -labeled dodecyl sulfuric acid (DSA), ^3H -labeled diethylenetriaminepentaacetic acid (H_5DTPA), and ^3H -labeled 2-ethyl-1-hexanol (2-EHOH) were obtained from the Amersham Corporation, Arlington Heights, Illinois.

Measurements of D. Distribution ratios, D, (defined as the concentration in the organic phase divided by the concentration in the aqueous phase) were measured at 25 and 50°C by a procedure described previously (5,6). The D's for HDBP and DSA were measured by reverse or back extraction to minimize the influence of traces of H_2MBP and H_2SO_4 , respectively. D's for H_2MBP , H_3PO_4 , and H_5DTPA were measured by forward extraction, after a preliminary extraction with a separate portion of organic phase, to minimize the effects of traces of HDBP in H_2MBP and $\text{HC}_2\text{H}_3\text{O}_2$ in H_5DTPA . In the case of the actinides, D's were usually measured by forward extraction because of the low values of D. When possible, reverse D's were measured to check reversibility.

All radiometric assaying was performed by conventional liquid scintillation counting techniques using a Beckman LS-100 automatic scintillation counter and Ready-Solv GP scintillation solution.

Counter-Current Liquid-Liquid Extractions. Two experimental arrangements were used to carry out counter-current liquid-liquid extractions. One system consisted of seven jacketed glass separatory vessels equipped with stainless steel centrifugal

stirrers. The vessels were maintained at 50°C by means of a constant temperature bath. The counter-current transfer of phases was performed manually. The other system consisted of an eight stage counter-current mini-centrifugal contactor (7). The eight stage mini-contactor has a continuous throughput and short phase contact times (~10 sec) and thus steady state conditions are attained rapidly. No provision was available for operating the centrifugal contactor at elevated temperatures; therefore, room temperature conditions were used for all experiments.

Flowsheet Testing. Na₂CO₃ scrub waste solutions were prepared by extracting measured amounts of U(VI) and Pu(IV) into dodecane solutions containing 0.02 M - 0.04 M HDBP and 0.0067 M - 0.0134 M H₂MBP. The resultant organic phase plus precipitates were then slurried with the required amount of Na₂CO₃ until all the precipitate dissolved.

All uranium and plutonium analyses were performed by isotopic dilution and radiometric techniques, respectively. HDBP and H₂MBP mixtures were analyzed by first separating the HDBP and H₂MBP from each other using a liquid-liquid chromatographic column containing n-decanol as the stationary phase and 8 M HNO₃ and 0.002 M NH₄OH as mobile phases. The separated HDBP and H₂MBP were then decomposed by oxidation and the resultant H₃PO₄ measured colorimetrically. NaDBP and Na₂MBP mixtures were analyzed by ion chromatography (8). Where feasible, DBP and MBP were analyzed radiometrically by spiking known quantities of HDBP and H₂MBP with the ³²P-labeled ester.

Results and Discussion

Dimerization of HDBP in Various Solvents. Dyrssen, *et al.* (9,10), has shown that polar solvents are better extractants for HDBP than non-polar solvents because of the formation of a stable hydrogen bonded complex between the polar groups of the solvent and the phosphoryl and acidic hydrogen groups of the HDBP. In order to ascertain the suitability of different solvents as extractants for HDBP and H₂MBP, measurements were made of the partitioning and dimerization constants of HDBP in a number of polar solvents.

The partitioning and dimerization constants, K_p and K₂, respectively, are defined by the following equations:

$$K_p = \frac{[\text{HA}]_{\text{org}}}{[\text{HA}]_{\text{aq}}} \quad (1)$$



$$K_2 = \frac{[H_2A_2]_{org}}{[HA]_{org}^2} \quad (3)$$

where $[HA]$ and $[H_2A_2]$ are the equilibrium concentrations of the monomeric and dimeric forms of HDBP. K_p and K_2 were calculated from the following equation derived by Dyrssen (9) and Hardy and Scargill (11):

$$D = \frac{K_p}{\phi} + \frac{2K_2K_p^2 C_{aq}}{\phi^2} \quad (4)$$

where D is the distribution ratio, C_{aq} is the total formula weight concentration of HDBP in equilibrium with the organic phase, and ϕ equals $(1 + K_a[H^+]^{-1})$. K_a is the acidity constant for HDBP, which has a value of 10^{-1} at 25°C and $\mu = 0.1$ (9). Plots of D vs. C_{aq} for HDBP using 2-ethyl-1-hexanol (2-EHOH), 2-ethyl-1-hexanoic acid (2-EHA), and p-diisopropylbenzene (p-DIPB) vs. 0.1 M HNO_3 at 25°C are shown in Figure 1. At low concentrations of C_{aq} , the horizontal asymptote gives

$$\log D = \log K_p \phi^{-1}. \quad (5)$$

The point of intersection of the two asymptotes gives the value for $\log 2K_pK_2/\phi$.

Values for K_p and K_2 for a variety of solvents are shown in Table I. Some data obtained by Dyrssen and Hay (10) and Hardy and Scargill (11) were included for comparison. The data in Table I show clearly that, as the partitioning constant increases, the dimerization constant decreases. Thus, those solvents which have the greatest ability to break the very stable HDBP dimer have the greatest tendency to extract the HDBP. Aliphatic alcohols show this property to the greatest extent. In the case of aliphatic alcohols the interaction between the solvent and HDBP is sufficiently strong that the D is independent of C_{aq} (see Figure 1). Thus, K_p divided by two gives D . The high K_p and low K_2 using aliphatic alcohols as solvents is due to the strong hydrogen bonds that form between the hydroxyl group of the alcohol and the phosphoryl and acidic hydrogen groups of HDBP. The probable structure of the alcohol-HDBP complex is shown in Figure 2.

It is interesting to note that the data in Figure 1 and Table I show that alcohols are better extractants for HDBP than are carboxylic acids. One might expect the reverse to be true because carboxylic acids probably form hydrogen-bonded complexes with HDBP which are similar in structure to the very stable HDBP dimer. Such structures have resonance stabilization and favorable hydrogen bond angles. However, one must consider the energy of association between the solvent molecules themselves. Association between solvent molecules must be broken in order for

Table I. Partition and dimerization constants for HDBP in various systems, 25°C.

System	$\log K_p$ (2σ)	$\log K_2$	Reference
2-ethyl-1-hexanol/0.1 M HNO_3	2.25 ± 0.03	<-0.2	This work
4-methyl-2-pentanol/0.1 M HNO_3	2.21 ± 0.05	<1	10
1-octanol/0.1 M HNO_3	2.16 ± 0.02	<1	This work
1-decanol/0.1 M HNO_3	2.15 ± 0.02	<1	This work
1-octanoic acid/0.1 M HNO_3	1.80 ± 0.02	N.D. ^a	This work
2-ethyl-1-hexanoic acid/0.1 M HNO_3	1.76 ± 0.02	0.54	This work
methyl isobutylketone/0.1 M HNO_3	1.36	1.19	10
isopropyl ether/0.1 M HNO_3	0.52	2.29	10
benzene/1 M HNO_3	-0.42	4.88	11
p-diisopropylbenzene/0.1 M HNO_3	-1.36	5.38	This work
kerosene/1 M HNO_3	-1.96	5.78	11
carbon tetrachloride/0.1 M HNO_3	-1.44	6.49	10

^aN.D. - Not Determined.

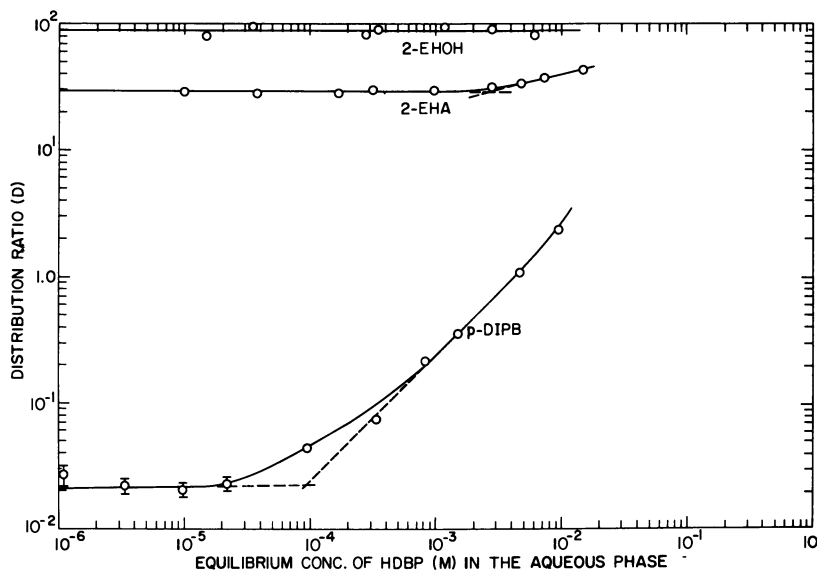
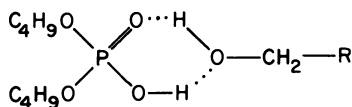


Figure 1. Distribution ratios of HDBP vs. equilibrium aqueous concentration of HDBP using 2-ethyl-1-hexanol (2-EHOH), 2-ethyl-1-hexanoic acid (2-EHA), and p-diisopropylbenzene (p-DIPB); aqueous phase = 0.1M HNO₃; T = 25°C.

HDBP-ALCOHOL



H₂MBP-ALCOHOL

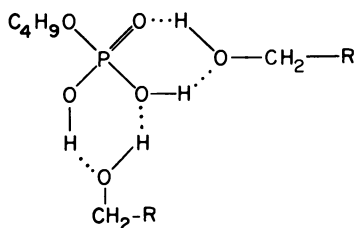


Figure 2. Structure of hydrogen-bonded complexes between an aliphatic alcohol and HDBP and H₂MBP

complexing with HDBP to take place. Carboxylic acids are much more strongly associated than alcohols (as indicated by differences in boiling points) because they form stable dimers analogous to dialkyl phosphoric acids (9). Thus, the difference in K_p and K_2 between alcohols and carboxylic acids may be explained, at least qualitatively, by the larger energy required to dissociate the carboxylic acids prior to the formation of the HDBP complex. There also might be some difference in the stabilities of the hydrogen bonded HDBP-alcohol and HDBP-carboxylic acid complexes which would either augment (alcohol more stable than carboxylic acid complex) or diminish (carboxylic acid more stable than alcohol complex) the difference between the two solvents.

A comparison of the constants in Table I for the 2-ethylhexyl and n-octyl isomers of the alcohol and carboxylic acid show a small but measurable difference in K_p . These results are difficult to explain from the standpoint of the relative contributions of steric and inductive effects. The branched chain isomers are less associated due to steric effects (as indicated by differences in boiling points) and form weaker acids due to inductive effects. Both of these effects would enhance the stability of the 2-ethylhexyl alcohol and carboxylic complexes with HDBP. However, space filling (Leybold-Hereaus) atom models show that steric effects also interfere to some degree with rotation around the hydroxyl and carboxyl groups. In addition, the enhanced electron density on the oxygens of the hydroxyl and carboxyl groups (due to inductive effects from branching in the alkyl chain) may not always increase hydrogen bond strength because the -OH and -COOH have both donor and acceptor properties. Thus, it is difficult to explain the difference in the n-octyl and 2-ethylhexyl isomers even qualitatively. However, the constants in Table I do not differ greatly for the two isomers and therefore selection of solvents would be based on other considerations.

Of the solvents listed in Table I, 2-ethyl-1-hexanol appears to be the best choice for processing the Na_2CO_3 scrub solutions. 2-EHOH has the highest K_p , is commercially available, and is less expensive than the straight chain alcohols. In addition, the D for H_2MBP using 2-EHOH is greater than one; all other non-alcoholic solvents have D's for H_2MBP much less than one. The flash point and water solubility of 2-EHOH are 85°C (12) and 0.10 parts of H_2O at 20°C (13), respectively.

Extraction of HDBP, H_2MBP , and H_3PO_4 . Figure 3 shows the D's for the extraction of HDBP, H_2MBP , and H_3PO_4 as a function of HNO_3 concentration in the aqueous phase using 2-EHOH. The order of extractability for the three compounds shown in Figure 3 is expected, since increasing the number of butyl groups and decreasing the number of hydrophilic groups decreases compatibility with the water structure and increases compatibility with the

organic phase. It is important to note the D's achieved for the extraction of H₂MBP using 2-EHOH. H₂MBP is miscible with H₂O in all proportions and therefore very difficult to extract into a water-immiscible solvent (11) unless a polar compound such as TBP is present in the organic phase. The probable structure of the H₂MBP-alcohol complex is shown in Figure 2.

Initial increases in D's for both HDBP and H₂MBP in the range of 0.1 M to 8 M HNO₃ are probably due to a combination of the diminution in the concentration of DBP⁻¹ and HMBP⁻¹ in the aqueous phase and to "salting out" effects from the HNO₃. Eventually the D's for both HDBP and H₂MBP decrease with increasing HNO₃ for donor oxygens in the 2-EHOH and phosphorous compounds. Figure 4 shows the extraction of HNO₃ by 2-EHOH and 2-EHA.

The effect of temperature on the D vs. HNO₃ curves is, in general, relatively small and insignificant from a practical standpoint. Increases in temperature would decrease the association of highly polar solvents, which may explain the higher D's at 50°C and low acidities. The extraction of HNO₃ by 2-EHOH is approximately 5% higher at 50°C than 25°C, which probably accounts for the lower D's at the higher temperature and acidities. The effect of macro concentrations (up to stoichiometric) of UO₂²⁺ on the D's of HDBP and H₂MBP from 3.5 M HNO₃ at 50°C was also found to be insignificant.

From a practical standpoint, extraction of a mixture of HDBP and H₂MBP from HNO₃ would be determined by the D's for H₂MBP. Nitric acid solutions in the 2 M to 6 M range are practical conditions from the standpoint of D's and nitric acid economy.

Extraction of DSA and H₅DTPA. Figure 3 also shows the D's for dodecyl sulfuric acid (DSA) (the acidic form of the commonly used detergent, sodium dodecyl sulfate) and diethylenetriamine-pentacetic acid (H₅DTPA). Both of these compounds could be constituents in a salt waste treatment facility of a fuel re-processing plant (1) and therefore were included in the study. DSA behaves similar to HDBP, as expected. Hydrogen-bonded complexes analogous to those shown in Figure 2 can be formed between the -OH group of the alcohol and the -OSO₃H radical of DSA. Cationic (quaternary ammonium salts) and neutral detergents are also strongly extracted by 2-EHOH. On the other hand, H₅DTPA is very poorly extracted because of the large number of hydrophilic groups and the absence of a long hydrocarbon group. In this respect, it is analogous to H₃PO₄, which has similar D's.

Interaction Effects of H₂MBP and HDBP. Hardy and Scargill (11) have shown that the presence of HDBP in kerosene has a pronounced effect on the extraction of H₂MBP. This behavior is due to hydrogen bonding of the two esters to each other. However, one would not expect interaction between HDBP and H₂MBP in a highly polar solvent, such as 2-EHOH, unless the concentration

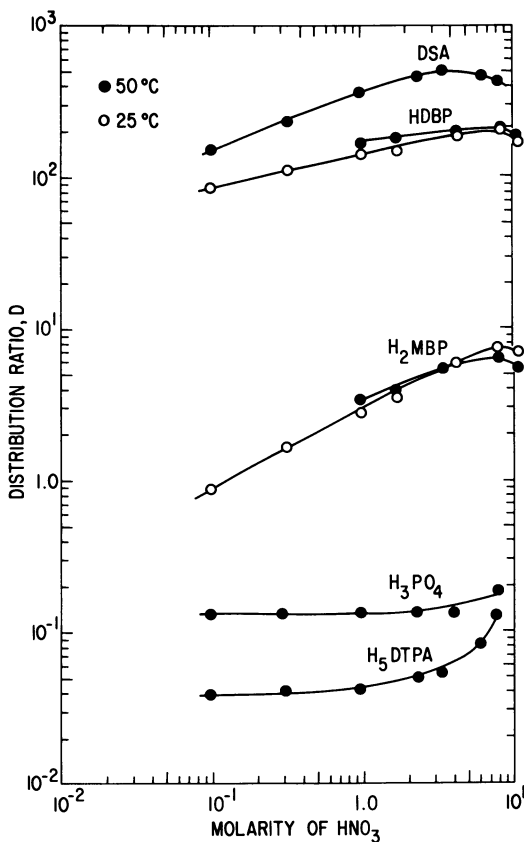


Figure 3. Distribution ratios of dibutyl phosphoric acid (HDBP), monobutyl phosphoric acid (H_2MBP), phosphoric acid (H_3PO_4), dodecyl sulfuric acid (DSA), and diethylenetriaminetetraacetic acid (H_5DTPA) vs. aqueous HNO_3 concentration; organic phase = 2-ethyl-1-hexanol; $T = 25^\circ$ and 50°C .

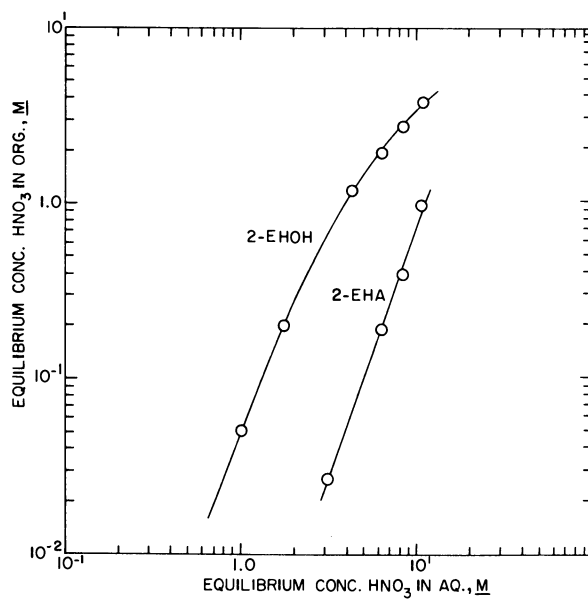


Figure 4. Equilibrium curve for the extraction of nitric acid using 2-ethyl-1-hexanol (2-EHOH) and 2-ethyl-1-hexanoic acid (2-EHA); $T = 25^\circ\text{C}$.

of one of the esters was above 0.1 M. The extraction of labeled H₂MBP was measured in 2-EHOH which contained unlabeled HDBP, 2 x 10⁻² M in concentration. No difference in the D for H₂MBP was found in the absence or presence of HDBP.

Extraction of NaDBP and Na₂MBP. The distribution ratios, D, of the sodium salts of DBP and MBP were measured between 0.25 M Na₂CO₃ and 2-EHOH. The data are shown in Table II below.

Table II. Distribution ratios, D, of NaDBP and Na₂MBP
Aqueous Phase - 0.25 M Na₂CO₃
Temperature 50°C

	<u>1st Ext.</u>	<u>2nd Ext.</u>
NaDBP	1.5 x 10 ⁻²	1.9 x 10 ⁻²
Na ₂ MBP	3.5 x 10 ⁻⁴	2.2 x 10 ⁻⁴

The low D's for the extraction of NaDBP and Na₂MBP from 2-EHOH afford a convenient method for stripping these compounds from the solvent.

Extraction of Actinides by HDBP and H₂MBP in 2-EHOH. The second objective in the development of a process for removing TBP degradation products from acidified Na₂CO₃ scrub solution is to effectively retain the actinides in the aqueous phase during the extraction of HDBP and H₂MBP. In order to achieve this objective, the DBP- and MBP-actinide complexes have to be effectively dissociated by bonding of solvent molecules to the coordinating groups of the HDBP and H₂MBP. Dyrssen, *et al.* (14), found that the D of Y(III) between a solution of 0.1 M HDBP in chloroform and 0.1 M HNO₃ could be reduced by four orders of magnitude by the addition of methylisobutyl carbinol up to 2 M in concentration. Mason, *et al.* (15,16), reported similar effects on the D's of certain actinides and lanthanides using HDEHP in 1-decanol and 2-ethyl-1-hexanoic acid.

Figure 5 shows the extraction of U(VI), Pu(IV), and Am(III) as a function of the concentration of HDBP and H₂MBP in 2-EHOH, at a constant HNO₃ concentration of 3.5 M. It can be seen that neither HDBP nor H₂MBP is an effective extractant in 2-EHOH for these actinides, although ester concentrations above 0.05 M give D's that are greater than one for Pu(IV). For comparison, the D for Pu(IV) using 0.02 M HDBP in p-diisopropyl benzene is approximately two orders of magnitude greater than when 2-EHOH is used as the diluent. The difference in D's is even greater when aliphatic diluents, *e.g.*, dodecane, are compared with 2-EHOH. As the concentrations of HDBP and H₂MBP decrease, the D's for U(VI) and Pu(IV) gradually approach that obtained in pure 2-EHOH

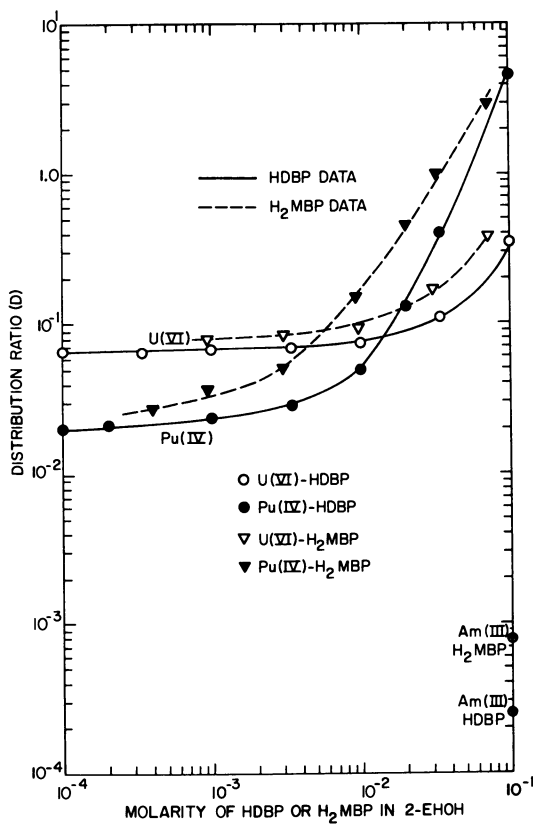


Figure 5. Distribution ratios of U (VI), Pu (IV), and Am (III) for HDBP and H₂MBP in 2-EHOH; aqueous phase = 3.5M HNO₃, T = 50°C.

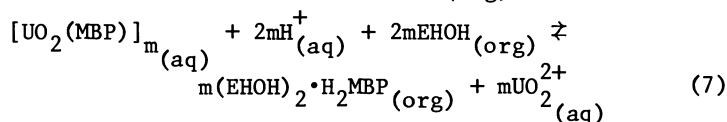
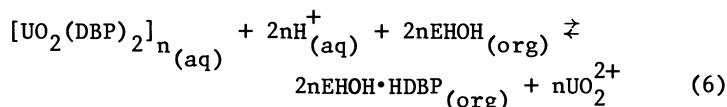
in equilibrium with 3.5 \underline{M} HNO_3 .

It is important to note that the D's for U(VI), Pu(IV), and Am(III) are higher for H_2MBP than HDBP. However, since the H_2MBP concentration produced by radiolysis and hydrolysis of TBP is always significantly less than HDBP (17), the net effect of the two esters on the D's is approximately the same.

Additional studies on the effect of HNO_3 concentration (in the 1 \underline{M} to 8 \underline{M} range) on the D's of U(VI) and Pu(IV), using fixed concentrations (0.02 \underline{M}) of H_2MBP and HDBP in 2-EHOH and using pure 2-EHOH, showed very poor extractions of both metal ions even at the lowest acid concentration. These studies also showed that 2-EHOH makes a significant contribution to the D's at the 0.02 \underline{M} ester concentration, especially for U(VI) at all acidities and for Pu(IV) at the high (6-8 \underline{M}) acidities. The highest D's were found for the Pu(IV)- H_2MBP system at 1 \underline{M} HNO_3 ($D = 1$). However, the addition of 0.05 \underline{M} $\text{H}_2\text{C}_2\text{O}_4$ to the 1 \underline{M} HNO_3 reduced the D to less than 0.1 for Pu(IV) and to less than 0.01 for U(VI).

Since the concentrations of HDBP and H_2MBP in Na_2CO_3 scrub waste solution will fluctuate (although in all probability H_2MBP would not exceed 0.01 \underline{M} (5)), the use of a small quantity of oxalic acid in the HNO_3 scrub solution would ensure an efficient removal of any Pu(IV) and U(VI) that extracts into 2-EHOH along with the HDBP and H_2MBP .

Flowsheet for Processing Na_2CO_3 Scrub Solutions. The flowsheet for processing Na_2CO_3 scrub solutions (the ARALEX process) is based on the use of 2-EHOH to extract TBP degradation products, primarily DBP and MBP, leaving the actinides in the aqueous phase raffinate. The raffinate can then be recycled into the HLLW and processed using DHDECMP (3). Equations describing the basic chemical equilibria, using uranyl-DBP and -MBP complexes as examples, are as follows:



where n and m equal the state of aggregation of the DBP and MBP complexes, respectively.

The feed solution for the process is the TBP- Na_2CO_3 -scrub waste solution. Many process-related variables determine the composition and volume of the Na_2CO_3 scrub solution; for example, the radiation and hydrolytic damage to the TBP extractant solutions, which, of course, depend on the cooling time of the fuel and residence time of the extractants in the LLE equipment, the

actinide and fission product composition of the organic extractants during stripping operations, and the relative flow rate of extractant and Na_2CO_3 scrub streams. Therefore, certain assumptions were made in selecting a reasonable composition and volume of the Na_2CO_3 waste to use in developing a flowsheet. First, the total quantity of actinides contained in the Na_2CO_3 scrub waste is ~ 6 Kg/MTHM (5). Uranium would total 5.9 Kg, and the remaining 0.1 Kg of actinides would consist of a mixture of Np, Pu, Am, and Cm (3). Second, the primary constituents of the Na_2CO_3 scrub waste (NaDBP, Na_2MBP , and the UO_2^{2+} -carbonato complex) must stay within solubility limits. Therefore, the uranyl complex and NaDBP concentrations should not exceed 0.01 M and 0.02 M, respectively, in the Na_2CO_3 solution, which requires a carbonate scrub volume of 2500 liters/MTHM. Third, the concentration of Na_2MBP is approximately one-third that of NaDBP, assuming no losses of H_2MBP during HNO_3 scrubbing (17). In addition to the above constituents, the Na_2CO_3 scrub waste will also contain a certain amount of NaHCO_3 and NaNO_3 from the neutralization of HNO_3 present in the TBP. Using data in references 1 and 2, 96 moles of NaHCO_3 and 96 moles of NaNO_3 will be formed in the Na_2CO_3 scrub solution from the neutralization reaction. However, neither the presence of variable amounts of NaHCO_3 and NaNO_3 nor actinides would alter the flowsheet in any significant detail. Thus, the Na_2CO_3 scrub waste used in the flowsheet development consists of 2500 liters/MTHM of 0.21 M Na_2CO_3 containing 6 Kg of actinides, 0.02 M NaDBP and 0.0067 M Na_2MBP (which are present as actinide complexes), 0.038 M NaHCO_3 , and 0.038 M NaNO_3 . Approximately 100 g of fission products, primarily Zr and Ru, are also present (1). Figure 6 shows a conceptual flowsheet based on one MTHM.

Flowsheet testing using counter-current liquid-liquid extraction was performed first using the eight stage mini-centrifugal contactor. The compositions and flow rates of the feed, organic phases, scrub, and raffinate are shown in Figure 7. (The feed solution was also 2×10^{-2} M in Zr(IV).) It can be seen from the flow diagram that the carbonate feed, 8 M HNO_3 , scrub solution from stage 5, and organic solution from stage 3 all meet and are mixed in stage 4. Thus, the neutralization of carbonate feed by HNO_3 and the extraction by 2-EHOH occur simultaneously. This technique avoids the extensive precipitation of actinide (VI and IV)-DBP and -MBP complexes which occurs when the carbonate waste solution is acidified prior to equilibration with 2-EHOH. The actinide (VI and IV)-DBP and -MBP precipitates (when they do form) will eventually dissolve and dissociate when mixed with 2-EHOH and HNO_3 solution, but this process requires several minutes.

Uranium(VI) was the only actinide present in the carbonate waste solution used in the counter-current run shown in Figure 7. Subsequent U(VI), HDBP, and H_2MBP analyses showed that steady state conditions had been already achieved after the collection

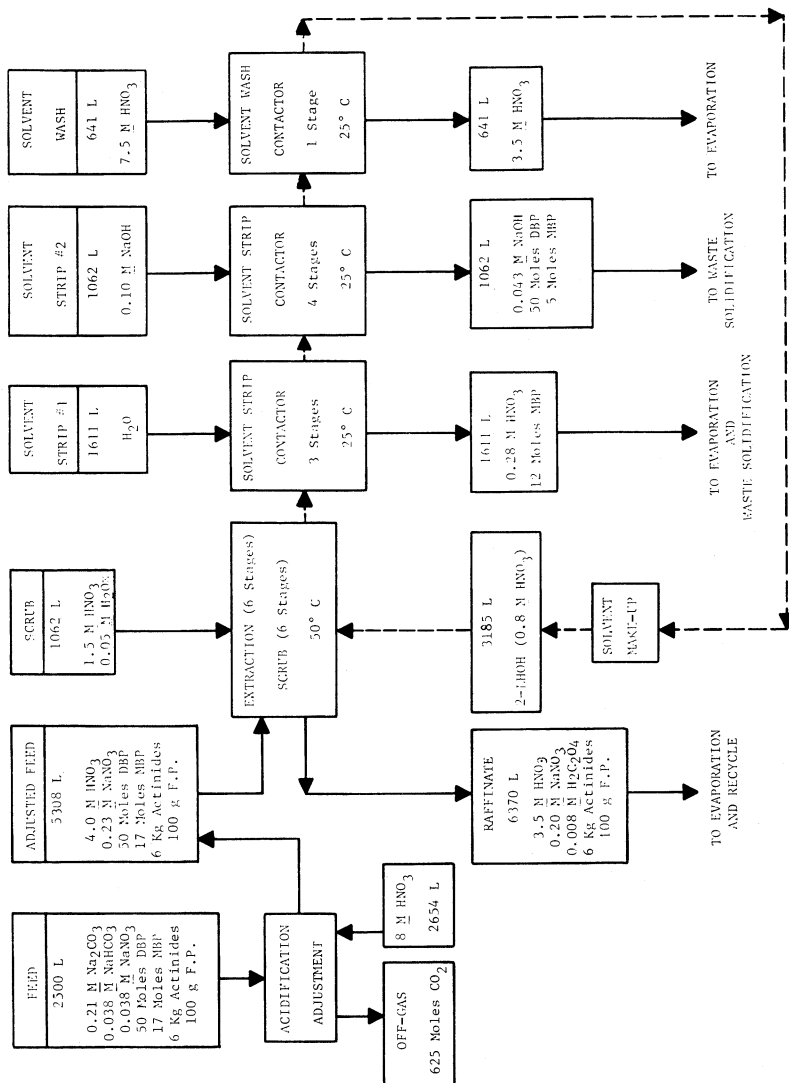


Figure 6. Conceptual flowsheet for the recovery of actinides from TBP-Na₂CO₃ scrub solutions; basis: one MTHM.

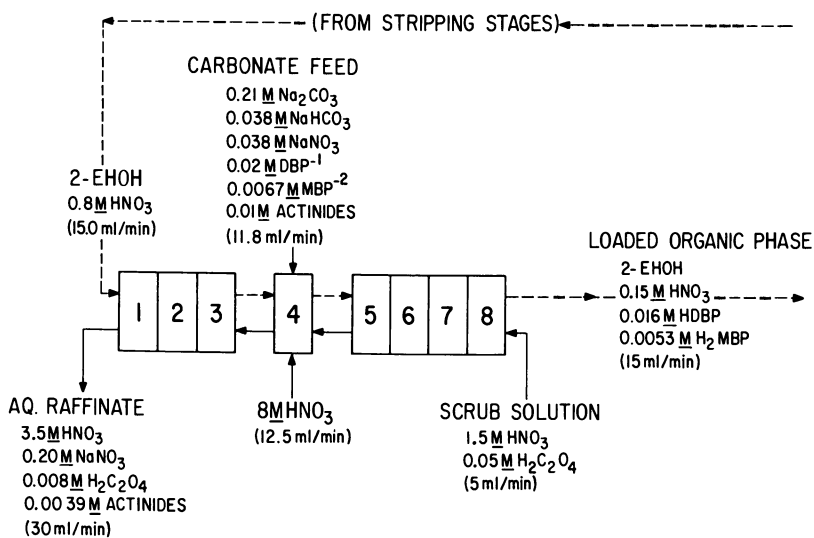


Figure 7. Eight-stage counter-current liquid-liquid extraction flow diagram for the extraction of HDBP and H_2MBP from Na_2CO_3 scrub waste solution; actinide = 0.01M U (VI); $T = 23^\circ\text{--}26^\circ\text{C}$.

of 450 ml (15 min run time) of raffinate. A total of over 3 liters of raffinate was collected before terminating the run. Only one part in 5×10^3 of the total uranium was present in the organic phase leaving stage 8. The decontamination factors for HDBP and H₂MBP from the raffinate were >100 and ≈ 20 , respectively. After completion of the run, the aqueous and organic phases were removed from the rotors and examined for insoluble material and interfacial precipitates. Stages 5 through 8 contained a small quantity of white precipitate in the organic phase, which is believed to be a Zr-MBP compound.

Additional studies on flowsheet testing were performed on carbonate feed solutions containing 0.01 M U(VI), 2.5×10^{-4} M Pu(IV), and 2×10^{-4} M Zr(IV). Preliminary experimental studies involving macro plutonium concentrations (10^{-4} M to 10^{-2} M) showed that polymeric Pu(IV) will extract into H₂MBP-alcohol mixtures. Although Pu(IV) polymer did not readily form during the preparation of the carbonate feed solutions, if insoluble U(VI)-DBP and -MBP complexes are formed on neutralization of the carbonate waste solution, some Pu(IV) (usually less than 10%) would be extracted by the 2-EHOH-HDBP-H₂MBP mixtures. This extractable plutonium (presumably Pu polymer) could not be readily removed by scrubbing with HNO₃-H₂C₂O₄ mixtures. In order to obviate this problem, diethylenetriaminepentaacetic acid (H₅DTPA) was added to the Na₂CO₃ scrub solution (prior to back extracting the actinide-DBP and -MBP complexes from TBP-nDD) in approximately the stoichiometric amount required to complex the actinides present. The presence of DTPA should prevent the formation of plutonium polymer during the transition from pH = 9 to less than pH = 0.3. Above 1 M in hydrogen ion concentration, H₅DTPA is no longer very effective as a chelating agent and thus does not affect the D's of actinides in the ARALEX process. In addition, DTPA in the Na₂CO₃ scrub also prevents the formation of plutonium hydroxide when macro concentrations of plutonium are present.

Figure 8 shows the flow diagram for a seven stage counter-current extraction run using the U(VI)-Pu(IV) carbonate (DTPA) waste solution. Jacketed separatory funnels maintained at 50°C were used for the test run. The carbonate feed solution was introduced into stage 4 while stirring the mixture of oxalic acid scrub, 8 M HNO₃, and 2-EHOH. No precipitation was observed in stage 4, but small quantities of interfacial precipitates were observed in stages 5-7. Phase disengagement (by gravity) was complete in less than 30 seconds. A total of 484 ml of raffinate (11 fractions) were collected. Only an average of one part of Pu (and U) from a total of 2×10^4 of each actinide was detected in the organic phases from stage 7. The HDBP and H₂MBP decontamination factors from the raffinate were >100 and ≈ 40 , respectively. Thus, the concentration of both HDBP and H₂MBP is $<10^{-4}$ M in the raffinate.

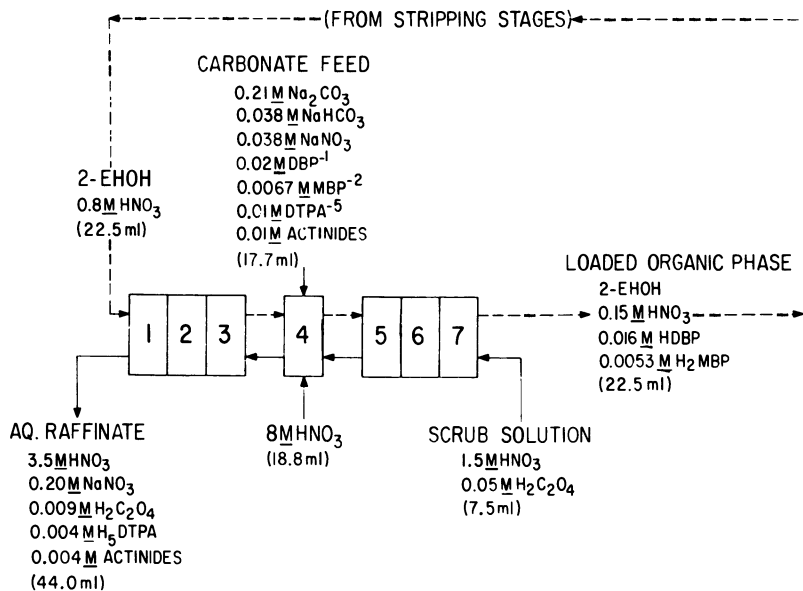


Figure 8. Seven-stage counter-current liquid-liquid extraction flow diagram for the extraction of HDBP and H_2MBP from Na_2CO_3 scrub waste solution; actinides = 0.01M U (VI) and $2.5 \times 10^{-4}\text{M}$ Pu (IV); $T = 50^\circ\text{C}$.

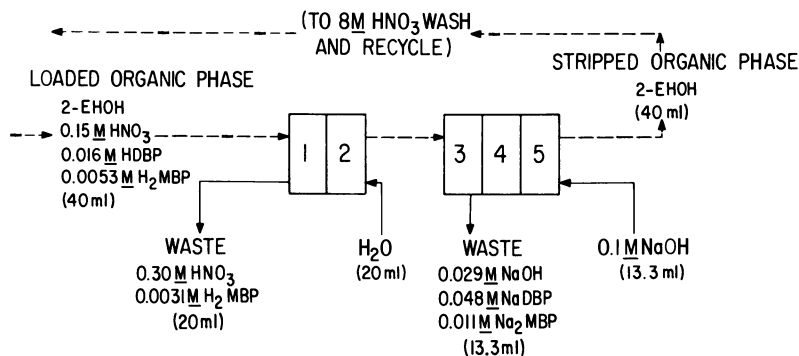


Figure 9. Five-stage counter-current liquid-liquid extraction flow diagram for the stripping of HDBP and H_2MBP from 2-ethyl-1-hexanol (2-EHOH); $T = 50^\circ\text{C}$.

The improvement in D.F. for uranium over that obtained using the 8 stage mini-centrifugal contactor was largely due to improved stage efficiency using the separatory funnels and higher temperature. However, the presence of DTPA chelating agent in the Na_2CO_3 scrub does ensure a good decontamination of plutonium from the organic phase. Improved decontamination factors for the actinides as well as the HDBP and H_2MBP could be achieved by increasing the number of stages. However, it would not be necessary to lower the concentrations of HDBP and H_2MBP in the raffinate well below the concentrations of these esters present in the TBP used to extract the actinides from the raffinate. Likewise, the desired level of decontamination of plutonium from the 2-EHOH would be governed by the levels of plutonium present in other waste streams.

Counter-current stripping of the HDBP and H_2MBP from the loaded 2-EHOH was performed using H_2O to remove excess HNO_3 and 0.1 M NaOH to remove the phosphorus esters. The flow diagram is shown in Figure 9. Separatory funnels at a temperature of 50°C were used for the stripping run. Complete phase disengagement required ~ 2 min (especially stage 3), but no emulsion or precipitate formation occurred. A total of 240 ml of stripped 2-EHOH was collected from stage 5. Decontamination of the 2-EHOH from the NaDBP and Na_2MBP was 350 and $\gg 100$, respectively. After stripping, the 2-EHOH is recycled.

The recovery of U(VI) and Pu(IV) from the acidic raffinates obtained from the alcohol extraction process can be readily carried out with TBP or preferably DHDECMP (3). (The latter extractant will also extract Am(III) and Cm(III).) The presence of H_5DTPA and dissolved 2-EHOH (solubility of 2-EHOH in 3.5 M HNO_3 at 50°C is 2.0×10^{-2} M) in the raffinate do not interfere with the extraction, or (in the case of 2-EHOH) with the stripping of actinides with TBP or DHDECMP. However, 2-EHOH would build up in recycled TBP or DHDECMP and, in the range of 5 to 10 weight % in these solvents, it will noticeably reduce the D's of the actinides. The build-up of 2-EHOH in the TBP or DHDECMP extractant solutions can be prevented by prior removal of the soluble 2-EHOH from the ARALEX raffinate. This can be accomplished by either steam stripping the raffinate or solvent scrubbing with dodecane or DIPB. The alcohol extraction process was not tested using neptunium, americium, or curium in the carbonate waste solution since Np(IV) and (VI) are similar to Pu(IV) and U(VI), and Np(V), Am(III), and Cm(III) are considerably less complexed than the tetra- and hexavalent actinides.

The ARALEX process can also be used to extract detergents from aqueous solutions containing actinides; for example, contaminated laundry solutions. Detergents from all three classes (anionics such as alkyl sulfates and alkyl benzene sulfonates; cationics such as N-benzyl-N-alkyl dimethyl ammonium chloride; and nonionics such as polyoxyethylenated alkyl phenols) are

readily extracted by 2-EHOH from acidic and neutral (and in some cases alkaline) solutions. Once the detergent is extracted from the actinides, the acidified raffinate may be evaporated or processed directly for actinide recovery. However, detergents of the types listed above cannot be back-extracted from the 2-EHOH and thus one would have to incinerate the loaded organic phase. In addition, the ARALEX process can be used to scrub residual TBP from various product streams such as americium and curium nitrate solutions, thus preventing the eventual precipitation of phosphates. The D's for TBP from dilute (0.17 M) to concentrated (8 M) HNO₃ solutions using 2-EHOH are in the range of 8×10^3 to 5×10^3 , respectively, at 25°C and 50°C.

Summary and Conclusions

A flowsheet for the recovery of actinides from TBP-Na₂CO₃ scrub waste solutions has been developed, based on batch extraction data, and tested, using laboratory scale counter-current extraction techniques. The process, called the ARALEX process, utilizes 2-ethyl-1-hexanol (2-EHOH) to extract the TBP degradation products (HDBP and H₂MBP) from acidified Na₂CO₃ scrub waste leaving the actinides in the aqueous phase. Dibutyl and monobutyl phosphoric acids are attached to the 2-EHOH molecules through hydrogen bonds. These hydrogen bonds also diminish the ability of the HDBP and H₂MBP to complex actinides and thus all actinides remain in the aqueous raffinate. Dilute sodium hydroxide solutions can be used to back-extract the dibutyl and monobutyl phosphoric acid esters as their sodium salts. The 2-EHOH can then be recycled.

After extraction of the acidified carbonate waste with 2-EHOH, the actinides may be readily extracted from the raffinate with DHDECMP or, in the case of tetra- and hexavalent actinides, with TBP.

The ARALEX process is relatively simple and involves inexpensive and readily available chemicals. The ARALEX process can also be applied to other actinide waste streams which contain appreciable concentrations of polar organic compounds that interfere with conventional actinide ion exchange and liquid-liquid extraction procedures. One such application is the removal of detergents from laundry or clean-up solutions contaminated with actinides.

Acknowledgments

The authors wish to acknowledge the assistance of Dr. Walter H. Delphin, now with DuPont de Nemours, Inc., for help in the preparation of the ³²P-labeled HDBP and H₂MBP, and the assistance of Anton A. Ziegler and Herbert Diamond for their help with the counter-current liquid-liquid extraction experiments involving

the mini-centrifugal contactor, and jacketed separatory funnels, respectively. The authors also wish to thank Florence Williams for performing the ion chromatographic analyses of the HDBP and H₂MBP. We especially thank Dr. D. William Tedder of ORNL for many helpful discussions throughout the course of this project, as well as Dr. J. O. Blomeke (ORNL) and Dr. Martin J. Steindler (ANL) for securing the funding which made portions of this project possible.

Literature Cited

1. Croff, A. G.; Tedder, D. W.; Drago, J. P.; Blomeke, J. O.; Perona, J. J. "A Preliminary Assessment of Partitioning and Transmutation as a Radioactive Waste Management Concept", ORNL/TM-5808, 1977; p. 51.
2. Richardson, G. L. "The Effect of High Solvent Irradiation Exposure on TBP Processing of Spent LMFBR Fuels", HEDL-TME 73-51, 1973; Appendix A.
3. Tedder, D. W.; Finney, B. C.; Blomeke, J. O. in "Actinide Separations"; Navratil, J. D.; Schulz, W. W. (Editors); American Chemical Society: Washington, D.C. 1979; p. 381.
4. Bahner, C. T.; Shoun, R. R.; McDowell, W. J. "Impurities that Cause Difficulty in Stripping Actinides from Commercial Tetraalkylcarbamoylmethyl Phosphonates"; ORNL-TM-5878, 1977.
5. Horwitz, E. P.; Mason, G. W.; Bloomquist, C. A. A.; Steindler, M. J. in "Actinide Partitioning and Transmutation Program Progress Report for Period October 1, 1977 to March 31, 1978"; Tedder, D. W.; Blomeke, J. O. (Compilers); ORNL-TM-6480, 1978; p. 65.
6. Delphin, W. H.; Horwitz, E. P. Anal. Chem., 1978, 50, 843.
7. Steindler, M. J., (Compiler), "Chemical Engineering Division Fuel Cycle Programs Progress Report, January-September, 1977", Section I.A.4; ANL-78-11, 1978.
8. Lash, R. P.; Hill, C. J. "Ion Chromatographic Determination of Dibutylphosphoric Acid in Nuclear Fuel Reprocessing Streams", Presented at the Second National Symposium on Ion Chromatographic Analyses of Environmental Pollutants: Raleigh, N.C., 1978.
9. Dyrssen, D. Acta Chem. Scand., 1957, 11, 1771.
10. Dyrssen, D.; Hay, L. D. Acta Chem. Scand., 1960, 14, 1091.
11. Hardy, C. J.; Scargill, D. J. Inorg. Nucl. Chem., 1959, 11, 128.
12. Marsden, C. (Compiler and Ed.); Maun, S. (Collaborator), "Solvents Guide", 2nd Ed.; Interscience Publishers: New York, 1963, Vol. 3.
13. Lange, N. (Compiler and Ed.); Forker, G., (Assistant), "Handbook of Chemistry", 7th Ed.; Handbook Publishers, Inc.: Sandusky, Ohio, 1949.
14. Dyrssen, D.; Ekberg, S. Acta Chem. Scand., 1959, 13, 1909.

15. Mason, G. W.; McCarty Lewey, S.; Peppard, D. F. J. Inorg. Nucl. Chem., 1978, 40, 1423.
16. McCarty Lewey, S.; Mason, G. W.; Peppard, D. F. J. Inorg. Nucl. Chem., 1978, 40, 1427.
17. Burger, L. L.; McClanahan, E. D. Ind. Eng. Chem., 1958, 50, 153.

RECEIVED May 14, 1979.

Work performed under U.S. Government contract number W-31-109-eng-38.

Dissolution of Plutonium Dioxide—A Critical Review

JACK L. RYAN and LANE A. BRAY

Pacific Northwest Laboratory, Battelle Memorial Institute, Richland, WA 99352

A major problem in the nuclear industry is the dissolution of refractory plutonium dioxide. Of all of the metal oxides capable of producing reasonably concentrated solutions in dilute acids, plutonium dioxide is one of the most, if not the most, difficult to dissolve. The difficult task of dissolution of PuO_2 on a process scale has been largely confined to scrap reprocessing and recovery problems related to plutonium metal production (1) along with some special situations such as in reprocessing of $^{238}\text{PuO}_2$ scrap in isotopic generator production. Use of mixed oxide fuels, either in LWR's or in breeder reactors, will require improved methods to dissolve plutonium dioxide for irradiated fuels reprocessing. This is particularly true if fuels are made by blending, pressing, and sintering separately prepared uranium dioxide with plutonium dioxide (the current method of choice of the fuel manufacturers) since this never appears to produce material which is completely converted to solid solution even after irradiation.

Overview of the PuO_2 Dissolution Problem and Methods

Several methods have been studied for the dissolution of PuO_2 . The most widely used method in the past is the use of nitric acid containing a small concentration (typically $<0.2 \text{ M}$) of fluoride usually added as HF. Although the use of HNO_3 -HF to dissolve PuO_2 or PuO_2 containing fuel residues is undesirable as pointed out by Nicholson (2), it is preferable to most of the other methods which have been used. Other options have been used only on a laboratory or limited process scale and will be mentioned only briefly here.

Gilman (3) has reviewed PuO_2 dissolution methods up to 1968, and Cleveland (1) has reviewed methods up to about 1970. Aqueous methods, other than HNO_3 -HF, include use of acids such as HI, HBr, and HCl containing SnCl_2 . These appear to act through a combination of strong acid and reducing properties. Phosphoric acid at 200°C and, on an analytical scale, HCl-HClO_4 at high temperature and pressure have been used. Because of their extreme

0-8412-0527-2/80/47-117-499\$05.00/0

© 1980 American Chemical Society

corrosiveness or incompatibility with plutonium processing in nitric acid, these methods find only very limited application.

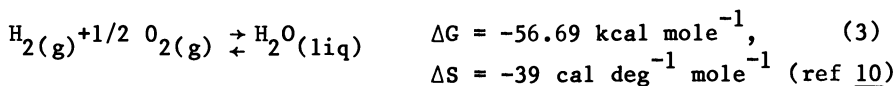
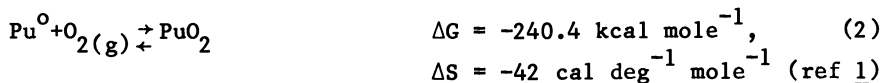
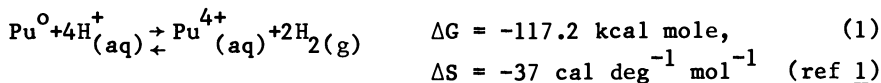
Pyrochemical methods include reduction of PuO_2 to Pu-Al alloy in a salt bath followed by dissolution of the alloy (1), vacuum or carbothermic reduction of PuO_2 to Pu_2O_3 followed by dissolution of the Pu_2O_3 (4), halogenation to PuX_3 or PuOX (3), and several fusion methods (1,3,4). Fusion agents include NH_4HF_2 , $\text{K}_2\text{S}_2\text{O}_7\text{-NaF}$, $\text{Na}_2\text{S}_2\text{O}_7\text{-K}_2\text{S}_2\text{O}_7$, and $\text{Na}_2\text{O}_2\text{-NaOH}$. Further work (6) has been done on the $\text{Na}_2\text{O}_2\text{-NaOH}$ fusion method in adapting it to rendering PuO_2 containing incinerator ash soluble. Of the fusion methods, the $\text{Na}_2\text{O}_2\text{-NaOH}$ mixture is probably by far the most attractive since it adds only sodium ion to the final process solution. It operates by oxidation of PuO_2 to Pu(VI) and/or Pu(VII) in the melt. It requires some care if organic matter is present with the PuO_2 , and if appreciable silica is present, viscous fusion mixtures and precipitation of silica on dissolution of the fusion mixture in nitric acid can occur. Adaptation of any of these pyrochemical methods to dissolution of PuO_2 in irradiated fuels reprocessing would be extremely difficult.

Direct dissolution of PuO_2 in nitric acid or nitric acid containing additives such as HF or Ce(IV) is by far preferable for irradiated fuel reprocessing. Nicholson (2) has very correctly pointed out that fuels reprocessors desire to dissolve irradiated fuels to low terminal nitric acid concentrations ($<4 \text{ M}$). On the other hand, most studies of PuO_2 dissolution by $\text{HNO}_3\text{-HF}$ have been aimed at high PuO_2 content scrap reprocessing and have involved $\geq 8 \text{ M HNO}_3$. Also, because of the extreme difficulty of removing the very fine (particle sizes down to $<1 \mu\text{m}$ (7)) PuO_2 and heat producing (^{106}Ru) fission product solids, it would be most desirable to dissolve all the PuO_2 in the bulk dissolver solution containing all the uranium. The rest of this paper will be devoted to dissolution in HNO_3 , $\text{HNO}_3\text{-HF}$, or $\text{HNO}_3\text{-Ce(IV)}$ solutions.

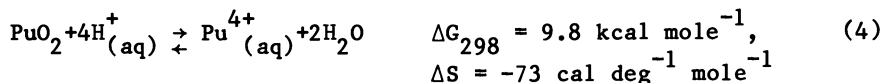
Dissolution of PuO_2 in Nitric Acid

Despite the fact that the dissolution of PuO_2 in pure nitric acid solution is extremely slow, only two sources of quantitative data appear to be available (8,9). Uriarte and Rainey (8) report a dissolution rate, R , in $\text{mg cm}^{-2} \text{ min}^{-1}$ of $R = 1.1 \times 10^{-7} [\text{HNO}_3]^4$ in the range $7\text{-}14 \text{ M HNO}_3$ where $[\text{HNO}_3]$ is the molar concentration of HNO_3 . In complete disagreement with this, Horner et al. (9) report almost no effect of nitric acid concentration on dissolution rate in the range 2 to 16 M HNO_3 with the rate being about $1.5 \times 10^{-5} \text{ mg cm}^{-2} \text{ min}^{-1}$, a value coinciding with that obtained by extrapolation of Uriarte and Rainey's work to 3.4 M HNO_3 . Both of these groups used high fired, presumably low surface area, PuO_2 . Although a difference in numerical values of rates might be explained on the basis of oxide used (difference in surface area measurement techniques), this does not account for the extremely large difference in nitric acid dependence.

It is important that, although apparently not recognized by workers in the field, at lower acidities (<5 M), such as those of most interest to fuels reproprocessors, plutonium dioxide is thermodynamically practically insoluble. Combining the following reactions and thermodynamic data:



gives:



Assuming constant ΔH , one obtains:

$$\Delta G_{373} = 15.3 \text{ kcal mole}^{-1}$$

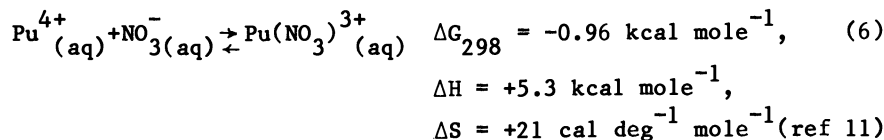
$$K_{298} = 6.7 \times 10^{-8}$$

$$K_{373} = 1.1 \times 10^{-9} \text{ for reaction (4).}$$

Assuming that $\alpha_{\text{Pu}^{4+}} = [\text{Pu}^{4+}(\text{aq})]$ and that $\alpha_{\text{H}^+} = \alpha_{\text{HNO}_3}^{\pm}$ gives:

$$K_{373} = \frac{[\text{Pu}^{4+}(\text{aq})]}{(\alpha_{\text{HNO}_3}^{\pm})^4 (\alpha_{\text{H}_2\text{O}})^2} = 1.1 \times 10^{-9} \quad (5)$$

For the reaction:



Resulting in:

$$\Delta G_{373} = -2.53 \text{ kcal mole}^{-1} \text{ and:}$$

$$K_{373} = 30.2 = \frac{a_{\text{Pu}(\text{NO}_3)_3^{3+}}}{(a_{\text{NO}_3^-})(a_{\text{Pu}^{4+}})} \quad (7)$$

Again, assuming unit activity coefficients for $\text{Pu}(\text{NO}_3)_3^{3+}$ and Pu^{4+} , that $a_{\text{NO}_3^-} = a_{\text{HNO}_3}$, and combining equations (5) and (7) gives:

$$[\text{Pu}(\text{NO}_3)_3^{3+}] = (30.2)(1.1 \times 10^{-9})(a_{\text{HNO}_3}^+)^5(a_{\text{H}_2\text{O}})^2. \quad (8)$$

Using the activity coefficient data of Davis and de Bruin (12) and assuming activity coefficients at 100°C are the same as those at 25°C since there appears (13) to be little variation between 0°C and 25°C, gives the calculated thermodynamic solubility curve for PuO_2 in Figure 1. Figure 1 indicates that $\text{Pu}(\text{IV})$ solutions above about 1 g Pu/L and below 5 M HNO_3 are thermodynamically unstable with respect to crystalline PuO_2 (but they are not unstable with respect to the kinetically more readily formed but less thermodynamically stable hydrated plutonium dioxide). It should be emphasized that error in ΔG_{373} for reactions (4) or (6) will change the results by a factor of 3.8 per kcal mole⁻¹ of error. Of the thermodynamic data used, the entropy data for reaction (6) is the most suspect since it is based on old, limited, and perhaps uncertain data (14). Some error is to be expected due to the assumptions regarding activity coefficients and a positive deviation at high acidities is expected due to neglect of higher nitrate complexes.

We have carried out limited experiments on the dissolution of PuO_2 in 4 M HNO_3 at 100°C (Figure 2). Using oxide prepared by firing $\text{Pu}(\text{III})$ oxalate for 2 hours at 900°C in air and having a surface area of 4.47 m²/g (BET method) at about 2.0 to 5.2 mg PuO_2 per ml solvent, we obtained about 1.4% dissolution of the Pu and about 2.8% of the ²⁴¹Am (present to the extent of about 1% in this oxide) in less than two hours (possibly less than 15 minutes). This was followed by no further dissolution (within experimental error) over a period of five hours more. Although this coincides closely with the solubility value from Figure 1, it also coincides closely with dissolution of plutonium to one-half of one unit cell depth over the entire surface and dissolution of ²⁴¹Am to one unit cell depth over the entire surface since 2.76% of the PuO_2 is in the surface unit cells with oxide having a surface area of 4.47 m²/g. Since one-half of the actinide atoms in the surface unit cells are in the surface layer, such behavior might suggest that the surface plutonium layer has been altered allowing easy dissolution and making the second layer accessible to selective leaching of the much more soluble ²⁴¹Am. This same behavior was observed with a different, but identically prepared and fresher

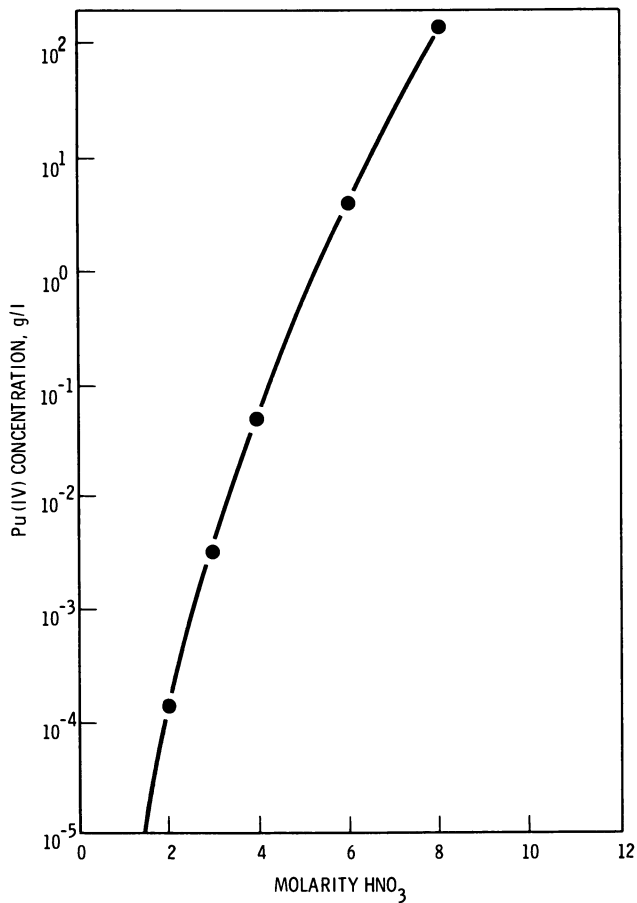


Figure 1. Thermodynamically calculated solubility of PuO_2 in HNO_3 .

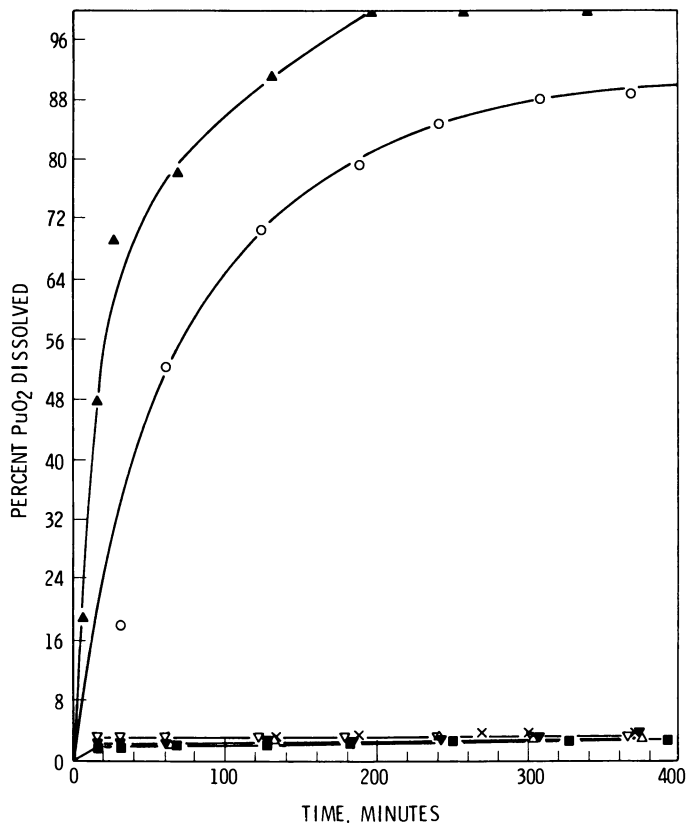


Figure 2. Dissolution of 0.13 g of 900°C fired PuO_2 (surface area = 4.47 m^2/g) using several different 50-ml stirred solutions at 100°C: (▲) 4M HNO_3 + 0.05M HF; (○) 4M HNO_3 + 0.05M HF + 0.005M Zr (IV); (△) 4M HNO_3 ; (▼) 4M HNO_3 + 0.05M HF + 0.025M Zr (IV); (■) 4M HNO_3 + 0.05M HF + 0.05M Zr (IV); (▽) 4M HNO_3 + 0.05M HF + 0.05M Zr metal (-80 mesh); and (×) synthetic dissolver solution [0.85M U (VI) + 4M HNO_3 + 0.05M HF + 0.0066M Zr (IV)].

(3 months old) batch of oxide.

Another experiment was performed at 100°C in which the 4 M HNO₃ solvent was replaced after two hours and again after four hours. In the first two hours, 2.8% of the ²⁴¹Am again dissolved (Pu was not separately determined). In each of the second and third two-hour intervals about 0.14% of the ²⁴¹Am dissolved. Within the limits of the counting statistics (²⁴¹Pu was determined by γ -counting at about 150 keV) the amount of Pu dissolved was also about 0.14%. This corresponds to a dissolution rate of 2.6×10^{-7} mg min⁻¹ cm⁻² which is about 60-fold lower than that reported by Horner et al. (9) for PuO₂ microspheres and 100-fold lower than that obtained by extrapolation to 4 M HNO₃ of Uriarte and Rainey's (8) results for PuO₂ pellets. If their very low surface areas are correct, this difference is not readily explainable.

Although the above experiments neither confirm nor reject the calculated solubilities shown in Figure 1, they do indicate that an initial relatively high dissolution rate is followed by a much lower rate. Such difference is not explainable on the basis of change in surface area. Since only the surface layer of PuO₂ dissolved readily, surface hydration might be suspected as a causative factor. Hydration of PuO₂ is not thermodynamically favorable, but the surface monolayer may be expected to react differently due to different thermodynamic properties. Also, radiolysis of adsorbed water to make oxidative free radicals might be a factor since we know that ²³⁸PuO₂ rather rapidly converts to amorphous and finally to polymeric hydrated PuO₂ in pure water.

Despite the fact that the oxide used had been made and stored in a low humidity atmosphere, we refired a sample of the oxide under the same firing conditions at which it was originally prepared and carried out a two hour dissolution immediately afterward. The amount of ²⁴¹Am dissolved was reduced to 27% of that before and no ²⁴¹Pu was detected indicating (for the counting conditions used) $\leq 0.2\%$ PuO₂ dissolved. This tends to support a surface hydration hypothesis, but further work would be needed to confirm this.

The low calculated solubility of PuO₂ at < 5 M HNO₃ indicates that care must be exercised in studying and interpreting dissolution rates in this acid region. It also leads to the prediction that fluoride might be required not only as a catalyst to increase the dissolution rate but also might be required to act as a stoichiometric reagent to complex Pu(IV) and to thereby increase equilibrium PuO₂ solubility. An estimate of this effect using the published value (15) of the formation constant for the monofluoro complex of Pu(IV), estimated values for the difluoro and trifluoro complexes based on data (15) for Th(IV) and U(IV), estimated entropies of formation based on published data (16) for Th(IV), U(IV), and Np(IV), the ionization constant for HF (15), and assuming unit activity coefficients for HF and F⁻ indicates that addition of 0.05 M HF to 4 M HNO₃ would be expected to

increase PuO_2 solubility four- to five-fold over that (48 mg Pu/L) shown in Figure 1. Although we did choose values of equilibrium constants measured at the higher ionic strengths available, they were not for 4 M HNO_3 and such calculations can only be considered to be rough approximations. We have, in fact, actually dissolved PuO_2 in 4 M HNO_3 -0.05 M HF to about ten times this estimated value. At higher nitric acid concentrations, the equilibrium solubility of PuO_2 is much higher as seen in Figure 1, and fluoride is expected to act only as a catalyst in increasing dissolution rate.

Dissolution of PuO_2 in HNO_3 - HF

Several fairly basic studies (8, 17, 18, 19) of the kinetics of dissolution of PuO_2 by HNO_3 -HF mixtures and other studies (20, 21, 22, 23) of the dissolution of chemically similar ThO_2 have been made. The principal things that can be said about this work are that there is little agreement between the various workers, and that the dissolution of ThO_2 by HNO_3 -HF is considerably easier and possibly mechanistically somewhat different from the dissolution of PuO_2 . The earlier of the PuO_2 work (8) finds the dissolution rate to increase by the 1.4th power of HF molarity at constant acidity, and by the 4th power of the total HNO_3 molarity. Barney (17) found the rate to be first order in the total HF not complexed to Pu(IV), first order in oxide surface area, and to be independent of acid concentration in the range 4-12 M. He found that the rate decreased with increasing amount of PuO_2 dissolved because fluoride was tied up by complexing with Pu(IV) in solution, and this effect increased with decreasing acidity due to formation of higher fluoro complexes at lower acidities. At 4 M HNO_3 the rate was extremely slow after a ratio of about 1 Pu/2.5 HF was reached. Tallent and Mailen (19) also found the rate to be first order in uncomplexed HF concentration, but, unlike Barney, they found the rate to also be first order in mean ionic activity of HNO_3 (second order if F^- instead of HF is the reacting species). They also recognized the effect of dissolved Pu(IV) in decreasing dissolution rates and did experiments aimed at eliminating this effect by oxidation of the Pu(IV) to Pu(VI) which forms much weaker fluoro complexes. The rates were increased by too large an extent to be attributable only to decrease of fluoride complexing, however. Despite the rather wide difference in conclusions with regard to effect of acidity on dissolution rate, the absolute rates (measured early in dissolution) were in rather good agreement for dissolution in 8-10 M HNO_3 - 0.05 M HF at 100°C. The values of Tallent and Mailen (18) for low surface area (0.012 m^2/g) microspheres, of Barney (17) for oxide produced by burning Pu metal (2.9 m^2/g), and our own unpublished data for oxide obtained by calcining Pu(III) oxalate at 900°C (4.47 m^2/g) all are in the range 1 to 9×10^{-3} mg PuO_2 min^{-1} cm^{-2} . The somewhat higher values of Uriarte and Rainey (8) are probably

due to the use of geometrical surface areas for pellets of only 90% theoretical density.

Takeuchi (22) obtained dissolution rates $>1 \text{ mg ThO}_2 \text{ cm}^{-2} \text{ min}^{-1}$ in 6 M HNO_3 - 0.035 M HF at only 70°C , a rate about one thousand times that for PuO_2 under the same conditions. Despite considerable evidence (24, 25, 26, 27) of inhibition of ThO_2 dissolution by complexing of F^- by Zr(IV) , Th(IV) , Al(III) , Be(II) , and Fe(III) (decreasing in the order shown) Shying et al. (20) have observed moderately high ThO_2 dissolution rates with 6.5 M HNO_3 and $\leq 0.005 \text{ M HF}$ at 25°C . At virtually all of their experimental points, Th(IV) in solution greatly exceeds the HF concentration, in some cases by a factor of ten. Under these conditions, very low PuO_2 dissolution rates would be expected based on Barney's (17) results. In fact, Barney's data indicates that at 6 M HNO_3 and $\text{Pu/F} > 0.5$, dissolution is very slow at 35°C and even at 10 M HNO_3 and 100°C dissolution of PuO_2 almost stops at $\text{Pu/F} = 2$. This again indicates much more rapid dissolution of ThO_2 than of PuO_2 since Th(IV) forms a stronger complex with fluoride than does Pu(IV) (15). Takeuchi et al. (22) under conditions where the $[\text{HF}]$ concentration in solution is large compared to the Th concentration, find the dissolution rate to be much less than first order in HF concentration, and find that the rate is proportional to $K_1 [\text{HF}] / (1 + K_1 [\text{HF}])$. This observation was for the same range of HF concentrations (0.01 to 0.05 M) for which the PuO_2 dissolution rate was found to be first order in uncomplexed $[\text{HF}]$. They also found a very low dependence on total acidity, as did Barney (17) for PuO_2 dissolution. Their dissolution rates were proportional to $K_2 [\text{HNO}_3] / (1 + K_2 [\text{HNO}_3])$ where HNO_3 is the concentration of unionized nitric acid. Shying et al. (20) found the dissolution rate at low HF concentrations, $< 0.005 \text{ M}$, and Th/F ratios > 1 to be less than first order in total fluoride concentration in solution (after correcting for fluoride adsorbed on the ThO_2 surface) approaching first order at the lower concentrations studied. We found that their rates can also be represented by an equation of the type $r = kK [\text{HF}] / (1 + K [\text{HF}])$. Shying et al. (21) report the dissolution rate in HNO_3 - HF solutions under the conditions noted above to be second order in mean ionic activity of HNO_3 , after correction for change in fluoride activity with HNO_3 concentration, a conclusion later reached by Tallent and Mailen for PuO_2 .

It appears on the basis of the above cited literature that there is little overall agreement between the more basic studies of PuO_2 and ThO_2 dissolution in both HNO_3 and in HNO_3 - HF solutions. It is difficult to review this work and to determine which conclusions, if any, are the closest to being correct. Some of the work is based on relatively limited experimental data with no evidence of its reproducibility. Thus, for example, Tallent and Mailen (18) carried out only eight PuO_2 dissolutions to determine both the fluoride and acid dependence of the dissolution rate. The number of samples taken per run ranged from three

to six (usually four) with first sampling times varying between 0.43 and 1.8 hours, and final sampling times up to 23 hours with dissolution proceeding to almost 100% of the initial PuO_2 in some cases. Despite continually changing curvature in these dissolution versus time plots, they have estimated initial dissolution rates and have determined exact first order dependences on HF concentration and on mean ionic activity of HNO_3 . We would suggest that there cannot be much reliability to the result. Barney's (17) study is much more careful in this regard in that he has measured seven or eight points in the first 60 minutes of dissolution and has used a large PuO_2 to solvent ratio. At his highest dissolution rates, all measurements were below about 10% dissolution to minimize change in surface area with time. Under these conditions of large PuO_2 surface area and rapidly increasing solution Pu(IV) concentration, the HF concentration not complexed by Pu(IV) was determined by assuming formation of only the one-to-one PuF^{3+} complex which is a reasonable assumption at 10 M HNO_3 .

The experimental approach of Takeuchi et al. (22) in their study of ThO_2 is probably the best. They have used a small measured surface area of a high density (99% of theoretical) ThO_2 pellet with sufficient volume of dissolvent that there was never sufficient Th dissolved to complex much of the HF. Solution samples were taken at approximately 10 minute intervals for about 100 minutes, and all dissolution plots were straight lines. Shying et al. (20, 21) measured dissolution rates of ThO_2 under conditions where the Th in solution was almost always in excess of total fluoride (up to 10-fold excess) with the ratio varying. At the acidities they used, (2 to 6.5 M) the fluoride must be strongly tied up by complexing to Th(IV) since Th is efficiently removed from anion exchange columns by 8 M HNO_3 -0.01 M HF (28). Tallent and Mailen (19) have shown a 100-fold decrease in PuO_2 dissolution rate when Th equal to the total fluoride is added to 8M HNO_3 -0.1 M HF. Thus, regardless of whether F^- , HF, ThF^{3+} , ThF_2^{2+} , etc., is the kinetically controlling fluoride species, the results cannot be meaningful since none of these can be directly proportional to total fluoride in solution (corrected for adsorbed fluoride) with Th/F varying from 0.23 to 10 (21) and acidities varying from 2 to 6.5 M HNO_3 .

It is tempting to speculate that dissolution of PuO_2 in HNO_3 -HF is similar to that for ThO_2 except in degree. The equation, $r = kK[\text{HF}]/(1+K[\text{HF}])$ as proposed by Takeuchi et al. (22) approaches a first order rate as $[\text{HF}]$ decreases. It is at these low HF concentrations, where the ThO_2 dissolution rates approach first order in $[\text{HF}]$, that the absolute ThO_2 rates approach those for PuO_2 at higher HF concentrations where the PuO_2 dissolution rate has been studied and found to be first order in HF concentration. The faster dissolution of ThO_2 compared to PuO_2 is not surprising in view of the difference in basicities, metal oxygen bond strengths, and related tendency of the oxides to hydrate.

Effects of Metallic Impurities on Dissolution in HNO₃-HF

Metallic impurities which complex fluoride strongly will, if present in quantities approaching the total fluoride concentration, markedly influence PuO₂ dissolution by lowering free F⁻ and HF activities. At the low terminal dissolution acidities desired in fuels reprocessing, metals which form stronger fluoro complexes than those of Pu(IV), will, if present in quantities equal to or greater than the total fluoride, effectively lower the thermodynamic solubility of PuO₂ to that in pure HNO₃ (Figure 1). Zirconium, which is both a fission product and cladding material, is an example of this type since both its first and second fluoro complex formation constants are greater than the first constant for Pu(IV).

All metallic ions which complex fluoride to an appreciable extent at the acidities and fluoride concentrations of interest can be expected to decrease dissolution rates through lowering of F⁻ and HF activities. Molen (29) showed that the rate of PuO₂ dissolution decreases with increasing PuO₂ to solvent (12 M HNO₃ - 0.1 M CaF₂) ratio. Harmon (30) noted that at 6 to 7 M HNO₃, the dissolution rate of PuO₂ is markedly decreased by the presence of an excess of U(VI) and Fe(III) and attributed this to lowered fluoride activity. The effects (24, 25, 26, 27) of Zr(IV), Th(IV), Al(III), Be(II), and Fe(III) on ThO₂ dissolution were noted earlier. Barney (17) studied the rate decrease caused by complexation of fluoride by dissolving Pu(IV). At high acidities (~10 M), he found only the PuF³⁺ complex needed to be considered, but at lower acidities higher complexes were also important.

Tallent and Mailen (19) have studied the dissolution of PuO₂ in 8 M HNO₃-0.1 M HF in the presence of a variety of fluoride complexing metallic ions, several of which might be expected to be present in process solutions. They adequately demonstrated a very large decrease in dissolution rate upon addition of metallic ions which complex fluoride strongly (2000-fold in the case of 0.1 M Zr), but they have given a totally incorrect quantitative interpretation of their data. They assumed that only the mono-fluoro complexes need be considered and carried out their experiments with equal concentrations of HF and metallic ion present. Under these conditions it can be shown that it is only because of higher complexes that such drastic reductions in dissolution rate (presumably due to corresponding reductions in HF and F⁻ activity) can occur. They have also neglected the fact that HF is a weak acid only slightly ionized in 8 M HNO₃, have incorrectly derived equations for fluoride activity in the presence of metallic ions, and have used published activity coefficient data for HF incorrectly.

The effects of various fluoride complexing metal ions at 25°C can be roughly estimated from their complex formation constants (15) assuming, as has been concluded (17), that at any given acidity the PuO₂ dissolution rate is first order with respect to free

(uncomplexed to metal) fluoride or HF concentration. Metallic ions present in irradiated fuel dissolver solution which are known to form complex fluorides (or form insoluble fluorides) are uranium (a bulk constituent), plutonium, zirconium (a fission product and a fuel cladding material), trivalent actinides, and lanthanides. Other fission products such as Nb, Mo, and Sb form fluoro complexes, but quantitative data is lacking.

Assuming unit activity coefficients for HF in 4 M HNO₃, equal activity coefficients for the metallic ions and the metal fluoro complexes, and that α_{H^+} and $\alpha_{NO_3^-}$ are equal to mean ionic activities given in ref. (12), it is predicted that Sr at dissolver solution levels will have virtually no effect on fluoride activity in 4 M HNO₃-0.05 M HF. If the total lanthanides plus trivalent actinides are assumed to act like Ce(III), they are not expected to lower fluoride activity in 4 M HNO₃ except above about 0.15 M HF where precipitation of the Ln(An)F₃ may occur. Addition of 1 M U(VI) to 4 M HNO₃-0.05 M HF will reduce free HF (and F⁻) and presumably PuO₂ dissolution rate by 5.6-fold at 25°C under the above assumptions and correcting for the nitrate complexing (11) of the uranium. Because the uranium is present in large excess, a very large amount of fluoride would be required to counteract this effect. This estimate is in reasonably close agreement with the experimental results of Harmon (30) in 6 M HNO₃ where the effect of uranium would be predicted to be about a factor of two less.

Zirconium forms a series of strong fluoro complexes, both the monofluoro and difluoro complexes being stronger than the monofluoro complex of Pu(IV). If only the monofluoro complex of Zr(IV) is considered, the predicted lowering of HF or fluoride activity in 4 M HNO₃-0.05 M HF on addition of 0.05 M Zr would be 75-fold. If the monofluoro and difluoro complexes are considered the predicted lowering of fluoride and HF activity and presumably lowering of PuO₂ dissolution rate would be 1000-fold. Including the higher fluoro complexes in the calculation would result in even larger predicted decrease in dissolution rate.

Based on estimates similar to those above, it can be predicted that large amounts of fluoride would be required to obtain PuO₂ dissolution rates in irradiated fuel dissolver solutions that are comparable to those in pure HNO₃-HF solutions. Because of the effect of the large excess of uranium, it is probably not feasible to add sufficient fluoride (since it is undesirable in later processing and waste storage steps) to reach a dissolution rate more than several-fold lower than in pure HNO₃-HF.

The above predictions were experimentally confirmed as shown in Figure 2. It can be seen from Figure 2 (the percent PuO₂ dissolved was determined by gamma counting ²⁴¹Am) that the presence of even half as much Zr as HF reduces the PuO₂ dissolution rate, within the limits of the ²⁴¹Am counting method, to that of pure HNO₃ alone. It can also be seen that Zr metal fines, as expected from chopping of zirconium clad fuel, are as

effective as Zr initially in solution. Even one tenth as much Zr as HF decreases the dissolution rate appreciably. The dissolution rate in a synthetic dissolver solution (comparable to that expected in 30,000 MWD/ton mixed oxide fuel) containing only about one eighth as much Zr as HF is also reduced for practical purposes to that in pure HNO₃.

It appears from the above results that in order to reasonably rapidly dissolve PuO₂ residues from mixed oxide fuel in a reasonable period, undesirably large amounts of HF would be required. An alternative is to separate PuO₂ residues (along with fission product solids and, in the case of LWR fuels, Zr cladding fines) from the nitric acid dissolver solution, and to dissolve this material in a separate HNO₃-HF solution. Depending upon the amount of Zr fines, and the amount and composition of the fission product solids, this might still require several times as much fluoride on a molar basis, as the amount of PuO₂ dissolved. A severe disadvantage to this approach is the difficulty of filtering or centrifuging solids. Not only are they extremely fine, but because of the high fission product ruthenium content and resulting high heat generation rate, it would also be difficult to maintain stable filter or centrifuge cakes.

Dissolution in HNO₃-Ce (IV)

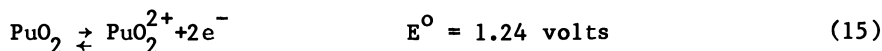
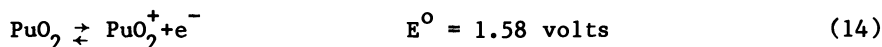
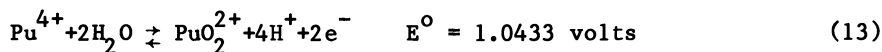
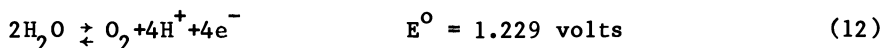
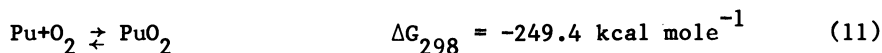
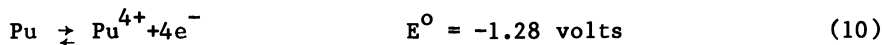
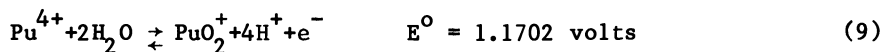
In 1961, A. S. Wilson (31) received a patent for a process of dissolving PuO₂ in nitric acid containing cerium ions. Wilson's work consisted of two dissolution experiments using cerous ion in 15.7 M HNO₃ and two control experiments in the absence of cerium. The very reactive PuO₂ used was prepared by a short calcining of the oxalate at 400-500°C. The PuO₂ dissolution rate (to 20% dissolution) was increased about five-fold due to the presence of Ce. The scatter was very large between the two control experiments. Wilson proposed, but did not prove, that the cerium acted as an oxidation catalyst in the process.

Uriarte and Rainey (8) studied the effect of Ce(IV) on PuO₂ dissolution at varying Ce(IV) and HNO₃ concentrations. They stated that "With 0.005 to 0.1 M Ce(IV) in 4 M HNO₃, the dissolution rate was approximately proportional to the first power of the ceric ion concentration. At lower Ce(IV) concentrations, the rates were the same as those in nitric acid alone." Although they, unlike Wilson, adequately demonstrated that Ce(IV) increases the dissolution rates of PuO₂ at various acidities, neither of their above conclusions is justified on the basis of their data. Their large experimental scatter, their lack of control of Ce(IV)/Ce(III) ratio, their lack of a measurement of the dissolution rate in pure 4 M HNO₃, and comparison of their results to an extrapolation to 4 M HNO₃ of their data for dissolution in pure 7-14 M HNO₃ make these conclusions untenable. Their claim that the rate in 7, 10, and 14 M HNO₃ in the presence of Ce(IV) is the same as in nitric acid alone is also clearly not supported by

their own data.

In more recent studies, Horner et al. (9) and Harmon (30) conclude that Ce(III) is completely ineffective in promoting PuO₂ dissolution except at very high acidities (>12 M) where some oxidation to Ce(IV) causes a modest increase in dissolution rate over that in pure HNO₃. They found Ce(IV) to be most effective at about 4 M HNO₃. Horner et al. (9) found the rate with 0.1 M Ce(IV) to be about 2000 times that which they reported for pure HNO₃. Their reported rates decrease rapidly both above and below 4 M HNO₃. At low Ce(IV) concentrations, they report the rate to be first order in Ce(IV) concentration, but their data is too limited to justify such a conclusion. They also found that the Ce(IV)/Ce(III) ratio is a very important factor influencing the dissolution rate with the rate at a ratio of 0.25 being 28-fold lower than in the absence of any initial Ce(III). From this, they conclude that a solution potential of about 1.38 volts would be needed for practical dissolution of PuO₂ microspheres. They propose ozone or electrolytic regeneration to maintain high Ce(IV)/Ce(III) ratio but have apparently pursued this only to the extent of brief and unsuccessful experiments with ozone. They have briefly examined other oxidants, such as persulfate, permanganate, and dichromate, but do not appear to have seriously considered the oxidation-reduction kinetics of these oxidants as compared to Ce(IV).

By properly combining the standard oxidation potentials and/or free energies (1, 10) of reactions (9) through (12) or (10) through (13) one obtains the standard potentials for oxidative dissolution of PuO₂ as PuO₂⁺ or PuO₂²⁺ as given in reactions (14) and (15):



From the potentials of reactions (14) and (15), it can be seen that PuO₂²⁺ will be the final product of oxidative dissolution.

Despite this, the dissolution can probably be expected to go through reaction (14) and thus, even though Pu(V) is unstable in the solution and need not reach unit activity, a solution potential within about 0.2 volts of that of reaction (14) might reasonably be expected to be required. This correlates closely with the 1.38 volts estimated by Horner et al. (9). It can be seen from the above that only very strong oxidants should be capable of dissolving PuO₂, and if these are further limited to those which are generally kinetically fast, Ce(IV) may be the only relatively stable example.

Horner et al. (9) have observed that in dissolution of irradiated fuels residues, ruthenium present as fission product Ru metal, destroys the Ce(IV) probably through formation of volatile RuO₄ followed by its decomposition to solid RuO₂ and return from the dissolver condenser to the solution. The RuO₂ is then again oxidized to RuO₄. Elimination of this problem will require removal of ruthenium from the solution. It should be noted that other fission products such as iodine are oxidized to high oxidation states by Ce(IV) and also will consume Ce(IV).

Conclusions

Traditional methods of dissolution of PuO₂ do not lend themselves to dissolution of the PuO₂ present in irradiated reactor fuels when it is not in solid solution with UO₂. Plutonium dioxide is insoluble both from a thermodynamic and kinetic standpoint in the terminal nitric acid concentrations desired for dissolver solutions. Pyrochemical dissolution methods would be very difficult with the high activity levels involved and would generally add appreciably to high level waste volumes. Use of nitric acid-hydrofluoric acid at tolerable levels of fluoride is severely limited by fluoride complexing by uranium and fission products. In dissolution in HNO₃ solutions of Ce(IV), various fission products consume Ce(IV). Despite this, the lack of other desirable alternatives makes it appear that further work on oxidative dissolution might be warranted.

Acknowledgment

This work was performed under U.S. Department of Energy Contract EY-76-C-06-1830.

Literature Cited

1. Cleveland, J. M., "The Chemistry of Plutonium," Gordon and Breach, New York, 1970.
2. Nicholson, E. L., USERDA Rep. ORNL/TM-5903 (1977).
3. Gilman, W. S., USAEC Rep. MLM-1264, (1965) and USAEC Rep. MLM-1513, (1968).

4. Deaton, R. L.; and Silver, G. L., Radiochem. Radioanal. Lett., (1972) 10, 277.
5. Angeletti, L. M.; and Bartscher, W. J., Anal. Chim. Acta., (1972) 60, 238-241.
6. Partridge, J. A.; and Wheelwright, E. J., USERDA Rep. BNWL-B-419 (1972).
7. "Composite Quarterly Report Light Water Reactor Fuel Recycle, Jan - March 1977," USERDA Rep. DPST-LWR-76-2-3 (1977).
8. Uriarte, A. L.; and Rainey, R. H., USAEC Rep. ORNL-3695 (1965).
9. Horner, D. E.; Crouse, D. J.; and Mailen, J. C., USERDA Rep. ORNL/TM-4716 (1977).
10. Latimer, W. M., "The Oxidation States of the Elements and Their Potentials in Aqueous Solutions," 2nd ed., Prentice Hall, Englewood Cliffs, N.J., 1952, pp. 30 and 39.
11. Jones, A. D.; and Choppin, G. R., Actinides Rev., (1969) 1, 311-336.
12. Davis, W. Jr.; and de Bruin, H. J., J. Inorg. Nucl. Chem., (1964) 26, 1069.
13. Landolt-Bornstein, "Physikalisch-Chemische Tabellen," Julius Springer, Berlin, 1963, Erg IIIc, pp. 2141 and 2145.
14. Zebroski, E. L.; and Neumann, F. K., USAEC Rep., KAPL-184, (1949); quoted by Hindman, J. C., Nat. Nuclear Energy Ser., IV-14A (1954) p. 339.
15. Sillén, L. G.; and Martell, A. E., "Stability Constants of Metal-Ion Complexes," The Chemical Society, London, 1964, pp. 259-261.
16. Choppin, G. R.; and Unrein, P. J., in "Transplutonium Elements," eds. Mueller, W.; and Lindner, R., North-Holland Publ. Co., Amsterdam, 1976, pp. 97-100.
17. Barney, G. S., USAEC Rep. ARH-SA-255 (Sept. 1976).
18. Tallent, O. K.; and Mailen, J. C., Nucl. Tech. (1977) 32, 167.
19. Tallent, O. K.; and Mailen, J. C., Nucl. Tech. (1977) 34, 416.
20. Shying, M. E.; Florence, T. M., and Carswell, D. J., J. Inorg. Nucl. Chem., (1970) 32, 3493.
21. Shying, M. E.; Florence, T. M.; and Carswell, D. J., J. Inorg. Nucl. Chem., (1972) 34, 213.
22. Takeuchi, T.; Hanson, C. K.; and Wadsworth, M. E., J. Inorg. Nucl. Chem., (1971) 33, 1089.
23. Takeuchi, T.; and Kowamura, K., J. Inorg. Nucl. Chem., (1972) 34, 2497.
24. Bond, W. D., USAEC Rep. ORNL-2519 (1958).
25. Farrell, M. S.; and Isaacs, S. R., AAEC Rep. E-143 (1965).
26. Blanco, R. E.; Ferris, L. M.; Flanary, J. R.; Kitts, F. G.; Rainey, R. H.; and Roberts, J. J., USAEC Rep. TID-7583 (1959) 234.
27. Ferris, L. M.; and Kibbey, A. H., USAEC Rep. ORNL-3143 (1961).
28. Ryan, J. L., USAEC Rep., HW-59193 REV (1959).
29. Molen, G. T., USAEC Rep. RFP-922 (1967).
30. Harmon, H. D., USAEC Rep. DP-1371 (1975).
31. Wilson, A. S., U.S. Patent 3,005,682 (1961).

RECEIVED September 4, 1979.

Recent Savannah River Experience and Development With Actinide Separations

M. C. THOMPSON, G. A. BURNEY, and J. M. McKIBBEN

Savannah River Laboratory, E. I. du Pont de Nemours and Company,
Aiken, SC 29801

Savannah River Laboratory (SRL) and Savannah River Plant (SRP) have been involved in actinide separations for 25 years. Work continues to upgrade processes and to initiate new processes. This report summarizes the work since 1971 (1) except for the changes in enriched uranium processing reported in 1977 (2). The following topics are discussed: recovery of americium and curium; reduction of wastes by substituting hydroxylamine nitrate (HAN) for ferrous sulfamate (FeSA) during partitioning of plutonium and uranium; a solvent extraction flowsheet for recovery of ^{238}Pu and ^{237}Np ; and improved separation of ^{238}Pu and ^{237}Np with macroporous ion exchange resins.

Recovery of Americium and Curium

Large-scale purification of americium, curium, and californium with pressurized cation exchange has been planned at SRP for many years (1). Initial work involved SRP batch extractions to isolate a crude actinide-lanthanide fraction followed by solvent extraction and ion exchange in the SRL high level caves (1). For large-scale purification, a single step was substituted for batch extraction and solvent extraction. Plant Purex solvent (30 vol % tri-n-butyl phosphate in n-paraffin) was used to minimize flush time and cross-contamination of solvent.

Laboratory Tests

A solvent extraction cycle similar to that used in the earlier work was selected (1). The flowsheet (Figure 1) was first demonstrated in laboratory miniature mixer-settlers.

Before solvent extraction, the feed was treated with manganous nitrate and less than equivalent permanganate to convert plutonium to Pu(VI). Tests in miniature mixer-settlers with synthetic feed solution but not containing Cf showed acceptably small concentrations of actinides in the aqueous waste (1AW) and organic raffinate (1CW) streams, and also acceptable separation of plutonium from curium and americium.

0-8412-0527-2/80/47-117-515\$05.00/0

© 1980 American Chemical Society

These results (Table 1) show that additional valence adjustment of the feed to reduce Pu from Pu(VI) to the more extractable Pu(IV) was not necessary. Plutonium in the Cm-Am stream (1BP) varied from 2 to 7.8% of feed Pu. In the 1C mixer-settler, 0.01M HAN back-extracted Pu efficiently, even when the flow of HAN was reduced 50%, and although the feed concentration of Pu in the test solutions was ~ 10 times that expected in plant operation.

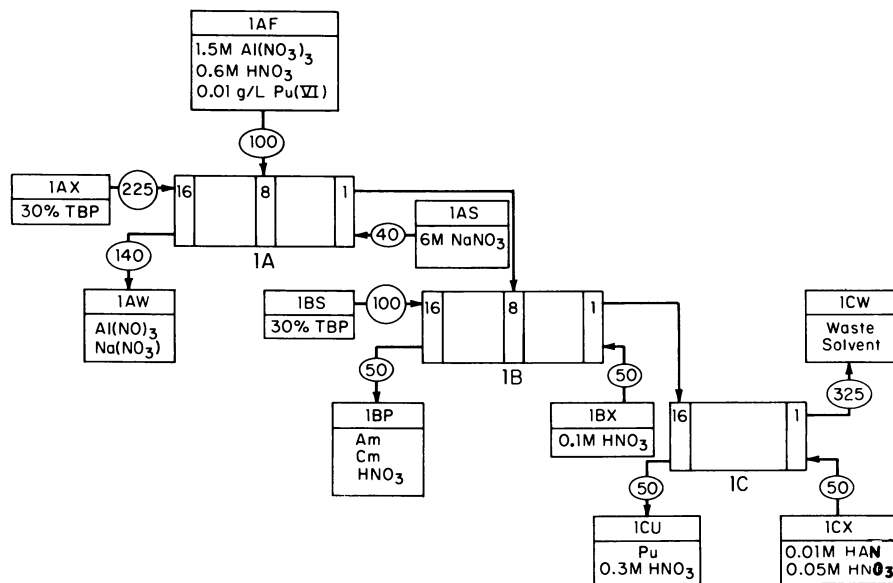


Figure 1. Solvent extraction flowsheet for laboratory miniature mixer settlers

Table 1. Laboratory Tests of Am and Cm Recovery With Synthetic Feed Solution

	% of Feed		
	Pu	Am	Cm
Raffinates			
Aqueous 1AW	<0.05	<0.05	<0.05
Organic	0.002	0.002	0.04
Product Solutions			
Cm-Am 1BP	<8	~ 100	~ 100
Pu 1CU	95	0.1	0.2

Plant Test

After the successful laboratory tests, a plant test was made with some changes from routine operation. The first cycle contactor in the plant is an 18-stage centrifugal contactor with the scrub entering Stage 1. To decrease entrainment of the 6M NaNO₃ scrub, the IAS was introduced into Stage 2 with Stage 1 acting as a centrifugal separator. The 1B mixer-settler was changed to allow the aqueous product to be washed with pure n-paraffin in Stages 18 and 17. The 1BS was introduced then at Stage 16 instead of Stage 18. The n-paraffin wash removed tributyl phosphate (TBP) dissolved in the aqueous and lowered the phosphate content of the resulting product from 140 to 6 mg/L when no actinides were in the feed.

The entrainment of IAS was determined in a separate run with potassium nitrate as a tracer. The concentration due to entrainment was 0.055 vol %; the contribution due to both entrainment and solubility was equivalent to 0.073 vol %, a value slightly less than the desired maximum of 0.1 vol %.

The hot run was made with the feed solution obtained by dissolving highly irradiated Pu-Al alloy in HNO₃ with mercuric ion catalyst. Uranium was added to the solution to produce a typical Purex feed. Uranium and most of the plutonium were recovered by the normal Purex process. The aqueous waste containing Am, Cm, Cf, fission products, Al, and Hg was evaporated; and acid was stripped to produce the feed (Table 2). The results are as expected from the laboratory tests: excellent recovery of Pu, Am, and Cm but low decontamination factors (DF).

Table 2. Plant Tests of Am and Cm Recovery With a Typical Concentrated Waste Feed Solution

Al(NO ₃) ₃ , M	1.5			
HNO ₃ , M	0.75			
Pu, g	468			
Am, g	74			
Cm, g	50			
Gamma, Ci	2.3×10^5			
Element or Isotope	Endstream, %			
	1AW	1BP	1CU	1CW
Pu	0.02	0.6	98.5	-
Am	-	100	-	-
Cm	-	100	-	-
¹⁴⁴ Ce	-	100	-	-
^{134,137} Cs	100	-	-	-
¹⁰⁶ Ru- ¹⁰⁶ Rh	29.7	17.9	47.3	5.1
⁹⁵ Zr- ⁹⁵ Nb	50	50	-	-
Gross Gamma DF	-	8.5	8.5	-

Analyses of sodium in the lBP showed 556 mg/L, which was equivalent to an entrainment of IAS of 0.09 vol %, higher than the cold run but less than 0.1 vol %. Phosphate concentration in the lBP solution was 13.1 mg/L.

Since the test, the flowsheet has been run six times in three campaigns to recover a total of ~6.1 kg Am and 2.3 kg Cm. The overall recovery of Am and Cm was >99%. The alpha and gamma content of these solutions was up to 10 times higher than in the test solution. The sodium concentration in the lBP varied from 420 to 526 mg/L which was lower than obtained in the test. The phosphate content of the lBP solution varied with the alpha activity in the feed or product. This result shows that the phosphate concentration is a function of alpha radiolysis. The range of the alpha particle is short; therefore, the radiolysis is probably occurring in the organic phase while Am and Cm are extracted. From the slope of the line in Figure 2, an alpha energy of 5.8 MeV for ^{244}Cm , and 10 minutes residence time in the organic phase, the G value was calculated to be 0.16 molecule per 100 electron volts. The product of radiolysis was assumed to be monobutylphosphoric acid since the n-paraffin wash should remove all TBP and dibutylphosphoric acid.

In all tests, the gamma activity of the solvent increased to extremely high levels. To remove the activity from the solvent (mostly ^{106}Ru), the wash time was extended and the 1B and 1C mixer-settlers were used as washers (Figure 3). Washed solvent follows the same trend as unwashed and never quite reaches the level prior to the run. Solutions of Na_2CO_3 , $\text{Na}_2\text{CO}_3\text{-NaOH}$, and 0.1M HNO_3 were used to wash the solvent.

The Am and Cm were combined in a single tank after evaporation and will be separated when time becomes available in the SRP cation exchange facility.

Waste Reduction Through Use of Hydroxylamine Nitrate

Ferrous sulfamate has been the reductant for plutonium during partitioning of uranium and plutonium in the Purex process at SRP since startup. In recent years, a desire to reduce waste volumes has led to studies of alternative reductants or combinations of FeSA with other reductants. The FeSA in the Pu strip solution produces $\text{Fe}(\text{OH})_3$ and Na_2SO_4 in neutralized waste; these compounds account for a large percentage of the solid material in Purex low activity waste. In an effort to reduce these wastes, we investigated HAN as a substitute for part or all of the FeSA in the Purex first cycle.

Earlier work at Savannah River had shown that HAN was a good Pu reductant at low acidity and indicated that HAN with $\text{Fe}(\text{NO}_3)_3$ catalysis might be substituted for FeSA during partitioning of U and Pu (3).

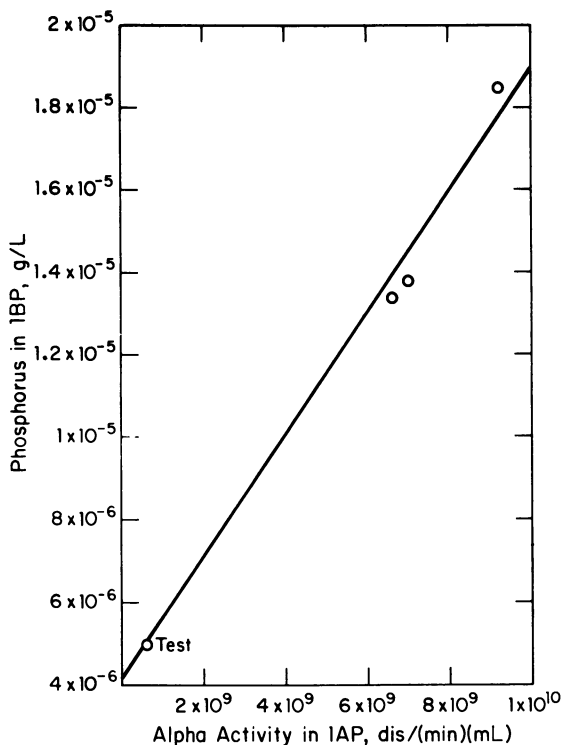
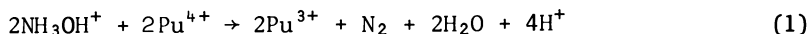


Figure 2. Phosphorus in IBP as a function of α activity in IAP

Laboratory Tests

Barney has studied reactions of hydroxylamine and plutonium and gives the following overall reaction (4):



when hydroxylamine concentration exceeds plutonium concentration. Richardson and Swanson confirmed the acid dependence under the latter conditions (5). Richardson also demonstrated Pu partitioning with HAN-N₂H₄ mixtures in miniature centrifugal contactors for breeder fuel compositions (5). Thus, we anticipated FeSA could be completely replaced. However, in tests at SRL, plutonium was shown to reflux in all tests except when 0.05M FeSA was present in addition to HAN.

The test results for plutonium are shown in Figures 4, 5, and 6. In the test with HAN alone, the Pu split evenly between the Pu and U products. Figure 4 shows that most of the Pu is reduced in the first stage, the only stage where the acidity is

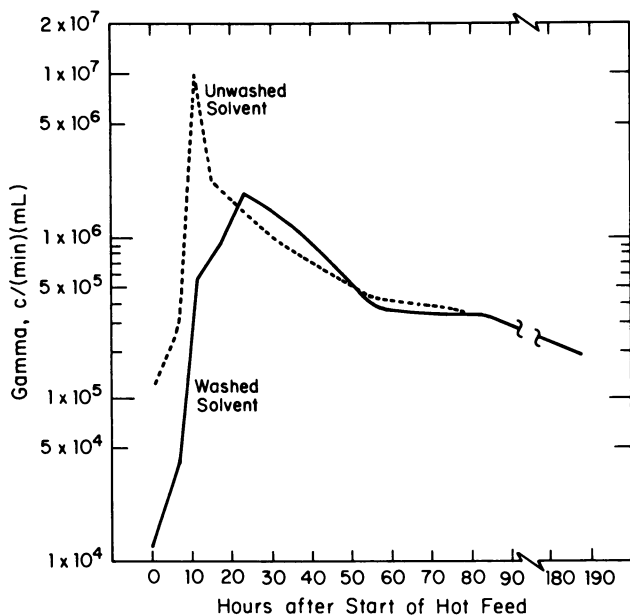


Figure 3. γ Activity of first cycle solvent: 0–10.3 hr, hot feed; 10.3–18.8 hr, product removal; 18.8–92 hr, washing with 1B and 1C mixer settlers and solvent washers; 92–188 hr, washing with solvent washer only.

<0.5M; reduction with HAN is best at low acidity (3,4). Absence of a NO_2 scavenger also contributes to the poor performance of HAN alone, because the Pu^{3+} is not protected from reoxidation by HNO_2 . Adding N_2H_4 to react with HNO_2 improved performance (Figure 4) but did not prevent some reflux. The Pu profile calculated with the SEPHIS computer program modified by Richardson (5) to include kinetics of reduction by HAN shows the expected result. Richardson achieved agreement between his experimental results in centrifugal contactors and the modified SEPHIS (5). The difference between Richardson's tests and our tests is the residence time for mixer-settlers versus centrifugal contactors. The modified SEPHIS program does not include kinetics for the reoxidation of Pu so the time effect could not be modeled. If residence time is a factor, SRP would have even more reoxidation because the residence time is much longer than for SRL miniature mixer-settlers.

Ferric nitrate could be used to catalyze the reduction of plutonium by hydroxylamine during partitioning (3). A laboratory test with a mixture of $\text{Fe}(\text{NO}_3)_3$ and HAN resulted in Pu reflux (Figure 5). Using $\text{Fe}(\text{NO}_3)_2$ instead of $\text{Fe}(\text{NO}_3)_3$ merely shifted the point of reflux toward the feed stage. The reflux must be caused by NO_2 because a plant test at Hanford with $\text{Fe}(\text{NO}_3)_2$ and N_2H_4 was successful except when excess NO_2 entered the partitioning column (6).

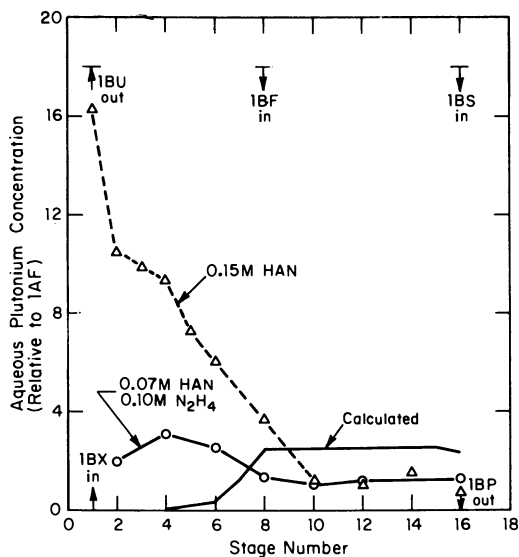


Figure 4. Aqueous Pu with hydroxylamine nitrate and hydrazine

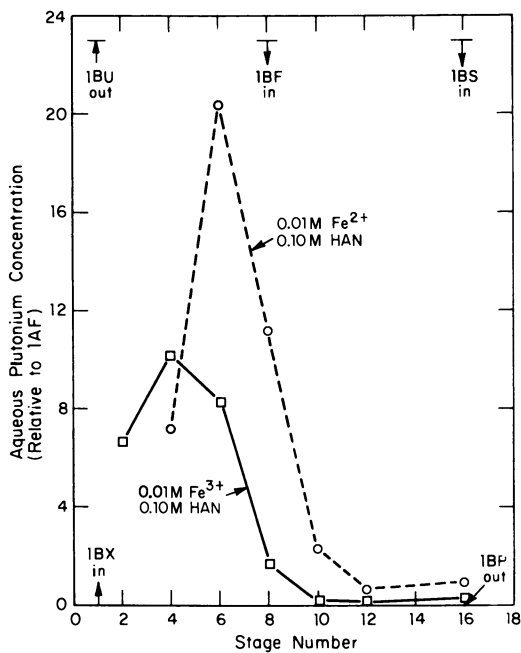


Figure 5. Aqueous Pu with mixtures of ferrous or ferric nitrate and hydroxylamine nitrate

Therefore, further tests were made with mixtures of FeSA and HAN. With 0.01M FeSA, Pu refluxed at the feed stage, but to a much lower extent than with $\text{Fe}(\text{NO}_3)_2$ (Figure 6). Increasing the FeSA to 0.05M gave good partitioning and showed the feasibility for testing in the plant.

SRP personnel did not want to handle hydrazine and hydrazoic acid which results from reaction of hydrazine with nitrous acid:

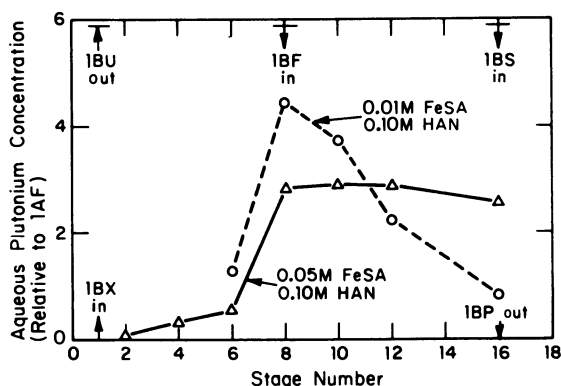
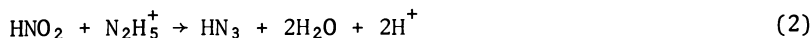


Figure 6. Aqueous Pu with mixtures of ferrous sulfamate and hydroxylamine nitrate

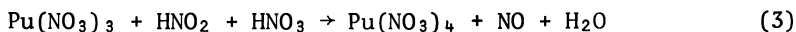
Plant Tests

A series of tests were made to determine how much of the FeSA could be replaced under plant conditions. Tests were started with normal FeSA concentration; then, FeSA was slowly replaced with HAN. Operation was stable for several days in all tests and resulted in a significant reduction in stored waste volume from the subsequent Pu purification cycle (Table 3). During the last 16-hr segment of the first test, FeSA was reduced to 0.05M with 0.035M HAN. After a period of continued stable operation, the neutron monitors on the mixer-settler showed increasing neutron emission indicative of a buildup in Pu. When the neutron monitors reached the operating limit, the cycle was shut down and, subsequently, flushed with FeSA under normal operating conditions. Samples of IBP were taken 5½ hr before reflux and 2 hr after the start of reflux. The samples were not analyzed until the following day and showed 0.03M and 0.02M for both sulfamate ion and hydroxylamine and 0.04M ferrous in the respective samples. Since the samples waited some hours prior

Table 3. Plant Tests of U-Pu Partitioning With Mixtures of HAN and FeSA

	Normal Operation	Test 1	Test 2	Test 3
First cycle operation, days	-	4.2	2.0	4.3
Scrub HNO ₃ , M	3.0	3.0	2.2	2.2
Strip concentration, M				
Fe ²⁺	0.12	0.08	0.08	0.07
NH ₂ SO ₃ ⁻	0.25	0.17	0.17	0.15
NH ₃ OH(NO ₃)	-	0.056	0.056	0.049
Products concentration, M				
Fe ²⁺	0.06	0.07	0.07	0.07
NH ₂ SO ₃ ⁻	0.14	0.08	0.10	0.07
NH ₃ OH(NO ₃)	-	0.03	0.04	0.025
Stored waste, L/MTU	309	206	206	177

to analysis and were identical, it was assumed that the results do not indicate the Fe²⁺ ion concentration in the mixer-settler. Most of the Fe³⁺ ion present in the initial samples would be reduced to Fe²⁺ prior to sample analysis. Sulfamate analyses indicate increased destruction which would be expected if plutonium is reoxidized from Pu(III) to Pu(IV) by nitrous acid when sulfamate concentrations get low:



Reduction by HAN is slow at 2.3-2.5M HNO₃ in the center of the mixer-settler. Therefore, Fe²⁺ would be the principal reductant and more should be consumed as reflux increases. However, subsequent reduction by HAN prevented measurement of Fe²⁺ so the HAN concentration should be indicative of increased Pu concentrations. The analyses showed that 0.01M more HAN was consumed after the start of reflux. Assuming that 2 moles of ferric are reduced per mole of hydroxylamine, the ferric ion concentration was 0.02M lower after reflux than before reflux. Lowering Fe²⁺ and NH₂SO₃⁻ was sufficient to obtain Pu reflux similar to that observed in laboratory tests with 0.01M FeSA.

Subsequent tests were made at lower 1A scrub acid concentration because most of the acid in the 2B contactor comes from the acid in the organic phase from the 1A contactor. Since Equation 1 shows an inverse fourth power dependence on acid concentration, the scrub acid was lowered to 2.2M. Good partitioning was observed and it was possible to lower both the FeSA and HAN concentrations. Tests at lower scrub acid and lower FeSA concentration will be made to further reduce waste volume.

Solvent Extraction Separation of Neptunium and Plutonium

Laboratory studies were made to design a solvent extraction flowsheet for the recovery, decontamination, and partitioning of ^{237}Np and ^{238}Pu from irradiated neptunium targets. Replacing anion exchange processing of these targets by solvent extraction in SRP operations would reduce cost and waste volume, and would increase the production rate of ^{238}Pu (7). The valence of Np and Pu must be adjusted to provide species of both elements that are extractable with TBP and may thereby be removed from inextractable fission products. The extractability of Np and Pu valence states into TBP decreases in the order: $\text{Pu(IV)} > \text{Np(VI)} > \text{Np(IV)} \sim \text{Pu(VI)} \gg \text{Np(V)} \sim \text{Pu(III)}$. Np(V) and Pu(III) are relatively inextractable. Stabilization of extractable valences is difficult because of the high specific activity of ^{238}Pu and the chemical effects of plant dissolver solution (2 g/L ^{237}Np , 0.4 g/L ^{238}Pu , 1.2M Al^{3+} , 4.6M NO_3^- , 1M H^+ , and fission products).

Thermodynamic calculations and batch extraction tests showed that the Np(IV)-Pu(IV) and Np(VI)-Pu(VI) systems are unstable for solution concentrations practical for solvent extraction. Products of radiolysis provide a mechanism for oxidation of Np(IV) and reduction of Np(VI) and Pu(VI). Batch extraction experiments showed that the reaction rates of destabilizing reactions are fast enough that the systems cannot be stabilized for a practicable time for plant processing (8).

Investigations then centered on methods for producing the appropriate valences in situ in the mixer-settlers during processing (9),

Iodine (including ^{131}I when short-cooled targets are processed) can be removed in head end by in situ precipitation with MnO_2 (10). MnO_2 oxidizes both neptunium and plutonium to M(VI). Therefore initial tests were made with Np(VI) and Pu(VI) produced by in situ precipitation of MnO_2 .

Laboratory tests showed that FeSA added as a sidestream to the extraction section of the mixer-settler lowered Np losses. After Pu(VI) and residual Np(VI) were extracted, FeSA was added to reduce inextractable Np(V) to extractable Np(IV) in situ. Any unextracted Pu(VI) will be lost by reduction to inextractable Pu(III). In some tests, urea was added after MnO_2 removal to stabilize Np(VI). Tests demonstrated that >99% of the Np can be recovered within 24 hr after valence adjustment, with or without urea as a stabilizer; however, Pu losses were high.

Additional tests were made to determine the optimum sidestream position. Np losses increased (except for the unexplained high losses in test with FeSA into Stage 11), and Pu losses decreased as the FeSA sidestream was moved to higher stages (Figure 7), providing more stages for Pu(VI) extraction before the remaining Pu is reduced to inextractable Pu(III).

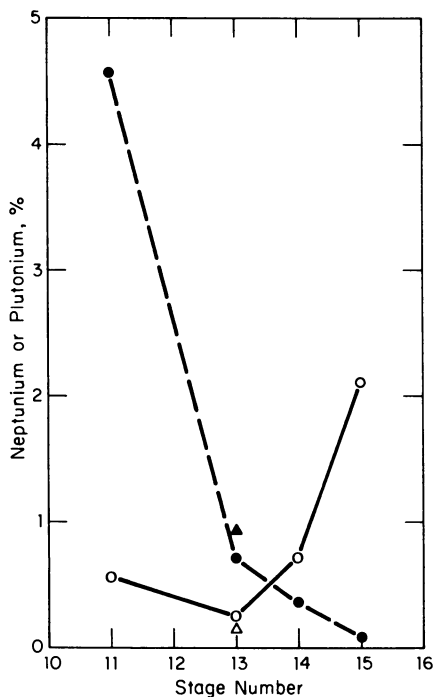


Figure 7. Np and Pu losses to waste as a function of stage of 0.35M ferrous sulfate addition: simulated feed: (○) Np, (●) Pu; plant feed: (△) Np, (▲) Pu.

Table 4. Laboratory Tests of ^{237}Np - ^{238}Pu Flowsheet With Plant Feed Solution

Fission Product	Decontamination Factor ^a
^{103}Ru	9.2×10^5
$^{134}, ^{137}\text{Cs}$	1×10^5
^{144}Ce	$>7.2 \times 10^5$
^{95}Zr	$>4.7 \times 10^2$

a. Ratio of activity in IAF to activity in IAP.

Because total actinide losses were minimized by introducing FeSA into Stage 13, a test with plant dissolver solution was made with the same conditions. Extractant and scrub flows were increased. Np and Pu losses (Figure 7) differ from tests with simulated feed because the FeSA concentration was increased to 0.50M.

Decontamination from fission products was good except for ^{95}Zr (Table 4) and is comparable to that achieved in reprocessing irradiated enriched uranium fuels (2).

Similar tests were made after adjustment to Np(IV) and Pu(IV) and with no valence adjustment. Results were similar in both cases because radiolysis rapidly oxidizes Np(IV) to Np(V).

Losses of Np and Pu as low as 0.15% and 0.25% were observed in tests with simulated feed and a 0.50M FeSA sidestream in Stage 11.

Higher Np losses (2.36%) were obtained in a test with plant feed because of increased radiolysis from fission products present in plant feed.

A mixer-settler test with a nitrite sidestream into Stage 15 was made because nitrate oxidation of neptunium with catalytic amounts of NO_2^- has been used to obtain Np(VI) (11,12). The concentration of HNO_2 must be carefully controlled because it forms during the oxidation reaction, and excess HNO_2 causes reduction of Np(VI) to Np(V). NO_2^- should be between 5×10^{-4} and $1 \times 10^{-3}\text{M}$; above $1 \times 10^{-3}\text{M}$, Np losses increase rapidly (12). Although preliminary mixer-settler tests with a NO_2^- sidestream established that NO_2^- was between 5×10^{-4} and $1 \times 10^{-3}\text{M}$ throughout the bank, NO_2^- could not be controlled with ^{238}Pu present, and Np losses of 17 to 33% were observed.

Partitioning of Neptunium and Plutonium

Neptunium and plutonium are partitioned by reducing Pu(IV) or Pu(VI) to inextractable Pu(III); neptunium is simultaneously reduced to Np(IV). Neptunium is kept in the organic phase by adjusting the acid in the aqueous strip solution (1BX) and the organic-to-aqueous flow ratio to maintain the extraction factor of neptunium greater than one.

Table 5 gives the results of partitioning tests with both the M(IV) and M(VI) combinations. For the M(VI) case, 0.06M and 0.08M FeSA are ~80% and 105%, respectively, of the stoichiometric amount of reductant necessary to completely reduce Np and Pu. The higher Pu loss might be caused by too low a $\text{Fe}^{2+}/\text{Fe}^{3+}$ ratio in the scrub section of the mixer-settler. When enriched U solutions were processed, $\text{Fe}^{2+}/\text{Fe}^{3+}$ ratios less than 0.18 led to oxidation of Pu(III) and Np(IV) (13). The $\text{Fe}^{2+}/\text{Fe}^{3+}$ ratio of 0.054 in the scrub section would allow oxidation and re-extraction of Pu. Np loss is not changed because most of the Np does not reach the scrub section. Rather than increase waste

Table 5. Partitioning of Neptunium and Plutonium

Temp, °C	N_2H_4 , M	FeSA, M	Pu Product, % Np	Np Product, % Pu
Np(VI)-Pu(VI)				
30-35	0	0.06	0.59	0.96
30-35	0	0.08	0.01	1.9
45	0.10	0.08	0.01	0.32
Np(IV)-Pu(IV)				
30-35	0	0.06	0.04	0.25
30-35	0	0.08	0.05	0.29
45	0.15	0.08	0.07	0.06

volumes by additional FeSA, N_2H_4 was added to act as both a reducing agent and a NO_2^- scavenger. Increasing the temperature to enhance the rate of N_2H_4 reduction reactions resulted in lower Pu losses although not as low as desired. Pu remaining in the first cycle Np product would be rejected to waste in the second Np cycle.

For the M(IV) case, 0.06M FeSA represents a tenfold stoichiometric excess so 0.08M FeSA does not lower Pu losses.

Second Plutonium Cycle

The plutonium product from the first cycle (1BP) must be further purified and concentrated before precipitation as Pu(III) oxalate (14). Concentrations of 3 to 8 g/L Pu and 0.5 to 1.5M HNO_3 are desired for precipitation in plant operation. Radiolysis of the solvent by ^{238}Pu to form nonstrippable plutonium dibutyl phosphate (DBP) complexes was expected to be the main problem with second Pu cycle operation. Thus, the second Pu cycle was tested to demonstrate that solutions in the desired concentration range could be readily extracted and stripped.

Two miniature mixer-settler tests were made with feed composition similar to that expected from the 1BP. The results (Table 6) demonstrate that ^{238}Pu can be extracted and stripped with small losses to waste and solvent. Losses of plutonium to the 2AW are dependent on the flow ratio of 2AX/2AF. The loss to the waste solvent (2BW) is dependent on flow of the solvent (2AX). Lowering the 2AX flow increases the loss to 2BW caused by radiolysis. The lower flow increases the ^{238}Pu concentration and the ^{238}Pu residence time in the solvent giving a higher total radiation dose. Thus, the increase in loss to 2BW was less than expected even though the total dose increased a factor of ~ 3 (increase in time and concentration is equal to the ratio of 2AX flow rates, 1.78 to 1 and therefore the increase is 1.78^2). The poor mass balance obtained in the first test in-

Table 6. Second Plutonium Cycle Tests With ^{238}Pu

Stream	Flow, mL/min	Composition
2AF	2.0	~ 1.0 g/L ^{238}Pu , $> 4.1M$ HNO_3
2AX	α	30% vol % TBP
2AS	0.60	0.70M HNO_3
2BX	0.40	0.01M HNO_3 , 0.056M HAN

α . 2AX Flow, mL/min	Plutonium, %		
	2AW	2BP	2BW
1.78	0.002	68.5	0.05
1.00	0.06	98.8	0.08

icates that steady state operation may not have been attained or that Pu reflux occurred in the 2B mixer-settler. The product from the second Pu cycle (2BP) contained 5.0 g/L ^{238}Pu and $\sim 0.6\text{M}$ HNO_3 , which is within the desired concentration range for oxalate precipitation.

The stability of the Pu product was tested by dividing the solution into two equal portions, washing one portion with 1 vol % n-paraffin, and leaving the other untreated. Within 24 hr, solids formed in the unwashed portion of solution. No solids formed in the n-paraffin washed portion for more than a month. The solids were not analyzed, but are believed to be Pu DBP compounds formed by radiolytic decomposition of dissolved and entrained TBP.

This process has not been used in the plant because the following work improved capacity enough to cover future requirements for ^{238}Pu .

Ion Exchange Separation of Neptunium and Plutonium

Many kilograms of ^{238}Pu and ^{237}Np have been recovered and purified at SRP in the past by anion exchange in a nitrate system (7). Also, anion exchange is used to separate and concentrate ^{239}Pu and ^{237}Np from high levels of fission products and highly salted solutions in several plant processes.

Gel-type resins, which have a low surface area and no discrete pore structure, were used for more than a decade (Figure 8). Initially *Dowex* 1-X4 and *Dowex* 21K were used but later *Dowex* 1-X3 and *Dowex* 1-X2 were found to have better sorption and elution properties. Presently macroporous anion exchange resins are used for all SRP applications (15). These resins have a rigid pore structure and large surface area which permits faster diffusion of the bulky hexanitrate ions of the tetravalent actinides (Figure 8). Initial testing of *Dowex* MSA-1 macroporous anion resins (40 to 60 mesh) in the laboratory and also in SRP columns demonstrated that the throughput of the different systems could be increased 25 to 100% because of increased resin loading attainable and increased flow rates. Increased flow rates are attributed to more rigid structure so there is less shrinking and swelling and deformation of the particles, particularly when the solution composition is widely varied. The greatest increase in capacity was in the waste recovery processing of large volumes containing low concentration of products in the feed because of improved flow rates. Also, product loss was decreased and product quality improved by using macroporous resin.

Macroporous and gel-type resins have the same matrix; and they have similar radiation, thermal, and chemical stability. Since somewhat higher flow rates and product loading are attainable with macroporous resins without loss of efficiency, a larger

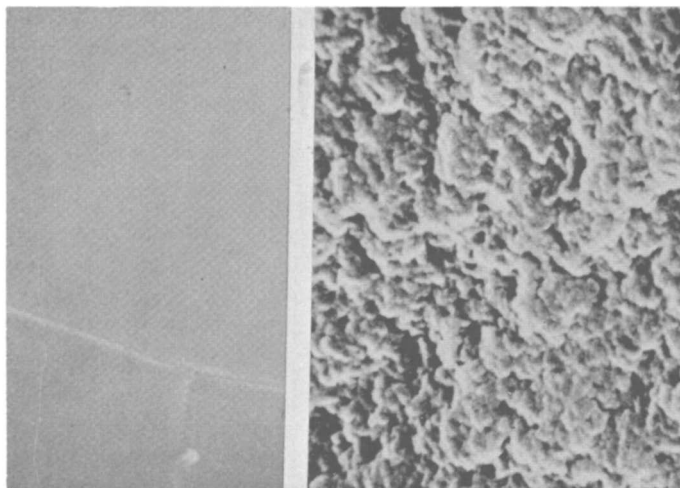


Figure 8. Scanning electron photomicrographs of anion exchange resin: Left, Dowex MSA-1 (11,000 \times); Right, Dowex I-X2 (21,000 \times).

quantity of product can be processed per unit volume of resin before the resin capacity is depleted.

The resin batches tested initially were all made on a pilot scale of 0.71 to 1.4m³ by the manufacturer. When large quantities were ordered (\sim 14m³), the resin was produced in production-scale equipment with some variation in process conditions and the properties of the resin for actinide processing were only nominally better than gel-type resin. The throughput was increased only 0 to 25%.

Because of supply problems in the past few years, resins from other manufacturers have been investigated. *Ionac* A-641 has been used for some applications at SRP and results approximate those obtained with production-grade *Dowex* MSA-1.

The process most sensitive to resin quality is separation of ²³⁸Pu from ²³⁷Np. Data comparing the separation with several different resins are given in Table 7.

The process procedure is as follows:

- Adjust the feed to \sim 8M NO₃⁻.
- Adjust the feed to 0.05M Fe(NH₂SO₃)₂ and then heat the feed at \sim 50°C for \sim 30 minutes.
- Feed the column at a controlled flow rate.
- After cosorption of Np and Pu anionic complexes, elute Pu(III) selectively with 5.4M HNO₃-0.05M N₂H₄ - 0.05M Fe(NH₂SO₃)₂.
- Elute Np(IV) with 0.35M HNO₃.

Table 7. Separation of ^{238}Pu and ^{237}Np by Anion Exchange

Resin Bed: 120 mL (0.75 in. ID by 16 in. long)
 Feed: 4 g Np/L - 1 g Pu/L (volume varied for different loading)

Resin	Mesh Size	Actinide Load, g ^a		Flow, mL/(cm ²)(min)			Product Purity Ratio, %	
		Pu	Np	Sorption	Elution		Np/Pu	Pu/Np
<i>Dowex</i> ^b								
1-X3	40-60	0.8	2.4	2.8	2.5	2	0.5	0.2
1-X3	40-60	1.2	4.2	2.8	2.5	2	3.72	0.26
	Granular ^c							
MSA-1	40-60	1.1	3.6	6	5	4	0.1	0.1
	Bead							
MSA-1	40-60 ^c	1.2	4.2	2.8	2.5	2	0.25	0.08
MSA-1	20-50 ^e	1.1	2.8	2.8	2.5	2	0.3	0.1
MSA-1	30-50 ^d	0.8	2.8	2.8	2.5	1.5	0.6	0.5
MSA-1	20-50 ^d	0.8	2.9	2.8	2.5	1.5	1.2	0.7
<i>Ionac</i> ^e								
A641	20-50	0.7	2.7	2.8	2.5	1.5	1.0	1.9

a. Loadings were made to maintain some free resin on the 120-mL column. Free resin is necessary to get product separation.

b. Trademark of Dow Chemical Co.

c. Resin produced on a pilot scale by the manufacturer.

d. Resin produced on a production scale by the manufacturer.

e. Trademark of Ionac Chemical Co.

Acknowledgment

The information contained in this article was developed during the course of work under Contract No. AT(07-2)-1 with the U.S. Department of Energy.

Literature Cited

1. Orth, D. A.; McKibben, J. M.; Prout, W. E.; Scotten, W. C. p. 534 in *Proc. Intern. Solvent Extraction Conference, 1971*, Society of Chemical Industry; London (1971).
2. Thompson, M. C. *Intern. Solvent Extraction Conference, 1977* (to be published in the proceedings).
3. McKibben, J. M.; Bercaw, J. E. AEC Report DP-1248, E. I. du Pont de Nemours & Co., Savannah River Laboratory, Aiken, SC (1971).
4. Barney, G. S. *J. Inorg. Nucl. Chem.*, 1976, **38**, 1977.
5. Richardson, G. L.; Swanson, J. L. ERDA Report HEDL-TME-75-31, Westinghouse Hanford Co., Hanford Engineering Development Laboratory, Richland, WA (1975).

6. Walser, R. L. AEC Report ARH-SA-69, Atlantic Richfield Hanford Co., Richland, WA (1970).
7. Groh, H. J.; Schlea, C. S. p. 517 in *Progress in Nuclear Energy, Series III. Process Chemistry Vol. 4*, Pergamon Press; London (1970).
8. Thompson, G. H.; Thompson, M. C. ERDA Report DP-1452, E. I. du Pont de Nemours & Co., Savannah River Laboratory, Aiken, SC (1977).
9. Thompson, G. H.; Thompson, M. C. ERDA Report DP-1460, E. I. du Pont de Nemours & Co., Savannah River Laboratory, Aiken, SC (1977).
10. Thompson, G. H.; Kelley, J. A. ERDA Report DP-1373, E. I. du Pont de Nemours & Co., Savannah River Laboratory, Aiken, SC (1975).
11. Siddall, T. H.; Dukes, E. K. *J. Am. Chem. Soc.*, 1959, **81**, 790.
12. Benedict, G. E.; McKenzie, T. R.; Richardson, G. L. AEC Report HW-SA-1963, General Electric Co., Hanford Atomic Products Operations, Richland, WA (1960).
13. Thompson, M. C.; Burney, G. A.; Hyder, M. L. ERDA Report DP-1396, E. I. du Pont de Nemours & Co., Savannah River Laboratory, Aiken, SC (1976).
14. Porter, J. A.; Symonds, A. E. AEC Report DP-981, E. I. du Pont de Nemours & Co., Savannah River Laboratory, Aiken, SC (1965) (Declassified 1971).
15. Thompson, G. H.; Burney, G. A. AEC Report DP-1333, E. I. du Pont de Nemours & Co., Savannah River Laboratory, Aiken, SC (1973).

RECEIVED June 20, 1979.

Research sponsored by the U.S. Department of Energy under contract number AT(07-2)-1.

Separation of Long-Lived α -Emitters from Highly Radioactive Solutions in the Thorium-Uranium Fuel Cycle

U. WENZEL, C. L. BRANQUINHO, D. HERZ, and G. RITTER

Institute of Chemical Technology, Kernforschungsanlage Jülich, G.m.b.H.,
Federal Republic of Germany

Spent Th-U fuel of the HEU (highly enriched uranium) type contains about 40 % of the original fissile and 90 % of the original fertile material. In the most developed -mixed (Th,U)₂O₂-fuel concept, both valuables shall be recycled. U and the corresponding Th portion will be refabricated without cooling time under remote conditions while the remaining Th (~ 50 %) will be stored for 20 years, until its radioactivity, mainly produced by ²²⁸Th and its daughter products, will not exceed that of natural Th. After this period, Th can be used for the cold fuel fabrication.

In this concept, the transuranium elements are considered as waste, due to their quantity and value (table 1), since they contribute only 0.6 % to the total spent fuel and from that amount only 5 % (²³⁹Pu and ²⁴¹Pu) are fissionable nuclides.

Element	Th	U	Np	Pu	FP	TP
Portion [%]	79.4	10	0.4	0.2	10	< 0.1
Isotope	²³² U	²³³ U	²³⁴ U	²³⁵ U	²³⁶ U	²³⁸ U
Portion [%]	0.01	26.8	15.7	7	42	8.5
Isotope	²³⁷ Np	²³⁸ Pu	²³⁹ Pu	²⁴⁰ Pu	²⁴¹ Pu	²⁴² Pu
Portion [%]	100	70.3	13	9.7	2.7	4.3

Table 1: Elemental and Isotopic Composition of Spent (Th,U)₂O₂ Fuel after 15 Reactor Cycles (1)

(TP = Transplutonium Elements)

0-8412-0527-2/80/47-117-533\$05.00/0
© 1980 American Chemical Society

On the other hand, Np and Pu are very radiotoxic elements and the long-term hazard potential (fig. 1) of a final HTGR-waste deposit is especially determined by ^{237}Np and ^{238}Pu (2), while the other actinides, apart from the non-recovered U, are of minor importance. Hence, alternative solutions for their disposal are now discussed and investigated (1).

The fuel cycle concept is much more influenced by the chemical behaviour of the actinides during the reprocessing of the Th-containing fuel. It could be demonstrated during the first hot operations (3), that Np ends up quantitatively in the waste stream, but Pu is distributed in the product streams (90 % in the Th-, 10 % in the U-stream). These facts contradict strongly the above mentioned fuel cycle strategy, since Pu is no waste component and the Pu-contaminated Th cannot be used for the fresh fuel fabrication with respect to its high specific α -activity.

In order to keep the original fuel cycle concept, the reprocessing has to be extended by:

- predecontamination of the Th-stream from Pu during the extraction
- isolation of Pu and eventually Np.

Great interventions into the existing and already tested reprocessing schemes should be avoided during the accomplishment of these requirements.

Extraction Behaviour of the Transuranium Elements during Reprocessing

The two cycle THOREX-process was chosen as reference scheme in our studies (fig. 2). This process consists of two stages which are connected discontinuously (4):

- the predecontamination stage with an acid feed including co- and simultaneous backextraction of Th and U and separation of the bulk of fission products
- the partition stage with an acid deficient feed including co- and selective backextraction of Th and U.

Without interventions, the extraction behaviour of Np and Pu is established by the development of NO_x during the dissolution, they are oxidized to the nonextractable Np(V) and the extractable Pu(IV) and follow hence the fission product (Np) and the heavy metal stream (Pu).

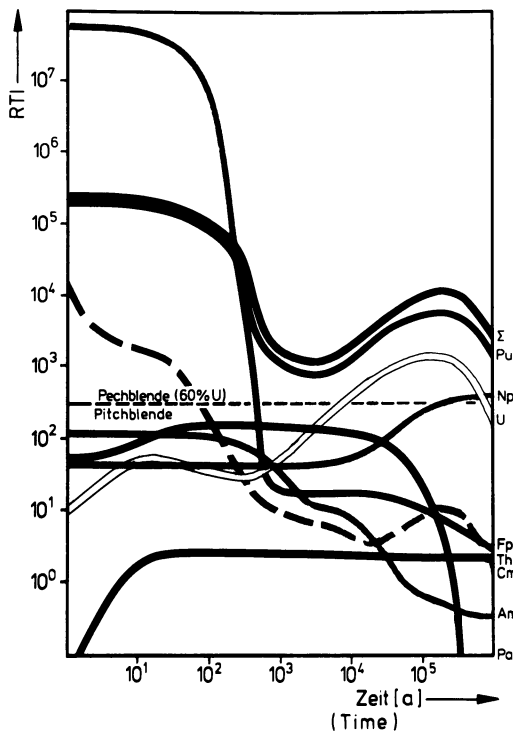


Figure 1. Radiotoxicity index of the HTGR waste after fifteen reactor cycles (99% recovery of Th and U)

The chemical behaviour of both actinides is simply modified by stabilizing oxidation states of different extractability. Table 2 shows the effects of some redox agents.

Redox Agents	Oxidation state	Extractability	Oxidation state	Extractability
	Np		Pu	
NO_x	Np(V)	non-extractable	Pu(IV)	extractable
VO_4^{3-}	Np(VI)	extractable	Pu(IV)	extractable
Fe^{2+}	Np(IV)	extractable	Pu(III)	non-extractable
$\text{Cr}_2\text{O}_7^{2-}$	Np(VI)	extractable	Pu(VI)	extractable
N_2H_4	Np(IV)	extractable	Pu(III)	non-extractable
U^{4+}	Np(IV)	extractable	Pu(III)	non-extractable

Table 2: Oxidation States and Extractability of Np and Pu in the Presence of Several Redox Agents

Other changes in the extractability of the actinides are performed using complexing agents. The distribution coefficients of Pu(IV) with various citric acid concentrations is demonstrated for the system TBP/ HNO_3 in table 3 and figure 3. The range of the HNO_3 concentrations corresponds to that of the waste effluents from the coextraction steps of the THOREX-process.

Nitric Acid [Mol/l]	Citric Acid [Mol/l]					
	0	0.05	0.1	0.2	0.3	1
1.3	2.65	0.93	0.55	0.22		
1.5	4.15	1.8	1.1		0.12	
2.0	7.4		2.6			0.08

Table 3: Distribution Coefficients of Pu(IV) in the System 30 % TBP-Dodecane/ HNO_3 in Dependence on the Citric Acid Concentration

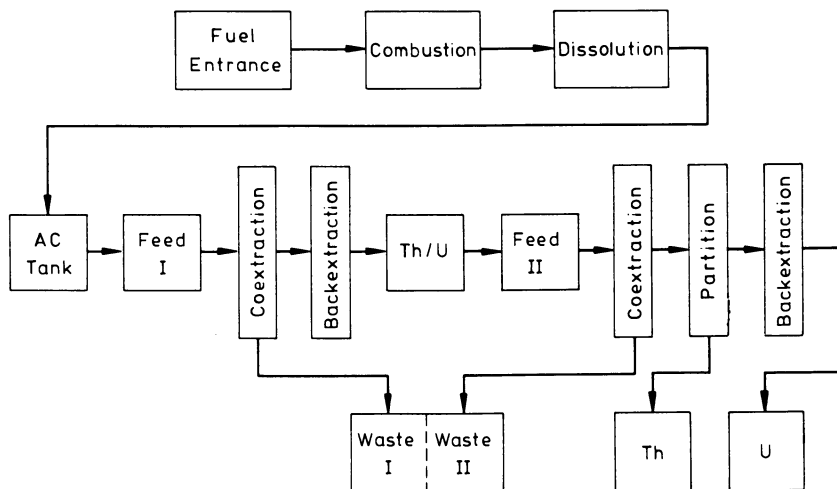


Figure 2. Two-cycle Thorex process

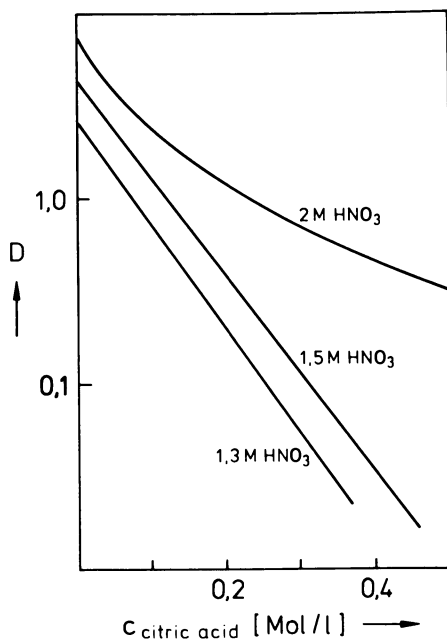


Figure 3. Distribution coefficients of Pu (IV) in a nitric acid-citric acid mixture

The influence of the redox agents on the actinide extraction behaviour was investigated with glove box shielded mixer-settlers and simulated THOREX-feed solutions. The results (5) are summarized in table 4. The yields of Np and Pu in the mentioned process streams were always quantitative.

Process Stage Intervention	End Stream	
	Np	Pu
Acid Feed no Intervention	Waste I	Th-U Stream
Acid Feed $\text{Fe}(\text{NH}_2\text{SO}_3)_2$ in Scrub	Th-U Stream	Waste I
Acid Feed $(\text{NH}_4)_3\text{VO}_4$ in Scrub	Th-U Stream	Th-U Stream
Acid Deficient Feed $(\text{NH}_4)_3\text{VO}_4$ in Scrub $\text{Fe}(\text{NH}_2\text{SO}_3)$ in Strip	Th-Stream	Th-Stream

Table 4: Consequences of THOREX-Process Interventions on the Actinide Extraction Behaviour

Actinide Disposal

A final concept has not been approved for the actinide disposal in the Th-U fuel cycle, but, in principle, three alternatives may be considered:

- ultimate storage in a waste deposit and toleration of the long-term hazard enhancement
- burn-off by recycling the actinides through a reactor of the same reactor line
- incineration in a high-flux reactor or a fast breeder.

Each of these alternatives requires the combination of the actinides (i.e. Np and Pu) in one of the reprocessing end streams. For the ultimate storage the appropriated stream is clearly the high level radioactive waste, while the isolation of the actinides is presupposed in both other cases, regarding the intermediate storage of the Th-product, and this additional separation process should be connected with an predecontaminated reprocessing stream as starting solution.

Based on the results of the extraction behaviour studies (table 4), the alternatives of the actinide disposal will be discussed with respect to the necessary interventions into the reprocessing scheme. The most compatible points between reprocessing and actinide separation will be illustrated (fig. 4).

Final Storage of the Actinides

The actinides as trace components will not take any penalty on the already tested waste management procedures (denitration, calcination, vitrification), provided that Np and Pu can be retained in the aqueous waste stream. Without changes of the THOREX flow-sheet, the 1st feed solution contains Np(V) and Pu(IV). Consequently, Np ends up in the waste stream, while Pu following the heavy metal, can be withdrawn with the aqueous phase of the 2nd coextraction step with reducing agents and thus combined with Np (hatched arrow) for the further waste treatment.

Actinide Recycling through the Reactor

Assuming the hot refabrication of the total heavy metal (Th + U), no actinide separation will be required. Under these circumstances, Np and Pu will be oxidized with VO_4^{3-} to an extractable valence state during both coextraction steps (cross-hatched arrow) and distributed between the Th- and the U-product stream.

Assuming a partial hot refabrication of the heavy metal (U + the corresponding Th amount), Np and Pu must be isolated and, hence, combined quantitatively in a single process stream. The simultaneous refabrication of Np, Pu and U requires the retention of the transuranium elements in the U-product stream, which has not been accomplished during the extraction until now. Presumably, a predecontamination of the Th-product from Pu will be needed with respect to the further use of this component in the fresh fuel fabrication after the intermediate storage time and, therefore, the starting solutions for an actinide separation are restricted to the following process streams:

- fuel solution (thin full arrow)

The separation of the actinides will be carried out before the actual partition of the fuel constituents without intervening into the extraction flow sheet, but the high fission product dose rate will be very disadvantageous.

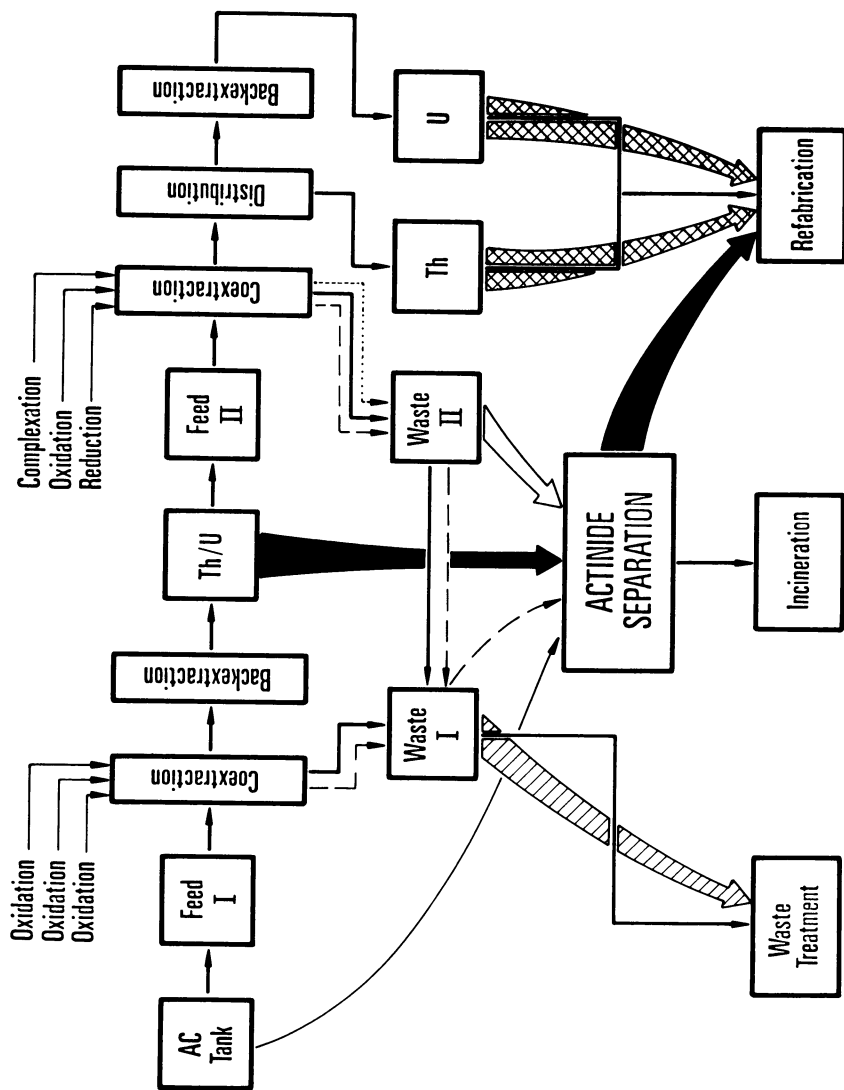


Figure 4. Alternatives of actinide removal and disposal

- waste I (thin broken arrow)
The combination of the actinides in the waste stream has been already discussed. The high dose rate will complicate the separation, too.
- Th-U stream (solid arrow)
Stabilized as extractable compounds (VO_4^{3-} -oxidation during the first cycle coextraction) the actinides will follow the heavy metal and can be separated from the intermediate product stream of the first cycle. This stream has a low fission product concentration, and the THOREX-process is discontinued anyhow at that step, but, of course, the insertion of a new component amidst an established process will cause unfavourable consequences.
- waste II (open arrow)
After co- and backextraction of the actinides in the first cycle, Np is reduced to non-extractable Np(V) by the development of NO_x . Pu can be retained in the aqueous phase with a complexing agent like citric acid (see table 3), which must not interfere with the Th/U coextraction. This stream has a low fission product content and its use as starting solution for the actinide separation will not cause additional interventions into the THOREX flow-sheet. It must be noted, however, that the demonstration of this process variant by mixer-settler runs is still to be carried out.

Provided the feasibility of the Np/Pu combination in waste II, this stream is the most suitable starting solution for the actinide separation; otherwise, the Th-U stream may be chosen.

After the actinide separation, Np and Pu will be recombined with U and the corresponding Th-amount for the refabrication process which will not suffer considerable changes by the presence of the transuranium elements.

Incineration

The incineration of actinides in a fast breeder will probably require a new fuel cycle with completely remote fabrication, re-processing and refabrication of the actinide fuel. The recently developed high flux irradiation facilities may become more economical for the actinide incineration. Concerning the re-processing, an actinide separation is indispensable and, thus, the actinides will be treated during the extraction in the same way as mentioned above.

Separation of the Actinides

Contrary to their influence on the Th-U fuel cycle, Np and Pu are only trace components of the spent fuel. Furthermore, the actinide separation will be carried out mainly to purify the re-processing end streams from Np and Pu, and not to recover both elements.

Under these premises, methods like the extraction chromatography with a high separation power should be favoured over those with a high separation capacity like the extraction.

Separation System

Tetravalent actinides are well extractable from HNO_3 -solutions into tertiary amines. The solvent (alamine 336, ~ 95 % TOA) is polymerized into polystyrene (6) forming together with the matrix, the separation compound (Lewextrel -type). The distribution coefficient (K_D) of the actinides are nearly independent in the range $2 \text{ M HNO}_3 \leq [\text{HNO}_3] \leq 6 \text{ M HNO}_3$; these coefficients are compiled in table 5

Aqueous Phase	K_D			
	Th(IV)	U(VI)	Np(IV)	Pu(IV)
Infinitively Diluted	200	<0.01	$4.6 \cdot 10^3$	$1.9 \cdot 10^4$
30 g Th/l 3 g U/l	1.3	<0.01	110	520

Table 5: Actinide Distribution Coefficient in the System
TOA / 2 M HNO_3

and the technical data of the Lewextrel-resin are summarized in table 6.

composition (weight %)	37.5 % TOA; 23.4 % DVB; 39.1 % styrene
density	0.96 g/cm^3
grain size	< 0.1 mm
average interstitial volume	47 %
capacity	0.15 m Mol/ml resin

Table 6: Technical Data of the Lewextrel -TOA resin

The chromatographic support does not show any synergistic effect on the separation.

This separation system enables the purification of all THOREX-reprocessing end streams from Np and Pu, requiring only small variations of the feed adjustment procedure.

Separation Process

The extraction chromatography is a discontinuous process, It consists of the following steps:

- preparation of the column to the separation conditions
- feed adjustment of the starting solution
- sorption of Np and Pu on the chromatographic compound
- desorption of Np and Pu from the chromatographic compound
- regeneration of the column.

The process was tested with a separation unit shielded by a glove box. Based on the results (1,7,8,9), a hot cell bench scale plant is now under construction (fig. 5). The starting solution (Th-U intermediate product stream from the reprocessing) is introduced into the hot cell with the transport container and pumped into the feed tank. The feed adjustment is carried out by adding HNO_3 conc. through the chemical reagent supply tube from outside, Np is stabilized with $\text{Fe}(\text{NH}_2\text{SO}_3)_2$, Pu with NO_x , the simultaneous stabilization in the tetravalent state can be performed with a definite $\text{Fe}^{2+}/\text{Fe}^{3+}$ mixture (10). Subsequently the feed solution passes through the column, Np and Pu are absorbed on the resin, the purified Th-U stream is collected in the product tank, Np and Pu are eluted from the column with 0.1 M HNO_3 / 0.1 M citric acid through the chemical reagent supply tube and are collected in the Np-Pu tank. The hot cell waste management is accomplished with the transport container.

The process is controlled with a flow rate meter (FIRC = Flow Indicator Recorder Controller) governing the gear-pump, and an on-line Np/Pu analyser (CoRC = Concentration Recorder Controller) (scintillation is used in the glove box experiments while polarography is under development for the hot cell plant) which discontinues the process at a definite Np/Pu concentration in the column effluent.

In the glove box experiments, 30 l Th-U stream/h (corresponding to 0.5 m³ per day) could be purified from Np and Pu.

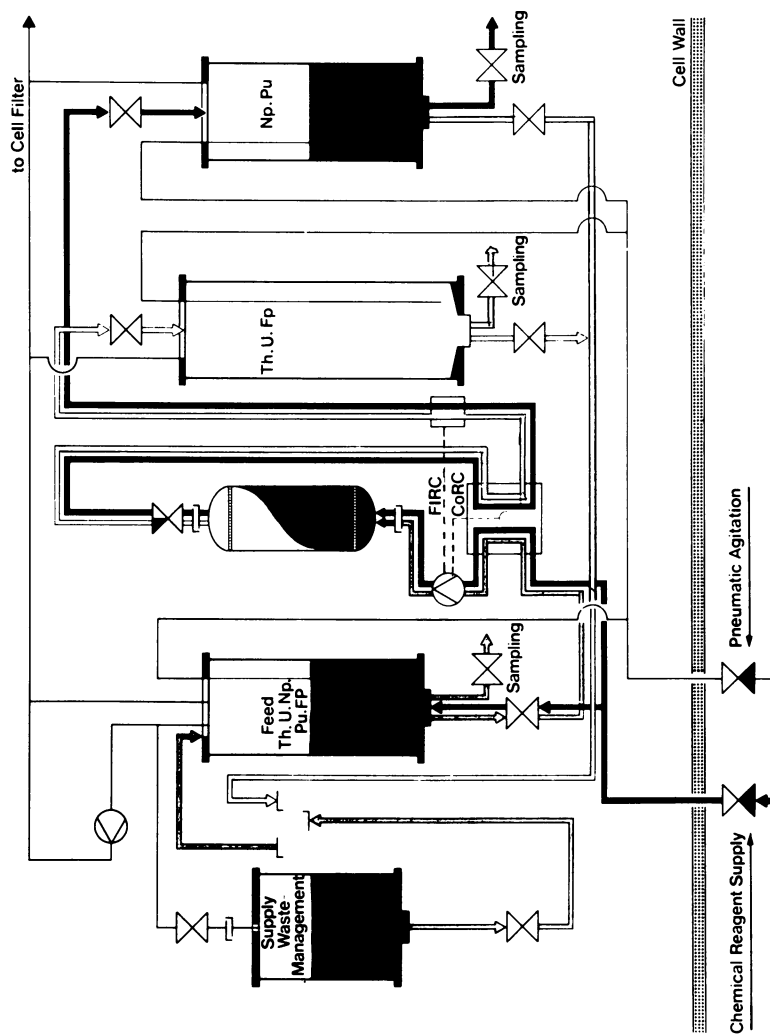


Figure 5. Hot cell separation unit for actinide removal

Summary

In the Th-U fuel cycle, Np and Pu are valueless components of the spent fuel. They have to be considered, however, during the spent nuclear fuel management. Both elements can be guided simultaneously into definite process streams by stabilizing extractable oxidation states during the reprocessing of spent Th-U fuel. With respect to an actinide separation, the intermediate Th-U product and the predecontaminated waste of the second THOREX-cycle are the best suited starting solutions. An extraction chromatographic process is suggested as separation method and its technical implementation is presented for the purification of the reprocessing end streams from Np and Pu.

Literature cited:

- 1 Wenzel U.; JÜL-Report, 1979, in press
- 2 Wenzel U.; Laser M.; Merz E.; Trans. Am. Nucl. Soc., 1975, 22, 350
- 3 Wenzel U.; Riedel H.J.; VI. Int. Symp. Mikrochem., 1970, E, 271
- 4 Schäfer L.; Wojtech B.; Kaiser G.; Merz E.; Sckuhr P.; AED-CONF-71-100-22, 1971
- 5 Wenzel U.; Branquinho C.L.; Herz D.; Ritter G.; JÜL-CONF., 1979, 30, 42
- 6 Kröbel R.; Mayer A.; DBP-2244306, 1974
- 7 Herz D.; Kankura R.; Wenzel U.; JÜL-1212, 1975
- 8 Kankura R.; JÜL-1372, 1977
- 9 Ritter G.; KFA-ICT-IB-412/77, 1977
- 10 Gourisse D.; Chesné A.; Analyt. Chim. Acta, 1969, 45, 321

RECEIVED May 18, 1979.

Laboratory and Pilot Plant Studies on Conversion of Uranyl Nitrate to Uranium Hexafluoride

I. J. URZA and D. C. KILIAN

Exxon Nuclear Company, Inc., 2955 George Washington Way, Richland, WA 99352

Exxon Nuclear Company has conducted various development programs to support the design and licensing of a commercial nuclear fuel reprocessing plant. The uranium conversion portion of the reprocessing plant will use fluidized-bed processes for conversion of uranyl nitrate hexahydrate (UNH) to uranium hexafluoride (UF_6). This paper describes the laboratory and pilot plant studies conducted at Oak Ridge National Laboratory (1) for Exxon Nuclear Company on the conversion of UNH to UF_6 and on the purification of UF_6 .

Laboratory Studies

Experimental laboratory studies on the removal of residual nitrate from UO_3 and the fluorination and sorption of technetium on MgF_2 were conducted to support the pilot plant work. These studies covered a wide range of conditions and were used primarily to guide the pilot plant effort rather than to determine quantitative thermodynamic and kinetic data.

Removal of Residual Nitrate From UO_3 : Uranium trioxide produced by thermal decomposition of uranyl nitrate solution in a fluidized-bed contains a small amount (usually about 0.4 to 1.0 wt%) of residual nitrate. If UO_3 is to be converted to UF_6 for feed to a gaseous diffusion enrichment plant, the nitrate content of the UO_3 must be reduced to meet UF_6 purity specifications. Fluorination of UO_3 in the presence of nitrate results in formation of nitrosyl and nitryl hexafluorouranates and heptafluorouranates (NO_xUF_y where $x = 1$ or 2 and $y = 6$ or 7) (2). These compounds form x potentially troublesome solids.

The removal of residual nitrate from UO_3 was studied as a function of time and temperature under nitrogen, air and hydrogen-nitrogen atmospheres. The procedure used for these tests was to place a UO_3 sample (10g) in a vertical 2.54 cm diameter by 30.5 cm long stainless steel reactor, heat it to the desired temperature, and then start the gas flow. When the test was terminated, the sample was cooled and sampled for analysis.

American Chemical
Society Library
0-8412-0527-2/80/47-117-54/\$05.00/0
© 1980 American Chemical Society

1155 16th St. N. W.

In Actinide Separations; Navratil, J., et al.;
ACS Symposium Series; American Chemical Society: Washington, DC, 1980.

Data from tests with typical UO_3 product produced in the pilot plant fluidized-bed calciner led to the following general conclusions:

1. Sparging of UO_3 with nitrogen, air or hydrogen at temperatures above 450°C is effective in lowering the nitrate content of UO_3 .

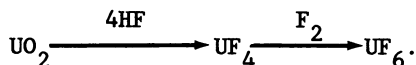
2. Treatment with hydrogen gives the highest nitrate removal rates and lowest residual nitrate but as expected, results in the highest conversion of UO_3 to U_3O_8 and UO_2 .

3. Treatment with nitrogen at temperatures above 550°C also causes significant decomposition of UO_3 to the lower oxides.

4. An air sparge is nearly as effective as nitrogen for nitrate removal at temperatures above 550°C and significantly suppresses the decomposition of UO_3 .

Fluorination and Sorption of Technetium on Magnesium

Fluoride: Trace quantities of technetium will accompany the uranium through the Purex solvent extraction process, the conversion of UNH to UO_3 and the fluorination of UO_3 . The technetium in the UO_3 will be fluorinated (probably to TcF_6) and will volatilize with the gaseous UF_6 product. The technetium must be removed to meet gaseous diffusion plant feed specifications. Gollither et al. (3) developed the use of MgF_2 for removal of technetium from UF_6 . The process was demonstrated on both a laboratory and production scale at the Paducah Gaseous Diffusion Plant where UF_6 is produced by the hydrofluorination process,



The objectives of the laboratory studies were: (1) to study the behavior of volatile technetium compounds produced by direct fluorination of UO_3 with elemental fluorine; (2) to study the technetium sorption characteristics of MgF_2 ; and (3) to determine the feasibility of repeated regeneration of MgF_2 by desorption of technetium with fluorine.

A batch of $\text{UO}_3\text{-Tc}_2\text{O}_7$ calcine was prepared in the laboratory by adding ammonium pertechnetate (NH_4TcO_4) to UNH which was then thermally denitrated at 350°C . Alumina was subsequently added to form a granular product.

The technetium losses due to volatilization during the calcination process were negligible. The analyzed technetium concentration was 1060 ppm (based on U) and the calculated concentration based on the ammonium pertechnetate input was 1070 ppm. This concentration is more than 10 times that expected in the fuel reprocessing plant UO_3 .

The ^{99}Tc used in this work was analyzed directly by beta scintillation counting. Analyses of samples were carried out using a radiochemical separation procedure, with perhenate as carrier, and beta proportional counting. Samples, which were always run in duplicate, generally showed a spread of <10%.

The major equipment items used in the fluorination-sorption tests included a fluorination reactor, an auxiliary reactor, a MgF₂ sorption reactor and a UF₆ cold trap. The fluorinator and the sorption reactor consisted of a 2.54 cm diameter nickel tube mounted vertically with a sieve plate at the bottom to support the bed. The fluorination, auxiliary and sorption reactors were heated with a tube furnace.

In each run, 100g of UO₃-Al₂O₃ containing 29g of UO₃ was added to the fluorination reactor. The 10.2 cm static bed was heated to 450°C with a nitrogen purge before starting each run. After the fluorine flow was started, the temperature at the reaction zone increased to 500-525°C. The reaction zone was followed with a movable thermocouple located in the bed. The off-gas from the fluorinator was routed to the sorption reactor either directly or after passing through the auxiliary reactor. In the runs when the auxiliary reactor was used, excess fluorine was added at the reactor inlet to promote conversion of volatile Tc₂O₇, TcO₃F or TcOF₄ (if these compounds were formed). The MgF₂ bed used in the sorption reactor consisted of 7-g sections of -4 +12 mesh MgF₂ which had been dried several hours at temperatures ranging from 125 to 550°C. Tests were conducted with MgF₂ bed depths of 2.54 to 15.2 cm (each 7-g section occupied about 2.54 cm of the reactor length). The sections were separated by nickel screens. The off-gas from the sorption reactor was passed through the stainless steel UF₆ cold trap to collect UF₆.

A total of 13 batch fluorination-sorption runs were made in this study with fluorine concentrations of 33 and 100%. The fluorination reactor bed temperature was maintained at 500°C and the MgF₂ sorption reactor temperature was maintained at 100°C in each run. When the auxiliary reactor was used, fluorine was added between the fluorinator and the auxiliary reactor to provide a minimum of 15% excess fluorine. The auxiliary reactor temperature was controlled at 500°C. Magnesium fluoride which was preconditioned with fluorine at 400-550°C and at 100 to 125°C was tested during these runs. The MgF₂ treated at the lower temperature was more effective for technetium removal.

Analyses of the effectiveness of technetium collection on MgF₂ was complicated by poor technetium material balances. The average overall material balance for runs in which the equipment was washed was 81%. The technetium collected on the MgF₂ ranged from 13 to 87% of the input; however, based on the amount of technetium found in the UF₆ product downstream of the MgF₂ bed, removal of >99% of the technetium from the UF₆ was achieved.

Repeated regeneration of MgF₂ by desorption of technetium with fluorine was tested at 350 and 500°C. The same MgF₂ bed was used during these tests. At the completion of each fluorination run, the MgF₂ was desorbed. The off-gas was passed through a cold trap to collect the desorbed technetium. Less than 10% of the technetium was desorbed at 350°C, but essentially all of the technetium was desorbed at 500°C.

The following conclusions were drawn from results of the technetium fluorination-sorption studies:

1. Greater than 99% of the technetium and uranium was volatilized from the fluorinator in all fluorination tests.

2. Excess fluorine in the fluorinator off-gas does not appear to improve the collection efficiency of MgF_2 for technetium compounds.

3. Greater than 99% of volatile technetium compounds produced by direct fluorination of UO_3 can be removed from UF_6 by passing the off-gas through a bed of MgF_2 .

4. Desorption tests confirmed that technetium removal from MgF_2 with fluorine is possible but optimum temperature, time and effects of repeated sorption-desorption cycles were not adequately defined.

5. Pretreatment conditioning of MgF_2 significantly affects technetium sorption capacity.

Uranium Calcination Pilot Plant Studies

The objectives of the uranium calcination development program were to:

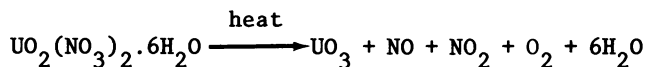
1. Test the performance of a rectangular uranium calcination vessel.

2. Produce fluidized-bed UO_3 product suitable for fluorination.

3. Verify operating and design parameters needed for start of detailed design.

4. Determine the behavior of technetium and ruthenium during calcination and the removal rate of residual nitrate by heat treatment of UO_3 .

Process Description: Uranium trioxide is produced by thermal decomposition of uranyl nitrate hexahydrate (UNH) by the following endothermic reaction:



$$\Delta H = 150 \text{ kcal/g-mole @ } 300^\circ\text{C}$$

The reaction is accomplished by spraying UNH into a bed of fluidized UO_3 particles at a temperature of about 300°C . The UNH is deposited on the UO_3 particles and decomposed. Fluidized-bed reactors are well suited for this process because high rates of heat and mass transfer are required between the solid and fluid. Under normal operating conditions, UO_3 produced in a fluidized-bed is granular, free flowing material with a particle size distribution suitable for subsequent fluidized-bed operations (4). The UO_3 is a chemically stable, mildly hygroscopic solid with a crystal density of 7.3 g/cm^3 .

The use of fluidized-beds for producing UO_3 has been studied extensively by various investigators (4-9) at pilot plant and production scale. The effects of operating variables such as temperature, feed composition, feed rate, and superficial velocity, have been investigated extensively.

A simplified flowsheet of the uranium calcination pilot plant is shown in Figure 1. Uranyl nitrate hexahydrate was prepared in two steam heated feed tanks. The UNH, which has a freezing point of about 65°C and a boiling point of 120°C, was pumped into the calciner through an air atomized feed nozzle. The UNH was calcined to UO_3 in the fluidized-bed calciner using preheated air as the fluidizing gas. The UO_3 product overflowed continuously by gravity from the calciner to the product vessel where the weight was monitored with a load cell.

Off-gas from the calcination process was passed through sintered-metal filters located in the upper section of the calcination vessel. The process off-gas was then cooled in the off-gas condenser where most of the NO_2 released in the denitration process was recovered as nitric acid and collected in the condensate tank. Uncondensed vapors were passed successively through the de-entrainer, the off-gas preheater, the HEPA filter, and then vented to the off-gas system.

Description of Equipment: The dimensions of the rectangular calcination vessel (15.2 cm x 12.7 cm) were selected to test geometric parameters that are important to the design of a plant-scale slab unit, thereby reducing uncertainties involved in scaleup.

The fluidized-bed section of the calciner contained the air distributor plate, the bed drainage outlet, the feed nozzle, the product overflow line, and the bed charging line. An expanded filter section containing porous stainless steel filters and the off-gas vent line was located directly above the fluidized-bed section.

The UNH feed tanks had a volume of 227 liters each; the vessels were jacketed for 15 psig steam and contained steam coils for 125 psig steam. A positive displacement metering pump was used to feed the UNH.

The off-gas condenser was a shell-and-tube (water-cooled) heat exchanger; a 260 liter capacity stainless steel tank was used to collect condensate; and a stainless steel wire-mesh de-entrainer, a shell-and-tube (steam-heated) preheater and a HEPA filter were used in the off-gas system.

The principal process instrumentation included: (1) thermocouples to monitor the temperature at various locations; (2) a flow controller to measure the air flow rate to the calciner; and (3) differential-pressure transmitters to monitor the pressure drop across the distributor plate, the fluidized-bed and the sintered-metal filters.

Results of Calcination Runs: Fifteen calcination runs were made using UNH feed concentrations ranging from 512 to 1172 g U/L and feed rates ranging from 150 to 419 mL/min. A total of 2540 kg of UO_3 was produced during these runs.

During the first two runs, dilute UNH feed (500 gU/L) and a low feed rate (150 mL/min) was used to test the operation of the system. In the subsequent runs, the UNH feed rate was progressively increased to 230, 315 and 419 mL/min and the UNH concentration was increased to 900 and 1200 g U/L.

During the first 8 runs, excessive particle growth and a progressive increase in pressure drop across the off-gas filters caused operational problems. These problems were resolved by enlarging and heating the filter housing, increasing the filter area and modifying the filter blowback system. The calcination system operated satisfactorily during the last 7 runs; the run length was limited by the UNH feed supply rather than process instabilities. Caking of UO_3 around the feed nozzle was evident in most runs but did not cause operational problems.

During the last 7 runs (9 thru 15) 1900 kg of UO_3 was produced in 76 hours of operation. The operating conditions and results of these runs are summarized in Table 1. The average particle diameter of the UO_3 bed material remained in the desired range (about 0.25 mm) for good fluidization of the bed. The maximum UO_3 production rate tested was 1,770 kg/hr- m^2 (based on the fluidized-bed cross section) during run 14.

The UO_3 product was typical of UO_3 produced in fluidized-beds at other facilities. The UO_3 was granular, free flowing material with a bulk density of 3.7 to 4.1 g/cm³ and a tap density of 3.9 to 4.2 g/cm³. The average nitrate content ranged from 0.37 to 0.92 wt% and the water content ranged from 0.02 to 0.25 wt%. The U_3O_8 content was less than 0.2 wt%.

Removal of Residual Nitrate: Product from runs 4 and 15 was heat treated at a bed temperature of 600°C and a superficial fluidizing air velocity of 30.5 cm/sec to study the removal of residual nitrate. The nitrate content was reduced to less than 0.05 wt% in 3 hours. Most of the nitrate removal occurred during the first hour of heat treatment. Less than 1% of the UO_3 decomposed to U_3O_8 and the particle size was not affected significantly.

Behavior of Technetium and Ruthenium: A pilot plant test was conducted to study the behavior of technetium and ruthenium in the uranium calcination process. The UO_3 product from these tests was used in subsequent fluorination studies. The UNH feed was spiked with ⁹⁹Tc (as ammonium pertechnetate) and nonradioactive ruthenium (as ruthenium nitrate), and then denitrated under normal run conditions. As expected, most of the technetium was found in the UO_3 product as technetium oxide. Over half of the ruthenium (RuO_4) was volatilized and found in the condensate from the off-gas.

TABLE 1
SUMMARY OF DATA FOR CALCINATION RUNS 9 THROUGH 15

<u>Run Number</u>	<u>UNH Feed Conc. g U/l</u>	<u>Feed Rate ml/min</u>	<u>Bed Temp. C°</u>	<u>Run Duration hrs</u>
9	1125	315	300	3.0
10	1145	315	300	8.4
11	1160	315	300	9.3
12	1100	315	300	12.4
13	1130	290	300	16.0
14	1145	315	300	15.9
15	1130	419	300	11.4

<u>Run Number</u>	<u>Avg. UO₃ Prod. Rate kg/hr-m²</u>	<u>UO₃ Produced kg</u>	<u>Avg. UO₃ Particle Size (mm)</u>	
			<u>Beginning</u>	<u>End</u>
9	1,320	77	0.25	0.25
10	1,200	195	0.23	0.25
11	1,270	229	0.30	0.25
12	1,120	269	0.23	0.23
13	1,090	337	0.28	0.30
14	1,320	406	0.25	0.28
15	1,770	390	0.28	0.25

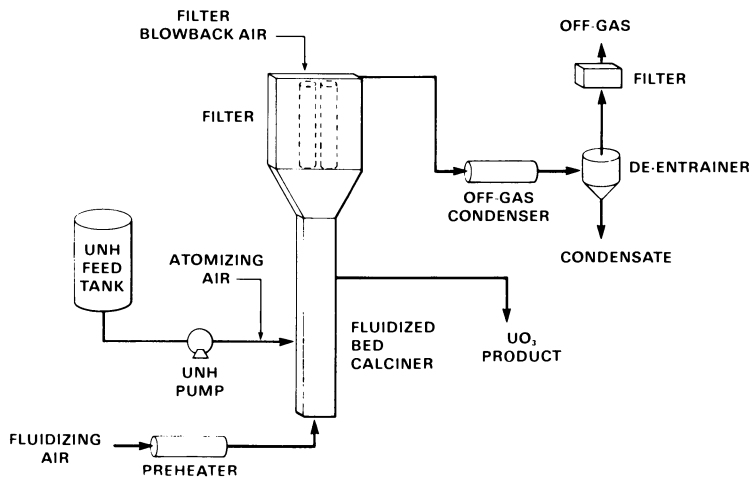


Figure 1. Simplified flowsheet of the U calcination pilot plant

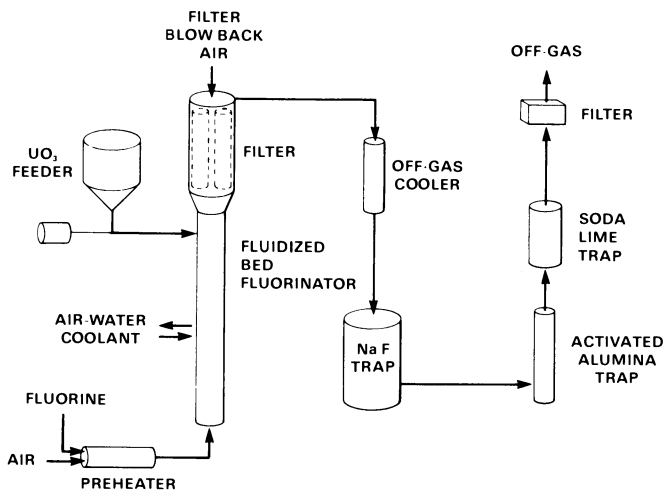


Figure 2. Simplified flowsheet of the fluorination pilot plant

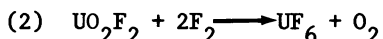
Uranium Fluorination Pilot Plant Studies

Uranium trioxide can be converted to UF₆ by a one-step, direct fluorination process, or by the hydrofluorination process which involves three steps: (1) reduction of UO₃ to UO₂ with hydrogen; (2) conversion of UO₂ to UF₄ with HF; and (3) fluorination of UF₄ with elemental fluorine. The one-step direct fluorination process was selected by ENC as the reference process for the commercial fuel reprocessing plant.

The objectives of the uranium fluorination development program were to:

1. Demonstrate direct fluorination of UO₃ in a fluidized-bed on a pilot plant scale.
2. Test the performance of fluorination equipment and define the range of acceptable design parameters.
3. Study methods of increasing fluorine utilization.
4. Study the behavior of technetium during fluorination and subsequent sorption on MgF₂.
5. Study fluorine disposal techniques.

Process Description: Uranium trioxide is directly fluorinated to UF₆ with elemental fluorine in a highly exothermic reaction ($\Delta H = 215$ kcal/g-mole at 450°C). Iwasaki (10) conducted laboratory studies on the kinetics and mechanism of direct fluorination of UO₃ powder to UF₆ with gaseous fluorine. The reaction was reported to take place in two steps:



The fluorination of U₃O₈ and UO₂ with fluorine gas has been studied in pilot plant facilities at Argonne National Laboratories (11), the Oak Ridge Gaseous Diffusion Plant (12), and by Russian investigators (13).

A simplified flowsheet of the fluorination pilot plant is shown in Figure 2. During the continuous fluorination runs, UO₃ was fed into a fluidized-bed of alumina (Al₂O₃) and UO₃ contained in the fluorinator. The feed was metered to the fluorinator at a rate equivalent to the UO₃ reaction rate. Preheated fluorine in the fluidizing gas was used to convert UO₃ solids to volatile UF₆. The fluorination reaction is highly exothermic; therefore, cooling must be provided to control the bed temperature. The fluorinator was cooled by injecting water into external cooling coils purged with air.

Description of Equipment: The major equipment pieces in the fluorination pilot plant were the fluorinator, the UO₃ feeder, the NaF traps and the activated alumina traps. The fluorination vessel was constructed of Monel and consisted of a fluidized-bed and an expanded filter section. The expanded filter section was

located directly above the fluidized-bed section and contained Monel sintered metal filters and the off-gas line. The fluidized-bed section contained the fluidizing gas distributor plate, the bed drainage outlet, and the bed feed inlet. The vessel was heated with electrical heaters and water-cooled with cooling coils attached to the outer vessel wall. Uranium trioxide was metered to the fluorinator with a solids screw-type feeder.

Three NaF traps were used to remove UF_6 from the fluorinator off-gas. Each trap contained about 50 kg of NaF pellets. Calrod heaters on the outer vessel surface were used to heat the traps.

Gaseous fluorine was obtained in 18,400 liter steel tank trailers. The composition of the gas, as received, was typically 90 to 95% fluorine, 5% HF, and 1 to 2% nitrogen-oxygen. The HF was removed by passing the gas through a NaF trap.

Four activated alumina traps were used for removal of fluorine from the process off-gas. The activated alumina traps were backed by a soda lime trap.

The fluorination system included the following process instrumentation: (1) thermocouples to monitor the temperature at various locations; (2) flow controllers and indicating rotameters to measure gas flow to the fluorinator; (3) differential-pressure transmitters to monitor the pressure drop across the distributor plate, fluidized-bed, and the sintered-metal filters; and (4) a duPont 400 photometric analyzer to continuously monitor fluorine in the off-gas.

Results of Fluorination Runs: Five batch and 11 continuous fluorination runs were made. The effects of temperature, UO_3 concentration, and fluorine concentration in the fluidizing gas were investigated to determine a suitable range of operation and to identify any instabilities associated with the process or deficiencies in equipment design.

In the batch fluorination runs, UO_3 was added to the fluorinator to make up initial concentrations ranging from 10 to 35 wt% UO_3 in Al_2O_3 . The UO_3 was fluorinated with F_2 concentrations up to 35 volume percent. Initially, low concentrations of reactants (UO_3-F_2) were used until the behavior of the reaction and bed temperature control were established. The fluorinator off-gas fluorine concentration versus the average fluidized-bed temperature for the batch runs is shown in Figure 3.

The following conclusions were among those drawn from the batch runs:

1. The reaction of UO_3 with F_2 was initiated readily at bed temperatures greater than 400°C.
2. Fluorine utilization greater than 95% was achieved at an average bed temperature of 500°C.
3. Substantial localized cooling was required to control the bed temperature at normal fluorination rates.

In the continuous fluorination runs, the UO_3 feeder was used to maintain the desired UO_3 concentration in the fluidized-bed. A total of 168 kg of UO_3 was fluorinated during 31 hours of

operation. Thermal and kinetic steady-state conditions were achieved rapidly, therefore, several bed temperatures and UO₃ concentrations were tested during the same run. Data from fluorination tests with a bed of 100% UO₃ are shown in Figure 4. The unreacted fluorine in the off-gas is shown as a function of the average bed temperature. Results of these tests led to the following conclusions:

1. The UO₃ produced by fluidized-bed calcination is suitable for direct fluidized-bed fluorination.
2. There was no evidence of sintering of the bed diluent (Al₂O₃) under the conditions tested.
3. The reaction rate is strongly dependent on temperature. The UO₃-F₂ reaction is initiated at about 350°C; at about 500°C, essentially all of the fluorine is reacted with UO₃.
4. Activated alumina and soda lime were found to be suitable for fluorine disposal; soda lime tends to cake at high reaction rates.

Runs With Technetium-Spiked UO₃: Two continuous uranium fluorination runs were made to determine the behavior of technetium in the pilot-plant fluorination system. Fluidized-bed-produced UO₃ containing 300 μg of technetium per gram of UO₃ was fluorinated and then separated from UF₆ by passing the volatile fluorination products through a static bed of MgF₂.

During the first run, about 95% of the technetium contained in UO₃ was leached from the first 35.6 cm of the MgF₂ trap with dilute nitric acid. A negligible amount was detected on the remaining 45.7 cm of the trap. Only a trace was accounted for downstream of the MgF₂ trap or between the fluorinator and the MgF₂ trap. The second run was made under similar conditions to verify results of the first run.

During the second run, about 75% of the technetium that was contained in UO₃ was recovered from the MgF₂. The technetium concentration was high at the top of the MgF₂ bed where first contact was made with the fluorinator off-gas. The overall technetium material balance for these tests was 84%.

Proper conditioning of MgF₂ for removal of impurities (mostly water) proved to be important in reducing the uranium loading of the MgF₂.

ACKNOWLEDGEMENTS

The authors wish to acknowledge the significant technical contributions of E. L. Youngblood (Oak Ridge National Laboratory) who was responsible for installation and operation of the Calcination and Fluorination Pilot Plants and of G. I. Cathers (Oak Ridge National Laboratory) who conducted the laboratory studies.

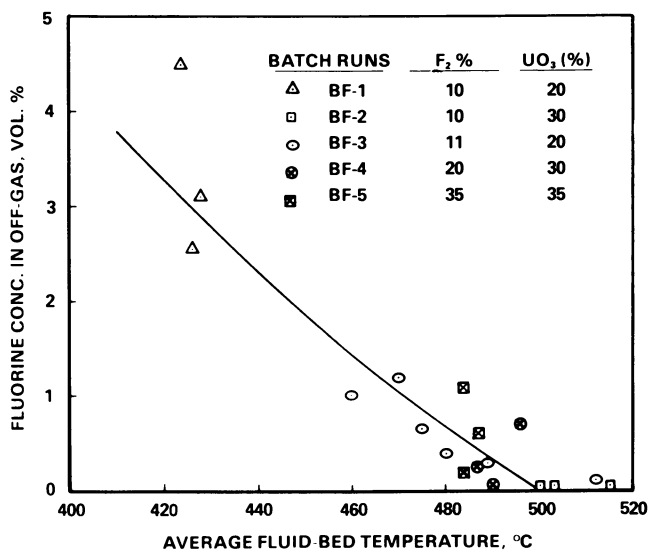


Figure 3. Fluorine concentration in the fluorinator off-gas vs. bed temperature during batch fluorination runs

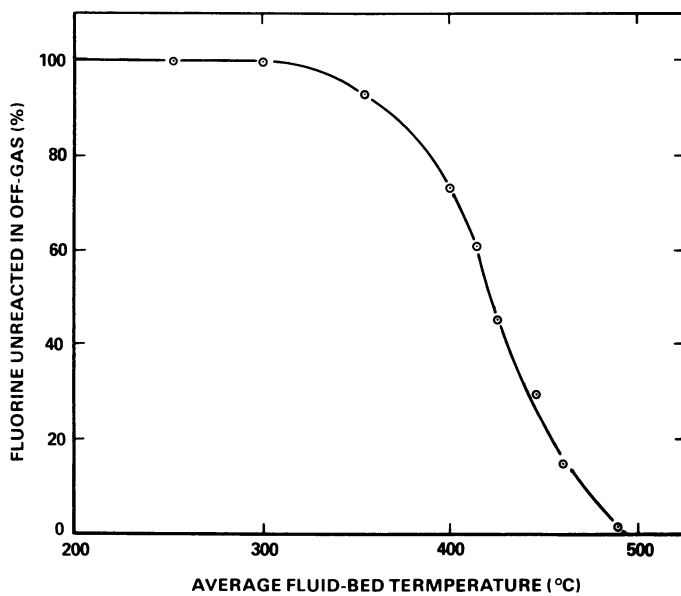


Figure 4. Fluorine unreacted in the fluorinator off-gas vs. bed temperature

REFERENCES

1. E. L. Youngblood, I. J. Urza, G. I. Cathers, Laboratory and Pilot-Plant Studies on the Conversion of Uranyl Nitrate Hexahydrate to UF₆ by Fluidized-Bed Processes, ORNL/TM-5913 (June, 1977).
2. O. A. Vita, The Determination of Bound Nitrogen in Uranium Hexafluoride with an Ammonia Electrode, *Analytical Chimica Acta*, 81 (1976) 45-52.
3. W. R. Gollither et al., Separation of Technetium-99 From Uranium Hexafluoride, TID-18290 (1960).
4. S. N. Robinson and J. E. Todd, Plant Scale Fluid-Bed Denitrator, MCW-1509, Mallinckrodt Chemical Works, Weldon Spring, MO (1966).
5. A. A. Jonke, N. M. Levitz, and E. J. Petkus, Fluidized-Bed Process for the Production of Uranium Tetrafluoride (Green Salt) From Uranyl Nitrate, Interim Report, ANL-5363 (December 30, 1954).
6. S. Semecek and W. T. Trask, The Integrated Fluid-Bed System, MCW-1478 (June 10, 1963).
7. W. J. Bjorklund and G. F. Offutt, First Product Denitration Campaign With Enriched Uranium at ICPP, IN-1475 (June 1971).
8. R. W. Lambert and J. M. Dotson, "Fluidized-bed Applications in the Midwest Fuel Recovery Plant," *Chemical Engineering Progress Symposium Series*, Vol. 66 No. 105, 175-179.
9. A. G. Fane, B. G. Charlton and P. G. Alfredson, The Thermal Denitration of Uranyl Nitrate in a Fluidized-bed Reactor, Australian Atomic Energy Commission Establishment Lucas Heights.
10. M. Iwasaki, "Kinetic Studies of the Fluorination of Uranium Oxides by Fluorine," *J. Inorg. Nucl. Chem.* 26, 1853-1861 (1964).
11. L. J. Anastasia et al., The Fluorination of UO₂-PuO₂ in a 2-inch Diameter Fluid-bed Reactor, ANL-7372, Argonne National Laboratory (December 1967).
12. D. C. Brater et al., "Preparation of Uranium Hexafluoride," Prog. Nucl. Energy, Ser. 3, 2 (1958).
13. O. G. Lebedev et al., Investigation of the Stability of the Fluorination Process of Uranous-Uranic Oxide in a Fluidized Bed, IAE-2328, Moscow (1973); translated May 1975, ORNL-tr-2938.

RECEIVED May 21, 1979.

Separation of Actinides from High Active Waste by Means of Counter Current Ion Migration

B. A. BILAL, F. HERRMANN, K. METSCHER, B. MÜHLIG,
CH. REICHMUTH, and B. SCHWARZ

Nuclear Chemistry Division, Hahn-Meitner-Institut für Kernforschung, Berlin,
Federal Republic of Germany, D-1000 Berlin 39

The use of nuclear power as energy source is determined by the safe handling and deposition of the nuclear waste. High active waste solutions must be transformed into stable solid form which is suitable for final disposal. The separation of the actinides from the waste before its solidification (e.g. vitrification) is advantageous (or may be even necessary) from two points of view:

1. The isolation of the long-lived and highly dangerous transuranium elements reduces the control time over the waste from the scale of millions to that of hundreds of years, since about 300 years are 10 x the half life time of the longest lived fission product Sr-90. The potential danger is reduced in the same scale.
2. No long-time experience exists about the stability and leaching of glasses containing the high α -active actinides.

Most processes are developed for separation of an individual actinide or certain groups of actinides (e.g. U, Np and Pu by TBP extraction) from the waste. These processes are usually based on liquid/liquid extraction and ion exchange technique. More or less complicated processes lead to the separation of only one transuranium element. In these processes the radiolytic destruction of the organic solvent or the ion exchanger causes some difficulties.

Using the counter current ion migration process (1-6), all the actinides in the waste are separated as group or individual in one stage yielding a high decontamination factor ($\approx 10^6$). The separation takes place in aqueous medium, which is less sensitive to the radiation effects than organic substances. The radiation products of the carboxylic acid solution (mainly acetic

0-8412-0527-2/80/47-117-561\$05.00/0

© 1980 American Chemical Society

acid) used as a counter current liquid are nearly chemical indifferent. The separated actinides are of high purity and are suitable for recycling in reactors (7). That means their concentration in the environment remains nearly stationary in circular process.

Principle of the Counter Current Ion Migration

In this separation process a flow of a suitable solvent is directed against the ionic mixture migrating in the electric field. If the flow rate is equal to the average migration velocity of the mixture, this remains stationary in the separation column, while the faster moving components migrate against the stream, and the slower components are gradually flushed back. In this way, it is possible, if necessary, to let the mixture migrate over a long distance relative to the solvent and so to obtain a very high separation factor. In most cases, non-isotopic ions are separated in very high purity. In some rare cases, in which the relative difference of the mobility is less than 1% (e.g. Lanthanides and some actinides) pure components are only obtained if the mobility difference is increased by additional effects, such as different complexation degree of the components by means of a suitable ligand.

Fig.1 shows a column type for discontinuous or batchwise separation process. A trough of polypropylene or another suitable material is divided vertically to the length axis (separation direction) by means of diaphragms of polypropylene gauze to prevent the thermal convection in this direction. The diaphragms are welded on polypropylene frames and are fitted like slides into plates of polypropylene through which the cooling pipes pass. The counter current liquid streams with a constant rate from the cathode to the anode if cations are to be separated and vice versa.

Holding the current strength and flow rate constant, a selfstabilization mechanism leads to the establishment of a stationary and constant concentration profile of the ionic mixture as a whole along the column. Within this profile the separation of the various components gradually takes place. The proceeding fractionation of the initial homogenous mixture leads on the other hand to the establishment of increasing concentration gradient of each component giving rise to opposite diffusion transport, causing remixing. The separation process is finished when the two transports

become equal. The separation time is not only a function of the mobility difference of the components, but also of the construction specification of the separation column. Finally, the components are obtained in zones which overlap slightly due to diffusion. The concentration of each ion in its pure zone is a function of its transport number, of the current strength and of the flow rate.

The column shown in fig.1 is also suitable for continuous separation of the mixture, but only in two fractions like the separation of the actinides as a group from the nuclear waste.

Processing of the High Active Waste (HAW)

The HAW of spent fuel reprocessing consists of a nitric acid ($\approx 4M$) solution of about 30 different ions, namely the actinides U, Np, Pu, Am and Cm, the fission products Cs, Rb, Sr, Ba, Mo, Nb, Zr, Te, Tc, Ru, Rh, Pd, Ag, Y, La, Ce, Pr, Nd, Pm, Sm, Eu, Gd, Tb and Dy and the corrosion products Mn, Cr, Ni and Fe. Table I presents the concentration of these components in a waste solution of reprocessing of fuel elements of light water reactors, supposing a burnup of 33000 Mwd/ton, a specific power of 30 Mw per ton Uranium (3,3% U-235), a cooling time of 1a and a waste volume of 500 litre/ton fuel. The last column of table I contains the chemical form of the components in the waste solution.

Fig.2 shows the flow sheet of the HAW processing. The use of the waste solution directly for separation leads to the dissipation of a very large part of the electric energy for the electrolytic transport of the hydrogen and nitrate ions. The concentration of the nitric acid is therefore reduced to about 0.05 M through denitration by means of formic acid. To prevent the hydrolysis and the precipitation of some components, particularly Pu, acetic acid is added as complexing agent to the solution before denitration. The elements Nb, Te and Mo partially precipitate as oxides. Se, Ag and Pd partially precipitate as metals. The rest of Mo, remaining in solution, is present as polymolybdate which does not precipitate Zr as Zr-polymolybdate, since the pH of the solution is still about 1.2. Due to the nitric oxides developed during the denitration the Pu is converted to Pu(IV) that forms stable positive charged acetato-formato-complexes, if the concentration

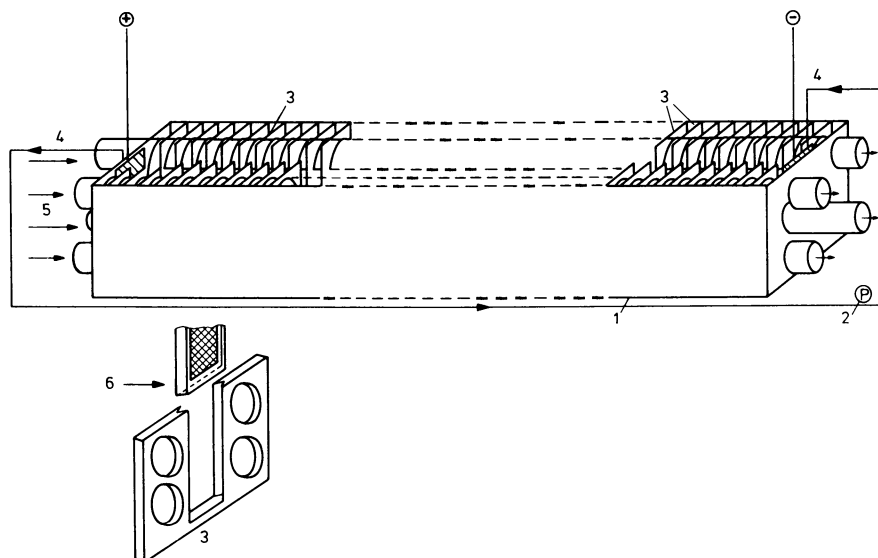


Figure 1. Column for discontinuous or batchwise separation: 1, outside walls; 2, pump; 3, plates for dividing the column in compartments; 4, counter current liquid; 5, cooling liquid; 6, frame with diaphragm.

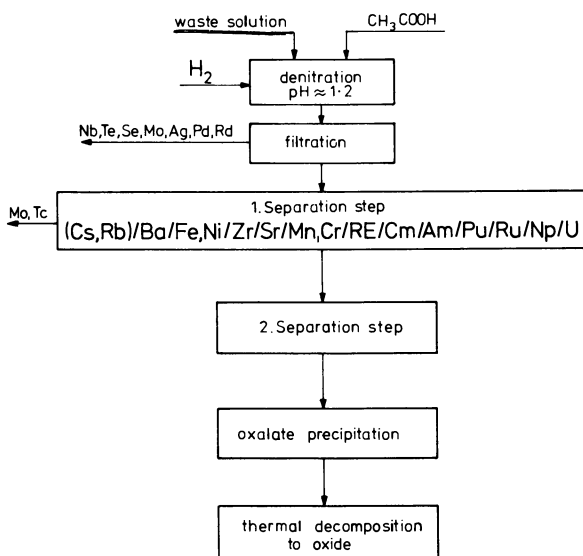


Figure 2. Flowsheet of the HAW processing

Table I. Concentration [g/l] and chemical form of the components in the waste solution.

element	C [g/l]	ion form	element	C [g/l]	ion form
U	0.84	UO_2^{2+}	Zr	5.30	Zr^{4+}
Np	1.52	NpO_2^+	Tc	1.70	TcO_4^-
Pu	0.09	Pu^{4+}	Ru	1.48	Ru(III)-NO-nitrato-nitro-complexes
Am	0.36	Am^{3+}	Rh	0.50	Rh(III)
Cm	0.06	Cm^{3+}	Pd	0.90	Pd(IV)-nitrate-complexes
Cs	2.60	Cs^+	Ag	0.12	Ag^+
Rb	0.44	Rb^+	Mn	1.1	Mn^{2+}
Sr	1.06	Sr^{2+}	Cr	0.01	Cr^{3+}
Ba	1.28	Ba^{2+}	Ni	0.004	Ni^{2+}
Y	0.5	Y^{3+}	Fe	0.05	Fe^{3+}
Rare Earths (RE)	11.40	RE^{3+}			
Mo	3.20	MoO_2^{2+}			
Nb	0.03	NbO_2^+			
Se	0.005	SeO_3^{2-}			
Te	0.40	TeO_3^{2-}			

of both the acetic and the formic acid is about 0.5 M. The stability of the Pu complexes over several days was examined previously by means of absorption spectroscopy. Neither a shift of the absorption band at $\lambda = 457 \text{ nm}$ nor new bands were found. If there is no interest to gain the elements Pd and Rh separately, they are precipitated in the denitration step by means of hydrogen gas which is activated on passing a plate of sinter glass on which Pd was already precipitated. Ru remains in the solution as Ru-NO-nitrato-nitro-complexes. Tc is present as the pertechnetate ion. All other components are present in the denitrated solution as simple or partially complexed cations. After filtration the multicomponent mixture is then separated in a column shown in fig.1. A mixture of acetic acid (0.5M) and nitric acid(0.05M) is used as counter current liquid (cathode \rightarrow anode).

Discontinuous Separation

One litre of waste solution containing the components at the concentration given in table I is processed according to figure 2. After about 1h operating time Mo and Tc are completely washed out of the column. After further 20h the maximum separation degree of the zones (cathode \rightarrow anode) Rb, Cs/Ba/Fe, Ni/Zr/Sr/Mn, Cr/RE/Cm/Am/Pu/Ru/Np/U is obtained (s.fig.3.I). The counter current overflow is highly decontaminated from all components and is therefore recycled (s.fig.1). The overlapping ranges of the actinides zones are sucked out of the first column and separated in a second one that has such a small cross section to get the largest spreading of the pure zones, but a small overlapping range. In a running batchwise separation, both columns are operated simultaneously. The pure zones of the actinides are then extracted out of the column and precipitated as oxalate. The overlapping zones are mixed again to the feed solution of the first separation step. More than 98% of the actinides are separated in the two steps and are decontaminated from the fission and corrosion products as well as from each other by the factor $>10^6$. The rare earths are decontaminated from each other by the factor $\approx 10^3$. The decontamination factor of the other fission products is about $>10^6$.

Separation Data 1.step: Length of the column. (L)=200 cm, free cross section (q)=5 cm², flow rate (V) = 40 ml/h, high voltage (U)=2000 V, current strength (I)=0.2 A, separation time (t)=21h. 2.step: L=200 cm, q=0.5cm², \dot{V} =4 ml/h, U=2000 V, I=0.02 A, t=21h.

Continuous Separation

Fig.4 shows schematically the arrangements used for continuous separation of the actinides as a group from the waste. A separation column (a) (L=100 cm) is connected to the vessel (b) containing the waste solution. Opposite to it there is a second column (c) (L=10 cm) having the same cross section. The counter current liquid (0.5M acetic acid + 0.05M nitric acid) streams from the cathode to the anode. The column (c) contains a zone of an ion of high mobility (e.g. K, Cs, Rb) to protect the components in (b) against cathode contact. In the column (a) the actinides as a group, Ru, Tc and Mo are separated from the other components.

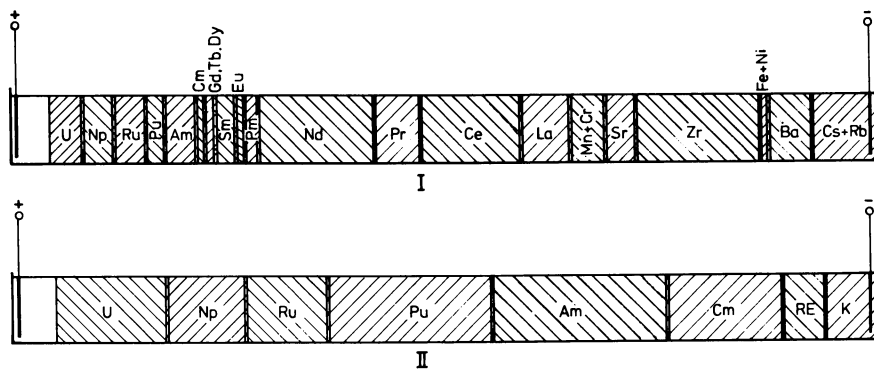


Figure 3. Stationary distribution of the separated components in a discontinuous process: I, first step; II, second step.

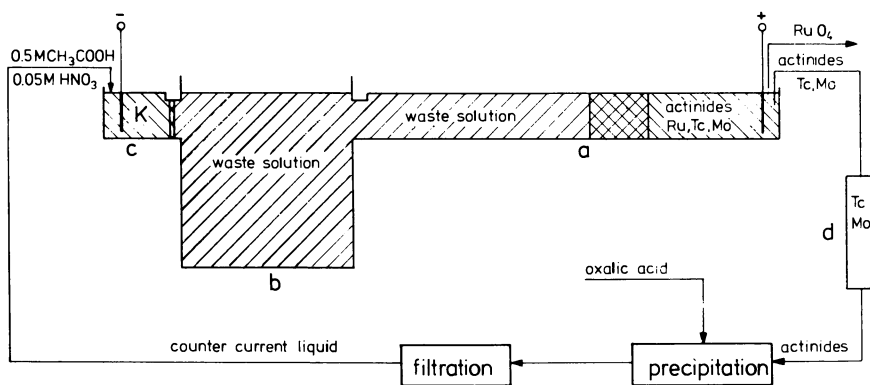


Figure 4. Equipment for continuous separation

Ru is quantitatively oxidized to the volatile RuO_4 on passing the anode chamber. The overflow passes an anion exchanger (d) to hold back Tc and Mo. The pure actinides are precipitated as oxalate which decomposes thermally to the oxides. The decontamination factor actinides/fission- and corrosion products is $\sim 10^6$.

The separation process starts as follows: First a discontinuous separation is carried out in the column (a) using the same values of I/q and \dot{V} as mentioned above. These values are then corrected to allow a continuous separation taking place between the REE- and Cm/Am-zones, where the condition

$$b_{E.u_{\text{REE}}} > v > b_{E.u_{\text{Cm/Am}}} \quad (1)$$

must be fulfilled. b_E is the electric field strength at the contact point between the column (a) and the vessel (b). Its value is given by the relation

$$E = I/q \kappa \quad , \quad (2)$$

where κ is the stationary conductivity of the solution in the vessel (b). The mobility u is determined from measurement of κ of the corresponding component in its pure zone obtained by means of discontinuous separation and calculation according to

$$u_i = \dot{V} \kappa / I \quad (3)$$

Separation Data q (of (a) and (c)) = 5 cm^2 ,
 $U = 1200 \text{ V}$, $I = 0.22 \text{ A}$, $\dot{V} = 25 \text{ ml/h}$, M (separated actinides [mole/d]) = 0.05 .

Estimation of Energy necessary for Separation

According to a linear extrapolation of the separation data, about 10^{-5} of the energy gained per one ton of fuel in light water reactors (s.above) must be used for the processing of its high active waste. This seems to be high. On the other hand, this method makes it possible to separate all the actinides simultaneously with a high decontamination factor. It is easy to operate the separation equipment automatically and so to have low personnel cost.

However, the development of the large scale technique and the construction of separation columns from

materials more resistant to radiation are still open to question.

Literature Cited

1. Brewer, A.K., Madorsky, S.L., and Westhaver, J.W., Science 1946 104, 156
2. Martin, H., Z.Naturforsch. 1949 4a, 28
3. Clusius K., Ramirez, E.R., Helv.Chim.Acta 1953 36, 1160
4. Wagener, K., Z.Elektrochem., Ber.Bunseges.Physik. Chem. 1960 64, 922
5. Wagener, K., "Report of the Hahn-Meitner-Institut für Kernforschung Berlin", Rept. HMI-B 44 (1965)
6. Bilal, B.A., Chem.Ing.Techn. 1970 42, 1090
7. Cunningham, G.W., IAEA-CN 36/561

RECEIVED May 14, 1979.

Polymolybdates as Plutonium (IV) Hosts

R. A. PENNEMAN

Los Alamos Scientific Laboratory, University of California, P. O. Box 1663,
Los Alamos, NM 87545

R. G. HAIRE and M. H. LLOYD

Oak Ridge National Laboratory, P. O. Box X, Oak Ridge, TN 37830

Dissolution of Zr-clad plutonium-bearing fuel can result in a residue which contains Pu, Zr and fission-product molybdenum. In addition, solutions of these elements can yield insoluble products on standing, or with further treatment such as extended heating. Initial data suggested that molybdates or polymeric molybdic acids were responsible for formation of the solids. In the case of polymeric molybdic acids, interstices in the matrix of MoO₆ octahedra could accept foreign ions, such as Pu(IV) and Zr(IV). It should be noted here that the ion size disparity between Zr(IV) and Pu(IV) will generally require that Zr and Pu occupy different coordination sites, with Pu(IV) demanding larger coordination. Recently, the existence of Zr molybdates, Pu molybdates and Zr-Pu molybdate mixtures (containing up to several percent Pu) have been identified; it was found that the individual Zr and Pu molybdate products were not isostructural. Detailed studies of the formations of these materials from aqueous media are still in progress (M. H. Lloyd and R. L. Fellows, results to be published).

A major concern is the association of Pu with the Zr-molybdenum precipitates, which results in relatively high losses of Pu. In an effort to determine the mechanism for the Pu association, several possibilities were explored. Presented here are chemical/structural considerations of the molybdenum systems, the experimental evidence collected to date on these materials and the initial conclusions that have been reached about them.

Chemical/Structural Considerations of the System

Jørgensen and Penneman (1) discussed the behavior of the translawrencium elements $Z = 104, 105$, etc. and called attention to the striking contrast in polymerization behavior, and characteristic aquo species of the hexavalent d- and f-block elements. For simple aquo ions, it turns out, empirically, that the total

0-8412-0527-2/80/47-117-571\$05.00/0

© 1980 American Chemical Society

In Actinide Separations; Navratil, J., et al.;

ACS Symposium Series; American Chemical Society: Washington, DC, 1980.

hydration energy of a given M^{+z} is $-z^2\kappa$, where κ is a characteristic constant for each transition group (2). However, oxo complexes of the (V) and (VI) states are more stable than accounted for by such a simple theory.

It is frequently argued that a specific property of 5f group M(VI) and M(V) is the formation of linear dioxo complexes, MO_2^{2+} and MO_2^+ . Their most striking property is the coexistence of oxo and aquo ligands, which is exceedingly rare in the rest of the elements. There are characteristic differences found frequently between the oxo ions of the V- and VI-valent actinides, uranium through americium, and those of the d elements in the same valence states.

- A. Actinyl V's and VI's give monomeric oxo cations in acid, in contrast to the d element proclivity towards polymerization (isopoly acid formation). Protactinium is similar to d elements in this regard.
- B. The actinyl(V) and (VI) oxo ions display trans orientation of the "yl" oxygens, rare in d-element compounds. Trans oxygen binding may require enhanced s participation, a relativistic effect found in the calculational efforts on superheavy elements.
- C. The "yl" oxygens are usually of higher bond order, with much shorter metal-oxygen bond lengths than the equatorial oxygen coordination (1.75 Å vs 2.45 Å).
- D. Actinyl ions require higher oxygen coordination (7-8) while d-block elements in the same valence state often have (4 or 6) oxygen coordination.

The structure of a typical oxygen coordination sphere around uranyl has six oxygens in the equatorial plane and two short oxygen bonds perpendicular to that plane. Bidentate oxygen-donors (with 2 oxygens attached to same element nitrate, carbonate) have a shorter bite than individual oxygens, and can be accommodated without puckering the equatorial oxygen ring; two nitrates and two water molecules are common (3). Hydroxyl groups replace water as the pH is increased. A structure containing dimeric units is known, with retention of the uranyl oxygens (4).

In contrast, hexavalent transition metals, such as molybdenum and tungsten, polymerize in acid by aggregation to specifically favored geometries containing oxide octahedra of MoO_6 and WO_6 (the iso poly acids) (5a). These oxide structures have cavities which accept foreign ions, to form heteropoly ions (5b). The central cavity is a tetrahedral site, often occupied by PO_4^{3-} , SiO_4^{4-} , etc, a fact utilized in phosphate precipitation:



The isolated MoO_6 octahedron is known only in condensed units, where the MoO_6 polyhedra share corners, edges and faces in combi-

nations, providing sites for hetero atoms with coordination numbers: 4, 6, 8, and 12. Although condensed units containing 6, 12, and 18 Mo or W atoms are common, others (containing 5, 9, 10, 11, or 17 M atoms) are formed by removal of one unit and also by dimerizing, eg., ($P_2Mo_5O_{23}$), (XM_9O_{32}), ($XM_{11}O_{39}$), ($X_2M_{17}O_{61}$).

Some known structures with guest metal ions in 4, 8 and 12 coordination are listed in the following table.

Known Structures			
	X-coordination	Ref.	X
$X^{n+}Mo_{12}O_{40}^{(8-n)-}$	4	(5)	Si, P, As, Zr, Ti
$X^{4+}W_{10}O_{36}H_2^{6-}$ or $X^{4+}W_{10}O_{36}^{8-}$	8	(6,7,8)	Ce, Th, U, Np, Pu
$X^{n+}Mo_{12}O_{42}^{(12-n)-}$	12	(9,10,11)	Ce, Th, U, Np

Since tetrahedral coordination is not appropriate for plutonium coordination by oxygen, it will not be discussed here.

If one removes from an octahedron the center metal M^{6+} and an apical oxygen, four planar oxygens remain available for coordination. If this is done from 2 W_6 units, there are 8 oxygens and a cation vacancy that can coordinate a large cation. The first example of such a structure contained Ce(IV), and later U(IV) (6-7). In these structures the 8-O's approximate an antiprism for Ce(IV) which is distorted in the U(IV) case.

The Mo_{12} unit provides a 12-coordinated site, an icosahedron of oxygens which can accommodate large cations; such a structure containing Ce(IV) was determined by Dexter and Silverton (9).

The sizes of the coordination cavities are illustrated by the following data:

(Experimental)

<u>M</u>	<u>M-O distances</u>	<u>Coord. No.</u>	<u>Material</u>	<u>Structure</u>
Ce^{IV}	2.38 - 2.40 Å	8	$CeW_{10}O_{36}H_2^{6-}$	O-antiprism
Ce^{IV}	2.51	12	$CeMo_{12}O_{42}^{8-}$	O-icosahedron
Ce^{IV}	2.50	12	$(NH_4)_2Ce(NO_3)_6$	
U^{IV}	2.29 - 2.32	8	$UW_{10}O_{36}^{8-}$	O-antiprism

Since there are no known structures of such compounds with plutonium, it is useful to utilize Zachariasen's rules (12) for estimating actinide-oxygen bond lengths which would be required in a particular coordination geometry.

Zachariasen's Bond Length - Bond Strength Relations (12).

1. A bond strength $\underline{s}_{ij} = \underline{s}_{ji}$ is assigned to a bond between the i 'th and j 'th atoms of a structure so that

$$\sum_j \underline{s}_{ij} = \underline{v}_i \quad , \quad \sum_i \underline{s}_{ij} = \underline{v}_j$$

where \underline{v}_i and \underline{v}_j are the valences of the two atoms.

2. The length of a bond \underline{D}_{AB} between two atoms of species \underline{A} and \underline{B} is a function only of the strength of the bond. A universal function $\underline{D}_{AB}(s)$, valid for all structures containing $\underline{A} - \underline{B}$ bonds, is postulated: $D = D_1 - B \ln s$ where D_1 is normalized to unit bond strength ($s=1$).

Zachariasen has tabulated D_1 and B values for d and f block oxides and halides (12). His bond length formulas for Ce-O distances in A are: Ce(III), $D_s = 2.18 - 0.338 \ln s$; and Ce(IV), $D_s = 2.117 - 0.326 \ln s$. We estimate the following values:

Cerium-Oxygen Distances, Å

	Coord.					
	D	s*	s*	s*	D	
Ce(III)-0	2.51	3/8	8	1/2	Ce(IV)-0	2.34
	2.65	1/4	12	1/3		2.48

s*: the bond strengths are divided equally among the Ce-O bonds in a given coordination, where actual bond distances are unknown. Note that reduction of Ce(IV) to Ce(III) in the 8-coordinated case would cause an opening of the cavity by increasing the Ce-O bond length from 2.34 to 2.51 Å and that the estimated Ce(IV)-O distance agrees well with the experimental measurements given earlier.

For plutonium, data from single crystal determinations are lacking. The following values are estimated as in the cerium case above using Zachariasen's formulas for plutonium: Pu(III)-O, $D_s = 2.142 - 0.35 \ln s$; and Pu(IV)-O, $D_s = 2.094 - 0.35 \ln s$.

Plutonium-Oxygen Distances, Å

	Pu(III)-O	Pu(IV)-O	
D, calcd	2.49	2.34	8-coord.
D, calcd	2.63	2.48	12-coord.

Here again, the expansion on reduction of Pu(IV) to Pu(III) would loosen the binding and open the oxygen cavity. Since base depolymerizes the polymolybdates, a basic reducing agent should break the plutonium-bearing framework. However, a good reducing agent would be required as the Pu(IV) is considerably stabilized (by 0.9V in $P_2W_{17}O_{61}^0$) (8).

We will have occasion to refer to such estimated Pu(IV)-O distances in the following section, in which the more extreme case of substituting Pu(IV) for Zr(IV) is discussed.

The Structures of Some Simple Molybdates

The "simple" molybdate salts have been the subject of study by several authors (13-24). There is still confusion as to their degree of common structural features; for example we question the unusual coordination polyhedra and the metal-oxygen distances in the structures of $Th(MoO_4)_2$ and $Hf(MoO_4)_2$ as deduced by Thoret (13). Likely the oxygen positions are in error since the metal-oxygen bond strengths from Zachariasen's formula give unreasonable valence sums for the coordinated metals. In contrast, we find the structure of the hydroxy zirconium polymolybdate hydrate (14) quite satisfactory when analyzed using Zachariasen's formulas. For atom numbering in the following analysis see Fig. 1, which was taken from reference 14. Using Zachariasen's values for molybdenum-oxygen bonds, and for zirconium-oxygen bonds, we find for $Zr(Mo_2O_7(OH)_2(H_2O)_2)$:

Summation of bond strengths around Mo and Zr.

<u>Neighbor</u>	<u>Distance</u>	<u>S_{ij}</u>	<u>Neighbor</u>	<u>Distance</u>	<u>S_{ij}</u>				
Mo-0	3	1.722	1.706	Zr-0	5	2.088	0.679		
	0	4	2.310	0.2627		0	5	2.088	0.679
	0	5	1.797	1.343		0	6	2.173	0.523
	0	6	1.755	1.538		0	6	2.173	0.523
	0	7	2.113	0.4918		0	7	2.175	0.520
	0	8	2.034	<u>0.6319</u>		0	7	2.175	0.520
						0	8	2.141	0.578
			$\Sigma Mo = 5.97$					$\Sigma Zr = 4.02$	

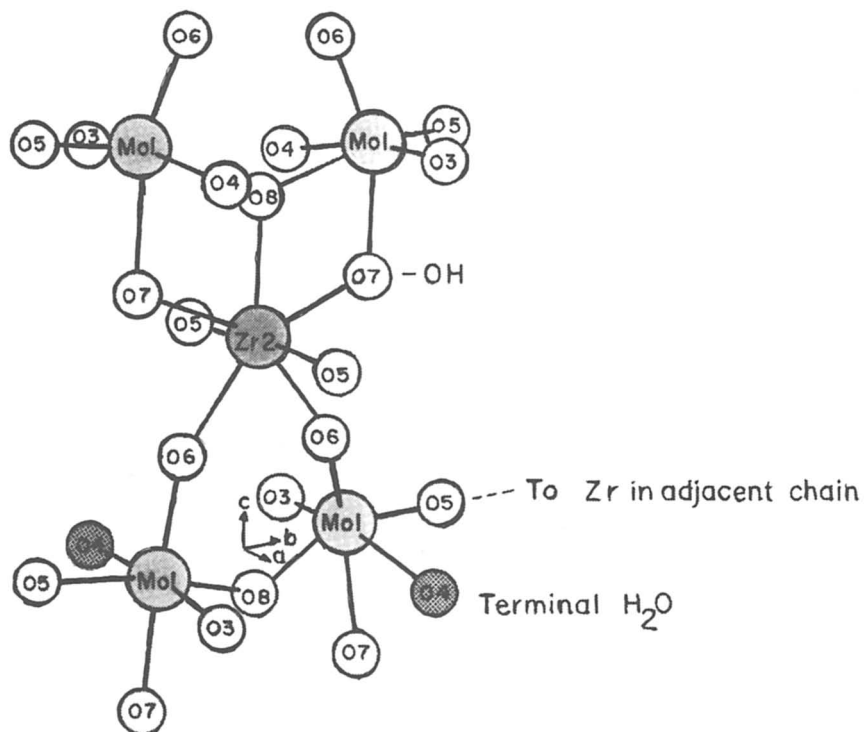


Figure 1. Structure of $ZrMo_2O_7(OH)_2(H_2O)_2$

Note that the seven Zr-O bond strengths are fairly uniform but that there is quite a range in Mo-O distances, with a resultant range in their bond strengths; in spite of this, they sum quite well for hexavalent molybdenum.

One of the useful extensions of Zachariasen's bond strength analysis is that by summing the oxygen bond strengths, as well as those of the metals, one can often tell which oxygens in the structure arise from coordinated water or hydroxyl. The O-H---O

bond strength is divided as follows: $O \xrightarrow{.83} H \xrightarrow{.17} O$.

Summation of bond strengths around the oxygens:

Bond Distance, Å	O	Σ , Metal-Oxygen only	Σ with H-Bonding
1.722	O ₃ -Mo	1.71	O ₃ = 1.71 + .17 + .17 = 2.05
2.310	O ₄ -Mo	0.26	O ₄ = 0.26 + .83 + .83 = 1.92
1.797, 2.088	O ₅ -Mo,Zr	2.02	
1.755, 2.173	O ₆ -Mo,Zr	2.06	
2.113, 2.175	O ₇ -Mo,Zr	1.01	O ₇ = 1.01 + .83 + .17 = 2.01
2.034, 2.141	O ₈ -Mo,Zr	1.84	

Thus, O₄ clearly originates from a water molecule, and is coordinated solely to Mo; O₇ is a hydroxyl oxygen which bridges Zr and Mo. The summation of oxygen bond strengths makes the assignments unequivocal.

Consequences of Substituting Pu(IV) for Zr in Zr Mo₂O₇(OH)₂·(H₂O)₂.

There is a direct link provided by O₅ between Zr in one chain and a Mo in the adjacent chain and the Zr-O bond vector is essentially aligned along the tetragonal *a* axis. Substitution of Pu(IV) for Zr(IV) at the same coordination number and bond strengths would involve an increase in the Pu(IV)-O₅ bond distance of 0.14 Å over the Zr(IV)-O₅ distance. This would clearly cause expansion between chains. Similarly, chain lengthening would result. Since Pu(IV) generally requires more than an oxygen coordination of seven, it would not seem likely that a solid solution will result over any extended range, nor that the then unknown Pu(IV) molybdate species would be isostructural with this Zr compound. This prediction has been borne out by the X-ray work which has shown that two different structures are involved.

Experimental Data on Zirconium Molybdate

In nitric acid solution containing uranium, plutonium, zirconium, molybdenum and other fission products, precipitation of zirconium molybdate occurs preferentially. Solutions containing only zirconium and molybdenum yield the "same" precipitated mater-

ial as solutions containing additionally uranium, plutonium, fission products, etc. The difference in this latter case is that the precipitate contains about 2 wt.% Pu or greater.

The precipitation of the zirconium-molybdenum material is a function of acid strength, temperature and time. The rate of precipitation is lower with lower temperatures, low zirconium concentrations and higher acid strengths. There also appears to be an induction period before the onset of precipitation. Discussed here is the characterization of the zirconium molybdate solids, as obtained separately from nitric acid solutions; chemical analyses, thermogravimetry and X-ray powder diffraction were used to characterize these solids.

Chemical analyses of the Zr-Mo precipitates yield a Mo/Zr mole ratio of two. Thermogravimetry on carefully air dried precipitates also provide a Mo/Zr mole ratio of two, based on the weight loss being MoO_3 and the final product being ZrO_2 . The data indicate 2.5 $\text{H}_2\text{O}/\text{Zr}$ in the original material. X-ray powder diffraction patterns of the initial precipitate show the material is identical to the compound reported by Clearfield and Blessing (14) to be $\text{ZrMo}_2\text{O}_7(\text{OH})_2(\text{H}_2\text{O})_2$. (tetragonal, $a_0 = 11.45(1)\text{\AA}$ and $c_0 = 12.49(1)\text{\AA}$). Heating this material leads to the formation of anhydrous $\text{Zr}(\text{MoO}_4)_2$, which on further heating decomposes to give monoclinic ZrO_2 . The anhydrous $\text{Zr}(\text{MoO}_4)_2$ material was indexed as having hexagonal symmetry, with $a_0 = 10.0\text{\AA}$ and $c_0 = 11.6\text{\AA}$, in agreement with lattice parameters for $\text{Zr}(\text{MoO}_4)_2$ reported by Trunov and Kovba (15a) and by Freundlich and Thoret (15b).

Experimental Data on Plutonium Molybdate

In the absence of zirconium, a plutonium-molybdenum compound can be precipitated from nitric acid solutions. The presence of zirconium in the same solution is detrimental to formation of this material, as zirconium molybdate is formed preferentially. However, the amount of Pu molybdate solids that form is a function of hydrogen ion concentrations; at 1M HNO_3 or less, solids form but at higher acid concentrations the quantity of precipitate decreases. At 3M HNO_3 solids are just barely detectable.

By chemical analyses, the plutonium molybdate precipitates contains 2 moles of molybdenum per mole of plutonium(IV). Based on thermogravimetry, the plutonium molybdate gradually loses ~2 moles of water to form an anhydrous $\text{Pu}(\text{MoO}_4)_2$. Continued heating of this compound results in a loss of MoO_3 ($>750^\circ\text{C}$) to yield fcc PuO_2 . X-ray powder diffraction of the carefully air dried plutonium molybdate precipitate provided data that were indexed as having orthorhombic symmetry, with $a_0 = 3.34$, $b_0 = 10.97$ and $c_0 = 6.32\text{\AA}$. The material appears to be isostructural with orthorhombic $\text{U}(\text{MoO}_4)_2$ ($a_0 = 3.36$, $b_0 = 11.08$, $c_0 = 6.42\text{\AA}$) reported by

C. Skvortsova and Sidorenko (16). The X-ray patterns obtained before and after the loss of water from the plutonium-molybdenum compound were identical, suggesting the waters were not important to the structure. Additional heating of the plutonium compound produced a new phase, also orthorhombic and identical to $\text{Pu}(\text{MoO}_4)_2$ reported by Tabuteau (17), by Prokoshin (18), and by Ustinov (19) ($a_0 = 9.42$, $b_0 = 10.05$, $c_0 = 13.98$ Å). This material is isostructural with the compounds $\alpha\text{-NpMo}_2\text{O}_8$ and $\alpha\text{-ThMo}_2\text{O}_8$ (20).

For prior work, having more application to process conditions, see ref. 25 and 26.

Precipitates from HNO_3 solutions containing Mo/Zr/Pu

The following table lists some analytical results on precipitates containing Mo, Zr and Pu. X-ray results are not available on these materials at present. In all cases, the amount of zirconium in the initial solution was in excess of the amount necessary to form $\text{ZrMo}_2\text{O}_7(\text{OH}_2)(\text{H}_2\text{O})_2$.

<u>Initial Concn. g/l</u>			<u>HNO_3, M</u>	<u>$\frac{\text{mg Pu}}{\text{mg (Zr+Mo)}}^*$</u>
<u>Mo</u>	<u>Zr</u>	<u>Pu</u>		
1.5	5.0	1.47	1	0.086
1.5	1.0	1.47	1	0.122
1	1.5	1.5	2	0.023
1	1.5	1.5	3	0.013
1	1.5	1.5	4	0.009

*Each value average of 5 experiments.

There is evidence that the Pu associated with the Zr-molybdate precipitates is not sorbed on the solid's surface but is an integral part of the material. This is borne out by the fact that the Pu cannot be leached out of the solid phase without destroying (dissolving it) it. Also, when the freshly prepared precipitate is added to Pu(IV) solutions, Pu is not carried down (sorbed) by the Zr solid phase.

Conclusions

1) Plutonium molybdate precipitated in the absence of Zr is a different structure (isostructural with $\text{U}(\text{MoO}_4)_2$ (16)) than the

$ZrMo_2O_7(OH)_2(H_2O)_2$ whose structure was determined by Clearfield and Blessing (14).

2) Because of the difference between Pu-O and Zr-O bond lengths ($\Delta = 0.14\text{\AA}$) at the same bond strength, it is expected that the $ZrMo_2O_7(OH)_2(H_2O)_2$ lattice will not accommodate extensive substitution of the larger Pu(IV) for Zr(IV).

3) The plutonium-bearing precipitate obtained from nitric acid solutions (containing molybdenum, zirconium and plutonium) gives an X-ray powder diffraction pattern not distinguishable from that of $ZrMo_2O_7(OH)_2(H_2O)_2$ precipitated without plutonium. However, since the Pu content is low, the Pu could be present either in the Pu molybdate structure or replacing Zr in the Zr molybdate structure and not be detected in the X-ray patterns.

4) Present data on the Zr and Pu molybdates have not provided evidence for the existence of heteropoly molybdate structures for those precipitates obtained from 1-5M HNO_3 .

5) Zachariasen's empirical rules relating bond strengths and bond lengths in 4f and 5f oxides is demonstrated to be useful when applied to the simple and complex molybdate structures (12).

Acknowledgments

We gratefully acknowledge the helpful comments of R. L. Fellows, Chemical Technology Division, Oak Ridge National Laboratory.

References

- Jørgensen, C. K.; Penneman, R. A., "Heavy Element Properties"; North-Holland Publishing Co., Amsterdam, 1976, p.117.
- Jørgensen, C. K., *Chimia (Switz.)*, 1969, **23**, 292.
- a. Taylor, J. C.; Mueller, M. H., *Acta Cryst.*, 1965, **19**, 536. b. Dalley, N. K.; Mueller, M. H.; Simonsen, S. H., *Inorg. Chem.*, 1971, **10**, 323. c. Eller, P. G.; Penneman, R. A. *Inorg. Chem.*, 1976, **15**, 2439.
- Aberg, M.; *Acta Chem. Scand.* 1969, **23**, 719-810.
- a. Cotton & Wilkinson, *Adv. Inorg. Chem.*, Interscience Publishers, Ed., 1966. b. Weakley, T. J. R., *Struct. Bonding*, 1974, **18**, 131-176.
- Iball, J.; Low, J. N.; Weakley, T. J. R., *J. Chem. Soc.*, Dalton Trans, 1974, 2021.
- Golubev, A. M.; Kazanskiĭ, L. P., *Dokl. Akad. Nauk SSSR*, 1975, **221**, 351, 826, *Zh. Neorg. Khim*, 1975, **20**, 867.
- Saprykin, *Dokl. Acad. Nauk* 1976, **228**, 649; *Radiokhim*, 1976, **18**, 101.
- Dexter, D. D.; Silverton, J. V., *J. Am. Chem. Soc.*, 1968, **90**, 3599.

10. Kazanskii, L. P.; Torchenkova, E. A.; Spitsyn, V. I., Dokl. Akad. Nauk SSSR, 1973, 201, 141.
11. Torchenkova, E. A.; Golubev, A. M., Dokl. Akad. Nauk SSSR, 1974, 216, 1073.
12. Zachariassen, W. H. "Bond Lengths in Oxygen and Halogen Compounds of d and f Elements." Journal of the Less-Common Metals, 1978, 62, 1-7.
13. Thoret, J., Rev. Chem. Min., 1974, 11, 237.
14. Clearfield, A.; Blessing, R. H. J. Inorg. Nucl. Chem., 1972, 34, 2643.
15. a. Trunov, V. K.; Kovba, L. M. Russian J. Inorg. Chem., 1967, 12, 1703. b. Freundlich, W.; Thoret, J. C.R. Acad. Sc. Paris, C, 1967, 265, 96.
16. Skvortsova, K. B.; Sidorenko, T. A. Zapiski, Vses. Mineralog. Obshch. 1965, 94, 548. (JCPDS 18-1425).
17. Tabuteau, A.; Pages, M.; Freundlich, W. Mater. Res. Bull., 1972, 7, No. 7, 691.
18. Prokoshin, A. D.; Ustinov, O. A.; Dogaev, Yu. D. Zavod. Lab. 1973, 3, 305.
19. Ustinov, O. A.; Novoselov, G. P.; Chebotarev, N. T.; Prokoshin, A. D.; Andrianov, M. A.; Matyushin, E. A. Radiokhimiya, 1976, 18, (No. 1), 115.
20. Freundlich, W.; Pages, M. C.R. Acad. Sc. Paris, C, 1969, 269, 392.
21. Golub, A. M.; Maksin, V.I.; Perepelitsa, A. P. Zhurnal Neorganicheskoi Khimii, 1975, 20, 867-870.
22. Brixner, L. H. J. Solid State Chem. 1973, 6, 550.
23. Srivastava, J. Radioanal. Chem., 1977, 40, 7.
24. Termes, S. C.; Pope, M. T. Transition Met. Chem. 1978, 3, 103.
25. Lloyd, M. H. "Solution Instabilities and Solids Formation in LWR Reprocessing Solutions." Trans. Am. Nuclear Soc. 1967, Vol. 24.
26. Lloyd, M. H. "Chemical Behavior of Plutonium in LWR Fuel Reprocessing Solutions." Conference: Plutonium Fuel Cycle Process, ANS National Topical Meeting, Miami, Florida, May 1977.

RECEIVED July 24, 1979.

INDEX

A

Absorption	
band of lanthanide ions, UV	136f
spectra	120
of solutions, extraction	122f
of trivalent actinide ions	133f
of trivalent lanthanide ions	133f
of uranyl sulfate solutions	122f
spectrum	
of nitric acid	262f
of uranium(IV) and uranium-	
(VI), UV-visible	269f
Acceptor reaction, Pu	195
Acetic acid as complexing agent	563
Acid(s)	
concentration on U-Pu separation,	
effect of	327
extraction, effect on metal ion	
extraction	75
in oxyanionic molten salt systems	243
recycle	391
-Thorex flowsheet	376
-Thorex process	371-376
Acidic properties of phosphorus-based	
extractants	89
Acidity, extraction of the actinide	
elements—effect of aqueous-	
phase	148
Actinides	
from acidic nuclear waste, parti-	
tioning of	395-409
alkyl phosphoric acid, extractants for	78
azide complexes, trivalent	132
bidentate extraction of	467-474
from bismuth into ammonium	
chloroaluminate, extraction of	184
in calcine	397f
complexes with orthophenanthro-	
line, formation constants of	
trivalent	139t
complexes, stability	134
concentration of PRF salt waste,	
reduction of precipitation-ion	
exchange process	22-24
di(2-ethylhexyl)phosphoric acid	
(HDEHP) extraction of tri-	
valent	147
diisodecylphosphoric acid extract-	
ant for trivalent	79
disposal alternatives	538-541
distribution	401f
coefficient	542t

Actinides (*continued*)

effect of H ₂ MEHP on separation	
factors for trivalent	448
effect of complexing agents on	
extractability of	536
elements, effect of aqueous-phase	
acidity on extraction	148
elution from ion-exchange resin	464t
extractants	
alkyl phosphoric acids	72
bidentate carbamoylmethylphos-	
phonates	73
development, comparison, and	
future	71-72
high-molecular-weight amines	76
extraction(s)	110f
of butyl phosphates from	475-494
by Dapex process	72
of detergents from aqueous solu-	
tions of	493-494
by dialkyl phosphoric acid	147
diketones	80
distribution data for	402
effect of redox agents on	538t
by H ₂ MBP and HDBP	485-487
reactions, trivalent	80
of trivalent	79, 103f
formation constants of azides com-	
plexes of trivalent	135t
HDEHP extraction of lanthanides-	414
HDEHP extraction of trivalent	448-450
from HAW, separation of	343
incineration of	541
ions with S donor ligands, com-	
plexes of	140
ions, absorption spectra of	
trivalent	133f
from irradiated nuclear fuels, sepa-	
ration of	337-339
lanthanide oxalates-HLLW,	
precipitation of	442-445
lanthanides partitioning, reverse	
Talspeak mode	414
liquid-liquid solvent extraction of	
trivalent	147
nuclides, preparation of	333-336
orthophenanthroline complexes,	
trivalent	137
oxidations and reductions, photo-	
chemical	269
oxides in molten alkali metal	
nitrates	233
chemistry of	235

Actinides (<i>continued</i>)	
partitioning	
from acidic waste, flowsheet for ..	407f
goals	382-383
partitioning flowsheets	381-392
photochemistry	253-265
photoseparation(s)	264t
processes	263
process waste solutions	24t
purification, effect of Al on ion exchange	467-469
quaternary ammonium salts	77
quantum efficiencies for redox reactions of	258t
recovery	
from acidified salt wastes	390f
flowsheet for	489f
from power reactor fuels	411-423
from scrub solutions	475-494
from treatment liquors	389
recycle	390f, 539
removal	
and disposal	540f
from high sodium waste	408t
hot-cell separation unit for	544f
from Zr-Al coprocess HAW	408t
from salt waste, precipitation-ion exchange removal of	23f
salts of the tertiary amines, extraction of	76
separation(s)	
complexing agents in	131
continuous and discontinuous	566
by dialkyl sulfioxides	77
effect of acid on	437
energy for	568
of fission products from	182
Hepex process—intergroup	79
from HAW	561-569
inorganic sorbents in	17
of man-made	71
nitrogen donor ligands in	131
oxalate precipitation	436-437
photochemical generation of reagents for	272
photochemical techniques	267-274
from Purex HAW, flowsheet of ...	346f
from Purex type HAW	
raffinates	427-439
requirements	398-399
starting solutions for	539-541
sulfur donor ligands in	131
Talspeak process of lanthanide—by tertiary amines	77
solution photochemistry	268
sorbent affinity for	30f
spectroscopy	255t
storage of	539
from titanate beds, elution of	27
from trivalent lanthanides, Tramex process, separation of trivalent	72
Actinium extraction by trioctylphosphine oxide-cyclohexane	74
Adsorption	
coefficient	4, 5t
equation, Np	4
of neptunium(V) on Dowex 1 resin	3
Agent, reducing, hydrazine	321
Air-monitoring sample, Pu-239 in	342f
Airox	
dry pyrochemical processing of oxide fuels	219
process	183
effect of temperature	226-230
proliferation resistance	219-220
pulverization of UO ₂ pellets	228t
for spent uranium oxide-based fuel	220-222
status of development	230
processed fuel, size distribution of ..	223t
processing, cladding after	221f
Alamine-336	77
Aliquat 336	
4(α,α -diocetyl) pyrocatechol, extraction by	108
extraction by	108-111
extraction from alkaline solution, advantages	111
-S chloride, TTA synergism with ...	81
Alkalinity on Eu extraction, effect of ..	112
Alkanes, extraction of U(VI) by bis-(di- <i>n</i> -hexylphosphinyl)	75
Alkyl amines extraction	72
Alkyl phosphoric acids, actinide extractants	72
Alkylpyrocatechols extractants	101
Alpha	
activity	518, 519f
from aqueous waste streams, bone char removal of	19
-bearing waste treatment	341-343
contaminants, residual	438-439
decay of Cm-242	422
emitters, separation from highly radioactive solutions	533-545
radiolysis	518
waste, retrievable	27
waste treatment, solid	385-387
Alumina	
column at 25°C, Pu elution from ...	13t
column preparation	9
effect of HF on Pu retention on	12t
plutonium retention from HNO ₃ on recovery of Pu by sorption onto	9-16
from uranyl nitrate solutions, sorption of Pu traces on	9
Aluminum	
dissolution of	423
on ion-exchange actinide purification, effect of	467-469
-magnesium alloy, recovery of Am from dissolved	472t

- Aluminum (*continued*)
 –magnesium residue, extraction
 chromatography recovery and
 purification of Am from 473t
 oxide–nitric acid medium, Pu in
 residues, processing flowsheet 468f
 zirconium-
 coprocess HAW, actinide
 removal from 408t
 HAW, pilot-plant tests on 409
 waste 396t
 extraction studies with 402–403
- Aluminum oxide–nitric acid medium,
 Pu in 10
- Aluminum-203, trace sorption of
 Pu(IV) onto 13
- Americium
 from aluminum–magnesium residue
 by solvent extraction, recovery
 and purification of 471t, 473t
 –curium
 cross-current stripping of 443f
 decontamination factors 169
 from HLLW, cross-current
 extraction of 443f
 from lanthanides, inorganic sor-
 bents use in separating 17
 recovery from HAW, flowsheet .. 415f
 separation 157
 in centrifugal contactor 169, 171t
 process, flowsheet of 170f
 Talspeak separation of 414
 decontamination 470–474
 diluent effects, extraction of 399–400, 408
 distribution coefficients, effect of
 oxidizing reagents on 168
 distribution ratios of 344f, 345
 effect of H₂MEHP concentration
 on the separation factor for 450t
 extraction 74
 from alkaline solutions by 4(α,α -
 diocylethyl) pyrocatechol .. 111
 from lithium chloride with tri-
 octylphosphine 74
 from nitric acid solutions 105t
 studies 158–160
 from high-level wastes, removal
 of 441–452
 ion-exchange process for 457
 kinetic studies 158
 oxide product, impurities in 472t
 with pressurized ion exchange,
 purification of 515
 recovery
 from α -radioactive aqueous waste,
 flowsheet for Pu and 342f
 from dissolved Al–Mg alloy 472t
 by ion exchange 466f
 plant test 517
 process 456f
 and purification 455–474
- Americium (*continued*)
 from resins 459–467
 from salt residues 466f
 separation from lanthanides .. 27–31, 345
 by tricaprylmethylammonium
 nitrate extraction, recovery of .. 417
 using a centrifugal contactor, selec-
 tive extraction of hexavalent ... 157
- Americium (III)
 cation by *bis*-2-ethylhexyl phos-
 phoric acid and *bis*-2,2-di-
 methylhexyl phosphoric acid,
 extraction of 79
 distribution
 coefficients of 141t
 coefficients, U(VI)O₂ and 165t
 ratio of Eu(III) 138f
 ratios of U(VI), Pu(IV), and 486f
 effect of ionic strength on oxidation
 rate of 162–164
 extraction 106f, 110, 113f
 kinetics of 79
 from lithium chloride by tertiary
 amines 76
 oxidation
 kinetics 160, 163f
 effects of nonoxidizable com-
 plexing agents 162
 rate, influencing factors 161t
 silver-catalyzed 160
- Americium (VI)
 concentration in organic phases 166f
 –curium (III) separation by extrac-
 tion chromatography 49t
 –curium (III) separation by solvent
 extraction 164–168
 dioxide, reduction rates of 172t
 fixation band 48
 procedure for extraction chroma-
 tography for separation of 47
- Americium-241
 dissolution in nitric acid 505
 from plutonium scrap, recovery
 of 417–418
 from PRF salt waste, metal
 hydroxide scavenging of 25
 recovery from aqueous raffinate 22
 recovery and purification, ion-
 exchange resins for 17
 sorption 26t
 Talspeak process, purification of ... 36
 tracers 398
- Americium 241/243 from HAW,
 recovery of 414–417
- Americium-243 recovery and purifi-
 cation, ion-exchange resins of 17
- Amex process, U extraction by 72
- Amines
 actinide extractants, high-molec-
 ular-weight 76
 actinides separation by tertiary 77

Amines (<i>continued</i>)	
alkyl	72
extraction of actinides by salts of tertiary	76
Ammonium chloroaluminate, extraction of actinides from Bi into	184
Ammonium salts, for actinide extraction	77
Amylhydroquinone reductant, 2,5-di-tert	361-363
Anion resin applications	17
Aquafor process	286
Aqueous reprocessing methods, spent reactor fuel, proliferation risks	178
Aralox process	476-494
Atom models, Leybold-Hereaus	481
Azide complexes, trivalent actinide and lanthanide	132
B	
Backextraction, Pu	310f
Bases in oxyanionic molten salt systems	243
Bed(s)	
design, bone char	21
titanate powder	25
elution of actinides from	27
Benzene solvents, DHDECMP-decallin-diisopropyl	400
Benzoylacetone, extraction of Pu(IV) by	80
Beta proportional counting	548
Bismuth	
carbide fuel, reprocessing in liquid	182
extraction of actinides from	184
phosphate process	279
Bond	
distances, Ce-O	574
distances, Pu-O	575
length-bond strength relations, Zachariassen's	574-575
strengths	
around molybdenum	575
around zirconium	575
metal-oxygen	577
Bone char	
bed design	21
calcium hydroxyapatite $[\text{Ca}_{10}(\text{PO}_4)_6(\text{OH})_2]$	17
decontamination of waste streams	19
physical properties of	18
removal from aqueous waste streams	
of alpha activity	19
of Pu-238 and Pu-239	19
Brønsted equation	164
C	
Cadmium-based reducing agents	182
Cadmium-magnesium alloys, solubilities in	212f, 213, 215f
Calcination	553t
Calcium recycle process	215f
electrolysis of calcium oxide	213-214
Calcium reduction, process parameters for	216
Californium with pressurized ion exchange, purification of	515
Carbamoylmethylphosphine (CMPs) extractants	75
bidentate	73
Carbamoylphosphonates (CPs) extractant	75
Catalyst	
ferrous nitrate	420-421
mercuric ion	517
Pu reduction	520-522
PD black	517
RH black	433
Caustic waste	433
decontamination, development of sorption system for	21
sorption of	21
treatment, plant-scale design for	21
Celestin reactors	33
Celite 545	34
Cell, electro-oxidation	314f
CEN-FAR processes	35
CEN-FAR TBP process; fixation, scrubbing, and elution	37
Centrifugal contactor(s)	
americium-curium separation	169, 171t
residence time for	520
selective extraction of hexavalent using a	157
Centrifugal separator	517
Cerium	
distribution coefficients for	192
as an oxidation catalyst	511-513
-oxygen bond distances	574
plutonium and uranium, distribution of	194f
Cerium(IV)	
/cerium(III) ratio effect on dissolution rate	512
consumption by fission products	513
effect on Ru	513
nitrates, tributyl phosphate extractant for	72
plutonium dissolution in nitric acid-	511-513
Chelating agent(s)	341, 457, 493
Chloride(s)	
distillation	347
effect in leachant	383
solutions, Ac extraction from	74
standard free energies of formation of	193t
by tertiary amines, Am(III) extraction from Li	76
Chromatographic separation, elution curve of	340f

- Chromatography
 column behavior 48-49
 extraction
 columns, characteristics of 34*t*
 for plutonium-irradiated targets .. 33
 reagents 34
 for separation of Am(VI) and
 Cm(III), procedure for 47
- Chromatography
 column elution 31
 extraction 33, 54*t*
 Am(VI)-Cm(III) separation by 49*t*
 characteristics of irradiated
 targets for 35*t*
 stationary phase—preparation of 34
 ion exchange 387-388, 441
 liquid 399
- Civex process 207, 220, 225, 272
- Cleanex
 feed solutions, composition of 154*f*
 feeds, iron impurity in 152
 process 147, 431
 advantages in batch process
 extractions 155
 chemistry 147-148
 equipment 149, 150*f*
 extraction 151
 feed adjustment 149, 151
 scrubbing 152
- CMP (*see* Phosphonate, dihexyl-*N,N*-
 diethyl carbonylmethylene)
- Column(s)
 breakthrough curve of Pu on
 aluminum oxide 11*f*
 electropulse 286
 laboratory scale 284*f*
 scale-up calculations for 297
 electroreduction 313*f*
 pulsed 308-312
 elution curve of Pu-239 from
 aluminum oxide 14*f*
 extraction chromatography 433
 for in-situ electroreduction,
 pulsed extraction 311*f*
 ion-exchange 343
 plutonium extraction in pulsed 437
 pulsed plate 409
 separation 564*f*
 for treatment of low-risk waste,
 bone char 20*f*
 uranium extraction in pulsed 437
- Complexing agent(s) 73, 450
 acetic acid as 563
 in actinide separations 131
 on Americium(III) oxidation
 kinetics, effects of 162
 effect on extractant selectivity 111
 on extractability of actinides,
 effect of 536
 on extraction, effect of 73, 108-109, 431
- Computer code, solvent extraction .. 354-355
- Concentration profiles
 for nitric acid 355
 for plutonium 355
 for thorium 355
- Contactor(s)
 centrifugal 159*f*
 electrolytic 285*f*
 tests 351-354
- Coordination
 cavities 573
 complexes, guest metal ions in 573
 sphere around uranyl, oxygen 572
- Core, axial blanket fuel assembly 198*t*
- Corrosion products 566
- Crucible turntable 196*f*
- Curium
 -americium
 cross-current stripping of 443*f*
 decontamination factors 169
 from high-level liquid waste,
 cross-current extraction of 443*f*
 from lanthanides, inorganic sor-
 bents in separating 17
 separation 157
 centrifugal contractor 169
 process, flowsheet of 170*f*
 in centrifugal contractor,
 results of 171*t*
 Talspeak 414
 and Einsteinium by dibutyl (di-
 ethylcarbamoyl)-phosphonate
 (DBDECP), extraction of 75
 from high-level wastes, removal
 of 441-452
 isotopic composition of 47*t*
 with pressurized ion exchange,
 purification of 515
 recovery
 from high-level waste, flowsheet
 for Am 415*f*
 plant test 517, 517*t*
 separation from lanthanides 27
- Curium (III)
 cation by *bis*-2-ethylhexyl phos-
 phoric acid and *bis*-2,2-di-
 methylhexyl phosphoric acid,
 extraction of 79
 procedure for extraction chroma-
 tography separation of 47
 separation by extraction chroma-
 tography, Am(VI)- 49*t*
 separation by solvent extraction,
 Am(VI)- 164
- Curium-242, alpha decay of 422
- Curium-244
 recovery from HAW 414-417
 recovery and purification, ion-
 exchange resins of 17
 Talspeak process, purification of 36
 tracer 148

Current efficiency in electropulse column	295	Dibutyl (diethylcarbamoyl) phosphonate extraction equation	75
Current-potential curves		Diethylenetriaminepentaacetic acid (DTPA)	389
determination of	317-319	Diketones extraction of actinides	80
for platinum	325f	Diluent effects, extraction of Am	399-400
cathode	318f	DIPB extractant, decalin-	409
for titanium cathode	320f	Diphosphine extractant, vinylene	75
Cyclohexane, actinium extraction from chloride solutions by tri-octylphosphine oxide-	74	Dissolution	
		disadvantages of F in plutonium oxide	510
		effects of metallic ions on	509-511
		in nitric acid-fluorhydric acid, plutonium dioxide	506-508
		in metal nitrate melt of the sodium diuranate	246
		in nitric acid	
		Americium-241	505
		-cerium(IV), plutonium dioxide	511-513
		-hydrofluoric acid, thorium dioxide	507
		plutonium dioxide	500-506
		of plutonium dioxide	
		acidic	499-500
		effect of fluoride on nitric acid	505-506
		kinetics	506
		pyrochemical	500
		standard potentials for oxidative rate, Ce(IV)/Ce(III) effect on	512
		rate, Ce(IV)/Ce(III) effect on	512
		Distribution	
		coefficient (s)	27, 37, 117, 127t, 134
		of acidic Pu(IV)	537f
		actinide	542t
		of americium (III)	141t
		for cerium	192
		determination of	400-402
		effect of oxidizing reagents on	
		Am	168t
		effect of oxidizing reagents on	
		U(VI)	165, 168t
		equation	28
		for H ₂ MEHP	450
		of metallic species	140
		of neodymium(III)	136f
		for plutonium	192
		of plutonium(IV)	536t
		temperature dependence of	126t
		temperature-effect on	125
		of tracer praseodymium ³⁺ , effect of DHDECMP impurities on	451t
		of trivalent TPE	106f
		uranium	74, 192
		of uranium(VI)	79, 140, 142f
		dioxide and Am(III)	165t
		data for DHDECMP and high sodium waste	405t
		data for extraction of actinides	402
D			
Dapex process	147, 431		
actinide extraction by	72		
DBDECMP (dibutyl- <i>N,N</i> -diethylcarbamylmethylenephosphonate)	398		
DBDECP (Dibutyl(diethylcarbamoyl) phosphonate)	75		
DBP (<i>see</i> Phosphate, dibutyl)			
Decalin			
-DIPB extractant	409		
-diisopropyl benzene solvents, DHDECMP-	400		
extractants, DHDECMP-	400		
Decladding	185, 197, 222, 244, 303		
Decomposition of uranyl nitrate, thermal	550-551		
Decontamination			
americium	470-474		
of caustic waste, pilot-plant test of filtration	23f		
development of a sorption system for caustic waste	21		
factor(s)	491, 493, 517, 525, 561, 566, 568		
americium	408		
americium-cerium	169		
effect of Zr on	347		
gamma	420-421		
for plutonium	474		
zirconium-95	375f		
fission product	187		
of Hanford PRF waste, sodium titanate	22-27		
incinerator ash	386-387		
of waste streams, bone char	19-31		
Denitration of HAW solutions	433		
Desorption			
effect of temperature on Pu	13		
from inorganic sorbents, nuclides ..	28		
of plutonium(IV) from uranyl nitrate	16		
of radionuclides from inorganic ion exchangers, nitric acid	31t		
DHDECMP (Phosphonate, dihexyl- <i>N,N</i> -diethylcarbamyl-methylene-)			
Dialkylthio phosphates	131		

- Distribution (*continued*)
- ratio(s) 482, 487
- of americium 344*f*, 345
- determination of 92
- effect of nitric acid concentration on 487
- of Eu(III)/Am(III) 138*f*
- extractants 482*f*
- of HDBP 480*f*
- measurements of 476
- of NaDBP 485*t*
- of Na₂MBP 485*t*
- nitric acid concentration profile and 357*f*
- of nuclide 91
- of plutonium 365, 367*f*
- effect of nitrous acid on 367*f*
- thorium concentration profile and 356*f*
- of Th(IV) extraction 92, 93*f*
- of U(VI), extraction 92, 93*f*
- of U(VI), Pu(IV), and Am(III) 486
- of Y(III) 485
- Donor reaction, plutonium 195
- Dowex 1 resin 7
- adsorption of Np(V) on 3
- Dowex 2 resin 7
- DSA (*see* Sulfuric acid, dodecyl)
- DTPA (diethylenetriamine pentaacetic acid) 389
- Dry processing of spent reactor fuel .. 177
- E**
- EDTA titration, U(VI) determination by 117-118
- Electrochemical partitioning 283
- Electrode reactions 304-305
- Electrolysis of calcium oxide, calcium recycle process 213-214
- Electrolytic contactors 285*f*
- Electrolytic reduction
- in situ 283
- of Pu(IV) 321-323
- separation of U and Pu by 317-330
- of U(VI) 321, 323
- Electron photomicrographs of ion-exchange resin, scanning 529*f*
- Electropulse column(s) 283, 286, 293*f*, 386
- design 292-294
- laboratory-scale 284*f*
- scale-up calculations for 297
- testing of 294
- for uranium-plutonium partition 291-300
- uranium transfer rate 297
- Electroredox of plutonium in power reactor fuel reprocessing 303-315
- Electroreduction, in-situ 303
- Electroreduction monocoil 319
- Eluting agent 13
- Elution of actinides from titanate beds 27
- Elution of radionuclides, effect of pH on 28
- Elutrient, HNO₃-FeSO₄ as an 12-13
- Energies of formation of chlorides, standard free 193*t*
- Energy for actinide separation 568
- Entrainment in aqueous phase, organic phase 153
- Equilibria, extraction 125
- Equipment, continuous separation 567*f*
- Ether(s)
- coordinative extractant 73
- extractants, disadvantages 71-72
- linkage in extractants 79
- Europium
- effect of H₂MEHP concentration on the separation factor for 450*t*
- extraction from alkaline solutions by 4(α,α -dioctylethyl) pyrocatechol 111
- extraction, effect of alkalinity on 112
- Europium(III)
- /americium(III), distribution ratio of 138*f*
- distribution coefficients of 141*t*
- extraction of 110*f*, 113*f*
- Evaporator, design 343
- Extinction coefficient 132
- Extractability of actinides, effect of complexing agents on 536
- Extractants
- for acidic degradation products, 2-ethylhexanol 388
- acidic properties of monoacidic phosphorus-based 89
- for actinides, alkyl phosphoric acids advantages of neutral phosphorus-based organic 97
- alkyl phosphoric acids, actinide 72
- alkylprocatechols 101
- bidentate carbamoylmethylphosphonates, actinide 73
- bis(2-ethylhexyl) phosphoric acid .. 398
- carbamoylmethylphosphonate (CMPs) 75
- carbamoylphosphonates (CPs) 75
- characteristics of tetraphenylmethylene phosphine 105
- concentration effect on element separation 112
- decalin-DIPB 409
- dependencies of extraction of Th(IV) and U(VI) 94
- development, comparison and future 71-72
- DHDECMP-decalin 400
- di-(2-ethylhexyl) phosphoric acid .. 343
- disadvantages, ether 71-72

Extractants (*continued*)

distribution ratios	482f
effect(s)	
of gamma irradiation on Pu	345
of hydrogen bonding in	144
of radiation on organic	153
radiolytic	400
ether linkage in	79
for HDBP, alcohol	478-481
for HDBP, carboxylic acid	478-481
high-molecular-weight amines	76
ion exchange	78
monodentate phosphate compounds, coordinative	73
organophosphorus bidentate	398
polydentate neutral organophosphorus	75
with preselected properties	101
purification	89
quaternary	91
selectivity	101
complexing agents, effect on	111
influencing factors	107
phosphorus-oxygen bond, effect on	107
steric influences	105-107
steric properties of	90
monoacidic phosphorus-based	89
structural considerations for	97
sulfonic acids, ion exchange	80
sulfoxides	77
in synergistic systems with TBP and and TOPO, pyrazolones	81
tetraalkyldiphosphinedioxides	75
tetraalkyldiphosphonates	75
of transplutonium elements by tetraphenylmethylene phosphine dioxide	104
tri-(2-ethylhexyl) phosphate (TEHP) use as	72
tributyl phosphate (TBP)	
advantages and disadvantages of	72
for cerium (IV) nitrates	72
for thorium nitrates	72
for uranyl nitrates	72
trihexyl phosphate (THP) use as	72
trioctylphosphine oxide (TOPO)	74
for trivalent actinides, diisodecylphosphoric acid	79
vinylene diphosphine	75
Extraction	
absorption spectra of solutions	122f
acetic acid, diethylenetriamine-penta-, (H_5 DTPA)	482
acid concentration, effect on	74
acid extraction, effect on metal ion	75
of the actinide elements, effect of aqueous-phase acidity	148

Extraction (*continued*)

actinide(s)	
by Aliquat 336 4(α,α -dioctylethyl) pyrocatechol	108
bidentate	467-474
from bismuth into ammonium chloroaluminate	184
by Dapex process	72, 110f
diketones	80
distribution data for	402
nitrates, TBP	73
phosphoric acid, dibutyl (HDBP)	485-487
phosphoric acid, monobutyl (H_2 MBP)	485-487
of actinium from nitrate media, use of trioctylphosphine oxide	74
by Aliquat 336	108-111
from alkaline solutions by 4- α,α -dioctylethyl pyrocatechol	
Am and Eu	111
by alkyl pyrocatechol	111-114
americium	74
of americium, diluent effects	399-400
of americium-curium from HLLW, cross-current	433f
of americium (III)	73, 106f, 110f, 113f
by Amex process, uranium	72
of aqueous solutions of uranyl salts	
by TOPO	127t
batch solvent	147
of butyl phosphates from actinides	475-494
capacity, structural modification—effect on	102
from chloride solutions by trioctylphosphine oxide-cyclohexane, actinium	74
chromatography	469, 542-543
americium (III)	166f
americium (VI)-curium (III) separation by	49t
solvent	164-168
characteristics of irradiated targets for	35t
column behavior	48-49
columns, characteristics of	34t
equipment, preparation of	34
for plutonium-irradiated targets	33
reagents	34
recovery and purification of Am from Al-Mg residue	473t
for separation of Am(VI) and Cm(III), procedure for	47
stationary phase preparation	34
Cleanex process	151
advantages in batch process	155
coefficient for trivalent metal, equilibrium	148

Extraction (*continued*)

column for in-situ electroreduction, pulsed	311f
computer code, solvent	354-355
concentration dependence of metals	109
constants	89, 98
counter-current	345-347, 491
liquid-liquid	476-477, 488
cross-current	442
of curium and einsteinium by DBDECP	75
of curium ³⁺ by <i>bis</i> -2-ethylhexyl phosphoric acid and <i>bis</i> -2,2- dimethylhexyl phosphoric acid	79
of detergents from aqueous solu- tions of actinides	493-494
dibutyl-butylphosphonate	398
distribution ratio of Th(IV)	93f
distribution ratio of U(VI)	93f
effect	
of alkalinity on Eu	112
of complexing agents	108-109
of redox agents on actinide	538t
of temperature on	482
efficiencies of TOPO for uranyl salts	125
equation, dibutyl (diethylcar- bamoyl) phosphonate	75
equilibria	125
equilibrium curve for HNO ₃	484
fission product	383
flow diagram, counter-current liquid-liquid	492f
flowsheet, solvent	524
for laboratory mixer settlers	516f
for neptunium	413f
Thorex	351
of hexavalent Am using a cen- trifugal contactor, selective	157
hot-cell studies of DHDECMP	442
hydroxyl groups, effect on alkaline ..	109
isothermal	118-120
kinetics of Am(III)	79
kinetics of Th(IV)	79
of lanthanides	110f
liquid-liquid	89, 199, 470
countercurrent	33
solvent	469
-actinides, HDEHP	414
by Aliquat 336 4(α,α -dioctylethyl) pyrocatechol	108
liquid-liquid	561
from lithium chloride by tertiary amines, Am(III)	76
from lithium chloride with trioctyl- phosphine, Am	74
mercury	406
methyl-isobutyl ketone	395
nitric acid dependency of U(VI) ..	96f

Extraction (*continued*)

from nitric acid solutions, Am	105t
of <i>bis</i> - <i>n</i> -octyl phosphoric acid, and <i>bis</i> -2,2-dimethylhexyl phos- phoric acid	79
phosphate, sodium dibutyl (NaDBP)	485
phosphate, sodium monobutyl (Na ₂ MBP)	485
of phosphoric acid	481-482
dibutyl	481-482
di(2-ethylhexyl) (HDEHP)	416, 431-433
monobutyl (H ₂ MBP)	481-482
by photochemical reduction, Pu solvent	270
pilot plant, solvent	372f
process, molten salt	455-474
of protactinium(IV) by benzoyl- actinide	77
in pulsed columns, Pu and U	437
quaternary ammonium salts, actinide	77
reactions, trivalent actinide	80
recovery of Am by triacrylmethyl- ammonium nitrate	417
recovery and purification of Am from Al-Mg residue by solvent ..	471t
scrub-strip studies, DHDECMP	404t
selectivity, steric factors influence on	77
separation of Am from the lantha- nides by solvent	345
separations, steric hindrance— importance in liquid-liquid	98
single-cycle	124f
solutions, IR spectra of	124f
solvent	71, 435-436, 515
stripping process	438
studies	
americium	158-160
on high sodium waste	403
of sulfuric acid, dodecyl	482
with zirconium-aluminum waste	402-403
systems, acidic	125-128
systems, synergistic solvent	80
tests on HAW solutions, HDEHP batch	435t
by <i>cis</i> -tetraphenylvinylenediphos- phine dioxide	76
by the <i>cis</i> -tetraolylvinylene diphos- phine dioxide	76
thenoyl trifluoroacetone (TTA)	80
of thorium into neutral phosphorus- based organic extractants	93t
of thorium(IV)	95f
acid solutions, TOPO	117
distribution ratios of the	92

Extraction (<i>continued</i>)	
of thorium(IV) (<i>continued</i>)	
extractant dependencies of	94
nitric acid dependencies of the	94, 96f
separation factors for the	92, 94
of transplutonium elements (TPE)	
from acid solution	101
from alkaline solutions	108
solvent	101-114
of transuranium elements	534-538
with tributyl phosphate (TBP)	279,
333, 351, 395, 398, 409, 421, 428-431	
countercurrent	429
solvent	388
by trioctylammonium nitrate, Pu	35
of trivalent actinides	79, 103f
bidentate	399
by dialkyl phosphoric acid,	
reactions	78
di(2-ethylhexyl) phosphoric acid	
(HDEHP)	147, 448-450
liquid-liquid solvent	147
of trivalent lanthanides	103f
di(2-ethylhexyl)phosphoric	
acid (HDEHP)	147, 448-450
liquid-liquid solvent	147
of uranium	
from acid, octaethyltetraamido-	
pyrophosphate (OETAPP)	76
into neutral phosphorus-based	
organic extractants	93t
synergistic systems of organo-	
phosphorus compounds in	81
of uranium (VI)	95f, 106f, 119f, 166f
acid solutions, TOPO	117
distribution ratios of the	92
extractant dependencies of	94
from mineral acids by <i>bis</i> -(di- <i>n</i> -	
hexylphosphinyl) alkanes	75
nitric acid dependencies of the	94
separation factors for the	92, 94
from sulfuric acid solution	
procedure	117-118
by tri- <i>n</i> -octyl phosphine	
oxide	117-128
with TOPO solvating reaction	118
synergistic	140
of uranyl nitrate, steric considera-	
tions in the	75
F	
Fast-breeder reactor fuels, repro-	
cessing diagram of	348f
FeSA (<i>see</i> Sulfamate, ferrous)	
Ferrous	
nitrate catalyst	420-421
sulfamate	469
sulfate-nitric acid as an elutriant	12-13
Filterometer	55
Filtration time(s)	
calculation of	55
effect of variables	60f
plutonium peroxide, effect	
digestion time on	62
of hydrogen peroxide on	62
of impurity concentration on	62
of temperature on	62
Fissile material(s)	351
dilution of	225
recycling	230
Fission product(s)	422, 488, 534, 566
behavior	241, 247
cerium(IV), consumption by	513
control, pyrometallurgical process	211
decontamination	187-188, 248-249, 347
effect of acidity on	352
factors for transplutonium	
fractions	43, 43t
elements, precipitation of	243
extraction	383
groups	183t, 192
half life of	561
heavy metal concentration	187
isotopes	411
in molten alkali metal nitrates	234
precipitation of	416
removal	224t
waste management, aqueous	395
zirconium	373, 525t
Flow diagram	
counter-current liquid-liquid	
extraction	492f
extractor phases	159f
for plant-scale bone char treatment	
of low-risk waste	20f
Flowsheet(s)	
partition cycle	374f
actinide partitioning	381-392
for actinide partitioning from	
acidic waste	407f
of actinide separation from Purex	
HAW	346f
for actinides recovery	489
of americium-curium separation	
process	170f
for americium recovery from HAW	415
development	395-409
for experimental runs on Talspeak	
Cycle	449f
of fluorination pilot plant	554f, 555
of HAW processing	563
of the HAW processing	564f
for laboratory mixer settlers, solvent	
extraction	516f
for neptunium, solvent extraction	413f
for partitioning of U and Pu	326f
plant tests of Np-237-Pu-238	525t
for precipitation of lanthanide	
oxalates	446f

- Flowsheet(s) (*continued*)
- for processing Al residues 468f
 - for processing sodium carbonate scrub solutions 487-494
 - proliferation resistant 287
 - for recovery of Pu traces 15f
 - solvent extraction 524
 - testing 477
 - equipment 371
 - tests 416
 - thorex solvent extraction 351
 - thorium 373
 - for thorium-based fuels 209f
 - for thorium-uranium-plutonium fuel, thorex 353f
 - tributyl phosphate (TBP) 418
 - of uranium calcination pilot plant .. 554f
 - for waste treatment 406
- Fluidized-bed processes 547-558
- Fluorhydric acid, PuO₂ dissolution in HNO₃- 506-508
- Fluoride
- effects of 375f
 - complexing metal ions on dissolution 509-511
 - in leachant 383
 - on nitric acid dissolution of PuO₂ 505-506
 - on thorium-uranium separation 371-373
 - in plutonium oxide dissolution, disadvantages of 510
 - volatility process 347
- Fluoridic-nitric acid solutions, Pu traces recovery by sorption onto alumina 9
- Fluorination
- pilot plant, flowsheet of 554f
 - reactor 549, 555-556
 - sorption procedure 549-550
 - technetium in pilot-plant 557
- Fluorine in fluorinator off-gas 558f
- Fluoro complexes, Zr 510
- Formation constants
- of azide(s) complexes
 - calculation of 132, 137
 - of trivalent actinide 135t
 - of trivalent lanthanide 135t
 - of trivalent actinide complexes with orthophenanthroline 139t
- Fuel(s)
- Airox dry pyrochemical processing of oxide 219
 - Airox process for spent U oxide-based 220
 - aqueous reprocessing of nuclear 345-347
 - assembly, core-axial blanket 198t
 - components, laser separation of reactor fuel 253
- Fuel(s) (*continued*)
- cycle(s)
 - concept 533-534
 - denatured 287
 - fast-breeder reactor 225
 - light-water reactor 222-224
 - thorium 207, 351, 371
 - uranium 533-545
 - decladding of spent 303
 - dissolution, spent 197
 - dry processing of light-water reactor 183
 - dry reprocessing of nuclear elemental and isotopic composition of spent Th-U 533t
 - enrichment, Civex process for 225
 - enrichment, Pyrocivex process for .. 225
 - flowsheet for thorium-based 209
 - heavy element separation for Th-U-Pu 351-368
 - manufacture, Pu recycled for 247
 - molten cadmium/salt reprocessing, carbide 182
 - nonaqueous reprocessing method for thorium-based 207-216
 - partitioning scheme for U_r-Pu-Th 288f
 - plutonium breeder 280
 - processing
 - carbide 182
 - molten salt oxidation-reduction processes for 233-250
 - pyrochemical 196f
 - pyrometallurgical method for the reprocessing of thorium-based 208-211
 - reaction rate of UO₂ 227f
 - recovery of actinides from power reactor 411-423
 - recycle requirements 248
 - recycle systems, reactor 177
 - recycling, fast-breeder reactors 177
 - reprocessing
 - advantages, PDPM in spent 179
 - applicability of photochemistry to 254
 - diagram of fast-breeder reactor .. 348f
 - electroredox of Pu in power reactor 303-315
 - in liquid bismuth, carbide 182
 - plutonium partitioning methods in power reactor fuel 279-288
 - reduction in 214-216
 - requirements, Th 208
 - salt transport processing of Th-U and U-Pu oxide and metal 182-183
 - separation of actinides from irradiated nuclear 337-339
 - size distribution of Airox processed 223t

Fuel(s) (<i>continued</i>)	
spent reactor	
dry processing of	177
proliferation risks, aqueous	
reprocessing methods	178
pyrochemical process for	177, 195-199
Salt Transport Process for U and Pu in	191-205
thorex flowsheet for Th-U-Pu	353f
tin process for reactor	184
zinc distillation process for spent mixed-oxide	185
zinc distillation of uranium oxide-plutonium oxide	186f
G	
Gamma	
activity	518
of first cycle solvent	520f
decontamination factor	420-421
irradiation on Pu extractants, effects of	345
radiation in fissile material	178
GAS CHROM Q	34
H	
Hafnium effect on Pu retention on alumina	12t
Half life of fission product	561
HAN (<i>see</i> Hydroxylamine nitrate)	
Hanford Plutonium Reclamation Facility (PRF) salt waste	22
reduction of actinide concentration of precipitation-ion-exchange process	22-24
Hanford Plutonium Reclamation Facility waste, sodium titanate decontamination of	22-27
HAW (<i>see</i> Waste, high activity)	
HDBP (<i>see</i> Phosphoric acid, dibutyl)	
HDEHP (Phosphoric acid, di(2-ethylhexyl)-)	431
H ₅ DTPA (Acetic acid, diethylenetriamine penta-) extraction of	482
HEPA filter treatment	385-386
Hepex process, intergroup actinide separation	79
Hexanol, 2-ethyl-, extractant for acidic degradation products	388
Hexylphosphinyl, di- <i>n</i> alkanes, extraction of U(VI) by <i>bis</i> -	75
H ₂ MBP (<i>see</i> Phosphoric acid, monobutyl)	
H ₂ MEHP (<i>see</i> Phosphoric acid, mono(2-ethylhexyl)-)	
Holding agents	292
Hot-cell separation unit for actinide removal	544f
Hydration, surface	505
Hydrazine	
aqueous Pu with HAN and holding reductant	521f
oxidation of	280
reducing agent	304
reducing agent	321
Hydrogen bonding in extractants, effect of	141
Hydrogen reductant for U-Pu partitioning	282
Hydrolytic damage to TBP extractant solutions	487-488
Hydroxide ion, selectivity of the	7
Hydroxyl groups, effect on alkaline extraction	109
Hydroxylamine nitrate (HAN)	
aqueous plutonium with ferrous sulfamate and	522f
effect of acidity on reduction rate of Pu(IV) by	361
and ferrous sulfamate, U-Pu partitioning with	523t
and hydrazine, aqueous Pu with plutonium reductant	521f
in primary U-Pu partitioning	352, 523
reaction mechanism and reduction kinetics of Pu-reductant	282
reductant	359
replacement of FeSA under plant conditions	522-523
waste reduction	518-523
Hydroxylamine salts reductants of Pu	282
Hyfrane 130	164
I	
Icosahedron geometry	573
Incinerator ash decontamination	386-387
Inductive effects	481
Infrared evaporating system for treatment of α -radioactive waste	344f
Infrared spectra	120
of extraction solutions	124f
Infrared spectroscopy	118
Iodine removal	524
Iodine, volatilization of	234
Ion	
exchange	561
actinide purification, effect of Al on	467-469
americium recovery by chromatographic separation of the transplutonium elements from lanthanides	337
chromatography	387-388, 441
effect of DHDECMP degradation products in	450
column	343
contactor, continuous	286

Ion (*continued*)

exchange (<i>continued</i>)	
elution curve of group separation by	338f
extractants	78
sulfonic acids-	80
plutonium recovery by	465f
process	
for americium	457
for plutonium	457
precipitation-reduction of	
actinide concentration of PRF salt waste	22-24
recovery of Ne	412
resin(s)	
actinide elution from	464t
properties of	457, 459, 467
recovery and purification	
for Am-241	17
of Am-243	17
of Cm-244	17
scanning electron photomicrographs of	529f
scheme for removal of actinides from salt waste, precipitation-	23f
separation	
of Am from lanthanides	345
of neptunium and plutonium	528-530
of plutonium-238 and neptunium-237 by	530t
of transuranium elements	337
with pressurized purification	
of americium	515
of californium	515
of curium	515
exchangers	
inorganic	18-19
nitric acid desorption of radionuclides from	28-31t
migration, countercurrent	561-569
Ionic exchange in sulfate-sulfuric acid solutions, Np(V)	3
Ionic exchanger, sodium titanate	25
Iron	
dissolution and filtration, selective ..	421
hydroxide precipitation	
decontamination of actinide-containing waste solutions ..	24
impurity in Cleanex feeds	152
targets, processing of irradiated Np-oxide-	419f
Irradiated targets for extraction chromatography, characteristics of ..	35t
Isobutyric acid element, α -hydroxy ..	423
Isothermal extraction	118-120
Isotopes	
fission product	411
production of heat source	411-423
transuranium	411

K

Ketone extraction, methyl-isobutyl	395
Kinetic(s)	
americium(III) oxidation	160, 163f
of fluorination of UO_3	555
of plutonium dioxide dissolution	506
of plutonium(IV) oxidation	363
studies, Am	158

L

Lanthanide(s)	
-actinides, HDEHP extraction of ..	414
-actinide separation, Talspeak process of	73
americium separation from	27
azide complexes, trivalent actinide ..	132
complexes, stability	134
curium separation from	27
elements, Pu chemical similarities with Th and	9
extraction of	110f
trivalent	103f
fixation	48
inorganic sorbents use in separating Am and Cm from	17
ion-exchange chromatographic separation of the transplutonium elements from	337
ion exchange separation of Am from ions with sulfur donor ligands, complexes of	140
ions, UV absorption band of	136f
oxalates	
flowsheet for precipitation of	446f
high-level liquid waste, precipitation of actinide-	442-445, 447t
partitioning reverse Talspeak mode, actinides-	414
separation	
conditions for transplutonium-	40t
preliminary operations to transplutonium/	37
of transplutonium elements from	35, 337-339
by solvent extraction, separation of Am from	345
sorbent affinity for	30f
trivalent	
complexes with orthophenanthroline, formation constants of ..	139t
di(2-ethylhexyl) phosphoric acid (HDEHP) extraction of	147, 448-450
effect of H_2MEHP on separation factors for	448
formation constants of azides	
complexes of	135t
ions, absorption spectra of	133f
liquid-liquid solvent extraction ..	147

- Neptunium (*continued*)
 oxide-iron targets, processing of
 irradiated 419f
 in perchloric acid, photoredox
 reactions of 259-261
 photochemistry of 254
 and plutonium
 combination in reprocessing and
 end streams 538-541
 ion-exchange separation 528-530
 partitioning 526-527
 purification of reprocessing end
 streams from 542
 recovery
 and separation of Np-237 and
 Pu-238 from irradiated 17
 by the Purex process 17
 solvent extraction flowsheet for 413f
 valence adjustment of 524
 Neptunium(IV)
 photo-oxidation of 260f
 Neptunium(V)
 adsorption in total sulfate 6f
 compounds 4
 on Dowex 1 resin, adsorption of 3
 ionic exchange in sulfate-sulfuric
 acid solutions 3
 photo-oxidation of 260f
 Neptunium-237
 by ion exchange, separation of
 Pu-238 and 530t
 from irradiated Np, recovery and
 separation of 17
 -plutonium-238 flowsheet, plant
 tests of 525t
 recovery of 412-414
 plutonium-238 from irradiated 418-421
 traced with Np-239 3
 Neptunium-239 tracer preparation 3
 Neutron absorption, parasitic 222
 Neutron cross section 222
 Nitrate(s)
 aqueous Pu with mixtures of
 ferrous or ferric 521f
 conversion, uranyl 547-558
 extraction, recovery of Am by
 tricaprylmethylammonium 417
 media, use of TOPO for the extrac-
 tion of Ac from 74
 molten
 plutonium dioxide in 237-239
 salt oxidation process 184
 uranium dioxide-plutonium
 dioxide in 238-239
 plutonium extraction by trioctyl-
 ammonium 35
 plutonium reduction catalyst,
 ferric 520-522
 removal of residual 552
 salting agent 428-429
 Nitrate(s) (*continued*)
 system, Pu(IV) separation from
 U in 76
 thermal decomposition of uranyl 550-551
 uranium dioxide in molten 235-239
 Nitric acid
 absorption spectrum of 262f
 -aluminum medium, Pu in 10
 americium extraction from 105f
 americium-241 dissolution in 505
 -cerium(IV), PuO₂ dissolution
 in 511-513
 concentration on distribution ratios,
 effect of 487
 concentration profile and distribu-
 tion ratio 357f
 concentration profiles for 355
 dependencies of the extraction of
 Th(IV) 94, 96f
 dependencies of the extraction of
 U(VI) 94, 96f
 desorption of radionuclides from
 inorganic ion exchangers 31t
 dissolution of PuO₂, effect of
 fluoride on 505-506
 electrolytic reduction of 319-321
 extraction, equilibrium curve for 484
 ferrous sulfate as an eluent 12-13
 fluorhydric acid, PuO₂ dissolution
 in 506-508
 -fluorhydric acid, ThO₂ dissolution
 of in 507
 plutonium dioxide, dissolution in 500-506
 reduction 304
 solubility of PuO₂ in 503f
 solubility of plutonium peroxide in
 solution(s), precipitates
 from molybdenum 579
 from plutonium 579
 from zirconium 579
 Nitric-fluoridic acid solutions, recov-
 ery of Pu traces from 9
 Nitrogen donor ligands 131
 Nitrous acid
 destruction in solvent phase, effect
 of sulfamic acid on 366f
 effect
 on distribution ratio of Pu 367f
 on oxidation of Pu(III) 365
 on plutonium purification 412
 stripping of Pu 345
 Nuclear
 fuel cycle, inorganic sorbents,
 disadvantages in 17
 magnetic resonance (NMR) 112, 123
 Nuclide(s)
 desorption from inorganic sorbents 28
 distribution ratio of 91
 preparation of actinides 333-336

O	
Octaethyltetraamidopyrophosphate (OETAPP) extraction of U from acid	76
Octahedral geometries	572
Off-gas condenser	551
Off-gas treatment	391
Opix process	441
Organophosphorus compounds	
bidentate	101
in extraction of U, synergistic systems of	81
reagent grouping of, neutral synthesis, tri-, tetra-, bidentate neutral	102
extractants	398
bidentate	75
polydentate neutral reagents, bidentate	398
Orthophenanthroline complexes, trivalent actinide and lanthanide ..	137
Oxal process	433, 436
engineering	439
Oxalate(s) precipitation	
of actinide-lanthanide HLLW ..	442-445
actinides separation	436-437
equipment for continuous	445
of lanthanide flowsheet for	446f
of lanthanide from synthetic HAW ..	447t
Oxidant, pentavalent V as an	412
Oxidation	
catalyst, Ce as an	511-513
kinetics of Pu(IV)	363
of $N_2H_5^+-U(IV)$, cycle electrolytic of plutonium(III), effect of nitrous acid on	365
potential shift	4
process, molten nitrate salt	184
rates, UO_2	226
reactions of uranium dioxide	244
and reductions, photochemical actinide	269f
states of plutonium in HND_3-HF ..	9-16
Oxygen	
bond strengths, metal-	577
coordination sphere around uranyl ..	572
partial pressure, effect on Airox process	226
P	
Palladium black catalysts	433
Palladium and rhodium precipitation ..	565
Partitioning method with FeSA	280
Partitioning scheme, prereduction	284f
PDPM (<i>see</i> Pyrochemical and dry processing methods)	
Peroxide precipitate, composition of Pu	51
Petrus cell	34
pH on sorption and elution of radionuclides, effect of	28
Phosphate(s)	
compounds, bidentate	75
compounds, coordinative extractants, monodentate	73
dialkyldithio dibutyl (DBP) on Zr separation from Th, effect of	376
dihexyl- <i>N,N</i> -diethyl carbonylmethylene, solvent recycle ..	389-391
extractant, <i>n</i> -tributyl-	371
extractant, tributyl advantages and disadvantages of for cerium(IV) nitrates- ..	72
for thorium	72
extraction	
of butyl from actinides	475-494
of sodium dibutyl	485
of sodium monobutyl	485
(TEHP) use as an extractant, tri-(2-ethylhexyl)	72
Phosphine dioxide, extractant characteristics of tetraphenylmethylene	105
of transplutonium elements by tetraphenylmethylene	104
Phosphine oxide, tri- <i>n</i> -octyl- (TOPO) extraction, acid solutions	
of thorium(IV)	117
of uranium(VI)	117
of uranium(VI) from sulfuric ..	117-128
extraction of aqueous solutions of uranyl salts by	127t
IR assignments for aqueous uranyl sulphate	123
NMR assignments for aqueous	123
pyrazolones extractants in synergistic systems with TBP and ..	81
solvating reaction, extraction of U(VI)	118
for uranium, solvation number of ..	120
for uranyl salts, extraction efficiencies of	125
Phosphonate	
dibutyl, butyl-, extraction	398
dibutyl- <i>N,N</i> -diethylcarbonylmethylene (DBDECMP)	398
dihexyl- <i>N,N</i> -diethylcarbonylmethylene, (DHDECMP) ..	383, 467
-decalin extractants	400
-decalin-diisopropyl benzene solvents	400
degradation products in ion-exchange chromatography, effects of	450
extraction	441, 469-470, 475
hot-cell studies of	442
-scrub-strip studies	404t

- Phosphonate (*continued*)
 and high sodium waste, distribution data for 405t
 impurities on distribution coefficient of tracer Pr^{3+} , effect of .. 451t
 purification 399
 wash with bisodium carbonate-potassium cyanide 405t
 esters, preparation of neutral 91
- Phosphoric acid(s)
 actinide extracts, alkyl 72
 dibutyl
 actinides extraction by 485-487
 alcohol extractants for 478-481
 carboxylic acid extractants for 478-481
 dimerization of 477-481
 distribution ratios of 480f
 extraction of 481-482
 hydrogen-bonded complexes of
 aliphatic alcohol and 480f
 interaction effects of 485
 partitioning and dimerization constants 479t
- di(2-ethylhexyl)-
 actinides 147
 batch extraction tests on HAW solutions 435t
 extraction 431-433
 of lanthanides-actinides 147, 414, 448-450
 process engineering 438-439
- extractant
 for actinides, alkyl phosphoric 78
bis(2-ethylhexyl) 398
 di-(2-ethylhexyl) 343
 diisodecyl- 343
 extraction of 481-482
 (HD(DIBM)P), *bis*(2,6-dimethyl-4-heptyl) 157
bis(hexoxyethyl) 79
 monobutyl
 actinides extraction by 485-487
 interaction effects of 485
- mono(2-ethylhexyl)-
 concentration on the separation factor for Am, effect of 450t
 concentration on the separation factor for Eu, effect of 450t
 distribution coefficient for 450
 on separation factors for trivalent actinides, effect of 448
 on separation factors for trivalent lanthanides, effect of 448
- reactions, extraction of a trivalent actinide by a dialkyl 78
- Phosphorus
 -based acids in ethanol, pK_a 's of 91
 -based organic extractants, advantages of neutral 97
 extraction of Th into neutral 93t
- Phosphorus (*continued*)
 extraction of U into neutral 93t
 -oxygen bond basicity of 90
 -oxygen bond, effect on extractant selectivity 107
 Phosphorus-32 tracer 477
- Photochemical
 coreduction of U(VI) and Pu(IV) 274
 generation of reagents 272
 methods, advantages 267
 reductant, TBP as 272
 reduction
 plutonium 256-257
 plutonium, solvent extraction by .. 270
 uranium 256-257
 separations, requirements for 267-268
 techniques 264-274
- Photochemistry
 actinide 253-265
 solution 268
 to fuel reprocessing, applicability of 254
 of plutonium 254
- Photoredox reactions of Np in HNO_3 261-263
- Photoredox reactions of Np in perchloric acid 259-261
- Photoreduction separation of Pu from U 256
- Photoreduction of uranyl to U(IV) 254
- Photoseparations, actinide 263, 264t
- Pilot treatment plant, caustic waste ... 21-22
- Platinum, current-potential curves for 325f
- Plutonium
 acceptor reaction 195
 advantages of peroxide precipitation of 51
 in an aluminum-203-nitric acid medium 10
 on aluminum oxide column, breakthrough curve of 11f
 -aluminum target, chemical treatment of dissolved 43
 and americium recovery from α -radioactive aqueous waste, flowsheet for 342f
 aqueous
 with FeSA and HAW 522f
 with hydroxylamine nitrate and hydrazine 521f
 with mixtures of ferrous or ferric nitrate 521f
 backextraction 310f
 electrolytic 308
 in electroreduction mixer settler .. 309t
 breeder fuel 280
 in cadmium/magnesium alloys, solubility of 212f
 chemical similarities with Th and lanthanide elements 9
 combination in reprocessing end streams, Np and 538-541

Plutonium (*continued*)

concentration	
in filtrate	
nitric acid, effect on	63
profile	9, 346f, 355, 358f, 364f
and distribution ratio	360f
from the Purex process solutions	9
costripping of U and	287
cycle tests, second	527t
decontamination factors for	474
desorption, effect of temperature on	13
dioxide	
dissolution	499-513
in nitric acid	500-506
-fluorhydric acid	506-508
-cerium(IV)	511-513
kinetics of	512
of pyrochemical	500
of standard potentials for	
oxidative	505-506
in molten nitrates	237-239
uranium dioxide-	238-239
in nitric acid, solubility of	503f
reactions and thermodynamic	
data at low acidities	501-502
thermodynamic solubility curve	502
dissolution	
of standard potentials for	
oxidative	506
distribution coefficients for	192
distribution ratio of	365, 367f
effect of nitrous acid on	367f
donor reaction	195
during denitration of HAW solu-	
tions, behavior of	434t
by electrolytic reduction, separation	
of U and	317-330
elution from alumina column	13t
enrichment	187
extractants, effects of γ -irradiation	
on	345
extraction in pulsed columns	437
extraction by trioctylammonium	
nitrate	35
flowsheet for partitioning of U and	326f
fuel, thorex flowsheet for Th-U-	353f
fuels, heavy element separation	
for Th-U-	351-368
hydroxylamine nitrate, reaction	
mechanism and reduction	
kinetics	282
hydroxylamine salts reductants	282
interference of Th-234 on measure-	
ments	10
ion-exchange process for	457
ion-exchange separation of Np	
and	528-530
-irradiated targets, extraction	
chromatography for	33
loss, calculated	362f

Plutonium (*continued*)

losses to waste	525f
in a mixer settler, electrolytic	
reduction of U and	327-330
molybdate experimental data	578-579
molybdate, precipitation of	578
in nitric acid-fluorhydric acid,	
oxidation states of	9-16
nitrous acid stripping of	345
in organic phase, oxidation of	368
oxidation states and extractability	
of	536t
oxidation states effect on sorption	12t
oxide	
dissolution of	504f
dissolution, disadvantages of	
fluoride in	510
fuel, zinc distillation of uranium	
oxide-	186f
salt transport process for	
uranium oxide-	196f
-oxygen bond distances	575
partition, electropulse column	
for U-	291-300
partitioning methods in power-	
reactor fuel reprocessing	279-288
partitioning, Np and	526-527
peroxide	
effect of H ₂ O ₂ on filtration time	62
on filtration time	
effect of digestion time	62
effect of impurity concentration	62
effect of temperature	62
in nitric acid, solubility of	52
precipitate	
composition of	51
crystalline forms	51
filterability of determination of	55
sulfate ion effect on	52
precipitation	
equipment for	55
experimental design	56
experimental procedure	56
general equation and coeffi-	
cients values	58t
reagents	54
recommended levels for major	
variables in	66t
variables and levels used in	
investigating	53t
photochemical reduction	256-257
photochemistry of	254
pK _a 's of phosphorus-based acids	
in ethanol	91
in power reactor fuel reprocessing,	
electroreox of	303-315
precipitates from HNO ₃ solutions	579
product purification and	
concentration	527-528
product stability	528

- Plutonium (*continued*)
- by the Purex Process, separation of U and 317-330
 - purification of reprocessing end streams from 542
 - purification, effect of nitrous acid on 412
 - Reclamation Facility (PRF), Hanford 22-27
 - recovery
 - by ion exchange 465f
 - from metallurgical scrap 22-27
 - by the Purex process 17
 - from salt residues 465f
 - from various resins 459-467
 - redox reactions 354
 - as reductant 518
 - ferrous sulfamate- 363
 - hydroxylamine nitrate 352
 - reduction by HAN 523
 - reduction catalyst, ferric nitrate 520-522
 - reflux, effect of FeSA on 519-522
 - retention from HNO₃ on alumina .. 10t
 - retention on alumina, effect of HF on 10t, 12t
 - scrap, recovery of Am-241 from 417-418
 - separation (s)
 - from air samples 339-341
 - effect of acid concentration on U- 327
 - from lanthanides 43t
 - uranium 307f
 - in electroreduction mixer settler 305, 306t
 - uranyl photoreduction 256
 - solvent extraction by photochemical reduction 270
 - sorption 26t
 - thorium, uranium-
 - fuel, partitioning scheme for 288f
 - partition in Mg alloy 210
 - traces
 - flowsheet for recovery of 15f
 - sorption onto alumina 9
 - transfer to aqueous phase, effect of U reduction efficiency on 300f
 - uranium-
 - partition tests 297-299
 - partition, electropulse column for 291-300
 - partitioning
 - equipment 286
 - with HAN and FeSA 523t
 - hydrogen reductant for 282
 - nonreductive 286
 - in Purex process 279-280
 - valence adjustment of 524
 - Plutonium(III)
 - effect of nitrous acid on oxidation of 365
 - electro-oxidation of 312-315
 - oxalate precipitation 527
 - oxidation 463
 - Plutonium(IV)
 - onto aluminum-203, trace sorption of 13
 - and americium(III), distribution ratios of U(VI) 486f
 - disproportionation 257
 - distribution coefficients of 536t
 - acidic 537f
 - electrolytic reduction of 321-323
 - by HAN, effect of acidity on reduction rate of 361
 - hosts, polymolybdates as 571-580
 - oxidation, kinetics of 363
 - photochemical coreduction of U(VI) and 274
 - reduction
 - electrolytic 324f
 - organic U(IV), aqueous 273t
 - plutonium(III) 323
 - rate 323
 - separation from U in nitrate system with uranium(IV), redox reaction of 292
 - by uranium(IV) and (V), reduction of 272
 - from uranyl nitrate, desorption of .. 16
 - Plutonium-236 daughters 422
 - Plutonium-238
 - from aqueous waste streams, bone char removal of 19
 - flowsheet, plant tests of Np-237- 525t
 - from irradiated Am-241, medical-grade 422-423
 - from irradiated Np, recovery and separation of 17, 418-421
 - and neptunium-237 ion-exchange, separation of 530t
 - specific activity of 524
 - Plutonium-239
 - in air-monitoring sample 342f
 - from aluminum oxide column, elution curve of 14f
 - from aqueous waste streams, bone char removal of 19
 - tracers 398
 - Plutonium-241 decay 417
 - Polymolybdates as Pu(IV) hosts 571-580
 - Potassium nitrate
 - eutectic, molten lithium and 235
 - fission products in sodium and 241-243
 - molten sodium and 237
 - Potential curves, current-
 - determination of 317-319
 - for platinum cathode 318f
 - for titanium cathode 320f
 - Potentiometry, complexometric 137
 - Praseodymium-142 tracer 445
 - Praseodymium³⁺, effect of DHDECMP impurities on distribution coefficient of tracer .. 451t

Precipitation	
-ion-exchange process reduction of actinide concentration of PRF salt waste	22-24
iron hydroxide decontamination of actinide-containing waste solutions by	24
-sodium titanate sorption	27
Prereduction partitioning scheme	284f
PRF (<i>see</i> Hanford Plutonium Reclamation Facility)	
Process	
calcium recycle	215f
parameters for calcium reduction	216
stationary distribution in discontinuous	567f
Proliferation resistance	
Airox process	219-220
pyrochemical processes	178
uranium-plutonium-thorium partition	210
resistant	
advantages, Z distillation process	185
flowsheets	287
process streams	207
risks, aqueous reprocessing methods, spent reactor fuel	178
Protactinium (IV) by benzoylacetone, extraction of	80
PuO ₂ (<i>see</i> Plutonium dioxide)	
Pulsed plate columns	409
Pulverization conditions	226
Pulverization, effect of temperature on degree of	229
Purex	
flowsheets	287
high-level waste, flowsheet of actinide separation from	346f
partitioning schemes	281f
process(es)	72, 89, 272, 279, 303, 343, 376, 427, 431, 437, 517-518, 548
disadvantages	291
neptunium recovery by the plutonium recovery by	17
separation of U and Pu by	317-330
solutions, concentration of Pu from	9
uranium-plutonium partitioning in	279-280
waste	27
solvent	515
type HAW raffinates, actinides separation from	427-439
Purification	
of americium-241, Talspeak process-	36
of curium-244, Talspeak process-	36
of reprocessing end streams from Np and Pu	542
Pyrazolones extractants in synergistic systems with TBP and TOPO	81
Pyrocatechol	
Americium extraction from alkaline solutions by Aliquat 336	111
Europium extraction from alkaline solutions by 4(α,α -dioctylethyl)	111
extraction	
of actinides by Aliquat 336	108
by alkyl	111-114
of lanthanides by Aliquat 336	108
Pyrochemical	
dry processing methods	191
program	
development of	180-181
objectives of the	177
separations processes	181-188
scale up	181
in spent fuel reprocessing, advantages	179-180
fuel processing	196f
process(es)	
construction materials for	203
design criteria	195
engineering concepts	199-202
plant capacity	203, 204f
proliferation resistance	178
size	198
for spent reactor fuels	195-199
volumes	198f
processing of oxide fuels, Airox dry	219
processing of spent reactor fuel	177
reduction of high-fired thoria	216
Pyrocivex process for fuel enrichment	220, 225
Pyrometallurgical method for reprocessing of Th-based fuels	208-211
Pyrometallurgical process, fission products control	211
Q	
Quantum efficiencies for redox reactions of actinides	258f
Quaternary extractants	101
R	
Radiation damage to TBP extractant solutions	487-488
Radiation on organic extractant, effect of	153
Radiolysis	
of adsorbed water	505
alpha	518
products	524
Radiolytic effects on extractant	400
Radionuclides, effect of pH on sorption and elution	28
Radionuclides from inorganic ion exchangers, HNO ₃ desorption	31f

- Radiotoxicity index of waste fuel 535f
- Raffinate, Am-241 recovery from
aqueous 22
- Reactions, extraction by dialkyl
phosphoric acid 78
- Reactor fuel reprocessing, potential 89
- Reactors, fuel recycling in fast-
breeder 177
- Recovery
of americium-241/243 from
HAW 414-417
of curium-244 from HAW 414-417
limitations, sorption 30
- Redox
agents 536t
on actinide extraction, effect of .. 538t
methods 9
process 279
reaction(s) 244-246
of actinides, quantum efficiencies 258t
plutonium 354
of plutonium(IV) with
uranium(IV) 292
- Reducing agent(s) 13, 527, 539
cadmium-based 182
ferrous sulfamate 279-280
holding reductants 280-282
- Reductant(s)
holding 363
of plutonium, hydroxylamine salts .. 282
for uranium-plutonium partition-
ing, hydrogen 282
- Reduction (s)
data, U electrolytic 296t
efficiencies, U 298f
efficiency on Pu transfer to aqueous
phase, effect of U 300f
electrolytic Pu(IV) 324f
in fuel reprocessing 214-216
of high-fired thoria, pyrochemical .. 216
of nitric acid, electrolytic 319-321
organic U(IV)-aqueous Pu(IV) 273t
oxide 187
parallel electrolytic 286
photochemical actinide oxidations
and 269f
of plutonium(IV), electrolytic 321-323
process, electrolytic 291
process parameters for calcium 216
rates of AmO₂ 172t
rates, UO₂ 226
of thorium-based fuels 208-210
of uranium dioxide, carbothermic .. 184
of uranium and plutonium in a
mixer settler, electrolytic 327-330
of uranium(VI), electro-
lytic 321, 323, 325f
- Reprocessing of nuclear fuel,
aqueous 345-347
- Reprocessing of nuclear fuel, dry 347
- Resin(s)
applications, anion 17
gel-type 463
macroporous 463, 528
preparation 4
properties 528
of ion-exchange 467
scanning electron photomicrographs
of ion-exchange 529f
- Rhodium black catalysts 433
- Rhodium precipitation, Pd and 565
- Ruthenium, effect on Ce(IV) 513
- Ruthenium in U calcination 552
- Ruthenium, volatilization of 234
- S**
- Salt
molten
oxidation-reduction processes for
fuel processing 233-250
redox process, requirements and
problems 248
systems, acids and bases in
oxyanionic 243
transport process 211
chemistry 192-195
for uranium oxide-plutonium
oxide 196f
for uranium and plutonium in
spent reactor fuels 191-205
- Salting agent(s) 77, 101, 361
nitrate 279, 428-429
- Scheme for HAW partitioning 430f
- Scrub solutions, actinides recovery
from 475-494
- Scrub solutions, flowsheet for process-
ing sodium carbonate 487-494
- Selectivity of the hydroxide ion 7
- Separation (s)
by dialkyl sulfoxides, actinide 77
by extraction chromatography,
Am(VI)-Cm(III) 47, 49t
factors
for chemical systems 36t
for the extraction of Th(IV) 92, 94
for the extraction of U(VI) 92, 94
of transplutonium elements 43
lanthanide(s)
conditions for transplutonium-
of plutonium from 43, 43t
of plutonium from lanthanides 162
by tertiary amines, actinides 77
of transplutonium elements from ... 35
- Silver (II) complexes 162
- Silver-catalyzed Am(III) oxidation .. 160
- Sodium
dibutyl phosphate, distribution
ratio of 485t
fluorine traps 556

Sodium (<i>continued</i>)	
monobutyl phosphate, distribution ratios of	485t
niobate, preparation and properties of	18-19
nitrate-potassium nitrate, fission products in	241-243
titanate	
decontamination of Hanford PRF waste	22-27
ionic exchanger	25
physical properties	18t
preparation and properties of	18-19
sorption, precipitation	27
synthesis of	18
zirconate, preparation and properties of	18-19
Solid-liquid phase separation	246
Solubility curve, PuO ₂ thermodynamic	502
Solvation number of TOPO for U	120
Solvent	
cleanup and recycle	389
extraction	71, 515
Purex	515
Sorbent(s)	
applications	19-31
inorganic	
in actinide separations	17
disadvantages in nuclear fuel cycle	17
nuclides desorption from	28
use in chromatographic separation of Am-Cm from rare earth ions	27
use in decontaminating liquid waste streams from actinides	17
use in separating Am and Cm from lanthanides	17
preparation	17-19
properties	17-19
source	17-19
Sorption	
of actinides	26t
onto alumina, recovery of plutonium traces by	9, 13
of caustic waste	21
effect of Pu oxidation states on	12
and elution of radionuclides, effect of pH on	28
precipitation, sodium titanate	27
procedure, fluorination-	549-550
quantitative	28
reactor	549
recovery limitations	30
system for caustic waste decontamination, development of	21
Spectrometry, alpha	9
Spectrophotometry	4, 118
Standard potentials for oxidative dissolution of PuO ₂	512
Steric	
considerations in the extraction of uranyl nitrate	75
effects	481
factors	572
influence on extraction selectivity	77
hindrance, importance in liquid-liquid extraction separations	98
influences, extractant selectivity	105
properties of the extractants	90
properties of phosphorus-based extractants	89
Stripping	
of americium-curium, cross-current	443f
coefficients, transcurium elements ..	152
counter-current	493
organic-phase modification and	152
Structural modification, effect on extraction capacity	102
Sulfamate, ferrous (FeSA)	469
and hydroxylamine nitrate, aqueous Pu with	522f
hydroxylamine nitrate replacement of	522-523
plutonium reductant	363
on plutonium reflux, effect of	519-522
as reductant	518
uranium-plutonium partitioning with HAN and	523t
Sulfate	
leach liquors, recovery of U from	76
solutions, absorption spectra of uranyl	122f
-sulfuric acid solutions, Np(V) ion-exchange in	3
Sulfonic acids, ion-exchange extractants	80
Sulfoxide(s)	
actinide separations by dialkyl	77
dioctyl, (DOSO)	78
dipentyl	78
di- <i>n</i> -pentyl, (DPSO)	77
diphenyl	78
extractants	77
Sulfur donor ligands	
in actinide separations	131
complexes of actinides ions and lanthanide ions	140
Sulfuric acid	
dodecyl (DSA), extraction of	482
solutions by TOPO, extraction of U(VI) from	117-128
solutions, Np(V) ionic exchange in sulfate-	3
Synergism with Aliquat 336-S chloride	81
Synergistic systems	
with adduct in aqueous phase	81
of organophosphorus compounds in U extraction	81

- Synergistic systems (*continued*)
 recovery of U from phosphoric acid 81
 solvent extraction 80
 with TBP and TOPO, pyrazolones
 extractants in 81
- Synthesis of sodium titanate 18
- T**
- Talspeak
 cycle, flowsheet 449f
 mode, actinides-lanthanides parti-
 tioning reverse 414
 process 33, 35, 431, 438, 441
 Curium-224 36
 kinetics of the 79
 purification of Am-241 36
 reverse 431, 435-436
 studies 448-450
 process of lanthanide-actinide
 separation 73
 separation of Am-Cu 414
- Tantalum sampling tubes 213
- Targets, processing of irradiated 419f
- TBP (*see* Tributyl phosphate)
- Techneium
 on magnesium fluoride, fluorination
 and sorption of 548-550
 in pilot-plant fluorination 557
 in uranium calcination 552
- Temperature
 dependence of distribution
 coefficient 126t
 effect of
 Airox process 226-230
 on degree of pulverization 229
 on plutonium desorption 13
 effect on distribution coefficient 125
- Tertiary treatment of low-risk waste
 stream 19
- Tetraalkylammonium thiocyanate 131
- Tetraalkyldiphosphinedioxides
 extractant 75
- Tetraalkyldiphosphonates extractant .. 75
- Tetrahydral holes 572
- cis*-Tetratolylylene diphosphine
 dioxide, extraction by 76
- Thenoyl trifluoroacetone (TTA) 80
 synergism with Aliquat 336-S
 chloride 81
- Thermocouple, chromel-alumel 213
- Thermosiphon/oxidizer apparatus 386
- Thiocyanate, tetraalkylammonium 131
- Thorex
 flowsheet for Th-U-Pu fuel 353f
 partition cycle flowsheet, acid-
 process(es) 89, 534
 acid- 371-376
 two-cycle 537f
 solvent extraction flowsheet 351
- Thoria, pyrochemical reduction of
 high-fired 216
- Thorium
 -based fuels
 flowsheet for 209f
 nonaqueous reprocessing method
 for 207-216
 pyrometallurgical method for the
 reprocessing of 208-211
 in cadmium-magnesium alloys,
 solubility of 212f, 213, 215f
 concentration profile and distribu-
 tion ratio 355, 356f
 dioxide, dissolution in HNO₃-HF .. 507
 effect of DBP on Zr separation from
 extraction into organic extractants .. 93t
 flowsheet 373
- fuel
 cycle(s) 207, 351, 371
 uranium-232 buildup in 207-208
 partitioning scheme for U-Pu 288f
 reprocessing, requirements 208
 and lanthanide elements, Pu
 chemical similarities with 9
 loss, calculated 362f
 partition
 cycle, U- 376
 in magnesium alloy, U-Pu- 210
 proliferation resistance of U-Pu- 210
 in sulfate systems, separation of 76
 tracers, purification 92
 tributyl phosphate, extractant for .. 72
- uranium
 fuel cycle 533-545
 fuel, elemental and isotopic
 composition of spent 533t
 -plutonium fuel, thorex flow-
 sheet for 353f
 -plutonium fuels, heavy element
 separation for 351-368
 separation in the acid-thorex
 process 371-376
 from uranium, aqueous reprocess-
 ing methods for separation 207
- Thorium (IV)
 acid solutions, TOPO extraction of .. 117
 extraction
 distribution ratio of 92, 93f
 kinetics of 79
 nitric acid dependency of 96f
 separation factors for 92, 94
- Thorium-234 interference measure-
 ments of Pu 10
- Tin, nitriding of U in molten 185
- Tin process for reactor fuels 184
- Titanate powder beds 25
- Titanium cathode, current-potential
 curves for 320f
- TOPO (*see* Phosphine oxide,
 tri-*n*-octyl-)

- Uranium (*continued*)
- fuel cycle, Th- 533-545
 - fuel, elemental and isotopic composition of spent Th- 533*t*
 - hexafluoride 547-558
 - in molten tin, nitriding of 185
 - in nitrate system, Pu(IV) separation from 76
 - non-aqueous reprocessing methods for separating Th from 207
 - oxide-plutonium oxide fuel, Z
 - distillation of 186*f*
 - oxide-plutonium oxide, salt transport process for 196*f*
 - partitioning equipment, Pu- 286
 - photochemical reduction 256-257
 - and plutonium
 - costripping of 287
 - by electrolytic reduction 317-330
 - flowsheet for partitioning of 326*f*
 - by the Purex Process 317-330
 - plutonium
 - fuel, thorex flowsheet for Th- 353*f*
 - fuels, heavy element separation for Th- 351-368
 - partition tests 297-299
 - partition, electropulse column 291-300
 - partitioning
 - hydrogen reductant for 282
 - in Purex process 279-280
 - with HAN and FeSA 523*t*
 - separation 307*f*
 - effect of acid concentration on in electroreduction mixer settler 305, 306*t*
 - thorium
 - fuel, partitioning scheme for 288*f*
 - partition in Mg alloy 210
 - partition, proliferation resistance 210
 - reduction efficiency(ies) 295, 297-299,
 - separation(s) 246
 - in the acid-thorex process, Th- .. 371
 - solar 271*t*
 - solvation number of TOPO for 120
 - from sulfate leach liquors, recovery of 76
 - in sulfate systems, separation of 76
 - thorium partition cycle 376
 - tracers, purification 92
 - transfer rate, electropulse column .. 297
 - trioxide
 - mechanism and kinetics of fluorination 555
 - removal of nitrate from 547-548
 - uranyl photoreduction separation of Pu from 256
 - from wet-process phosphoric acid with synergistic systems, recovery of 81
- Uranium(IV)
- absorption spectrum of 269*f*
 - Pu(IV) reduction 273*t*
 - cycle electrolytic oxidation of
 - $N_2H_5^+$ 326*f*
 - photoreduction of uranyl to 254
 - reduction of Pu(IV) by 272, 292
- Uranium(V)
- reduction of Pu(IV) by 272
- Uranium(VI)
- determination by EDTA titration 117-118
 - dioxide and Am(III) distribution coefficients 165*t*
 - disproportionation of 304
 - distribution coefficient(s) of 79, 140, 142*f*
 - effect of oxidizing reagents on 168
 - distribution ratios of extraction 92
 - effect of oxidizing reagents on distribution coefficients 165
 - electrolytic reduction 321, 323, 325*f*
 - extraction 106*f*, 119*f*, 126*f*
 - acid solutions, TOPO 117
 - distribution ratio of 93*f*
 - from mineral acids by *bis*-(di-*n*-hexylphosphinyl) alkanes 75
 - nitric acid dependency of 96*f*
 - separation factors for 92, 94, 166*f*
 - from sulfuric acid solution(s) by TOPO 117-128
 - synergistic 140
 - plutonium(IV), and Am(III), distribution ratios of 486
 - and plutonium(IV), photochemical coreduction of 274
 - ultraviolet-visible absorption spectrum of 269*f*
- Uranium-232 buildup in Th fuel cycle 207-208
- Uranium-236 enrichment of U reductant 280
- Uranyl
- ions, vibrational excitation of 270
 - nitrate
 - desorption of Pu(IV) from 16
 - solutions, sorption of Pu traces on alumina 9
 - steric considerations in extraction 75
 - photoreduction separation of Pu from U 256
 - salts, extraction efficiencies of TOPO 125
 - salts by TOPO, extraction of aqueous solutions 127*t*
 - sulfate
 - NMR assignments for aqueous 125
 - solutions, absorption spectra of .. 122*f*
 - TOPO, IR assignments for aqueous 123
 - tributyl phosphate extractant for 72
 - to uranium(IV), photoreduction of 254

V

Vacuum	
distillation, Mg separation by	197
distillation, Z separation by	197
transfer	149
Vanadium oxidant, pentavalent	412
Vibrational excitation from IR laser irradiation	270
Vortex mixer	92

W

Waste(s)	
actinide(s)	
recovery from acidified salt	390f
removal from high sodium	408t
removal from Zr-Al coprocess	
high-level	408t
separation from high activity	561-569
bone char column for treatment	
of low-risk	20f
cross-current extraction of Am-Cm	
from high-level liquid	443f
distribution data for DHDECMP	
and high sodium	405t
extraction studies on high sodium	403
extraction studies with Zr-Al	402-403
flowsheet	
for actinide partitioning from	
acidic	407f
of actinide separation from Purex	
high-level	346f
for americium-curium recovery	
from high-level	415f
for bone char treatment of low-risk	20f
for plutonium and americium	
recovery from α -radioactive	
aqueous	342f
fuel, radiotoxicity index for	535f
Hanford Plutonium Reclamation	
Facility (PRF) salt	22
hazard potential	534
high activity	
component ions	565t
direct partitioning	439
direct partitioning, HDEHP	
process for	438
partitioning solutions	433
partitioning, TBP process	429
processing, flowsheet of	563
raffinates, actinides separation	
from purex type	427-439
solutions	
behavior of Pu during denitration of	434t
denitration of	433
denitration-oxalate precipitation of	436t

Waste (continued)

high activity (continued)	
solutions (continued)	
phosphoric acid, di(2-ethylhexyl)-, batch extraction	
tests on	435t
synthetic	434t
high level waste, separation of	
actinides from	343
high sodium	405t
infrared evaporating system for	
treatment of α -radioactive	344f
management	381, 427
aqueous fission product	395
metal hydroxide scavenging of	
Am-241 from PRF salt	25
neptunium losses to	525f
nuclear fuel element solutions,	
TPE removal from	101
partitioning	427-439
of actinides from acidic	
nuclear	395-409
high-level liquid	384f
process scheme for high-activity	432f
pilot-plant test of filtration, bone	
char decontamination of caustic	23f
pilot-plant tests on Zr-Al high-level	409
plutonium losses to	525f
precipitation	
of actinide-lanthanide oxalates	
from high-level liquid	442-445
-ion-exchange scheme for	
removal of actinides from	
salt	23f
of lanthanide oxalates from	
synthetic high-level	447t
processing high-level liquid	442
processing, flowsheet of the high-activity	564f
Purex process	27
recovery of Am-241/243 from high-level	414-417
recovery of Cm-244 from high-level	414-417
reduction of actinide concentration	
of PRF salt precipitation-ion-exchange process	22-24
reduction, HAN	518-523
removal of Am from high-level	441-452
removal of Cm from high-level	441-452
retrievable alpha	27
retrievable transuranium	25
salts processing	455
sodium titanate decontamination of	
Hanford PRF	22-27
solution(s)	
actinide process	24t
composition of molten salt	
extraction	458t
composition, synthetic	444t

